Lille 1 University laboratory:
GEOSYSTEMES, UMR
8217 CNRS-Lille1

China University of
Geosciences (Wuhan):
Faculty of Earth Sciences

Le Phytoplancton de la limite Permien-Trias du Sud de la Chine

Ph.D. Candidate: LEI Yong

Major: Géosciences, Ecologie, Paléontologie et Océanographie

Supervisors: Dr. Thomas SERVAIS
Prof. FENG qinglai

Cité Scientifique 59655
VILLENEUVE D'ASCQ Cedex

388 Lumo Road, Hongshan District
Wuhan 430074, Hubei, P.R.China

Université des Sciences et Technologies de Lille1

Ecole doctorale des Sciences de la Matière, du Rayonnement et de l'Environnement
Laboratoire "Géosystèmes" - UMR CNRS 8217

Thèse présentée pour obtenir le titre de Docteur de l'Université de Lille1
Spécialité "Géosciences, Ecologie, Paléontologie et Océanographie"

Par Yong LEI

Le Phytoplancton de la limite Permien-Trias du Sud de la Chine

Thèse en co-tutelle dirigée par Thomas Servais (CNRS, Université de Lille1) et Feng Qinglai (China University of Geosciences)

Date de soutenance prévue: le 22 mai 2013, à Wuhan (Chine)
devant le jury composé de:

Sylvie CRASQUIN: CNRS, Université de Paris6, France; *Rapporteur*

FENG Qinlai: China University of Geosciences; *Directeur de thèse*

LI Jun: Nanjing Institute of Geology and Palaeontology; *Rapporteur*

Thomas SERVAIS: CNRS, Université de Lille1; *Directeur de thèse*

作者简介

雷勇，男，1985年出生于重庆市璧山县。于2004年入读中国地质大学（武汉）环境学院，学习生物科学。在2008年9月就读于本校地球科学学院的古生物学与地层学专业，两年之后提前攻读博士学位。期间，本人于2011年9月至2012年12月，在法国里尔一大进行博士联合培养学习一年。通过此次博士论文答辩之后，可以同时获得里尔一大和中国地质大学（武汉）的博士学位。攻读博士学位期间，学习8门课程，共修18个学分，其中学位课12学分，选修课6学分，平均成绩为83分。

在科研方面，本人积极与导师冯庆来教授和Thomas Servais研究员探讨有关二叠纪与三叠纪之交海洋浮游植物演变的问题。先后参与的科研项目有：中国石油化工股份有限公司海相油气勘探前瞻性项目“海相优质烃源岩形成的地球生物学过程”（编号: G0800-06-ZS-319）；国家自然科学基金重点项目：“放射虫和硅在华南新元古代和古生代烃源岩形成中的作用研究”（项目号：40839903）；国家自然科学基金项目：“重大地质突变期生物与环境协同演化”（项目号：40921062）

攻读博士学位期间（2008~2013年），现已公开发表学术论文8篇，其中以第一作者发表学术论文4篇，其中3篇为SCI。在投的学术论文3篇，文章具体目录如下：

Published or accepted papers:

[1]**雷勇**，冯庆来，桂碧雯. 安徽巢湖平顶山剖面上二叠统大隆组有机质富集的地球生物学模式. 古地理学报. 2010.(12): 202-211.

[2]**Lei, Y**., Servais, T., Feng, Q.L., He, W.H. The spatial (nearshore-offshore) distribution of latest Permian phytoplankton from the Yangtze Block, South China. **Palaeogeography, Palaeoclimatology, Palaeoecology. 2012. (363-364): 151-162.**

[3]**Lei, Y**., Servais, T., Feng, Q.L. The diversity of the Permian phytoplankton. **Review of Palaeobotany and Palynology. (In press. DOI: 10.1016/j.revpalbo.2013.03.004)**

[4]**Lei, Y**., Servais, T., Feng, Q.L., He, W.H. Latest Permian phytoplankton from the Yangtze Platform. **Palynology. (Accepted for publication)**

[5]聂小妹，**雷勇**，冯庆来，向宇. 四川广元上寺剖面长兴阶放射虫动物群演变及控制因素. 地质论评. 2012.(58): 809-815.

[6]徐国真，冯凡斌，**雷勇**，沈俊，冯庆来. 贵州安顺新民二叠系—三叠系界线剖面磁化率变化及古气候环境意义. 沉积学报. 2012.30(5):817-824.

[7]沈俊，周炼，冯庆来，张木辉，**雷勇**，张宁，喻建新，顾松竹．华南二叠纪-三叠纪之交初级生产力的演化以及大隆组黑色岩系初级生产力的定量估算．中国科学D辑. (Accepted for publication)

[8]SHEN Jun, ZHOU Lian, FENG QingLai, ZHANG Muhui, **LEI Yong**, ZHANG Ning, YU Jiangxin, GU Songzhu. Paleo-productivity evolution across the Permian-Triassic boundary and quantitative calculation of primary productivity of black rock series from Dalong Formation, South China. Chinese Science Bulletin D. (Accepted for publication)

Manuscripts:

[1]**Lei Yong** et al. Palynology and palynofacies of the Upper Permian to Lower Triassic of Shangsi (Sichuan, China). **Review of Palaeobotany and Palynology. (revised and under corrections)**

[2]**Lei Yong** et al. The phytoplankton community succession during the Permian-Triassic boundary in South China-one of the possible mechanism for the mass extinction. (To be submitted to Palaeogeography, Palaeoclimatology, Palaeoecology)

[3] JUN SHEN, **YONG LEI**, THOMAS J. ALGEO, QINGLAI FENG, THOMAS SERVAIS, JIANXIN YU, and LIAN ZHOU. Volcanic Effects on Microplankton during the Permian-Triassic Transition (Shangsi and Xinmin, South China). **(Submitted to Palaios)**

华南二叠纪与三叠纪之交的浮游植物

博士生：雷勇　　导师：Thomas Servais；冯庆来

摘　要

二叠纪与三叠纪之交的生物大灭绝是自显生宙以来地球上发生的最大一次集群灭绝事件，距今约252Ma。这次事件造成当时海洋生态系统中大约90%以上的物种灭绝。许多学者将这次灾难事件归因于环境的突变，如海洋的大范围缺氧、西伯利亚火山喷发以及海平面骤降等。而在统计生物多样性变化的时候，多数学者只关注海洋动物物种多样性的变化，对于遍布海洋的浮游植物却是知之甚少。甚至于一些研究浮游植物的学者也只是参与争论二叠纪与三叠纪之交的“真菌高峰”事件。而近年来，一系列关于二叠纪末期蓝细菌爆发的报道则引发了大家对海洋初级生产者的注意。因此，本文主要研究了华南地区二叠纪与三叠纪之交的疑源类，同时结合前人有关蓝细菌以及其它动物化石的数据，综合分析了二叠纪末生物大灭绝期间浮游植物群落的演替及其对生态环境的影响。

首先，笔者总结了二叠纪的疑源类化石。结果表明：相对于孢粉化石，二叠纪疑源类的研究程度较低，但是其物种多样性远远超出前人的预计。尽管具大型膜壳的疑源类化石在古生代中期以后就很少出现，但是具小型膜壳的类型在二叠纪的地层中仍然相当丰富。二叠纪的各个阶都可以发现 20-30 个疑源类化石属。而某些常见的属（如 *Micrhystridium* 和 *Veryhachium*）则被报道超过40余次。然而，我们还需要更多的数据才能找到二叠纪疑源类物种多样性的变化规律，而且需要对具小型膜壳的种类倍加留意。

本文选取的七个剖面均位于华南地区二叠纪与三叠纪之交的地层中，包括中寨剖面、凉风垭剖面、上寺剖面、甘溪剖面、峡口剖面以及东攀剖面。在这些剖面里找到了丰富且保存完好的疑源类化石。大部分化石的膜壳较小，其直径在20微米左右，如：*Micrhystridium*、*Veryhachium* 以及 *Leiosphaeridia*。同时也在上寺等剖面发现了一些具大型膜壳的疑源类化石，如 *Dictyotidium*（膜壳直径达80微米）。而这些化石基本都在其它晚二叠世的地层中报道过。

由于出现了十余种归属于 *Micrhystridium* 和 *Veryhachium* 的化石，且发现将其划归到物种级别较为困难。因此，本文从化石膜壳形态学的角度将 *Micrhystridium*/*Veryhachium* complex 类群划分为五类。其中，*Veryhachium cylindricum* 亚属代表具椭圆形膜壳的类型；*Veryhachium trispinosum* 亚属囊括具三角形膜壳的类群；而 *Veryhachium lairdii* 亚属则包含所有四边形膜壳的种类；*Micrhystridium pentagonale* 亚属涵盖五边形或者六边形膜壳的类群；而 *Micrhystridium breve* 亚属则包括具球形膜壳的物种。

为了研究华南地区二叠纪末期疑源类在海洋中的空间分布特征，文中选定六个剖面来分析。这些剖面囊括从近岸浅海到远岸深水的沉积环境。根据疑源类属种的生物多样性和物种的丰度，并结合前人的相关资料分析表明：（1）近岸地区的疑源类物种多样性较低，一般只有 2-4 种（如中寨和东攀剖面）；而相对远岸的大陆架地区物种多样性较高，可以达到 10 种左右（如煤山、上寺以及凉风垭剖面）；但是随着离岸距离的增加，大陆坡地区的疑源类物种多样性同样是较低的（如甘溪和峡口剖面）。（2）在疑源类化石属一级上，*Leiosphaeridia*、*Reduviasporonites* 以及 *Micrhystridium* 从近岸浅水环境到远岸深水地区均有分布；*Dictyotidium* 和 *Veryhachium* 更多地出现于开阔的海域。（3）*Schizosporis* 则只在上寺和煤山剖面的二叠纪与三叠纪之交的地层附近出现（海平面较低时），可能指示一种相对近岸浅水的环境。（4）在物种级别上，具短突起的 *Micrhystridium breve* 在近岸环境中占据绝对优势，且对营养盐的浓度较为敏感，其生物量的变化与 Fe 和 Al 元素的含量变化较为一致。而膜壳较大（直径约 80 微米）的球形疑源类如 *Dictyotidium reticulatum* 一般出现在浅水区域，膜壳较小（直径约 30 微米）的 *Leiosphaeridia* 则更多地分布在水体较深的环境中。同时，膜壳光滑的 *Leiosphaeridia minutissima* 在近岸占据优势，而膜壳具颗粒纹饰的 *Leiosphaeridia micrograniferа* 则在远岸较为丰富。（5）虽然链状疑源类 *Reduviasporonites* 出现在多个剖面，但是众多学者认为的二叠纪末期的“真菌高峰”在扬子板块的海相地层中并没有出现。需要指出的是，个体较大的 *Reduviasporonites chalastus*（单胞直径约 40 微米）常分布于近岸环境；而个体较小的 *Reduviasporonites catenulatus*（单胞直径约 15 微米）则更多地出现在远岸深水的区域。

基于疑源类化石与动物化石的生物多样性变化规律，文中将华南二叠纪与三叠纪之交的地层划分为较为明显的三个阶段。阶段 1 对应的牙形石生物带为 *Clarkina changxingensis* 带以及 *Clarkina yini* 带，此阶段的疑源类化石生物多样性是三个阶段中最高的，发现疑源类达 10 属 28 种。与第一阶段相比，阶段 2 的疑源类化石生物多样性出现大幅降低，只出现 7 属 11 种。其对应的牙形石生物带为 *Clarkina meishanensis* 带、*Hindeodus changxingensis* 带、*Clarkina taylorae* 带以及 *Hindeodus parvus* 带。而阶段 3 对应 *Isarcicella staeschei* 带和 *Isarcicella isarcica* 带，只有一种疑源类化石 *Leiosphaeridia minutissima* 零星地出现在凉风垭剖面和甘溪剖面。

二叠纪末期的生物大灭绝之前（阶段 1），海洋生态系统总体保持动态平衡，动物以及浮游植物都具有较高的生物多样性。但是，由于环境的突变（如大规模的火山喷发、海平面的骤降以及温度升高等），海洋生态系统的平衡被打破。大多数的动植物由于对环境的不适应而惨遭灭绝，而生命力极强的蓝细菌却在这适宜的环境中大面积爆发，成为最主要的初级生产者。然而，蓝细菌的爆发却给环境带来了持续性的恶化，首先是加大了海洋透光带中光衰减的程度；其次是加速了海水中的氧气消耗；同时也为海洋动物提供了有毒的且贫营养的食物。这三点影响对其它浮游植物以及大多数的海洋动物来说都是致命的。但是，不同物种对于这些影响的反应却是不一样的。总体来讲，疑源类等其它类型的浮游植物基本从近岸海域中消失，只分布在远岸的水域。而个体较大的动物则基本消失，体型较小的动物凭借其对蓝细菌以及恶劣环境较强的适应性而得以残存（阶段 2）。然而此次生物危机并未结束，随着温度的进一步升高以及无机营养盐的持续性输入，蓝细菌的爆发向远岸以及深水环境中扩

张（阶段 3；上寺剖面 28 层以及煤山剖面 29 层），致使大多数在前一阶段残存的种类也不能在这更为恶劣的环境中幸免而遭到灭绝，只剩下个别适应力极强的灾难种得以存活并繁盛（如双壳类的 *Claraia*）。

大规模的火山喷发可能是二叠纪末期生物大灭绝的导火索，其导致了生态环境的巨大变化，如温度升高等。本文认为：高温以及陆地风化的加强直接促使蓝细菌的持续性爆发。而蓝细菌的不断增殖则加深了海水的缺氧程度以及造成了其它浮游植物的大量减少。经过以上的变化，海洋的缺氧、高温以及食物的缺乏则是海洋动物灭绝的直接原因。

关键词：晚二叠世，早三叠世，生物大灭绝，疑源类，浮游植物

The phytoplankton at the Permian-Triassic boundary (PTB), South China

Ph.D. Candidate: Lei Yong Supervisors: Thomas Servais; Feng Qinglai

ABSTRACT

The end-Permian extinction event (252 Ma ago) is considered the greatest mass extinction in the history of the Earth, with over 90% of all marine species becoming extinct. Many authors try to explain the causes of this extinction, linking it to environmental catastrophes, such as ocean anoxia, Siberian trap volcanism, sea-level changes, etc., but the causal factors of the extinction still remain controversial. Most studies documented the extinction of marine metazoan groups, and usually ignore the fluctuations of the diversity of primary producers in the marine environments at the Permian-Triassic boundary (PTB), although the presence of a possible "fungal spike" in the Late Permian let to much debate. Recently, a series of papers analyzed the cyanobacterial changes during the PTB interval in South China. On the other hand, a few papers documented in the PTB strata the biodiversity changes of the acritarchs, which are considered to represent the major part of the organic-walled microphytoplankton in the Palaeozoic. The objective of the present study is to document the different phytoplankton communities (including acritarchs and cyanobacteria) in the Chinese PTB strata and to try to analyze the relationships between the mass extinction and the phytoplankton community changes at the PTB, South China.

Firstly, we present a synthesis of the Permian fossil record of acritarchs at a global scale. The revision shows that Permian acritarch descriptions have largely been neglected, compared to other palynomorph groups, such as spores and pollen grains. While larger organic-walled cysts, as known from the Lower and Middle Palaeozoic, are usually absent, many smaller acritarchs are commonly found in Permian palynological assemblages. During most of the Permian stages, acritarch show a genus richness of about 20 to 30 genera. Some genera, such as *Micrhystridium* and *Veryhachium*, have been reported in over 40 publications. Nevertheless, many Permian acritarchs still need to be documented in detail, and additional systematical studies, in particular of the very small taxa, are needed to fully understand the diversity and significance of Permian acritarch.

The description of new material includes the analyses of diverse and well-preserved latest

Permian phytoplankton assemblages from seven sections of the Yangtze Block (South China) from the localities Zhongzhai (Guizhou Province), Liangfengya (Chongqing City), Meishan (Zhejiang Province), Shangsi (Sichuan Province), Xiakou and Ganxi (Hubei Province) and Dongpan (Guangxi Province). Most of the species have been reported previously from other Late Permian sections elsewhere in the world. The South Chinese phytoplankton taxa are generally very small in size, usually displaying diameters of about 20 μm, and commonly include the genera *Micrhystridium*, *Veryhachium* and *Leiosphaeridia*. However, larger taxa with vesicles often exceeding 80μm in diameter, such as *Dictyotidium*, are also abundant in the Shangsi section.

The taxonomical descriptions of the acritarch assemblages include a reevaluation of the classification of two of the most common taxa. Due to the presence of large populations of *Micrhystridium* and *Veryhachium*, a simple classification scheme for the *Micrhystridium*/*Veryhachium* complex is proposed, based on the geometrical shape of the vesicle. We propose dividing the complex into five groups: the *Veryhachium cylindricum* group, representing all ellipsoidal specimens; the *Veryhachium trispinosum* group, with triangular shape vesicles; the *Veryhachium lairdii* group, with rectangular central bodies; the *Micrhystridium pentagonale* group, including all pentagonal specimens; and the *Micrhystridium breve* group, representing all spherical forms.

Subsequently, in order to analyze the spatial (palaeoecological) distribution of the organic-walled microphytoplankton in the Late Permian, the palynological material from six of the investigated sections from the Yangtze Block, South China, displaying different sediment facies types (from neritic to offshore palaeoenvironments, including basinal facies) has been investigated. Based on the diversity and relative abundance of acritarch species and genera, the new data from the Chinese Late Permian sections provide similar patterns as those described from other geological periods: (1) low diversities with 2 to 4 acritarch species occur in nearshore environments, whereas the higher diversities (more than ten acritarch species) appear in the offshore environments; (2) at the generic level, the genera *Leiosphaeridia*, *Reduviasporonites* and *Micrhystridium* are distributed widely, from nearshore facies corresponding to shallow water environments to offshore facies corresponding to deeper water settings, whereas some genera, such as *Dictyotidium* and *Veryhachium,* have a narrower distribution, occurring on the continental shelf and towards the basin, indicating open marine environments; (3) the genus *Schizosporis* only occurs around the PTB, when the sea level declined, probably indicating nearshore environments with shallow water settings; (4) at the specific level, the species *Micrhystridium breve,* displaying short spines, and *Leiosphaeridia minutissima* are indicative of neritic facies, whereas the other species of *Micrhystridium* and *Veryhachium* with longer spines (e.g., *Micrhystridium stellatum* and *Veryhachium hyalodermum*) and *Leiosphaeridia microgranifera* indicate more open marine environments. Big spherical acritarch species (over 80 μm in diameter), such as *Dictyotidium reticulatum*, indicate shallow water environments; (5) in the PTB strata, the relative abundance of the enigmatic *Reduviasporonites*, interpreted by some authors as a fungal spore, is never higher

than 14%, indicating that a ‘spike’ of *Reduviasporonites* did not occur in the Yangtze area. *Reduviasporonites chalastus* (40μm in length) obviously dominates in shelf environments of shallow water, whereas the smaller *Reduviasporonites catenulatus* (15μm in length) is more common in deeper water.

Another part of the present study concerns the interpretation of the phytoplankton changes in the investigated interval. Based on the analysis of the organic-walled microphytoplankton in the PTB strata of South China three different stages of acritarch communities around the PTB can be identified. Diverse (28 species attributed to 10 genera) and abundant acritarch assemblages occur in Stage 1, corresponding to the *Clarkina changxingensis* and *Clarkina yini* conodont biozones. Subsequently, moderately diverse acritarch assemblages (11 species in 7 genera) are present in Stage 2 at the Permian to Triassic transition, corresponding to the *Clarkina meishanensis*, *Hindeodus changxingensis*, *Clarkina taylorae* and *Hindeodus parvus* conodont biozones. Only one species (*Leiosphaeridia minutissima*) has been recorded in the Stage 3 possibly related to low biomass production, corresponding to the *Isarcicella staeschei* and *Isarcicella isarcica* conodont biozones.

During the end Permian, the marine ecosystem was balanced before the mass extinction (Stage 1; diverse and abundant metazoan and phytoplankton communities). However, this balance was perturbated by dramatic environmental changes (e.g., large-scale volcanic eruptions, drastic sea-level changes and higher sea-water temperatures), which most probably promoted cyanobacterial blooms at a worldwide scale, as recorded by the presence of lipid biomarkers and microbialites. The cyanobacterial proliferation possibly had very negative effects on the metazoan diversities, aggravated ocean anoxia, and reduced the abundance and diversity of other primary producers (increased light attenuation). Many species of different metazoan groups became extinct during the Stage 2 when the marine environments were perturbated (anoxic conditions and food-limitation), when only few primary consumers developed, in particular those with small sizes or/and those that were insensitive to the cyanobacterial toxin. Along with the rising temperature and intense inorganic nutrients (Fe and P), the cyanobacterial blooms proliferated in offshore and deep waters (bed 28 in Shangsi and bed 29 in Meishan), when the acritarchs (high quality food for metazoan) became rare. Many species of the primary consumers that survived the end Permian mass extinction disappeared during the earliest Triassic, probably due a degradation of the environmental conditions (high temperature, ocean anoxia and food deficiency). Only a few disaster taxa dominated in the ocean (e.g. the bivalve *Claraia*).

If the end Permian mass extinction was triggered by large-scale volcanic eruptions, important ocean anoxia, large food deficiency and high temperatures, we consider that the cyanobacterial blooms enhanced the ocean anoxia and food deficiency during the PTB. Nevertheless, the relationship between the mass extinction and cyanobacterial blooms are more complex than that we previously thought.

Key Words: End Permian, Early Triassic, mass extinction, acritarchs, phytoplankton

Le Phytoplancton de la limite Permien-Trias du Sud de la Chine

Candidat : Lei Yong
Directeurs de Thèse : Thomas Servais (Université de Lille1) ;
Feng Qinglai (China University of Geosciences) ;

Résumé

La fin du Permien (- 252 Ma) est marquée par la plus grande extinction de masse dans l'histoire de la Vie sur Terre, avec la disparition de plus de 90% des espèces marines. Beaucoup d'auteurs ont essayé d'expliquer les causes de cette extinction notamment en la mettant en relation avec des catastrophes écologiques tels qu'une anoxie des océans, un volcanisme des trappes en Sibérie, et/ou des fluctuations du niveau marin. Cependant, les facteurs causant cette extinction restent controversés. De nombreuses études ont documenté l'extinction des groupes de métazoaires marins, mais le plus souvent en ignorant les fluctuations de la diversité de la production primaire dans les environnements marins à la limite Permien/Trias (*Permian/Triassic boundary* - PTB), alors que la présence d'un possible « pic fongique » dans le Permien terminal a provoqué un important débat. Plus récemment, des travaux ont analysé les changements des cyanobactéries autour de la limite Permien/Trias en Chine. Quelques articles documentent aussi dans les couches de la PTB les changements de biodiversité des acritarches, qui représentent la majeure partie du microphytoplancton à paroi organique au Paléozoïque. L'objectif de l'étude présentée ici est de documenter les différentes communautés du phytoplancton (incluant les acritarches et les cyanobactéries) dans des couches de la limite Permien/Trias en Chine et d'essayer d'analyser les relations entre l'extinction de masse et les changements des communautés de phytoplancton au niveau de la PTB dans le sud de la Chine.

Tout d'abord, nous présentons une synthèse de l'enregistrement fossile des acritarches du Permien à l'échelle globale. Cette révision montre que les descriptions d'acritarches du Permien ont largement été négligées, en comparaison avec d'autres groupes de palynomorphes, tels que les spores ou les grains de pollen. Alors que les kystes à paroi organique de grande taille, qui étaient très abondant dans le Paléozoïque inférieur et moyen, sont habituellement absents, beaucoup d'acritarches de petite taille sont retrouvés dans les assemblages du Permien. Durant la plupart des étages du Permien, la richesse générique des acritarches est de 20 à 30 genres. Quelques genres,

comme *Micrhystridium* et *Veryhachium*, ont été signalés dans plus de 40 publications. Néanmoins, beaucoup d'acritarches du Permien ne sont pas encore documentés en détail, et des travaux systématiques supplémentaires, notamment concernant les très petits taxons, sont nécessaires pour réellement comprendre la diversité et l'importance des acritarches au Permien.

La description de nouveau matériel inclut les analyses des associations de phytoplancton bien préservé et diversifié du Permien teminal de sept coupes géologiques du bloc de Yangtze (sud de la Chine) provenant des localités Zhongzhai (Guizhou Province), Liangfengya (Chongqing City), Meishan (Zhejiang Province), Shangsi (Sichuan Province), Xiakou et Ganxi (Hubei Province), et Dongpan (Guangxi Province). La plupart des espèces rencontrées ont été signalées auparavant dans d'autres coupes géologiques du Permien terminal d'autres parties du monde. Les taxons du phytoplancton sont généralement de taille très petite, le plus souvent d'un diamètre autour de 20 μm, et ils incluent souvent les genres *Micrhystridium*, *Veryhachium* et *Leiosphaeridia*. Par contre, des taxons plus larges avec des corps centraux qui souvent dépassent des diamètres de 80 μm, comme *Dictyotidium*, sont également abondant dans la coupe de Shangsi.

Les descriptions des assemblages d'acritarches incluent une réévaluation de la classification de deux genres parmi les plus communs. Grâce à la présence de grandes populations de *Micrhystridium* et de *Veryhachium*, un simple schéma de classification, basé sur le contour géométrique du corps central, est proposé pour le « *complexe* à *Micrhystridium*/*Veryhachium*». Nous proposons de diviser ce « *complexe* » en cinq groupes : le groupe *Veryhachium cylindricum* pour représenter tous les spécimens ellipsoïdaux; le groupe *Veryhachium trispinosum* pour toutes les formes triangulaires; le groupe *Veryhachium lairdii* pour les formes avec des corps centraux rectangulaires; le groupe *Micrhystridium pentagonale* incluant tous les spécimens pentagonaux; et le groupe *Micrhystridium breve* représentant toutes les formes sphériques.

Ensuite, dans le but de comprendre la distribution spatiale (paléoécologique) du microphytoplancton à paroi organique du Permien terminal, le matériel palynologique de six coupes géologiques du bloc de Yangtze au sud de la Chine a été analysé. Ces coupes représentent des types de faciès sédimentaires différents (allant des paléoenvironnements néritiques à *offshore*, incluant également des faciès de bassin). Basées sur la diversité et l'abondance relative des genres et des espèces d'acritarches, les nouvelles données des coupes géologiques du Permien terminal de Chine fournissent des modes de distribution paléoécologiques comparables à ceux des autres périodes géologiques : (1) des faibles diversités de 2 à 4 espèces d'acritarches sont présentes dans des environnements près de la côte, tandis que les diversités plus élevées (plus de 10 espèces d'acritarches) sont présentes dans des environnement offshore ; (2) au niveau générique, les genres *Leiosphaeridia*, *Reduviasporonites* et *Micrhystridium* sont largement répandus, allant des faciès côtiers correspondant à des faibles profondeurs d'eau jusqu'au faciès distaux correspondant à des profondeurs d'eau plus grandes, tandis que d'autres genres, tels que *Dictyotidium* et *Veryhachium* ont des distributions plus restreintes, présents sur le shelf continental et vers le bassin, indiquant des conditions marines plus ouvertes ; (3) le genre *Schizosporis* n'est présent qu'autour de la PTB quand les niveaux marins sont très bas, indiquant probablement des environnements près des côtes avec des niveaux marins peu profonds ; (4) au niveau des espèces, *Micrhystridium breve,* avec des appendices courts, et *Leiosphaeridia minutissima*, indiquent des faciès néritiques, tandis que d'autres espèces de *Micrhystridium* et de *Veryhachium* avec des appendices plus longs (p.ex., *Micrhystridium stellatum* et *Veryhachium hyalodermum*), ainsi que *Leiosphaeridia microgranifera*, indiquent des environnement marins plus ouverts. Les espèces d'acritarches de grande taille (plus de 80 µm en diamètre), comme *Dictyotidium reticulatum*, indiquent des environnements à faible profondeur d'eau ; (5) dans les niveaux de la PTB, l'abondance relative de l'énigmatique *Reduviasporonites*, qui est interprété par quelques auteurs comme une spore fongique, ne dépasse jamais 14%, révoquant ainsi l'existence présumée d'un pic de *Reduviasporonites* dans la région du Yangtze. *Reduviasporonites chalastus* (40 µm en longueur) dominait clairement les environnements de plateforme peu profonds, tandis que *Reduviasporonites catenulatus*, plus petit (15 µm en longueur), est plus abondant dans des eaux plus profondes.

Une autre partie de notre étude concerne l'interprétation des changements du phytoplancton dans l'intervalle analysé. Basés sur l'analyse du microphytoplancton à paroi organique des couches géologiques autour de la PTB du sud de la Chine, trois étages distincts avec des communautés à acritarches différentes sont identifiés. Des assemblages avec des acritarches abondants et diversifiés (28 espèces appartenant à 10 genres) sont présents dans l'Etage 1, correspondant aux biozones à conodontes *Clarkina changxingensis* et *Clarkina yini*. Ensuite, des assemblages d'acritarches modérément diversifiés (11 espèces appartenant à 7 genres) sont présents dans l'Etage 2, près de la transition Permien/Trias, et correspondant aux biozones à conodontes *Clarkina meishanensis*, *Hindeodus changxingensis*, *Clarkina taylorae* et *Hindeodus parvus*. Une seule espèce (*Leiosphaeridia minutissima*) a été retrouvé dans l'Etage 3, peut-être liée à une production de biomasse réduite, correspondant aux biozones à conodontes *Isarcicella staeschei* et *Isarcicella isarcica*.

A la fin du Permien, les écosystèmes marins étaient bien équilibrés avant l'extinction de masse (Etage 1 ; communautés de métazoaires et de phytoplancton diversifiées et abondantes). Par contre, cet équilibre a été perturbé par des changements environnementaux dramatiques (p.ex., éruptions volcaniques à grande échelle, changements du niveau marin drastiques, températures de l'eau de mer plus élevées), ce qui a probablement favorisé des proliférations de cyanobactéries au niveau mondial, comme enregistrées par la présence de biomarqueurs lipides et de microbialites. La prolifération des cyanobactéries a probablement eu des effets très négatifs sur la diversité des métazoaires, aggravés par une anoxie des océans, et a réduit l'abondance et la diversité des autres producteurs primaires (atténuation de l'intensité de lumière). Beaucoup d'espèces de différents groupes de métazoaires se sont éteintes durant l'Etage 2 quand les conditions environnementales marines ont été perturbées (conditions d'anoxie et limitation de nutriments), quand seulement peu de consommateurs primaires se sont développés, en particulier ceux de taille réduite et/ou ceux qui n'étaient pas sensibles aux toxines des cyanobactéries. Lorsque les températures augmentaient et

que les nutriments inorganiques (Fe et P) étaient abondants, les cyanobactéries ont proliféré dans des milieux offshore et d'eaux profondes (couche 28 à Shangshi et couche 29 à Meishan), pendant que les acritarches (nutriment de grande qualité pour les métazoaires) devenaient rare. Beaucoup d'espèces des consommateurs primaires qui avaient survécu à l'extinction de masse à la fin du Permien disparaissaient dans le Trias le plus inférieur, probablement dû à une dégradation des conditions de l'environnement (température élevée, anoxie de l'océan, et déficience en nutriment). Seulement quelques taxons dominaient dans les océans (p.ex., le bivalve *Claraia*).

Si l'extinction de masse du Permien a été initiée par des éruptions volcaniques de grande envergure, une importante anoxie des océans, une grande déficience en nutriments et des températures élevées, nous considérons que les proliférations des cyanobactéries augmentaient l'anoxie des océans et la déficience en nutriments durant la PTB. Les relations entre l'extinction de masse et les proliférations des cyanobactéries sont plus complexes que ce qui était auparavant établi.

Mots-clés：Permien terminal, Trias inférieur, extinction de masse, acritarches, phytoplancton

目　录

Content

第一章 绪论

§1.1 二叠纪-三叠纪之交生物大灭绝的研究进展

1.1.1 生物大灭绝的过程分析

据古生物化石资料显示，二叠纪与三叠纪之交的生物大灭绝是自显生宙以来地球上发生的最大一次集群灭绝事件[1-3]，距今约252Ma[4]。自上世纪70年代开始，国内外众多的古生物学家对这一地质事件做了多方面的探索，发现这次事件造成当时海洋生态系统中大约90%以上的物种灭绝，同时造成近 70%的陆地生物灭绝[1-3]。而更多的研究则将焦点放在此次事件的过程上。

在华南地区，吴顺宝等[5]以及杨遵义等[6]对比了多条剖面的古生物化石资料，认为二叠纪与三叠纪之交的生物大灭绝并非单期次灭绝，而是由多期次的灭绝组成。Yin et al. (2007）则将煤山剖面二叠纪与三叠纪之交的生物灭绝过程分为三幕，序幕发生在24e层底部；主幕发生在25层底部；而尾幕则出现在28层底[7]。然而，由于采样精度等原因，在这之前的研究认为，煤山剖面的生物大灭绝事件是单幕式的灭绝事件，仅发生在 25 层底部[8]。而一些学者对单一门类的生物化石研究发现，多数门类的化石呈现出双幕式的灭绝模式。如方宗杰[9]提出，华南地区双壳类在二叠纪与三叠纪之交的大灭绝是双幕式的灭绝。此后，这种灭绝模式在放射虫[10]、有孔虫[11]以及腕足类[12, 13]等化石门类中均得到了很好的印证。就在最近，Song et al. (2012）在统计了华南地区二叠纪与三叠纪之交多个剖面共计17个门类500余种生物化石资料后，明确提出此次灭绝事件是双幕式的灭绝[14]。同时发现，第一幕的灭绝发生在二叠纪末期（煤山剖面25层底部），有57%的物种遭到灭绝；第二幕则发生在早三叠世初期（煤山剖面第28层顶部），共计71%的物种灭绝。

1.1.2 生物大灭绝的原因探讨

全球各地的地质学家对二叠纪与三叠纪之交大灭绝事件的研究除了讨论其过程，同时对大灭绝的原因也做了深层次的挖掘。到目前为止，尽管提出了众多的假说，如外星撞击[15-18]、海洋缺氧或硫化[19, 20]、大规模火山喷发[21]以及海平面变化[22]等，但是种种假说均不能完全解释此次大灭绝的原因。

1）外星撞击

地史时期的五次生物大灭绝中，白垩纪末期的生物大灭绝被认为是由于地外星体撞击所致[23]。而早期的研究者认为，外星撞击同样是二叠纪与三叠纪之交生物大灭绝的首要原因。

其主要的证据是发现部分界线粘土岩存在铱异常[15]、富勒烯及异常的稀有气体[24]、冲击石英以及铁质微球粒等记录[16-18]。然而，这些结果在后续的研究中并没有得到重现。同时，外星撞击的陨石坑也一直未被发现[25-27]。因此，这一假说并没有得到广泛的认可，还需要研究者找到更加强有力的证据。

2）大规模火山喷发

大规模的火山喷发可以带来一系列的生态环境变化。首先，炙热的岩浆可以导致大面积的森林火灾发生。其次，随岩浆喷出的高密度火山灰可以遮蔽阳光，对植物光合作用造成影响，进而影响动物的生存。第三，火山喷发将释放大量的气体物质，其中，高浓度的二氧化碳将加大全球碳排放，进而导致全球变暖；而二氧化硫和硫化氢等气体则可以形成酸雨以及破坏臭氧层，从而对地球生物造成伤害[28]。同时，二叠纪与三叠纪之交的众多剖面都可以找到数层由于火山喷发而形成的粘土岩。因此，大规模的火山喷发一直被多数地质学家认为是二叠纪末期生物大灭绝的主要原因。

殷鸿福等[29]很早就发现华南二叠纪与三叠纪之交的多个剖面都保存着火山粘土岩，并认为该地区强烈的火山活动可能是导致生物大灭绝的原因之一。而 Wignall 则分析了地史时期火山活动与生物灭绝的关系，并认为它们之间存在较好的联系[21]。因此，找到火山灰的来源则成为支持这一假说的直接证据。而发生于二叠纪至三叠纪的两个大火山岩省（峨眉山大火山岩省和西伯利亚大火山岩省）则成为学者们的关注焦点[30-36]。现有资料表明，峨眉山大火山岩省基本可以确定是发生于中二叠世，可能为中二叠世末期生物灭绝的主要原因，却与二叠纪末期的生物大灭绝无关[37]。目前，多数学者认为西伯利亚大火山岩省是二叠纪与三叠纪之交生物大灭绝的重要原因[30-32]。但是，这些猜测并没有精确的年代学数据支持。相反，个别数据显示，西伯利亚大火山岩省的主要喷发时间可能比此次生物大灭绝的时间更晚[34, 38]。因此，这个假说还需要更多的年代学数据来支撑。同时，现阶段对火山如何影响环境，进而造成生物灭绝的作用机制还不甚了解[39, 40]，需要更多的学者来做系统的研究。

3）海洋大范围缺氧

二叠纪与三叠纪之交的生物大灭绝的主体是好氧的海洋宏观生物，倘若海洋水体发生大范围的缺氧事件，势必会对这些生物的生存造成巨大的影响。Isozaki[19]认为晚二叠世至早三叠世期间，泛大洋一直处在缺氧的环境中。并指出此次海水缺氧事件的时间可能长达 20Ma，其不仅是二叠纪末期海洋生物大灭绝的原因，也影响了早三叠世动物的复苏。而 Grice et al.(2005）更是认为当时海洋的透光带中已经富集了硫化氢，由此证明此次缺氧的程度相当严重[20]。在这之后，多个剖面也相继报道了类似的现象[41-44]，更加证明了此次海水缺氧事件影响范围较大，甚至可能是全球性的。因此，海水缺氧事件可能是二叠纪末期海洋生物大灭绝的主要原因之一。

4）海平面升降

浅海地区是海洋生物生活的主要场所之一。海平面的骤降则会直接导致浅海地区面积的减少，从而影响到海洋生物的生存。由于泛大陆的聚合，从晚古生代开始，海平面出现一期明显的海退事件，而二叠纪末期达到当时海平面的最低值（图 1-1）。据图 1-1 可知，地史时期的五次生物大灭绝与海洋面积的缩减具有较强的相关性。二叠纪与三叠纪之交的海退始于长兴晚期，在全球多个剖面都有明显的沉积记录，煤山剖面在此期间则在第 24e 层底部出现

一个Ⅱ型层序界面[45]。Newell[22]较早地认识到此次海平面的降低是生物大灭绝的原因之一。然而，二叠纪末期的生物大灭绝并没有发生于此次海退事件期间，而是发生在处于海侵过程中的煤山 25 层[14]。因此，海退事件可能并不是其主要原因，而海退之后引发的海水大面积缺氧事件以及突发的大规模火山喷发事件才是二叠纪末期生物大灭绝的真正元凶[28]。

关于二叠纪末期的生物大灭绝的原因，还有很多其他的假说，如海洋倒转事件[46]、甲烷释放事件[47]、全球气候变化以及全球大火事件[13]等，然而过分地强调单一事件的作用并不能解决二叠纪末期生物大灭绝的所有问题。因此，多数学者更倾向于是多种因素的综合作用才导致了此次生物大灭绝事件的发生[7]。

§1.2 二叠纪疑源类研究进展

现代海洋浮游植物主要由三大类组成，钙质浮游植物（如钙藻），硅质浮游植物（如硅藻）和有机质壳浮游植物（如沟鞭藻等）。钙藻和硅藻等浮游植物出现并繁盛于中生代，而最早的有机质壳浮游植物则出现于前寒武纪[52]。同时，有机质壳浮游植物在早古生代达到繁盛的顶峰，特别是奥陶纪和泥盆纪[53, 54]。奥陶纪时期，由于海平面较高，大陆架分布广泛，导致作为初级生产者的浮游植物的生物量和生物多样性都极高，从而引起“奥陶纪生物大爆发”[51, 55]。而泥盆纪的浮游植物繁盛同样引发“Devonian nekton revolution”[56, 57]。由图 1-1 可知，浮游植物物种多样性的高低与地史时期海洋面积的大小呈较强的相关性。因此，从晚泥盆世开始到早石炭世，浮游植物的生物量和生物多样性都出现了巨大的降低。

于是，一些学者认为疑源类在这一时期出现缺失。而此阶段疑源类生物多样性的下降也与古环境的其它参数变化关系密切，如海洋营养盐的减少，大气中二氧化碳浓度的变化等[58, 59]。由于其它具有机质壳的浮游植物如沟鞭藻化石在晚三叠世才大量出现（图 1-1），因此，Riegel[58]称石炭纪和二叠纪疑源类化石的生物多样性和生物量降低的事件为“Phytoplankton Blackout”（从晚泥盆世开始，持续将近 130Ma）。但是，Servais et al.（2006）对此提出质疑，他认为疑源类壳体化石的缺失不足以说明浮游植物的不存在[60]。以现代大洋中的沟鞭藻为例，只有少量沟鞭藻的壳体可以保存为化石[61]。

Mullins and Servais[62]总结了石炭纪的浮游植物。他们发现，与早古生代浮游植物生物多样性相比，其在石炭纪的生物多样性一般较低，且从 Tournaisian 到 Serpukhovian 越来越低，在晚石炭世时，只有 1-3 种[62]。

现有的研究表明，二叠纪疑源类化石个体较小，其直径通常在 20 微米左右，很难在普通光学显微镜下进行研究。同石炭纪类似，二叠纪疑源类生物多样性同样很低，以致大多数的学者都着重研究生物多样性更高，个体体积更大的孢粉化石，只是零星的报道一些疑源类。因此在二叠纪地层的研究中，无论是化石带的报道，还是古环境的重建，孢粉化石组合的研究都比疑源类的研究更为深入。

生物亲缘关系方面，除了亲缘关系不明的疑源类，其它的一些浮游植物如绿藻已经在晚古生代出现[63]。它们大多应该归属于 Prasinophyceae、Chlorophyceae 和 Zygnemaphyceae。同时，一些菌孢也同样经常被报道。尤其是在二叠纪末生物大灭绝时期，一些学者认为出现

了菌孢繁盛的高峰[64-68]。

迄今为止，关于二叠纪的疑源类化石，只有两篇简短的总结文章[69, 70]。因此，本节首先查阅了超过 100 篇关于二叠纪浮游植物的报道，同时检索了 Fensome et al.（1990）总结的二叠纪疑源类的所有种类，期望总结二叠纪浮游植物多样性的变化规律[71]。同 Mullins and Servais [62]类似，本节研究的浮游植物包括了二叠纪所有的未知亲缘关系的海相疑源类化石，也有一些可疑的非海相的疑源类化石，同时也囊括了已知亲缘关系的藻类化石，如绿藻。

值得注意的是，本节的主要目的并不是讨论各类浮游植物的亲缘关系。所以对于某些亲缘关系存在争议的属种（如 *Leiosphaeridia* 和 *Polyedryxium*），都将其视为疑源类化石。

在研究二叠纪的地层时，尽管很多文章都提到了孢粉型化石组合，但是绝大多数都是研究孢粉化石，只有近 100 篇文章报道了浮游植物化石（包括疑源类和其它藻类）。图 1-2 摘录了这些文献中的关键信息，包括研究地区、地层时代、作者、时间、物种名等，其它信息将在文中详细叙述。但是，根据 Fensome et al.（1990）的分类意见，某些属种如 *Acanthotriletes* 被归为孢子化石而没有被收录进本节[71]。

本文参照国际地层委员会(ICS）划分二叠纪地层[72]。文中出现的所有物种，其种名都收录在附录 A 中。

1.2.1 早二叠世

1.2.1.1 Gzhelian/Asselian

在石炭纪与二叠纪之交（Gzhelian/Asselian），只有两篇文章描述了浮游植物。在阿根廷，距离 San José de Jáchal 29 公里处 Tupe 组的岩层中，Gutiérrez et al.（2006）报道了 3 种浮游植物化石 *Botryococcus braunii*、*Leiosphaeridia* sp.和 *Brazilea* spp. [73]。而 Gorter et al.（2008）在澳大利亚 Treachery 组也发现了三个属的疑源类化石（*Botryococcus*、*Baltisphaeridium* 和 *Ulanisphaeridium*）[74]。

1.2.1.2 Asselian 以及 Asselian/Sakmarian

在早二叠世 Asselian/Sakmarian，有 5 篇文章描述了浮游植物化石。在南极地区 Beacon 群地层中，Kent et al.（1990）发现了保存完好且丰度较高的孢粉型化石[75]。主要是一些孢子和花粉，但是同时也含有多种浮游植物化石，如 *Botryococcus* sp.、*Diexallophasis* sp.、*Leiosphaeridia* sp.、*Dictyotidium* sp.、*Tasmanites* sp.、*Brazilea scissa*、*Tetraporina* sp.和 *Quadrisporites horridus*。在南极 Heimefrontfjella 的北部，Lindström[76]同样描述了几种疑源类化石，包括 Acritarch sp. A、*Botryococcus braunii*、*Leiosphaeridia* spp.、*Lophosphaeridium* spp.、*Dictyotidium* sp.、*Tasmanites* sp. A、*Tetraporina gigantea*、*T. tetragona*、*T.* sp. A、*Brazilea scissa* 和 *Quadrisporites horridus*。

在阿根廷西部 La Rioja 省，Di Pasquo et al.（2010）研究了三个剖面的地层，报道了两个孢粉组合带，都产出疑源类化石 *Portalites gondwanensis*[77]。同时，他们认为其中一个化石带的时代应该是 Asselian 与 Sakmarian 之交[77]。

在乌拉圭这一时期的地层中，Beri et al.（2006）和 Beri et al.（2010）分别分析了来自

San Gregorio 组的 4 个岩芯样品（DCLS24）和 32 个采自 Cerro Pelado 组的样品[78, 79]。他们报道了多个属的浮游植物化石，如 *Deusilites*、*Leiosphaeridia*、*Micrhystridium*、*Pilasporites*、*Portalites*、*Brazilea*、*Tetraporina*、*Quadrisporites* 和 *Botryococcus*[78, 79]。

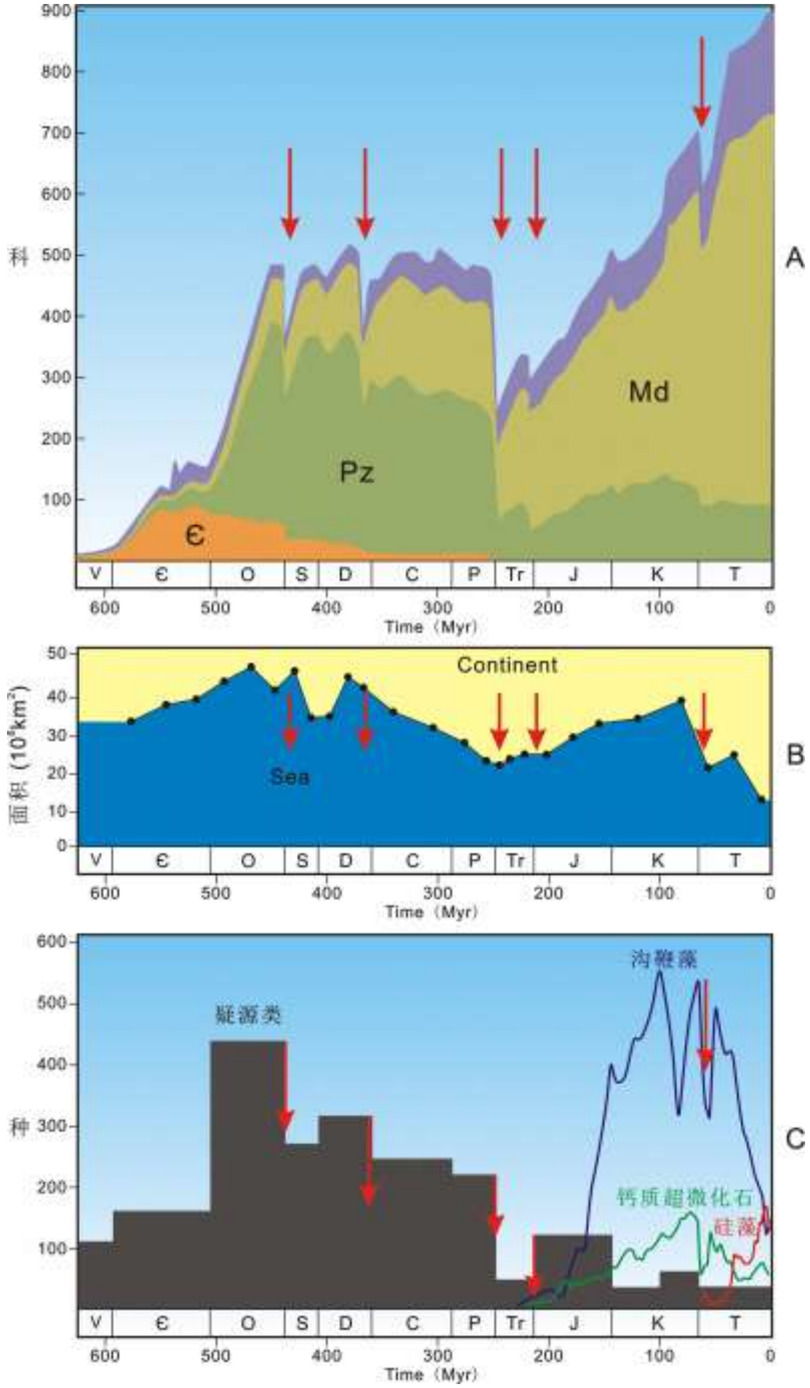

图 1-1 地史时期生物大灭绝与海平面以及浮游植物多样性变化的对比

红色箭头指示五次生物大灭绝；A：生物多样性变化来自[48]；B：海洋面积变化来自[49]；C：浮游植物多样性变化来自[50, 51]。

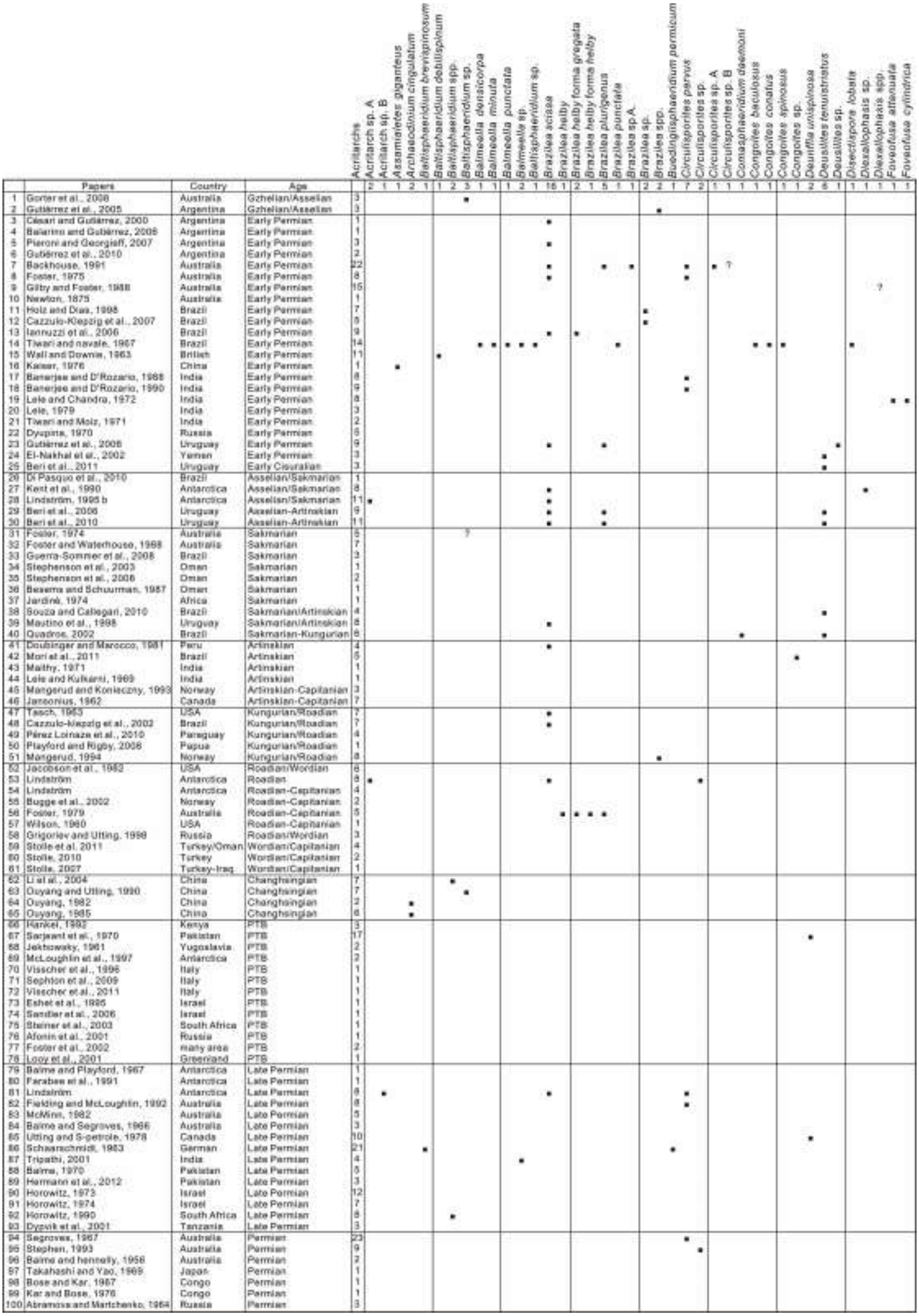

	Papers	Country	Age	Acritarchs	Acritarch sp. A	Acritarch sp. B	Assamialetes giganteus	Archaeodinium cingulatum	Baltisphaeridium brevispinosum	Baltisphaeridium debilispinum	Baltisphaeridium spp.	Baltisphaeridium sp.	Balmeella densicorpa	Balmeella minuta	Balmeella punctata	Balmeella sp.	Baltisphaeridium sp.	Brazilea sciasa	Brazilea helby	Brazilea helby forma gregata	Brazilea helby forma helby	Brazilea plurigenus	Brazilea punctata	Brazilea sp A.	Brazilea sp.	Brazilea spp.	Buedingiisphaeridium permicum	Circulisporites parvus	Circulisporites sp.	Circulisporites sp. A	Circulisporites sp. B	Comasphaeridium daemoni	Congoites baculosus	Congoites conatus	Congoites spinosus	Congoites sp.	Deunffia unispinosa	Deusilites tenuistriatus	Deusilites sp.	Disectispora lobata	Diexallophasis sp.	Diexallophasis spp.	Foveofusa attenuata	Foveofusa cylindrica
					2	1	1	2	1	1	2	3	1	1	1	2	1	16	1	2	1	5	1	1	2	2	1	7	2	1	1	1	1	1	1	1	2	6	1	1	1	1	1	1
1	Gorter et al., 2008	Australia	Gzhelian/Asselian	3								■																																
2	Gutiérrez et al., 2005	Argentina	Gzhelian/Asselian	3																						■																		
3	Césari and Gutiérrez, 2000	Argentina	Early Permian	1														■																										
4	Balarino and Gutiérrez, 2006	Argentina	Early Permian	1																																								
5	Pieroni and Georgieff, 2007	Argentina	Early Permian	3														■																										
6	Gutiérrez et al., 2010	Argentina	Early Permian	2																																								
7	Backhouse, 1991	Australia	Early Permian	22														■				■		■				■		■	?													
8	Foster, 1975	Australia	Early Permian	8														■										■																
9	Gilby and Foster, 1988	Australia	Early Permian	15																																						?		
10	Newton, 1875	Australia	Early Permian	1																																								
11	Holz and Dias, 1998	Brazil	Early Permian	7																					■																			
12	Cazzulo-Klepzig et al., 2007	Brazil	Early Permian	5																					■																			
13	Iannuzzi et al., 2006	Brazil	Early Permian	9														■		■																								
14	Tiwari and navale, 1967	Brazil	Early Permian	14									■	■	■	■	■						■										■	■	■					■				
15	Wall and Downie, 1963	British	Early Permian	11						■																																		
16	Kaiser, 1976	China	Early Permian	1			■																																					
17	Banerjee and D'Rozario, 1988	India	Early Permian	8																								■																
18	Banerjee and D'Rozario, 1990	India	Early Permian	9																								■																
19	Lele and Chandra, 1972	India	Early Permian	8																																							■	■
20	Lele, 1979	India	Early Permian	3																																								
21	Tiwari and Moiz, 1971	India	Early Permian	2																																								
22	Dyupina, 1970	Russia	Early Permian	5																																								
23	Gutiérrez et al., 2006	Uruguay	Early Permian	9														■				■																■						
24	El-Nakhal et al., 2002	Yemen	Early Permian	3																																	■							
25	Beri et al., 2011	Uruguay	Early Cisuralian	3																																	■							
26	Di Pasquo et al., 2010	Brazil	Asselian/Sakmarian	1																																								
27	Kent et al., 1990	Antarctica	Asselian/Sakmarian	8														■																							■			
28	Lindström, 1995 b	Antarctica	Asselian/Sakmarian	11	■													■																										
29	Beri et al., 2006	Uruguay	Asselian-Artinskian	9														■				■															■							
30	Beri et al., 2010	Uruguay	Asselian-Artinskian	11														■				■															■							
31	Foster, 1974	Australia	Sakmarian	5								?																																
32	Foster and Waterhouse, 1988	Australia	Sakmarian	7																																								
33	Guerra-Sommer et al., 2008	Brazil	Sakmarian	3																																								
34	Stephenson et al., 2003	Oman	Sakmarian	1																																								
35	Stephenson et al., 2008	Oman	Sakmarian	2																																								
36	Besems and Schuurman, 1987	Oman	Sakmarian	1																																								
37	Jardiné, 1974	Africa	Sakmarian	1																																								
38	Souza and Callegari, 2010	Brazil	Sakmarian/Artinskian	4																																	■							
39	Mautino et al., 1998	Uruguay	Sakmarian/Artinskian	8														■																										
40	Quadros, 2002	Brazil	Sakmarian-Kungurian	6																												■						■						
41	Doubinger and Marocco, 1981	Peru	Artinskian	4														■																										
42	Mori et al., 2011	Brazil	Artinskian	5																																■								
43	Maithy, 1971	India	Artinskian	1																																								
44	Lele and Kulkarni, 1969	India	Artinskian	1																																								
45	Mangerud and Konieczny, 1993	Norway	Artinskian-Capitanian	3																																								
46	Jansonius, 1962	Canada	Artinskian-Capitanian	7																																								
47	Tasch, 1963	USA	Kungurian/Roadian	7														■																										
48	Cazzulo-klepzig et al., 2002	Brazil	Kungurian/Roadian	7														■																										
49	Pérez Loinaze et al., 2010	Paraguay	Kungurian/Roadian	4																																								
50	Playford and Rigby, 2008	Papua	Kungurian/Roadian	1																																								
51	Mangerud, 1994	Norway	Kungurian/Roadian	8																						■																		
52	Jacobson et al., 1982	USA	Roadian/Wordian	8																																								
53	Lindström	Antarctica	Roadian	8	■													■											■															
54	Lindström	Antarctica	Roadian-Capitanian	4																																								
55	Bugge et al., 2002	Norway	Roadian-Capitanian	2																																								
56	Foster, 1979	Australia	Roadian-Capitanian	5															■	■	■	■																						
57	Wilson, 1960	USA	Roadian-Capitanian	1																																								
58	Grigoriev and Utting, 1998	Russia	Roadian/Wordian	3																																								
59	Stolle et al. 2011	Turkey/Oman	Wordian/Capitanian	4																																								
60	Stolle, 2010	Turkey	Wordian/Capitanian	2																																								
61	Stolle, 2007	Turkey-Iraq	Wordian/Capitanian	1																																								
62	Li et al., 2004	China	Changhsingian	7							■																																	
63	Ouyang and Utting, 1990	China	Changhsingian	7								■																																
64	Ouyang, 1982	China	Changhsingian	2				■																																				
65	Ouyang, 1985	China	Changhsingian	6				■																																				
66	Hankel, 1992	Kenya	PTB	3																																								
67	Sarjeant et al., 1970	Pakistan	PTB	17																																	■							
68	Jekhowsky, 1961	Yugoslavia	PTB	2																																								
69	McLoughlin et al., 1997	Antarctica	PTB	2																																								
70	Visscher et al., 1996	Italy	PTB	1																																								
71	Sephton et al., 2009	Italy	PTB	1																																								
72	Visscher et al., 2011	Italy	PTB	1																																								
73	Eshet et al., 1995	Israel	PTB	1																																								
74	Sandler et al., 2006	Israel	PTB	1																																								
75	Steiner et al., 2003	South Africa	PTB	1																																								
76	Afonin et al., 2001	Russia	PTB	1																																								
77	Foster et al., 2002	many area	PTB	2																																								
78	Looy et al., 2001	Greenland	PTB	1																																								
79	Balme and Playford, 1967	Antarctica	Late Permian	1																																								
80	Farabee et al., 1991	Antarctica	Late Permian	1																																								
81	Lindström	Antarctica	Late Permian	8		■												■										■																
82	Fielding and McLoughlin, 1992	Australia	Late Permian	8																								■																
83	McMinn, 1982	Australia	Late Permian	5																																								
84	Balme and Segroves, 1966	Australia	Late Permian	3																																								
85	Utting and S-petrole, 1978	Canada	Late Permian	10																																	■							
86	Schaarschmidt, 1963	German	Late Permian	21					■																		■																	
87	Tripathi, 2001	India	Late Permian	4												■																												
88	Balme, 1970	Pakistan	Late Permian	5																																								
89	Hermann et al., 2012	Pakistan	Late Permian	3																																								
90	Horowitz, 1973	Israel	Late Permian	12																																								
91	Horowitz, 1974	Israel	Late Permian	7																																								
92	Horowitz, 1990	South Africa	Late Permian	8							■																																	
93	Dypvik et al., 2001	Tanzania	Late Permian	3																																								
94	Segroves, 1967	Australia	Permian	23																								■																
95	Stephen, 1993	Australia	Permian	9																									■															
96	Balme and hennelly, 1956	Australia	Permian	2																																								
97	Takahashi and Yao, 1969	Japan	Permian	1																																								
98	Bose and Kar, 1967	Congo	Permian	1																																								
99	Kar and Bose, 1976	Congo	Permian	1																																								
100	Abramova and Martchenko, 1964	Russia	Permian	3																																								

图 1-2a 二叠纪疑源类文献记录（参考文献见正文）

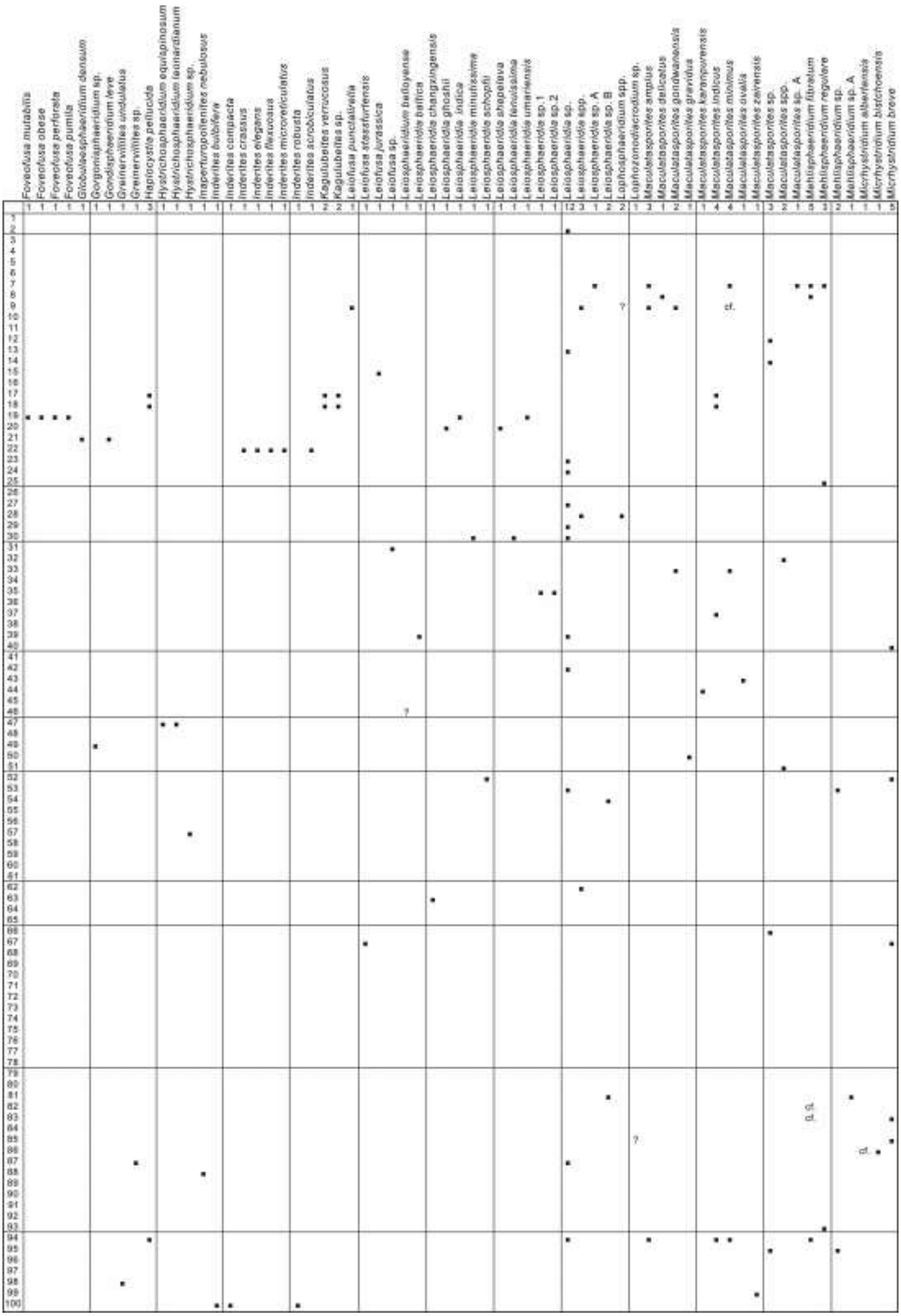

图 1-2b 二叠纪疑源类文献记录（接上图）

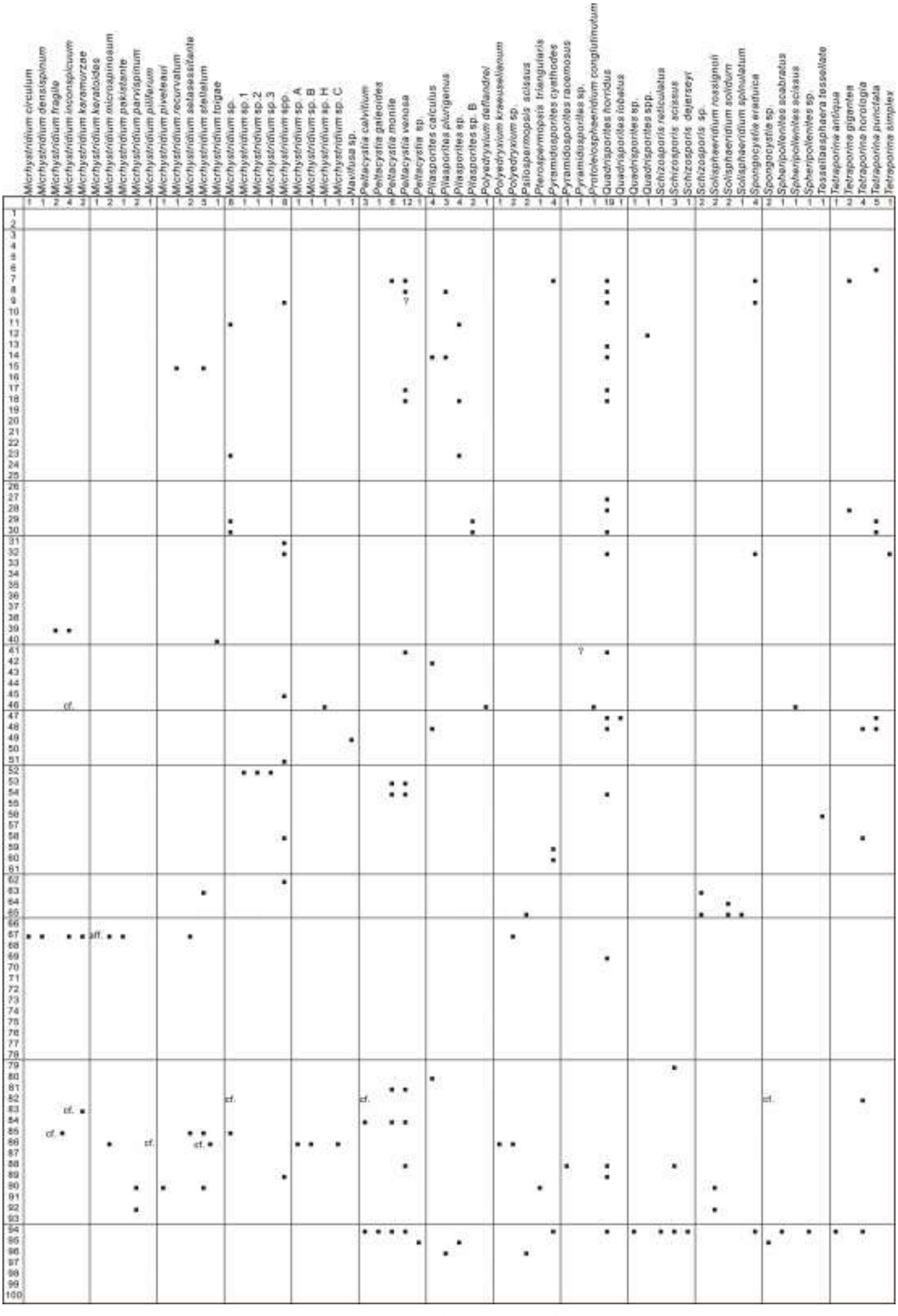

图 1-2c 二叠纪疑源类文献记录（接上图）

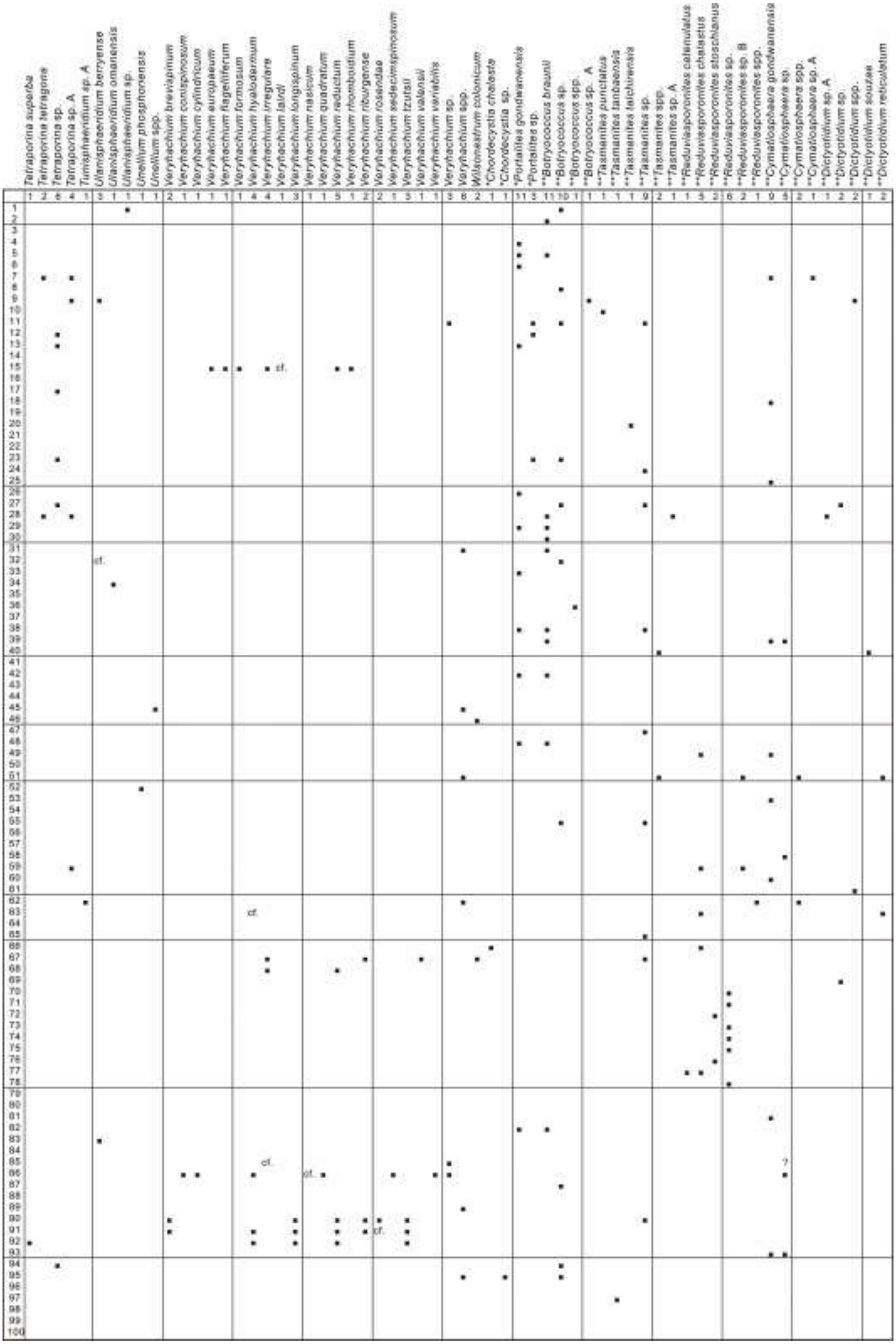

图 1-2d 二叠纪疑源类文献记录（接上图）

1.2.1.3 Sakmarian 以及 Sakmarian/Artinskian

大约有 10 篇文章报道了 Sakmarian 以及 Sakmarian/Artinskian 的浮游植物种类。在阿曼的 Al Khlata 地区的冰川沉积物中，Besems and Schuurman[80]描述了两个孢粉组合带，其中都含有藻类 *Botryococcus braunii*。而 Stephenson et al.（2003）认为，疑源类 *Ulanisphaeridium omanensis* 出现在最大海侵期的页岩里面[81]。在阿曼北部，Stephenson et al.（2008）报道了疑源类 *Leiosphaeridia* 出现在 Haushi 的灰岩层中[82]。

在巴西 Paraná 盆地，Quadros[83]记录了多种疑源类出现在石炭纪和二叠纪之交。而 *Deusilites tenuistriatus* 和新种 *Dictyotidium souzae* 出现在 Sakmarian/Artinskian 时期；*Tasmanites* spp. 出现于 Sakmarian-Kungurian；*Micrhystridium breve*、*M. toigae* 和 *Comasphaeridium daemoni* 仅现于 Kungurian。在这一地区北部，Souza and Callegari[84]报道了一个保存较好的孢粉植物化石组合，同时 *Botryococcus braunii*、*Deusilites tenuistriatus*、*Portalites gondwanensis* 和 *Tasmanites* sp.也存在其中。在 Paraná 盆地南部，Guerra-Sommer et al.（2008） 也发现了几种浮游植物化石，如 *Maculatasporites minimus*、*M. gondwanenssi* 和 *Portalites gondwanensis*[85]。

在澳大利亚，Foster[86]以及 Foster and Waterhouse[87]分别调查了 Waterloo 海湾和 Canning 盆地的孢粉组合，同时报道了几种浮游植物化石，包括 *Baltisphaeridium* sp.、*Leiofusa* spp.、*Micrhystridium* spp.、*Spongocystia eraduica*、*Ulanisphaeridium* sp. cf. *Ulanisphaeridium berryense*、*Veryhachium* spp.、*Tetraporina simplex*、*Maculatasporites* spp.、*Quadrisporites horridus*、*Botryococcus braunii* 以及 *B.* sp.

在乌拉圭 Arroyo Seco 地区 Melo 组地层中，Mautino et al.（1998）报道了三种浮游植物化石：*Botryococcus braunii*、*Cymatiosphaera gondwanensis* 和 *Micrhystridium fragile*[88]。而在非洲 Karroo 组地层中，Jardiné[89]只发现了一种疑源类 *Maculatasporites indicus*。

1.2.1.4 早二叠世晚期（Artinskian-Kungurian）

有四篇文章记录了 Artinskian 的浮游植物化石。在印度 Bihar 地区的 Karanpura 煤田南部，Leleand and Kulkarni[90]报道了两个孢粉组合带，同时描述了一个疑源类的新种 *Maculatasporites karanpurensis*。而在 Auranga 煤田中，Maithy[91]描述了另外一种疑源类 *Maculatasporites ovalis*。在秘鲁 Cuzco 地区，Doubinger and Marocco [92]报道了 4 种疑源类 *Pyramidosporites* sp.、*Brazilea scissa*、*Peltacystia venosa* 和 *Quadrisporites horridus*。而在巴西 Paraná 盆地南部，Mori et al.（2012）记录了 9 种疑源类化石[93]。值得注意的是，两种疑源类 *Congoites* sp.和 *Quadrisporites lobatus* 在二叠纪的记录中仅出现这一次。在挪威斯瓦尔巴群岛，Mangerud and Konieczny [94]分析了 16 个剖面的孢粉组合，发现最早的 *Kraeuselisporites* 化石组合带属于晚 Artinskian 到早 Capitanian。同时产出疑源类化石 *Micrhystridium* spp.、*Unellium* spp.和 *Veryhachium* spp.等[94]。

在 Kungurian 到 Roadian 的地层中，有 6 篇文章报道了浮游植物化石。在加拿大 Peace 河流域，Jansonius[95]描述了超过 20 种的疑源类化石。但是大多数化石出现在早三叠世，只有 6 种产出于 Kungurian 到 Capitanian。其中包括：*Micrhystridium inconspicuum*、*M.* sp.H.、 *Polyedryxium deflandrei*、*Protoleiosphaeridium conglutinutum*、*Spheripollenites scissus* 和一个新种 *Leiosphaeridium ?belloyense*。

在美国堪萨斯，Tasch[96]描述了疑源类的两个新种 *Hystrichosphaeridium leonardianum* 和 *H. equispinosum*。在挪威巴伦支海南部的芬马克台地，Mangerud[97]分析了二叠纪至早三叠世的孢粉型化石组合。其中 *Dyupetalum* sp. –*Hamiapollenites bullaeformis* 孢粉化石组合带属于 Kungurian 到 Roadian，产出 8 个属的浮游植物化石：*Micrhystridium*、*Veryhachium*、*Cymatiosphaera*、*Dictyotidium*、*Tasmanites*、*Brazilea*、*Maculatasporites* 和 *Reduviasporonites*。

在巴西南部 Candiota 煤田中，Cazzulo-Klepzig et al.（2002）发现了较为丰富的浮游植物化石，包括：*Botryococcus braunii*、*Portalites gondwanensis*、*Pilasporites calculus*、*Brazilea scissa*、*Tetraporina horologia*、*T. punctata* 和 *Quadrisporites horridus*[98]。同时利用 U/Pb 测定的年龄为 267.1 ±3.4 Ma，处于中二叠世[98]。

在巴拉圭 Paraná 盆地，Pérez Loinaze et al.（2010）分析了 5 个采自 Mallorquin-1 井的岩芯样品，发现 4 种疑源类化石 *Gorgonisphaeridium* sp.、*Navifusa* sp.、*Cymatiosphaera gondwanensis* 和 *Reduviasporonites chalastus*[99]。

在巴布亚新几内亚 Bird’s Head 地区 Ainim 组和 Aiduna 组，Playford and Rigby[100]报道了 5 种浮游植物化石，包括：*Mehlisphaeridium regulare*、*Cymatiosphaera gondwanensis*、*Maculatasporites indicus*、*Peltacystia venosa* 和 *Quadrisporites horridus*。

1.2.1.5 其它早二叠世疑源类化石记录

由于缺乏准确的时代信息，很多二叠纪疑源类化石记录不能做出上述具体的分类。其中有 23 篇报道疑源类化石的这类文章的时代只能归属到早二叠世或者早 Cisuralian[101]。值得一提的是，其中研究南美洲地区的多达 13 篇。Césari and Gutiérrez [102]分析了阿根廷西部地区晚石炭世至二叠纪的孢粉型化石带，发现 *Fusacolpites fusus*- *Vittatina subsaccata*（FS）和 *Lueckisporites*- *Weylandites*（LW）生物带处于早二叠世，同时报道了疑源类化石 *Brazilea scissa*。而在阿根廷 Paganzo 盆地 Tasa Cuna 组，Balarino and Gutiérrez[103]报道了另外一种疑源类化石 *Portalites gondwanensis*。同一地区的 Sauces 组，Pieroni and Georgieff[104]记录了 3 种疑源类化石：*Botryococcus braunii*、*Portalites gondwanensis* 和 *Brazilea scissa*。而最近在 Río Francia 组中，Gutiérrez et al.（2010）也发现了两种疑源类化石 *Portalites gondwanensis* 和 *Tetraporina punctata*[105]。

在巴西 Paraná 盆地，许多学者研究了此地区的孢粉型化石。Tiwari and Navale[106]描述了一个孢粉组合并报道了多达 14 种疑源类化石，其中包括 8 个新种：*Balmeella densicorpa*、*B. minuta*、*B. punctata*、*Brazilea crassa*、*B. punctata*、*Congoites baculosus*、*C. conatus*、*Disectispora lobata*。Paraná 盆地北部，Holz and Dias [107]记录了疑源类的 7 个属：*Micrhystridium*、*Pilasporites*、*Portalites*、*Veryhachium*、*Botryococcus*、*Tasmanites* 和 *Brazilea*。在相邻地区，Iannuzzi et al.（2006）报道了疑源类化石 *Leiosphaeridia*、*Portalites*、*Brazilea*、*Tetraporina* 和 *Quadrisporites*[108]。而 Cazzulo-Klepzig et al.（2007）注意到，疑源类化石 *Portalites*、*Brazilea*、*Tetraporina*、*Maculatasporites* 和 *Quadrisporites* 经常出现在巴西南部煤层的孢粉植物群中，但是 *Botryococcus* 却未被发现[109]。

在乌拉圭，Gutiérrez et al.（2006）从 San Gregorio 组的 4 孔钻井中发现了一些疑源类化石，包括 *Botryococcus*、*Portalites*、*Leiosphaeridia*、*Micrhystridium*、*Tetraporina*、*Pilasporites* 和 *Brazilea*[110]。而最近 Beri et al.（2011）从 San Gregorio 另外一组钻井中描述了其它一些浮游植物化石，如 *Deusilites tenuistriatus*、*Mehlisphaeridium regulare* 和 *Cymatiosphaera*[101]。它们产自 *Cristatisporites inconstans –Vittatina saccata* 孢粉化石带，其时代属于早 Cisuralian[101]。

在印度 Godavari 盆地，Tiwari and Moiz[111]描述了两个新种 *Globulaesphaeridium densum* 和 *Gondisphaeridium leve*。而在 Madhya Pradesh 地区，Lele and Chandra [112]则报道了一个疑源类的新属 *Foveofusa*，同时描述了 8 个新种，包括：*Foveofusa attenuate*、*F. cylindrical*、*F. mutabilis*、*F. obese*、*F. perforate*、*F. pumila*、*Leiosphaeridia indica* 以及 *L. umariensis*。在 Bihar 地区，Hutar 煤田中的 Talchir 组里，Lele and Shukla[113]报道了 3 个疑源类化石新种：*Leiosphaeridia ghoshii*、*L. shepeleva* 和 *Tasmanites talchirensis*。在 Rajmahal Hills 地区的 Chuparbhita 和 Hura 盆地，Banerjee and D'Rozario[114, 115]先后两次报道了一些疑源类和藻类化石，如：*Haplocystia*、*Pilasporites*、*Cymatiosphaera*、*Circulisporites*、*Kagulubeites*、*Maculatasporites*、*Peltacystia*、*Tetraporina* 和 *Quadrisporites horridus*。

在澳大利亚昆士兰中部地区的 Blair Athol 煤层，Foster[116]发现了丰富的微体植物化石，其中也包括一些疑源类化石：*Brazilea scissa*、*Circulisporites parvus*、*Maculatasporites delicates*、*Mehlisphaeridium fibratum*、*Peltacystia venosa*、*Pilasporites plurigenus*、*Quadrisporites horridus* 和 *Botryococcus* sp.。之后在 Arckaringa 盆地，Gilby and Foster[87]报道了更多的疑源类化石种类，包括 *Diexallophasis?* spp.、*Leiofusa punctalirella*、*Leiosphaeridia*. spp.、?*Lophosphaeridium* spp.、*Maculatasporites amplus*、*M. gondwanensis*、*M.* sp. cf. *M. minimus*、*Micrhystridium* spp.、*Peltacystia venosa*、*Quadrisporites horridus*、*Spongocystia eraduica*、*Tetraporina* sp. A、*Ulanisphaeridium berryense*、*Botryococcus* sp. A 和 *Dictyotidium* spp.。而在 Collie 盆地中的 Stockton 组，Backhouse[117]描述了 22 种浮游植物化石。其归属于 11 个疑源类化石属，包括：*Leiosphaeridia*、*Mehlisphaeridium*、*Pyramidosporites*、*Spongocystia*、*Cymatiosphaera*、*Brazilea*、*Circulisporites*、*Maculatasporites*、*Peltacystia*、*Tetraporina* 和 *Quadrisporites*。

在英国 Yorkshire 地区早二叠世的泥灰岩中，Wall and Downie[118]描述了 11 种疑源类化石，归属于 4 个属：*Baltisphaeridium*、*Leiofusa*、*Micrhystridium* 和 *Veryhachium*，其中包括两个新种 *Baltisphaeridium debilispinum* 和 *Veryhachium flagelliferum*。

在也门 Kolli 组的 Khalaqah 段中，El-Nakhal et al.（2002）报道了 3 个浮游植物属：*Leiosphaeridia*、*Deusilites* 和 *Tasmanites*[119]。同时他认为，疑源类 *Deusilites tenuistriatus* 和 *D. tentus* 应为同物异名[119]。

在华北太原组，Kaiser[120]描述了一个微体古植物群，同时也记录了一种疑源类 *Assamialetes giganteus*。

在俄罗斯乌拉尔地区，Dyupina[121]报道了一个疑源类新属 *Inderites*，并描述了 5 个新种 *Inderites crassus*、*I. elegans*、*I. flexuosus*、*I. microreticulatus* 和 *I. scrobiculatus*。

值得一提的是，在各个地质时期被广泛报道的一类疑源类化石 *Tasmanites* 是由 Newton [122]在澳大利亚被称为“White Coal”的地层中首先描述的。

1.2.2 中二叠世

在中-晚二叠世（瓜德鲁普统至乐平统），很少文章报道浮游植物。迄今为止，据统计，在中二叠世，一共只有十篇文章提及了疑源类化石。同时，也只有少数几篇文章涉及到Kungurian/Roadian的疑源类。在Roadian-Wordian的地层中，Wilson[123]在美国俄克拉荷马州记录了一种疑源类化石*Hystrichosphaeridium* sp.。在犹他州Phosphoria和Park City组中，Jacobson et al.（1982）描述了6种疑源类化石[124]。其中4种归属于*Micrhystridium*，另外两个为新种：*Leiosphaeridia schopfii*和*Unellium phosphoriensis*[124]。在俄罗斯Kolguyev岛，Grigoriev and Utting[125]报道了1种疑源类化石*Micrhystridium* spp.和两种绿藻化石*Cymatiosphaera* sp.与*Tetraporina horologia*。

中二叠世（Roadian –Capitanian）地层中，在澳大利亚昆士兰Rewan组的煤层中里，Foster[126]描述了5种疑源类化石：*Brazilea helbyi*、*B. helbyi* forma *gregata*、*B. helbyi* forma *helbyi*、*B. plurigena*和*Tessellaesphaera tessellate*。而在南极Dronning Maud Land地区Vestfjella山脉，Lindström[76, 127, 128]从62块样品中发现了3种疑源类化石（Acritarch sp. A、*Leiosphaeridia* sp.和*Mehlisphaeridium* sp.）和5种其它藻类化石（*Cymatiosphaera gondwanensis*、*Brazilea scissa*、*Circulisporites* sp.、*Peltacystia monile*和*P. venosa*）。在格林兰岛Norwegian大陆架中部的岩芯样品里，Bugge et al.（2002）报道了2个疑源类化石属：*Botryococcus*和*Tasmanites*[129]。

在土耳其Hazro地区Wordian-Capitanian的地层中，Stolle先后三次[130-132]报道了共计6种浮游植物化石：*Pyramidosporites cyathodes*、*Cymatiosphaera gondwanensis*、*Dictyotidium* spp.、*Tetraporina* sp. A、*Reduviasporonites chalastus*和*R*. sp. B。

1.2.3 晚二叠世

1.2.3.1 长兴期以及二叠纪与三叠纪之交

在二叠纪与三叠纪之交的地层中，有近17篇的文章报道了疑源类化石。在中国云南富源，Ouyang[133, 134]描述了一些疑源类化石，包括：*Archaeodinium cingulatum*、*Solisphaeridium solidurn*、*S. spinulatum*、*Tasmanites* sp.、*Psiloschizosporis scissus*和*Schizosporis* sp.。在煤山剖面，Ouyang and Utting[135]以及Li et al.（2004a）先后发现了共计6个疑源类化石属（*Baltisphaeridium*、*Leiosphaeridia*、*Micrhystridium*、*Veryhachium*、*Schizosporis*和*Tunisphaeridium*）和2个绿藻化石属（*Cymatiosphaera*和*Dictyotidium*），同时也发现了类似真菌的化石*Reduviasporonites*[69]。值得一提的是，Ouyang and Utting[135]在文中认为疑源类化石组合带*Leiosphaeridia changxingensis –Micrhystridium stellatum*出现在晚二叠世，并描述了一个新种*Leiosphaeridia changxingensis*。但是Li et al.（2004a）阐述了煤山剖面疑源类的变化趋势，没有提及化石带，也没有发现此种疑源类化石[69]。

在欧洲和非洲的一些二叠纪-三叠纪之交的地层中，Jekhowsky[136]描述了6种*Veryhachium*属的疑源类化石，其中包括两个新种：*Veryhachium ?irregulare*和*V. reductum*。在巴基斯坦西部Chhidru组，Sarjeant et al.（1970）报道了16种疑源类化石和一种绿藻化石

[137]。同时他强调，二叠纪的疑源类化石个体小且形态简单[137]。在肯尼亚 Maji ya Chumvi 组，Hankel[138]记录了两种疑源类化石 *Chordecystia chalasta* 和 *Reduviasporonites chalastus*。而在南极 Amery 群，McLoughlin et al.（1997）也报道了两种疑源类化石 *Dictyotidium* sp.和 *Quadrisporites horridus*[139]。

1.2.3.2 其它晚二叠世疑源类化石记录

和研究早二叠世地层一样，一些作者在研究晚二叠世的地层时，并不能得到确切的地层时代信息，只能归为晚二叠世。在南极地区 Prince Charles 山，Balme and Playford[140]报道了微体古植物组合带，其中产出疑源类化石 *Schizosporis scissus*。而在 Transantarctic 山中部，Farabee et al.（1991）记录了疑源类化石 *Pilasporites calculus*[141]。之后在 Vestfjella 山的三个剖面中，Lindström[127]详细分析了其孢粉组合，报道了较多疑源类化石：Acritarch sp. B、*Mehlisphaeridium* sp. A、*Leiosphaeridia* sp. B、*Cymatiosphaera gondwanensis*、*Brazilea scissa*、*Circulisporites parvus*、*Peltacystia monile* 和 *P. venosa*。

在德国 Franconian 海湾，Schaarschmidt[142]描述了 21 种浮游植物化石，归属于 6 个化石属：*Baltisphaeridium*、*Buedingiisphaeridium*、*Micrhystridium*、*Polyedryxium*、*Veryhachium* 和 *Cymatiosphaera*。同时他提到，这些疑源类化石的直径大都在 20 微米左右[142]。

在以色列 Negev 地区北部，Horowitz[143, 144]先后描述了 12 种疑源类化石，归属于 5 个属：*Micrhystridium*、*Pterospermopsis*、*Solisphaeridium*、*Veryhachium* 和 *Tasmanites*。而在南非 Karoo 地区，Horowitz [145]报道了 7 种疑源类化石和一种藻类化石。归属于 5 个属：*Baltisphaeridium*、*Micrhystridium*、*Solisphaeridium*、*Veryhachium* 和 *Tetraporina*。

在澳大利亚，Balme and Segroves[146]描述了三个疑源类新种，*Peltacystia calvitia*、*P. monilis* 和 *P. venosa*。而在悉尼盆地北部地区的煤层中，McMinn [147]报道了 5 种疑源类化石，包括：*Mehlisphaeridium* sp. cf. *M. fibratum*、*Micrhystridium breve*、*M.* sp. cf. *M. inconspicuum*、*M. karamurzae* 和新种 *Ulanisphaeridium berryense*。在昆士兰中部，Fielding and McLoughlin[148]记录了更多的疑源类化石，包括：*Botryococcus braunii*、*Mehlisphaeridium* sp. cf. *M. fibratum*、*Micrhystridium* sp.、*Portalites gondwanensis* cf. *Spongocystia* sp.、*Circulisporites parvus*、*Peltacystia* sp. cf. *P. calvitium* 和 *Tetraporina horologia*。

在印度，Tripathi[149]分析了 Rajmahal 盆地 Chuperbhita 煤田的 RCH-151 岩芯样品，发现了 4 个疑源类化石属 *Balmeella*、*Botryococcus*、*Greinervillites* 和 *Leiosphaeridia*。在坦桑尼亚 Kilombero 地区的 Karoo 超群，Dypvik et al.（2001）报道了 3 种疑源类化石 *Mehlisphaeridium regulare*、*Cymatiosphaera gondwanensis* 以及 *C.* sp.[150]。

在巴基斯坦 Surghar 和 Salt 山，Balme[151]发现了 5 种疑源类化石 *Inaperturopollenites nebulosus*、*Pyramidosporites racemosus*、*Peltacystia venosa*、*Quadrisporites horridus* 和 *Schizosporis scissus*。而在同一地区，Hermann et al.（2012）则报道了 3 种疑源类化石：*Micrhystridium* sp.、*Veryhachium* sp.和 *Quadrisporites horridus*[152]。

1.2.3.3 二叠纪末期的真菌高峰

在以色列二叠纪末的生物大灭绝期间，由于疑源类 *Reduviasporonites* 化石占据样品中

孢粉型化石的 95%以上，而且 Eshet et al.（1995）认为其为一种真菌，于是首先提出了二叠纪末期“真菌高峰”的概念[64]。紧接着，在意大利阿尔卑斯山南部，Visscher et al.（1996）报道了疑源类化石 *Reduviasporonites*，也认为它是一种真菌的菌孢[66]。由于此化石在二叠纪末期的大灭绝期间异常富集，他们同样认为此时出现了菌孢高峰[66]。之后在全球其它地区的二叠纪-三叠纪之交的地层中，Looy et al.（2001）、Steiner et al.（2003）以及 Sandler et al.（2006）先后也报道了真菌高峰的存在[65, 68, 153]。

然而，一些作者认为这类疑源类化石并非真菌化石。在俄罗斯，Afonin et al.（2001）描述了 *Reduviasporonites* 并认为其为一种藻类[154]。之后 Foster et al.（2002）采集了来自格陵兰岛、英国、中国、俄罗斯以及澳大利亚等地 PTB 的样品，总结并重新详细地描述了 *Reduviasporonites* 化石，并将其归为两个种 *Reduviasporonites catenulatus* 和 *R. chalastus*[155]。他们认为，这两个种都为链状，其最大的区别在于每一个单体胞囊的直径相差较大[155]。*Reduviasporonites catenulatus* 的个体较小，其长度一般在 20 微米以下；而 *R. chalastus* 个体较大，其长度在 20 至 60 微米之间。同时，他们还对 *Reduviasporonites* 做了化学分析，认为其更像是藻类而不是真菌[155]。

但是，Sephton et al.（2009）分析了 *Reduviasporonites* 的碳同位素和氮同位素等化学组成，明确地认为其来源于真菌[156]。而后，Visscher et al.（2011）通过形态等方面的证据，更加巩固了 *Reduviasporonites* 为真菌的结论[67]。关于 *Reduviasporonites* 是否为真菌的争论也许并未结束，应该还会有更多的学者加入研究的行列中。

1.2.4 其它二叠纪疑源类的报道

另外还有 7 篇文章报道了二叠纪疑源类化石，但是缺乏更为准确的地层信息，我们无法将其划分到以上各类。在澳大利亚的煤层中，Balme and Hennelly[157]以及 Stephen[158]报道了 2 种疑源类化石 *Brazilea plurigenus* 和 *Psiloschizosporis scissus*。在澳大利亚西部，Segroves[159]详细地描述了一些浮游植物种类。在俄罗斯 Pre-Caspian 地区，Abramova and Martchenko[160]描述了 3 个新种 *Inderites bulbiferus*、*I. compactus* 和 *I. robustus*。在刚果，Bose and Kar[161]描述了一个新属 *Greinervillites*，同时描述了新种 *Greinervillites undulatus*。同一地区，Kar and Bose[162]又记录了另外一个新种 *Maculatasporites zairensis*。在日本二叠纪的砂岩中，Takahashi and Yao[163]报道了一种疑源类化石 *Tasmanites tanbaensis*。

1.2.5 二叠纪疑源类的古地理分布

在早古生代的地层中，特别是奥陶纪和泥盆纪，疑源类不仅可以用于划分地层，同时也可以用来恢复古地理环境。疑源类古地理分区不仅存在于早-中奥陶世[164, 165]，同样也存在于志留纪[166]和泥盆纪[56, 167]。另一方面，近年来，研究疑源类古地理分布的学者越来越多[168-172]。他们发现，疑源类大都富集在大陆架附近；而离陆地越远，其多样性越低，符合近岸-远岸的分布规律。本文也将在第三章中重点讨论这个问题。

以上的数据表明，在二叠纪，共计 45 个浮游植物化石属出现在南半球中纬度地区，共

来自于 57 篇文章的资料（图 1-3）。也有 27 属在北半球低纬度地区，它们出自 12 篇文章。值得注意的是，二叠纪疑源类的数据量远远不够，还需要大量的研究工作，才能得到相对严谨的结果。同时，在北半球高纬度地区至今还未找到疑源类化石，中纬度地区也只有 11 个属被报道。而在南半球低纬度和高纬度地区，分别有 20 个和 17 个疑源类化石属被发现。如图 1-3 D 所示，尽管目前数据量较小，但是仍然可以明显看出疑源类化石的多样性高低与研究论文的数量成正相关。其较高的物种多样性来自于大量的研究工作，特别是在早二叠世（图 1-3）。

就疑源类化石属的古地理分布而言，*Cymatiosphaera* 分布最广，从北半球中纬度地区一直到南半球高纬度地区皆有发现。而另外一些属如 *Baltisphaeridium*、*Micrhystridium* 和 *Veryhachium* 分布在北半球中纬度地区至南半球中纬度地区。反之，*Leiosphaeridia*、*Dictyotidium*、*Tasmanites* 和 *Brazilea* 则只出现在北半球低纬度地区到南半球中纬度地区，而其它一些属的分布更窄。但是，也许只是因为调查研究的地区分布不均而导致了某些属种分布较窄。值得一提的是，尽管 *Portalites* 被报道了多达 14 次，但是其仅限于分布在南半球中纬度地区。

与 Li et al.（2004a）的结论类似，目前为止，由于二叠纪疑源类的数据量太小且大多数常见种都是世界性的广布种，而无法做生物古地理的研究[69]。

在古环境的重建方面，大多数二叠纪的有机质浮游植物都出现在砂岩、粉砂岩、泥岩和页岩中，即出现在近岸浅海或者潮坪环境。同时，多数研究孢粉的学者都着重调查陆地孢粉化石，而大都忽略了疑源类的研究。即使报道了疑源类，其在孢粉组合中含量也极低。然而此类近岸环境的有机质化石中应该包含较多海洋浮游植物，如绿藻类。只有少数几篇文章研究了远岸海洋环境的疑源类[69, 82, 92, 94, 135]。而这些文章中出现的疑源类大都是直径较小的种类，通常不超过 20 微米，皆为常见的疑源类种类，如 *Baltisphaeridium*、*Micrhystridium* 和 *Veryhachium*。

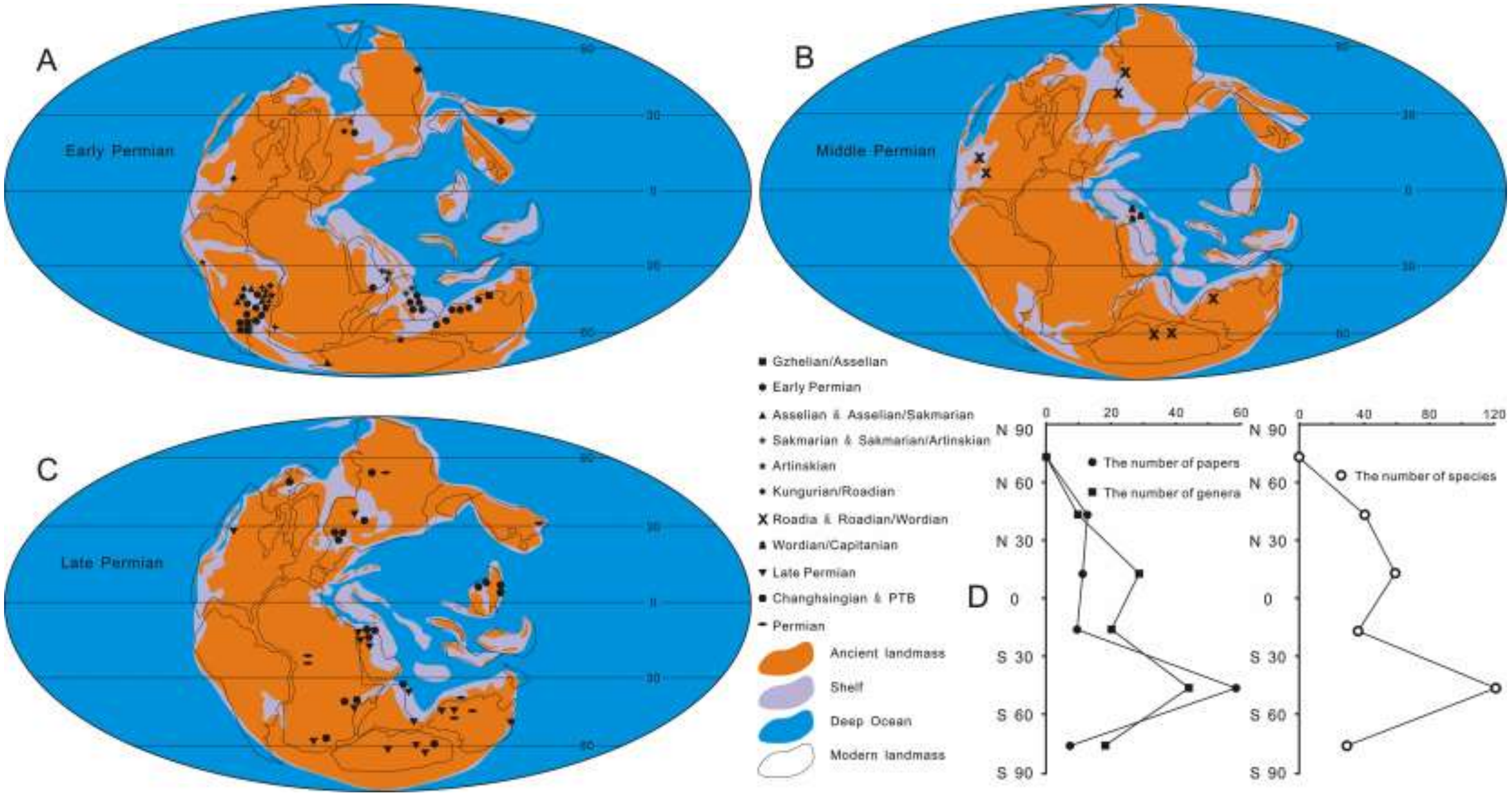

图 1-3 二叠纪疑源类的古地理分布图

A：早二叠世（290Ma）；B：中二叠世（265 Ma）；C：晚二叠世（255 Ma）；均改自[173]；D：二叠纪疑源类随纬度的变化规律

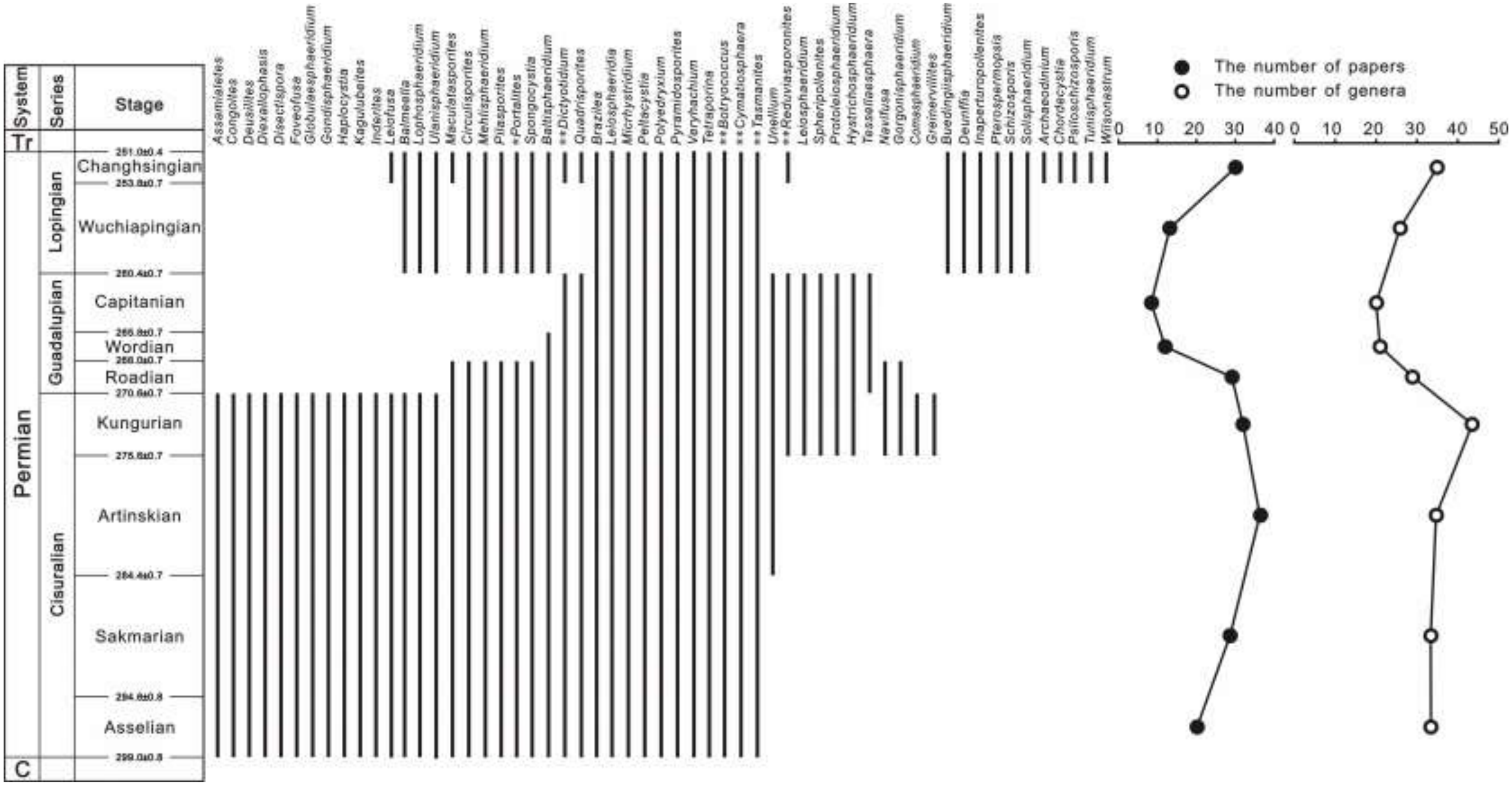

图 1-4 二叠纪疑源类化石属的多样性变化

二叠纪地层划分参考自[72]；*：真菌；**：藻类

1.2.6 二叠纪疑源类的物种多样性

以上结果显示，相对于早古生代，二叠纪疑源类的研究程度很低，很可能大部分的疑源类化石都未被发现。与石炭纪的浮游植物类似[62]，现在仍然有很多问题不能解决。首先，很多文章的详细地层时代不明（见上文）。其次，由于众多文献之间存在较长的时间间隔，故很多属种的描述不尽相同，同时许多生物亲缘关系也不能确定。第三，各个时代间隔内的研究程度不一致，导致无法准确评估整个二叠纪浮游植物物种多样性的变化趋势。因此，为了更好地评价二叠纪浮游植物物种多样性的相对变化，本文不仅统计了浮游植物化石属种的数量，同时也统计了各阶的研究论文数量。

在统计的时候，如果某一属种出现在两个阶之间（或者更多，如 Kungurian 和 Roadian），则其将被各计算一次，其结果如图 1-4 所示。同时，本文还统计了各属被报道的次数以及其包含的物种的数量（图 1-5）。

在早二叠世，浮游植物生物多样性程度较高，一般高于 30 个属（图 1-4）。而据现有的资料显示，中二叠世和晚二叠世早期（Roadian-Wuchiapingian），其多样性较低，只有大约 20 属。但是，有 36 属的浮游植物被报道于二叠纪末期长兴阶（图 1-4）。然而如图 1-4 所示，浮游植物的多样性与其报道的论文数量呈现较强的正相关，大量的研究集中在早二叠世与二叠纪末期，从而导致较多的浮游植物属种被发现。

在早二叠世，多样性最高的浮游植物组合由 Backhouse[117]报道于澳大利亚，共计 22 种浮游植物化石。其它报道浮游植物种类超过 10 种的文章有：Gilby and Foster（1988）[174]、Tiwari and Navale（1967）[106]、Beri et al.（2010）[79]、Lindström（1995）[76]、Mori et al.（2012）[93]以及 Wall and Downie（1963）[118]。而在中二叠世，所有报道疑源类的文章里，都未超过 10 种，最高仅有 8 种[97, 175]。在晚二叠世，疑源类多样性最高的为 Schaarschmidt（1963），其描述了 21 种化石，包括一种绿藻[142]。其次为 Sarjeant et al.（1970），报道了 16 种疑源类和 1 种绿藻[137]。而 Horowitz（1973）也记录了 10 种疑源类和 2 种绿藻[143]。

从图 3 可以看出，一些疑源类属在整个二叠纪都有报道，包括：*Botryococcus*、*Brazilea*、*Cymatiosphaera*、*Leiosphaeridia*、*Micrhystridium*、*Peltacystia*、*Polyedryxium*、*Pyramidosporites*、*Tasmanites*、*Tetraporina* 和 *Veryhachium*。某些属应该也出现于整个二叠纪，但是可能由于研究较为局限的等问题，在某一段时期内未被记录。如 *Baltisphaeridium* 在 Capitanian 缺失。然而，一些属的报道时间间隔较为局限，如 *Comasphaeridium* 和 *Greinervillites* 仅被发现于 Kungurian；*Archaeodinium*、*Chordecystia*、*Psiloschizosporis*、*Tunisphaeridium* 和 *Wilsonastrum* 仅报道于长兴阶。

由图 1-5 可以清楚得知，一些疑源类属在二叠纪地层中出现非常频繁。*Micrhystridium* 被报道次数高达 55 次，涉及 27 个化石物种；与其类似，有 22 个物种被归为 *Veryhachium*，也被报道了 46 次。还有一些种类出现频率较高，如 *Brazilea*、*Leiosphaeridia*、*Tetraporina*、*Maculatasporites*、*Peltacystia*、*Botryococcus* 和 *Quadrisporites* 被分别记录多达 20 次；*Reduviasporonites*、*Cymatiosphaera*、*Tasmanites*、*Portalites*、*Circulisporites* 和 *Mehlisphaeridium* 被报道也有十次以上。反之，*Chordecystia*、*Diexallophasis*、*Unellium*、*Archaeodinium*、*Deunffia*、 *Psiloschizosporis* 和 *Wilsonastrum* 只被发现 2 次；而 *Assamialetes*、*Buedingiisphaeridium*、*Comasphaeridium*、*Disectispora*、*Globulaesphaeridium*、*Gondisphaeridium*、*Gorgonisphaeridium*、*Inaperturopollenites*、*Leiosphaeridium*、*Navifusa*、*Protoleiosphaeridium*、*Pterospermopsis*、*Tessellaesphaera* 和 *Tunisphaeridium* 仅被报道过一次。

在种一级分类水平中，一些物种也较为常见。*Botryococcus braunii*、*Brazilea scissa*、*Peltacystia venosa*、*Portalites gondwanensis* 和 *Quadrisporites horridus* 出现了 10 次以上；*Brazilea plurigenus*、*Circulisporites parvus*、*Deusilites tenuistriatus*、*Mehlisphaeridium fibratum*、*Micrhystridium breve*、*M. stellatum*、*Peltacystia monile*、*Tetraporina punctata*、*Veryhachium reductum*、*Reduviasporonites chalastus* 和 *Cymatiosphaera gondwanensis* 也出现了 5 次以上。

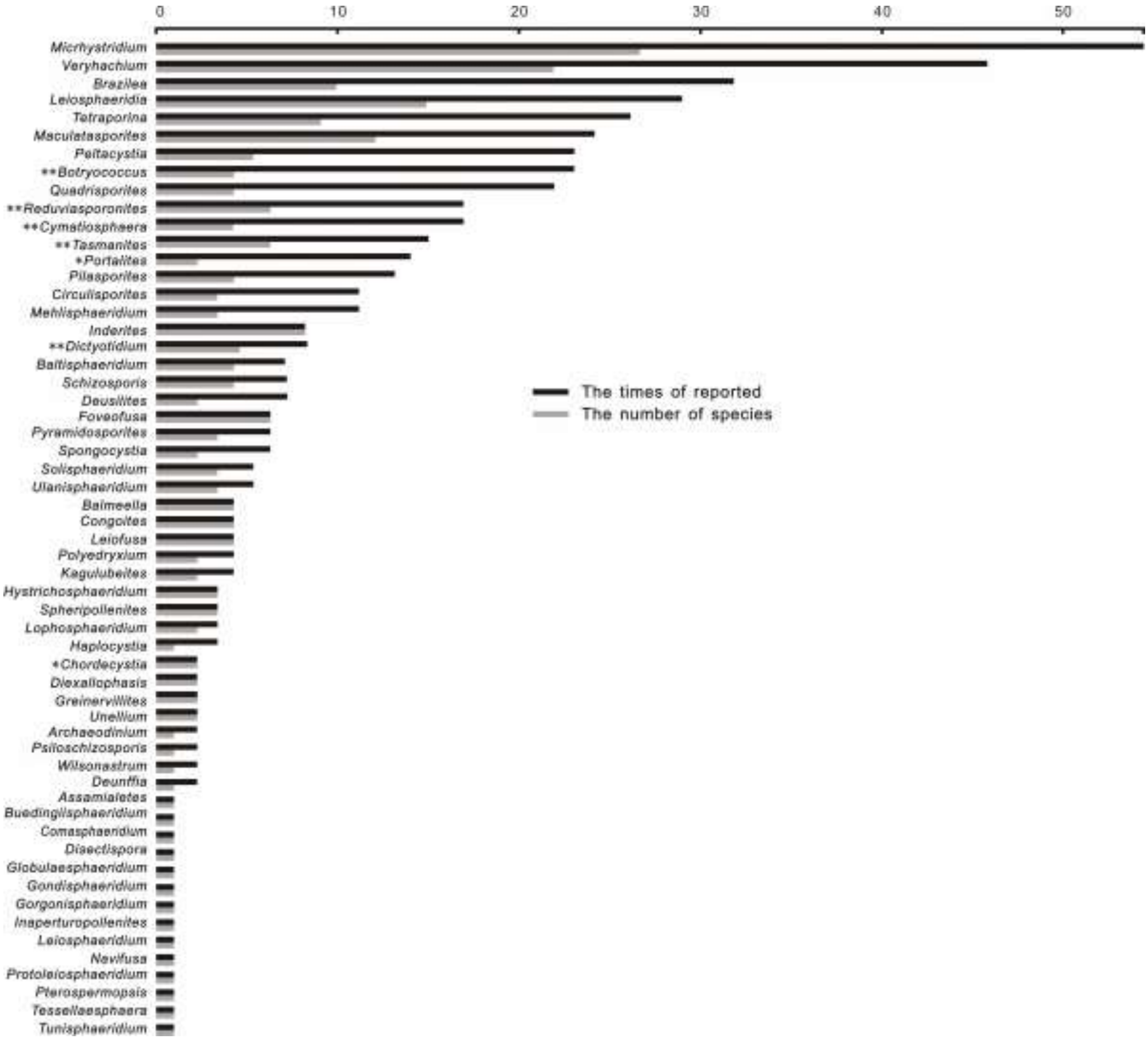

图 1-5 二叠纪疑源类化石各属被报道的次数以及各个属出现的物种数

*：真菌；**：藻类

§1.3 二叠纪与三叠纪之交生物大灭绝研究存在的不足以及本文的研究目的

前人在研究二叠纪末期的海洋生物大灭绝的时候，多是基于动物化石，对广布于海洋中的初级生产者研究较少。

1）通过近些年对蓝细菌的研究表明，蓝细菌在二叠纪末期的生物大灭绝期间出现两期异常的峰值，可能与大灭绝之后生态环境发生巨大变化有关。

2）研究发现[14, 176]，钙质藻类的生物多样性在煤山 25 层底部出现大幅度降低，仅有一种残存到早三叠世。

3）在二叠纪末期，对于海洋中主要的具有机质壳浮游植物（疑源类）的研究较少，而有关“真菌高峰”的讨论却持续近二十年。

基于这些因素，本文将主要采集华南地区二叠纪与三叠纪之交疑源类的资料，同时综合前人的其它数据，分析二叠纪末生物大灭绝期间浮游植物与生态环境的协同演化。

第二章 华南二叠纪与三叠纪之交的疑源类

§2.1 研究区地质背景

本文所涉及的二叠纪与三叠纪之交剖面共计七个，都位于华南地区扬子板块。分别为中寨剖面、煤山剖面、上寺剖面、凉风垭剖面、峡口剖面、甘溪剖面以及东攀剖面（图 2-1）。七个剖面囊括了海陆交互相、台地以及盆地相等沉积相。同时也涵盖了从近岸到远岸的古海洋环境（图 2-2），各剖面详细的地层对比见图 2-3。以下将逐一概述各个剖面的地质背景。

2.1.1 中寨剖面

中寨剖面（26°09.110N，105°17.113E）位于贵州省西部，六盘水市东南部，距离六枝特区 25 公里（图 2-1）[177]。该剖面自下而上连续沉积上二叠统龙潭组以及下三叠统飞仙关组。龙潭组出露近 30 米（野外层号为 1-27），而飞仙关组出露约 10 米（层号为 28-37）。龙潭组主要以砂岩和泥岩为主，也包括多层灰岩，产出双壳、腕足、介形虫、腹足类以及头足类等化石[178]。飞仙关组则以钙质泥岩为主，夹少量火山灰沉积以及灰岩，产出少量腕足以及大量的双壳类化石[178]。根据该剖面的沉积特征分析，其属于扬子台地西部的海陆交互相沉积（图 2-2）[177-179]。基于牙形石 *Hindeodus parvus* 的出现，Metcalfe and Nicoll [177]认为二叠纪与三叠纪之交的界限应该在 28 层的灰岩里。而 Shen et al.（2011）利用 U-Pb 测定第 29 层的粘土岩的年龄为距今 252.24 ±0.13 Ma[4]。

2.1.2 煤山剖面

煤山剖面（31°03N，119°54E）位于浙江省长兴县西北部约 25 公里处（图 2-1）。该剖面是全球界限层型的标准剖面，已于 2001 年被确定为全球二叠系-三叠系界限层型和点（GSSP），且以牙形石 *Hindeodus parvus* 首次出现的煤山 D 剖面 27c 层作为三叠纪的开始[180-182]。该剖面属于扬子板块东缘近大陆架碳酸盐台地沉积，水深在 30 至 60 米之间[180]。自下而上出露为长兴组和殷坑组。长兴组上部岩性以灰岩为主，夹少量泥岩。而殷坑组底部则以泥灰岩为主，夹少量灰岩以及火山灰沉积。根据 U-Pb 测年的数据，第 25 层和 28 层的绝对年龄为距今 252.28 ±0.08 Ma 和 252.10 ±0.06 Ma [4]。

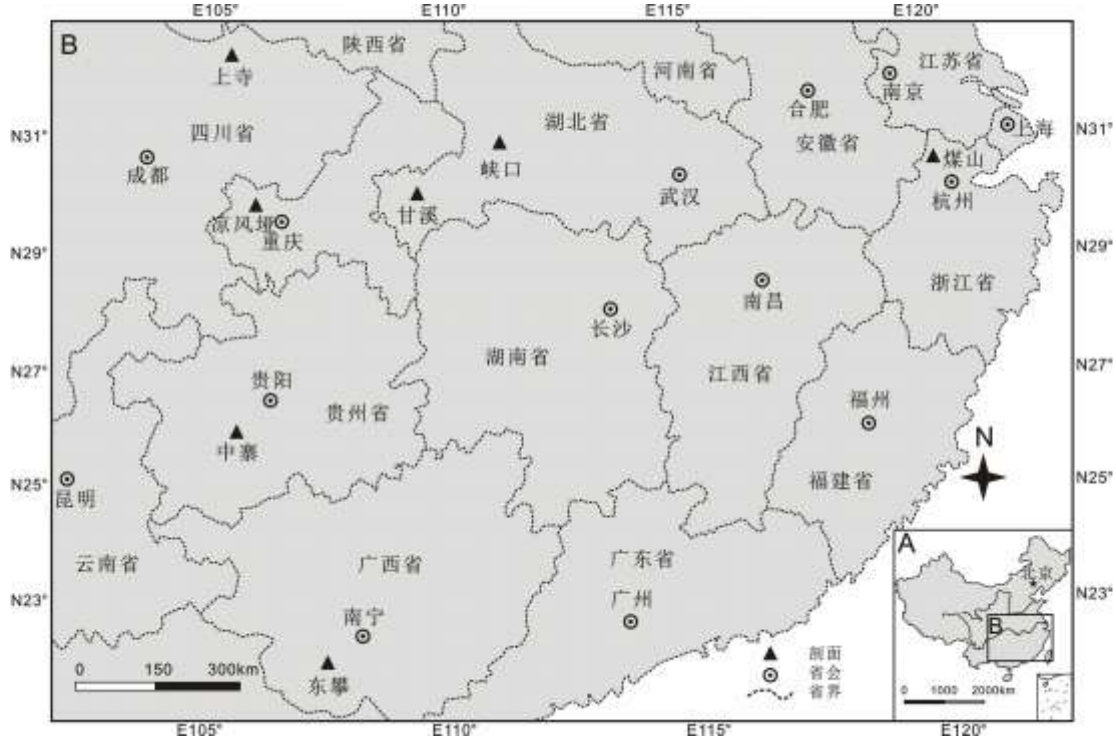

图 2-1 七个剖面所在的研究区地图

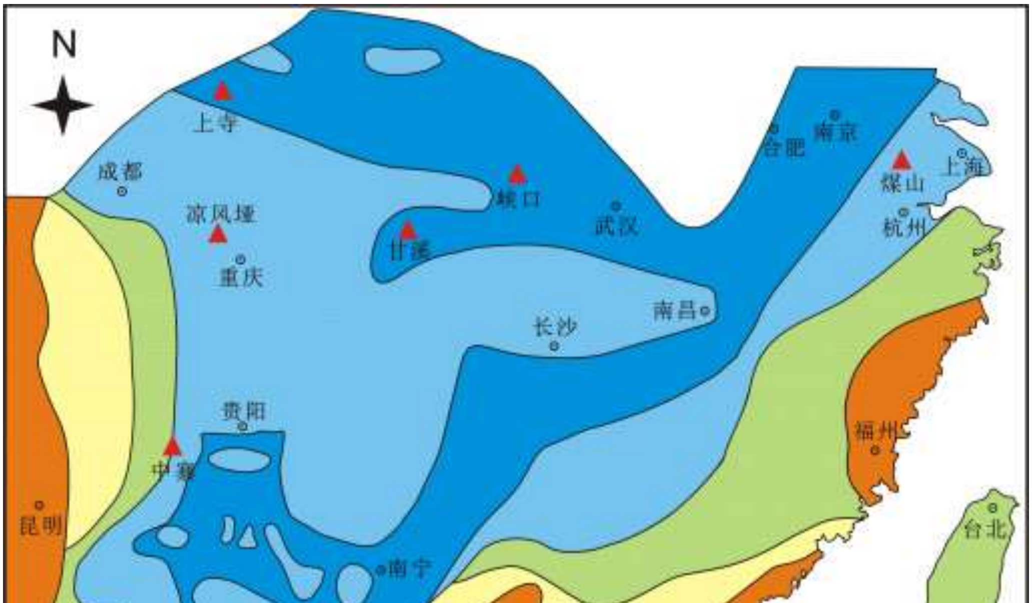

图 2-2 华南地区晚二叠世末期古地理图（改自[183]）

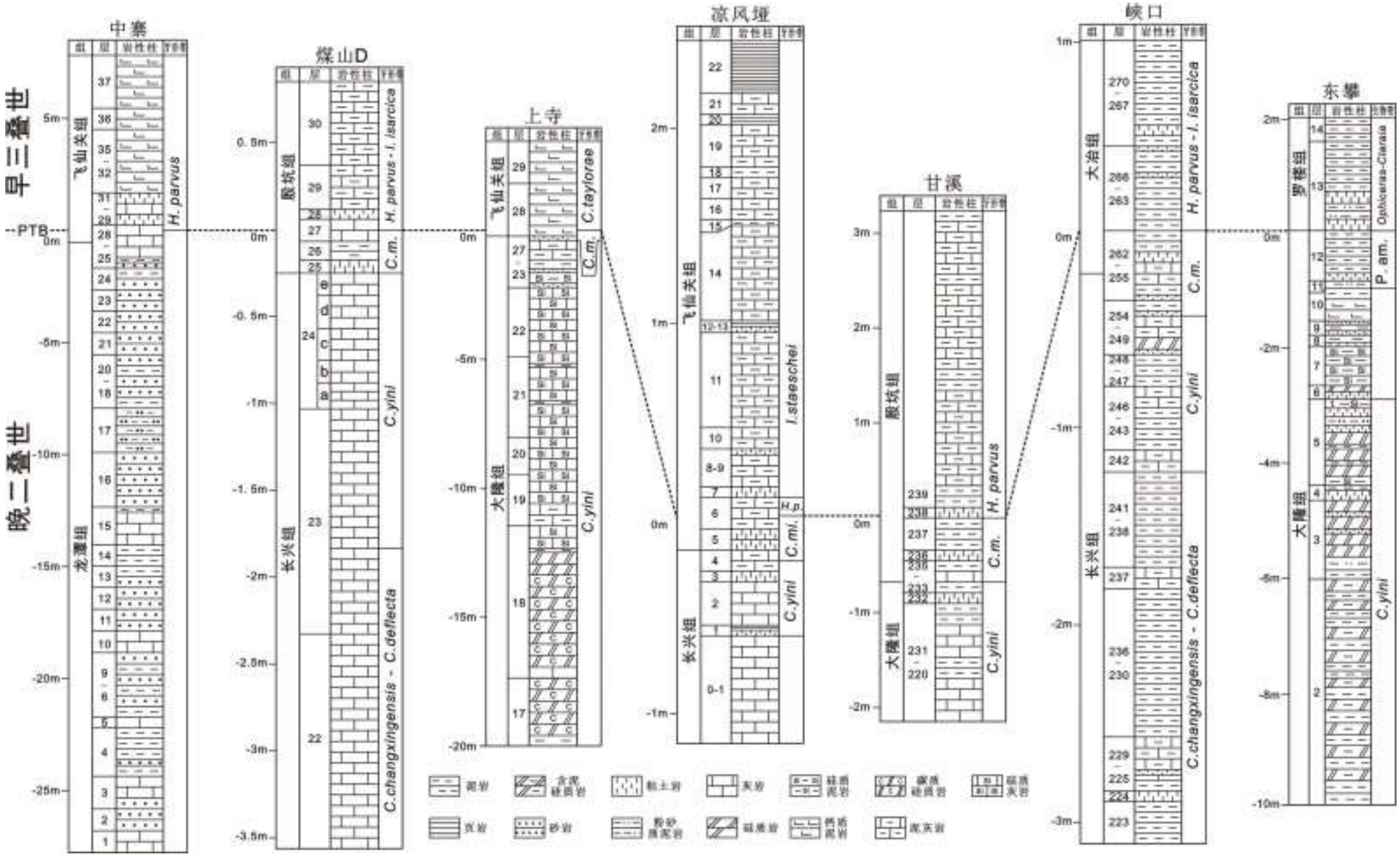

图 2-3 华南地区各研究剖面地层划分对比图 （划分依据见正文）

C.=Clarkina; *H.=Hindeodus*; *I.=Isarcicella*; *m.=meishanensis*; *mi.=microcuspidata*; P. am.= Permian ammonoids;

2.1.3 上寺剖面

上寺剖面位于四川省北部广元市剑阁县上寺村附近，处于上扬子西北部（图 2-1）[184, 185]。该剖面较完整地出露大隆组以及飞仙关组的一部分。从上世纪 80 年代开始，已有大量的地质工作者研究过该剖面，而本文将沿用李子舜等[186]划分的层位，以便于对比。大隆组包括 15 至 27 层，岩性以硅质灰岩为主，夹少量灰岩、泥岩以及火山灰沉积，产出化石包括放射虫、双壳、腕足以及菊石等。28 层以上为飞仙关组，岩性以钙质泥岩和泥灰岩为主，夹少量火山灰沉积，产出丰富的菊石。根据岩性以及其它沉积特征判断，该剖面沉积相变化较大，大隆组处于远大陆架至盆地相沉积，而飞仙关组则属于近岸的潮坪环境[186]。根据菊石带以及牙形石带，15-16 层为吴家坪晚期。而该剖面 PTB 的划分则具有较大的争议。若只依据 *Hindeodus parvus* 的首现，PTB 则将高于大灭绝界限 2-4 米[184-187]。而基于牙形石 hindeodid 和 gondolellid 的综合考虑，Jiang et al.（2011）认为 PTB 应该置于距 28 层底部 22 厘米处[188]。根据 U-Pb 测年数据，第 27 层的绝对年龄为距今 252.28 ±0.13 Ma[4]。

2.1.4 凉风垭剖面

凉风垭剖面位于重庆市中梁山地区，临近山洞村的一个采石场（图 2-1）。该剖面露头极好，晚二叠世长兴组与早三叠世飞仙关组下段沉积连续，界限清楚。长兴组以深灰色的厚层灰岩为主，上部夹几层火山灰沉积，产出丰富的腕足、有孔虫、珊瑚、腹足类以及介形虫等化石。飞仙关组则以泥质灰岩为主，夹少量页岩以及火山灰沉积，主要产出介形虫等化石。该剖面处于中上扬子台地内部，离陆地较远。根据牙形石 *Hindeodus parvus* 的首现，该剖面的 PTB 应置于第 6 层的灰岩里（夏文臣，个人交流）。

2.1.5 峡口剖面

峡口剖面（31°06.874N，110°48.221E）临近湖北省宜昌市兴山县峡口镇，处于扬子版块北部（图 2-1）[189]。该剖面露头较好，出露晚二叠世长兴组与早三叠世大冶组。长兴组上部（223 层-256 层）以薄层的泥岩以及泥质灰岩为主，而大冶组底部（257 层-270 层）则主要为泥岩，夹少量几层火山灰沉积。根据岩性等沉积特征判断，该剖面属于开阔的大陆架沉积，离陆地较远，海水较深（图 2-2）[189, 190]。根据最新的牙形石数据，*Hindeodus parvus* 的首现位于 262 层[39]。

2.1.6 甘溪剖面

甘溪剖面（30°07.4′N，109°26.8′E）位于湖北省，临近恩施市（图 2-1）。该剖面延公路分布，露头极好，连续沉积晚二叠世大隆组以及早三叠世殷坑组。大隆组上部（220 层至 233 层）以泥岩为主，夹少量灰岩及火山灰沉积。而殷坑组沉积厚度可达几百米，以中厚层灰岩

为主，夹少量泥岩以及火山灰沉积。根据牙形石 *Hindeodus parvus* 的首现，该剖面的 PTB 位于 238 层[191]。

2.1.7 东攀剖面

东攀剖面（22° 16.196N，107° 41.505E）位于广西省西部，南宁市以西约 80 公里，处于扬子板块的南部（图 2-1）[192]。该剖面连续出露晚二叠世大隆组上部以及早三叠世罗楼组下部。2 至 8 层以硅质岩和硅质泥岩为主，夹少量泥岩以及火山灰沉积，富含双壳，腕足，腹足，介形虫以及放射虫等化石。9 至 14 层则以泥岩为主，夹少量火山灰沉积，产出少量菊石、有孔虫以及放射虫等化石。Feng et al.（2007）认为大隆组处于大陆坡至盆地相（图 2-2）[10]。由于该剖面产出可以指示深水环境的放射虫 *Albaillella*，He et al.（2005）认为第 5 层的海水深度应该在 500 米左右[193]。而根据双壳以及菊石化石带，He et al.（2005, 2007a, b）以及 Feng et al.（2007）建议将 PTB 定在 12 层与 13 层之间[10, 192-194]。

§2.2 实验方法与结果

2.2.1 疑源类化石的实验室处理过程

大多数的疑源类被认为是海洋浮游植物，因此它们通常保存在海相的沉积岩地层中。目前在多种沉积岩中均能发现疑源类化石，但是多见于泥岩与页岩之中，然而早期的研究者却都热衷于在燧石薄片中寻找疑源类。采样时注意不宜采集已开始风化的露头样品。疑源类的外壁与其它孢粉型化石的外壁类似，都是由抗酸碱腐蚀的孢粉素形成。本文中，疑源类的实体化石均是运用标准的孢粉化石分离方法获得。

1）样品前处理

首先将采集到的样品用蒸馏水洗净，并除去风化或者污染的表面。然后将样品粉碎至直径为 2~5mm 的颗粒，根据岩性的不同，粒径要求也不一样。例如，钙质岩石以及页岩等在酸处理的时候反应强烈，不需要粉碎得过细。

2）实验步骤

1 加样：称取 50g 前处理完毕的样品放入 1000 毫升的塑料烧杯中（同时加入一粒石松孢子用于计算样品中疑源类的含量）;

2 加盐酸：将 36.5%的盐酸缓慢倒入烧杯中，同时用玻璃棒轻轻搅拌（防止反应过于强烈而形成大量的气泡使样品溢出，盐酸与样品质量的比例大约为 3:1）;

3 静置反应 24 小时，每隔 6 小时左右轻轻搅拌一次；

4 中和：加入过量蒸馏水，并在静置 4-6 小时之后倒出上层清液。此步骤将重复 3-4 次，直至杯中 ph 值为 7 左右；然后将样品晾干；

5 加氢氟酸：将 40%的氢氟酸缓慢倒入烧杯中，同时用玻璃棒轻轻搅拌，用量与盐酸相同；

6 重复步骤（3）；如果样品未能全部溶解，可以继续加入一定量的氢氟酸，再重复步骤（3），直至样品溶解完毕；

7 重复步骤（4）；

8 离心：将剩下的样品残渣倒入 50ml 的离心管之中，在转速为 2000 转/秒的离心机中离心 10 分钟左右，然后倒掉上层清液；

9 重液分离：将离心得到的样品静置 24 小时左右之后，加入密度为 2.2 左右的重液并搅拌均匀；然后离心 20 分钟，取上层浊液倒入 50ml 的玻璃烧杯中，并加入 5‰的醋酸溶液；

10 再离心：玻璃烧杯中的混合物静置 24 小时，然后倒去上层清液，将剩下的浑浊液倒入 10ml 的离心管之中，并加入蒸馏水，离心 10 分钟；重复 3-4 次，直至离心管中样品的 ph 值在 7 左右；

11 统计与鉴定：取少量离心管中的残留物制作成临时装片或者永久装片，然后利用生物显微镜进行疑源类的统计与鉴定。个别化石较多的样品则用毛笔在体视镜下挑取出疑源类化石，并利用电子扫描显微镜成像。

重液的配置：首先将锌粒（Zn）与氢碘酸（HI）在搪瓷盆中反应 24 小时，待反应完毕，按照需要的重液密度加入适量的固体碘化钾（KI）。配置密度为 2.2 的重液用量约为：Zn：HI：KI= 100 g：500 ml：500g。

§2.3 疑源类的研究结果

此次研究从扬子板块二叠纪与三叠纪之交的七条剖面采集了岩石样品共计 418 块。经实验室处理之后，在其中的 94 个样品中发现丰富的疑源类化石。同时，在中寨剖面和上寺剖面的较多样品中发现了大量的孢粉化石。各剖面的样品采集情况如表 2-1 所示。以下将对各个剖面的疑源类化石实验结果进行逐一介绍。实验数据见附录 B。

表 2-1：各剖面的样品采集数量以及含疑源类及孢粉的样品数量

样品数量/剖面	中寨	煤山	上寺	凉风垭	峡口	甘溪	东攀
采集样品	87	1	141	29	60	77	23
含疑源类样品	5	1	52	7	6	11	12
含孢粉样品	45	1	23	-	-	-	5

2.3.1 中寨剖面

由于中寨剖面属于海陆交互相，离陆地非常近，因此样品中的孢粉含量异常丰富。此次研究共在 45 个样品中鉴别出 16 属的孢粉化石，其中绝大部分是孢子化石，只有极少量的花粉（图 2-4）。孢粉组合中，以具较厚实的椭圆形壁的 *Punctatosporites* 和 *Laevigatosporites*

两个属占据绝对优势，其百分含量在整个剖面的平均值分别达 37.4%和 17.1%，而其它属都未超过 10%。在晚二叠世末期的 5 个样品中发现了少量的疑源类化石，包括：*Baltisphaeridium* sp.、*Micrhystridium breve*、*M. stellatum* 以及 *Reduviasporonites chalastus*。其中具短突起的 *Micrhystridium breve* 的含量最高，在 5 个样品中的平均值达到 58.6%。其次为 *Baltisphaeridium* sp.，达到 35.7%。

2.3.2 煤山剖面

Ouyang and Utting[135]以及 Li et al.（2004a）对煤山剖面的疑源类做了较为详细的调查[69]，共发现疑源类化石 13 种，隶属于 9 属，包括：*Baltisphaeridium*、*Cymatiosphaera*、*Dictyotidium*、*Leiosphaeridia*、*Micrhystridium*、*Veryhachium*、*Reduviasporonites*、*Schizosporis* 以及?*Tunisphaeridium*（图 2-5）。而此次研究中，煤山剖面 26 层的疑源类及其百分比分别为：*Dictyotidium reticulatum*（41.4%）、*Micrhystridium stellatum*（23.2%）、*Veryhachium hyalodermum*（16.0%）、*Reduviasporonites chalastus*（7.0%）以及 *Schizosporis* sp.（12.4%）。同时，煤山剖面的早三叠世也发现大量的孢粉化石。

2.3.3 上寺剖面

上寺剖面疑源类化石的物种多样性是七个剖面中最高的，共在 37 个样品中发现疑源类 20 种，隶属于 8 属（图 2-6）。包括：*Baltisphaeridium* sp.、*Dictyotidium reticulatum*、*D.* sp.、*Leiofusa* sp.、*Leiosphaeridia micrograníera*、*L. minutissima*、*Micrhystridium breve*、*M. fragile*、*M. pentagonale*、*M. stellatum*、*Reduviasporonites catenulatus*、*R. chalastus*、*Schizosporis scissus*、*S.* sp.、*Veryhachium cylindricum*、*V. hyalodermum*、*V. nasicum*、*V. quadratum*、*V. sedecimspinosum* 以及 *V.* sp. A。从属一级水平上看，球形疑源类 *Leiosphaeridia* 最为丰富，其相对含量达 50.8%；而具突起的 *Micrhystridium* 以及 *Veryhachium* 分别为 26.8%和 11.1%。在种一级水平上，*Leiosphaeridia micrograníera*、*L. minutissima*、*Micrhystridium breve*、*Dictyotidium reticulatum* 以及 *Veryhachium hyalodermum* 是最为常见的种。吴家坪晚期（15 层-16 层）几乎只出现膜壳较大的球形疑源类 *Dictyotidium reticulatum*（膜壳直径在 80 微米左右）；长兴期则以膜壳较小的球形疑源类 *Leiosphaeridia* 为主（膜壳直径在 30 微米左右）；但是在 PTB 附近，具突起的疑源类的丰度明显升高，特别是具短突起的 *Micrhystridium breve* 在 28 层异常富集（图 2-6）。值得一提的是，链状疑源类 *Reduviasporonites* 的丰度在 PTB 附近也较高，但是最高只有 14%。同时，25 层至 29 层中发现了大量的孢粉化石，甚至在 28 层顶部以后的地层中，只出现孢粉化石。根据上寺剖面孢粉型化石的特征，本文将其划分为 3 个孢粉型化石组合带（图 2-6）。

1）*Dictyotidium* 组合带（15 层-17 层）：主要出现在吴家坪晚期，位于牙形石带 *Neogondolella orienta* 带顶部以及 *Neogondolella yini* 带底部。该组合带中疑源类属种单一，只发现具大型膜壳的球形疑源类 *Dictyotidium reticulatum*，同时发现少量炭屑。

2）*Leiosphaeridia- Micrhystridium- Veryhachium* 组合带（17 层-25 层）：出现于长兴期，

包括牙形石带 *Neogondolella yini* 带和 *Neogondolella meishanensis* 带。其中，17 层顶部至 20 层底部缺乏孢粉型化石，而 20 层顶部至 25 层则以 *Leiosphaeridia*、*Micrhystridium*、*Veryhachium* 占优，也含有少量孢粉化石，如：*Leiotriletes*、*Lycopodiacidites* 以及 *Waltzispora*。

3）*Pteruchipollenites- Leiotriletes* 组合带（26 层-29 层）：主要位于二叠纪与三叠纪之交的地层中，包括牙形石带 *Hindeodus changxingensis* 带以及 *Hindeodus parvus* 带。该组合带主要以孢粉化石为主，包括：*Lycopodiacidites*、*Waltzispora*、*Indotriradites*、*Leiotriletes*、*Cycadopites*、*Tripartites*、*Propterisispora*、*Lueckisporites*、*Pteruchipollenites*、*Alisporites*、*Gardenasporites*、*Vitreisporites*、*Protohaploxypinus* 和 *Cordaitina*。其中，孢子、花粉以及疑源类三者的相对百分比为：43.7%、42.6%和 13.7%。同时，*Pteruchipollenites* 和 *Leiotriletes* 的含量分别达 18.4%以及 14.1%。而疑源类则以具短突起的 *Micrhystridium breve* 以及链状疑源类 *Reduviasporonites* 为主要类型。

2.3.4 凉风垭剖面

凉风垭剖面共计发现疑源类 8 种 3 属，包括：*Leiosphaeridia microgranifera*、*L. minutissima*、*Micrhystridium breve*、*M. pentagonale*、*M. stellatum*、*Veryhachium hyalodermum*、*V. quadratum* 以及 *V. sedecimspinosum*。在长兴组顶部火山灰沉积之后的泥岩中，*Micrhystridium* 和 *Veryhachium* 的丰度极高，与上寺剖面 25 层的疑源类分布类似（图 2-5）。而在早三叠世却只发现 *Leiosphaeridia minutissima* 一种疑源类化石。该剖面未发现孢粉化石。

2.3.5 峡口剖面

峡口剖面的疑源类物种多样性较低且生物量也不高，只在二叠纪末期的 6 个样品中发现 3 种疑源类化石（图 2-5），包括：*Dictyotidium reticulatum*、*Leiosphaeridia microgranifera* 以及 *Reduviasporonites catenulatus*。其中，*Leiosphaeridia microgranifera* 占据绝对优势，在六个样品中百分含量的平均值达 74.3%。

2.3.6 甘溪剖面

甘溪剖面的疑源类属种单一，只在早三叠世的十一个样品中发现了 *Leiosphaeridia minutissima*，且丰度不大（图 2-5）。含疑源类化石的层位几乎都是属于火山灰沉积之后出现的泥岩，且未发现孢粉化石。

2.3.7 东攀剖面

东攀剖面疑源类的物种多样性同样很低，只有 2 种 1 属（图 2-5），包括：*Leiosphaeridia microgranifera* 和 *L. minutissima*。但是，其生物量相对较高，且 *Leiosphaeridia microgranifera* 在 15 个样品中相对百分含量的平均值高达 93%。同时，东攀剖面也发现少量的孢粉化石。

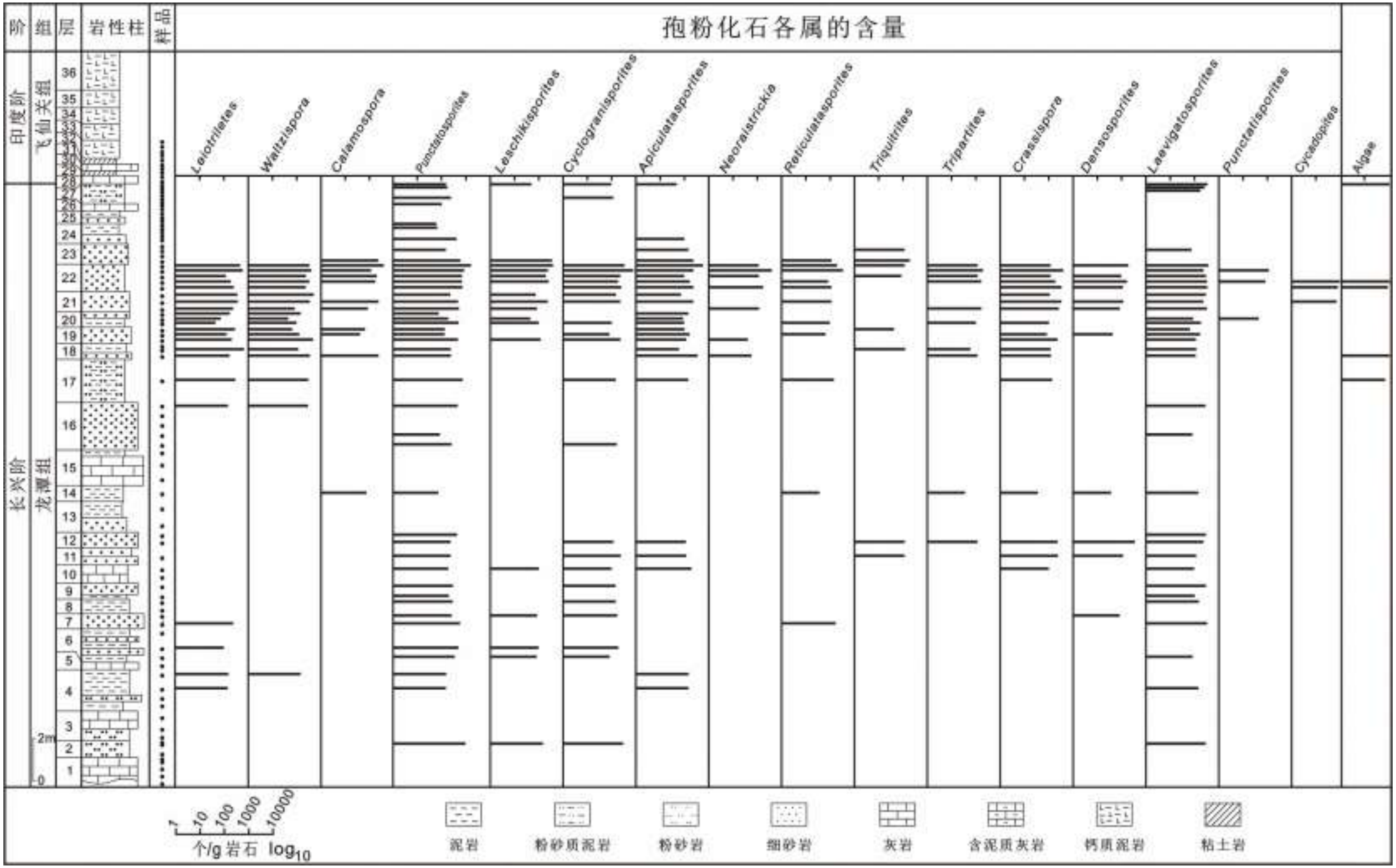

图 2-4 中寨剖面孢粉以及疑源类的丰度

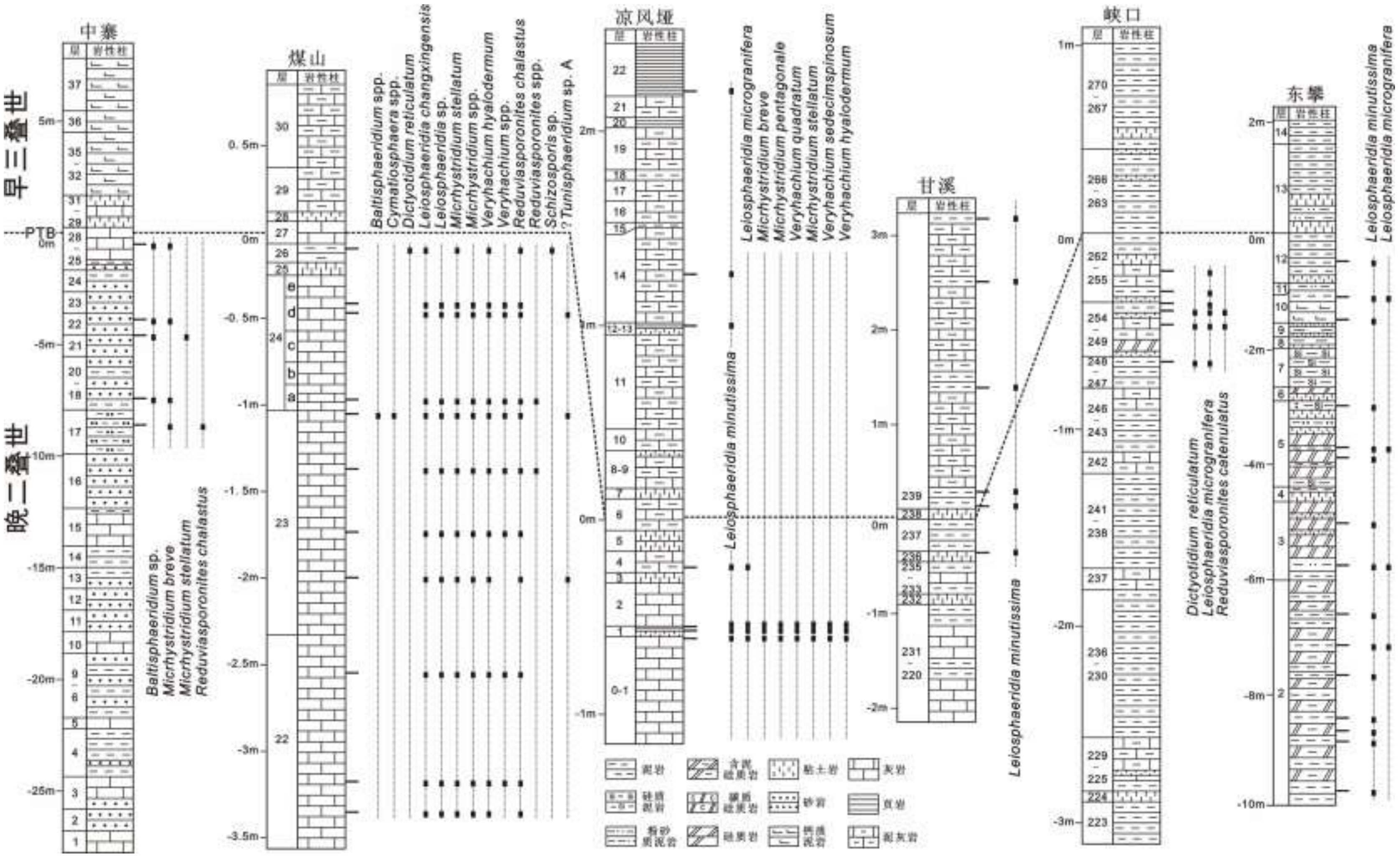

图 2-5 各剖面疑源类化石出现的层位 （PTB 的划分依据见正文）

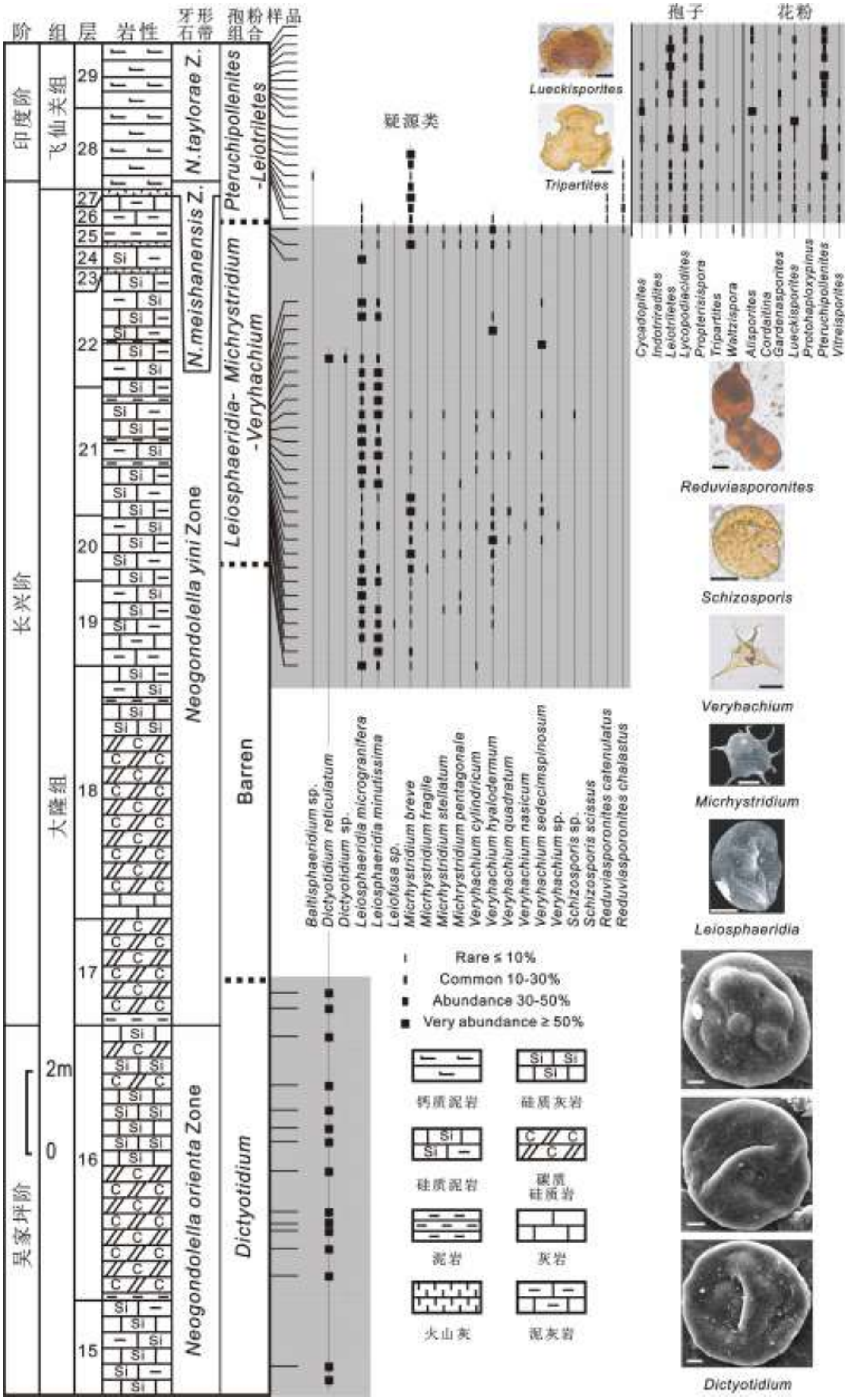

图 2-6 上寺剖面疑源类以及孢粉化石出现的层位和丰度（牙形石生物带来自[188]）

第三章 华南二叠纪与三叠纪之交疑源类生存空间的分布特征

§3.1 疑源类生存空间分布的研究现状

疑源类通常被认为是海洋浮游植物的胞囊，因此常见于海相地层，多产于泥岩和页岩之中，而少量出现在砂岩和灰岩中。非海相的疑源类也偶见于较新的地层之中。对于疑源类的研究，前人的重点都集中在化石的形态学上，很少关注其亲缘关系以及在古环境上的应用。目前讨论得较多的且应用广泛的是疑源类在古海洋中的空间分布研究。利用这些结果，可以反应研究区当时距离海岸的远近以及间接地反应其水体深度。而此类研究多集中在疑源类生物多样性最高的早古生代，其它时代偶见报道。

在前寒武纪，由于疑源类化石贫乏，因此其生态学的研究相对较少。Butterfield and Chandler[195]在研究加拿大 Baffin 岛 Agu Bay 组的浮游植物时，提出：不同的海洋环境（从局限浅海到深海）拥有不同的疑源类组合。（1）在近岸局限浅海的环境，主要以丝状和个体较小的球形疑源类为主，且其生物多样性较低；（2）在近岸开阔的环境中，以丝状和体型较大的疑源类（直径> 50 μm）为主，生物多样性较高；（3）在大陆架中部，海水较深地区（透光带中），以丰富的球形疑源类为主；（4）在外大陆架水体更深的区域（透光带以下），以小型的球形疑源类为主（直径<50 μm），且生物多样性较低；（5）而在大陆坡至洋盆，疑源类的多样性非常低。

在寒武纪和奥陶纪，疑源类的生态学研究变得非常普遍。在撒哈拉板块北部，Vecoli [170]记录了丰富的疑源类化石。同时，他分析了各类疑源类组合所对应的沉积环境。他总结到： leiosphaerid- Netromorphitae- *Veryhachium* 组合一般代表近岸、浅水的环境，且生物多样性较低；而 Polygonium- *Micrhystridium* 组合则可以指示局限的海洋环境。

在涉及到奥陶纪的地层中，有 5 篇文章调查了疑源类的分布规律。在美国 Midcontinent 中-晚奥陶世，Jacobson[168]认为：（1）leiosphaerid 组合代表了近岸浅水的环境；（2）peteinosphaerid- *Dicommopalla* 组合代表浅海环境；而 baltisphaerid- veryhachid- *Polygonium* 则代表开阔海域。在美国印第安纳州的晚奥陶世 Eden 页岩，Colbath[196]鉴别出两个疑源类组合，同时提出一个疑源类丰度变化的模型。在中国南部扬子板块早奥陶世大湾组，Xu[197]报道了一个代表深水海洋环境疑源类组合，其属种包括 *Striatotheca*、*Coryphidium*、*Pirea*、*Acanthodiacrodium*、*Dasydiacrodium* 和 *Arbusculidium filamentosum*。扬子板块中-晚奥陶世，Li et al.（2004b）研究了疑源类从近岸到远岸的分布规律[171]。研究结果显示：（1）从近岸到远岸，疑源类的丰度和多样性波动较大；（2）近岸环境，疑源类生物多样性较低（约有

10 种），而远岸多样性较高（近 40 种）[171]。同一地区，Yan and Li[198]利用聚类分析和主成分分析的方法鉴别出十个不同的疑源类组合，且认为它们由不同的环境因素控制。分析表明：*Stelliferidium* 组合出现在内大陆架地区；*Baltisphaeridium- Leiosphaeridia* 组合、*Baltisphaeridium- Peteinosphaeridium* 组合、*Cymatiogalea* 组合、*Polygonium* 组合以及 *Stelliferidium- Leiosphaeridia* 组合代表外大陆架；*Baltisphaeridium* 组合、*Leiosphaeridia* 组合、*Peteinosphaeridium* 组合以及 *Rhopaliophora* 组合则指示深水的页岩盆地。

在志留纪地层中，有 7 篇文章分析了疑源类的空间分布。Smith and Saunders[199]总结了疑源类的分布与沉积相的关系。他们认为：（1）疑源类大多沉积于连续的开阔海域而很少出现在河流沉积物中；（2）实体化石保存的完整程度可以反映其沉积环境：化石保存完好，说明其沉积于开阔的深水区域，而如果化石多为碎片，则其沉积在近岸；（3）疑源类的分布直接受到洋流的控制。在威尔士地区，有四篇文章对疑源类的分布规律做了详尽的研究[169, 200-202]。Dorning[169]识别出三个疑源类组合：分别可以指示近岸，远岸和深水。近岸组合中疑源类多样性较低，通常包括 5-15 种；远岸大陆架的组合中，其多样性最高，达 25-60 种；而深水组合与近岸组合类似，多样性很低，为 2-15 种。紧接着，Dorning [200]和 Dorning and Bell[201]又鉴别出四个疑源类组合，包括：*Leiosphaeridia wenlockia* 组合、*Leiofusa tumida* 组合、*Micrhystridium intonsurans* 组合以及 *Salopidium granuliferum* 组合。它们分别出现在礁灰岩相，近大陆架，远大陆架开阔海洋以及大陆架深水区域[200, 201]。而 Richardson and Rasul[202]认为，疑源类与牙形石化石的组合可以指示海相沉积。同时，sporomorphs、micrhystrids 和 tasmanitids 则出现在近岸环境中。在利比亚 Rhadames 盆地，Al-Ameri[203]认为 tasmanitids 和 *Veryhachium lairdi* 可以指示泻湖环境。在瑞典哥特兰岛 Ludlow 地区的志留纪地层中，Stricanne et al.（2004）通过三个不同的生态学类别，定性和定量地分析了疑源类的近岸-远岸分布规律[172]。其中，在大陆架上，具刺疑源类丰富，而球形疑源类减少。在属一级水平上，*Micrhystridium* 和 *Dilatisphaera* 更多的出现在近岸环境，而 *Evittia*、*Percultisphaera* 和 *Oppilatala* 则出现在远岸。同时，*Micrhystridium* 里具长刺或者刺较为复杂的类型通常出现在大陆架上[172]。

有三篇文章调查了泥盆纪疑源类的生态分布情况。在加拿大 Alberta 地区，Staplin[204]认为疑源类的丰度与距生物礁的距离有关。球形疑源类的分布较为广泛；具薄刺的类型则一般繁盛于生物礁附近；而具厚刺或者壳体为多面体的类型通常只分布在远离生物礁的区域[204]。在德国西部地区晚泥盆世，Riegel[205]报道称疑源类在近岸浅海相对贫乏，而在远洋较为繁盛。在美国爱荷华州 Rapid 群 Cedar Valley 组，Wicander and Wood[206]分析了孢粉型化石中疑源类与孢粉的比例。结果显示，疑源类与孢粉的相对丰度反映了近岸-远岸的变化，高丰度的疑源类组合通常指示海相且远岸的沉积环境[206]。

古生代以后的地层中，由于疑源类的多样性急剧下降，其生态学的研究也相对减少。在英格兰和南威尔士地区的侏罗纪地层中，Wall[207]认为疑源类的分布由环境控制：在封闭的近岸环境中，具刺疑源类繁盛（富含 *Micrhystridium* 和 *Baltisphaeridium*）；而在开阔的大洋环境里，以 *Veryhachium*、*Leiofusa*、*Metaleiofusa* 和 *Domasia* 为主。

以上的研究表明：（1）与现代大洋浮游藻类的分布特征类似，疑源类在近岸浅水环境中生物多样性较低，而在相对较为远岸的大陆架地区其生物多样性则非常高。但是不同时代的

地层中，即使处于同一古环境位置，疑源类的生物多样性也有很大的差别。（2）具较短突起的或者球形疑源类常出现于近岸环境；而具较长突起的类型则通常出现于远岸地区。这些研究结果大都是基于疑源类丰富的早古生代，而本文则将在晚二叠世地层中继续开展类似的研究，从而探求疑源类在海洋中的空间分布特征。

§3.2 华南二叠纪-三叠纪之交疑源类的近岸-远岸分布特征

现代海洋中藻类（如：沟鞭藻、硅藻以及颗石藻等）的分布与海水的一系列参数有关，如水温、透光带的光照强度、ph值、营养盐的浓度、盐度以及氧气含量等[208-211]。与之类似，疑源类在古海洋中的分布也应当与这些条件的变化有关[171, 212]。但是，现在还很难在老地层中还原这些参数。因此，疑源类的生态学研究也相对落后。从上一节的资料可见，已有较多的文献在研究早古生代疑源类的空间分布状况。但是，由于之前的一些学者认为疑源类生物多样性在晚古生代较低（特别是石炭纪和二叠纪），以致很少有人关注这一时期疑源类的古生态学信息。本章将利用在华南地区晚二叠世得到的疑源类数据来恢复疑源类在海洋中的分布情况。

本章选取晚二叠世疑源类较为丰富的6个研究剖面，包括：中寨、煤山、上寺、凉风垭、峡口以及东攀剖面。中寨剖面位于扬子板块西部，为海陆交互相沉积[177-179]。煤山剖面位于扬子板块东缘，其岩相为近大陆架台地[180]。上寺剖面处于扬子板块北缘，自吴家坪期开始，由斜坡相逐渐转变为深水盆地相[186]。同煤山剖面一样，上寺剖面在晚二叠世末期至早三叠世发现大量的孢粉化石。因此，这两个剖面受到陆源影响较大，离陆地较近。凉风垭剖面也处于扬子板块北部，为浅水开阔台地沉积（夏文臣，个人交流）。峡口剖面位于扬子板块中部，处于开阔地台的大陆架远端[189, 190]。凉风垭与峡口剖面均未发现孢粉化石，因此，认为它们距离陆地较远。而位于扬子板块南部的东攀剖面则处于大陆坡至盆地相，其临近康滇古陆，受陆源影响较大，样品中也发现较多的孢粉化石[10, 193]。为了便于讨论，基于岩相的变化以及距离陆地的远近，我们将六个剖面做如下处理（图3-1）。而以下将从属和种两个级别来分别探讨疑源类生物多样性的近岸-远岸分布规律。

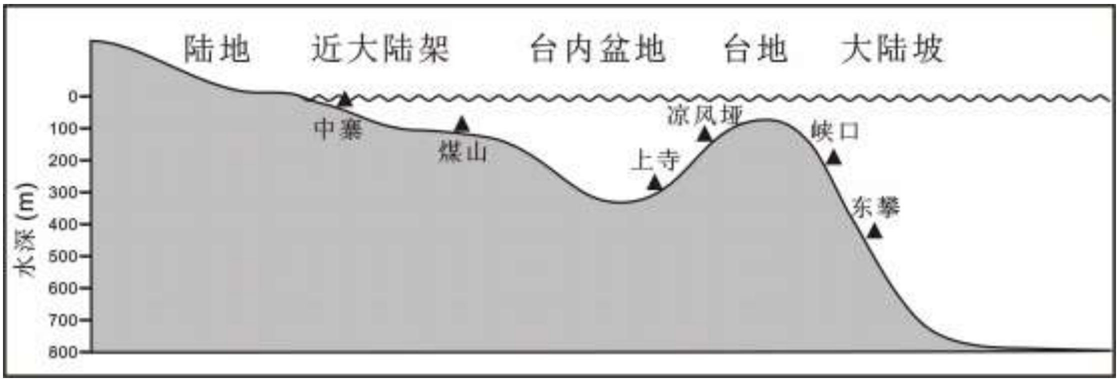

图3-1 二叠纪-三叠纪之交各剖面的沉积相

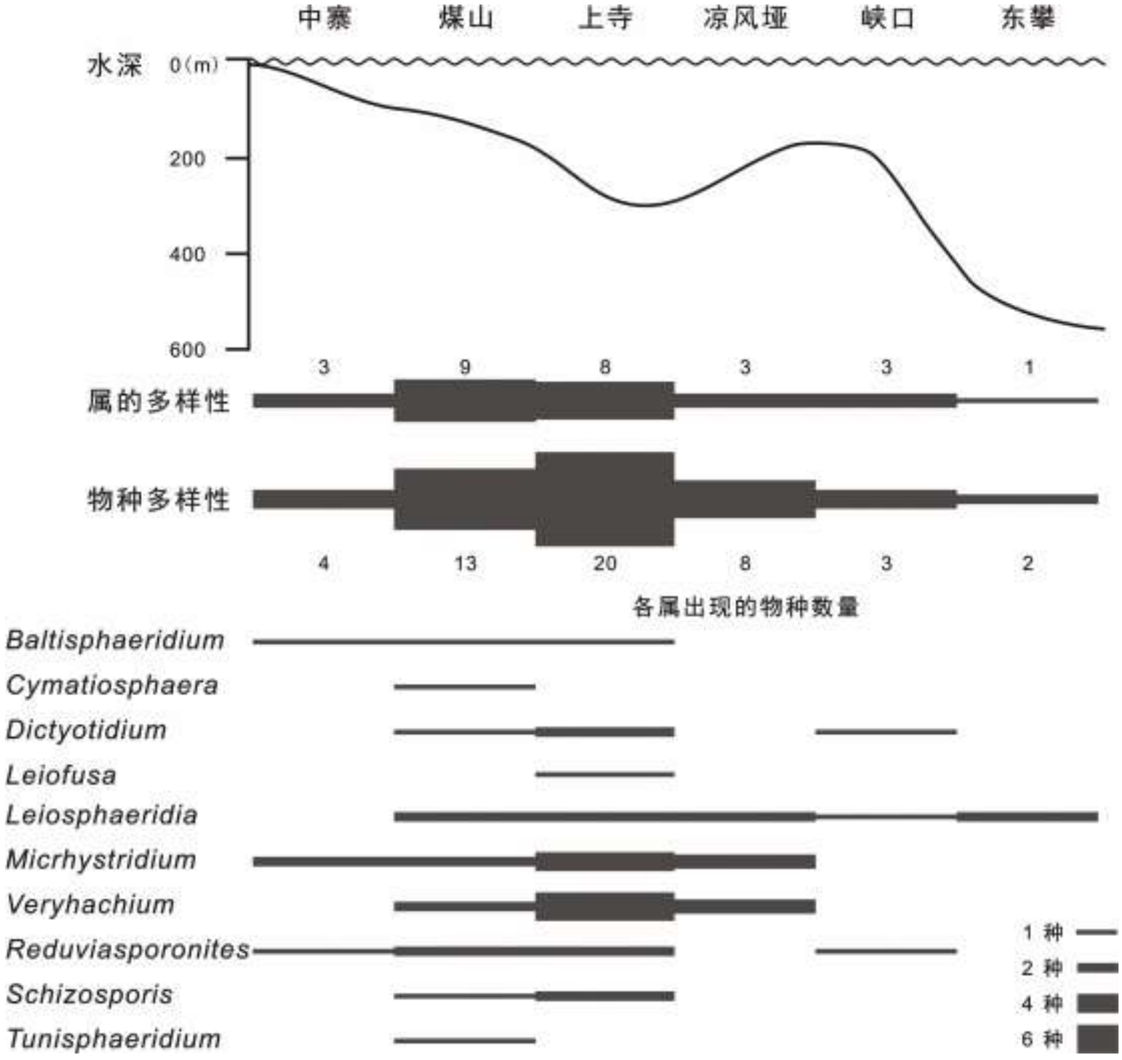

图3-2 疑源类各属在研究区的分布情况

3.2.1 疑源类属一级的近岸-远岸分布特征

如图 3-2 所示，离陆地最近的剖面（中寨和东攀）的疑源类物种多样性最低。一般只有 2-4 种，隶属于 4 个疑源类化石属。但是，距离陆地相对较远的剖面（煤山和上寺剖面）疑源类物种多样性非常高。其中，上寺剖面的疑源类达到了 8 属 20 种。然而，随着与陆地距离的进一步拉大，凉风垭以及峡口剖面的疑源类物种多样性反而逐步降低。凉风垭剖面共发现疑源类 8 种，而峡口只有 3 种。

本文的结果重现了早古生代疑源类的分布特征[169-171, 195, 205, 206]，即：疑源类多样性符合近岸-远岸的分布规律。近岸地区，疑源类多样性低，而相对远岸的大陆架地区其多样性较高。然而在大陆坡以及深海盆地附近，随着与陆地距离的拉大，疑源类多样性是逐步降低的。

值得注意的是，Dorning [169]以及 Li et al.（2004b）[171]在研究早古生代的地层时发现，

疑源类在远岸地区可以达到 25 至 60 种之多，即使在近岸地区也仍有十余种。而晚二叠世的地层中，处于远岸区域的上寺剖面也只有 20 种疑源类被发现。但是，在绪论中已经分析到，疑源类在地史时期的分布是不均匀的。早古生代是疑源类生物多样性的顶峰时期，奥陶纪有报道的疑源类就高达 400 余种[51]，而二叠纪的疑源类至今也只有 200 余种被发现（见绪论）。因此，笔者认为，疑源类生物多样性的背景值是造成疑源类物种多样性在不同时代、同一类型的沉积相中差别较大的原因。

在疑源类的属一级别，一些属的出现较为偶然，如 *Cymatiosphaera*、*Leiofusa* 以及?*Tunisphaeridium* 仅在一个剖面被发现。而另一些属（如 *Leiosphaeridia*、*Reduviasporonites* 和 *Micrhystridium*）却是常见的种类，从近岸的浅水环境到大陆坡等深水地区都有发现（图 3-2）。还有一些属（如 *Dictyotidium* 和 *Veryhachium*）基本只在远岸较深水的环境中出现，指示开阔的海域；而 *Schizosporis* 则只在上寺和煤山剖面的二叠纪与三叠纪之交的地层附近出现（海平面较低时），可能指示一种相对近岸浅水的环境。

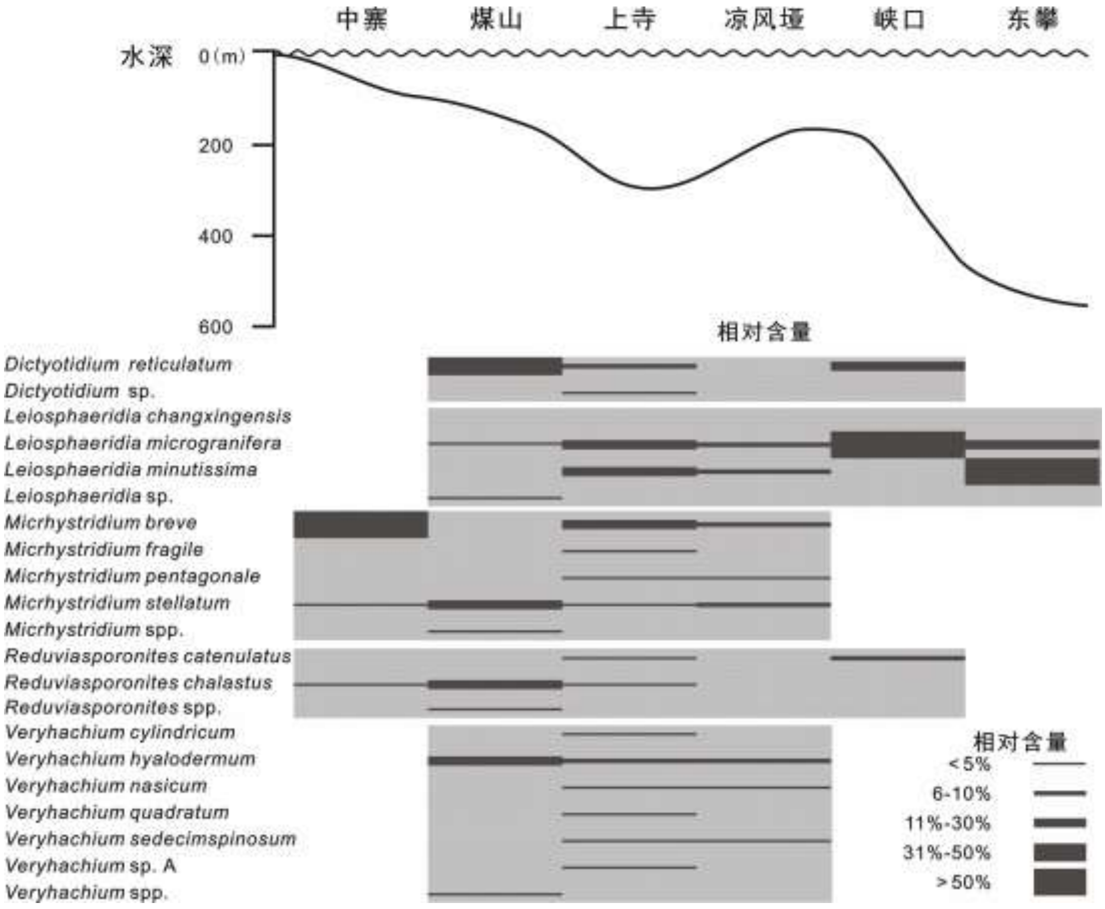

图 3-3 疑源类的主要物种在研究区的分布特征

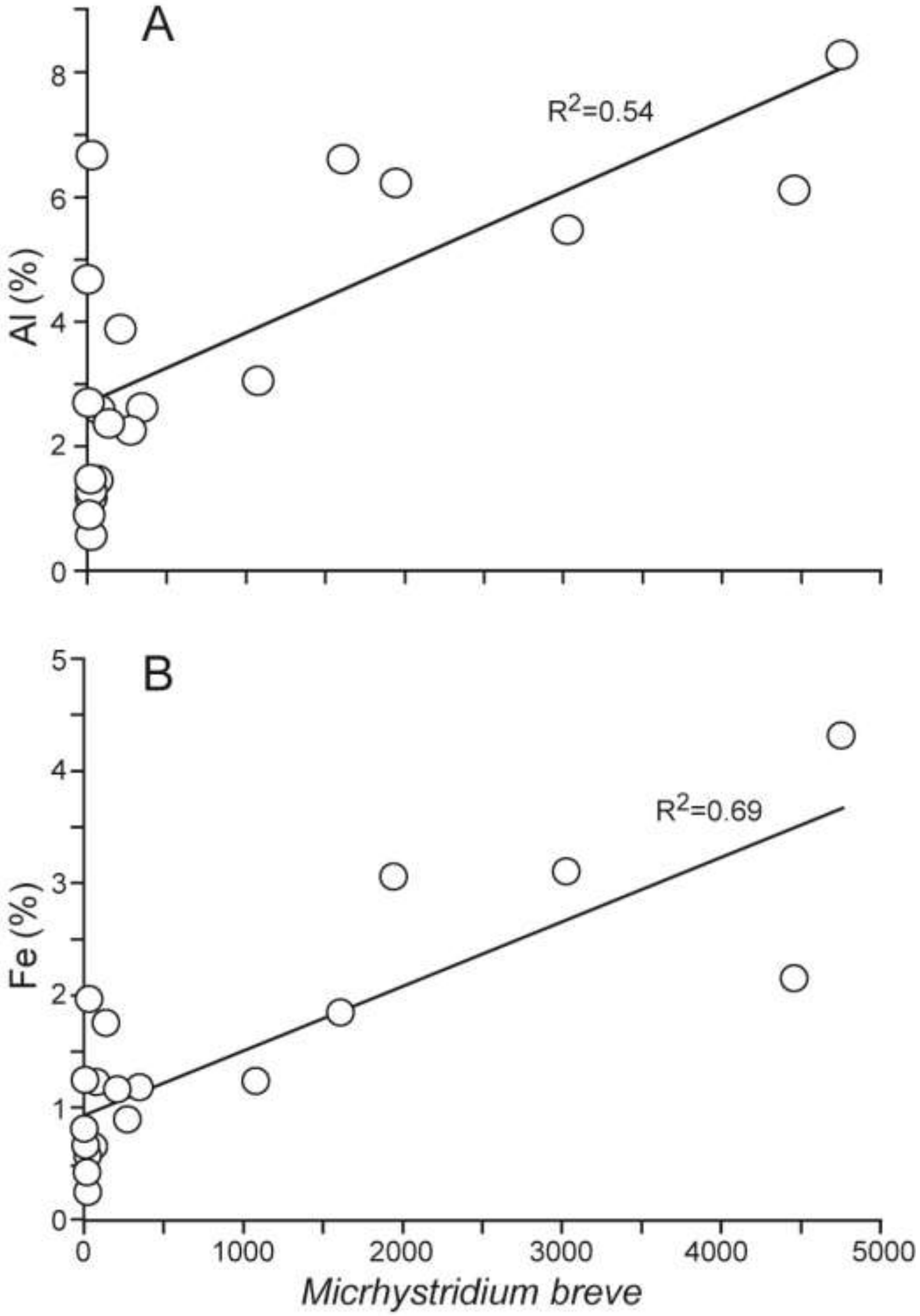

图 3-4 疑源类 *Micrhystridium breve* 的丰度与 Al、Fe 元素含量的相关性比较

3.2.2 疑源类种一级的近岸-远岸分布特征

3.2.2.1 具刺疑源类

在二叠纪的地层中，小型的具刺疑源类（*Micrhystridium*和*Veryhachium*）是被报道得最多的疑源类属（见第一章）。而本文的研究中，共计十种疑源类归为这两个属，超过发现的所有疑源类种类的三分之一。值得注意的是，在中寨剖面以及上寺剖面的PTB附近地层中，具较短突起（一般2~4微米）的*Micrhystridium breve*在近岸、局限的环境中占据巨大优势（图3-3）。而具较长突起（5微米及以上）的*Micrhystridium*和*Veryhachium*则大多出现在更为远岸的开阔海域。如*Micrhystridium stellatum*和*Veryhachium hyalodermum*在上寺、煤山以及凉风垭剖面都较为丰富。而类似的现象在早古生代的地层中也有发现[168, 170-172, 200, 202, 203, 207]，特别是Stricanne et al.（2004）在Gotland的志留纪地层中同样观察到具短突起与长突起的*Micrhystridium*的相对丰度随近岸-远岸的变化规律[172]。Servais et al.（2004）在其它一些疑源类属种的形态学研究中也注意到类似的现象[54]。而现生沟鞭藻的研究中，Mertens et al.（2009）则将此类现象与海水的盐度以及温度的变化相联系[213]。然而，上寺剖面二叠纪末期具短突起疑源类的繁盛却与营养盐的大量输入有关。

在二叠纪末期，华南多个剖面出现多期火山灰的沉积[29]。经证实，这些火山灰大都来自于西伯利亚火山的喷发[30-32]。而随着海平面的降低，陆源物质（如Al、Fe）同火山灰带来的营养盐（如Fe，N，P等）大量地涌入海洋中[214, 215]。这些含有大量营养盐的陆源碎屑会极大地促进浮游植物的生长，同时，也可能促进蓝细菌的爆发（将在下一章中详述）。而这种促进作用在上寺剖面表现得尤为显著。如图3-4所示，*Micrhystridium breve*与Al和Fe含量的线性相关性（R^2）都在0.5以上，呈现较强的线性相关。特别是在二叠纪与三叠纪之交的25层至28层，*Micrhystridium breve*与Fe元素含量的变化保持一致。在此阶段，由于海平面的下降，上寺剖面已经距离陆地较近[186]。25层中已经发现一些孢粉化石，而28层以后，几乎都是以孢粉化石占主导地位（图2-6）。因此，在25层至28层，由于环境的剧烈变化，上寺剖面的疑源类群落由之前的具长突起以及球形疑源类为主的类群逐渐转变为以具短突起的*Micrhystridium breve*为主的群落。在此适宜的条件下，*Micrhystridium breve*的生物量随着大量营养盐的涌入而迅速增加。

3.2.2.2 球形疑源类

Dorning[169]在研究志留纪的疑源类时指出，球形疑源类更多地出现在近岸或者盆地相的环境中。在前寒武纪地层的研究中，Butterfield and Chandler[195]认为具小型膜壳的球形疑源类一般出现在近岸或者外大陆架地区，而具较大且无纹饰膜壳的球形疑源类则多出现于大陆架中部。Yan and Li[198]在调查了华南中-晚奥陶世的疑源类之后发现，球形疑源类*Leiosphaeridia*组合一般出现在深水环境的盆地页岩相。

在本文中，*Leiosphaeridia*更多地出现在开阔的海域，如处于远大陆架、大陆坡或者盆地相的上寺、峡口以及东攀剖面。从物种级别分析，膜壳表面具颗粒纹饰的*Leiosphaeridia microgranifera*一般发现于远岸的环境中，如峡口和上寺剖面；而膜壳表面光滑的

*Leiosphaeridia minutissima*则在受陆源影响较大的东攀剖面占据绝对优势。

具大型膜壳的另外一种球形疑源类*Dictyotidium reticulatum*（通常膜壳的直径在80微米以上且一般被认为是一种绿藻）在上寺剖面的吴家坪期、长兴期的22层、煤山剖面的26层以及峡口剖面PTB的附近层位都大量出现（图2-5和3-3）。而这些层位都是海平面较低的时期，因此，此种疑源类可能指示一种浅水的环境。

3.2.2.3 链状疑源类

被大量学者争论的链状疑源类*Reduviasporonites*在扬子板块的二叠纪末期也有发现。尽管其生物亲缘关系现在还没有统一的看法，但是随着在全球各地的相继报道，其无疑也是二叠纪末期一类重要的疑源类类型。*Reduviasporonites*在此前的报道中一般都是出现在近岸、靠近陆相的区域，如以色列的Yamin组[64]，意大利阿尔卑斯山南部的Tesero剖面[66]，以及南非的Karoo超群[65]等。其峰值（*Reduviasporonites*的含量占据孢粉型化石总量的90%以上）一般认为是在PTB以上1-3米的位置[64]，其它层位也有少量出现。而本文所调查的剖面除中寨剖面处于海陆交互相之外，其余剖面都是典型的海相沉积。虽然*Reduviasporonites*在中寨、煤山、上寺以及峡口剖面的样品中都有出现，但是其百分含量却很低，远远不及“真菌高峰”的百分比（图3-3）。含量最高的为14%，位于上寺剖面的28层，二叠纪与三叠纪之交过渡层中。物种级别上看，个体较大的*Reduviasporonites chalastus*（单个膜壳的长度为40微米左右，宽度在20微米左右）常分布在近岸的环境中，如中寨和煤山剖面；而个体较小的*Reduviasporonites catenulatus*（单个膜壳的长度为10~20微米，宽度约10微米）则更多地出现在远岸深水的区域，如上寺和峡口剖面（图3-3）。

§3.3 本章小结

本章研究的6条二叠纪与三叠纪之交的剖面囊括了海陆交互相、近大陆架、远大陆架以及大陆坡等沉积相。通过对扬子板块的6条剖面的疑源类定性和定量的分析发现，疑源类的属和物种的多样性都符合近岸-远岸的分布规律（图3-5）。并初步得到以下结论：

1）扬子板块二叠纪末期，近岸地区的疑源类物种多样性较低，一般只有2-4种；而远岸的物种多样性较高，可以达到10-20种左右。

2）从疑源类属一级来看，*Leiosphaeridia*、*Reduviasporonites*和*Micrhystridium*从近岸浅水环境到远岸深水地区均有分布；*Dictyotidium*和*Veryhachium*更多地出现于开阔的海域；而*Schizosporis*则只在上寺25层和煤山剖面的26层出现（海平面较低时），可能指示一种相对近岸浅水的环境。

3）在种一级别，具短突起的*Micrhystridium breve*在近岸环境中占据绝对优势，且对营养盐的浓度较为敏感，其生物量的变化与Fe元素的含量变化较为一致。而具较长突起的其它种类的*Micrhystridium*以及*Veryhachium*（如*Micrhystridium stellatum*和*Veryhachium hyalodermum*）则较多地出现在远岸环境中。

4）膜壳较大（直径约80微米）的球形疑源类如*Dictyotidium reticulatum*一般出现在浅

水区域，而膜壳较小（直径约 30 微米）的 *Leiosphaeridia* 则更多地分布在水体较深的环境中。同时，膜壳光滑的 *Leiosphaeridia minutissima* 在近岸占据优势，而膜壳具颗粒纹饰的 *Leiosphaeridia micrograniferа* 则在远岸较为丰富。

5）虽然链状疑源类 *Reduviasporonites* 出现在多个剖面，但是众多学者认为的二叠纪末期的“真菌高峰”在扬子板块的海相地层中并没有出现。需要指出的是，个体较大的 *Reduviasporonites chalastus* 常分布于近岸环境；而个体较小的 *Reduviasporonites catenulatus* 则更多地出现在远岸深水的区域。

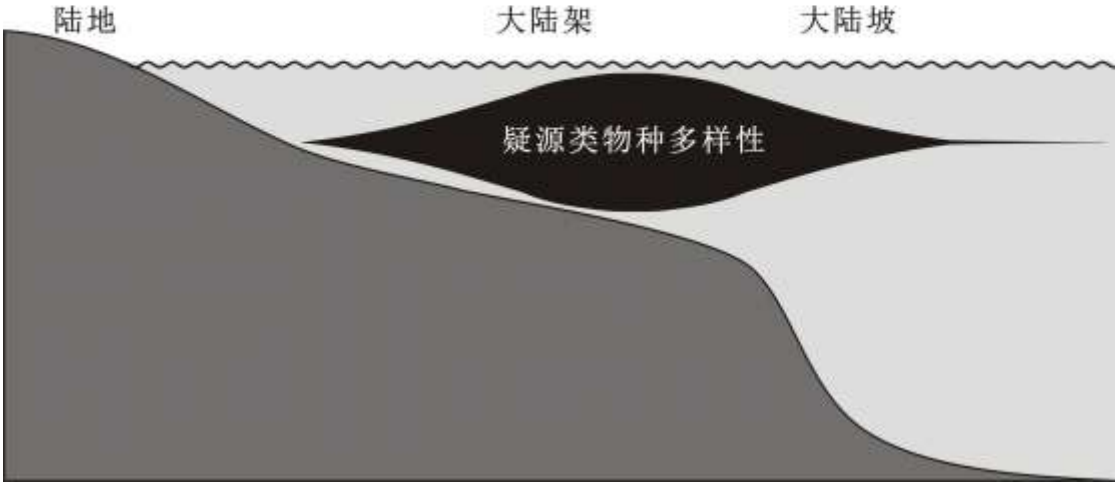

图 3-5 疑源类近岸-远岸的分布规律示意图

第四章 华南二叠纪与三叠纪之交浮游植物群落的演替及其对生态系统的影响

§4.1 蓝细菌爆发对现代海洋生态系统的影响

蓝细菌生存在地球上已经超过 35 亿年[216]，同时也是现代大洋中最为常见的光合固氮菌之一[217, 218]。然而，蓝细菌的间歇性爆发却给淡水生态系统以及海洋生态系统带来了巨大的生态危机[218, 219]。例如，近年来巢湖夏季频频爆发的蓝藻水华使昔日的饮用水水源遭到重度污染[220]，而自从 20 世纪以来，几乎每年夏天波罗的海都会出现蓝藻爆发，给当地的生态环境以及社会经济造成了巨大的损害[221]。

由于多数蓝细菌都具有漂浮能力，因此它们可以在不同的水深环境中迅速繁殖[219, 222]。而蓝细菌的持续性爆发会加快海洋透光带中光衰减的速度[223, 224]，进而造成其它需要进行光合作用的初级生产者（如：硅藻和海草等）以及珊瑚等的生物量急剧降低[225, 226]。

对于海洋中的动物而言，一些蓝细菌会产生大量的毒素。根据不同的作用部位，这些毒素可以划分为：肝毒素（微囊藻素、节球藻素和拟柱饱藻毒素），神经毒素（类毒素和蛤蚌毒素）以及一些皮肤毒素等[219]。而这些毒素都是蓝细菌产生的次级代谢产物，对蓝细菌自身无害，却会增加浮游动物的死亡率或者使浮游动物失去繁殖能力等[227-229]。更为严重的是，这些毒素都是生物毒素，可以通过食物链传递，从而威胁到更高营养级的海洋动物（如鱼类）甚至是水鸟等[218, 228-230]。

另一方面，即使不产生毒素，蓝细菌的爆发也会对生态系统造成极大的破坏。在蓝细菌爆发期间，由于其通常在海洋表层大量繁殖且具有漂浮能力，因此只有极少量的蓝细菌被动物摄食以及沉积到大洋底部。然而，蓝细菌在死亡之后，其残体从海水表层即开始分解，消耗掉大量的氧气，致使海水中的溶解氧急剧减少，从而严重威胁到鱼类以及其它动物的生存[231-234]。

但是，蓝细菌在海洋中的爆发也需要多方面的条件。首先是需要大量的营养元素（如磷和铁等）[235, 236]，其次是需要较高的温度和较为封闭的环境[226, 237, 238]。只有在以上条件都达到的前提下，蓝细菌才会迅速繁殖。因此，多数的蓝细菌爆发事件都集中在夏季，且常出现在半封闭的海湾环境中。

§4.2 华南二叠纪与三叠纪之交浮游植物群落的演化及其对海洋生态系统的影响

4.2.1 华南二叠纪与三叠纪之交海洋蓝细菌的爆发及其诱因

在现代大洋中，两类丝状蓝细菌（*Lyngbya* 和 *Trichodesmium*）和一类球形蓝细菌（*Synechococcus*）是造成蓝细菌爆发的主要元凶[226]。*Lyngbya* 一般固着在海草、珊瑚或者大型海藻等底栖生物表面。但在平静的海洋环境中，它也能利用其漂浮能力在海洋表面迅速增殖[226]。*Trichodesmium* 是一类缺乏异形胞的蓝细菌，主要出现在营养盐较为缺乏的热带以及亚热带远洋环境中，但是在陆源输入较大的近岸环境容易形成水华[226]。丝状蓝细菌是主要的光合固氮蓝细菌，它们利用自身的漂浮能力，能够利用海洋表层的营养盐并进行光合作用，从而迅速繁殖[219, 222]。它们的限制性营养元素均为铁和磷，其适宜温度一般为 20° 至 30°[226]。相对而言，球形蓝细菌 *Synechococcus* 则常出现在更为开阔的海域中[239]。其形成的蓝藻水华面积经常达到 100 平方公里以上，而且能够持续数月之久[223, 224]。同时，*Synechococcus* 可以在超过 30° 的海水中生长[240]，而磷是其最主要的限制性营养元素。

与之类似，在二叠纪与三叠纪之交的钙质微生物岩地层中，通常也会发现丝状蓝细菌（*Renalcis* 或者 *Epiphyton* 以及 *Rivularia*）和球形蓝细菌两类化石[241-243]。含这两类蓝细菌化石的钙质微生物岩在华南二叠纪末的生物大灭绝之后迅速增加[38]。而 Kershaw et al.（2007）认为，微生物岩在早三叠世的古特地斯洋有着广泛的分布（图 4-1）[244]。同时，在煤山和上寺剖面，蓝细菌的生物标志化合物（二甲基霍烷）的丰度在二叠纪末期的生物大灭绝之后也出现两个明显的峰值[38, 245]。由此可以证实，二叠纪与三叠纪之交的海洋中的确出现了蓝细菌爆发的事件。

Joachimski et al.（2012）测试了煤山和上寺剖面牙形石化石的氧同位素，利用这些数据，他们估算了当时海水的温度，其结论认为这两个剖面在二叠纪末期的大灭绝之后，海水温度升高，从 25° 迅速上升至 30° 左右（图 4-2）[246]。同时，由于大范围的火山爆发以及陆源风化的加强，大量的营养盐（含 Fe、P 元素）由陆地源源不断地输送到海洋中[214, 215, 246]。从上述分析可知，种种适宜的环境条件导致了蓝细菌在二叠纪末期的生物大灭绝之后迅速爆发。

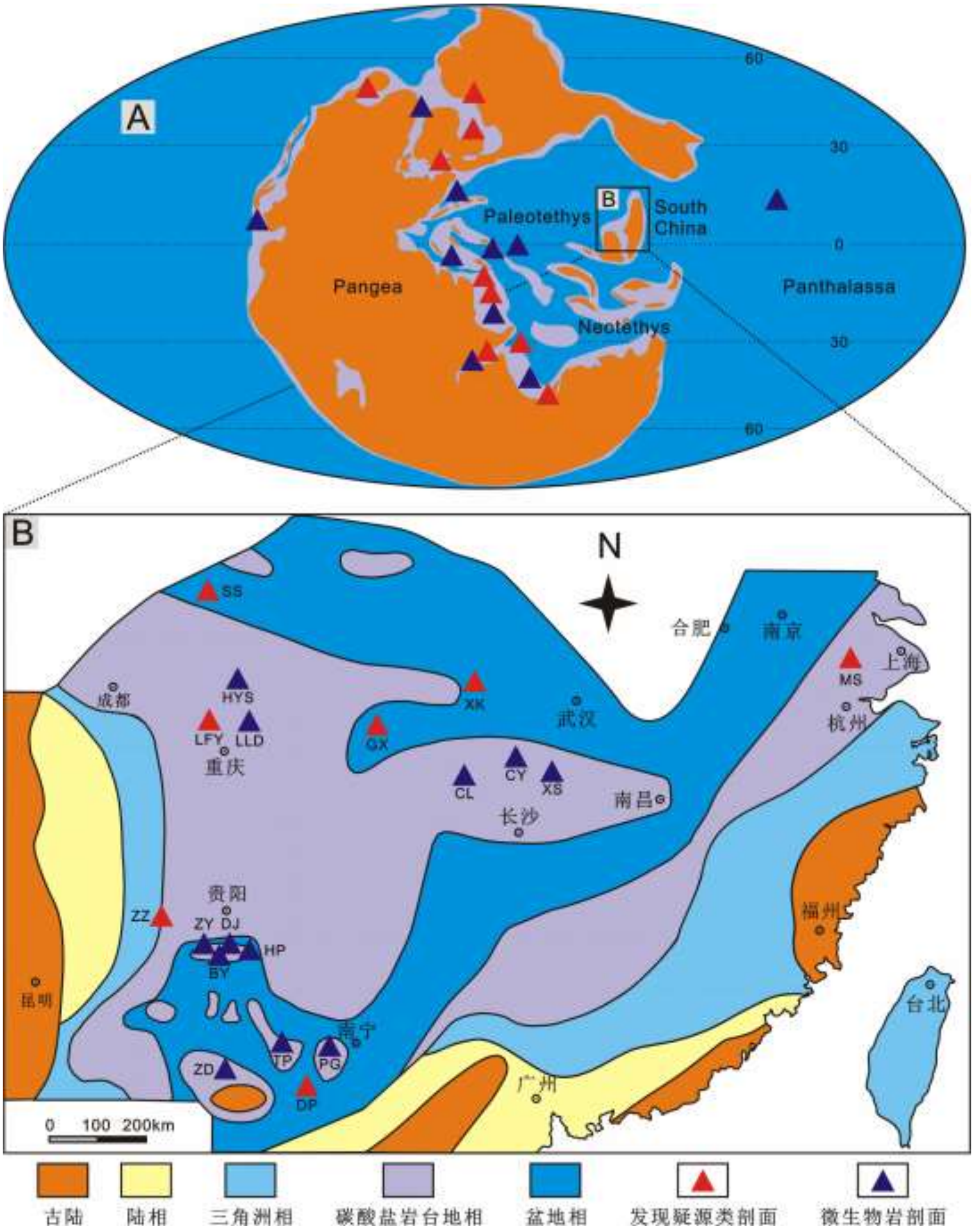

图 4-1 二叠纪-三叠纪之交疑源类与蓝细菌的分布图

A：古地理图改自[173]，微生物岩数据来自[244]；

B：古地理图改自[183]，微生物岩数据来自[38]。

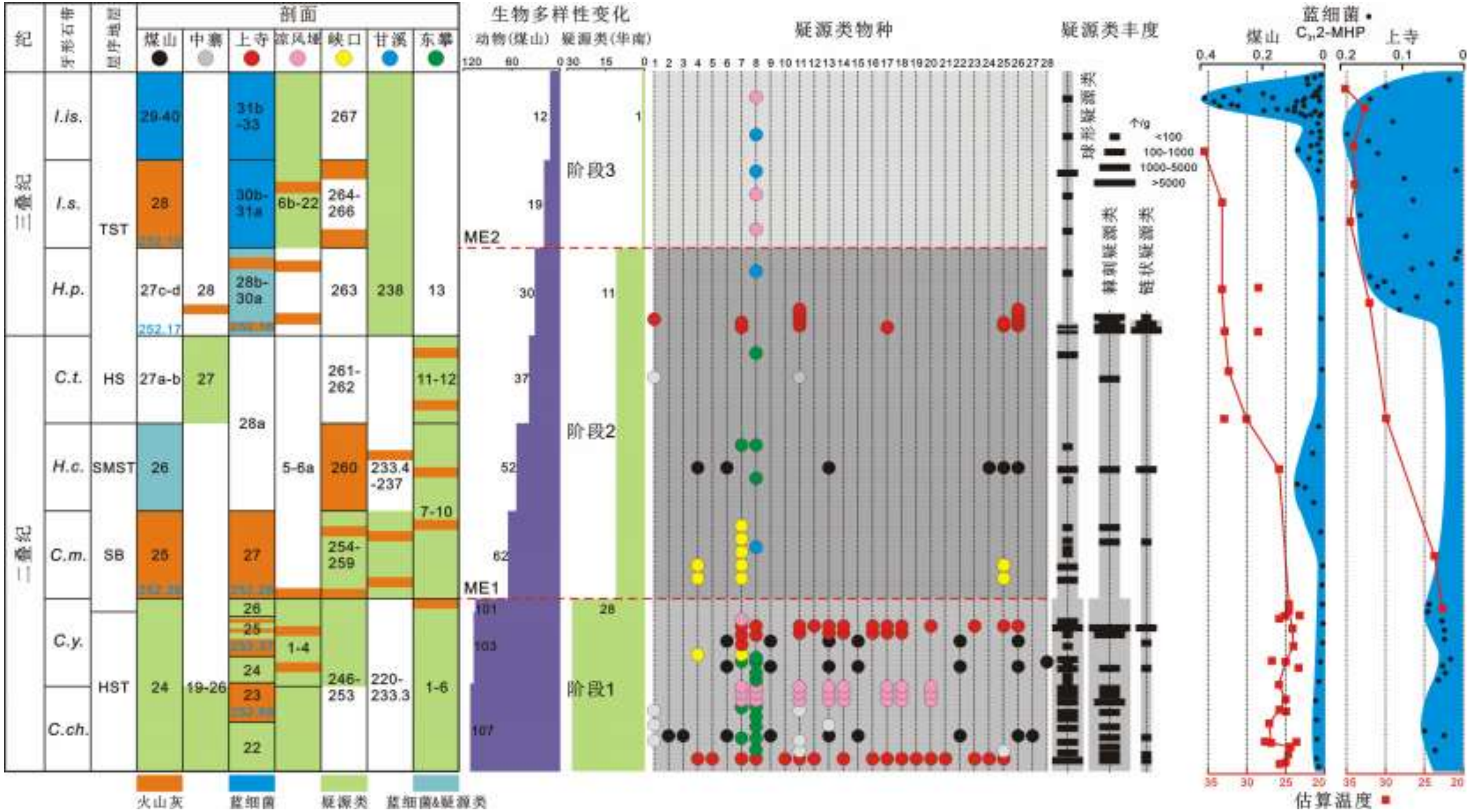

图 4-2 华南二叠纪-三叠纪之交浮游植物与后生动物化石生物多样性对比

ME: mass extinction. *I. is.*: *Isarcicella isarcica*; *I. s.*: *I. staeschei*; *H. p.*: *Hindeodus parvus*; *H. c.*: *H. changxingensis*; *C. t.*: *Clarkina taylorae*; *C. m.*: *C. meishanensis*; *C.y.*: *C. yini*; *C. ch.*: *C. changxingensis*. 各剖面地层划分见正文；牙形石带以及层序地层资料来自[247]；动物化石多样性来自[8]；煤山剖面蓝细菌资料来自[247]；上寺剖面蓝细菌来自（谢树成，个人交流）；海水温度来自[246]。

4.2.2 华南二叠纪与三叠纪之交疑源类的变化及原因分析

与之相反，从二叠纪末至早三叠世，疑源类的生物多样性和丰度在华南地区却出现了明显的降低（图 4-2）。如图 4-2 所示，笔者将二叠纪与三叠纪之交的这段地层按照煤山剖面的牙形石生物带来构建，并未依据地层的实际厚度。图中，动物化石生物多样性的数据来自煤山剖面[8]，而疑源类的数据则来自华南地区的七个剖面。动物与疑源类化石的生物多样性变化较为一致，可以划分为较为明显的三个阶段（图 4-2）。阶段 1 对应的牙形石生物带为 *Clarkina changxingensis* 带以及 *Clarkina yini* 带，此阶段疑源类化石的生物多样性是最高的，发现疑源类达 10 属 28 种。与第一阶段相比，阶段 2 的疑源类化石生物多样性出现大幅降低，只出现 7 属 11 种。其对应的牙形石生物带为 *Clarkina meishanensis* 带、*Hindeodus changxingensis* 带、*Clarkina taylorae* 带以及 *Hindeodus parvus* 带。而最后一个阶段对应 *Isarcicella staeschei* 带和 *Isarcicella isarcica* 带，只有一种疑源类化石 *Leiosphaeridia minutissima* 零星地出现在凉风垭剖面和甘溪剖面。

本文第三章分析了疑源类的近岸-远岸分布规律，认为疑源类在远岸的环境中的生物多样性一般高于近岸环境[171]。而在长兴阶末期，华南出现一期较大幅度的海退事件，造成阶段 2 初期的海平面低于阶段 1。因此，阶段 1 末期（煤山剖面 24 层顶部）疑源类生物多样性降低的因素极有可能是海平面的下降。正常情况下，在阶段 2 至阶段 3 期间，疑源类的生物多样性将随着海平面的回升而增加。然而，实际情况却大相径庭，疑源类的多样性仍然是降低的。因此，必定还有其它重要原因导致了这个结果。

如图 4-2 所示，从阶段 1 至阶段 3，疑源类的丰度大体上是降低的。但是，疑源类在上寺剖面的 28 层和煤山剖面的 26 层（阶段 2）尽管属种较少，其生物量却很高。值得注意的是，疑源类在火山灰之后的深色页岩或者泥岩中尤其富集，其生物多样性与生物量都较其它层位高，如煤山剖面 26 层，上寺剖面 25 层和 28 层以及凉风垭剖面的 1 层。其原因为，在火山喷发之后，大量的营养盐（如 Fe、N、P 等）沉降到海水中[215, 248, 249]，而这些营养元素正是海洋中浮游植物生长的限制性元素，由此造成浮游植物的大量繁殖[250-252]。然而，这种对疑源类的促进作用在阶段 3 的类似环境中却未能得到体现，如在上寺剖面的第 30 层以及煤山剖面的 29 层均未发现疑源类化石。但是，其促进作用并不是没有体现，而是作用的主体发生了改变。由图 4-2 可知，蓝细菌的繁盛正是始于以上两个层位，而下一节将分析其中的具体原因。另一方面，具有较大争议的链状疑源类的丰度在华南是比较低的（不超过 14%），远远达不到“真菌高峰”（90%以上）的程度[64-68, 153, 156]。因此，“真菌高峰”在华南二叠纪末期并没有出现。

4.2.3 华南二叠纪-三叠纪之交浮游植物群落演化对生态系统的影响

在二叠纪末期的生物大灭绝之前，动物和疑源类都具有非常高的生物多样性和丰度（图 4-2 和 4-3）[8]。然而，随着大规模的火山喷发以及海洋缺氧事件的发生，海洋中动物的生物多样性急剧降低[19, 31-33, 253]。与此同时，由蓝细菌主导的钙质微生物岩却大面积地出现在浅

海水域中[38]。而在这些钙质微生物岩中往往只能发现极少量的动物化石，如双壳类、介形虫以及个体较小的腹足类等[241, 242]。

Sun et al.（2012）测试了早三叠世牙形石的氧同位素，并估算了当时海水中的温度[176]。其分析认为，早三叠世 Smithian 晚期，高温是大量动植物从赤道生态系统中消失的罪魁祸首[176]。但是他们也注意到，Smithian 晚期的海水温度高达 40 度，而二叠纪末期的海水温度只有 25 度[176, 246]。因此，高温并不是二叠纪末期生物大灭绝的首要因素。然而，这个温度已经达到了蓝细菌爆发的适宜温度（20° 至 30°），加之二叠纪末期海水中富集了大量的 N、P、Fe 等浮游植物限制性元素（见上文），因此，蓝细菌得以急速增殖，广布二叠纪末期的海洋，最后以钙质微生物岩的形式保存在地层中[38, 244]。

在后生动物的食谱中，蓝细菌是一类低营养的食物，而其中的一些蓝细菌更具有较强的毒性（见前文）[254, 255]。FerrÃo-Filho et al.（2001）在实验室的动物喂养实验中证实，即使是不具有毒性的蓝细菌种类（*Synechococcus elongatus*）也不能很好地支撑浮游动物（*Moinodaphnia macleayi*）的生长[234]。但是，只需要在其食物中加入少量的绿藻（营养价值高），此类浮游动物的营养缺乏症状就会消失[234]。然而，不同的物种对蓝细菌的忍受能力却是不一样的，这已在浮游动物、双壳类以及腹足类的实验中得到证实[218, 234, 256]。而 Limén and Ólafsson[257]将个体较大的双壳类和体型较小的介形虫混养在一起，同时让食物成为其限制性因素。他们发现，在食物缺乏的情况下，个体较大的双壳类的物种多样性和丰度都急剧降低，而体型较小的介形虫则几乎没有受到影响[257]。由此表明，在食物缺乏的环境中，体型较小的初级消费者更容易在种间竞争中胜出[257]。

回溯到二叠纪末期的生物大灭绝之前，海洋生态系统总体保持平衡，动物以及浮游植物都具有较高的生物多样性（图 4-2，阶段 1）。浮游植物中，蓝细菌和链状的疑源类均较少，主要出现球形以及具刺的疑源类，其丰度极高（图 4-3，阶段 1）。然而，由于环境的突变，如大规模的火山喷发、海平面的骤降以及温度升高等（图 4-3，阶段 2）[31-33, 176, 246]，海洋生态系统的平衡被打破。大多数的动植物由于对环境的不适应而惨遭灭绝，而生命力极强的蓝细菌却在这适宜的环境中大面积爆发，成为主要的初级生产者（图 4-2 和 4-3，阶段 2）。然而，蓝细菌的爆发却给环境带来了持续性的恶化，首先是加大了海洋透光带中光衰减的程度；其次是加速了海水中的氧气消耗（图 4-3）；同时也为海洋中的动物提供了有毒的且贫营养的食物（见前文 4.1 节）。这三点影响对其它浮游植物以及大多数的海洋动物来说都是致命的。但是，不同物种对于这些影响的反应却是不一样的。总体来讲，疑源类等其它类型的浮游植物基本从近岸海域中消失，只分布在远岸的水域，其总体的丰度是降低的。其中，球形疑源类丰度降低，具刺疑源类以及链状疑源类的丰度升高（图 4-3，阶段 2）。而个体较大的动物则基本消失，体型较小的后生动物凭借其对蓝细菌以及恶劣环境较强的适应性而得以残存[258-262]。

然而此次生物危机并未结束，随着温度的进一步升高以及无机营养盐的持续性输入，蓝细菌的爆发向远岸以及深水环境中扩张，导致疑源类等其它浮游植物的多样性和丰度都急剧降低，致使大多数在前一阶段残存的动物也不能在这更为恶劣的环境中幸免而遭到灭绝（图 4-2 和 4-3；阶段 3；上寺剖面 28 层以及煤山剖面 29 层），只剩下个别适应力极强的灾难种得以存活并繁盛（如双壳类的 *Claraia*）[261]。

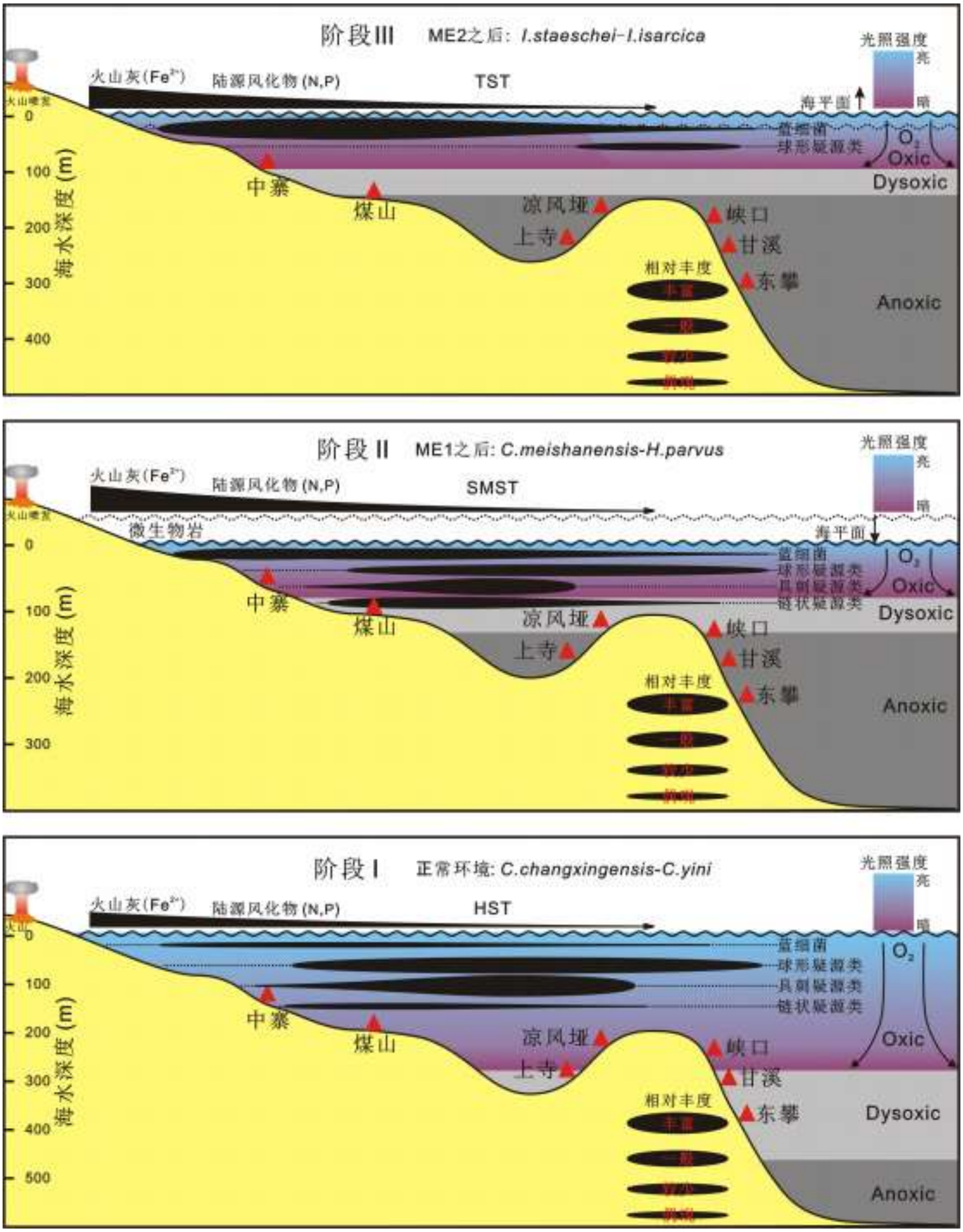

图 4-3 华南地区二叠纪-三叠纪之交海洋浮游植物与环境演变的示意图

I.: *Isarcicella*; *H.*: *Hindeodus*; *C.*: *Clarkina*

§4.3 本章小结

1）在华南地区二叠纪与三叠纪之交的地层中，疑源类的生物多样性与后生动物生物多样性的变化较为一致，都是逐步降低的，并且可以划分为明显的三个阶段；但是蓝细菌的丰度在生物大灭绝之后却出现了明显的升高。

2）如果认为大规模的火山喷发是二叠纪末期生物大灭绝的导火索，而海洋的缺氧、高温以及食物的缺乏是动物灭绝的直接原因；那么，本文认为高温以及陆地风化的加强是蓝细菌持续性爆发的诱因，而蓝细菌的增殖则加深了海水的缺氧程度以及造成了其它浮游植物的减少。

第五章 疑源类化石的分类及系统描述

§5.1 *Micrhystridium/Veryhachium* complex 的划分

具突起的小型疑源类 *Micrhystridium* 以及 *Veryhachium* 在整个显生宙的地层中都十分常见。它们各自已有超过 200 个物种被记录[71]。正是由于如此多的物种存在，因此它们被称作“waste-basket”属，类似的属还包括：*Baltisphaeridium*、*Multiplicisphaeridium* 以及 *Polygonium* [263]。多数孢粉学家在鉴定物种的时候，将膜壳为多角形且具多枚突起的疑源类划分到 *Micrhystridium* 中，而将膜壳呈多角形且具八枚及以下突起的疑源类划归 *Veryhachium*。值得注意的是，由于这类化石个体在形态上呈现出一定规律的渐变性，因此在进行种一级别的鉴定时，就显得尤为困难。

二叠纪的 *Micrhystridium* 一般呈球形或者椭球形，膜壳上具数量不等，长短不一的突起。但是突起的外形比较类似，几乎都不分叉，基部较宽，顶端渐尖且封闭。*Micrhystridium* 的膜壳一般小于 20 微米，而其它膜壳较大且具突起的疑源类则一般归为 *Baltisphaeridium* 或者 *Multiplicisphaeridium*。*Veryhachium* 多为膜壳较小且呈多角形的疑源类，一般具少于 8 枚突起。突起的外形与 *Micrhystridium* 类似，都较为简单，一般不分叉。

如前文所述，*Micrhystridium* 和 *Veryhachium* 在二叠纪的地层中是被报道次数最多的属。归属于 *Micrhystridium* 的 27 种疑源类共计被报道了 55 次，同时，*Veryhachium* 也被报道了 46 次，共包括 22 种。在种一级水平上，*Micrhystridium breve*、*M. stellatum* 以及 *Veryhachium reductum* 是最常见的物种。

尽管众多学者在过去几十年里不断地对这两个属或者归属于它们的物种进行修订，但是它们的属征还是具有很大的争议[263, 264]。由于在鉴别物种的时候不易将新的化石鉴定到种一级别，因此，许多作者就使用 *Micrhystridium/ Veryhachium* complex 来表示这一特定类群的疑源类化石[58, 64, 69, 118, 264-266]。

由于许多作者已经对 *Micrhystridium* 和 *Veryhachium* 做过多次综述和修订，因此本文的目的并不是对它们进行总结或者修订，而是根据它们的形态特征，为二叠纪的 *Micrhystridium* 和 *Veryhachium* 提出一个简单可行的分类方案。

此次在扬子板块二叠纪与三叠纪之交的地层中，根据前人所描述的物种鉴别特征，共发现十个物种可以归到 *Micrhystridium* 和 *Veryhachium*。但是，由于这些物种之间只具有细微的差别，因此很难区分，且很多物种极有可能是同物异名。为了能够更为容易地区分这些物种，本文建议将它们划分为五个不规范的类群，而划分依据只是其膜壳的几何形态而不考虑突起的数量以及形态变化。

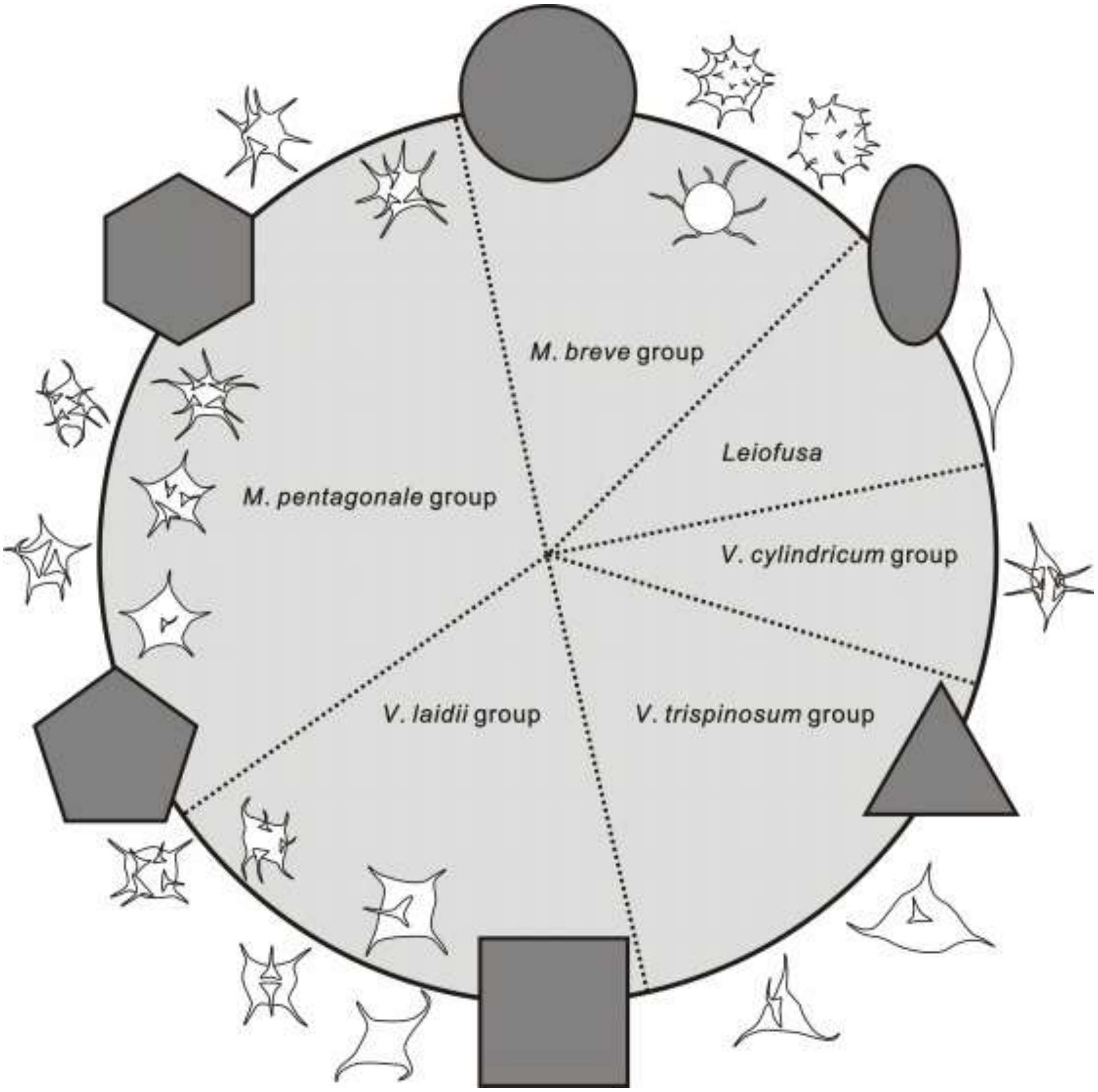

图 5-1 *Micrhystridium/Veryhachium complex* 分类示意图

Servais et al.（2007）总结了奥陶纪 *Veryhachium* 的主要形态类型，同时沿用了前人的提议，根据膜壳的几何外形，将 *Veryhachium* 划分为两个不规范的类群：*Veryhachium trispinosum* 亚属以及 *Veryhachium lairdii* 亚属。前者包括了所有具三角形膜壳的 *Veryhachium* 化石种类，而后者则囊括了所有具四边形膜壳的 *Veryhachium* 物种[263]。

与之相比，二叠纪 *Veryhachium* 的类型较多样，且很多类型与 *Micrhystridium* 存在较为明显的渐变。因此，本文将沿用 Servais et al.（2007）的提议，且另外增加 *Veryhachium cylindricum* 亚属，其包括膜壳为椭圆形的 *Veryhachium*[263]。同时，再添加 *Micrhystridium pentagonale* 和 *Micrhystridium breve* 两个亚属。前者涵盖了膜壳为五边形或者六边形的

Micrhystridium 或者 *Veryhachium* 的种类；而后者则包括了所有具球形膜壳的 *Micrhystridium*。

本文中，*Veryhachium cylindricum* 亚属只含有 *Veryhachium cylindricum* 一种。*Veryhachium trispinosum* 亚属包括 *Veryhachium hyalodermum* 以及 *V.* sp.两个具三角形膜壳的物种。而 *Veryhachium lairdii* 亚属则包含了 *Veryhachium nasicum*、*V. quadratum* 以及 *V. sedecimspinosum* 三个物种。*Micrhystridium pentagonale* 亚属涵盖 *Micrhystridium pentagonale* 和 *M. stellatum*；而 *Micrhystridium breve* 亚属则包括了 *Micrhystridium fragile* 以及 *M. breve* 两个物种。需要指出的是，此分类为一种开放性的分类系统，任何真实存在于化石膜壳的其它几何类型都可以添加入本系统中。如图 5-1 所示为这两个属物种的假想图，而图版 2 和图版 3 则为本文所观察到的化石类型。可见，这些几何形态的膜壳都真实的出现在化石上，且其渐变的特征令它们无法被准确地鉴定到种。而本文提出的分类系统可以较为容易地解决这个问题。

本文所提出的分类方式只是基于形态学角度对 *Micrhystridium*/*Veryhachium* complex 类群的化石做出快速而方便的划分，而并不能反映它们真正的生物亲缘关系。因此，未来的研究应当利用生物化学等方法（如基于生物标志化合物）对疑源类的膜壳做细致的分析，从而得到更为准确的生物关系图谱。值得注意的是 Grice et al.（2005）以及 Hays et al.（2011）对只含有 *Micrhystridium* 与 *Veryhachium* 复合物的岩石进行了生物化学的研究，并认为 C33 *n*-alkylcyclohexane 可能是它们的生物标志化合物[267, 268]。然而，目前测试的结果几乎都是基于全岩的测试，即使找到了某一类生物标志化合物，也不能将其与特定种类的化石进行一一对应。因此，测试特定种类疑源类的生物标志化合物显得尤为重要。

完成类似工作的关键是在利用浸解法得到实体化石残留物之后，对疑源类化石进行分离纯化。目前的技术有两种：一种是在体视镜下，利用显微操作仪挑选出特定的疑源类种类。这种方法是最直接有效的方式，其纯度很高，但是效率较为低下，适用于化石膜壳较大，化石丰度较高的样品。Sephton et al.（2009）利用此项技术挑取出链状的疑源类化石 *Reduviasporonites*，并对其做了详细的化学分析，包括碳同位素、氮同位素以及生物标志化合物的分析等，从而认为它更像是一种真菌类生物[156]。另一种方法是利用流式细胞仪进行分离。这种方法的原理是利用疑源类化石自发荧光的特性，使用流式细胞仪将具有荧光的化石与不具荧光的杂质分离。其优点是效率高，可重复性强，对膜壳较小的疑源类尤其适用。其缺点是纯度较低，不能分离出某一特定种类的化石。但是，我们可以利用化石直径的差别，先利用不同孔径的筛网将疑源类按照直径的大小分类。然后，对不同类别分别进行纯化。因此，这种方法对样品的要求较高，需要事先找到合适的样品。其样品的特征为：以一种疑源类为主，或者几种疑源类的直径有较大的差别。Talyzina et al.（2000）利用这种方法纯化了早寒武世的疑源类样品，并从这些分离出的样品中找到了沟鞭藻的生物标志化合物[269]。但是他们制备的样品纯度较低，仍然未能将特定生物标志化合物与疑源类一一对应。然而，更为精细的工作将是以后一个重要的研究方向。

§5.2 疑源类化石的系统描述

根据 Colbath and Grenfell[63]的分类，本文将 *Dictyotidium*、*Leiosphaeridia* 以及 *Schizosporis* 作为绿藻。尽管众多学者对 *Reduviasporonites* 的生物亲缘关系做了大量的讨论，但是并没有形成共识。因此，文中仍将其作为一种疑源类。

Algae
Division Chlorophyta Pascher, 1914
Class Prasinophyceae Christensen, 1962
Order Not assigned
Family Pterosphaeridiaceae Mädler, 1963
Genus *Dictyotidium* Eisenack, 1955, emend. Staplin, 1961
模式种： *Dictyotidium dietyotum* (Eisenack, 1938) Eisenack, 1955

Dictyotidium reticulatum Schulz, 1965

图版 2，图 1-12
Dictyotidium reticulatum Schulz, 1965, p. 278, 图版 23, 图 12-14

描述：膜壳为球形至椭球形，表面覆盖网状纹饰。网状纹饰呈规则或者不规则的六边形，边长 4~10 微米。膜壳的壁常形成单条或者多条呈笔直或者略微弯曲的褶皱。膜壳常具有横裂等脱囊结构，将膜壳分为整体相连的两部分。

测量数据：膜壳直径为 52(76)110 μm（从左至右依次为：最小值，平均值，最大值。以下皆同）, 45（样本量）

讨论：此类较大的球形膜壳在古生代及以前的地层中十分常见，但是在二叠纪地层中却较少出现。同一时期，与之类似的是 *Leiosphaeridia changxingesis* Ouyang and Utting, 1990，但是两者膜壳表面的纹饰有较为明显的区别。前者覆盖规则或者不规则的网状纹饰，而后者却为较为粗糙的表面，颗粒状或者有微孔。

文献记载：二叠纪，中国[135]、挪威[97]；三叠纪，德国[270]、西班牙[271]

产出层位：此种疑源类在上寺剖面的吴家坪期和 22 层占据绝对优势。其它剖面如煤山 26 层和峡口剖面等也有出现。

Dictyotidium sp.

图版 6，图 15-16

描述：膜壳呈球形，表面由较为规则的四边形或者六边形紧密连接而形成。其边长为 2-4 微米。而四边形或者六边形的内部通常被矿物充填。膜壳通常不具有褶皱和开口

测量数据： 膜壳直径为 30(36)42 μm, 5（样本量）

讨论：当前种的膜壳几乎没有受到成岩过程中压实作用的影响而仍保持近球形的原状。与 *Dictyotidium reticulatum* 相比，当前种的膜壳直径只有后者的三分之一左右。由于发现的个体有限，未能找到已知的种类与之对应。

产出层位：上寺剖面 22 层。

Genus *Leiosphaeridia* Eisenack, 1958, emend. Downie and Sarjeant, 1963

模式种： *Leiosphaeridia baltica* Eisenack, 1958

Leiosphaeridia micrograniferα (Staplin, 1961) Downie and Sarjeant, 1965

图版 5, 图 11-22

Protoleiosphaeridium micrograniferα Staplin, 1961, p.405, 图版 48, 图 4

Leiosphaeridia micrograniferα (Staplin, 1961) Downie and Sarjeant, 1965, p.124

描述：膜壳椭球形至亚球形。膜壳表面具有较为密集的颗粒状纹饰，其颗粒通常近圆形，直径为 0.5 微米左右。膜壳壁单层，较薄，约 1 微米，常形成笔直或者弯曲的多条褶皱，偶见开口。

测量数据： 膜壳直径为 25(32)40 μm, 14（样本量）;

讨论：当前种与 *Leiosphaeridia granulosa* Staplin, 1961 较为相似，而当前种的膜壳较后者更大。但是膜壳上颗粒状纹饰的单个颗粒的直径却明显小于后者，当前种的为 0.5 微米左右，而后者的通常为 1 微米。

文献记载：早志留世，宾夕法尼亚[272]；晚泥盆世，加拿大[204]

产出层位：上寺与峡口剖面的晚二叠世多个层位均较为丰富。

Leiosphaeridia minutissima (Naumova, 1949) Jankauskas, 1989

图版 6，图 1-14

Leiosphaeridia minutissima Naumova, 1949, p. 52-53, 图版 1, 图. 1-2, 图版 2, 图 1-2

Leiosphaeridia minutissima (Naumova, 1949) Jankauskas, 1989, p. 79-80, 图版 9, 图 1-4, 11

描述：膜壳球形至亚球形，表面光滑，不具其它纹饰。膜壳壁单层且较薄，常形成笔直或者弯曲的多条褶皱，未见开口。

测量数据： 膜壳直径为 25(31)40 μm, 23（样本量）

讨论：当前种膜壳的大小与 *Leiosphaeridia micrograniferα* 较为一致，且常一起出现。但是两者膜壳的壁有显著的区别。当前种的壁是光滑的，而后者具有粒状纹饰。

文献记载：新元古代，加拿大[195]、刚果[273]、捷克 [274]、印度[275]、俄罗斯[276-278]；埃迪卡拉纪，波兰[279]、乌克兰[280]、乌拉圭[281]；寒武纪，捷克[282, 283]、俄罗斯[284]

产出层位：在上寺、凉风垭、东攀、甘溪等剖面的多个层位较为丰富。

Class Zygnematophyceae Round, 1971

Order Zygnematales Borge and Pascher 1913

Family Zygnemataceae Kützing, 1843

Genus *Schizosporis* Cookson and Dettmann, 1959, emend. Pierce, 1976

模式种：*Schizosporis reticulatus* Cookson and Dettmann, 1959

Schizosporis scissus (Blame and Hennelly, 1956) Hart, 1965

图版 5，图 8-10

Laevigatosporites scissus Blame and Hennelly, 1956, p. 56, 图版 1, 图 6-9

Spheripollenites scissus (Blame and Hennelly, 1956) Jansonius, 1962, p. 82, 图版 16, 图 8

Schizosporis scissus (Blame and Hennelly, 1956) Hart, 1965, p. 14

描述：膜壳球形至椭球形。膜壳壁薄，厚约 1 微米，表面光滑，没有明显的褶皱。常具中裂等开口将膜壳分隔成相似的两部分。

测量数据：膜壳直径为 25(36)45 μm, 5（样本量）

讨论：当前种的膜壳壁比 *Micrhystridium*、*Veryhachium* 以及 *Leiosphaeridia* 的壁都明显厚一些，但是又不及 *Dictyotidium* 壁的厚度。常具有较为明显的脱囊结构是容易被鉴别的特征。

文献记载：二叠纪，南极[140, 141]、澳大利亚[157, 159]、巴基斯坦[151]；三叠纪，加拿大([95]

产出层位：在上寺 25 层中较为常见，煤山个别层位偶见。

Schizosporis sp.

图版 5，图 1-7

描述：膜壳几乎都为球形，表面密集分布着 0.5~1 微米长的突起。突起中空，简单不分叉，顶端封闭。膜壳常具中裂等脱囊结构，并将膜壳分隔成相似的两个部分。

测量数据： 膜壳直径为 20(23)25 μm, 8（样本量）

讨论：当前种与 *Schizosporis scissus* 以及 *Leiosphaeridia microgranifera* 都较为类似。当前种同 *Schizosporis scissus* 一样具有中裂等脱囊结构，而 *Leiosphaeridia microgranifera* 很少发现有开口。它们的膜壳表面也有明显的区别。当前种具有密集的短刺；*Schizosporis scissus* 是光滑的；而 *Leiosphaeridia microgranifera* 则是具有颗粒状纹饰，且常具有不规则的褶皱。

产出层位： 发现于上寺剖面的 21 层和 25 层。

Acritarcha Evitt, 1963

Genus *Baltisphaeridium* Eisenack, 1958, emend. Eisenack, 1969

模式种： *Baltisphaeridium* (as *Ovumhispidum*) *longispinosum* Eisenack, 1931

Baltisphaeridium **sp.**

图版 4，图 1

描述：膜壳球形至亚球形，表面覆盖较为密集的突起。突起简单，坚实，不分叉，顶端封闭，长度为 2-4 微米。膜壳壁较薄，厚约 1 微米，单层，无开口。

测量数据：膜壳直径为 25(35)42 µm, 4（样本量）；突起长度：2-4 µm

讨论：当前种与 *Micrhystridium* 以及 *Veryhachium* 都具有突起。然而，当前种的个体明显大于 20 微米而不能归为 *Micrhystridium*。而其突起的数量较多，也不能归为 *Veryhachium*。由于发现的个体数量较少，不能将其准确地命名。

产出层位：偶见于中寨和上寺的个别样品中。

Genus *Leiofusa* Eisenack, 1938

模式种： *Leiofusa fusiformis* Eisenack, 1938

Leiofusa **sp.**

图版 4，图 2

描述：膜壳呈纺锤形，表面光滑。膜壳壁薄，未见开口。膜壳两端均有一较长的突起。突起中空，简单，不分叉，顶端封闭，长约为膜壳主体的一半。

测量数据： 膜壳直径为 35 µm, 1（样本量）；突起长度：17 µm

讨论：当前种的膜壳明显比 *Micrhystridium* 和 *Veryhachium* 的膜壳大。但是，它们的突起的外形几乎是一致的。只是当前种的突起比后两者的较长。由于只发现了一个样本，因此未能将其鉴定到种。

产出层位：出现在上寺 21 层。

Genus *Micrhystridium* Deflandre, 1937, emend. Sarjeant and Stancliffe, 1994

模式种： *Micrhystridium inconspicuum* (Deflandre, 1935) Deflandre, 1937

Micrhystridium breve **Jansonius, 1962**

图版 4，图 13-24

Micrhystridium breve Jansonius, 1962, p. 85, 图版 16, 图 62, 63, 66

描述：膜壳球形至椭球形，表面光滑具 20~40 枚突起。突起简单，中空，不分叉，顶端封闭，长 2~5 微米。膜壳壁单层且薄，一般厚 0.5~1 微米，偶见简单的开口。

测量数据： 膜壳直径为 15(17)21 µm, 23（样本量）；突起长度：2-5 µm

讨论：Sarjeant et al. (1970)认为 *Micrhystridium breve* 与 *M. recurvatum* forma *brecispinosa* Valensi, 1953 应该为同物异名[137]。当前种的特征较为明显，膜壳具有密集的短刺，可以很容易地将其与其它种类相区别。

文献记载：二叠纪，巴基斯坦[137]、加拿大[285]、澳大利亚[147]、美国[124]、巴西[83]；三叠纪，加拿大[95, 286-288]、西伯利亚[289]；志留纪，加拿大[290]

产出层位：常见于近岸的环境中，出现在中寨，上寺以及凉风垭剖面。在上寺剖面的 25 和 28 层尤为丰富。

Micrhystridium fragile Deflandre, 1947

图版 4，图 5

Micrhystridium fragile Deflandre, 1947, p. 8, fig. 13-18

描述：膜壳球形至亚球形，表面光滑，具十枚左右的突起。突起较为细小而易弯曲，中空，顶端封闭。突起的长度可达 10-15 微米，通常超过其膜壳的直径。

测量数据： 膜壳直径为 9(11)12 μm, 4（样本量）；突起长度：11-15 μm

讨论：当前种的膜壳主体（不包括突起）直径非常小，只有约 10 微米。而其突起的形态也较为特殊，比 *Micrhystridium* 其它种类的突起较为细小。

文献记载：二叠纪，乌拉圭[88]、英格兰[291]；三叠纪，英格兰[292]；侏罗纪，英格兰[207, 293, 294]、以色列[291]

产出层位：偶见于上寺 21-25 层。

Micrhystridium pentagonale Stockmans and Willière, 1963

图版 3，图 18-20

Micrhystridium pentagonale Stockmans and Willière, 1963, p. 470-471, 图版 3, 图 32

描述：膜壳呈五角形，表面光滑，可见简单的开口。一般附着 5-9 枚突起，其中 5 枚从膜壳的五个角延伸出来，其余的 1-4 枚突起附着在膜壳中央。突起简单，中空，基部较宽，顶端渐尖而封闭，其长度一般只有膜壳直径的一半左右。

测量数据： 膜壳直径为 12(14)17 μm, 15（样本量）；突起长度：4-10 μm

讨论：当前种膜壳的形状与 *Micrhystridium stellatum* 类似，但是更接近规则的五角形。后者的突起可以更多，也更为细长。

文献记载：志留纪，比利时[295]；石炭纪，土耳其[296];

产出层位：常见于在上寺剖面的 21-25 层，偶见于凉风垭剖面。

Micrhystridium stellatum Deflandre, 1945

图版 4，图 6-12

Micrhystridium stellatum Deflandre, 1945, p. 65, 图版 3, 图 16-19

描述：膜壳为多角形，常为五边形或者六边形，表面光滑，具不定数量的突起，一般为 8-12 枚。突起简单，中空，顶端渐尖而封闭，长度为膜壳直径的一半至一倍。

测量数据： 膜壳直径为 13(16)18 μm, 15（样本量）；突起长度：6-15 μm

讨论：当前种在地史时期十分常见，世界各地均有报道。其典型的特征为多角形的膜壳以及细长的突起。在前文已将其与 *Micrhystridium pentagonale* 做过比较。

文献记载：奥陶纪，美国[297]；志留纪，英格兰[169]、法国[298]、瑞典[299, 300]；泥盆纪，利比亚[301]、波兰[302]；石炭纪，中国[303]、土耳其[296]；二叠纪，英国[118]、中国[135]、德国[142]、以色列[143]；三叠纪，英格兰[292]

产出层位：常见于中寨，煤山，上寺以及凉风垭剖面。

Genus *Reduviasporonites* Wilson, 1962, emend. Foster, 2002

模式种： *Reduviasporonites catenulatus* Wilson, 1962

长期以来，*Reduviasporonites* 被许多作者认为是一种真菌化石。但是一些作者将其归为一种绿藻[154, 155]。由于它的亲缘关系尚存疑问，因而在此将其仍划归为疑源类。值得注意的是，许多支持其为真菌化石的作者认为在二叠纪与三叠纪之交的地层中存在一段 *Reduviasporonites* 的高峰[64, 66-68]。然而，在本文的研究过程中，笔者始终未能在华南 PTB 附近发现此类现象。在华南地区各剖面，*Reduviasporonites* 化石的百分含量最高仅为 14%（上寺剖面），远远低于“真菌高峰”的百分量（大于 90%）。

***Reduviasporonites catenulatus* Wilson, 1962, p. 94-95, 图版：1, 图 1-6**

图版 7，图 12-17

描述：膜壳整体为两节或多节组成的链状，单个膜壳呈亚球形或者椭球形，表面光滑或具褶皱，节与节之间的连接处明显比膜壳其它部位厚。单个膜壳长约 20 微米，其长宽比为 1:1 至 1:2。

测量数据：膜壳直径为 8(15)20 μm, 17（样本量）

讨论：关于此类疑源类生物属性的争论已经持续十余年，最新的资料倾向于其为真菌。Foster et al. (2002)对它们做了详细的描述以及分类研究[155]。而当前种与 *Reduviasporonites chalastus* 的相似度非常高。其最大的区别只是在于当前种的单个膜壳要小于后者。

文献记载：二叠纪，澳大利亚[155]、美国[304, 305]；白垩纪，加拿大[306]

产出层位：常见于上寺与峡口剖面。

***Reduviasporonites chalastus* (Foster, 1979) Elsik, 1999**

图版 7，图 1-11,18-23

Chordecystia chalasta Foster, 1979, p. 109-110; pl 41, 图 3-9;

? *Brazilea helbyi* forma *gregata* Foster, 1979, p. 112; 图版 41, 图 1-2.

Tympanicysta stoschiana Balme, 1980, p. 22-24; 图版 1, 图 3-7; Afonin et al., 2001, p. 484-486, 图 1; 2A-C, E,F.

Reduviasporonites stoschianus (Balme) Elsik, 1999, p. 40; 图版 1, 图 1-24.

? *Reduviasporonites stoschianus* (Balme) Elsik, 1999; Wood and Elsik, 1999, p.46-48; 图版：1,

图 1-9; 图版 2, 图 1-7.

描述：膜壳整体为两节或多节组成的链状，单个膜壳亚球形或者近四边形，表面光滑或者具褶皱节与节之间的连接处明显比膜壳其它部位厚。单个膜壳长约 40 微米，其长宽比为 2:1 至 6:1。

测量数据： 膜壳直径为 15(36)65 μm, 19（样本量）

讨论：当前种单个膜壳的个体明显大于 *Reduviasporonites catenulatus*，其余特征都类似。

文献记载：二叠纪，澳大利亚[126, 155]、中国[135]、丹麦[307]、伊拉克[130]、肯尼亚[138]、巴拉圭[99]、秘鲁[308]、俄罗斯[154]、土耳其[131]、美国[305]

产出层位：常见于中寨、煤山以及上寺剖面的二叠纪与三叠纪之交的过渡层中。

Genus *Veryhachium* Deunff, 1954, emend. Sarjeant and Stancliffe, 1994

模式种： *Veryhachium trisulcum* (Deunff, 1954) Deunff, 1959

Veryhachium cylindricum Schaarschmidt, 1963

图版 3，图 21-25

Veryhachium cylindricum Schaarschmidt, 1963, p. 64, 图版 18, 图 8-10

描述：膜壳为长椭球形，表面光滑，多具 6 枚对称的突起。突起简单，中空，基部较宽，可达 5-10 微米，顶端渐尖而封闭，长约 10 微米。其中两枚突起沿膜壳长轴延伸，剩下的四枚突起对称地分布于短轴上下。

测量数据： 膜壳直径为 15(18)22 μm, 13（样本量）；突起长度：8-12 μm

讨论：当前种的形态较为特别，整体两轴对称。尤其是它的突起基部宽大，而且分布均匀，易于识别，而一枚位于长轴端的突起常脱落。

文献记载：二叠纪，德国[142]

产出层位：常见于上寺剖面 21-25 层。

Veryhachium hyalodermum (Cookson, 1955) Schaarschmidt, 1963

图版 3，图 1-8

Veryhachium hyalodermum Cookson, 1956, p. 188-189, 图版 1, 图 12-16

Veryhachium hyalodermum (Cookson, 1956) Schaarschmidt, 1963, p. 62-63

描述：膜壳扁平，呈三角形，表面光滑，具 4 枚突起，偶见开口。突起简单，中空，基部略宽，顶部渐尖而封闭。其中三枚突起随膜壳的三个角延伸，其余一枚突起较短位于膜壳中央。

测量数据： 膜壳直径为 10(12)14 μm, 25（样本量）；突起长度：9-15 μm

讨论：*Veryhachium* 中有多个物种都只具有 4 枚突起，比如 *Veryhachium ceratioides* Stockmans and Willière, 1962、*V. europaeum* Stockmans and Willière, 1960 以及 *V. leonense* Cramer, 1964 等。实际上，这些物种之间的区别很模糊，也很难界定。而当前种的突起一般较后几种更为

细长。

文献记载：二叠纪，中国[135]、德国[142]、以色列[144]、南非[145]；始新世，澳大利亚[309]

产出层位：常见于上寺剖面 21-25 层，以及煤山和凉风垭剖面。

***Veryhachium nasicum* (Stockmans and Willière, 1960) Stockmans and Willière, 1962**

图版 3，图 9-12

Stellinium nasicum Stockmans and Willière, 1960, p. 3, 图版 1, 图 3

Veryhachium nasicum (Stockmans and Willière, 1960) Stockmans and Willière, 1962, p. 52

描述：膜壳扁平，成规则或者不规则的四边形，表面光滑，一般具 5 枚突起。突起简单，中空，基部略宽，顶部渐尖而封闭。其中四枚突起延膜壳四角伸展，剩下一枚突起附着在膜壳中部。

测量数据： 膜壳直径为 17(19)22 μm, 21（样本量）；突起长度：5-9 μm

讨论：*Veryhachium* 中也有多个物种具有四边形的膜壳，而被许多作者称为 *Veryhachium lairdii* group。当前种地史时期分布较广，其突起也易于识别。

文献记载：泥盆纪，比利时[310]、中国[303]、利比亚[311]；石炭纪，俄罗斯[301]；二叠纪，德国[142]

产出层位：常见于上寺剖面 21-25 层，以及凉风垭剖面。

***Veryhachium quadratum* Schaarschmidt, 1963**

图版 4，图 4

Veryhachium quadratum Schaarschmidt, 1963, p. 63, 图版 17, 图 8-10.

描述：膜壳多角形，表面光滑，具 5-8 枚较短的突起。突起中空，顶端较钝，近圆弧状，多延膜壳的边缘分布。突起一般宽约 2 微米，长 1-2 微米。

测量数据： 膜壳直径约为 20 μm, 2（样本量）；突起长度：1-2 μm

讨论：当前种与 *Veryhachium* 的其它物种区别较大。其突起十分短小，一般只有 1-2 微米，易于鉴别。

文献记载：二叠纪，德国[142]

产出层位：偶见于上寺剖面 21 层。

***Veryhachium sedecimspinosum* Staplin, 1961**

图版 3，图 13-17

Veryhachium sedecimspinosum Staplin, 1961, p414, 图版 49, 图 9-11

描述：膜壳呈规则或者不规则的四边形，表面光滑，具 6-8 枚突起。突起简单，中空，基部较宽，顶端渐尖而封闭。其中 4 枚突起延膜壳的四个角伸展，剩下的突起（一般为 2-4 枚）附着在膜壳中部，一般对称分布。

测量数据：膜壳直径为 15(16)17 μm, 4（样本量）；突起长度：7-13 μm

讨论：当前种与 *Veryhachium nasicum* 非常相似，都具有相同形态的膜壳，突起的形态也是类似的。唯一的不同点只是当前种的突起为 6-8 枚，而后者只有 5 枚。实际上，他们很可能就是一个物种，只是人为地将其划分为不同种类。

文献记载：泥盆纪，加拿大[204]；二叠纪，德国[295]

产出层位：常见于上寺和凉风垭剖面。

***Veryhachium* sp.**

图版 4，图 2

描述：膜壳近三角形，表面光滑，具 3 至 6 枚突起。突起较短，简单，中空，顶端渐尖而封闭。其中三枚突起延膜壳的三角伸展，其余的突起则附着在膜壳中央。

测量数据： 膜壳直径约为 25 μm, 3（样本量）；突起长度约 5 μm

讨论：当前种的膜壳与 *Veryhachium hyalodermum* 类似，呈三角形。但是前者的个体明显大于后者。而后者的突起长度却明显长于前者。由于样本量较少，未能将其准确分类。

产出层位：偶见于上寺剖面 21 层。

第六章 结论以及研究展望

为了探索二叠纪与三叠纪之交生物大灭绝期间浮游植物与生态环境的演变，本文以具有机质壳的浮游植物化石疑源类为重点研究对象，在华南二叠纪的有关地层中选取了七条地质剖面。经研究得到以下结论：

1）经过对二叠纪疑源类化石的文献综述表明：二叠纪疑源类化石的研究程度较低，但是已经报道的疑源类化石数量已达 55 属、230 种（其中包含 77 个未定种），远远超过前人对二叠纪疑源类数量的统计。二叠纪疑源类主要以长地史分布的属种为主，如 *Micrhystridium*、*Veryhachium*、*Leiosphaeridia* 以及 *Brazilea* 等。而且大多数疑源类的膜壳都较小，直径约 20 微米。

2）在空间尺度上，本文所研究的七条剖面涵盖了海陆交互相、近大陆架、远大陆架以及大陆坡等沉积相。经过对疑源类定性以及定量的研究发现，疑源类的属和物种的多样性都符合近岸-远岸的分布规律。近岸地区的疑源类物种多样性较低，一般只有 2-4 种（如中寨和东攀剖面）；而较远岸的大陆架地区物种多样性较高，可以达到 20 种左右（如煤山、上寺以及凉风垭剖面）；但是随着离岸距离的增加，大陆坡地区的疑源类物种多样性同样是较低的（如甘溪和峡口剖面）。

3）在疑源类化石属一级上，*Leiosphaeridia*、*Reduviasporonites* 以及 *Micrhystridium* 从近岸浅水环境到远岸深水地区均有分布；*Dictyotidium* 和 *Veryhachium* 更多地出现于开阔的海域；而 *Schizosporis* 则只在上寺剖面 25 层和煤山剖面 26 层出现（海平面较低时），可能指示一种相对近岸浅水的环境。

4）在物种级别上，具短突起的 *Micrhystridium breve* 在近岸环境中占据绝对优势，且对营养盐的浓度较为敏感，其生物量的变化与 Fe 和 Al 元素的含量变化较为一致。而具较长突起的其它种类的 *Micrhystridium* 以及 *Veryhachium*（如 *Micrhystridium stellatum* 和 *Veryhachium hyalodermum*）则较多地出现在远岸环境中。同时，本文从化石膜壳形态学的角度对 *Micrhystridium/Veryhachium complex* 类群做了简单的分类。其中，*Veryhachium cylindricum* 亚属包括 *Veryhachium cylindricum* 一种；*Veryhachium trispinosum* 亚属包括 *Veryhachium hyalodermum* 以及 *V.* sp.两个具三角形膜壳的物种；而 *Veryhachium lairdii* 亚属则包含了 *Veryhachium nasicum*、*V. quadratum* 以及 *V. sedecimspinosum* 三个物种；*Micrhystridium pentagonale* 亚属涵盖 *Micrhystridium pentagonale* 和 *M. stellatum*；而 *Micrhystridium breve* 亚属则包括了 *Micrhystridium fragile* 以及 *M. breve* 两个物种。

5）膜壳较大（直径约 80 微米）的球形疑源类如 *Dictyotidium reticulatum* 一般出现在浅水区域，而膜壳较小（直径约 30 微米）的 *Leiosphaeridia* 则更多地分布在水体较深的环境中。同时，膜壳光滑的 *Leiosphaeridia minutissima* 在近岸占据优势，而膜壳具颗粒纹饰的 *Leiosphaeridia microgranifera* 则在远岸较为丰富。

6）虽然链状疑源类 *Reduviasporonites* 出现在多个剖面，但是众多学者认为的二叠纪末期的“真菌高峰”在扬子板块的海相地层中并没有出现。需要指出的是，个体较大的 *Reduviasporonites chalastus* 常分布于近岸环境；而个体较小的 *Reduviasporonites catenulatus* 则更多地出现在远岸深水的区域。

7）时间尺度上：在华南地区二叠纪与三叠纪之交的地层中，疑源类的生物多样性与动物生物多样性的变化较为一致，都是逐步降低的，并且可以划分为明显的三个阶段。阶段 1 的疑源类生物多样性丰富，发现疑源类 10 属 28 种，其止于煤山剖面 24 层顶；而阶段 2 疑源类生物多样性开始下滑，共计 7 属 11 种，其止于煤山剖面 27 层顶；而阶段 3 疑源类物种多样性极低，只发现 1 种化石。但是蓝细菌化石的丰度在生物大灭绝之后的阶段 2 和阶段 3 均出现两个明显的峰值。其原因可能是适宜的环境条件（如：不断上升的海水温度以及火山喷发和陆地风化带来的大量营养盐）导致了蓝细菌的不断增殖并使其迅速成为生物大灭绝之后浅海环境中最主要甚至唯一的初级生产者。

8）大规模的火山喷发可能是二叠纪末期生物大灭绝的导火索，其导致了生态环境的巨大变化，如温度升高等。本文认为：高温以及陆地风化的加强直接促使蓝细菌的持续性爆发。而蓝细菌的不断增殖则加深了海水的缺氧程度以及造成了其它浮游植物的大量减少。经过以上的变化，海洋的缺氧、高温以及食物的缺乏则是海洋动物灭绝的直接原因。

在本文的写作以及研究的过程中，笔者认识到一些当前二叠纪疑源类研究存在的不足：

1）从二叠纪疑源类综述可以看出，中二叠世疑源类的研究基础是非常薄弱的，需要更多学者去探索。

2）本文的研究手段还过于传统，在以后更为精细的工作中，需要利用生物化学测试等方法分析疑源类膜壳中保存下来的化学信号，进而探讨疑源类的生物亲缘关系。

3）当前对于大规模的火山喷发对生物的影响过程还缺乏了解，需要更多的古生物学者结合地球化学等资料来综合分析，从而更加明晰生物与环境的协同演化过程，为保护如今的地球生态环境作出应有的贡献。

致 谢

五年的博士学习时光转瞬即逝，回首走过的岁月，一路的辛苦与汗水换来的不仅仅是一纸文凭，更是知识与成长。在论文即将完成之时，感触颇多。

首先，诚挚地感谢我的导师冯庆来教授，其严谨的治学之道、务实的工作作风以及乐观的生活态度是我在学习、工作和生活中的榜样。在论文的设计、野外采样、实验处理以及论文的定稿过程中，冯老师都悉心指导。在生活中遇到困难时，冯老师也给予我最大的帮助与支持。同时，我也要郑重地感谢我的另外一个导师 Thomas Servais 研究员。在他热心地帮助下，我才能有机会到法国里尔一大进行交流学习。在他细致地指导下，我更加深入地了解了自己的研究方向，进而完成了多篇学术论文的撰写。

感谢地学院何卫红教授几年来在学习上以及生活中的教导与帮助；感谢喻建新教授在疑源类实验室处理以及鉴定时给予的帮助。同时由衷地感谢王永标教授、谢树成教授、黄俊华教授、夏文臣教授以及张宁教授，他们在野外工作中给予了我莫大的帮助和指导。同样感谢袁爱华、杨文强、吴俊、刘桂春、张阳、张磊、石敏、沈俊、胡庆、向宇、冯凡斌、石磊、徐国真、聂小媚、马强芬、钱鑫等，他们在野外工作，室内实验以及生活学习中的帮助使得本人能够更好地完成工作和学习计划。

感谢 Taniel Danelian 教授、Nicolas Tribovillard 教授以及 Stephanie ninive 女士在里尔一大对我的帮助和支持。同时感谢 Elisabeth Locatelli 女士帮我找到众多的珍贵文献，让我得以较为全面地认识和总结二叠纪的疑源类。

还要感谢南京古生物研究所的李军老师和东京大学的 Yukio Isozaki 教授等对本人在博士期间发表的论文提出的宝贵意见和建议。

感谢我的母亲多年来对我的帮助与支持；同样感谢我的妻子张芳对我的关心、支持与守候。

最后，谨以此文献给我在天堂的父亲，感谢您的养育之恩。

参考文献

[1] Erwin D. The great Paleozoic crisis: Life and death in the Permian. Critical Moments in Paleobiology and earth History Series. Columbia University Press, New York, 1993. p. 1-327.

[2] Erwin D H, Bowring S A, Jin Y G. End-Permian mass extinctions: a review. Catastrophic events and mass extinctions: impacts and beyond, 2002,356:363-383.

[3] Raup D M, Sepkoski Jr J J. Mass extinctions in the marine fossil record. science, 1982,215(4539):1501-1503.

[4] Shen S Z, Crowley J L, Wang Y, et al. Calibrating the end-Permian mass extinction. science, 2011,334(6061):1367-1372.

[5] 吴顺宝, 李庆, 王薇薇. 四川华蓥山二叠纪与三叠纪之交沉积特征及动物群变化. 现代地质, 1988,2(3):375-385.

[6] 杨遵仪, 吴顺宝, 殷鸿福, et al. 华南二叠--三叠纪过渡期地质事件: 地质出版社：北京, 1991.

[7] Yin H F, Feng Q L, Lai X L, et al. The protracted Permo-Triassic crisis and multi-episode extinction around the Permian-Triassic boundary. Global and Planetary Change, 2007,55(1-3):1-20.

[8] Jin Y G, Wang Y, Wang W, et al. Pattern of marine mass extinction near the Permian-Triassic boundary in South China. science, 2000,289(5478):432-436.

[9] 方宗杰. 从华南二叠纪-三叠纪礁生态系的演变探讨与灭绝-残存-复苏相关的几个问题. in: 戎嘉余, 方宗杰, (Eds), 生物大灭绝与复苏: 来自华南古生代和三叠纪的证据 合肥: 中国科学技术大学出版社, 2004:475-572.

[10] Feng Q L, He W H, Gu S Z, et al. Radiolarian evolution during the latest Permian in South China. Global and Planetary Change, 2007,55(1-3):177-192.

[11] Song H J, Tong J N, Chen Z Q. Two episodes of foraminiferal extinction near the Permian–Triassic boundary at the Meishan section, South China. Australian Journal of Earth Sciences, 2009,56(6):765-773.

[12] Chen Z. Extinction–survival–recovery of brachiopod faunas during the Permian–Triassic transition. Albertiana, 2005,33:23-26.

[13] Chen Z, McNamara K. End-Permian extinction and subsequent recovery of the Ophiuroidea (Echinodermata). Palaeogeography, Palaeoclimatology, Palaeoecology, 2006,236(3):321-344.

[14] Song H J, Wignall P B, Tong J N, et al. Two pulses of extinction during the Permian-Triassic crisis. Nature Geoscience, 2012,6:52-56.

[15] Xu D Y, Ma S L, Chai Z F, et al. Abundance variation of iridium and trace elements at the Permian/Triassic boundary at Shangsi in China. Nature, 1985,314(6007):154-156.

[16] Kaiho K, Kajiwara Y, Nakano T, et al. End-Permian catastrophe by a bolide impact: evidence of a

gigantic release of sulfur from the mantle. Geology, 2001,29(9):815.

[17] Basu A R, Petaev M I, Poreda R J, et al. Chondritic meteorite fragments associated with the Permian-Triassic boundary in Antarctica. science, 2003,302(5649):1388-1392.

[18] Becker L, Poreda R, Basu A, et al. Bedout: a possible end-Permian impact crater offshore of northwestern Australia. science, 2004,304(5676):1469-1476.

[19] Isozaki Y. Permo-Triassic boundary superanoxia and stratified superocean; records from lost deep sea. science, 1997,276(5310):235-238.

[20] Grice K, Cao C Q, Love G D, et al. Photic zone euxinia during the Permian-Triassic superanoxic event. science, 2005,307(5710):706-709.

[21] Wignall P B. Large igneous provinces and mass extinctions. Earth-Science Reviews, 2001,53(1-2):1-33.

[22] Newell N D. Revolutions in the history of life. Geological Society of America Special Paper, 1967,89:63-91.

[23] Alvarez L W, Alvarez W, Asaro F, et al. Extraterrestrial cause for the Cretaceous-Tertiary extinction. Science, 1980,208(4448):1095-1108.

[24] Becker L, Poreda R, Hunt A, et al. Impact event at the Permian-Triassic boundary: evidence from extraterrestrial noble gases in fullerenes. science, 2001,291(5508):1530.

[25] Xu L, Lin Y T, Shen W J, et al. Platinum-group elements of the Meishan Permian–Triassic boundary section: evidence for flood basaltic volcanism. Chemical Geology, 2007,246(1):55-64.

[26] Farley K A, Mukhopadhyay S, Isozaki Y, et al. An extraterrestrial impact at the Permian-Triassic boundary? science, 2001,293(5539):2343.

[27] Farley K, Ward P, Garrison G, et al. Absence of extraterrestrial ^{3}He in Permian–Triassic age sedimentary rocks. Earth and Planetary Science Letters, 2005,240(2):265-275.

[28] 罗根明. 二叠纪—三叠纪之交的微生物地质过程和 CNS 生物地球化学循环: 中国地质大学, 2012.

[29] 殷鸿福, 黄思骥, 张克信, et al. 华南二叠纪一三叠纪之交的火山活动及其对生物绝灭的影响. 地质学报, 1989,63(2):169-181.

[30] Svensen H, Planke S, Polozov A G, et al. Siberian gas venting and the end-Permian environmental crisis. Earth and Planetary Science Letters, 2009,277(3):490-500.

[31] Renne P R, Black M T, Zichao Z, et al. Synchrony and causal relations between Permian-Triassic boundary crises and Siberian flood volcanism. science, 1995,269(5229):1413.

[32] Kamo S L, Czamanske G K, Amelin Y, et al. Rapid eruption of Siberian flood-volcanic rocks and evidence for coincidence with the Permian–Triassic boundary and mass extinction at 251 Ma. Earth and Planetary Science Letters, 2003,214(1):75-91.

[33] Reichow M K, Pringle M S, Al'Mukhamedov A I, et al. The timing and extent of the eruption of the Siberian Traps large igneous province: Implications for the end-Permian environmental crisis. Earth and Planetary Science Letters, 2009,277(1-2):9-20.

[34] Saunders A, Reichow M. The Siberian Traps and the End-Permian mass extinction: a critical

review. Chinese Science Bulletin, 2009,54(1):20-37.

[35] Renne P R, Basu A R. Rapid eruption of the Siberian Traps flood basalts at the Permo-Triassic boundary. Science, 1991,253(5016):176.

[36] Lo C H, Chung S L, Lee T Y, et al. Age of the Emeishan flood magmatism and relations to Permian–Triassic boundary events. Earth and Planetary Science Letters, 2002,198(3):449-458.

[37] Wignall P B, Sun Y D, Bond D P G, et al. Volcanism, mass extinction, and carbon isotope fluctuations in the Middle Permian of China. science, 2009,324(5931):1179-1182.

[38] Xie S C, Pancost R D, Wang Y B, et al. Cyanobacterial blooms tied to volcanism during the 5 my Permo-Triassic biotic crisis. Geology, 2010,38(5):447-450.

[39] Shen J, Algeo T J, Hu Q, et al. Negative C-isotope excursions at the Permian-Triassic boundary linked to volcanism. Geology, 2012,40:963-966.

[40] Shen J, Algeo T J, Zhou L, et al. Volcanic perturbations of the marine environment in South China preceding the latest Permian mass extinction and their biotic effects. Geobiology, 2012,10(1):82-103.

[41] Hays L E, Beatty T W, Henderson C M, et al. Evidence for photic zone euxinia through the end-Permian mass extinction in the Panthalassic Ocean (Peace River Basin, Western Canada). Palaeoworld, 2007,16(1):39-50.

[42] Nabbefeld B, Grice K, Twitchett R J, et al. An integrated biomarker, isotopic and palaeoenvironmental study through the Late Permian event at Lusitaniadalen, Spitsbergen. Earth and Planetary Science Letters, 2010,291(1):84-96.

[43] Luo G M, Huang J H, Xie S C, et al. Relationships between carbon isotope evolution and variation of microbes during the Permian–Triassic transition at Meishan Section, South China. International Journal of Earth Sciences, 2010,99(4):775-784.

[44] Luo G M, Wang Y b, Grice K, et al. Microbial-algal community changes during the latest Permian ecological crisis: Evidence from lipid biomarkers at Cili, South China. Global and Planetary Change, 2013:http://dx.doi.org/10.1016/j.gloplacha.2012.1011.1015.

[45] 张克信, 童金南, 殷鸿福, , et al. 浙江长兴二叠系—三叠系界线剖面层序地层研究. 地质学报, 1996,70(3):270-281.

[46] Gruszczynski M, Hoffman A, Malkowski K, et al. Seawater strontium isotopic perturbation at the Permian-Triassic boundary, West Spitsbergen, and its implications for the interpretation of strontium isotopic data. Geology, 1992,20(9):779-782.

[47] Berner R A. Examination of hypotheses for the Permo-Triassic boundary extinction by carbon cycle modeling. Proceedings of the National Academy of Sciences, 2002,99(7):4172.

[48] Sepkoski Jr J J. A kinetic model of Phanerozoic taxonomic diversity. III. Post-Paleozoic families and mass extinctions. Paleobiology, 1984:246-267.

[49] Ronov A B. Phanerozoic transgressions and regressions on the continents: a quantitative approach based on areas flooded by the sea and areas of marine and continental deposition. American Journal of Science, 1994,294(7):777-801.

[50] Falkowski P G, Katz M E, Knoll A H, et al. The Evolution of Modern Eukaryotic Phytoplankton.

science, 2004,305(5682):354-360.

[51] Servais T, Lehnert O, LI J, et al. The Ordovician Biodiversification: revolution in the oceanic trophic chain. Lethaia, 2008,41(2):99-109.

[52] Katz M E, Finkel Z V, Grzebyk D, et al. Evolutionary trajectories and biogeochemical impacts of marine eukaryotic phytoplankton. Annual review of ecology, evolution, and systematics, 2004:523-556.

[53] Moldowan J M, Dahl J, Jacobson S R, et al. Chemostratigraphic reconstruction of biofacies: molecular evidence linking cyst-forming dinoflagellates with pre-Triassic ancestors. Geology, 1996,24(2):159.

[54] Servais T, Stricanne L, Montenari M, et al. Population dynamics of galeate acritarchs at the Cambrian-Ordovician transition in the Algerian Sahara. Palaeontology, 2004,47(2):395-414.

[55] Servais T, Owen A W, Harper D A T, et al. The Great Ordovician biodiversification event (GOBE): the palaeoecological dimension. Palaeogeography, Palaeoclimatology, Palaeoecology, 2010,294(3):99-119.

[56] Le Hérissé A, Servais T, Wicander R. Devonian acritarchs and related forms. COURIER-FORSCHUNGSINSTITUT SENCKENBERG, 2000:195-205.

[57] Klug C, KrÖGer B, Kiessling W, et al. The Devonian nekton revolution. Lethaia, 2010,43(4):465-477.

[58] Riegel W. The Late Palaeozoic phytoplankton blackout -Artefact or evidence of global change. Review of Palaeobotany and Palynology, 2008,148(2-4):73-90.

[59] Strother P K, Servais T, Vecoli M. The effects of terrestrialization on marine ecosystems: the fall of CO_2. Geological Society, London, Special Publications, 2010,339(1):37-48.

[60] Servais T, Nützel A, Mullins G L. Was there a phytoplankton blackout in the late Paleozoic? Palynology, 2006,30:228.

[61] Head M J. Modern dinoflagellate cysts and their biological affinities. Palynology: principles and applications, 1996,3:1197-1248.

[62] Mullins G L, Servais T. The diversity of the Carboniferous phytoplankton. Review of Palaeobotany and Palynology, 2008,149(1-2):29-49.

[63] Colbath G K, Grenfell H R. Review of biological affinities of Paleozoic acid-resistant, organic-walled eukaryotic algal microfossils (including "acritarchs"). Review of Palaeobotany and Palynology, 1995,86(3-4):287-314.

[64] Eshet Y, Rampino M R, Visscher H. Fungal event and palynological record of ecological crisis and recovery across the Permian-Triassic boundary. Geology, 1995,23(11):967-970.

[65] Steiner M B, Eshet Y, Rampino M R, et al. Fungal abundance spike and the Permian-Triassic boundary in the Karoo Supergroup (South Africa). Palaeogeography, Palaeoclimatology, Palaeoecology, 2003,194(4):405-414.

[66] Visscher H, Brinkhuis H, Dilcher D L, et al. The terminal Paleozoic fungal event: evidence of terrestrial ecosystem destabilization and collapse. Proceedings of the National Academy of Sciences of the United States of America, 1996,93(5):2155-2158.

[67] Visscher H, Sephton M A, Looy C V. Fungal virulence at the time of the end-Permian biosphere crisis? Geology, 2011,39(9):883-886.

[68] Looy C V, Twitchett R J, Dilcher D L, et al. Life in the end-Permian dead zone. Proceedings of the National Academy of Sciences of the United States of America, 2001,98(14):7879.

[69] Li J, Cao C Q, Servais T, et al. Later Permian acritarchs from Meishan (SE China) in the context of Permian palaeobiogeography and palaeoecology. Neues Jahrbuch für Geologie und Paläontologie, Monatshefte, 2004:427-448.

[70] Traverse A. Permo-Triassic Palynofloras. Paleopalynology, 2007:275-287.

[71] Fensome R A, Palynologists A A o S. Acritarchs and fossil prasinophytes: an index to genera, species and infraspecific taxa: American Association of Stratigraphic Palynologists Foundation, 1990.

[72] Gradstein F M, Ogg J G, Smith A G, et al. A new geologic time scale, with special reference to Precambrian and Neogene. Episodes, 2004,27(2):83-100.

[73] Gutiérrez P R, Cisterna G A, Balarino L, et al. Formación Tupe (Carbonífero Superior-Pérmico inferior) en la mina La Delfina (Cuesta de Huaco, San Juan): contenido paleontológico. Ameghiniana, 2005,42(4):32-33.

[74] Gorter J D, Poynter S E, Bayford S W, et al. Glacially influenced petroleum plays in the Kulshill Group (Late Carboniferous Early Permian) of the southeastern Bonaparte Basin, Western Australia. The APPEA Journal, 2008,48(1):69-113.

[75] cKent L, Lindström S, Guy-Ohlson D. An Early Permian palynoflora from Milorgfjella, Dronning Maud Land, Antarctica. Antarctic Science, 1990,2(4):331-344.

[76] Lindström S. Early Permian palynostratigraphy of the northern Heimefrontfjella mountain-range, Dronning Maud Land, Antarctica. Review of Palaeobotany and Palynology, 1995,89(3-4):359-415.

[77] Di Pasquo M, Vergel M M, Azcuy C L. Pennsylvanian and Cisuralian palynofloras from the Los Sauces area, La Rioja Province, Argentina: Chronological and paleoecological significance. International Journal of Coal Geology, 2010,83(2-3):276-291.

[78] Beri Á, Gutiérrez P R, Cernuschi F, et al. Palinología del Pérmico Inferior en la perforación DCLS-24 (Formación San Gregorio), departamento de Cerro Largo, Uruguay. Parte I: esporas, algas, prasinofitas y acritarcas Ameghiniana, 2006,43(1):227-244.

[79] Beri Á, Martínez Blanco X, Mourelle D. A synthesis of palynological data from the Lower Permian Cerro Pelado Formation (Paraná Basin, Uruguay): A record of warmer climate stages during Gondwana glaciations. Geologica Acta, 2010,8(4):419-429.

[80] Besems R E, Schuurman W M L. Palynostratigraphy of Late Paleozoic glacial deposits of the Arabian Peninsula with special reference to Oman. Palynology, 1987(11):37-53.

[81] Stephenson M, Osterloff P, Filatoff J. Integrated palynological biozonation of the Permian of Saudi Arabia and Oman: progress and problems. GeoArabia, 2003,8:467-496.

[82] Stephenson M H, Angiolini L, Leng M J, et al. Abrupt environmental and climatic change during the deposition of the Early Permian Haushi limestone, Oman. Palaeogeography, Palaeoclimatology, Palaeoecology, 2008,270(1-2):1-18.

[83] Quadros L P. Acritarcos e tasmanites do Permo-Carbonífero da bacia do Paraná. Revista do Instituto Geológico, 2002,23(1):39-50.

[84] Souza P, Callegari L. An Early Permian Palynoflora from the Itararé Subgroup, Paraná Basin, Brazil. Revista española de micropaleontología, 2010,36(3):439-450.

[85] Guerra-Sommer M, Cazzulo-Klepzig M, Menegat R, et al. Geochronological data from the Faxinal coal succession, southern Paraná Basin, Brazil: A preliminary approach combining radiometric U-Pb dating and palynostratigraphy. Journal of South American Earth Sciences, 2008,25(2):246-256.

[86] Foster C. Stratigraphy and palynology of the Permian at Waterloo Bay, Yorke Peninsula, South Australia. Transactions of the Royal Society of South Australia, Incorporated, 1974,98:29-42.

[87] Foster C B, Waterhouse J B. the Granulatisporites confluens Oppel-zone and early Permian marine faunas from the Grant Formation on the Barbwire terrace, Canning Basin, Western Australia. Journal of the Geological Society of Australia, 1988,35(2):135-157.

[88] Mautino L R, Vergel M D M, Anzótegui L M. Palinologia de la Formacion Melo (Permico inferior) en Arroyo Seco, Departamento Rivera, Uruguay, Parte V: Granos de polen, acritarcas E Incertae sedis. Ameghiniana, 1998,35(3):299-314.

[89] Jardiné S. Microflores des formations du Gabon attribuées au Karroo. Review of Palaeobotany and Palynology, 1974,17(1-2):75-112.

[90] Lele K M, Kulkarni S. Two miospore assemblages from the Argada sector, south Karanpura coalfield, Bihar, with remarks on their probable age. The Palaeobotanist, 1969,17(3):288-293.

[91] Maithy P. Fossil flora from Barakar stage in Auranga Coalfield. The Palaeobotanist, 1971,19(1):70-76.

[92] Doubinger J, Marocco R. Contenu palynologique du groupe Copacabana (Permien Inférieur et Moyen) sur la bordure sud de la cordillère de Vilcabamba, Région de Cuzco (Pérou). Geologische Rundschau, 1981,70(3):1086-1099.

[93] Mori A L O, de Souza P A, Marques J C, et al. A new U–Pb zircon age dating and palynological data from a Lower Permian section of the southernmost Paraná Basin, Brazil: Biochronostratigraphical and geochronological implications for Gondwanan correlations. Gondwana Research, 2012,21(2–3):654-669.

[94] Mangerud G, Konieczny R. Palynology of the Permian succession of Spitsbergen, Svalbard. Polar research, 1993,12(1):65-93.

[95] Jansonius J. Palynology of Permian and Triassic sediments, Peace River area, western Canada. Palaeontographica Abteilung B, 1962,110(1-4):35-98.

[96] Tasch P. Hystrichosphaerids and dinoflagellates from the Permian of Kansas. Micropaleontology, 1963,9(3):332-336.

[97] Mangerud G. Palynostratigraphy of the Permian and lowermost Triassic succession, Finnmark Platform, Barents Sea. Review of Palaeobotany and Palynology, 1994,82(3-4):317-349.

[98] Cazzulo-klepzlg M, Guerra-Sommer M, Formoso N, et al. Geochemical and palynological evidence for the age determination of Permian coals, southern Brazil. Journal of South American Earth

Sciences, 2002,15(3):375-380.

[99] Pérez Loinaze V S, Césari S N, López Gamundí O, et al. Palynology of the Permian San Miguel Formation (Western Paraná Basin, Paraguay): Gondwanan biostratigraphic correlations. Geologica Acta, 2010,8(4):483-493.

[100] Playford G, Rigby J F. Permian palynoflora of the Ainim and Aiduna formations, West Papua. Revista española de micropaleontología, 2011,40(1-2):1-57.

[101] Beri Á, Gutiérrez P, Balarino L. Palynostratigraphy of the late Palaeozoic of Uruguay, Paraná Basin. Review of Palaeobotany and Palynology, 2011,167(1-2):16-29.

[102] Césari S N, Gutiérrez P R. Palynostratigraphy of Upper Paleozoic sequences in central-western Argentina. Palynology, 2000,24(1):113.

[103] Balarino M L, Gutiérrez P R. Palinología de la Formación Tasa Cuna (Pérmico Inferior), Córdoba, Argentina: sistemática y consideraciones bioestratigráficas Ameghiniana, 2006,43(2):437-460.

[104] Pieroni E M, Georgieff S M. Reconsideración estratigráfica del Neopaleozoico de los alrededores del dique Los Sauces, La Rioja. Revista de la Asociación Geológica Argentina, 2007,62(1):105-115.

[105] Gutiérrez P R, Correa G A, Carrevedo M L. Primer registro de palinomorfos de edad pérmica en la Formación Río Francia (Paleozoico Superior, San Juan, Argentina). Revista del Museo Argentino de Ciencias Naturales, 2010,12(2):203-216.

[106] Tiwari R S, Navale G K B. Pollen and spore assemblage in some coals of Brazil. Pollen et Spores, 1967,9(3):583-605.

[107] Holz M, Dias M E. Taphonomy of palynological records in a sequence stratigraphic framework: an example from the Early Permian Paraná Basin of southern Brazil. Review of Palaeobotany and Palynology, 1998,99(3-4):217-233.

[108] Iannuzzi R, dos Santos Scherer C M, de Souza P A, et al. Afloramento Morro do Papaléo, Mariana Pimentel, RS. Registro ímpar da sucessão sedimentar e florística pós-glacial do Paleozóico da Bacia do Paranά, 2006,2.

[109] Cazzulo-Klepzig M, Guerra-Sommer M, Menegat R, et al. Peat-forming environment of permian coal seams from the faxinal coalfield (Paraná Basin) in southern Brazil, based on palynology and palaeobotany. Revista brasileira de paleontologia, 2007,10(2):117-127.

[110] Gutiérrez P R, Beri Á, Balarino M L, et al. Palinología del Pérmico Inferior en la perforación CLS-24 (Cerro Largo Sur), departamento de Cerro Largo, Uruguay. Parte II: granos de polen Ameghiniana, 2006,43(3):611-635.

[111] Tiwari R S, Moiz A A. Palynological study of Lower Gondwana (Permian) coals from the Godavari Basin, India. The Palaeobotanist, 1971,19(1):95-106.

[112] Lele K M, Chandra A. Palynology of the marine intercalations in the lower Gondwana of Madhya Pradesh, India. The Palaeobotanist, 1972,19(3):253-262.

[113] Lele K M, Shukla M. Studies in the Talchir flora of India; 12, Palynology of the Talchir Formation of Hutar Coalfield, Bihar. Geophytology, 1979,10(1-2):231-238.

[114] Banerjee M, D'Rozario A. Palynostratigraphy and environment of deposition in the Lower

Gondwana sediments of Chuparbhita coalfield, Rajmahal Hills. Jour Palaeontol Soc India, 1988,33:73-90.

[115] Banerjee M, D'Rozario A. Palynostratigraphic correlation of lower Gondwana sediments in the Chuparbhita and Hura Basins, Rajmahal Hills, Eastern India. Review of Palaeobotany and Palynology, 1990,65(1-4):239-255.

[116] Foster C B. Permian plant microfossils from the Blair Athol Coal Measures, central Queensland, Australia. Palaeontographica Abteilung B: Palaeophytologie, 1975,154(5-6):121-171.

[117] Backhouse J. Permian palynostratigraphy of the Collie Basin, Western Australia. Review of Palaeobotany and Palynology, 1991,67(3-4):237-314.

[118] Wall D, Downie C. Permian hystrichospheres from Britain. Palaeontology, 1963,5(4):770-784.

[119] El-Nakhal H A, Stephenson M H, Owens B. New Late Carboniferous-Early Permian palynological data from glacial sediments in the Kooli Formation, Republic of Yemen. Micropaleontology, 2002,48(3):222.

[120] Kaiser H. Die permische Mikroflora der Cathaysia-Schichten von Nordwest-Schansi, China. Palaeontographica Abteilung B, 1976,159(4-6):83-157.

[121] Dyupina G V. Akritarkhi terrigennykh otlozheniy nizhney permi srednego Urala, Acritarchs from lower Permian terrigenous deposits of the central Urals (in Verkhnepaleozoyskiye terrigennyye otlozheniya Urala). Akademiya Nauk SSSR, Ural'skiy Filial, Institut Geologii i Geokhimii, Trudy, 1970,88:47-60.

[122] Newton E T. On “Tasmanite” and Australian “White Coal”. Geological Magazine (Decade II), 1875,12(08):337-342.

[123] Wilson L. A Permian hystrichosphaerid from Oklahoma. Oklahoma Geology Notes, 1960,20:170.

[124] Jacobson S R, Wardlaw B R, Saxton J D. Acritarchs from the Phosphoria and Park City Formations (Permian, Northeastern Utah). Journal of Paleontology, 1982,56(2):449-458.

[125] Grigoriev M, Utting J. Sedimentology, palynostratigraphy, palynofacies and thermal maturity of Upper Permian rocks of Kolguyev Island, Barents Sea, Russia. Bulletin of Canadian Petroleum Geology, 1998,46(1):1-11.

[126] Foster C B. Permian plant microfossils of the Blair Athol Coal Measures, Baralaba Coal Measures, and basal Rewan Formation of Queensland. Geological Survey of Queensland Publications, 1979(372):1-244.

[127] Lindström S. Late Permian palynology of Fossilryggen, Vestfjella, Dronning Maud Land, Antarctica. Palynology, 1996:15-48.

[128] Lindström S. Palynology of Permian shale, clay and sandstone clasts from the Basen till in northern Vestfjella, Dronning Maud Land. Antarctic Science, 2005,17(1):87-96.

[129] Bugge T, Ringas J, Leith D, et al. Upper Permian as a new play model on the mid-Norwegian continental shelf: Investigated by shallow stratigraphic drilling. AAPG Bulletin, 2002,86(1):107.

[130] Stolle E. Regional Permian palynological correlations: Southeast Turkey-Northern Iraq. Comunicações Geológicas, 2007,94:125-143.

[131] Stolle E. Recognition of southern Gondwanan palynomorphs at Gondwana's northern margin—and biostratigraphic correlation of Permian strata from SE Turkey and Australia. Geological Journal, 2010,45(2-3):336-349.

[132] Stolle E, Yalçin M N, Kavak O. The Permian Kas Formation of SE Turkey—palynological correlation with strata from Saudi Arabia and Oman. Geological Journal, 2011,46:561-573.

[133] Ouyang S. Upper Permian and Lower Triassic palynomorphs from eastern Yunnan, China. Canadian Journal of Earth Sciences, 1982,19(1):68-80.

[134] Ouyang S. Palynology of Upper Permian and Lower Triassic strata of Fuyuan district, Eastern Yunan. Palaeontologia sinica, 1986,169(9):1-122.

[135] Ouyang S, Utting J. Palynology of upper Permian and lower Triassic rocks, Meishan, Changxing County, Zhejiang Province, China. Review of Palaeobotany and Palynology, 1990,66(1-2):65-103.

[136] Jekhowsky B. Sur quelques hystrichospheres Permo-Triassiques d'Europe et d'Afrique. Revue de Micropaléontologie, 1961,3(4):207-212.

[137] Sarjeant W A S, Kummel B, Teichert C. Acritarchs and tasmanitids from the Chhidru Formation, uppermost Permian of West Pakistan. Stratigraphical Boundary Problems: Permian and Triassic of West Pakistan University of Kansas, Department of Geology, Special Publication, 1970,4:277-304.

[138] Hankel O. Late Permian to early triassic microfloral assemblages from the Maji y a Chumvi Formation, Kenya. Review of Palaeobotany and Palynology, 1992,72(1-2):129-147.

[139] McLoughlin S, Lindstr m S, Drinnan A N. Gondwanan floristic and sedimentological trends during the Permian-Triassic transition: new evidence from the Amery Group, northern Prince Charles Mountains, East Antarctica. Antarctic Science, 1997,9(3):281-298.

[140] Balme B E, Playford G. Late Permian plant microfossils from the Prince Charles Mountains, Antarctica. Revue de Micropaléontologie, 1967,10(3):179-192.

[141] Farabee M J, Taylor E L, Taylor T N. Late Permian palynomorphs from the Buckley Formation, central transantarctic mountains, Antarctica. Review of Palaeobotany and Palynology, 1991,69(4):353-368.

[142] Schaarschmidt F. Sporen und Hystrichosphaerideen aus dem Zechstein von Büdingen in der Wetterau. Palaeontographica Abteilung B, 1963,113(1-4):38-91.

[143] Horowitz A. Late Permian palynomorphs from southern Israel. Pollen et Spores, 1973,15(2):315-341.

[144] Horowitz A. Espéces du genre *Veryhachium* du Permo-Trias du Sud d'Israel. Revue de Micropaléontologie, 1974,17(2):75-80.

[145] Horowitz A. Palynology and paleoenvironment of uranium deposits in the Permian Beaufort Group, South Africa. Ore Geology Reviews, 1990,5(5-6):537-540.

[146] Balme B E, Segroves K L. *Peltacystia* gen. nov.: a microfossil of uncertain affinities from the Permian of Western Australia. Journal of the Royal Society of Western Australia, 1966,49(1):26-31.

[147] McMinn A. Late Permian acritarchs from the northern Sydney Basin. Journal and Proceedings of the Royal Society of New South Wales115, 1982,115:79-86.

[148] Fielding C, McLoughlin S. Sedimentology and palynostratigraphy of Permian rocks exposed at Fairbairn Dam, central Queensland. Australian Journal of Earth Sciences, 1992,39(5):631-649.

[149] Tripathi A. Permian, Jurassic and Early Cretaceous palynofloral assemblages from subsurface sedimentary rocks in Chuperbhita Coalfield, Rajmahal Basin, India. Review of Palaeobotany and Palynology, 2001,113(4):237-259.

[150] Dypvik H, Hankel O, Nilsen O, et al. The lithostratigraphy of the Karoo supergroup in the Kilombero Rift Valley, Tanzania. Journal of African Earth Sciences, 2001,32(3):451-470.

[151] Balme B E. Palynology of Permian and Triassic strata in the Salt range and Surghar range, West Pakistan. Special Publication - University of Kansas, Department of Geology, 1970,4:305-453.

[152] Hermann E, Hochuli P A, Bucher H, et al. Uppermost Permian to Middle Triassic palynology of the Salt Range and Surghar Range, Pakistan. Review of Palaeobotany and Palynology, 2012.

[153] Sandler A, Eshet Y, Schilman B. Evidence for a fungal event, methane-hydrate release and soil erosion at the Permian-Triassic boundary in southern Israel. Palaeogeography, Palaeoclimatology, Palaeoecology, 2006,242(1-2):68-89.

[154] Afonin S A, Barinova S S, Krassilov V A. A bloom of *Tympanicysta* Balme (green algae of zygnematalean affinities) at the Permian-Triassic boundary. Geodiversitas, 2001,23(4):481-487.

[155] Foster C B, Stephenson M H, Marshall C, et al. A revision of *Reduviasporonites* Wilson 1962: description, illustration, comparison and biological affinities. Palynology, 2002,26(1):35-58.

[156] Sephton M A, Visscher H, Looy C V, et al. Chemical constitution of a Permian-Triassic disaster species. Geology, 2009,37(10):875-878.

[157] Balme B E, Hennelly J P F. Monolete, monocolpate, and alete sporomorphs from Australian Permian sediments. Australian Journal of Botany, 1956,4(1):54-67.

[158] Stephen M. Plant fossil distributions in some Australian Permian non-marine sediments. Sedimentary Geology, 1993,85(1-4):601-619.

[159] Segroves K L. Cutinized microfossils of probable nonvascular origin from the Permian of Western Australia. Micropaleontology, 1967,13(3):289-305.

[160] Abramova S A, Martchenko O F. Opyt primeneniya palinologicheskogo metoda issledovaniya pri izuchenii solyanykh kupolov Prikaspiya (experimental applications of palynological methods of investigation to the study of salt-domes in the Pre-Caspian region). Vsesoyuznyi Nauchno-Issledovatelskii Institut Galurgii, Moskva, Trudy, 1964:49-52.

[161] Bose M, Kar R. Palaeozoic Sporae dispersae from Congo IV. On some new miospore genera. Mus Roy Afr Cent Tervuren, Belg Ann, 1967:241-263.

[162] Kar R K, Bose M N. Palaeozoic sporae dispersae from Zaire (Congo);XII, Assise a couches de houille from Greinerville region. Musee Royal de l'Afrique CentraleSerie in 8 (super 0) , Sciences Geologiques, 1976(77):23-133.

[163] Takahashi K. Plant microfossils from the Permian sandstone in the southern marginal area of the Tanba belt. Transactions and Proceedings of the Palaeontological Society of Japan New Series, 1969,73:41-48.

[164] Li J, Servais T. Ordovician acritarchs of China and their utility for global palaeobiogeography. Bulletin de la Societe Geologique de France, 2002,173(5):399-406.

[165] Servais T, Li J, Molyneux S G, et al. Ordovician organic-walled microphytoplankton (acritarch) distribution: the global scenario. Palaeogeography, Palaeoclimatology, Palaeoecology, 2003,195(1-2):149-172.

[166] Le Hérissé A, Gourvennec R. Biogeography of upper Llandovery and Wenlock acritarchs. Review of Palaeobotany and Palynology, 1995,86(1-2):111-133.

[167] Le Hérissé A, Gourvennec R, Wicander R. Biogeography of Late Silurian and Devonian acritarchs and prasinophytes. Review of Palaeobotany and Palynology, 1997,98(1-2):105-124.

[168] Jacobson S R. Acritarchs as paleoenvironmental indicators in Middle and Upper Ordovician rocks from Kentucky, Ohio and New York. Journal of Paleontology, 1979,53(5):1197-1212.

[169] Dorning K J. Silurian acritarchs from the type Wenlock and Ludlow of Shropshire, England. Review of Palaeobotany and Palynology, 1981,34(2):175-203.

[170] Vecoli M. Palaeoenvironmental interpretation of microphytoplankton diversity trends in the Cambrian-Ordovician of the northern Sahara Platform. Palaeogeography, Palaeoclimatology, Palaeoecology, 2000,160(3-4):329-346.

[171] Li J, Servais T, Yan K, et al. A nearshore-offshore trend in acritarch distribution from the Early-Middle Ordovician of the Yangtze Platform, South China. Review of Palaeobotany and Palynology, 2004,130(1-4):141-161.

[172] Stricanne L, Munnecke A, Pross J, et al. Acritarch distribution along an inshore-offshore transect in the Gorstian (lower Ludlow) of Gotland, Sweden. Review of Palaeobotany and Palynology, 2004,130(1-4):195-216.

[173] Ziegler A M, Hulver M L, Rowley D B. Permian world topography and climate. *In*: Martini, I P (ed) Late glacial and postglacial environmental changes-Quaternary, Carboniferous-Permian and Proterozoic, 1996:111-146.

[174] Gilby A R, Foster C B. Early Permian palynology of the Arckaringa Basin, South Australia. Palaeontographica Abteilung B: Palaeophytologie, 1988,209(4-6):167-191.

[175] Lindström S. Early Late Permian palynostratigraphy and palaeo-biogeography of Vestfjella, Dronning Maud Land, Antarctica. Review of Palaeobotany and Palynology, 1995,86(1-2):157-173.

[176] Sun Y D, Joachimski M M, Wignall P B, et al. Lethally Hot Temperatures During the Early Triassic Greenhouse. science, 2012,338(6105):366-370.

[177] Metcalfe I, Nicoll R S. Conodont biostratigraphic control on transitional marine to non-marine Permian-Triassic boundary sequences in Yunnan-Guizhou, China. Palaeogeography, Palaeoclimatology, Palaeoecology, 2007,252(1-2):56-65.

[178] He W H, Shi G R, Gao Y Q, et al. A new Early Triassic microgastropod fauna from the Zhongzhai Section, Guizhou, southwestern China. Proceedings of the Royal Society of Victoria, 2008,120(1):157-166.

[179] Peng Y Q, Zhang S X, Yu T X, et al. High-resolution terrestrial permian-triassic

eventostratigraphic boundary in western Guizhou and eastern Yunnan, southwestern China. Palaeogeography, Palaeoclimatology, Palaeoecology, 2005,215(3-4):285-295.

[180] Yin H F, Zhang K X, Tong J N, et al. The global stratotype section and point (GSSP) of the Permian-Triassic boundary. Episodes, 2001,24(2):102-114.

[181] Jiang H S, Lai X L, Luo G M, et al. Restudy of conodont zonation and evolution across the P/T boundary at Meishan section, Changxing, Zhejiang, China. Global and Planetary Change, 2007,55(1-3):39-55.

[182] Zhang K X, Tong J N, Shi G R, et al. Early Triassic conodont-palynological biostratigraphy of the Meishan D Section in Changxing, Zhejiang Province, South China. Palaeogeography, Palaeoclimatology, Palaeoecology, 2007,252(1-2):4-23.

[183] Feng Q, Gu S, Hu W, et al. Latest Permian Entactinaria (Radiolaria) from southern Guangxi, China. Journal of Micropalaeontology, 2007,26(1):19-37.

[184] Wignall P B, Hallam A, Lai X L, et al. Palaeoenvironmental changes across the Permian/Triassic boundary at Shangsi (N. Sichuan, China). Historical Biology, 1995,10(2):175-189.

[185] Lai X L, Yang F Q, Hallam A, et al. The Shangsi section, candidate of the Global Stratotype section and point of the Permian-Triassic boundary. In: Yin, H F (Ed), The Palaeozoic-Mesozoic Boundary Candidates of Global Stratotype Section and Point of the Permian-Triassic Boundary China University of Geosciences Press, Wuhan, 1996:113-124.

[186] 李子舜, 詹立培, 朱秀芳, et al. 古生代—中生代之交的生物绝灭和地质事件—四川广元上寺二叠系—三叠系界线和事件的初步研究. 地质学报, 1986(1):1-17.

[187] Nicoll R S, Metcalfe I, Cheng-Yuan W. New species of the conodont genus Hindeodus and the conodont biostratigraphy of the Permian-Triassic boundary interval. Journal of Asian Earth Sciences, 2002,20(6):609-631.

[188] Jiang H S, Lai X L, Yan C B, et al. Revised conodont zonation and conodont evolution across the Permian–Triassic boundary at the Shangsi section, Guangyuan, Sichuan, South China. Global and Planetary Change, 2011,77(3–4):103-115.

[189] Wang G Q, Xia W C. Conodont zonation across the Permian Triassic boundary at the Xiakou section, Yichang city, Hubei Province and its correlation with the Global Stratotype Section and Point of the PTB. Canadian Journal of Earth Sciences, 2004,41(3):323-330.

[190] 王正允. 湖北兴山大峡口二叠系沉积相及层序地层特征. 江汉石油学院学报, 1998,20(3):1-7.

[191] Mutwakil N, Xia W C, Zhang N. Late Permian (Changhsingian) conodont biozonation and the basal boundary, Ganxi section, western Hubei Province, south China. Canadian Journal of Earth Sciences, 2006,43(2):121-133.

[192] He W H, Feng Q L, Weldon E A, et al. A late Permian to early Triassic bivalve fauna from the Dongpan Section, southern Guangxi, South China. Journal of Paleontology, 2007,81(5):1009-1019.

[193] He W H, Shen S Z, Feng Q L, et al. A late Changhsingian (Late Permian) deepwater brachiopod fauna from the Talung Formation at the Dongpan section, southern Guangxi, South China. Journal of

Paleontology, 2005,79(5):927-938.

[194] He W H, Shi G R, Feng Q L, et al. Brachiopod miniaturization and its possible causes during the Permian–Triassic crisis in deep water environments, South China. Palaeogeography, Palaeoclimatology, Palaeoecology, 2007,252(1):145-163.

[195] Butterfield N J, Chandler F W. Paleoenvironmental distribution of Proterozoic microfossils, with an example from the Agu Bay Formation, Baffin Island. Palaeontology, 1992,35(4):943-957.

[196] Colbath G K. Abundance fluctuations in Upper Ordovician organic-walled microplankton from Indiana. Micropaleontology, 1980,26(1):97-102.

[197] Xu W. Depth zonation of Arenigian acritarchs in South China. Chinese Science Bulletin, 1997,42(3):248-251.

[198] Yan K, Li J. The palaeoenvironmental implication of Early-Middle Ordovician acritarch communities from South China. Chinese Science Bulletin, 2010,55(10):957-964.

[199] Smith N, Saunders R. Paleoenvironments and their control of acritarch distribution; Silurian of east-central Pennsylvania. Journal of Sedimentary Research, 1970,40(1):324.

[200] Dorning K. The organic palaeontology of Palaeozoic carbonate environments. Micropalaeontology of Carbonate Environments Ellis Horwood, Chichester, England, 1987:256-265.

[201] Dorning K, Bell D. The Silurian carbonate shelf microflora: acritarch distribution in the Much Wenlock Limestone Formation. In: Hart, M.B. (Ed.),. Micropalaeontology of Carbonate Environments Ellis Horwood, Chichester, England, 1987:266-287.

[202] Richardson J, Rasul S. Palynofacies in a Late Silurian regressive sequence in the Welsh Borderland and Wales. Journal of the Geological Society, 1990,147(4):675-686.

[203] Al-Ameri T K. Acid-resistant microfossils used in the determination of Palaeozoic palaeoenvironments in Libya. Palaeogeography, Palaeoclimatology, Palaeoecology, 1983,44(1-2):103-116.

[204] Staplin F L. Reef-controlled distribution of Devonian microplankton in Alberta. Palaeontology, 1961,4(3):392-424.

[205] Riegel W. Phytoplankton from the upper Emsian and Eifelian of the Rhineland, Germany--A preliminary report. Review of Palaeobotany and Palynology, 1974,18(1-2):29-39.

[206] Wicander R, Wood G D. The use of microphytoplankton and chitinozoans for interpreting transgressive/regressive cycles in the Rapid Member of the Cedar Valley Formation (Middle Devonian), Iowa. Review of Palaeobotany and Palynology, 1997,98(1-2):125-152.

[207] Wall D. Microplankton, pollen, and spores from the Lower Jurassic in Britain. Micropaleontology, 1965,11(2):151-190.

[208] Devillers R, De Vernal A. Distribution of dinoflagellate cysts in surface sediments of the northern North Atlantic in relation to nutrient content and productivity in surface waters. Marine Geology, 2000,166(1):103-124.

[209] Pospelova V, Chmura G L, Walker H A. Environmental factors influencing the spatial distribution of dinoflagellate cyst assemblages in shallow lagoons of southern New England (USA). Review of

Palaeobotany and Palynology, 2004,128(1-2):7-34.

[210] Pospelova V, de Vernal A, Pedersen T F. Distribution of dinoflagellate cysts in surface sediments from the northeastern Pacific Ocean (43–25°N) in relation to sea-surface temperature, salinity, productivity and coastal upwelling. Marine Micropaleontology, 2008,68(1–2):21-48.

[211] Bouimetarhan I, Marret F, Dupont L, et al. Dinoflagellate cyst distribution in marine surface sediments off West Africa (17-6 N) in relation to sea-surface conditions, freshwater input and seasonal coastal upwelling. Marine Micropaleontology, 2009,71(3-4):113-130.

[212] Stricanne L, Servais T. A statistical approach to classification of the Cambro-Ordovician galeate acritarch plexus. Review of Palaeobotany and Palynology, 2002,118(1-4):239-259.

[213] Mertens K N, Ribeiro S, Bouimetarhan I, et al. Process length variation in cysts of a dinoflagellate, *Lingulodinium machaerophorum*, in surface sediments: Investigating its potential as salinity proxy. Marine Micropaleontology, 2009,70(1):54-69.

[214] Sheldon N D. Abrupt chemical weathering increase across the Permian–Triassic boundary. Palaeogeography, Palaeoclimatology, Palaeoecology, 2006,231(3):315-321.

[215] Algeo T J, Twitchett R J. Anomalous Early Triassic sediment fluxes due to elevated weathering rates and their biological consequences. Geology, 2010,38(11):1023-1026.

[216] Schopf J W. Microfossils of the Early Archean Apex chert: new evidence of the antiquity of life. science, 1993,260(5108):640-646.

[217] Capone D G, Zehr J P, Paerl H W, et al. *Trichodesmium*, a globally significant marine cyanobacterium. science, 1997,276(5316):1221-1229.

[218] Wiegand C, Pflugmacher S. Ecotoxicological effects of selected cyanobacterial secondary metabolites a short review. Toxicology and Applied Pharmacology, 2005,203(3):201-218.

[219] Briand J F, Jacquet S, Bernard C, et al. Health hazards for terrestrial vertebrates from toxic cyanobacteria in surface water ecosystems. Veterinary research, 2003,34(4):361-377.

[220] 方凤满, 金高洁, 高超. 巢湖蓝藻爆发多要素预测模型研究. 地理科学, 2010,30(5):760-765.

[221] Kahru M, Savchuk O, Elmgren R. Satellite measurements of cyanobacterial bloom frequency in the Baltic Sea: interannual and spatial variability. Marine Ecology Progress Series, 2007,343:15-23.

[222] Walsby A, Dubinsky Z, Kromkamp J, et al. The effects of diel changes in photosynthetic coefficients and depth of Planktothrix rubescens on the daily integral of photosynthesis in Lake Zürich. Aquatic Sciences-Research Across Boundaries, 2001,63(3):326-349.

[223] Phlips E J, Badylak S. Spatial variability in phytoplankton standing crop and composition in a shallow inner-shelf lagoon, Florida Bay, Florida. Bulletin of Marine Science, 1996,58(1):203-216.

[224] Phlips E J, Badylak S, Lynch T C. Blooms of the picoplanktonic cyanobacterium Synechococcus in Florida Bay, a subtropical inner-shelf lagoon. Limnology and Oceanography, 1999:1166-1175.

[225] Hall M O, Durako M J, Fourqurean J W, et al. Decadal changes in seagrass distribution and abundance in Florida Bay. Estuaries and Coasts, 1999,22(2):445-459.

[226] O'Neil J M, Davis T W, Burford M A, et al. The rise of harmful cyanobacteria blooms: The potential roles of eutrophication and climate change. Harmful algae, 2012,14:313-334.

[227] DeMott W R, Zhang Q X, Carmichael W W. Effects of toxic cyanobacteria and purified toxins on the survival and feeding of a copepod and three species of Daphnia. Limnology and Oceanography, 1991:1346-1357.

[228] Engström-Öst J, Lehtiniemi M, Green S, et al. Does cyanobacterial toxin accumulate in mysid shrimps and fish via copepods? Journal of Experimental Marine Biology and Ecology, 2002,276(1–2):95-107.

[229] Golubic S, Abed R M M, Palińska K, et al. Marine toxic cyanobacteria: Diversity, environmental responses and hazards. Toxicon, 2010,56(5):836-841.

[230] Karlson A M L, Mozūraitis R. Deposit-feeders accumulate the cyanobacterial toxin nodularin. Harmful algae, 2011,12(0):77-81.

[231] Heiskanen A S, Kononen K. Sedimentation of vernal and late summer phytoplankton communities in the coastal Baltic Sea. Archiv fur Hydrobiologie Stuttgart, 1994,131(2):175-198.

[232] Sellner K, Olson M, Kononen K. Copepod grazing in a summer cyanobacteria bloom in the Gulf of Finland. Hydrobiologia, 1994,292(1):249-254.

[233] Vahtera E, Conley D J, Gustafsson B G, et al. Internal ecosystem feedbacks enhance nitrogen-fixing cyanobacteria blooms and complicate management in the Baltic Sea. AMBIO: A journal of the Human Environment, 2007,36(2):186-194.

[234] FerrÃo-Filho A S, Azevedo S M F O, DeMott W R. Effects of toxic and non-toxic cyanobacteria on the life history of tropical and temperate cladocerans. Freshwater Biology, 2001,45(1):1-19.

[235] Bianchi T S, Engelhaupt E, Westman P, et al. Cyanobacterial blooms in the Baltic Sea: Natural or human-induced? Limnology and Oceanography, 2000:716-726.

[236] Boyd P W, Law C S, Wong C, et al. The decline and fate of an iron-induced subarctic phytoplankton bloom. Nature, 2004,428(6982):549-553.

[237] Kanoshina I, Lips U, Leppänen J M. The influence of weather conditions (temperature and wind) on cyanobacterial bloom development in the Gulf of Finland (Baltic Sea). Harmful algae, 2003,2(1):29-41.

[238] Posch T, Koster O, Salcher M M, et al. Harmful filamentous cyanobacteria favoured by reduced water turnover with lake warming. Nature Clim Change, 2012,advance online publication.

[239] Zwirglmaier K, Jardillier L, Ostrowski M, et al. Global phylogeography of marine *Synechococcus* and *Prochlorococcus* reveals a distinct partitioning of lineages among oceanic biomes. Environmental microbiology, 2008,10(1):147-161.

[240] Moore L R, Post A F, Rocap G, et al. Utilization of different nitrogen sources by the marine cyanobacteria Prochlorococcus and Synechococcus. Limnology and Oceanography, 2002:989-996.

[241] Lehrmann D J. Early Triassic calcimicrobial mounds and biostromes of the Nanpanjiang basin, South China. Geology, 1999,27(4):359-362.

[242] Wang Y B, Tong J N, Wang J S, et al. Calcimicrobialite after end-Permian mass extinction in South China and its palaeoenvironmental significance. Chinese Science Bulletin, 2005,50(7):665-671.

[243] Jiang H X, Wu Y S, Cai C F. Filamentous cyanobacteria fossils and their significance in the

Permian-Triassic boundary section at Laolongdong, Chongqing. Chinese Science Bulletin, 2008,53(12):1871-1879.

[244] Kershaw S, Li Y, Crasquin-Soleau S, et al. Earliest Triassic microbialites in the South China block and other areas: Controls on their growth and distribution. Facies, 2007,53(3):409-425.

[245] Xie S C, Pancost R D, Yin H F, et al. Two episodes of microbial change coupled with Permo/Triassic faunal mass extinction. Nature, 2005,434(7032):494-497.

[246] Joachimski M M, Lai X L, Shen S Z, et al. Climate warming in the latest Permian and the Permian–Triassic mass extinction. Geology, 2012,40(3):195-198.

[247] Yin H, Xie S, Luo G, et al. Two episodes of environmental change at the Permian–Triassic boundary of the GSSP section Meishan. Earth-Science Reviews, 2012,115(3):163-172.

[248] Ayris P, Delmelle P. Volcanic and atmospheric controls on ash iron solubility: A review. Physics and Chemistry of the Earth, Parts A/B/C, 2012,45–46:103-112.

[249] Lindenthal A, Langmann B, Paetsch J, et al. The ocean response to volcanic iron fertilisation after the eruption of Kasatochi volcano: a regional scale biogeochemical ocean model study. Biogeosciences Discuss, 2012,9:9233-9257.

[250] Abraham E R, Law C S, Boyd P W, et al. Importance of stirring in the development of an iron-fertilized phytoplankton bloom. Nature, 2000,407(6805):727-730.

[251] Duggen S, Olgun N, Croot P, et al. The role of airborne volcanic ash for the surface ocean biogeochemical iron-cycle: a review. Biogeosciences, 2010,7(3):827-844.

[252] Olgun N, Duggen S, Croot P L, et al. Surface ocean iron fertilization: The role of airborne volcanic ash from subduction zone and hot spot volcanoes and related iron fluxes into the Pacific Ocean. Global Biogeochemical Cycles, 2011,25(4):GB4001.

[253] Wignall P, Twitchett R. Oceanic anoxia and the end Permian mass extinction. science, 1996,272(5265):1155-1158.

[254] Hairston N, Holtmeier C, Lampert W, et al. Natural selection for grazer resistance to toxic cyanobacteria: evolution of phenotypic plasticity? Evolution, 2007,55(11):2203-2214.

[255] Nascimento F J A, Karlson A M L, Näslund J, et al. Settling cyanobacterial blooms do not improve growth conditions for soft bottom meiofauna. Journal of Experimental Marine Biology and Ecology, 2009,368(2):138-146.

[256] Lance E, Brient L, Carpentier A, et al. Impact of toxic cyanobacteria on gastropods and microcystin accumulation in a eutrophic lake (Grand-Lieu, France) with special reference to Physa (= Physella) acuta. Science of the total environment, 2010,408(17):3560-3568.

[257] Limén H, Ólafsson E. Ostracod species-specific utilisation of sediment detritus and newly settled cyanobacteria, *Aphanizomenon* sp., in the Baltic Sea: evidence from stable carbon isotopes. Marine Biology, 2002,140(4):733-738.

[258] He W H, Twitchett R J, Zhang Y, et al. Controls on body size during the Late Permian mass extinction event. Geobiology, 2010,8(5):391-402.

[259] Algeo T J, Chen Z Q, Fraiser M L, et al. Terrestrial–marine teleconnections in the collapse and

rebuilding of Early Triassic marine ecosystems. Palaeogeography, Palaeoclimatology, Palaeoecology, 2011,308(1):1-11.

[260] Song H J, Tong J N, Chen Z Q. Evolutionary dynamics of the Permian–Triassic foraminifer size: Evidence for Lilliput effect in the end-Permian mass extinction and its aftermath. Palaeogeography, Palaeoclimatology, Palaeoecology, 2011,308(1):98-110.

[261] Chen Z Q, Benton M J. The timing and pattern of biotic recovery following the end-Permian mass extinction. Nature Geoscience, 2012,5(6):375-383.

[262] Luo G, Lai X, Shi G R, et al. Size variation of conodont elements of the Hindeodus-Isarcicella clade during the Permian-Triassic transition in South China and its implication for mass extinction. Palaeogeography, Palaeoclimatology, Palaeoecology, 2008,264(1-2):176-187.

[263] Servais T, Vecoli M, Li J, et al. The acritarch genus *Veryhachium* Deunff 1954: taxonomic evaluation and first appearance. Palynology, 2007,31(1):191-203.

[264] Sarjeant W A S, Stancliffe R P W. The Micrhystridium and Veryhachium complexes (Acritarcha: Acanthomorphitae and Polygonomorphitae); a taxonomic reconsideration. Micropaleontology, 1994,40(1):1-77.

[265] Visscher H, Brugman W A. Ranges of selected palynomorphs in the Alpine Triassic of Europe. Review of Palaeobotany and Palynology, 1981,34(1):115-128.

[266] Van de Schootbrugge B, Bailey T R, Rosenthal Y, et al. Early Jurassic climate change and the radiation of organic-walled phytoplankton in the Tethys Ocean. Paleobiology, 2005,31(1):73-97.

[267] Grice K, Twitchett R J, Alexander R, et al. A potential biomarker for the Permian-Triassic ecological crisis. Earth and Planetary Science Letters, 2005,236(1-2):315-321.

[268] Hays L E, Grice K, Foster C B, et al. Biomarker and isotopic trends in a Permian-Triassic sedimentary section at Kap Stosch, Greenland. Organic Geochemistry, 2011,43:67-82.

[269] Talyzina N M, Moldowan J M, Johannisson A, et al. Affinities of Early Cambrian acritarchs studied by using microscopy, fluorescence flow cytometry and biomarkers. Review of Palaeobotany and Palynology, 2000,108(1-2):37-53.

[270] Schulz E. Sporae dispersae aus der Trias von Thüringen. Abhandlungen des ZGI, 1965,1:257-287.

[271] Besems R E. Aspects of middle and late triassic palynology. 2. Preliminary palynological data from the hornos--siles formation of the prebetic zone, NE province of Jaen (Southeastern Spain). Review of Palaeobotany and Palynology, 1981,32(4):389-400.

[272] Johnson N G. Early Silurian palynomorphs from the Tuscarora Formation in central Pennsylvania and their paleobotanical and geological significance. Review of Palaeobotany and Palynology, 1985,45(3-4):307-359.

[273] Gaucher C, Germs G J B. Recent advances in South African Neoproterozoic-Early Palaeozoic biostratigraphy: correlation of the Cango Caves and Gamtoos Groups and acritarchs of the Sardinia Bay Formation, Saldania Belt. South African Journal of Geology, 2006,109(1-2):193-214.

[274] Vavrdová M. Proterozoic acritarchs from the Precambrian-Cambrian transition in southern

Moravia (Mìnín-1 borehole, Czech Republic). Bulletin of Geosciences, 2008,83(1):85-92.

[275] Bhat G M, Ram G, Koul S. Potential for oil and gas in the Proterozoic carbonates (Sirban Limestone) of Jammu, northern India. Geological Society, London, Special Publications, 2009,326(1):245-254.

[276] Maslov A V. Riphean and Vendian sedimentary sequences of the Timanides and Uralides, the eastern periphery of the East European Craton. Geological Society, London, Memoirs, 2004,30(1):19-35.

[277] Stanevich A M, Maksimova E N, Kornilova T A, et al. Microfossils of the late Proterozoic Debengdinskaya Formation of the Olenekskiy uplift. Bulletin of the Томск Polytechnic University, 2007,311(1):9-14.

[278] Vorob'eva N G, Sergeev V N, Knoll A H. Neoproterozoic Microfossils from the Northeastern Margin of the East European Platform. Journal of Paleontology, 2009,83(2):161-196.

[279] Moczydłowska M. The Ediacaran microbiota and the survival of Snowball Earth conditions. Precambrian Research, 2008,167(1-2):1-15.

[280] Leonov M V, Ragozina A L. Upper Vendian assemblages of carbonaceous micro-and macrofossils in the White Sea Region: systematic and biostratigraphic aspects. Geological Society, London, Special Publications, 2007,286(1):269-275.

[281] Gaucher C, Blanco G, Chiglino L, et al. Acritarchs of Las Ventanas Formation (Ediacaran, Uruguay): Implications for the timing of coeval rifting and glacial events in western Gondwana. Gondwana Research, 2008,13(4):488-501.

[282] Konzalová O F M. Microfossils of the Paseky Shale (Lower Cambrian, Czech Republic). Journal of the Czech Geological Society, 1995,40(4):55-66.

[283] Steiner M, Fatka O. Lower Cambrian tubular micro-to macrofossils from the Paseky Shale of the Barrandian area (Czech Republic). Paläntologische Zeitschrift, 1996,70(3):275-299.

[284] Naumova S N. Spores of the Lower Cambrian. Izvestiya Akademiya Nauk SSSR, Seriya Geologicheskaya, 1949,4:49-56.

[285] Utting J. Geological Survey of Canada, Open File 593. Natural Resources Canada. Natural Resources Canada1978.

[286] Utting J, Spina A, Jansonius J, et al. Reworked miospores in the Upper Paleozoic and Lower Triassic of the northern circum-polar area and selected localities. Palynology, 2004,28(1):75.

[287] Utting J, Zonneveld J P, MacNaughton R B, et al. Palynostratigraphy, lithostratigraphy and thermal maturity of the Lower Triassic Toad and Grayling, and Montney formations of western Canada, and comparisons with coeval rocks of the Sverdrup Basin, Nunavut. Bulletin of Canadian Petroleum Geology, 2005,53(1):5-24.

[288] Zonneveld J P, Beatty T W, MacNaughton R B, et al. Sedimentology and ichnology of the Lower Triassic Montney Formation in the Pedigree-Ring/Border-Kahntah River area, northwestern Alberta and northeastern British Columbia. Bulletin of Canadian Petroleum Geology, 2010,58(2):115-140.

[289] Ilyina N V, Egorov A Y. The Upper Triassic of northern Middle Siberia: stratigraphy and

palynology. Polar Research, 2008,27(3):372-392.

[290] Collom C J, Hills L V. Geological Survey of Canada, Open File 3833. Natural Resources Canada: Natural Resources Canada, 1999.

[291] Sarjeant W A S. Microplankton from the Ampthill Clay of Melton, South Yorkshire. Palaeontology, 1962,5(3):478-497.

[292] Van de Schootbrugge B, Tremolada F, Rosenthal Y, et al. End-Triassic calcification crisis and blooms of organic-walled 'disaster species'. Palaeogeography, Palaeoclimatology, Palaeoecology, 2007,244(1-4):126-141.

[293] Porter R. Palynological evidence for Jurassic microplankton provinces in Great Britain. Review of Palaeobotany and Palynology, 1988,56(1-2):21-39.

[294] Stancliffe R P W. Acritarchs and other non-Dinophycean marine Palynomorphs from the Oxfordian (Upper Jurassic) of Skye, Western Scotland and Dorset, Southern England. Palynology, 1990,14(1):175-192.

[295] Stockmans F, Willière Y. Les *Hystrichosphères* ou mieux les Acritarches du Silurien Belge. Sondage de la Brasserie Lust à Courtrai (Kortrijk). Bulletin de la Société belge de Géologie, de paléontologie et d' hydrologie1963.

[296] Higgs K T, Finucane D, Tunbridge I P. Late Devonian and early Carboniferous microfloras from the HakkarI Province of southeastern Turkey. Review of Palaeobotany and Palynology, 2002,118(1-4):141-156.

[297] Eley B E, Legault J A. Palymorphs from the Manitoulin Formation (Early Llandovery) of southern Ontario. Palynology, 1988,12(1):49-63.

[298] Deflandre G. Microfossiles des calcaires siluriens de la Montagne Noire. Annales de Paléontologie1945.

[299] Gelsthorpe D N. Microplankton changes through the early Silurian Ireviken extinction event on Gotland, Sweden. Review of Palaeobotany and Palynology, 2004,130(1-4):89-103.

[300] Stricanne L, Munnecke A, Pross J. Assessing mechanisms of environmental change: Palynological signals across the Late Ludlow (Silurian) positive isotope excursion (δ^{13}C, δ^{18}O) on Gotland, Sweden. Palaeogeography, Palaeoclimatology, Palaeoecology, 2006,230(1-2):1-31.

[301] Marhoumi R, Rauscher R. Un plancton Dévonien de la Méseta orientale au Maroc. Review of Palaeobotany and Palynology, 1984,43(1-3):237-253.

[302] Filipiak P. Lower Famennian phytoplankton from the Holy Cross Mountains, Central Poland. Review of Palaeobotany and Palynology, 2009,157(3-4):326-338.

[303] Gao L D. Late Devonian and Early Carboniferous acritarchs from Nyalam county, Xizang (Tibet), China. Review of Palaeobotany and Palynology, 1986,47(1-2):17-30.

[304] Wilson L R. A Permian fungus spore type from the Flowerpot Formation of Oklahoma. Oklahoma Geology Notes, 1962,22(4):91-96.

[305] Elsik W C. *Reduviasporonites* Wilson 1962: Synonymy of the fungal organism involved in the late Permian crisis. Palynology, 1999:37-41.

[306] Kalgutkar R M, Braman D R. Santonian To ?Earliest Campanian (Late Cretaceous) Fungi from the Milk River Formation, Southern Alberta, Canada. Palynology, 2008,32(1):39.

[307] Balme B E. Palynology of Permian-Triassic boundary beds at Kap Stosch, East Greenland. Meddelelser om Grønland1979.

[308] Wood G D, Elsik W C. Paleoecologic and stratigraphic importance of the fungus Reduviasporonites stoschianus from the'Early-Middle'Pennsylvanian of the Copacabana Formation, Peru. Palynology, 1999,23:43-53.

[309] Cookson I C. Additional Microplankton from Australian Late Mesozoic and Tertiary Sediments. Marine and Freshwater Research, 1956,7(1):183-191.

[310] Stockmans F, Willière Y. *Hystrichosphères* du Dévonien belge (Sondage de l'Asile d'alienés à Tournai). Senckenbergiana Lethaea, 1960,41:1-11.

[311] Moreau-Benoit A. Acritarches et chitinozoaires du Dévonien moyen et supérieur de Libye occidentale. Review of Palaeobotany and Palynology, 1984,43(1-3):187-216.

图版与图版说明

图版 1

各研究剖面野外露头 PTB 附近的照片

图版 2

比例尺均为 10 微米；1-9 为扫描电镜照片，10-12 为光学显微镜照片；
样品均来自上寺剖面/SS292-4
1-12：*Dictyotidium reticulatum* Schulz, 1965

图版 3

比例尺均为 10 微米；均为光学显微镜照片；
样品号：
1-7、9-15、17-25：上寺剖面/SS25-E；
8、16：凉风垭剖面/LFY-1-A
1-8：*Veryhachium hyalodermum* (Cookson, 1955) Schaarschmidt, 1963
9-12：*Veryhachium nasicum* (Stockmans and Willière, 1960) Stockmans and Willière, 1962
13-17：*Veryhachium sedecimspinosum* Staplin, 1961
18-20：*Michrystridium pentagonale* Stockmans and Willière, 1963
21-25：*Veryhachium cylindricum* Schaarschmidt, 1963

图版 4

比例尺均为 10 微米；均为光学显微镜照片；
样品号：
1：中寨剖面/ZZ22-2；
2：上寺剖面/SS289-1-2；
3-5、8：上寺剖面/SS290-7；
6-7、9、19-24：上寺剖面/SS25-E；
10-12：凉风垭剖面/LFY-1-B；
13-18：上寺剖面/TS28-18
1：*Baltisphaeridium* sp.
2：*Leiofusa* sp.
3：*Veryhachium* sp.
4：*Veryhachium quadratum* Schaarschmidt, 1963
5：*Michrystridium fragile* Deflandre, 1947
6-12：*Michrystridium stellatum* Deflandre, 1945
13-24：*Michrystridium breve* Jansonius, 1962

图版 5

比例尺均为 10 微米；均为光学显微镜照片；

样品号：

1-10：上寺剖面/SS25-E；

11-16：上寺剖面/SS290-8-1；

17-22：上寺剖面/SS291-2.

1-7：*Schizosporis* sp.

8-10：*Schizosporis scissus* (Blame and Hennelly, 1956) Hart, 1965

11-22：*Leiosphaeridia microgranifera* (Staplin, 1961) Downie and Sarjeant, 1965

图版 6

比例尺均为 10 微米；1-14、17-19 为光学显微镜照片，15-16 为扫描电镜照片；

样品号：

1-4：东攀剖面/DP2-G；

5-8：东攀剖面/DP5-B；

9-14：上寺剖面/SS25-E；

15-16：上寺剖面/SS292-4；

17-18：煤山剖面/MS-26；

19：上寺剖面/SS16-26

1-14：*Leiosphaeridia minutissima* (Naumova, 1949) Jankauskas, 1989

15-16：*Dictyotidium* sp.

17-19：foraminifera linings

图版 7

比例尺均为 10 微米；均为光学显微镜照片；

样品号：

1-6、11、14、23：上寺剖面/TS28-17；

12-13：峡口剖面/XK254-1；

16-17：中寨剖面/ZZ19-3；

7-10、15、18-22：上寺剖面/TS28-18

1-11、18-23：*Reduviasporonites chalastus* (Foster, 1979) Elsik, 1999

12-17：*Reduviasporonites catenulatus* Wilson, 1962

图版 8

比例尺均为 10 微米；8 为扫描电镜照片，其余均为光学显微镜照片；

样品号：

1、4、9：中寨剖面/ZZ-40；

2-3、10、12、16、19：中寨剖面/ZZ-61；
5-8、11、13：中寨剖面/ZZ-37；
14-15、17-20：中寨剖面/ZZ-90
1-3：*Tripartites cristatus* Dybova and Jachowicz, 1957
4-8：*Triquitrites sinensis* Ouyang, 1962
9-13：*Leiotriletes exiguus* Ouyang and Li, 1980
14-15：*Waltzispora strictura* Ouyang and Li, 1980
16-20：*Neoraistrickia* sp.

图版 9

比例尺均为 10 微米；均为光学显微镜照片；
样品号：
1-4、8-9：中寨剖面/ZZ-5；
5-7、18-20：中寨剖面/ZZ-94；
10-13：中寨剖面/ZZ-37；
14-17：中寨剖面/ZZ-61
1-5：*Crassispora orientalis* Oyang and Li, 1980
6-9：*Densosporites* sp.
10-20：*Cyclogranisporites* sp.

图版 10

比例尺均为 10 微米；均为光学显微镜照片；
样品号：
1、3-4、6：中寨剖面/ZZ-5；
2、5、7-9、11-12、15：中寨剖面/ZZ-94；
10、16：中寨剖面/ZZ-37；
13-14：中寨剖面/ZZ-51
1-5：*Laevigatosporites lineolatus* Ouyang, 1962
6-12：*Punctatisporites pistilus* Ouyang, 1986
13-16：*Punctatosporites* sp.

图版 11

比例尺均为 10 微米；均为光学显微镜照片；
样品号：
1-2、5-9、15-16：中寨剖面/ZZ-56；
3-4：中寨剖面/ZZ-60；
10-12：中寨剖面/ZZ-37；
13-14、19-20：中寨剖面/ZZ-94；

17-18：中寨剖面/ZZ-61

1-3：*Apiculatasporites perirugosus* (Ouyang and Li, 1980) Ouyang,1982

4-12：*Lycopodiacidites* sp.

13-20：*Calamospora* sp.

图版 12

比例尺均为 10 微米；均为光学显微镜照片；

样品号：

1-2、13：上寺剖面/TS28-16；

3-6：中寨剖面/ZZ-37；

7-8：中寨剖面/ZZ-57；

9-10：中寨剖面/ZZ-5；

11-12、14-18：上寺剖面/TS-18；

19-20、23-25：上寺剖面/TS-14；

21-22、26：上寺剖面/TS-10；

1-18：*Cycadopites* sp.

19：*Tripartites cristatus* Dybova and Jachowicz, 1957

20：*Waltzispora* sp.

21：*Proterisispora sparsus* Ouyang and Li, 1980

22：*Indotriradites reidii* Foster 1979

23-24：*Dictyophyllidites barrisii* Couper, 1958

25：*Leiotriletes* sp.

26：*Proterisispora* sp.

图版 13

比例尺均为 10 微米；均为光学显微镜照片；

样品号：

1、6-7、11-12：上寺剖面/TS-14；

2-5、8、10、13：上寺剖面/TS-10；

9、14-15：上寺剖面/TS-11

1-6、10-12：*Alisporites* sp.

7-9：*Lueckisporites virkkiae* (Potonié and Klaus, 1954) Klaus, 1963

13-14：*Protohaploxypinus* sp.

15：*Platysaccus* sp.

图版 1

中寨

煤山

上寺

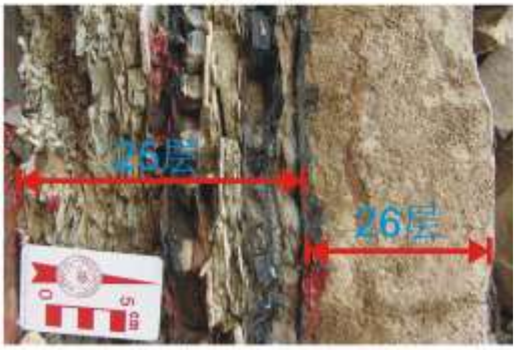

上寺25-26层

凉风垭

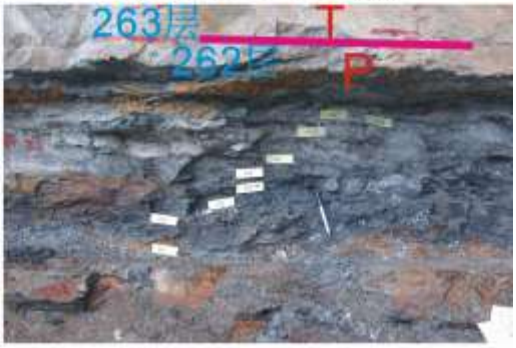

峡口

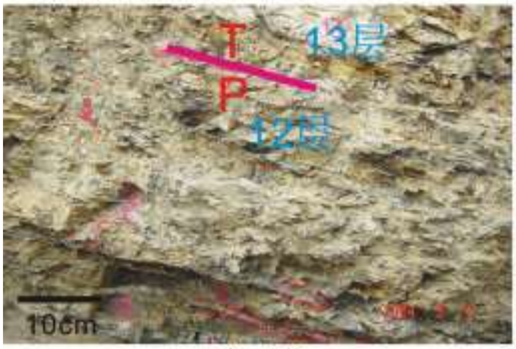

东攀

甘溪

图版 2

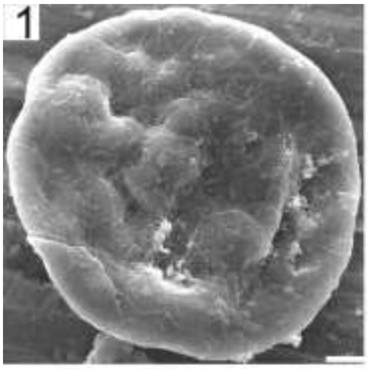
1

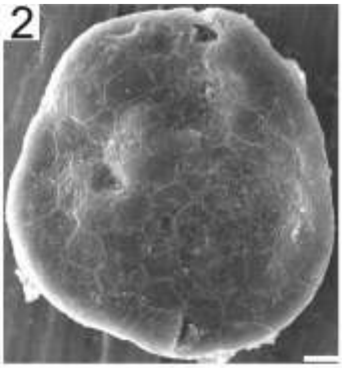
2

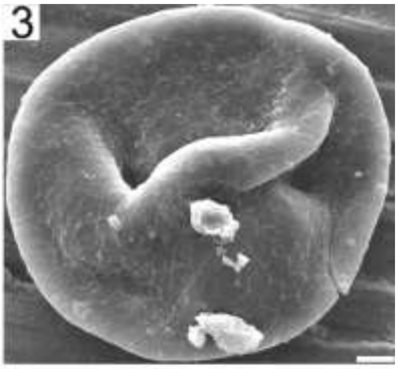
3

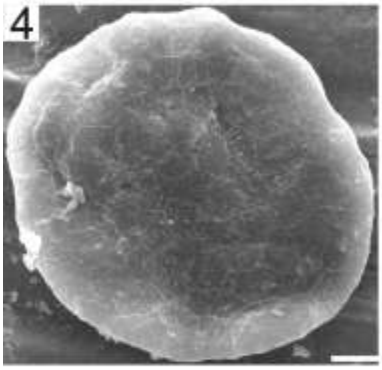
4

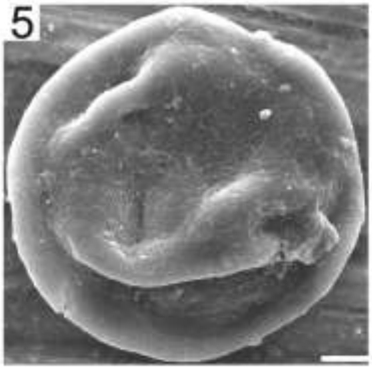
5

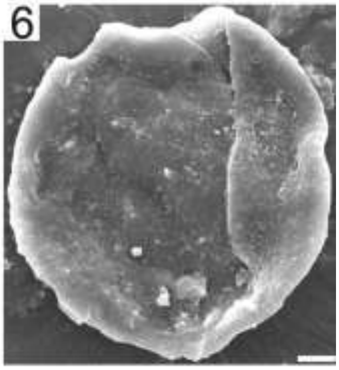
6

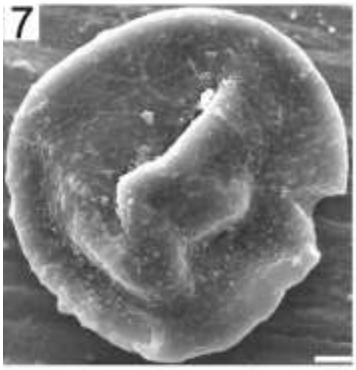
7

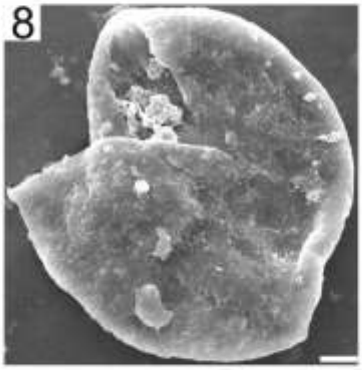
8

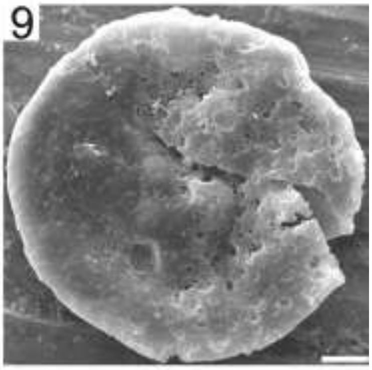
9


10


11

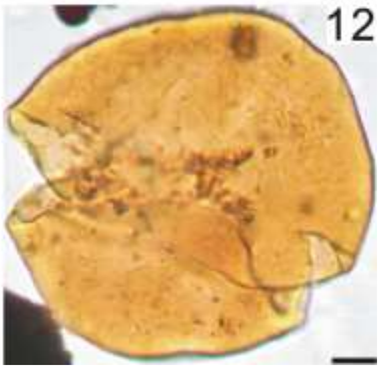
12

图版 3

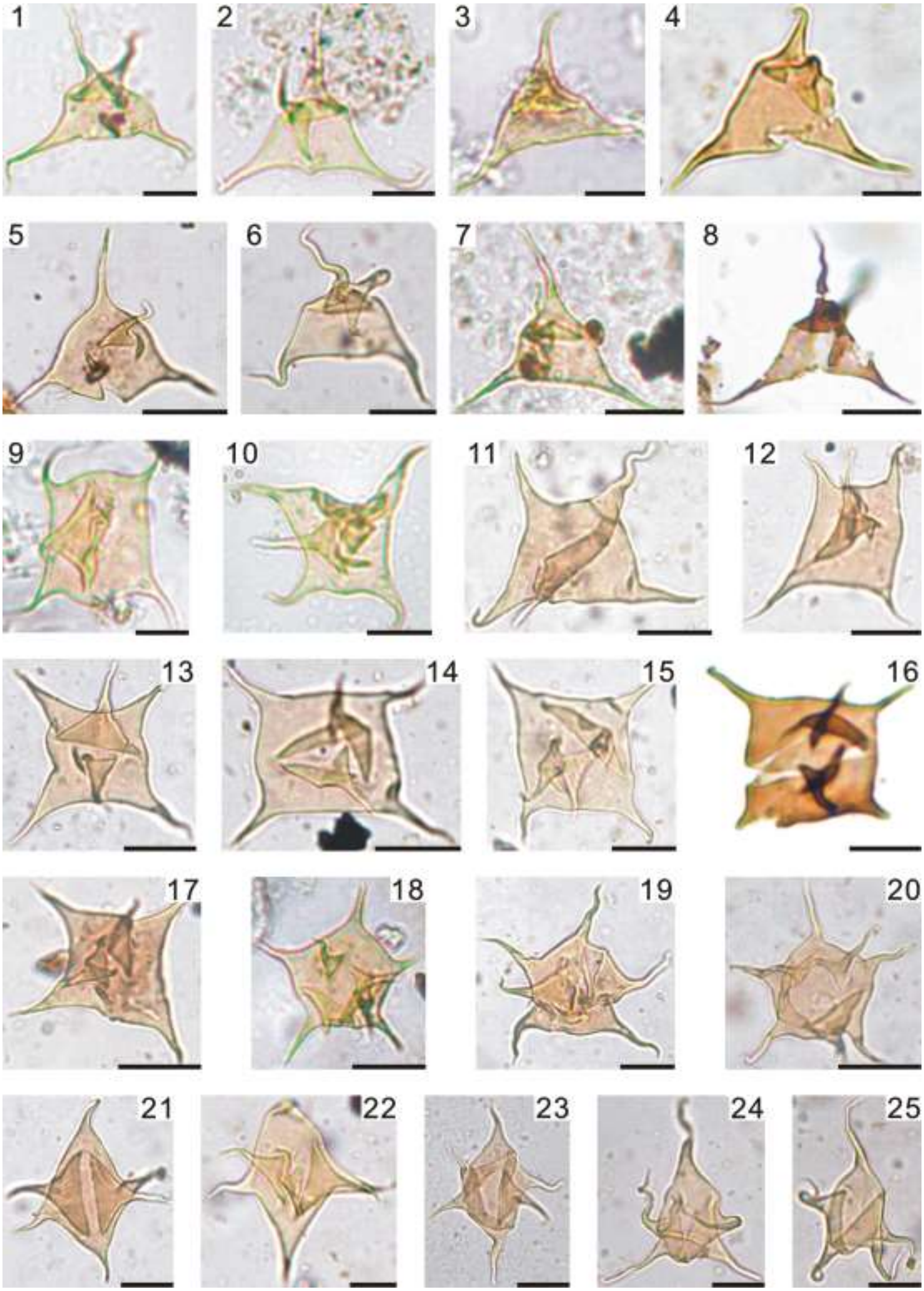

图版 4

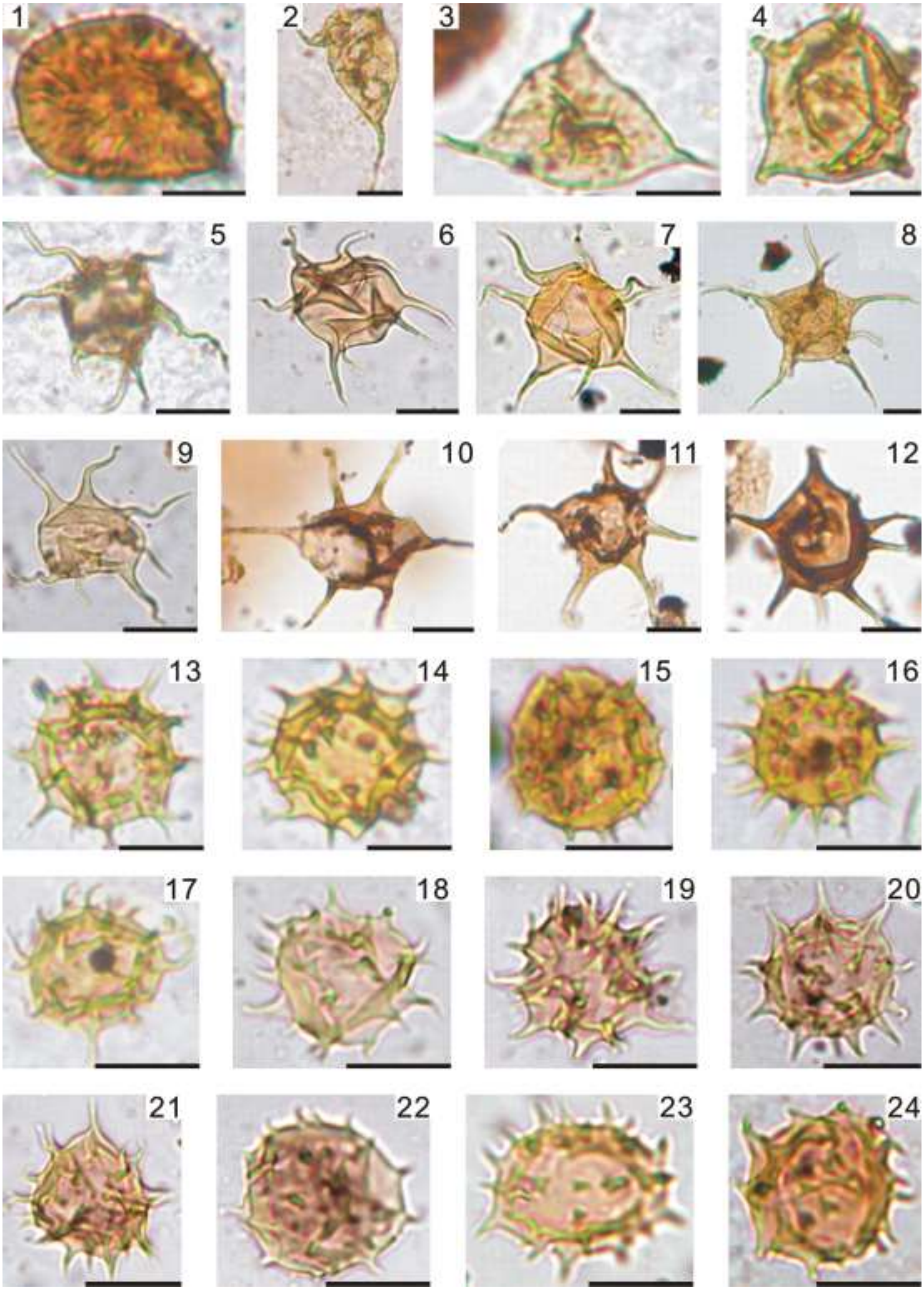

图版 5

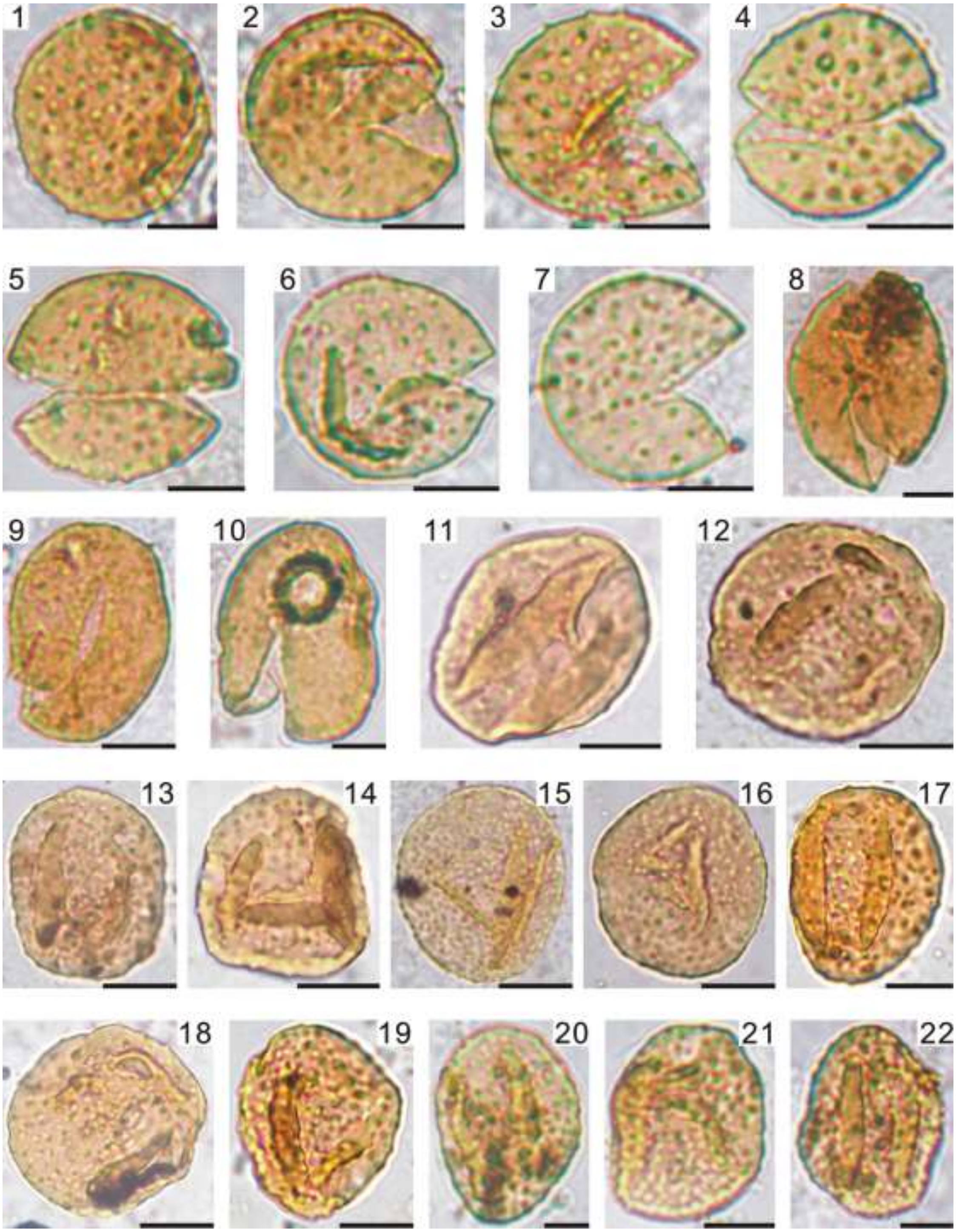

图版 6

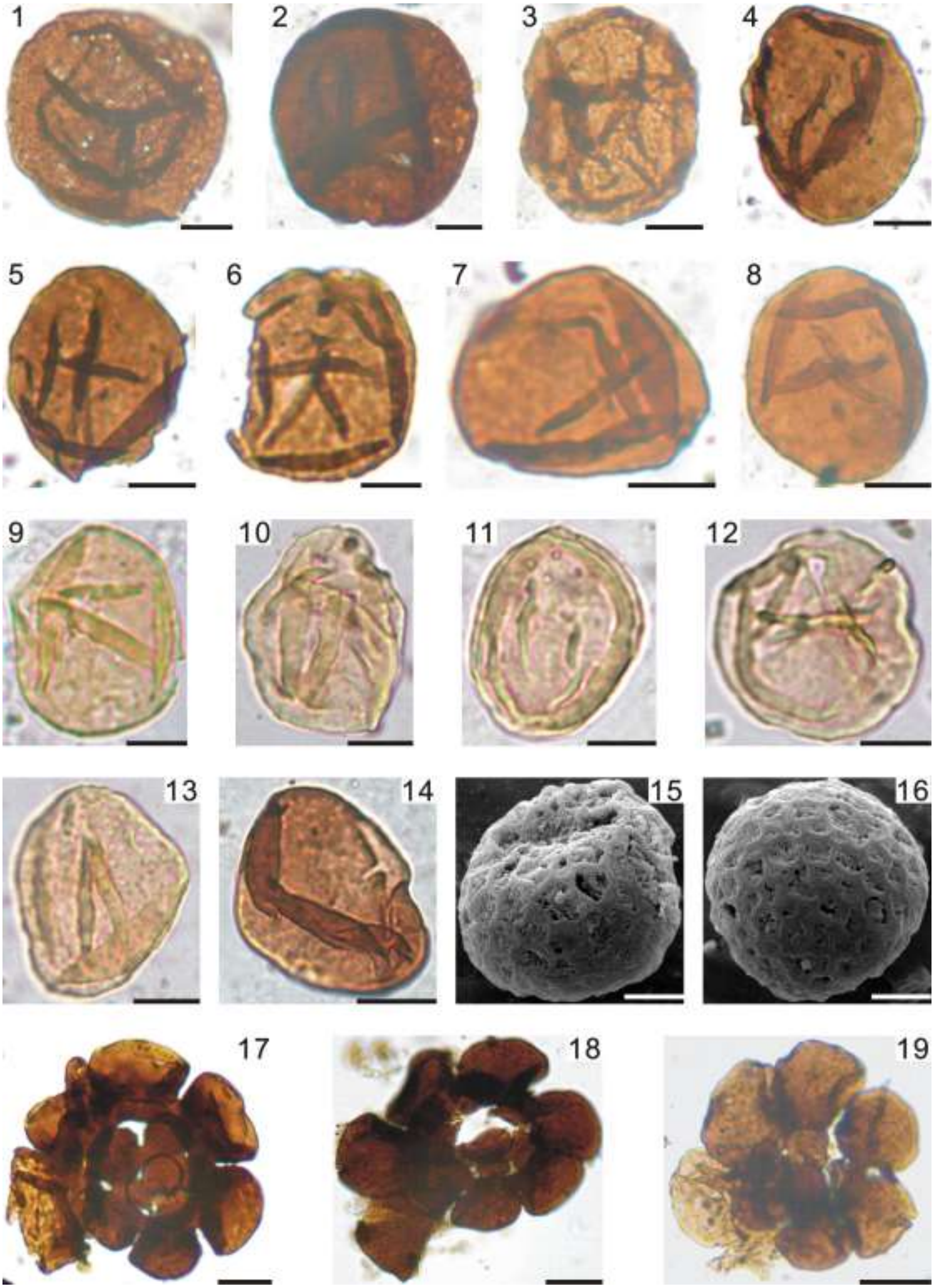

图版 7


1


2


3


4


5


6


7


8


9


10


11


12


13

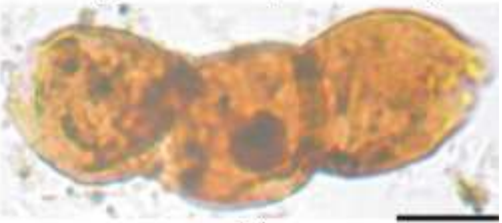
14


15


16


17


18


19


20


21

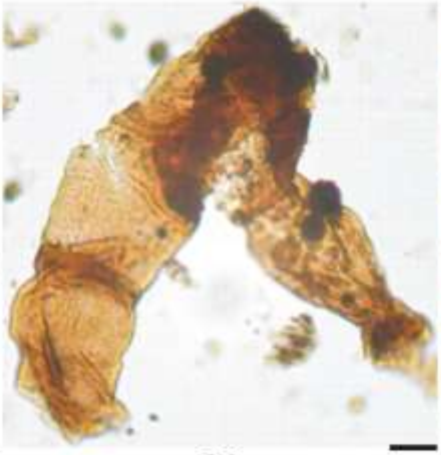
22


23

图版 8

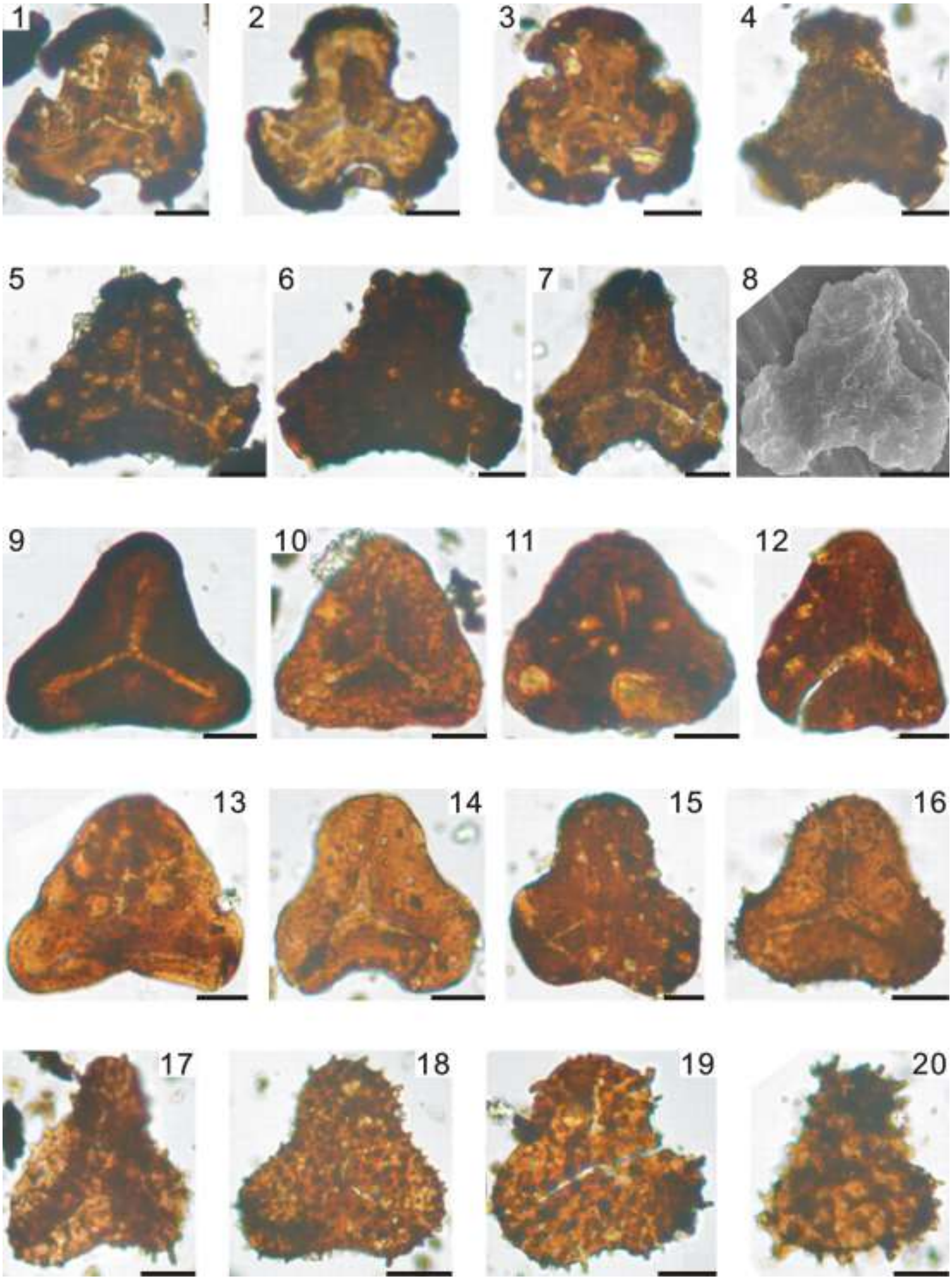

图版 9

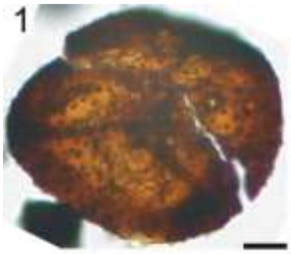
1

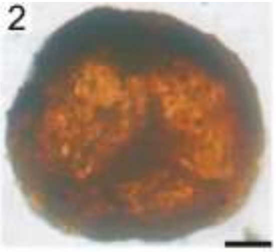
2


3

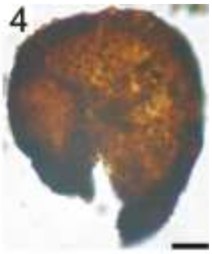
4

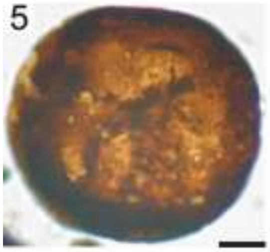
5

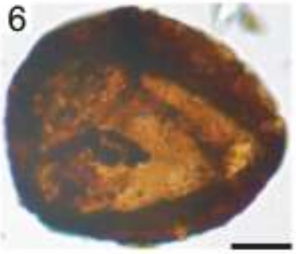
6

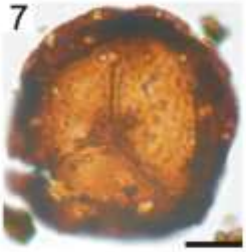
7


8

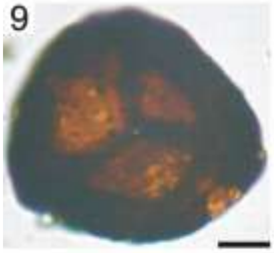
9


10

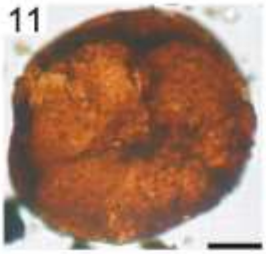
11

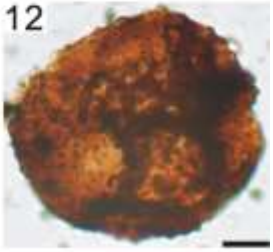
12


13

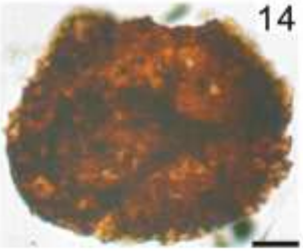
14

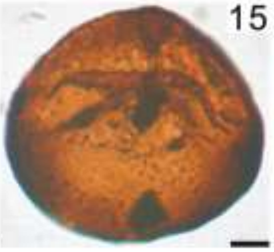
15


16


17


18

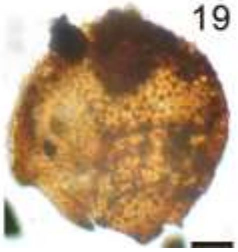
19

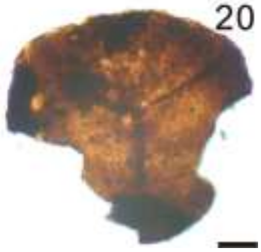
20

图版 10

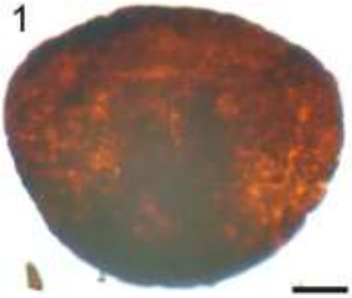
1

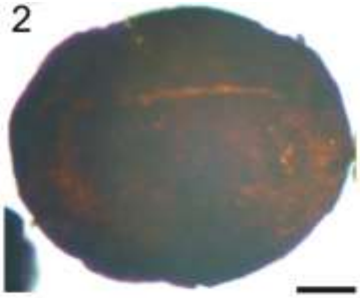
2


3


4

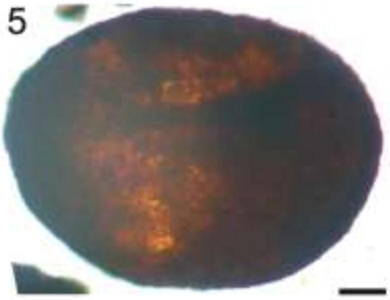
5

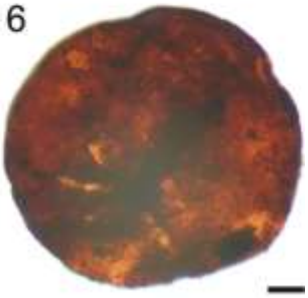
6

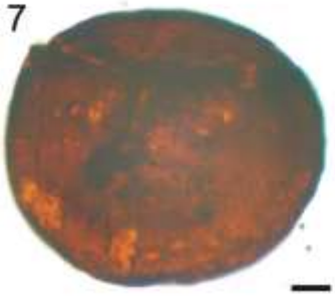
7


8

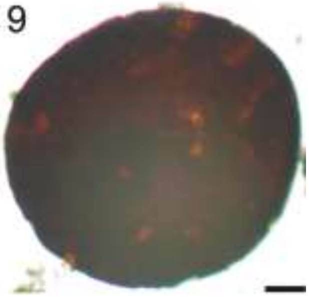
9

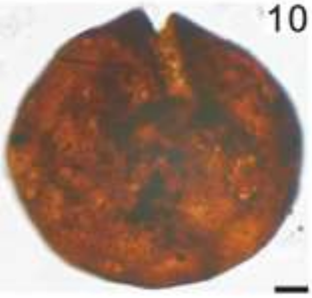
10

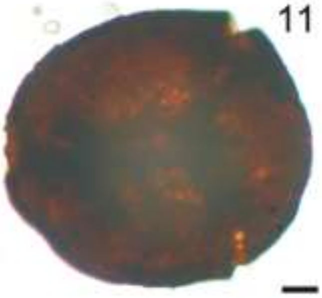
11

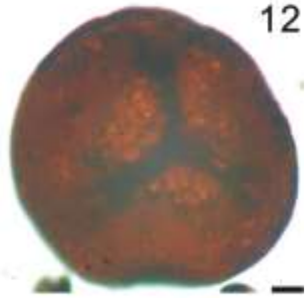
12

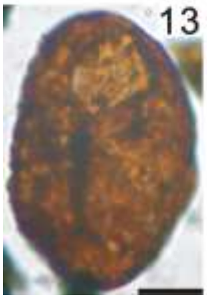
13

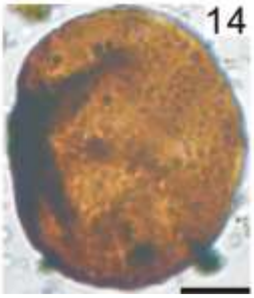
14


15


16

图版 11

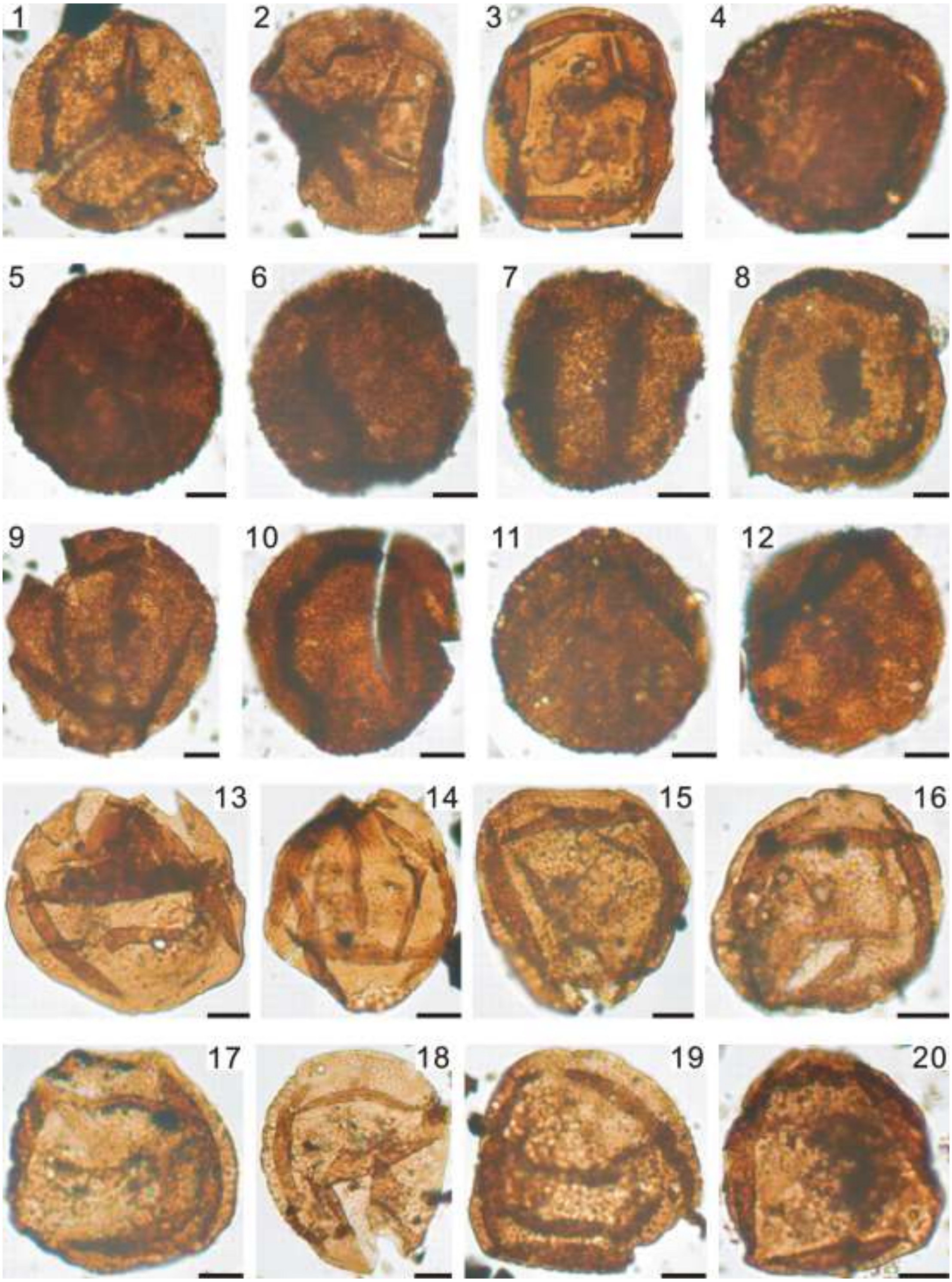

图版 12

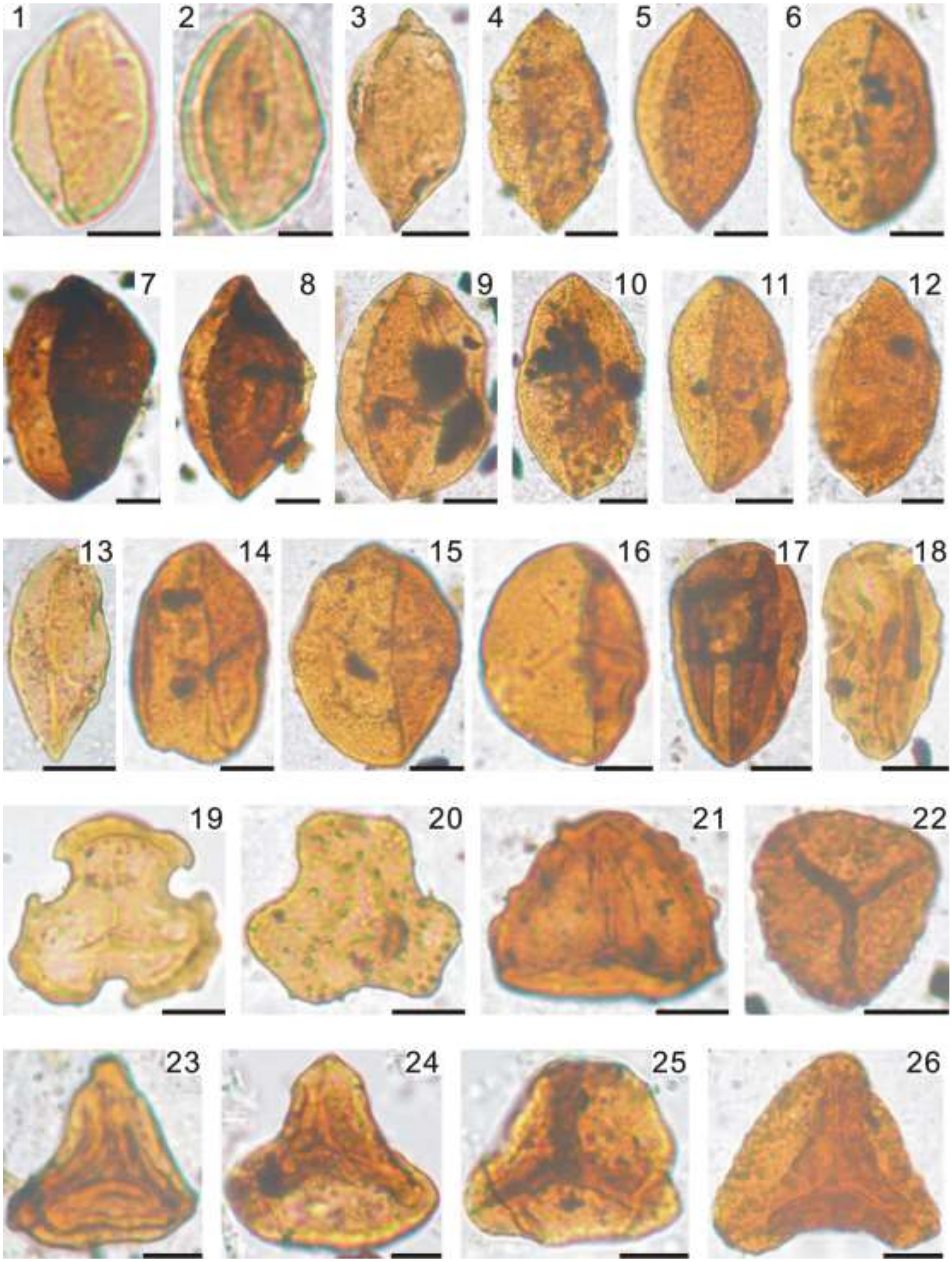

图版 13

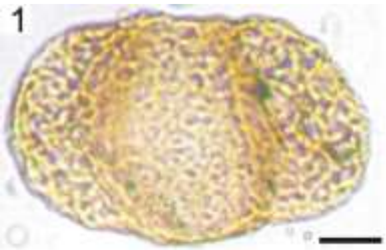
1

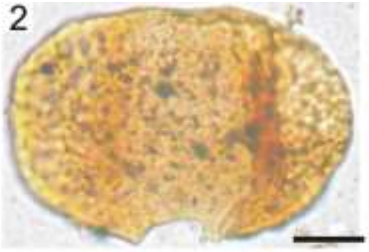
2

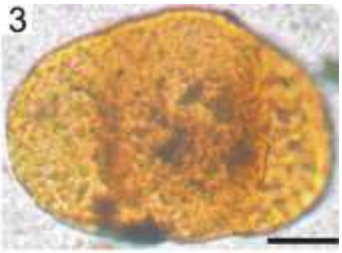
3

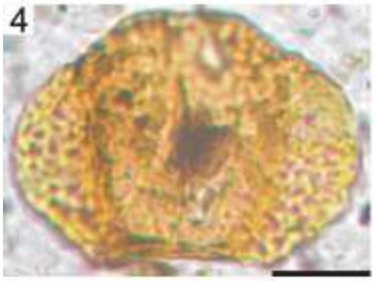
4

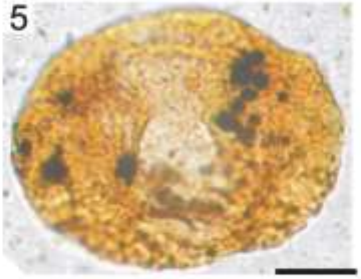
5

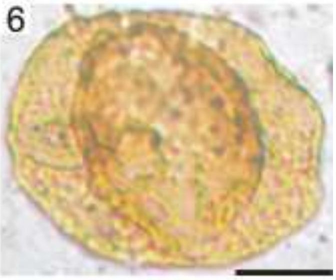
6

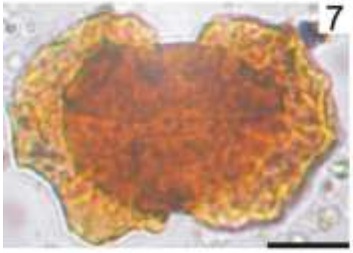
7

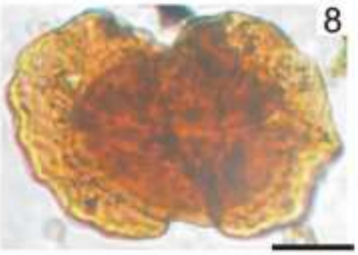
8

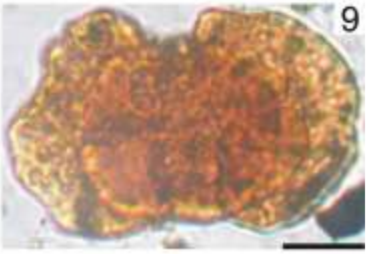
9

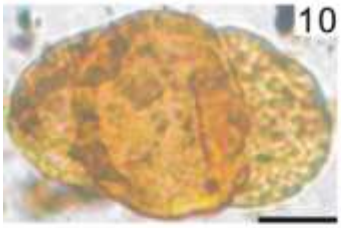
10

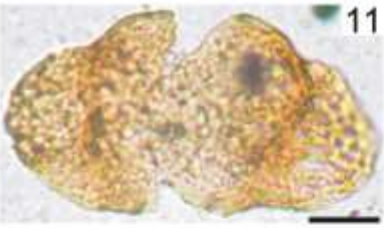
11

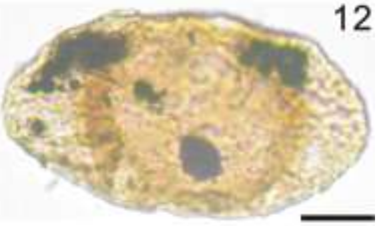
12

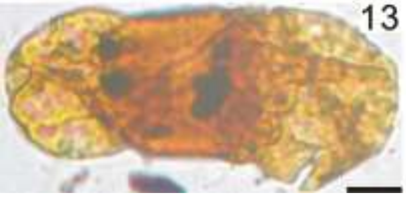
13

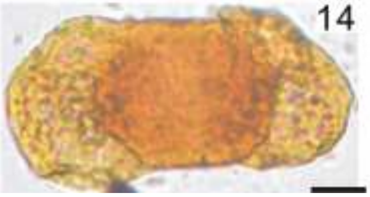
14

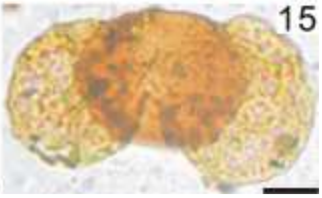
15

附录 A：二叠纪疑源类属种目录

（55 属、230 种，含 77 个未定种）

Acritarchs and Incertae Sedis
Acritarch sp. A (Lindström, 1995 a; Lindström, 1995 b)
Acritarch sp. B (Lindström, 1996)
Genus *Assamialetes* Singh, 1975
Assamialetes giganteus (Kaiser, 1976) Fensome et al., 1990
Genus *Archaeodinium* Ouyang, 1979
Archaeodinium cingulatum Ouyang, 1979
Genus *Baltisphaeridium* (Eisenack, 1958) Eisenack, 1969
Baltisphaeridium brevispinosum (Eisenack, 1931) Eisenack, 1959
Baltisphaeridium debilispinum Wall and Downie, 1963
Baltisphaeridium spp. (Li et al., 2004; Horowitz, 1990)
Baltisphaeridium sp. (Foster, 1974; Gorter et al., 2008; Shu and Utting, 1990; Lei et al., 2012)
Genus *Balmeella* Pant and Mehra, 1963
Balmeella densicorpa Tiwari and Navale, 1967
Balmeella minuta Tiwari and Navale, 1967
Balmeella punctata Tiwari and Navale, 1967
Balmeella sp. (Tripathi, 2001)
Genus *Buedingiisphaeridium* Schaarschmidt, 1963
Buedingiisphaeridium permicum Schaarschmidt, 1963
Genus *Brazilea* Tiwari and Navale, 1967
Brazilea crassa Tiwari and Navale, 1967
Brazilea scissa (Balme and Hennelly, 1956) Foster, 1975
Brazilea helbyi Foster, 1979
Brazilea helby forma *gregata* Foster, 1979
Brazilea helbyi forma *helbyi* Foster, 1979
Brazilea plurigenus (Balme and Hennelly, 1956) Foster, 1979

Brazilea punctata Tiwari and Navale, 1967
Brazilea sp A. (Backhouse, 1991)
Brazilea sp. (Cazzulo-Klepzig et al., 2007; Holz and Dias, 1998)
Brazilea spp. (Gutiérrez et al., 2005; Mangerud, 1994)
Genus *Circulisporites* de Jersey, 1962
Circulisporites parvus de Jersey, 1962
Circulisporites sp. (Lindström, 1995 a; Stephen, 1993)
Circulisporites sp. A (Backhouse, 1991)
Circulisporites sp. B (Backhouse, 1991)
Genus *Comasphaeridium* Staplin and Jansonius et Pocock, 1965
Comasphaeridium daemoni Quadros, 2002
Genus *Congoites* Sah, 1967
Congoites baculosus Tiwari and Navale, 1967
Congoites conatus Tiwari and Navale, 1967
Congoites spinosus Tiwari and Navale, 1967
Congoites sp. (Mori et al., 2011)
Genus *Deunffia Downie*, 1960
Deunffia unispinosa (Schön, 1967) Sarjeant, 1970
Genus *Deusilites* Hemer and Nygreen, 1967
Deusilites tenuistriatus Gutiérrez and Césari et Archangelsky, 1997
Deusilites sp. (Gutiérrez et al., 2006)
Genus *Disectispora* Tiwari and Navale, 1967
Disectispora lobata Tiwari and Navale, 1967
Genus *Diexallophasis* Loeblich, 1970
Diexallophasis sp. (Kent et al., 1990)
Genus *Foveofusa* Lele and Chandra, 1972
Foveofusa attenuata Lele and Chandra, 1972
Foveofusa cylindrica Lele and Chandra, 1972
Foveofusa mutabilis Lele and Chandra, 1972

Foveofusa obese Lele and Chandra, 1972
Foveofusa perforata Lele and Chandra, 1972
Foveofusa pumila Lele and Chandra, 1972
Genus *Globulaesphaeridium* Tiwari and Moiz, 1971
Globulaesphaeridium densum Tiwari and Moiz, 1971
Genus *Gorgonisphaeridium* Staplin and Jansonius et Pocock, 1965
Gorgonisphaeridium sp. (Pérez Loinaze et al., 2010)
Genus *Gondisphaeridium* Tiwari and Moiz, 1971
Gondisphaeridium leve Tiwari and Moiz, 1971
Genus *Greinervillites* Bose and Kar, 1967
Greinervillites sp. (Tripathi, 2001)
Genus *Haplocystia* Segroves, 1967
Haplocystia pellucida Segroves, 1967
Genus *Hystrichosphaeridium* Deflandre, 1937
Hystrichosphaeridium leonardianum Tasch, 1963
Hystrichosphaeridium equispinosum Tasch, 1963
Hystrichosphaeridium sp. (Wilson, 1960)
Genus *Inaperturopollenites* Pflug and Thomson, 1953
Inaperturopollenites nebulosus Balme, 1970
Genus *Inderites Abramova* and Martchenko, 1964
Inderites bulbifera Abramova and Martchenko, 1964
Inderites compacta Abramova and Martchenko, 1964
Inderites crassus Dyupina, 1970
Inderites elegans Dyupina, 1970
Inderites flexuosus Dyupina, 1970
Inderites microreticulatus Dyupina, 1970
Inderites robusta Abramova and Martchenko, 1964
Inderites scrobiculatus Dyupina, 1970
Genus *Kagulubeites* Bose and Maheshwari, 1968

Kagulubeites verrucosus Bose and Maheshwari, 1968
Kagulubeites sp. (Banerjee and D'Rozario, 1988; Banerjee and D'Rozario, 1990)
Genus *Leiofusa* Eisenack, 1938
Leiofusa punctalirella Loeblich, 1970
Leiofusa stassfurtensis Schön, 1967
Leiofusa jurassica (Schön, 1967) Sarjeant, 1970
Leiofusa sp. (Lei et al., 2012)
Leiofusa spp. (Foster, 1974)
Genus *Leiosphaeridium* Staplin, 1961
Leiosphaeridium belloyense Jansonius, 1962
Genus *Lophosphaeridium*(Timofeev, 1959) Downie, 1963
Lophosphaeridium spp. (Gilby and Foster, 1988; Lindstrm, 1995 b)
Lophosphaeridium sp. (Utting and S-petrole, 1978)
Genus *Maculatasporites* Tiwari, 1964
Maculatasporites amplus Segroves, 1967
Maculatasporites delicates Foster, 1975
Maculatasporites gondwanensis Tiwari, 1964
Maculatasporites gravidus Playford and Rigby, 2011
Maculatasporites indicus Tiwari, 1964
Maculatasporites karanpurensis Lele and Kulkarni, 1969
Maculatasporites minimus Segroves, 1967
Maculatasporites zairensis Kar and Bose, 1976
Maculatasporites sp. (Cazzulo-Klepzig et al., 2007; Hankel, 1992; Stephen, 1993)
Maculatasporites spp. (Foster and Waterhouse, 1988; Mangerud, 1994)
Maculatasporites sp A. (Backhouse, 1991)
Genus *Mehlisphaeridium* Segroves, 1967
Mehlisphaeridium fibratum Segroves, 1967
Mehlisphaeridium regulare Anderson, 1977
Mehlisphaeridium sp. (Lindström, 1995 a; Stephen, 1993)
Mehlisphaeridium sp. A (Lindström, 1996)
Genus *Micrhystridium* (Deflandre, 1937) Sarjeant and Stancliffe, 1994

Micrhystridium albertensis Staplin, 1961
Micrhystridium bistchoensis Staplin, 1961
Micrhystridium breve Jansonius, 1962
Micrhystridium circulum Schön, 1967
Micrhystridium densispinum Valensi, 1953
Micrhystridium fragile Deflandre, 1947
Micrhystridium inconspicuum (Deflandre, 1935) Deflandre, 1937
Micrhystridium karamurzae Sarjeant, 1970
Micrhystridium keratoides Spode, 1964
Micrhystridium microspinosum Schaarschmidt, 1963
Micrhystridium pakistante Sarjeant, 1970
Micrhystridium parvispinum Deflandre, 1946
Micrhystridium pentagonale Stockmans and Willière, 1963
Micrhystridium piliferum Deflandre, 1937
Micrhystridium piveteaui Valensi, 1963
Micrhystridium recurvatum Valensi, 1953
Micrhystridium setasessitante Jansonius, 1962
Micrhystridium stellatum Deflandre, 1945
Micrhystridium toigae Quadros, 2002
Micrhystridium sp. (Beri et al., 2006; Beri et al., 2010; Fielding and McLoughlin, 1992; Gutiérrez et al., 2006; Holz and Dias, 1998; Utting and S-petrole, 1978)
Micrhystridium sp.1 (Jacobson et al., 1982)
Micrhystridium sp.2 (Jacobson et al., 1982)
Micrhystridium sp.3 (Jacobson et al., 1982)
Micrhystridium spp. (Foster, 1974; Foster and Waterhouse, 1988; Gilby and Foster, 1988; Grigoriev and Utting, 1998; Hermann et al., 2012; Li et al., 2004; Mangerud, 1994; Mangerud and Konieczny, 1993;)
Micrhystridium sp. A (Schaarschmidt, 1963)
Micrhystridium sp. B (Schaarschmidt, 1963)
Micrhystridium sp. C (Schaarschmidt, 1963)
Micrhystridium sp. H (Jansonius, 1962)
Genus *Navifusa* Combaz and Lange et Pansart, 1967
Navifusa sp. (Pérez Loinaze et al., 2010)
Genus *Peltacystia* Balme and Segroves, 1966
Peltacystia calvitium Balme and Segroves, 1966

Peltacystia galeoides Segroves, 1967
Peltacystia monilis Balme and Segroves, 1966
Peltacystia venosa Balme and Segroves, 1966
Peltacystia sp. (Stephen, 1993)
Genus *Pilasporites* Balme and Hennelly, 1956
Pilasporites calculus Balme and Hennelly, 1956
Pilasporites plurigenus Balme and Hennelly, 1956
Pilasporites sp. (Banerjee and D'Rozario, 1990; Gutiérrez et al., 2006; Holz and Dias, 1998; Gutiérrez et al., 2006)
Pilasporites sp. B (Beri et al., 2006; Beri et al., 2010)
Genus *Polyedryxium* Deunff, 1954
Polyedryxium deflandrei Deunff, 1954
Polyedryxium kraeuselianum Schaarschmidt, 1963
Polyedryxium sp. (Sarjeant et al., 1970; Schaarschmidt, 1963)
Genus *Psiloschizosporis* Jain, 1968
Psiloschizosporis scissus (Balme and Henn, 1956) Ouyang, 1985
Genus *Pyramidosporites* Segroves, 1967
Pyramidosporites cyathodes Segroves, 1967
Pyramidosporites racemosus Balme, 1970
Genus *Pterospermopsis* Wetzel, 1952
Pterospermopsis triangularis Horowitz, 1973
Genus *Protoleiosphaeridium* Timofeev, 1959
Protoleiosphaeridium conglutinatum Timofeev, 1959
Genus *Quadrisporites* Hennelly, 1959
Quadrisporites horridus(Hennelly, 1959) Potonié and Lele, 1961
Quadrisporites lobatus (Tiwari and Navale, 1967) Ybert, 1975
Quadrisporites sp. (Segroves, 1967)
Quadrisporites spp. (Cazzulo-Klepzig et al., 2007)
Genus *Reduviasporonites* (Wilson, 1962) Foster, 2002

Reduviasporonites catenulatus Wilson, 1962
Reduviasporonites chalastus (Foster, 1979) Elsik, 1999
Reduviasporonites stoschianus (Balme, 1980) Elsik, 1999
Reduviasporonites sp. (Eshet et al., 1995; Visscher et al., 1996; Looy et al., 2001; Steiner et al., 2003; Sandler et al., 2006; Sephton et al., 2009)
Reduviasporonites sp. B (Mangerud, 1994; Stolle et al. 2011)
Reduviasporonites spp. (Li et al., 2004)
Genus *Solisphaeridium* Staplin and Jansonius et Pocock, 1965
Solisphaeridium rossignoli Glikson, 1966
Solisphaeridium solidurn Ouyang and Li, 1980
Solisphaeridium spinulatum Ouyang, 1985
Genus *Spongocystia* Segroves, 1967
Spongocystia eraduica Segroves, 1967
Spongocystia sp. (Fielding and McLoughlin, 1992; Stephen, 1993)
Genus *Spheripollenites* Coupcr, 1958
Spheripollenites scabratus Coupcr, 1958
Spheripollenites scissus (Balme and Hennelly, 1956) Jansonius, 1962
Spheripollenites sp. (Segroves, 1967)
Genus *Tessellaesphaera* Foster, 1979
Tessellaesphaera tessellata Foster, 1979
Genus *Tetraporina* Naumova, 1939
Tetraporina antiqua Naumova, 1950
Tetraporina gigantea (Bose and Maheshwari, 1968) Backhouse, 1991
Tetraporina horologia (Staplin, 1960) Playford, 1963
Tetraporina punctata (Tiwari and Navale, 1967) Kar and Bose, 1976
Tetraporina simplex Anderson, 1977
Tetraporina superba Anderson, 1977
Tetraporina tetragona Anderson, 1977
Tetraporina sp. (Banerjee and D'Rozario, 1988; Cazzulo-Klepzig et al., 2007; Gutiérrez et al., 2006; Iannuzzi et al., 2006; Kent et al., 1990; Segroves, 1967)
Tetraporina sp. A (Backhouse, 1991; Gilby and Foster, 1988; Lindstrm, 1995 b; Stolle et al. 2011)

Genus *Tunisphaeridium* Deunff and Evitt, 1968
Tunisphaeridium sp. A (Li et al., 2004)
Genus *Ulanisphaeridium* McMinn, 1982
Ulanisphaeridium berryense McMinn, 1982
Ulanisphaeridium omanensis Stephenson and Osterloff et Filatoff, 2003
Ulanisphaeridium sp. (Gorter et al., 2008)
Genus *Unellium* Rauscher, 1969
Unellium phosphoriensis Jacobson, 1982
Unellium spp. (Mangerud and Konieczny, 1993)
Genus *Veryhachium* (Deunff, 1954) Sarjeant and Stancliffe, 1994
Veryhachium brevispinum Horowitz, 1972
Veryhachium conispinosum Schaarschmidt, 1963
Veryhachium cylindricum Schaarschmidt, 1963
Veryhachium europaeum Stockmans and Willière, 1960
Veryhachium flagelliferum Wall, 1963
Veryhachium formosum Stockmans and Willière, 1960
Veryhachium hyalodermum (Cookson, 1955) Schaarschmidt, 1963
Veryhachium irregulare Jekhowsky, 1961
Veryhachium lairdi (Deflandre, 1946) Downie, 1959
Veryhachium longispinum Horowitz, 1972
Veryhachium nasicum (Stockmans and Willière 1960) Stockmans and Willière 1962
*Veryhachium quad*ratum Schaarschmidt, 1963
Veryhachium reductum (Deunff, 1959) Jekhowsky, 1961
Veryhachium rhomboidium Downie, 1959
Veryhachium riburgense Brosius and Bitterli, 1961
Veryhachium rosendae Cramer, 1964
Veryhachium sedecimspinosum Staplin, 1961
Veryhachium tzutsii Horowitz, 1972
Veryhachium valensii (Valensi, 1953) Downie and Sarjeant, 1964
Veryhachium variabilis Schaarschmidt, 1963
Veryhachium sp. (Holz and Dias, 1998; Schaarschmidt, 1963; Utting, 1978)
Veryhachium sp. A (Lei et al., 2012)
Veryhachium spp. (Foster, 1974; Hermann et al., 2012; Li et al., 2004; Mangerud, 1994;

Mangerud and Konieczny, 1993; Stephen, 1993)
Genus *Wilsonastrum* Jansonius, 1962
Wilsonastrum colonicum Jansonius, 1962
Fungi?
Genus *Chordecystia* Foster, 1979
Chordecystia chalasta Foster, 1979
Chordecystia sp. (Stephen, 1993)
Genus *Portalites* Hemer and Nygreen, 1967
Portalites gondwanensis Nahuys and Alpern et Ybert, 1968
Portalites sp. (Cazzulo-Klepzig et al., 2007; Gutiérrez et al., 2006; Holz and Dias, 1998)
Division Chlorophyta Pascher, 1914
Class Chlorophyceae Kützing, 1843
Order Chlorococcales Marchand, 1895
Family Dictyosphaeriaceae West, 1916
Genus *Botryococcus* Kützing, 1849
Botryococcus braunii Kützing, 1849
Botryococcus sp. (Bugge et al., 2002; Foster, 1975; Foster and Waterhouse, 1988; Gorter et al., 2008; Gutiérrez et al., 2006; Holz and Dias, 1998; Kent et al., 1990; Segroves, 1967; Stephen, 1993; Tripathi, 2001)
Botryococcus spp. (Besems and Schuurman, 1987)
Botryococcus sp. A (Gilby and Foster, 1988)
Class Zygnematophyceae Round, 1971
Order Zygnematales Borge and Pascher, 1913
Family Zygnemataceae Kützing, 1843
Genus *Schizosporis* (Cookson and Dettman, 1959) Pierce, 1976
Schizosporis reticulatus Cookson and Dettman, 1959
Schizosporis dejerseyi Segroves, 1967
Schizosporis scissus (Balme and Hennelly, 1956) Hart, 1965
Schizosporis sp. (Shu, 1985; Shu and Utting, 1990; Lei et al., 2012)
Order Not assigned
Family Not assigned

Genus *Tasmanites* Newton, 1875
Tasmanites punctatus Newton, 1875
Tasmanites tanbaensis Takahashi and Yao, 1969
Tasmanites talchirensis Lele, 1979
Tasmanites sp. (Bugge et al., 2002; El-Nakhal et al., 2002; Holz and Dias, 1998; Horowitz, 1973; Kent et al., 1990; Sarjeant et al., 1970; Shu, 1985; Souza and Callegari, 2010; Tasch, 1963)
Tasmanites spp. (Mangerud, 1994; Quadros, 2002)
Tasmanites sp. A (Lindstrm, 1995 b)
Division Prasinophyta Christensen, 1962
Class Prasinophyceae Christensen, 1962
Order Not assigned
Family Pterosphaeridiaceae Mädler, 1963
Genus *Cymatiosphaera* Wetzel, 1933
Cymatiosphaera gondwanensis (Tiwari, 1965) Backhouse, 1991
Cymatiosphaera sp. (Dypvik et al., 2001; Grigoriev and Utting, 1998; Mautino et al., 1998; Schaarschmidt, 1963; Utting and S-petrole, 1978)
Cymatiosphaera spp. (Li et al., 2004; Mangerud, 1994)
Cymatiosphaera sp. A (Backhouse, 1991)
Genus *Dictyotidium* (Eisenack, 1955) Staplin, 1961
Dictyotidium souzae Quadros, 2002
Dictyotidium reticulatum Schulz, 1965
Dictyotidium sp. A (Lindstrm, 1995 b)
Dictyotidium sp. (Kent et al., 1990; McLoughlin et al., 1997; Lei et al., 2012)
Dictyotidium spp. (Gilby and Foster, 1988; Stolle, 2007)
Genus *Leiosphaeridia* (Eisenack, 1958) Downie and Sarjeant, 1963
Leiosphaeridia baltica Eisenack, 1958
Leiosphaeridia changxingensis Ouyang Shu and Utting, 1990
Leiosphaeridia ghoshii (Lele, 1979) Fensome et al., 1990
Leiosphaeridia indica Lele and Chandra, 1972
Leiosphaeridia micrograniferа (Staplin, 1961) Downie and Sarjeant, 1965
Leiosphaeridia minutissima (Naumova, 1949) Jankauskas, 1989
Leiosphaeridia schopfii Jacobson, 1982
Leiosphaeridia shepeleva (Lele, 1979) Fensome et al., 1990

Leiosphaeridia tenuissima Eisenack, 1958
Leiosphaeridia umariensis Lele and Chandra, 1972
Leiosphaeridia sp.1 (Stephenson et al., 2008)
Leiosphaeridia sp.2 (Stephenson et al., 2008)
Leiosphaeridia sp. (Beri et al., 2006; Beri et al., 2010; El-Nakhal et al., 2002; Gutiérrez et al., 2005; Kent et al., 1990; Iannuzzi et al., 2006; Lindström, 1995 a; Mautino et al., 1998; Mori et al., 2011; Segroves, 1967; Tripathi, 2001)
Leiosphaeridia spp. (Gilby and Foster, 1988; Li et al., 2004; Lindstrm, 1995 b)
Leiosphaeridia sp. A (Backhouse, 1991)
Leiosphaeridia sp. B (Lindström, 1996; Lindström, 2005)

附录 B：华南二叠纪-三叠纪之交疑源类数据

样品号/物种名	*Baltisphaeridium* sp.	*Dictyotidium reticulatum*	*Dictyotidium* sp.	*Leiofusa* sp.	*Leiosphaeridia micrograniferа*	*Leiosphaeridia minutissima*	*Micrhystridium breve*	*Michrystridium fragile*	*Michrystridium pentagonale*	*Michrystridium stellatum*	*Reduviasporonites catenulatus*	*Reduviasporonites chalastus*	*Schizosporis* sp.	*Schizosporis scissus*	*Veryhachium cylindricum*	*Veryhachium hyalodermum*	*Veryhachium nasicum*	*Veryhachium quadratum*	*Veryhachium sedecimspinosum*	*Veryhachium* sp.
中寨剖面																				
ZZ-27-6	80						108	188												
ZZ-22-3	76						224	300												
ZZ-22-2	180							210		30										
ZZ-20-1	60						180	240												
ZZ-19-3							120	120			20									
煤山剖面																				
MS-26		230								128	39		69			89				
上寺剖面																				
TS28b-10							1867													
TS28b-11							1944					17								

样品号/物种名	*Baltisphaeridium* sp.	*Dictyotidium reticulatum*	*Dictyotidium* sp.	*Leiofusa* sp.	*Leiosphaeridia microgranifera*	*Leiosphaeridia minutissima*	*Micrhystridium breve*	*Michrystridium fragile*	*Michrystridium pentagonale*	*Michrystridium stellatum*	*Reduviasporonites catenulatus*	*Reduviasporonites chalastus*	*Schizosporis* sp.	*Schizosporis scissus*	*Veryhachium cylindricum*	*Veryhachium hyalodermum*	*Veryhachium nasicum*	*Veryhachium quadratum*	*Veryhachium sedecimspinosum*	*Veryhachium* sp.
TS28b-13	25						315					18								
TS28b-14							4751					105								
TS28a-16							1815				35	74								
TS28a-17					32		3025				268	854								
TS28a-18					51		3333				160	1017				48				
SS-25e					850	254	4455	126	230	321		118	76	50	126	3130	237		168	
SS-25c					86	10	1609		10	15					224	714	167			
SS-25a					8															
SS293-6					450	162													5	
SS293-3					86	45										6				
SS292-12																23				
SS292-6																			14	
SS292-4		1980	330		350	366														
SS292-2					2327	3200														
SS292-1					980	1948														
SS291-7					3230	7693														

样品号/物种名	*Baltisphaeridium* sp.	*Dictyotidium reticulatum*	*Dictyotidium* sp.	*Leiofusa* sp.	*Leiosphaeridia microgranifera*	*Leiosphaeridia minutissima*	*Micrhystridium breve*	*Michrystridium fragile*	*Michrystridium pentagonale*	*Michrystridium stellatum*	*Reduviasporonites catenulatus*	*Reduviasporonites chalastus*	*Schizosporis* sp.	*Schizosporis scissus*	*Veryhachium cylindricum*	*Veryhachium hyalodermum*	*Veryhachium nasicum*	*Veryhachium quadratum*	*Veryhachium sedecimspinosum*	*Veryhachium* sp.
SS291-6					5560	7903	24			55			15		36	50			72	
SS291-5					1380	3432									65					
SS291-4					270	111														
SS291-3					2200	1820	25													
SS291-2					2390	3045	78			14					25	24	10		33	
SS291-1					540	185	7									79				
SS290-10					330	372									21					
SS290-9					23	44	348			25						25			22	
SS290-8-1					16		275			45						67	56		56	
SS290-7					870	848	1078	36	15	380					72	549		36		36
SS290-6					29		65									127				
SS290-5					130		211		13	4						49				
SS290-4					140	53	138	14								28				
SS289-3					2107	1657	26									26				
SS289-2					320	358	32		16	15						38				
SS289-1-2				35	790	834	11									34				

样品号/物种名	*Baltisphaeridium* sp.	*Dictyotidium reticulatum*	*Dictyotidium* sp.	*Leiofusa* sp.	*Leiosphaeridia microgranifera*	*Leiosphaeridia minutissima*	*Micrhystridium breve*	*Michrystridium fragile*	*Michrystridium pentagonale*	*Michrystridium stellatum*	*Reduviasporonites catenulatus*	*Reduviasporonites chalastus*	*Schizosporis* sp.	*Schizosporis scissus*	*Veryhachium cylindricum*	*Veryhachium hyalodermum*	*Veryhachium nasicum*	*Veryhachium quadratum*	*Veryhachium sedecimspinosum*	*Veryhachium* sp.
SS288-42					390	854														
SS288-37					26		4													
SS288-34					250	66	21		5											
SS276-3		228																		
SS276-1		821																		
SS274-1		1368																		
SS274-1		410																		
SS16-31		219																		
SS16-28		182																		
SS16-26		219																		
SS16-23		156																		
SS16-16		2893																		
SS16-14		463																		
SS16-12		547																		
SS16-8		109																		
SS16-4		1127																		

样品号/物种名	*Baltisphaeridium* sp.	*Dictyotidium reticulatum*	*Dictyotidium* sp.	*Leiofusa* sp.	*Leiosphaeridia microgranifera*	*Leiosphaeridia minutissima*	*Micrhystridium breve*	*Michrystridium fragile*	*Michrystridium pentagonale*	*Michrystridium stellatum*	*Reduviasporonites catenulatus*	*Reduviasporonites chalastus*	*Schizosporis* sp.	*Schizosporis scissus*	*Veryhachium cylindricum*	*Veryhachium hyalodermum*	*Veryhachium nasicum*	*Veryhachium quadratum*	*Veryhachium sedecimspinosum*	*Veryhachium* sp.
SS15-7		199																		
SS15-5		328																		
凉风垭剖面																				
LFY-22-B						58														
LFY-14-D						35														
LFY-13						89														
LFY-4-A					26	97														
LFY-1-B					58	226	52		42	141						108		28	99	
LFY-1-A					38	85	22		12	55						31		10	41	
LFY-7 下					126	456	223		168	335						201		56	134	
峡口剖面																				
XK257-2					88															
XK256					39															

样品号/物种名	*Baltisphaeridium* sp.	*Dictyotidium reticulatum*	*Dictyotidium* sp.	*Leiofusa* sp.	*Leiosphaeridia microgranifera*	*Leiosphaeridia minutissima*	*Micrhystridium breve*	*Michrystridium fragile*	*Michrystridium pentagonale*	*Michrystridium stellatum*	*Reduviasporonites catenulatus*	*Reduviasporonites chalastus*	*Schizosporis* sp.	*Schizosporis scissus*	*Veryhachium cylindricum*	*Veryhachium hyalodermum*	*Veryhachium nasicum*	*Veryhachium quadratum*	*Veryhachium sedecimspinosum*	*Veryhachium* sp.
XK254-2					78															
XK254-1		78			99						34									
XK252		80			98						56									
XK248-2		67			89															
甘溪剖面																				
GX-37						160														
GX-32						218														
GX-29						149														
GX-25						100														
GX-20						59														
GX-18						364														
GX-17						24														
GX-13						107														
GX-7						39														
GX239						37														
GX236						53														

样品号/物种名	*Baltisphaeridium* sp.	*Dictyotidium reticulatum*	*Dictyotidium* sp.	*Leiofusa* sp.	*Leiosphaeridia microgranifera*	*Leiosphaeridia minutissima*	*Micrhystridium breve*	*Michrystridium fragile*	*Michrystridium pentagonale*	*Michrystridium stellatum*	*Reduviasporonites catenulatus*	*Reduviasporonites chalastus*	*Schizosporis* sp.	*Schizosporis scissus*	*Veryhachium cylindricum*	*Veryhachium hyalodermum*	*Veryhachium nasicum*	*Veryhachium quadratum*	*Veryhachium sedecimspinosum*	*Veryhachium* sp.
东攀剖面																				
DP12-B						124														
DP10-B					35	55														
DP10-A						68														
DP5-C						70														
DP5-B					22	89														
DP5-A						90														
DP3-B						56														
DP3-A					56	140														
DP2-I						190														
DP2-H					23	110														
DP2-G						280														
DP2-E						190														

A ppendix C: The papers and unpublished manuscripts

(1)Manuscript 1. Pages 121-195.
Lei, Y., Servais, T., Feng, Q.L. The diversity of the Permian phytoplankton. **Review of Palaeobotany and Palynology.**
(In press. DOI: 10.1016/j.revpalbo.2013.03.004)

(2) Manuscript 2. Pages 196-218.
Lei Yong et al. Palynology and palynofacies of the Upper Permian to Lower Triassic of Shangsi (Sichuan, China). **Review of Palaeobotany and Palynology.**
(revised and under corrections)

(3) Manuscript 3. Pages 219-231.
Lei, Y., Servais, T., Feng, Q.L., He, W.H. The spatial (nearshore-offshore) distribution of latest Permian phytoplankton from the Yangtze Block, South China. **Palaeogeography, Palaeoclimatology, Palaeoecology. 2012. (363-364): 151-162.**

(4) Manuscript 4. Pages 232-249.
Lei Y., et al. The phytoplankton community succession during the Permian-Triassic boundary in South China-one of the possible mechanism for the mass extinction. (To be submitted to Palaeogeography, Palaeoclimatology, Palaeoecology)

(5) Manuscript 5. Pages 250-278.
Lei, Y., Servais, T., Feng, Q.L., He, W.H. Latest Permian phytoplankton from the Yangtze Platform. **Palynology. (Accepted for publication)**

(6) Manuscript 6. Pages 279-309.
JUN SHEN, **YONG LEI**, THOMAS J. ALGEO, QINGLAI FENG, THOMAS SERVAIS, JIANXIN YU, and LIAN ZHOU. Volcanic Effects on Microplankton during the Permian-Triassic Transition (Shangsi and Xinmin, South China).
(Submitted to Palaios)

Paper 1: (section 1.2)

Lei, Y., Servais, T., Feng, Q.L. The diversity of the Permian phytoplankton. Review of Palaeobotany and Palynology. (In press)
DOI:10.1016/j.revpalbo.2013.03.004

Accepted Manuscript

The diversity of the Permian phytoplankton

Yong Lei, Thomas Servais, Qinglai Feng

PII: S0034-6667(13)00046-8
DOI: doi: 10.1016/j.revpalbo.2013.03.004
Reference: PALBO 3448

To appear in: *Review of Palaeobotany and Palynology*

Received date: 11 February 2012
Revised date: 3 August 2012
Accepted date: 12 March 2013

Please cite this article as: Lei, Yong, Servais, Thomas, Feng, Qinglai, The diversity of the Permian phytoplankton, *Review of Palaeobotany and Palynology* (2013), doi: 10.1016/j.revpalbo.2013.03.004

The diversity of the Permian phytoplankton

Yong Lei[1,2*], **Thomas Servais**[2], **Qinglai Feng**[1]

[1] *State Key Laboratory of Geo-processes and Mineral Resources, China University of Geosciences, Wuhan 430073, China*

[2] *UMR 8217 Géosystèmes, CNRS-Université Lille1, Cité Scientifique, F-59655 Villeneuve d'Ascq, France*

***Corresponding author**, E-mail: leiyongdida@163.com; Tel: +86-13485387952

Thomas SERVAIS, E-mail: thomas.servais@univ-lille1.fr;

Fax: +33-320436900; Tel: +33-320337220

Qinglai FENG, E-mail: qinglaifeng@cug.edu.cn;

Fax: +86-027-67883002; Tel: +86-027-67883006

Abstract. The Palaeozoic fossil record of organic-walled microphytoplankton is represented by the acritarchs, organic-walled microfossils (OWMs) considered mostly as the resting cysts of phytoplanktonic organisms, although the biological affinities of the acritarchs are, by definition, unknown. Acritarchs appear in the Precambrian and reach their highest diversity in the Lower and Middle Palaeozoic (Cambrian to Devonian). After a drastic diversity drop in the Devonian, they are considered to be of very low diversity in the Upper Palaeozoic (Carboniferous to Permian), where some authors claim the presence of a 'phytoplankton blackout' due to nutrient depletion in the oceans. Here we present a synthesis of the Permian fossil record of acritarchs. The revision shows that Permian acritarch descriptions have largely been neglected, compared to other palynomorph groups, such as spores and pollen grains. While larger organic-walled cysts, as known from the Lower and Middle Palaeozoic, are usually absent, many smaller acritarchs are commonly found in Permian palynological assemblages. In addition, several OWMs interpreted as fungal spores have been described, but also possible green algae, including chlorophycean, prasinophycean or zygnematophyceaen algae. During most of the Permian stages, OWMs show genus richness of about 20 to 30 genera. Some genera, such as *Micrhystridium* and *Veryhachium*, have been reported in over 40 publications. Nevertheless, many Permian acritarchs still need to be documented in detail, and additional systematical studies, in particular of the very small taxa, are needed to fully understand the diversity and significance of Permian phytoplankton.

Keywords: Permian, phytoplankton, acritarch, diversity

1. Introduction

The modern marine phytoplankton is dominated by three algal groups: calcareous coccolithophorids, siliceous diatomsand organic-walled dinoflagellates. While the calcareous and siliceous phytoplankton only diversified in the Mesozoic, the presence of organic-walled microphytoplankton in the fossil record dates back to the

Precambrian (e.g., Katz et al., 2004). Organic-walled microphytoplankton have largely been recorded from the Palaeozoic, whereas siliceous microplankton seems absent and calcareous phytoplanktonic organisms only possibly exist since the early Palaeozoic, probably due to preservation problems (Munnecke and Servais, 2008). The highest diversities of organic-walled phytoplankton are recorded in the Lower and Middle Palaeozoic, with a possible maximum of diversity being reached during the Ordovician and Early Devonian (e.g., Molyneux et al., 1996; Strother, 1996; Servais et al., 2004). During the Ordovician, sea levels were very high, and the epicontinental shelves had their greatest extension, triggering the 'Great Ordovician Biodiversification Event' with abundant phytoplankton playing an important role at the base of newly established trophic webs (Servais et al., 2008, 2010). The abundant and diverse phytoplankton present in the Devonian oceans (Le Hérisse et al., 2000) was also involved in the 'Devonian nekton revolution' (Klug et al. 2010). It was only during the Late Devonian and towards the Devonian-Carboniferous boundary that acritarch diversity dramatically dropped (e.g., Mullins and Servais, 2008).

Acritarchs were considered to become almost absent in the Carboniferous and Permian, because larger cysts are no longer observed in the fossil record. This drop of diversity of resting cysts in the fossil record has been related to different palaeoenvironmental conditions, such as nutrient changes in the oceans, or changes in pCO_2 (see recent discussions in Riegel, 2008; Strother, 2008; Strother et al., 2010). Riegel (1996, 2008) named this Late Palaeozoic interval with a virtual absence of organic-walled phytoplankton the 'Phytoplankton Blackout', because (after the Late

Devonian acritarch 'extinction' and a 130 million year period of absence of large phytoplanktonic cysts in the fossil record) organic-walled dinoflagellate cysts are only recorded since the Triassic and did not strongly diversify before the Late Triassic and Jurassic. Servais et al. (2006) questioned the existence of a 'phytoplankton blackout', because the absence of resting cysts in the fossil record does not necessarily imply the absence of the phytoplankton in the Late Palaeozoic oceans. In the modern oceans, only a minor part of the dinoflagellates produce resting cysts that are fossilisable (e.g., Head, 1996).

Mullins and Servais (2008) reviewed the diversity of the Carboniferous phytoplankton, and noted that phytoplankton diversity declined significantly from the Tournaisian to the Serpukhovian. Phytoplankton diversity in the Late Carboniferous was generally very low, with typically only 1-3 species being documented in each assemblage (Mullins and Servais, 2008).

Permian acritarch studies have generally been neglected. Most palynological investigations focus on spores and pollen grains that are usually abundant and diverse in Permian palynological assemblages. These plant-derived microfossils, that are much larger in size than phytoplankton in the same assemblages, are easier to observe and to describe (in particular with the light microscope). For these reasons pollen and spores became of great importance, not only for Permian palynostratigraphy, but also for palaeogeographical and palaeoenvironmental reconstructions.

Permian acritarchs recovered in palynological slides are generally very small in size, usually not reaching the diameter of 20 μm. They are therefore more difficult to study in detail with the light microscope. Permian acritarchs, similar to those from the Carboniferous, are generally considered to be of low diversity and low abundance, and they are not a significant component in biostratigraphic and palaeobiogeographic studies.

In addition to acritarchs, organic-walled microorganisms related to the green algae (Divisions Chlorophyta and Prasinophyta) have been documented in the Late Palaeozoic (e.g., Colbath and Grenfell, 1995). These morphotypes probably include prasinophytes and various chlorophyte groups, including members of the Hydrodictiaceae, Botryococcaceae and members of the Zygnemataceae. In addition, fungal palynomorphs have been reported, in particular in the Late Permian, with an animated debate about a fungal spike in the late part of the Permian that might have been implicated in the Permian-Triassic extinction event (e.g. Eshet et al., 1995; Steiner et al., 2003).

A consistent summary of Permian phytoplankton has never been published and only two short reviews of Permian acritarchs have been presented (Li et al., 2004a; Traverse, 2007). Here we summarize the current knowledge on Permian organic-walled phytoplankton, with the aim to understand if significant diversity changes can be observed and if the geographical distribution of the assemblages allows any palaeobiogeographical interpretation. We try to bring all literature data together, by reviewing all taxa listed by Fensome et al. (1990) and by compiling the more recent literature published after the compilation of the catalogue of Fensome et al. (1990). Like Mullins and Servais (2008), we review all OWMs of unknown affinities ('acritarchs'), includingtaxa such as the possibly non-marine genus *Mehlisphaeridium*, but also possible prasinophycean, chlorophycean, zygnemataceaen and hydrodictyaceaen algae that are described in the literature. In addition, several taxa of OWMs from the Permian have been tentatively attributed to fungal spores (Eshet et al., 1995; Visscher et al., 1996; Sephton et al., 2009; Visscher et al., 2011).

It is beyond the scope of the present paper to discuss the possible biological affinities of all the different taxa described in the Permian. The genera *Leiosphaeridia* and *Polyedryxium*, regarded as prasinophytes by several authors, are here considered as acritarchs (i.e., organic-walled microfossils of unknown biological affinities). We do not propose any new attribution to biological groups and consider most taxa as 'acritarchs', i.e. organisms of unknown biological affinity. A few taxa are herein attributed to the green algae, following current consensus of their affinities in the literature(Colbath and Grenfell, 1995).

2. The Permian phytoplankton record

Although many papers mention acritarchs in palynological assemblages (particularly in works dedicated to Permian spores and pollen grains), only about one hundred publications concern descriptions of acritarchs, prasinophytes, chloryphycean, zygnemataceaen and hydrodictyaceaen algae from Permian strata. Figure 1 summarizes the descriptions of marine organic-walled palynomorphs and probable phytoplankton in the individual papers on Permian palynology. For each individual article, the authors, the country from which the assemblages were described, and the biostratigraphical age that was provided in the study are indicated in Figure 1. Following Fensome et al. (1990), we do not include miospores or other taxa (such as *Acanthotriletes*) that have been incorrectly assigned to the acritarchs.

Stratigraphy follows the Permian stratigraphical subdivisions of the International Commission on Stratigraphy (ICS), based on Gradstein et al. (2004). A stratigraphic scheme of the Permian is provided within Figure 3. A comprehensive list of all Permian acritarch taxa (including author names) is provided in Appendix 1.

2.1. Early Permian (Cisuralian)

2.1.1. Gzhelian/Asselian

Only two papers have described organic-walled microplankton from Carboniferous-Permian boundary strata (Gzhelian/Asselian). In Argentina, Gutiérrez et al. (2005) identified *Botryococcus braunii*, *Leiosphaeridia* sp. and specimens attributed to *Brazilea* spp., from the Tupe Formation, located south of the Mina La Delfina locality, about 29 km northeast of San José de Jáchal. Gorter et al. (2008) reported the three genera *Botryococcus*, *Baltisphaeridium* and *Ulanisphaeridium* from the Treachery Formation, Lower Kulshill Group, Australia.

2.1.2 Asselian and Asselian/Sakmarian

Five studies mention phytoplankton from earliest Permian strata. In Antarctica, Kent et al. (1990) studied the palynology of the Beacon Supergroup sedimentary rocks exposed at Milorgfjella, Dronning Maud Land, and found a relatively rich and well preserved palynoflora, dominated by spores and pollen grains, but also including *Botryococcus* sp., *Diexallophasis* sp., and *Leiosphaeridia* sp., two prasinophytes (*Dictyotidium* sp., *Tasmanites* sp.), together with *Brazilea scissa*, *Tetraporina* sp. and *Quadrisporites horridus*.

Lindström (1995b) described several acritarchs from three localities in the northern Heimefrontfjella, Antarctica (namely A and C in Milorgfjella and Lidkvarvet in Sivorgfjella), including the taxa: Acritarch sp. A, *Botryococcus braunii*, *Leiosphaeridia* spp., *Lophosphaeridium* spp., *Dictyotidium* sp., *Tasmanites* sp. A, *Tetraporina gigantea*, *T. tetragona*, *T.* sp. A, *Brazilea scissa*, and *Quadrisporites horridus*.

Di Pasquo et al. (2010) studied three outcrops of the Libertad and Sauces Formations from the Los Sauces area in the Province La Rioja, western Argentina, and defined two assemblage zones, yielding the acritarch *Portalites gondwanensis*. They considered that the age of the assemblage 2 was of Asselian/Sakmarian.

Two studies described phytoplankton taxa from the Asselian to Artinskian in Uruguay. Beri et al. (2006) analyzed four samples of borehole DCLS24 from the San Gregorio Formation. Subsequently, Beri et al. (2010) analyzed 32 outcrop samples and thirty borehole samples from the Cerro Pelado Formation, including the acritarch genera *Deusilites*, *Leiosphaeridia*, *Micrhystridium*, *Pilasporites*, and *Portalites*, but also the genera *Brazilea* and *Tetraporina*, as well as *Quadrisporites* and *Botryococcus*.

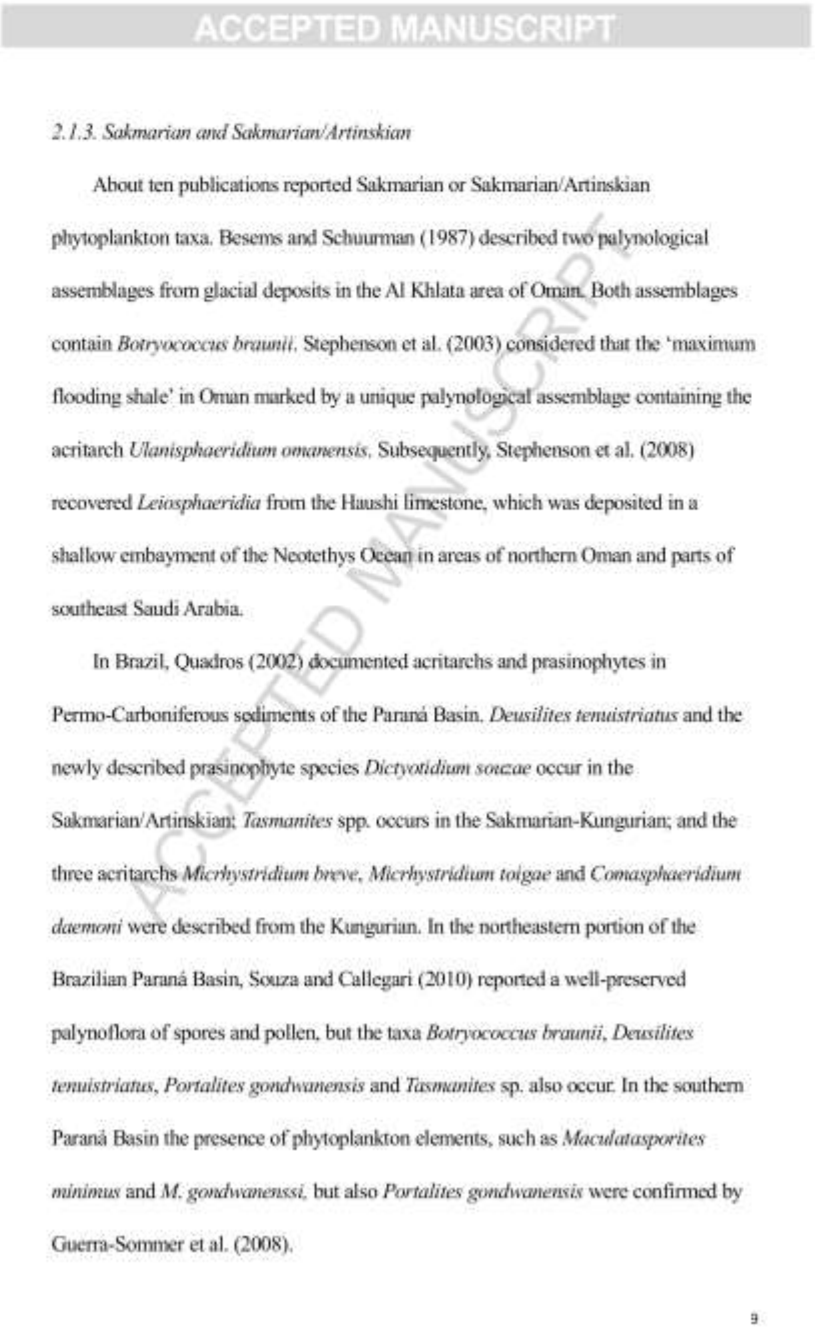

2.1.3. Sakmarian and Sakmarian/Artinskian

About ten publications reported Sakmarian or Sakmarian/Artinskian phytoplankton taxa. Besems and Schuurman (1987) described two palynological assemblages from glacial deposits in the Al Khlata area of Oman. Both assemblages contain *Botryococcus braunii*. Stephenson et al. (2003) considered that the 'maximum flooding shale' in Oman marked by a unique palynological assemblage containing the acritarch *Ulanisphaeridium omanensis*. Subsequently, Stephenson et al. (2008) recovered *Leiosphaeridia* from the Haushi limestone, which was deposited in a shallow embayment of the Neotethys Ocean in areas of northern Oman and parts of southeast Saudi Arabia.

In Brazil, Quadros (2002) documented acritarchs and prasinophytes in Permo-Carboniferous sediments of the Paraná Basin. *Deusilites tenuistriatus* and the newly described prasinophyte species *Dictyotidium souzae* occur in the Sakmarian/Artinskian; *Tasmanites* spp. occurs in the Sakmarian-Kungurian; and the three acritarchs *Micrhystridium breve*, *Micrhystridium toigae* and *Comasphaeridium daemoni* were described from the Kungurian. In the northeastern portion of the Brazilian Paraná Basin, Souza and Callegari (2010) reported a well-preserved palynoflora of spores and pollen, but the taxa *Botryococcus braunii*, *Deusilites tenuistriatus*, *Portalites gondwanensis* and *Tasmanites* sp. also occur. In the southern Paraná Basin the presence of phytoplankton elements, such as *Maculatasporites minimus* and *M. gondwanenssi*, but also *Portalites gondwanensis* were confirmed by Guerra-Sommer et al. (2008).

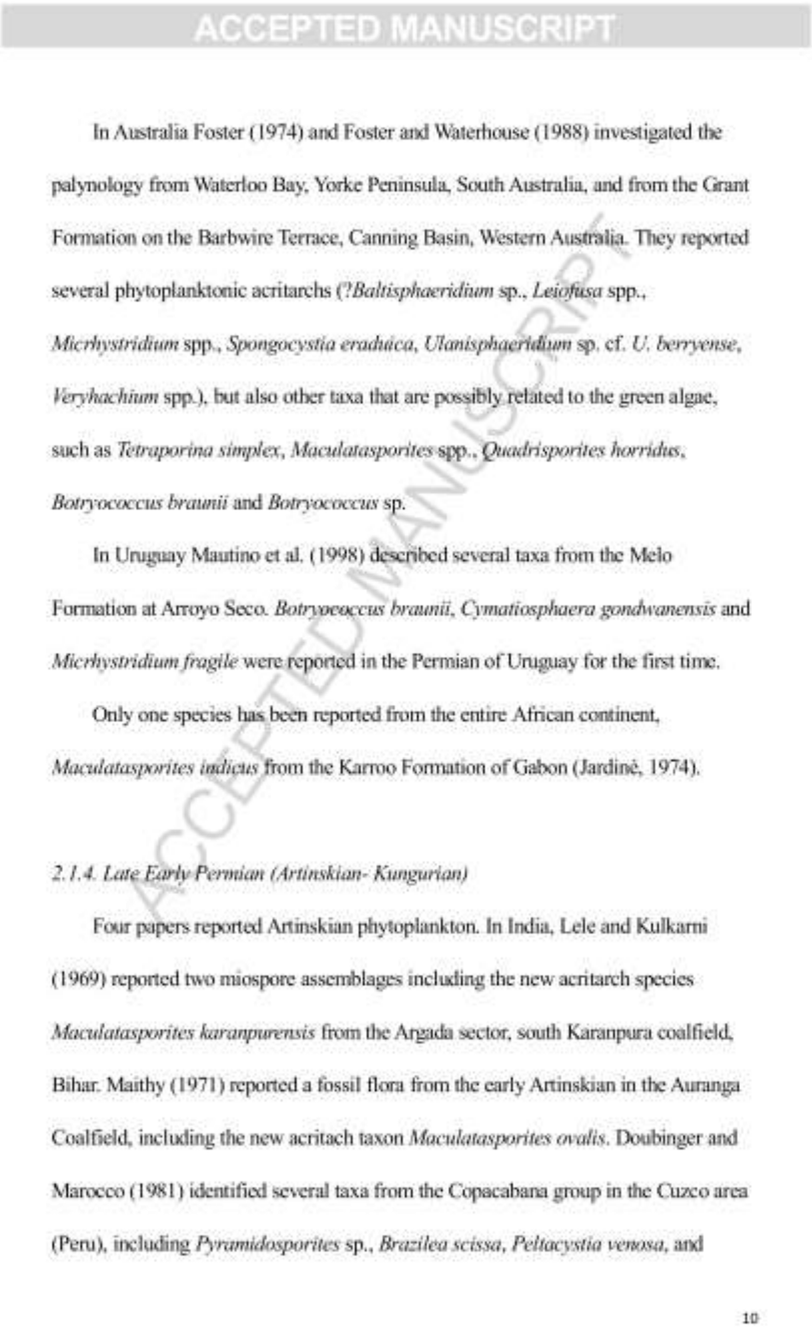

In Australia Foster (1974) and Foster and Waterhouse (1988) investigated the palynology from Waterloo Bay, Yorke Peninsula, South Australia, and from the Grant Formation on the Barbwire Terrace, Canning Basin, Western Australia. They reported several phytoplanktonic acritarchs (?*Baltisphaeridium* sp., *Leiofusa* spp., *Micrhystridium* spp., *Spongocystia eraduica*, *Ulanisphaeridium* sp. cf. *U. berryense*, *Veryhachium* spp.), but also other taxa that are possibly related to the green algae, such as *Tetraporina simplex*, *Maculatasporites* spp., *Quadrisporites horridus*, *Botryococcus braunii* and *Botryococcus* sp.

In Uruguay Mautino et al. (1998) described several taxa from the Melo Formation at Arroyo Seco. *Botryococcus braunii*, *Cymatiosphaera gondwanensis* and *Micrhystridium fragile* were reported in the Permian of Uruguay for the first time.

Only one species has been reported from the entire African continent, *Maculatasporites indicus* from the Karroo Formation of Gabon (Jardiné, 1974).

2.1.4. Late Early Permian (Artinskian- Kungurian)

Four papers reported Artinskian phytoplankton. In India, Lele and Kulkarni (1969) reported two miospore assemblages including the new acritarch species *Maculatasporites karanpurensis* from the Argada sector, south Karanpura coalfield, Bihar. Maithy (1971) reported a fossil flora from the early Artinskian in the Auranga Coalfield, including the new acritach taxon *Maculatasporites ovalis*. Doubinger and Marocco (1981) identified several taxa from the Copacabana group in the Cuzco area (Peru), including *Pyramidosporites* sp., *Brazilea scissa*, *Peltacystia venosa*, and

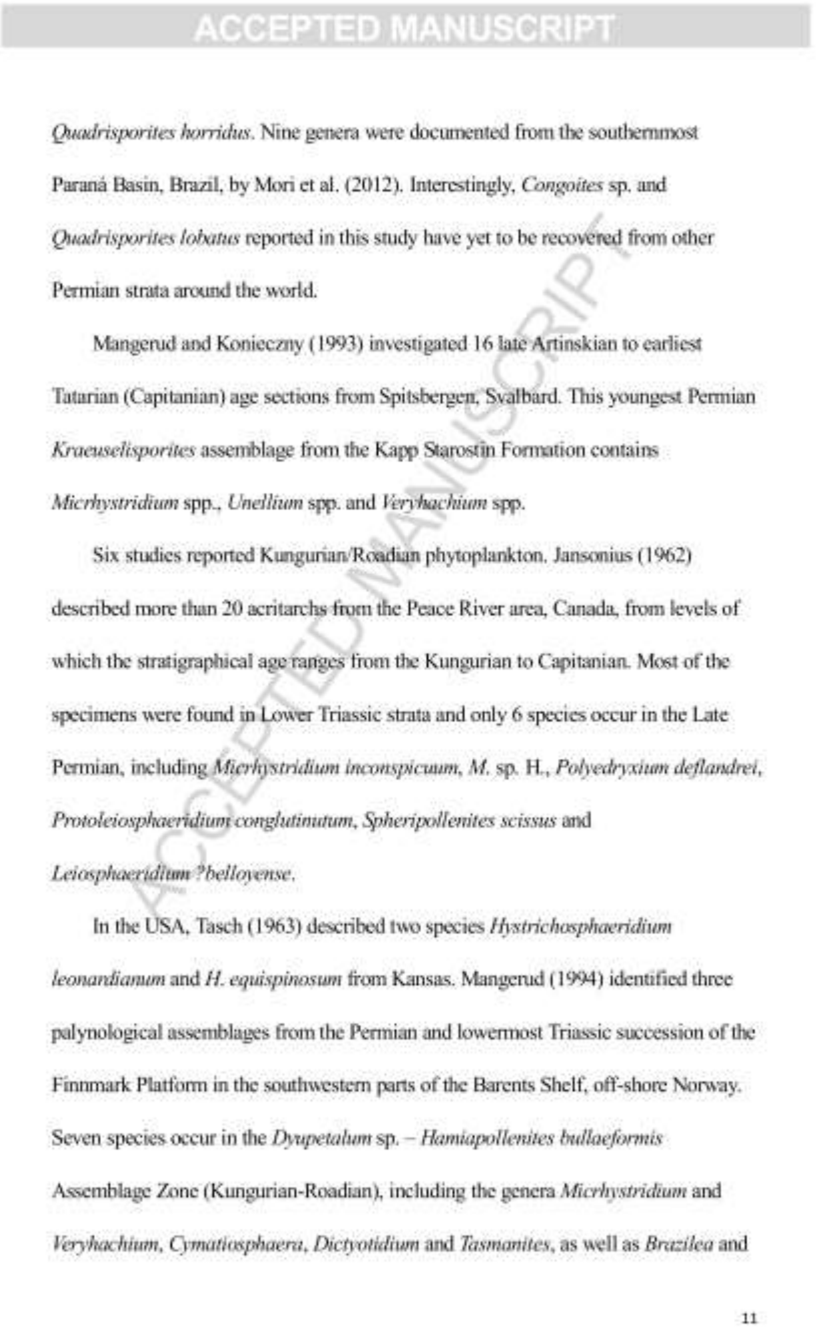

Quadrisporites horridus. Nine genera were documented from the southernmost Paraná Basin, Brazil, by Mori et al. (2012). Interestingly, *Congoites* sp. and *Quadrisporites lobatus* reported in this study have yet to be recovered from other Permian strata around the world.

Mangerud and Konieczny (1993) investigated 16 late Artinskian to earliest Tatarian (Capitanian) age sections from Spitsbergen, Svalbard. This youngest Permian *Kraeuselisporites* assemblage from the Kapp Starostin Formation contains *Micrhystridium* spp., *Unellium* spp. and *Veryhachium* spp.

Six studies reported Kungurian/Roadian phytoplankton. Jansonius (1962) described more than 20 acritarchs from the Peace River area, Canada, from levels of which the stratigraphical age ranges from the Kungurian to Capitanian. Most of the specimens were found in Lower Triassic strata and only 6 species occur in the Late Permian, including *Micrhystridium inconspicuum*, *M.* sp. H., *Polyedryxium deflandrei*, *Protoleiosphaeridium conglutinatum*, *Spheripollenites scissus* and *Leiosphaeridium ?belloyense*.

In the USA, Tasch (1963) described two species *Hystrichosphaeridium leonardianum* and *H. equispinosum* from Kansas. Mangerud (1994) identified three palynological assemblages from the Permian and lowermost Triassic succession of the Finnmark Platform in the southwestern parts of the Barents Shelf, off-shore Norway. Seven species occur in the *Dyupetalum* sp. – *Hamiapollenites bullaeformis* Assemblage Zone (Kungurian-Roadian), including the genera *Micrhystridium* and *Veryhachium*, *Cymatiosphaera*, *Dictyotidium* and *Tasmanites*, as well as *Brazilea* and

Maculatasporites, together with the enigmatic *Reduviasporonites*.

In southern Brazil, Cazzulo-Klepzig et al. (2002) studied the coal-bearing strata of the Candiota Coalfield. The assemblages include *Botryococcus braunii*, *Portalites gondwanensis*, *Pilasporites calculus*, *Brazilea scissa*, *Tetraporina horologia*, *T. punctata* and *Quadrisporites horridus*. The absolute age determination from a tonstein interbedded in the Candiota Upper Coal Seam, using U/Pb, indicated an age of 267.1±3.4 Ma, thus possibly indicating a Middle Permian age.

In Paraguay, Pérez Loinaze et al. (2010) analyzed five samples from three levels in cores of the Mallorquin-1 well, Paraná Basin. They recovered *Gorgonisphaeridium* sp., *Navifusa* sp., *Cymatiosphaera gondwanensis*, and *Reduviasporonites chalastus*.

More recently, in West Papua, Playford and Rigby (2011) documented five species of phytoplankton from the Bird's Head region (Ainim Formation) and the Central Ranges of the Bird's Body region (Aiduna Formation), including the acritarch *Mehlisphaeridium regulare*, the prasinophyte *Cymatiosphaera gondwanensis*, and *Maculatasporites indicus*, *Peltacystia venosa*, and *Quadrisporites horridus*.

2.1.5. Other Early Permian acritarchs records

Many other records come from Permian strata that are not precisely dated. Twenty-three studies have reported phytoplankton from Early Permian strata, but the lack of precise stratigraphical information means that they can only be assigned to the Early Permian or Early Cisuralian (Beri et al., 2011). Thirteen of these investigations were published based on South American material. Lower Carboniferous to Permian palynological zones were described from sections in central-western Argentina by Césari and Gutiérrez (2000), with the uppermost *Fusacolpites fusus-Vittatina subsaccata* (FS) and *Lueckisporites-Weylandites* (LW) biozones indicating an Early Permian age. Only one taxon was cited: *Brazilea scissa*. In the Paganzo Basin, Argentina, Balarino and Gutiérrez (2006) described another acritarch, *Portalites gondwanensis*, from the Tasa Cuna Formation. Pieroni and Georgieff (2007) reported *Botryococcus braunii* and *Portalites gondwanensis*, but also *Brazilea scissa* from the Sauces Formation. More recently, Gutiérrez et al. (2010) documented *Portalites gondwanensis* and *Tetraporina punctata* from the Rio Francia Formation.

In the Paraná Basin, Brazil, Tiwari and Navale (1967) reported one pollen and spore assemblage, including 14 species of acritarchs, with eight new species *Balmeella densicorpa*, *B. minuta*, *B. punctata*, *Brazilea crassa*, *Brazilea punctata*, *Congoites baculosus*, *C. conatus*, *Disectispora lobata*. Holz and Dias (1998) reported the genera *Micrhystridium*, *Pilasporites*, *Portalites* and *Veryhachium*, but also *Botryococcus*, as well as *Tasmanites* and *Brazilea* from samples investigated from the northeastern region of the Rio Grande do Sul State. Iannuzzi et al. (2006) documented the acritarchs *Leiosphaeridia* and *Portalites*, *Brazilea* and *Tetraporina*, and *Quadrisporites* from the Itararé and Rio Bonito units. Cazzulo-Klepzig et al. (2007) noted that the genera *Portalites*, *Brazilea*, *Tetraporina*, *Maculatasporites* and *Quadrisporites* were commonly found in south Brazilian coal palynofloras, but *Botryococcus* was not recorded.

In Uruguay, Gutiérrez et al. (2006) described some acritarchs from four side well

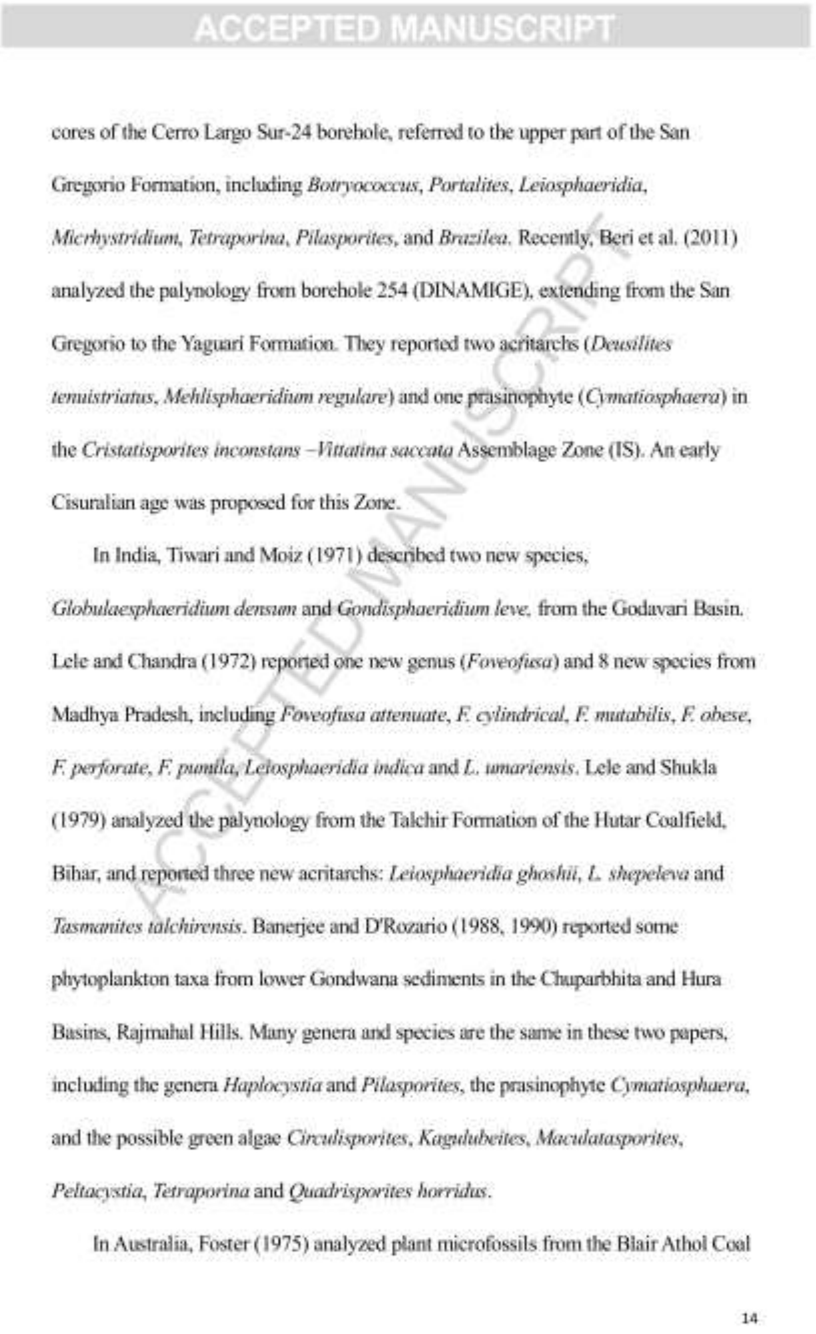

cores of the Cerro Largo Sur-24 borehole, referred to the upper part of the San Gregorio Formation, including *Botryococcus*, *Portalites*, *Leiosphaeridia*, *Micrhystridium*, *Tetraporina*, *Pilasporites*, and *Brazilea*. Recently, Beri et al. (2011) analyzed the palynology from borehole 254 (DINAMIGE), extending from the San Gregorio to the Yaguari Formation. They reported two acritarchs (*Deusilites tenuistriatus*, *Mehlisphaeridium regulare*) and one prasinophyte (*Cymatiosphaera*) in the *Cristatisporites inconstans* –*Vittatina saccata* Assemblage Zone (IS). An early Cisuralian age was proposed for this Zone.

In India, Tiwari and Moiz (1971) described two new species, *Globulaesphaeridium densum* and *Gondisphaeridium leve*, from the Godavari Basin. Lele and Chandra (1972) reported one new genus (*Foveofusa*) and 8 new species from Madhya Pradesh, including *Foveofusa attenuate*, *F. cylindrical*, *F. mutabilis*, *F. obese*, *F. perforate*, *F. pumila*, *Leiosphaeridia indica* and *L. umariensis*. Lele and Shukla (1979) analyzed the palynology from the Talchir Formation of the Hutar Coalfield, Bihar, and reported three new acritarchs: *Leiosphaeridia ghoshii*, *L. shepeleva* and *Tasmanites talchirensis*. Banerjee and D'Rozario (1988, 1990) reported some phytoplankton taxa from lower Gondwana sediments in the Chuparbhita and Hura Basins, Rajmahal Hills. Many genera and species are the same in these two papers, including the genera *Haplocystia* and *Pilasporites*, the prasinophyte *Cymatiosphaera*, and the possible green algae *Circulisporites*, *Kagulubeites*, *Maculatasporites*, *Peltacystia*, *Tetraporina* and *Quadrisporites horridus*.

In Australia, Foster (1975) analyzed plant microfossils from the Blair Athol Coal

Measures, central Queensland, and reported eight acritarchs: *Brazilea scissa*, *Circulisporites parvus*, *Maculatasporites delicates*, *Mehlisphaeridium fibratum*, *Peltacystia venosa*, *Pilasporites plurigenus*, *Quadrisporites horridus* and *Botryococcus* sp. Gilby and Foster (1988) analyzed the palynology of the Arckaringa Basin and reported a high number of acritarch species, including *Diexallophasis?* spp., *Leiofusa punctalirella*, *Leiosphaeridia.* spp., ?*Lophosphaeridium* spp., *Maculatasporites amplus*, *M. gondwanensis*, *M.* sp. cf. *M. minimus*, *Micrhystridium* spp., *Peltacystia venosa*, *Quadrisporites horridus*, *Spongocystia eraduica*, *Tetraporina* sp. A, *Ulanisphaeridium berryense*, *Botryococcus* sp. A and *Dictyotidium* spp. Backhouse (1991) described 22 phytoplankton species from the Collie Coal Measures and the underlying glacigene Stockton Formation, in the Collie Basin, including five acritarchs from the four genera *Leiosphaeridia*, *Mehlisphaeridium*, *Pyramidosporites*, and *Spongocystia*, two prasinophytes (*Cymatiosphaera gondwanensis* and *Cymatiosphaera* sp. A), and fourteen species attributed to the five genera *Brazilea*, *Circulisporites*, *Maculatasporites*, *Peltacystia* and *Tetraporina*, together with the species *Quadrisporites horridus*. By comparing the palynological results with previously published palynological studies from Western Australian strata with marine faunas, an age range of uppermost Carboniferous/Asselian to Early Late Permian was suggested for the Permian of the Collie Basin.

In Great Britain, Wall and Downie (1963) described eleven acritarchs attributed to four genera (*Baltisphaeridium*, *Leiofusa*, *Micrhystridium* and *Veryhachium*) from Lower Permian marls of Yorkshire, including two new species (*Baltisphaeridium* *debilispinum* and *Veryhachium flagelliferum*).

In Yemen, El-Nakhal et al. (2002) reported that the acritarchs *Leiosphaeridia* and *Deusilites* and the prasinophyte *Tasmanites* are common in the Khalaqah Member of the Kolli Formation, and that *Deusilites tenuistriatus* should be considered a junior synonym of *Deusilites tentus*.

In China, Kaiser (1976) documented a microflora from Taiyuan, with one acritarch, *Assamialetes giganteus*.

In Russia, Dyupina (1970) described five new species of the genus *Inderites* from the Urals: *Inderites crassus*, *I. elegans*, *I. flexuosus*, *I. microreticulatus* and *I. scrobiculatus*.

Interestingly, the widely cited taxon *Tasmanites* was first described from Permian strata in Australia by Newton (1875) who erected the type-species *Tasmanites punctatus* based on descriptions of an assemblage from the 'White Coal'.

2.2.Middle Permian (Guadalupian)

Only ten studies concern phytoplankton from the Middle Permian (Guadalupian) and the lower part of the Upper Permian (Lopingian) , although a few papers report palynomorphs from Kungurian/Roadian strata, spanning the Lower-Middle Permian boundary. In Roadian-Wordian strata, Wilson (1960) reported *Hystrichosphaeridium* sp. from Oklahoma. Jacobson et al. (1982) described six species of acritarchs (including four species of *Micrhystridium* and two new species: *Leiosphaeridia schopfii* and *Unellium phosphoriensis*) from well-dated samples in the Permian

Phosphoria and Park City Formations in northeastern Utah, USA. In Russia, Grigoriev and Utting (1998) documented acritarchs related to *Micrhystridium* spp., the prasinophyte *Cymatiosphaera* sp., together with *Tetraporina horologia* from Kolguyev Island.

Foster (1979) described five new species from Middle Permian (Roadian –Capitanian), Blair Athol Coal Measures, Baralaba Coal Measures, and the basal Rewan Formation of Queensland, Australia, including *Brazilea helbyi*, *B. helbyi* forma *gregata*, *B. helbyi* forma *helbyi*, *B. plurigena* and *Tessellaesphaera tessellate*. Lindström (1994, 1995a) analyzed the palynology of 62 samples from the southern section of a sedimentary sequence exposed at Fossilryggen in the Vestfjella mountain range in Dronning Maud Land, Antarctica. He recovered three acritarchs (Acritarch sp. A, *Leiosphaeridia* sp. and *Mehlisphaeridium* sp.), the prasinophyte *Cymatiosphaera gondwanensis*, and *Brazilea scissa*, *Circulisporites* sp., *Peltacystia monile*, and *P. venosa*. Subsequently, Lindström (2005) reported *Leiosphaeridia* sp. B, *Peltacystia monile* and *P. venosa*, and *Quadrisporites horridus* from northern Vestfjella. In Norway, Bugge et al. (2002) reported *Botryococcus* and *Tasmanites* from core samples on the eastern margin of the mid-Norwegian shelf.

Stolle published three studies on Wordian-Capitanian strata from Turkey (Stolle, 2007; Stolle et al., 2010; Stolle et al., 2011) from Wordian-Capitanian strata from Turkey, She found *Pyramidosporites cyathodes*, *Cymatiosphaera gondwanensis* and *Dictyotidium* spp., and *Tetraporina* sp. A, *Reduviasporonites chalastus* and *R.* sp. B from the Kas and Gomaniibrik formations in the Hazro outcrop area.

2.3. Late Permian (Lopingian)

2.3.1. Changhsingian and the Permian-Triassic Boundary (PTB)

Seventeen papers have described acritarchs from the latest Permian Changhsingian Stage and from Permian-Triassic Boundary strata. In China, Ouyang (1982, 1985) described three acritarchs (*Archaeodinium cingulatum*, and the two new species *Solisphaeridium solidurn* and *S. spinulatum*), together with *Tasmanites* sp., *Psiloschizosporis scissus* and *Schizosporis* sp. from eastern Yunnan. Ouyang and Utting, (1990) and Li et al. (2004a) reported five acritarch genera (*Baltisphaeridium*, *Leiosphaeridia*, *Micrhystridium*, *Veryhachium* and *Tunisphaeridium*), two prasinophyte genera (*Cymatiosphaera* and *Dictyotidium*), and *Reduviasporonites* and *Schizosporis* from the Meishan section, Zhejiang Province, that serves as the Global Boundary Stratotype Section and Point (GSSP) for the PTB. While Ouyang and Utting (1990) mentioned the presence of a *Leiosphaeridia changxingensis* –*Micrhystridium stellatum* Assemblage Zone and described a new species (*Leiosphaeridia changxingensis*), Li et al. (2004a) did not propose assemblage zones or new species, but tried to understand the phytoplankton community changes before the PTB.

Covering the Permian-Triassic transitional interval, Jekhowsky (1961) described six species of *Veryhachium* (including two new taxa: *Veryhachium ?irregulare* and *V. reductum*) from Europe (former Yugoslavia) and Africa (Tunisia, Libya, Madagascar), whereas Sarjeant et al. (1970) described sixteen acritarchs and one prasinophyte from the Chhidru Formation, in West Pakistan. Sarjeant et al. (1970) noted that the Permian acritarchs are uniformly small and of simple morphology. Hankel (1992) documented *Chordecystia chalasta* and *Reduviasporonites chalastus* from the Maji ya Chumvi Formation, Kenya. McLoughlin et al. (1997) reported *Dictyotidium* sp. and *Quadrisporites horridus* from the Amery Group, in Antarctica.

2.3.2. Other Late Permian acritarchs records

Similarly to the studies of Early Permian strata, several authors have reported phytoplankton from Late Permian strata, but the lack of precise stratigraphical information permits assignment only to the Late Permian. From the Antarctic area, Balme and Playford (1967) studied plant microfossils from the Prince Charles Mountains, and recorded *Schizosporis scissus*. *Pilasporites calculus* was documented from the Buckley Formation of the Central Transantarctic Mountains by Farabee et al. (1991). Lindström (1996) analyzed the palynology from three sections at Fossilryggen in the Vestfjella mountain range, and recorded Acritarch sp. B, *Mehlisphaeridium* sp. A, *Leiosphaeridia* sp. B, *Cymatiosphaera gondwanensis*, *Brazilea scissa*, *Circulisporites parvus*, *Peltacystia monile*, and *P. venosa*.

In Germany, Schaarschmidt (1963) described five acritarch genera (*Baltisphaeridium*, *Buedingiisphaeridium*, *Micrhystridium*, *Polyedryxium*, *Veryhachium*) and the prasinophyte genus *Cymatiosphaera*, including 21 species (seven of them were newly established) from the coast of the Franconian bay. In addition, he noted that most of the acritarchs were smaller than 20 μm.

In Israel, Horowitz (1973) described 12 species from two boreholes in the northern Negev, including four acritarchs (*Micrhystridium*, *Pterospermopsis*, *Solisphaeridium* and *Veryhachium*) and *Tasmanites*. Subsequently, Horowitz (1974) described seven acritarchs attributed to the genus *Veryhachium* from the same boreholes. Furthermore, Horowitz (1990) reported seven acritarchs and a possible zygnemataceaen alga from the Karoo region of the Republic of South Africa, belonging to *Baltisphaeridium*, *Micrhystridium*, *Solisphaeridium*, *Veryhachium* and *Tetraporina*.

From Australia, Balme and Segroves (1966) described three new species, including *Peltacystia calvitia*, *P. monilis* and *P. venosa*. McMinn (1982) described five acritarchs from the coal measure sequences of the Northern Sydney Basin, including *Mehlisphaeridium* sp. cf. *M. fibratum*, *Micrhystridium breve*, *M.* sp. cf. *M. inconspicuum*, *M. karamurzae* and the new species *Ulanisphaeridium berryense*. Fielding and McLoughlin (1992) studied the sedimentology and palynology from the vicinity of Fairbairn Dam, near the town of Emerald in central Queensland, and documented *Botryococcus braunii*, *Mehlisphaeridium* sp. cf. *M. fibratum*, *Micrhystridium* sp., *Portalites gondwanensis*, cf. *Spongocystia* sp., *Circulisporites parvus*, *Peltacystia* sp. cf. *P. calvitium* and *Tetraporina horologia*.

In India, the occurrence of four genera, including *Balmeella*, *Botryococcus*, *Greinervillites* and *Leiosphaeridia*, was reported from the Borehole RCH-151, in the Chuperbhita Coalfield, Rajmahal Basin, by Tripathi (2001). From Tanzania, the taxa *Mehlisphaeridium regulare*, *Cymatiosphaera gondwanensis* and *C.* sp. were documented from the Karoo Supergroup in the Kilombero Rift Valley by Dypvik et al. (2001).

From Pakistan, Balme (1970) reported on an assemblages of spores and pollen from the Surghar Range and Salt Range, which included five acritarchs, two of them were newly established: *Inaperturopollenites nebulosus*, *Pyramidosporites racemosus*, *Peltacystia venosa*, *Quadrisporites horridus* and *Schizosporis scissus*. Hermann et al. (2012) recently analyzed the uppermost Permian to Middle Triassic palynology from the Salt Range and Surghar Range, reporting the acritarchs *Micrhystridium* sp. and *Veryhachium* sp., but also *Quadrisporites horridus* from the late Permian strata.

2.3.3. The possible presence of a fungal spike in the Late Permian

In Italy, Visscher et al. (1996) reported the genus *Reduviasporonites* from the Southern Alps and interpreted this palynomorph as a fungal spore. Because of the massive occurrence of *Reduviasporonites* they suggested the presence of a fungal event just before the Permian-Triassic Boundary (PTB) and considered this event as very important component of the mass extinction. More recently, Sephton et al. (2009) analyzed the geochemical composition of *Reduviasporonites* from the PTB section of Tesero in the Southern Alps. They suggest that *Reduviasporonites* is indeed of fungal origin, according to results of organic chemistry analyses, including studies of carbon and nitrogen isotopes, as well as C/N ratios. Very recently, Visscher et al. (2011) confirmed this conclusion regarding the interpretation of the taxon *Reduviasporonites*.

It was in Israel that Eshet et al. (1995) first defined a 'fungal spike', with the genus *Reduviasporonites* making up to 95% of the palynomorphs in palynological assemblages recovered within the widespread claystone horizon that marks the PTB locally. In South Africa, Steiner et al. (2003) reported a one meter thick 'fungal abundance spike' in the southern Karoo Supergroup, with high abundances of *Reduviasporonites*. Sandler et al. (2006) reported a 'fungal event' at the PTB from two cores, the Makhtesh Qatan 2 (core 9) and Avedat 1 (core 5) drill holes in Israel.

Several authors have subsequently criticized these interpretations and the attribution of *Reduviasporonites* to the fungi. In European Russia, Afonin et al. (2001) reported *Tympanicysta stoschianus* at the Permian-Triassic boundary on the left bank of the Kichmenga River near Nedubrovo Village, Vologda region. This taxon, very similar to *Reduviasporonites*, was interpreted to be of algal origin. Subsequently, Foster et al. (2002) suggested that *Tympanicysta stoschiana* is a junior synonym of *Reduviasporonites chalastus*. Foster et al. (2002) reviewed the genus *Reduviasporonites* Wilson 1962 in detail, and described two species, *Reduviasporonites catenulatus* and *Reduviasporonites chalastus*, from several sections from Greenland, Britain, China, Saudi Arabia, Russia and Australia. Foster et al. (2002) also suggested that this palynomorph is most likely of algal, rather than fungal origin.

Several other authors reported *Reduviasporonites* (see Figure 1). In East Greenland, for example, Looy et al. (2001) found abundant spores and pollen grains in a palynological assemblage from the Schuchert Dal Formation, Jameson Land and Scoresby Land, that also included *Reduviasporonites*.

It appears that the debate as to whether *Reduviasporonites* is of algal or fungal origin and if a 'fungal event' really existed, will probably continue in the next years.

2.4. Other Permian acritarch records

There are another seven papers reporting phytoplankton from Permian strata with no precise stratigraphical information. Balme and Hennelly (1956) described two new species (*Brazilea plurigenus* and *Psiloschizosporis scissus*) from Australian coals. In Russia, Abramova and Martchenko(1964) reported three new species from the Pre-Caspian region, including *Inderites bulbiferus*, *I. compactus* and *I. robustus*. From Congo, Bose and Kar (1967) described one new genus with the new species *Greinervillites undulatus* whereas Kar and Bose (1976) reported the new species *Maculatasporites zairensis* from the same country (then named Zaire). In Japan, Takahashi and Yao (1969) reported some plant microfossils from the Permian sandstone in the southern marginal area of the Tanba belt, with the new species *Tasmanites tanbaensis*. Segroves (1967) described in detail the phytoplankton from western Australia, whereas Stephen (1993) investigated Australian Permian coal measure strata.

3. Palaeogeographical and palaeoenvironmental distribution of Permian phytoplankton

Acritarchs are well known to provide not only useful biostratigraphical data from the Palaeozoic rocks, but also palaeobiogeographical and palaeoenvironmental information, in particular between the Ordovician and Devonian. An acritarch provincialism is particularly obvious in the Early-Middle Ordovician (e.g., Li and Servais, 2002; Servais et al., 2003), but also present in the Silurian (e.g., Le Hérissé and Gourvennec, 1995) and Devonian (e.g., Le Hérissé et al., 1997, 2000). On the other hand, inshore-offshore variations of acritarch assemblages and palaeoenvironmental changes have been discussed for many years, and it is generally accepted that highest abundances and diversities are recorded on the shelves, with lower diversity acritarch assemblages present in nearshore and offshore environnements (e.g., Jacobson, 1979; Dorning, 1981; Vecoli, 2000; Li et al., 2004b; Stricanne et al., 2004). It is thus particularly interesting to understand if palaeobiogeographical or palaeoenvironnemental signals can also be provided by the Permian acritarchs.

Our literature review shows that 45 genera were reported in 57 papers published from southern middle palaeolatitudes, whereas 27 genera were documented in 12 papers from northern low palaeolatitudes (Figure 2). However, the Permian dataset is far from being complete. There are no documents of phytoplankton from northern high palaeolatitudes and only eleven genera are reported from northern middle palaeolatitudes. In addition, there are twenty and seventeen genera, respectively, described from southern low palaeolatitudes and from southern high palaeolatitudes. As illustrated in Figure 2D, it is obvious that the dataset is far from being complete, but it is also clearly illustrated that the number of investigations correlates with the number of described taxa. The diversity 'peak' in the southern hemisphere is clearly related to the greater number of publications and the higher number of investigated areas and samples, in particular for the Early Permian (Figure 2A).

It appears that the genus *Cymatiosphaera* has been documented widely, from northern middle palaeolatitudes to southern high palaeolatitudes. Some 'classical' acritarch genera (*Baltisphaeridium*, *Micrhystridium*, *Veryhachium*) were reported from almost all intervals between northern middle palaeolatitudes to southern middle palaeolatitudes, and they seem virtually cosmopolitan. On the other hand, the genera *Leiosphaeridia*, *Dictyotidium*, *Tasmanites* and *Brazilea* are present between northern low palaeolatitudes to southern middle palaeolatitudes, but the datasets are most probably not complete. Many genera have a narrower distribution, but this is probably the result of limited documentation and does not reflect a palaeobiogeographical distribution. However, most interestingly, the genus *Portalites* was documented fourteen times and seems to be only distributed in southern middle palaeolatitudes.

Our results support the conclusion by Li et al. (2004a), that Permian acritarch data are too sparse to support palaeobiogeographical interpretations. Most of the common acritarch taxa seem to have a cosmopolitan distribution. The distribution of taxa that might be attributed to different (green) algae groups does also not allow any palaeobiogeographical interpretation so far.

In terms of palaeoenvironmental distribution, most of the Permian organic-walled phytoplankton was reported from (nearshore) shallow marine or lagoonal environments. Most palynological investigations of Permian rocks focus on the study of plant-derived palynomorphs, which are necessisarily of terrestrial origin. Acritarchs are usually only described as minor components of these assemblages. These nearshore environments sometimes include high numbers of larger sized OWMs that are probably related to freshwater green algae. As already indicated by Colbath and Grenfell (1995) several of these OWMs may have different biological affinities and all are not necessarily attributable to the marine phytoplankton. As the biological affinities remain mostly unknown, it is difficult to estimate the ratio of freshwater forms.

Only a few papers investigated assemblages from more offshore marine environments (e.g., Doubinger and Marocco, 1981; Ouyang and Utting, 1990; Mangerud and Konieczny, 1993; Li et al., 2004a; Stephenson et al., 2008). These studies mostly document large numbers of smaller sized acritarchs (usually smaller than 20 µm), including high numbers of the 'common' taxa *Baltisphaeridium*, *Micrhystridium* and *Veryhachium*, that are considered as typically marine forms, probably resting cysts of phytoplankton.

4. Permian phytoplankton diversity

Relatively few studies focus on the description of the marine organic-walled phytoplankton of the Late Palaeozoic and most probably the major part of the phytoplankton still remains undescribed. Similar to the Carboniferous (Mullins and Servais, 2008), there are still a number of barriers to estimating the Permian phytoplankton diversity. Firstly, there is a lack of precise age control in some studies (see above). Secondly, taxonomic consistency and/or accuracy remain in many cases uncertain. Detailed revision is needed for most of the Permian taxa- that were described many years ago when biometrical and variability studies were not yet common. Thirdly, the number of investigations and the variable duration of the Permian stages continue to effect those diversity calculations that are possible to date accurately. Finally, another bias in our dataset may be the reworking of older palynomorphs in younger sediments. However, it is often impossible to distinguish reworked from "*in situ*" specimens. Most of the published biodiversity studies do not take into account this possible bias. In order to illustrate relative diversity fluctuations through Permian tome., we compared the number of described taxa with the number of samples and investigations for each stratigraphic stage.

Taxa that occur in two (or more) stages are counted as occurring in both (or all) stages. The resulting 'total diversity' is illustrated in Figure 3. In addition, we counted the number of species and the number of times that species were reported in every genus (Figure 4).

Early Permian, over 30 phytoplankton genera are recorded (Figure 3). Taxon richness appears to drop in the Middle to lower Upper Permian, with only about twenty phytoplankton genera described between the Roadian to Wuchiapingian. However, there are 36 genera recorded in the uppermost Permian, in the Changhsingian stage (Figure 3). There seems to be a clear correlation between the number of investigations and the number of taxa recorded, the high diversities in the Lower and uppermost Permian correlating with the greater number of investigations (Figure 3).

The most diverse phytoplankton assemblage occurs in the Early Permian of Australia, with twenty-two phytoplankton species described by Backhouse (1991). The investigations of Gilby and Foster (1988), Tiwari and Navale (1967), Beri et al. (2010), Lindström (1995b), Mori et al. (2011), and Wall and Downie (1963), report over ten species in each Early Permian assemblage. The number of Middle Permian phytoplankton species in a single study never exceeds ten, with the highest records of eight species in the papers by Lindström (1995a) and Mangerud (1994). Schaarschmidt (1963) describe 21 phytoplankton species from the Late Permian, including one prasinophyte. This maximum is followed by the description of 16 acritarchs and one prasinophyte from western Pakistan by Sarjeant et al. (1970) and the recording of ten acritarchs and two prasinophytes from Israel by Horowitz (1973). Detailed taxonomic revisions would be needed to determine if these higher diversities recorded in the Permian are simply artifact of taxonomic splitting.

Some phytoplankton taxa occur in all Permian stages, including the genera *Botryococcus*, *Brazilea*, *Cymatiosphaera*,, *Leiosphaeridia*, *Micrhystridium*, *Peltacystia*, *Polyedryxium*, *Pyramidosporites*, *Tasmanites*, *Tetraporina*, *and Veryhachium* (Figure 3). *Some genera are found* in almost all stages, except in the Wuchiapingian (*Dictyotidium* and *Quadrisporites*). On the other hand, *Baltisphaeridium* is reported from all stages except from the Capitanian. This may suggest that these taxa are present during the entire Permian, but not yet recorded from the Capitanian and Wuchiapingian, respectively. On the contrary, *Comasphaeridium* and *Greinervillites* are only found in the Kungurian, and

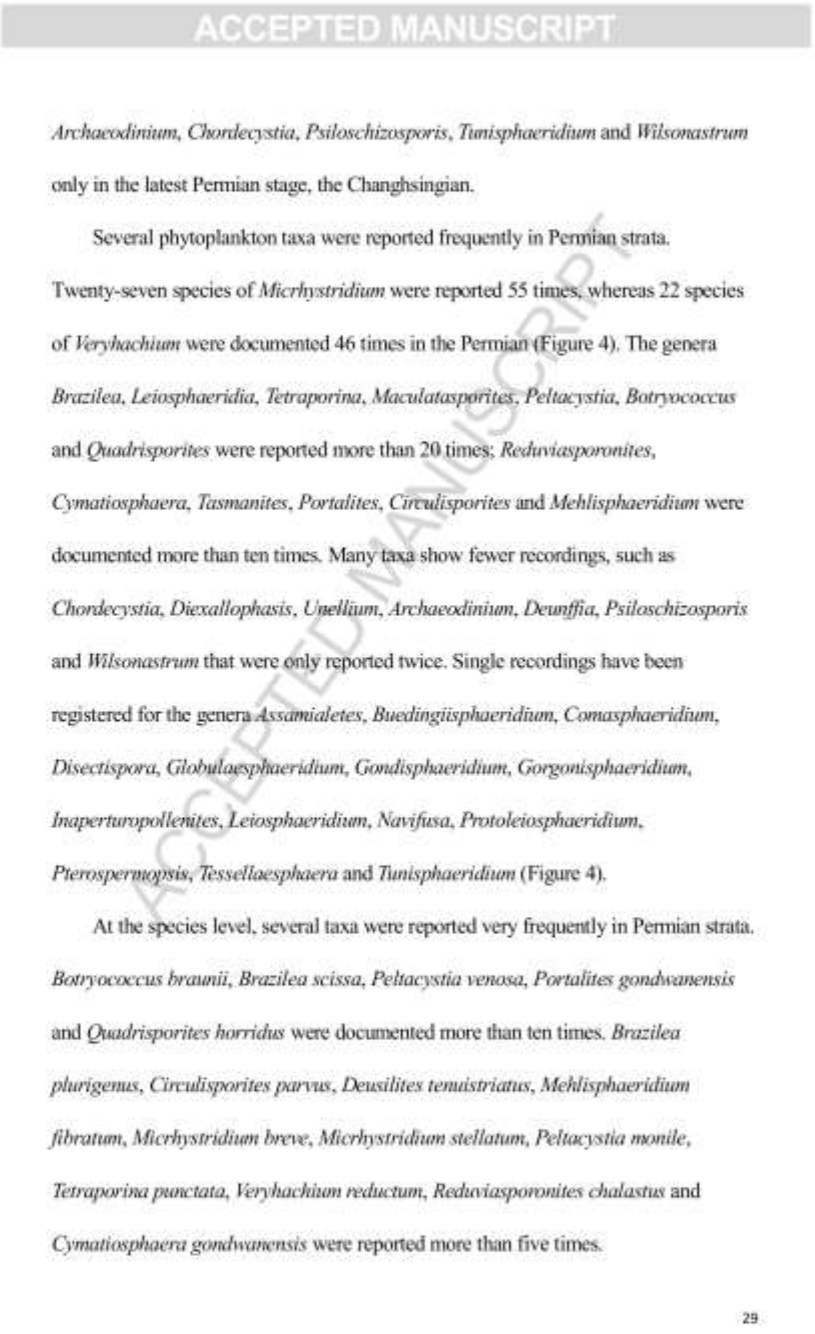

Archaeodinium, *Chordecystia*, *Psiloschizosporis*, *Tunisphaeridium* and *Wilsonastrum* only in the latest Permian stage, the Changhsingian.

Several phytoplankton taxa were reported frequently in Permian strata. Twenty-seven species of *Micrhystridium* were reported 55 times, whereas 22 species of *Veryhachium* were documented 46 times in the Permian (Figure 4). The genera *Brazilea*, *Leiosphaeridia*, *Tetraporina*, *Maculatasporites*, *Peltacystia*, *Botryococcus* and *Quadrisporites* were reported more than 20 times; *Reduviasporonites*, *Cymatiosphaera*, *Tasmanites*, *Portalites*, *Circulisporites* and *Mehlisphaeridium* were documented more than ten times. Many taxa show fewer recordings, such as *Chordecystia*, *Diexallophasis*, *Unellium*, *Archaeodinium*, *Deunffia*, *Psiloschizosporis* and *Wilsonastrum* that were only reported twice. Single recordings have been registered for the genera *Assamialetes*, *Buedingiisphaeridium*, *Comasphaeridium*, *Disectispora*, *Globulaesphaeridium*, *Gondisphaeridium*, *Gorgonisphaeridium*, *Inaperturopollenites*, *Leiosphaeridium*, *Navifusa*, *Protoleiosphaeridium*, *Pterospermopsis*, *Tessellaesphaera* and *Tunisphaeridium* (Figure 4).

At the species level, several taxa were reported very frequently in Permian strata. *Botryococcus braunii*, *Brazilea scissa*, *Peltacystia venosa*, *Portalites gondwanensis* and *Quadrisporites horridus* were documented more than ten times. *Brazilea plurigenus*, *Circulisporites parvus*, *Deusilites tenuistriatus*, *Mehlisphaeridium fibratum*, *Micrhystridium breve*, *Micrhystridium stellatum*, *Peltacystia monile*, *Tetraporina punctata*, *Veryhachium reductum*, *Reduviasporonites chalastus* and *Cymatiosphaera gondwanensis* were reported more than five times.

5. Conclusions

About 100 studies have reported acritarchs and green algae (Prasinophyceae, Zygnemataceae and Hydrodictyaceae) from Permian strata. More than half of these publications concerned strata of the Early Permian, and only ten papers reported Middle Permian phytoplankton. The majority of the descriptions are from localities that were located in southern middle Permian palaeolatitudes. Most studies focused on terrestrial,plant-derived palynomorphs described from palaeoenvironments, located at the margins of the Gondwanan supercontinent. More than twenty papers were reported from South America, with a high number of publications from Brazil, Argentina, Uruguay and Paraguay. On the other hand, only twenty-five papers concern the Permian northern hemisphere and very few papers document high palaeolatitudes.

The dataset on Permian phytoplankton is both inconsistent and in taxon richness curve strongly correlates with the number of investigations. The relatively high phytoplankton diversities in the Early and latest Permian can be correlated with the greater number of investigations: 45 and 36 phytoplankton genera are described in the Kungurian and Changhsingian stages, but only 20 genera, respectively, in the Wordian and Capitanian stages. Therefore, we do not propose that this high-low-high pattern characterizes the permain record. The most common recorded genera are *Micrhystridium* and *Veryhachium*. These are most probably open marine phytoplankton cysts, but many palynomorphs thought to belong to freshwater green algae.

If small marine acritarchs (usually smaller than 20 µm) were to be described in detail, they might reveal a much higher morphological diversity than previously recorded. This is the case with diverse, but commonly ignored, small Cretaceaous acritarchs described by Habib and Knapp (1982) and Schrank (2003). However, given the present state of knowledge, the record of Permian acritarchs, when examined in detail, continues to support more general studies which have remarked on a dearth of cyst-forming phytoplankton during the Carboniferous-Triassic interval ever since the pioneering work of Helen Tappan (Tappan, 1980).

Acknowledgments

We are particularly grateful to Paul Strother, Thijs Vandenbroucke and Marco Vecoli, who greatly helped improving this paper with their detailed review. We acknowledge the help of Elisabeth Locatelli (Géosystèmes, Lille, France) for finding Permian references. This work was supported by National Science Foundation of China (NSFC) project no. 40839903, 40921062, the Chinese 973 (2011CB808800), and 111 programmes (B08030) and by grants of the University of Lille1 ("Allocation Présidentielle" and "Bonus Qualité Recherche") and the Conseil Régional du Nord (France).

References

Abramova, S.A., Martchenko, O.F., 1964. Opyt primeneniya palinologicheskogo metoda issledovaniya pri izuchenii solyanykh kupolov Prikaspiya (experimental applications of palynological methods of investigation to the study of salt-domes in the Pre-Caspian region). Vsesoyuznyi Nauchno-Issledovatelskii Institut Galurgii, Moskva, Trudy, 49-52.

Afonin, S., Barinova, S., Krassilov, V., 2001. A bloom of *Tympanicysta* Balme (green algae of zygnematalean affinities) at the Permian-Triassic boundary. Geodiversitas 23, 481-487.

Backhouse, J., 1991. Permian palynostratigraphy of the Collie Basin, Western Australia. Review of Palaeobotany and Palynology 67, 237-314.

Balarino, M.L., Gutiérrez, P.R., 2006. Palinología de la Formación Tasa Cuna (Pérmico Inferior), Córdoba, Argentina: sistemática y consideraciones bioestratigráficas. Ameghiniana 43, 437-460.

Balme, B., 1970. Palynology of Permian and Triassic strata in the Salt Range and Surghar Range, West Pakistan (In: Stratigraphic boundary problems; Permian and Triassic of West Pakistan). University of Kansas, Department of Geology 4, 305-453.

Balme, B.E., Hennelly, J.P.F., 1956. Monolete, monocolpate, and alete sporomorphs from Australian Permian sediments. Australian Journal of Botany 4, 54-67.

Balme, B., Playford, G., 1967. Late Permian plant microfossils from the Prince Charles Mountains, Antarctica. Revue de Micropaléontologie 10, 179-192.

Balme, B., Segroves, K., 1966. *Peltacystia* gen. nov.: a microfossil of uncertain affinities from the Permian of Western Australia. Journal of the Royal Society of Western Australia 49, 26-31.

Banerjee, M., D'Rozario, A., 1988. Palynostratigraphy and environment of deposition in the Lower Gondwana sediments of Chuparbhita coalfield, Rajmahal Hills. Journal of the Palaeontological Society of India 33, 73-90.

Banerjee, M., D'Rozario, A., 1990. Palynostratigraphic correlation of lower Gondwana sediments in the Chuparbhita and Hura Basins, Rajmahal Hills, Eastern India. Review of Palaeobotany and Palynology 65, 239-255.

Beri, Á., Gutiérrez, P.R., Cernuschi, F., Balarino, M.L., 2006. Palinología del Pérmico Inferior en la perforación DCLS-24 (Formación San Gregorio), departamento de Cerro Largo, Uruguay. Parte I: esporas, algas, prasinofitas y acritarcas Ameghiniana 43, 227-244.

Beri, Á., Martínez Blanco, X., Mourelle, D., 2010. A synthesis of palynological data from the Lower Permian Cerro Pelado Formation (Paraná Basin, Uruguay): A record of warmer climate stages during Gondwana glaciations. Geologica Acta 8, 419-429.

Beri, Á., Gutiérrez, P., Balarino, L., 2011. Palynostratigraphy of the late Palaeozoic of Uruguay, Paraná Basin. Review of Palaeobotany and Palynology 167, 16-29.

Besems, R.E., Schuurman, W.M.L., 1987. Palynostratigraphy of Late Paleozoic glacial deposits of the Arabian Peninsula with special reference to Oman. Palynology 11, 37-53.

Bose, M., Kar, R., 1967. Palaeozoic Sporae dispersae from Congo IV. On some new miospore genera. Musée royal de l'afrique central, Annales. Série in 8, sciences géologiques, 87-98.

Bugge, T., Ringas, J., Leith, D., Mangerud, G., Weiss, H., Leith, T., 2002. Upper Permian as a new play model on the mid-Norwegian continental shelf: Investigated by shallow stratigraphic drilling. AAPG Bulletin 86, 107.

Césari, S.N., Gutiérrez, P.R., 2000. Palynostratigraphy of Upper Paleozoic sequences in central-western Argentina. Palynology 24, 113.

Cazzulo-Klepzig, M., Guerra-Sommer, M., Formoso, N., Calarge, L., 2002. Geochemical and palynological evidence for the age determination of Permian coals, southern Brazil. Journal of South American Earth Sciences 15, 375-380.

Cazzulo-Klepzig, M., Guerra-Sommer, M., Menegat, R., Simas, M.W., Mendon a Filho, J.G., 2007. Peat-forming environment of permian coal seams from the faxinal coalfield (Paraná Basin) in southern Brazil, based on palynology and palaeobotany. Revista Brasileira de Paleontologia 10, 117-127.

Colbath, G.K., Grenfell, H.R. 1995. Review of biological affinities of Paleozoic acid-resistant, organic-walled eukaryotic algal microfossils (including "acritarchs"). Review of Palaeobotany and Palynology 86, 287-314.

Di Pasquo, M., Vergel, M.M., Azcuy, C.L., 2010. Pennsylvanian and Cisuralian palynofloras from the Los Sauces area, La Rioja Province, Argentina: Chronological and paleoecological significance. International Journal of Coal Geology 83, 276-291.

Dorning, K.J., 1981. Silurian acritarch distribution in the Ludlowian shelf sea of South Wales and the Welsh Borderland. In: Neale, J.W., Brasier, M.D. (eds.), Microfossils from Recent and Fossil Shelf Seas. Ellis Horwood, Chichester, pp. 31-36.

Doubinger, J., Marocco, R., 1981. Contenu palynologique du groupe Copacabana (Permien Inférieur et Moyen) sur la bordure sud de la cordillère de Vilcabamba, Région de Cuzco (Pérou). Geologische Rundschau 70, 1086-1099.

Dypvik, H., Hankel, O., Nilsen, O., Kaaya, C., Kilembe, E., 2001. The lithostratigraphy of the Karoo supergroup in the Kilombero Rift Valley, Tanzania. Journal of African Earth Sciences 32, 451-470.

Dyupina, G.V., 1970. Akritarkhi terrigennykh otlozheniy nizhney permi srednego Urala (Acritarchs from lower Permian terrigenous deposits of the central Urals) In: Verkhnepaleozoyskiye terrigennyye otlozheniya Urala. Akademiya Nauk SSSR, Ural'skiy Filial, Institut Geologii i Geokhimii, Trudy 88, 47-60.

El-Nakhal, H.A., Stephenson, M.H., Owens, B., 2002. New Late Carboniferous-Early Permian palynological data from glacial sediments in the Kooli Formation, Republic of Yemen. Micropaleontology 48, 222.

Eshet, Y., Campino, M.R., Visscher, H., 1995, Fungal event and palynological record of ecological crisis and recovery across the Permian-Triassic boundary. Geology 23, 967-970.

Farabee, M.J., Taylor, E.L., Taylor, T.N., 1991. Late Permian palynomorphs from the Buckley formation, central transantarctic mountains, Antarctica. Review of

Palaeobotany and Palynology 69, 353-368.

Fensome R.A., Williams, G.L., Sedley Barss, M., Freeman, J.M., Hill J.M., 1990. Acritarchs and fossil Prasinophites: An index to genera, species and intraspecific taxa. American Association of Stratigraphic Palynologists Foundation 25, 1-771.

Fielding, C., McLoughlin, S., 1992. Sedimentology and palynostratigraphy of Permian rocks exposed at Fairbairn Dam, central Queensland. Australian Journal of Earth Sciences 39, 631-649.

Foster, C.B., 1974. Stratigraphy and palynology of the Permian at Waterloo Bay, Yorke Peninsula, South Australia. Transactions of the Royal Society of South Australia 98, 29-42.

Foster, C.B., 1975. Permian plant microfossils from the Blair Athol Coal Measures, central Queensland, Australia. Palaeontographica. Abteilung B: Palaeophytologie 154, 121-171.

Foster, C.B., 1979. Permian plant microfossils of the Blair Athol Coal Measures, Baralaba Coal Measures, and basal Rewan Formation of Queensland. Geological Survey of Queensland, 1-244.

Foster, C.B., Waterhouse, J., 1988. The *Granulatisporites confluens* Oppel-zone and early Permian marine faunas from the Grant Formation on the Barbwire terrace, Canning Basin, Western Australia. Journal of the Geological Society of Australia 35, 135-157.

Foster, C.B., Stephenson, M.H., Marshall, C., Logan, G.A., Greenwood, P.F., 2002. A revision of *Reduviasporonites* Wilson 1962: description, illustration, comparison and biological affinities. Palynology 26, 35-58.

Gilby, A.R., Foster, C.B., 1988. Early Permian palynology of the Arckaringa Basin, South Australia. Palaeontographica. Abteilung B: Palaeophytologie 209, 167-191.

Gorter, J., Poynter, S., Bayford, S., Caudullo, A., 2008. Glacially influenced petroleum plays in the Kulshill Group (Late Carboniferous Early Permian) of the southeastern Bonaparte Basin, Western Australia. The APPEA Journal 48, 69-113.

Gradstein, F.M., Ogg, J.G., Smith, A.G., Bleeker, W., Lourens, L.J., 2004. A new geologic time scale, with special reference to Precambrian and Neogene. Episodes 27, 83-100.

Grigoriev, M., Utting, J., 1998. Sedimentology, palynostratigraphy, palynofacies and thermal maturity of Upper Permian rocks of Kolguyev Island, Barents Sea, Russia. Bulletin of Canadian Petroleum Geology 46, 1-11.

Guerra-Sommer, M., Cazzulo-Klepzig, M., Menegat, R., Formoso, M.L.L., Basei, M.S., Barboza, E.G., Simas, M.W., 2008. Geochronological data from the Faxinal coal succession, southern Paraná Basin, Brazil: A preliminary approach combining radiometric U-Pb dating and palynostratigraphy. Journal of South American Earth Sciences 25, 246-256.

Gutiérrez, P.R., Cisterna, G., Balarino, L., Coturel, E., Desjardins, P., 2005. Formación Tupe (Carbonífero Superior-Pérmico inferior) en la mina La Delfina (Cuesta de Huaco, San Juan): contenido paleontológico. Ameghiniana 42, 32-33.

Gutiérrez, P.R., Beri, Á., Balarino, M.L., Cernuschi, F., 2006. Palinología del Pérmico Inferior en la perforación CLS-24 (Cerro Largo Sur), departamento de Cerro Largo, Uruguay. Parte II: granos de pollen. Ameghiniana 43, 611-635.

Gutiérrez, P.R., Correa, G.A., Carrevedo, M.L., 2010. Primer registro de palinomorfos de edad pérmica en la Formación Río Francia (Paleozoico Superior, San Juan, Argentina). Revista del Museo Argentino de Ciencias Naturales 12, 203-216.

Habib, D., Knapp, S.D., 1982. Stratigraphic utility of Cretaceous small acritarchs. Micropaleontology, 28: 335-371, Tulsa.

Hankel, O., 1992. Late Permian to early triassic microfloral assemblages from the Maji ya chumvi formation, Kenya. Review of Palaeobotany and Palynology 72, 129-147.

Head, M., 1996. Modern dinoflagellate cysts and their biologicalaffinities. In: Jansonius, J., McGregor, D.C. (eds.), Palynology: Principles and Applications, American Association of Stratigraphic Palynologists Foundation, pp. 1197–1248.

Hermann, E., Hochuli, P.A., Bucher, H., Roohi, G., 2012. Uppermost Permian to Middle Triassic palynology of the Salt Range and Surghar Range, Pakistan. Review of Palaeobotany and Palynology 169, 61-95.

Holz, M., Dias, M.E., 1998. Taphonomy of palynological records in a sequence stratigraphic framework: an example from the Early Permian Paraná Basin of southern Brazil. Review of Palaeobotany and Palynology 99, 217-233.

Horowitz, A., 1973. Late Permian palynomorphs from southern Israel. Pollen et Spores 15, 315-341.

Horowitz, A., 1974. Especes du genre Veryhachium du Permo-Trias du Sud d'Israel. Revue de Micropaléontologie 17, 75-80.

Horowitz, A., 1990. Palynology and paleoenvironment of uranium deposits in the Permian Beaufort Group, South Africa. Ore Geology Reviews 5, 537-540.

Iannuzzi, R., dos Santos Scherer, C.M., de Souza, P.A., Holz, M., Caravaca, G., Adami-Rodrigues, K., Tybusch, G.P., de Souza, J.M., Smaniotto, L.P., Fischer, T.V., 2006. Afloramento Morro do Papaléo, Mariana Pimentel, RS. Registro ímpar da sucessão sedimentar e florística pós-glacial do Paleozóico da Bacia do Paraná 2.

Jacobson, S.R., 1979. Acritarchs as paleoenvironmental indicators in Middle and Upper Ordovican rocks from Kentucky, Ohio and New York. Journal of Paleontology 53, 1197-1212.

Jacobson, S.R., Wardlaw, B.R., Saxton, J.D., 1982. Acritarchs from the Phosphoria and Park City Formations (Permian, Northeastern Utah). Journal of Paleontology 56, 449-458.

Jansonius, J., 1962. Palynology of Permian and Triassic sediments. Peace River area, Western Canada. Palaeontographica 110, 35-98.

Jardiné, S., 1974. Microflores des formations du Gabon attribuées au Karroo. Review of Palaeobotany and Palynology 17, 75-112.

Jekhowsky, de, B., 1961. Sur quelques hystrichospheres Permo-Triassiques d'Europe et d'Afrique. Revue de Micropaléontologie 3, 207-212.

Kaiser, H., 1976. Die permische Mikroflora der Cathaysia-Schichten von

Nordwest-Schansi, China. Palaeontographica. Abteilung B: Palaeophytologie 159, 83-157.

Kar, R.K., Bose, M.N., 1976. Palaeozoic sporae dispersae from Zaire (Congo); XII, Assise a couches de houille from Greinerville region. Musée royal de l'afrique central, Annales. Série in 8, Sciences Geologiques, 23-133.

Katz, M.E., Finkel, Z.V., Grzebyk, D., Knoll, A.H., Falkowski, P.G., 2004. Evolutionnary trajectories and biogeochemical impacts of marine eukaryotic phytoplankton. Annual Review of Ecology, Evolution and Systematics 35, 523-556.

Kent, L., Lindstrom, S., Guy-Ohlson, D., 1990. An Early Permian palynoflora from Milorgfjella, Dronning Maud Land, Antarctica. Antarctic Science 2, 331-344.

Klug, C., Kröger, B., Kiessling, W., Mullins, G.L., Servais, T., Fryda, J., Korn, D., Turner, S., 2010. The Devonian Nekton Revolution. Lethaia 43, 465-477.

Le Hérissé, A., Gourvennec, R., 1995. Biogeography of upper Llandovery and Wenlock acritarchs. Review of Palaeobotany and Palynology 86, 111-133.

Le Hérissé, A., Gourvennec, R., Wicander, R., 1997. Biogeography of Late Silurian and Devonian acritarchs and prasinophytes. Review of Palaeobotany and Palynology 98, 105-124.

Le Hérissé, A., Servais, T., Wicander, R., 2000. Devonian acritarchs and related forms. Courier Forschungs-Institut Senckenberg 220, 195-205.

Lele, K.M., Chandra, A., 1972. Palynology of the marine intercalations in the lower Gondwana of Madhya Pradesh, India. The Palaeobotanist 19, 253-262.

Lele, K.M., Kulkarni, S., 1969. Two miospore assemblages from the Argada sector, south Karanpura coalfield, Bihar, with remarks on their probable age. The Palaeobotanist 17, 288-293.

Lele, K.M., Shukla, M., 1979. Studies in the Talchir flora of India; 12, Palynology of the Talchir Formation of Hutar Coalfield, Bihar. Geophytology 10, 231-238.

Li, J., Servais, T., 2002. Ordovician acritarchs of China and their utility for global palaeobiogeography. Bulletin de la Société géologique de France 173, 399-406.

Li, J., Servais, T., Brocke, R., 2002. Chinese Palaeozoic acritarch research: Review and Perspectives. Review of Palaeobotany and Palynology 118, 181-193.

Li, J., Cao, C., Servais, T., Zhu, Y., 2004a. Later Permian acritarchs from Meishan (SE China) in the context of Permian palaeobiogeography and palaeoecology. Neues Jahrbuch für Geologie und Paläontologie, Monatshefte 2004, 427-448.

Li, J., Servais, T., Yan, Y., Zhu, H., 2004b. A nearshore-offshore trend in the acritarch distribution of the EarlyMiddle Ordovician of the Yangtze Platform, S-China. Review of Palaeobotany and Palynology 130, 141-161.

Lindström, S., 1994. Late Palaeozoic palynology of western Dronning Maud Land, Antarctica. Lund Publications in Geology 121, 1-33.

Lindström, S., 1995a. Early Late Permian palynostratigraphy and palaeo-biogeography of Vestfjella, Dronning Maud Land, Antarctica. Review of Palaeobotany and Palynology 86, 157-173.

Lindström, S., 1995b. Early Permian palynostratigraphy of the northern Heimefrontfjella mountain-range, Dronning Maud Land, Antarctica. Review of

Palaeobotany and Palynology 89, 359-415.

Lindström, S., 1996. Late Permian palynology of Fossilryggen, Vestfjella, Dronning Maud Land, Antarctica. Palynology, 15-48.

Lindström, S., 2005. Palynology of Permian shale, clay and sandstone clasts from the Basen till in northern Vestfjella, Dronning Maud Land. Antarctic Science 17, 87-96.

Looy, C.V., Twitchett, R.J., Dilcher, D.L., Van Konijnenburg-Van Cittert, J.H.A., Visscher, H., 2001. Life in the end-Permian dead zone. Proceedings of the National Academy of Sciences of the United States of America 98, 7879-7883.

Maithy, P., 1971. Fossil flora from Barakar stage in Auranga Coalfield. The Palaeobotanist 19, 70-76.

Mangerud, G., 1994. Palynostratigraphy of the Permian and lowermost triassic succession, Finnmark Platform, Barents sea. Review of Palaeobotany and Palynology 82, 317-349.

Mangerud, G., Konieczny, R., 1993. Palynology of the Permian succession of Spitsbergen, Svalbard. Polar Research 12, 65-93.

Mautino, L., Vergel, M., Anzótegui, L., 1998. Palinologia de la Formacion Melo (Permico inferior) en Arroyo Seco, Departamento Rivera, Uruguay, Parte V: Granos de polen, acritarcas E Incertae sedis. Ameghiniana 35, 299-314.

McLoughlin, S., Lindström, S., Drinnan, A.N., 1997. Gondwanan floristic and sedimentological trends during the Permian-Triassic transition: new evidence from the Amery Group, northern Prince Charles Mountains, East Antarctica.

Antarctic Science 9, 281-298.

McMinn, A., 1982. Late Permian acritarchs from the northern Sydney Basin. Journal and Proceedings of the Royal Society of New South Wales 115, 79-86.

Mori, A.L.O., de Souza, P.A., Marques, J.C., Lopes, R.C., 2012. A new U-Pb zircon age dating and palynological data from a Lower Permian section of the southernmost Paraná Basin, Brazil: biochronostratigraphical and geochronological implications for Gondwanan correlations. Gondwana Research 21, 654-669.

Molyneux, S.G., Le Hérissé, A., Wicander, R., 1996. Paleozoic phytoplankton. In: Jansonius, J., McGregor, D.C. (eds.), Palynology: Principles and Applications, American Association of Stratigraphic Palynologists Foundation, pp. 493-529.

Mullins, G.L., Servais, T., 2008. The diversity of the Carboniferous phytoplankton. Review of Palaeobotany and Palynology 149, 29-49.

Munnecke, A., Servais, T., 2008. Palaeozoic calcareous plankton: evidence from the Silurian of Gotland. Lethaia 41, 185-194

Newton, E.T., 1875. On "Tasmanite" and Australian "White Coal". Geological Magazine 12, 337-342.

Ouyang, S., 1982. Upper Permian and Lower Triassic palynomorphs from eastern Yunnan, China. Canadian Journal of Earth Sciences 19, 68-80.

Ouyang, S., 1985. Palynology of Upper Permian and Lower Triassic strata of Fuyuan District, eastern Yunnan. Palaeontologia Sinica, new series A, no.9 (whole no.169), 1-122. (In Chinese with English summary.)

Ouyang, S., Utting, J., 1990. Palynology of upper Permian and lower Triassic rocks, Meishan, Changxing County, Zhejiang Province, China. Review of Palaeobotany and Palynology 66, 65-103.

Pérez Loinaze, V., Césari, S.N., López Gamundi, O., Buatois, L., 2010. Palynology of the Permian San Miguel Formation (Western Paraná Basin, Paraguay): Gondwanan biostratigraphic correlations. Geologica Acta 8, 483-493.

Pieroni, E.M., Georgieff, S.M., 2007. Reconsideración estratigráfica del Neopaleozoico de los alrededores del dique Los Sauces, La Rioja. Revista de la Asociación Geológica Argentina 62, 105-115.

Playford, G., Rigby, J.F., 2011. Permian palynoflora of the Ainim and Aiduna formations, West Papua. Revista española de micropaleontologia 40, 1-57.

Quadros, L.P., 2002. Acritarcos e tasmanites do Permo-Carbonífero da bacia do Paraná. Revista do Instituto Geológico 23, 39-50.

Riegel, W., 1996. The geologic significance of the Late Paleozoic phytoplankton blackout. IX IPC Meeting, Houston,Texas, U.S.A., Abstracts, pp. 133–134.

Riegel, W., 2008. The Late Palaeozoic phytoplankton blackout--Artefact or evidence of global change. Review of Palaeobotany and Palynology 148, 73-90.

Sarjeant, W.A.S., Kummel, B., Teichert, C., 1970. Acritarchs and tasmanitids from the Chhidru Formation, uppermost Permian of West Pakistan. Stratigraphical Boundary Problems: Permian and Triassic of West Pakistan. University of Kansas, Department of Geology, Special Publication 4, 277-304.

Sandler, A., Eshet, Y., Schilman, B., 2006. Evidence for a fungal event, methane-hydrate release and soil erosion at the Permian-Triassic boundary in southern Israel. Palaeogeography, Palaeoclimatology, Palaeoecology 242, 68-89.

Schaarschmidt, F., 1963. Sporen und Hystrichosphaerideen aus dem Zechstein von Büdingen in der Wetterau. Palaeontographica Abteilung B 113, 38-91.

Schrank, E., 2003. Small acritarchs from the Upper Cretaceous: taxonomy, biological affinities and palaeoecology. Review of Palaeobotany and Palynology 123, 199-235.

Segroves, K.L., 1967. Cutinized microfossils of probable nonvascular origin from the Permian of Western Australia. Micropaleontology 13, 289-305.

Sephton, M.A., Visscher, H., Looy, C.V., Verchovsky, A.B., Watson, J.S., 2009. Chemical constitution of a Permian-Triassic disaster species. Geology 37, 875-878.

Servais, T., Li, J., Molyneux, S.G., Raevskaya, E., 2003. Ordovician organic-walled microphytoplankton (acritarch) distribution: the global scenario. Palaeogeography, Palaeoclimatology, Palaeoecology 195, 149-172.

Servais, T., Li, J., Stricanne, L., Vecoli, M., Wicander, R., 2004. Acritarchs. In: Webby, B., Droser, M., Paris, F., Percival, I. (eds), The Great Ordovician Biodiversification Event. Columbia University Press, New York, pp. 348-360.

Servais, T., Nützel, A., Mullins, G., 2006. Was there a phytoplankton blackout in the late Paleozoic? Palynology 30, 228.

Servais, T., Lehnert, O., Li, J., Mullins, G.L., Munnecke, A., Nützel, A., Vecoli, M. 2008. The Ordovician Biodiversification: revolution in the oceanic trophic chain.

Lethaia 41, 99-109.

Servais, T., Owen, A.W., Harper, D.A.T, Kröger, B. & Munnecke, A., 2010. The Great Ordovician Biodiversification Event (GOBE): the palaeoecological dimension. Palaeogeography, Palaeoclimatology, Palaeoecology 294, 99-119.

Souza, P., Callegari, L., 2010. An early Permian palynoflora from the Itararé Subgroup, Paraná Basin, Brazil. Revista española de micropaleontologia 36, 439-450.

Steiner, M.B., Eshet, Y., Rampino, M.R., Schwindt, D.M., 2003. Fungal abundance spike and the Permian-Triassic boundary in the Karoo Supergroup (South Africa). Palaeogeography, Palaeoclimatology, Palaeoecology 194, 405-414.

Stephen, M., 1993. Plant fossil distributions in some Australian Permian non-marine sediments. Sedimentary Geology 85, 601-619.

Stephenson, M., Osterloff, P., Filatoff, J., 2003. Integrated palynological biozonation of the Permian of Saudi Arabia and Oman: progress and problems. GeoArabia 8, 467-496.

Stephenson, M.H., Angiolini, L., Leng, M.J., Brewer, T.S., Berra, F., Jadoul, F., Gambacorta, G., Verna, V., Al Beloushi, B., 2008. Abrupt environmental and climatic change during the deposition of the Early Permian Haushi limestone, Oman. Palaeogeography, Palaeoclimatology, Palaeoecology 270, 1-18.

Stolle, E., 2007. Regional Permian Palynological correlations: Southeast Turkey – Northern Iraq. Comunicações Geológicas 94, 125-143.

Stolle, E., 2010. Recognition of southern Gondwanan palynomorphs at Gondwana's

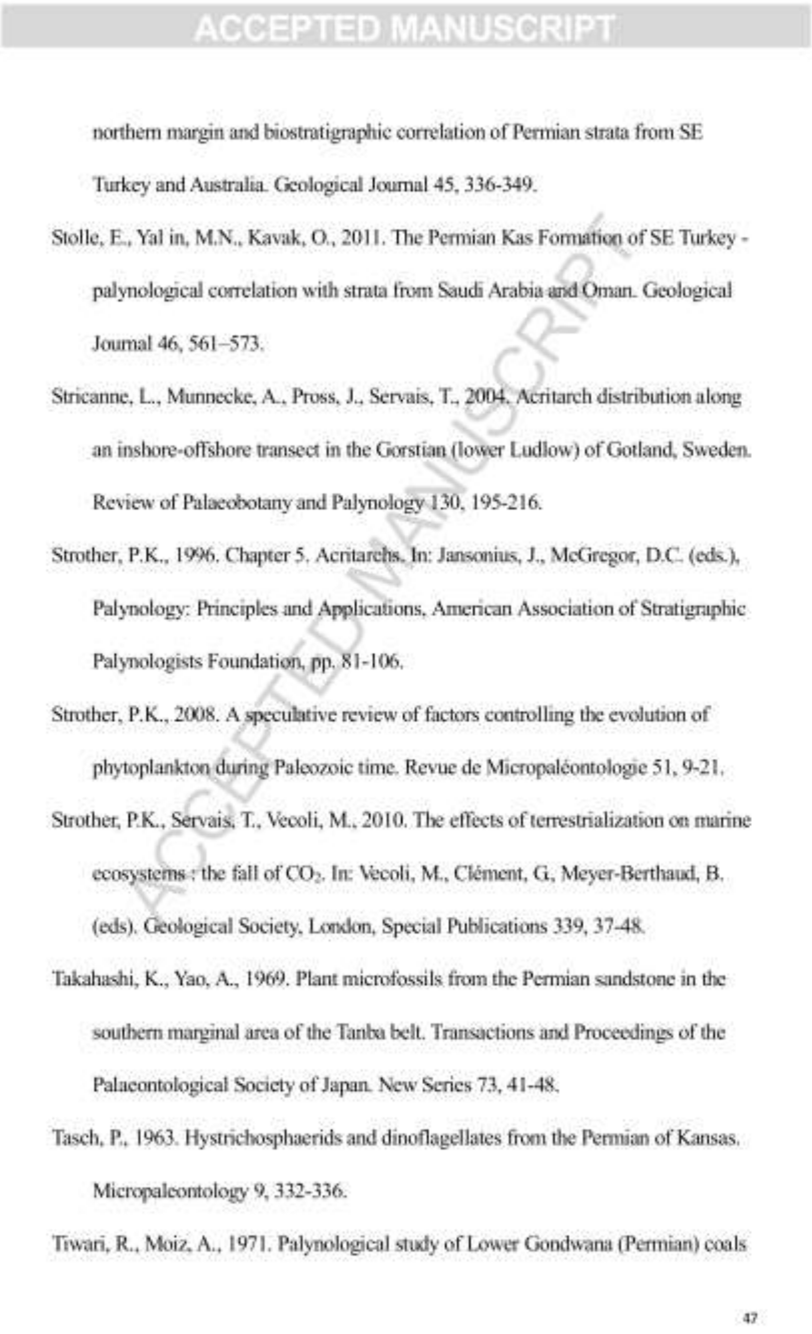

northern margin and biostratigraphic correlation of Permian strata from SE Turkey and Australia. Geological Journal 45, 336-349.

Stolle, E., Yal in, M.N., Kavak, O., 2011. The Permian Kas Formation of SE Turkey - palynological correlation with strata from Saudi Arabia and Oman. Geological Journal 46, 561–573.

Stricanne, L., Munnecke, A., Pross, J., Servais, T., 2004. Acritarch distribution along an inshore-offshore transect in the Gorstian (lower Ludlow) of Gotland, Sweden. Review of Palaeobotany and Palynology 130, 195-216.

Strother, P.K., 1996. Chapter 5. Acritarchs. In: Jansonius, J., McGregor, D.C. (eds.), Palynology: Principles and Applications, American Association of Stratigraphic Palynologists Foundation, pp. 81-106.

Strother, P.K., 2008. A speculative review of factors controlling the evolution of phytoplankton during Paleozoic time. Revue de Micropaléontologie 51, 9-21.

Strother, P.K., Servais, T., Vecoli, M., 2010. The effects of terrestrialization on marine ecosystems : the fall of CO_2. In: Vecoli, M., Clément, G., Meyer-Berthaud, B. (eds). Geological Society, London, Special Publications 339, 37-48.

Takahashi, K., Yao, A., 1969. Plant microfossils from the Permian sandstone in the southern marginal area of the Tanba belt. Transactions and Proceedings of the Palaeontological Society of Japan. New Series 73, 41-48.

Tasch, P., 1963. Hystrichosphaerids and dinoflagellates from the Permian of Kansas. Micropaleontology 9, 332-336.

Tiwari, R., Moiz, A., 1971. Palynological study of Lower Gondwana (Permian) coals from the Godavari Basin, India. The Palaeobotanist 19, 95-106.

Tiwari, R.S., Navale, G.K.B., 1967. Pollen and spore assemblage in some coals of Brazil. Pollen et Spores 9, 583-605.

Traverse, A., 2007. Permo-Triassic Palynofloras. Paleopalynology, 275-287.

Tripathi, A., 2001. Permian, Jurassic and Early Cretaceous palynofloral assemblages from subsurface sedimentary rocks in Chuperbhita Coalfield, Rajmahal Basin, India. Review of Palaeobotany and Palynology 113, 237-259.

Vecoli, M., 2000. Palaeoenvironmental interpretation of microphytoplankton diversity trends in the Cambrian-Ordovician of the northern Sahara Platform. Palaeogeography, Palaeoclimatology, Palaeoecology 160, 329-346.

Visscher, H., Brinkhuis, H., Dilcher, D., Elsik, W., Eshet, Y., Looy, C., Rampino, M., Traverse, A., 1996. The terminal Paleozoic fungal event: evidence of terrestrial ecosystem destabilization and collapse. Proceedings of the National Academy of Sciences of the United States of America 93, 2155-2158.

Visscher, H., Sephton, M.A., Looy, C.V., 2011. Fungal virulence at the time of the end-Permian biosphere crisis? Geology 39, 883-886.

Utting, J., 1978. Geological Survey of Canada, Open File 593. Natural Resources Canada, 1-17.

Wall, D., Downie, C., 1963. Permian hystrichospheres from Britain. Palaeontology 5, Part 4, 770-784.

Wilson, L., 1960. A Permian hystrichosphaerid from Oklahoma. Oklahoma Geology Notes 20, 170.

Ziegler, A. M., Hulver, M. L., Rowley, D. B., 1997. Permian world topography and climate. In: Martini, I. P. (ed.). Late glacial and postglacial environmental changes: Quaternary, Carboniferous-Permian and Proterozoic. Oxford, Oxford University Press, 111–146.

Figure captions

Figure 1. (a,b,c,d) Organic-walled microphytoplankton cited in Permian palynological papers. All taxa are here considered as acritarches, i.e., of unknown biological affinities, except species marked as (*) representing possible fungi and as (**) representing possible green algae.

Figure 2. Palaeogeographical distribution of Permian phytoplankton. Palaeogeographical reconstruction for the Early Permian (2A) (290 Ma), Middle Permian (2B) (265 Ma) and Late Permian (2C) (255 Ma) after Ziegler et al. (1997). 2D illustrates the numbers of published papers and recovered genera and species for the different palaeolatitudes.

Figure 3. The phytoplankton generic diversity in the Permian. Stratigraphical scale after Gradstein et al. (2004). * Fungi; ** Algae

Figure 4. Number of records of Permian phytoplankton genera in literature, and number of records of species in every genus. * Fungi; ** Algae

Table caption

Appendix 1. The list of Permian acritarch taxa

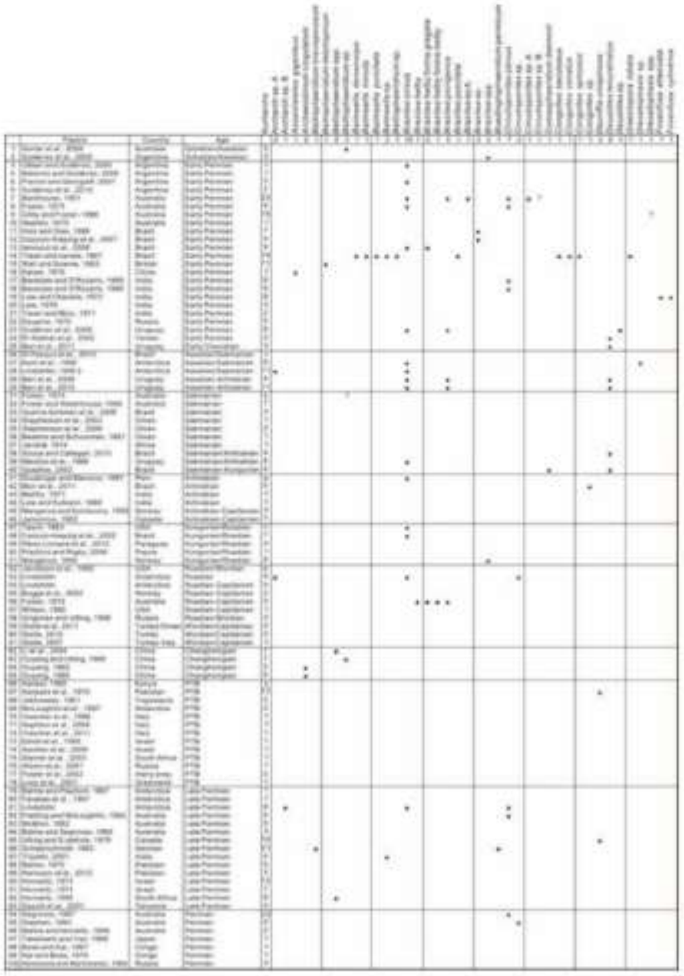

Figure 1a

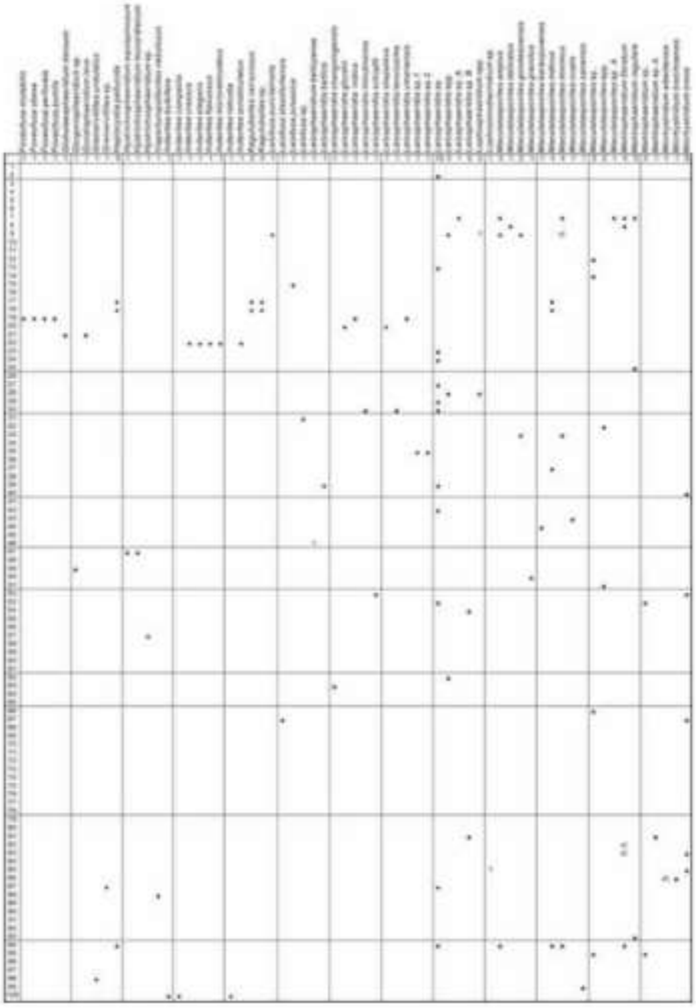

Figure 1b

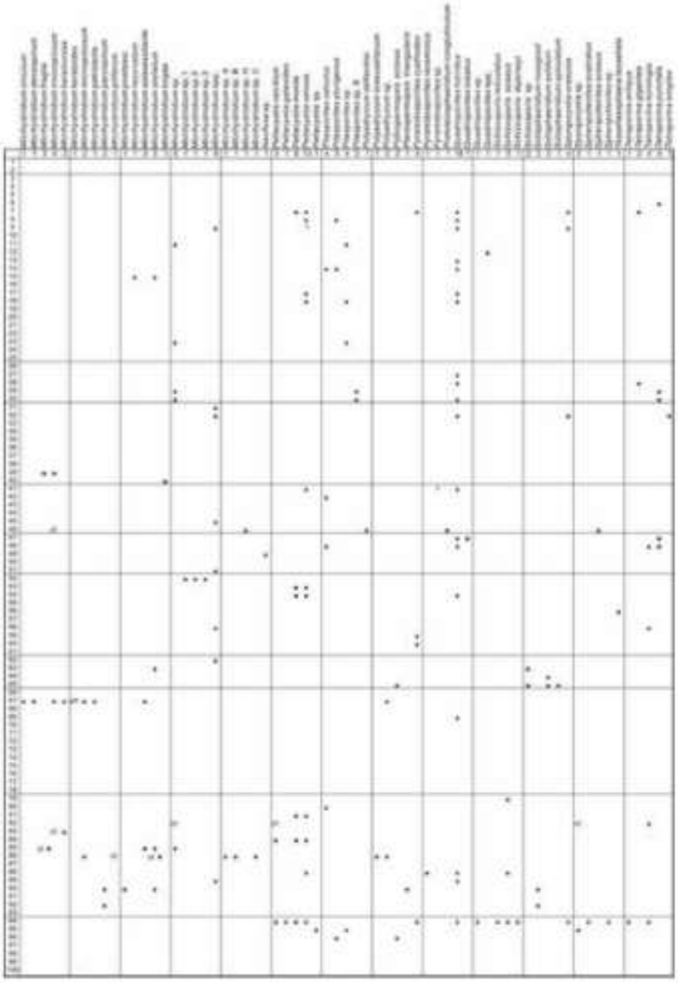

Figure 1c

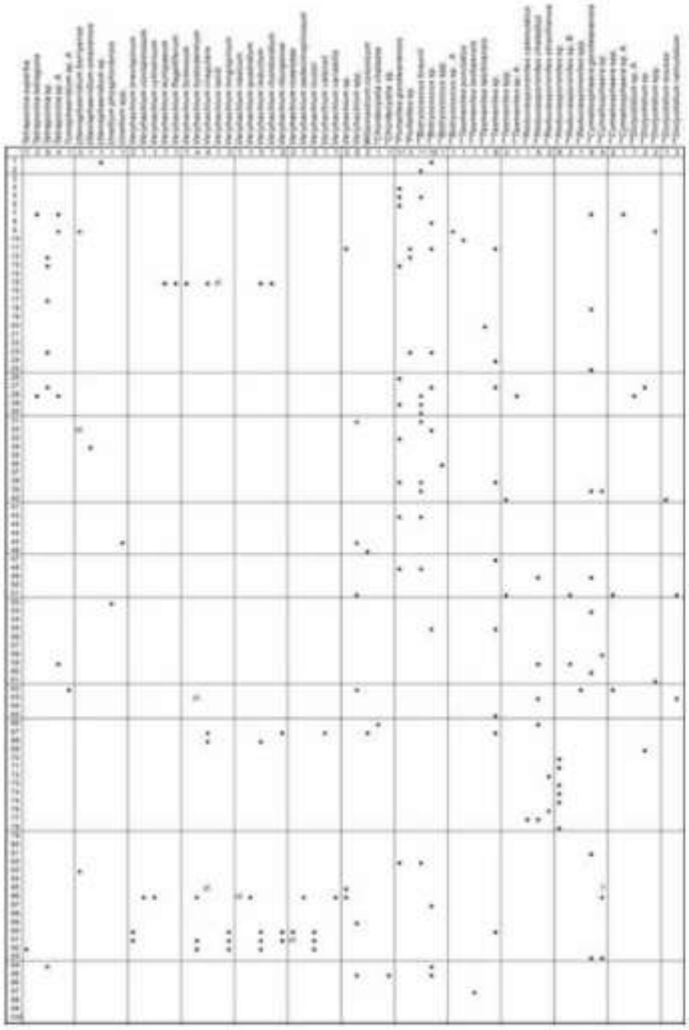

Figure 1d

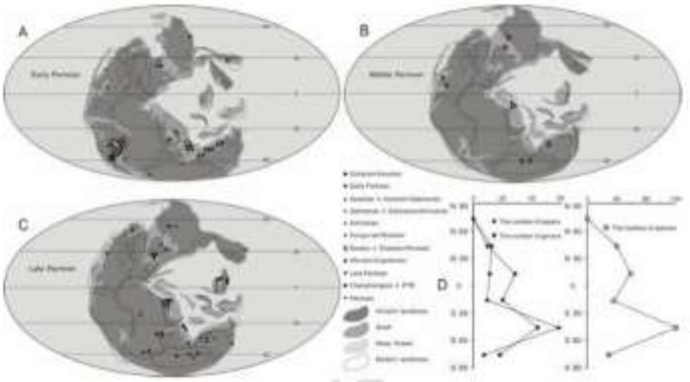

Figure 2

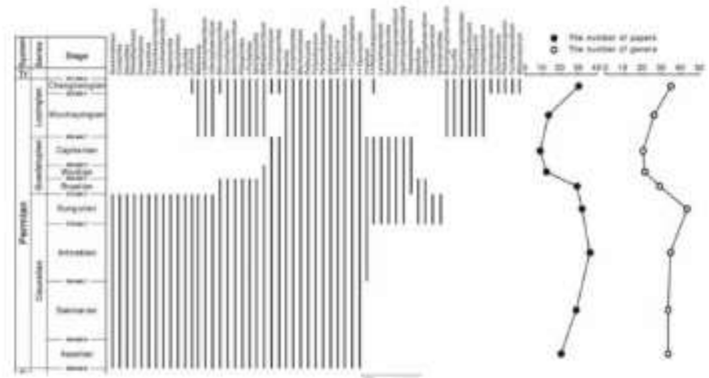
The number of papers
The number of genera
System
Series
Stage
Permian
Lopingian
Guadalupian
Cisuralian
Changhsingian
Wuchiapingian
Capitanian
Wordian
Roadian
Kungurian
Artinskian
Sakmarian
Asselian
0 10 20 30 40
0 10 20 30 40 50

Figure 3

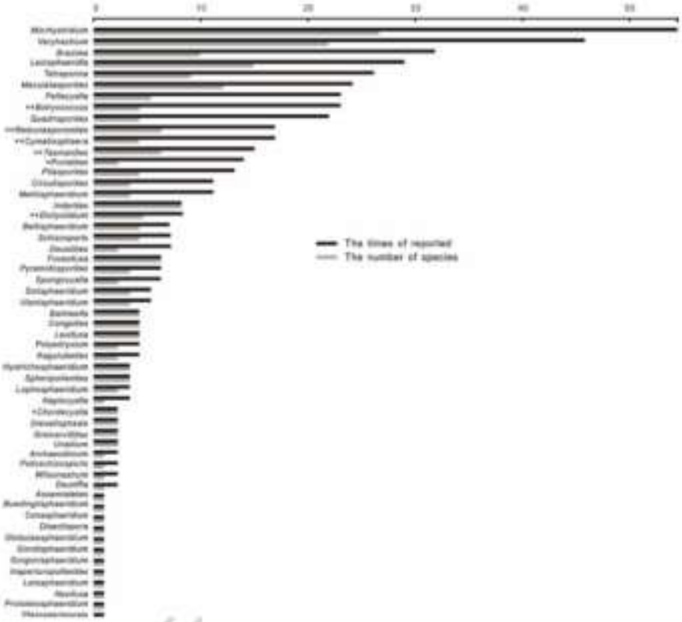
0
10
20
30
40
50
Micrhystridium
Veryhachium
Brazilea
Leiosphaeridia
Tetraporina
Maculatasporites
Peltacystia
++Botryococcus
Quadrisporites
++Reduviasporonites
++Cymatiosphaera
++Tasmanites
Pilasporites
Circulisporites
++Dictyotidium
Baltisphaeridium
Schizosporis
Deusilites
Solisphaeridium
Polyedryxium
Hystrichosphaeridium
Lophosphaeridium
Unellium
The times of reported
The number of species

Figure 4

Appendix

Acritarchs and Incertae Sedis
Acritarch sp. A (Lindström, 1995 a; Lindström, 1995 b)
Acritarch sp. B (Lindström, 1996)
Genus *Assamialetes* Singh, 1975
Assamialetes giganteus (Kaiser, 1976) Fensome et al., 1990
Genus *Archaeodinium* Ouyang, 1979
Archaeodinium cingulatum Ouyang, 1979
Genus *Baltisphaeridium* (Eisenack, 1958) Eisenack, 1969
Baltisphaeridium brevispinosum (Eisenack, 1931) Eisenack, 1959
Baltisphaeridium debilispinum Wall and Downie, 1963
Baltisphaeridium spp. (Li et al., 2004; Horowitz, 1990)
Baltisphaeridium sp. (Foster, 1974; Gorter et al., 2008; Shu and Utting, 1990)
Genus *Balmeella* Pant and Mehra, 1963
Balmeella densicorpa Tiwari and Navale, 1967
Balmeella minuta Tiwari and Navale, 1967
Balmeella punctata Tiwari and Navale, 1967
Balmeella sp. (Tripathi, 2001)

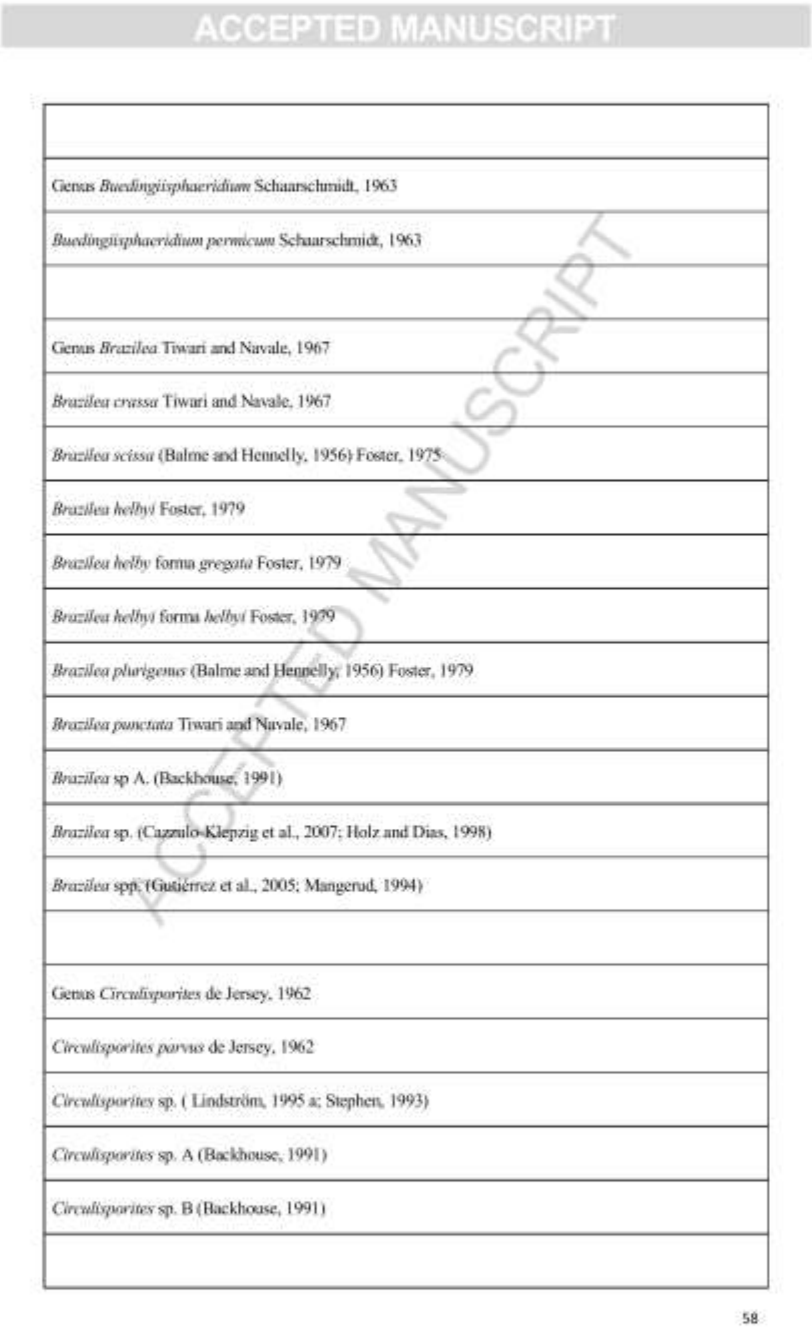

Genus *Buedingiisphaeridium* Schaarschmidt, 1963
Buedingiisphaeridium permicum Schaarschmidt, 1963
Genus *Brazilea* Tiwari and Navale, 1967
Brazilea crassa Tiwari and Navale, 1967
Brazilea scissa (Balme and Hennelly, 1956) Foster, 1975
Brazilea helbyi Foster, 1979
Brazilea helby forma *gregata* Foster, 1979
Brazilea helbyi forma *helbyi* Foster, 1979
Brazilea plurigenus (Balme and Hennelly, 1956) Foster, 1979
Brazilea punctata Tiwari and Navale, 1967
Brazilea sp A. (Backhouse, 1991)
Brazilea sp. (Cazzulo-Klepzig et al., 2007; Holz and Dias, 1998)
Brazilea spp. (Gutiérrez et al., 2005; Mangerud, 1994)
Genus *Circulisporites* de Jersey, 1962
Circulisporites parvus de Jersey, 1962
Circulisporites sp. (Lindström, 1995 a; Stephen, 1993)
Circulisporites sp. A (Backhouse, 1991)
Circulisporites sp. B (Backhouse, 1991)

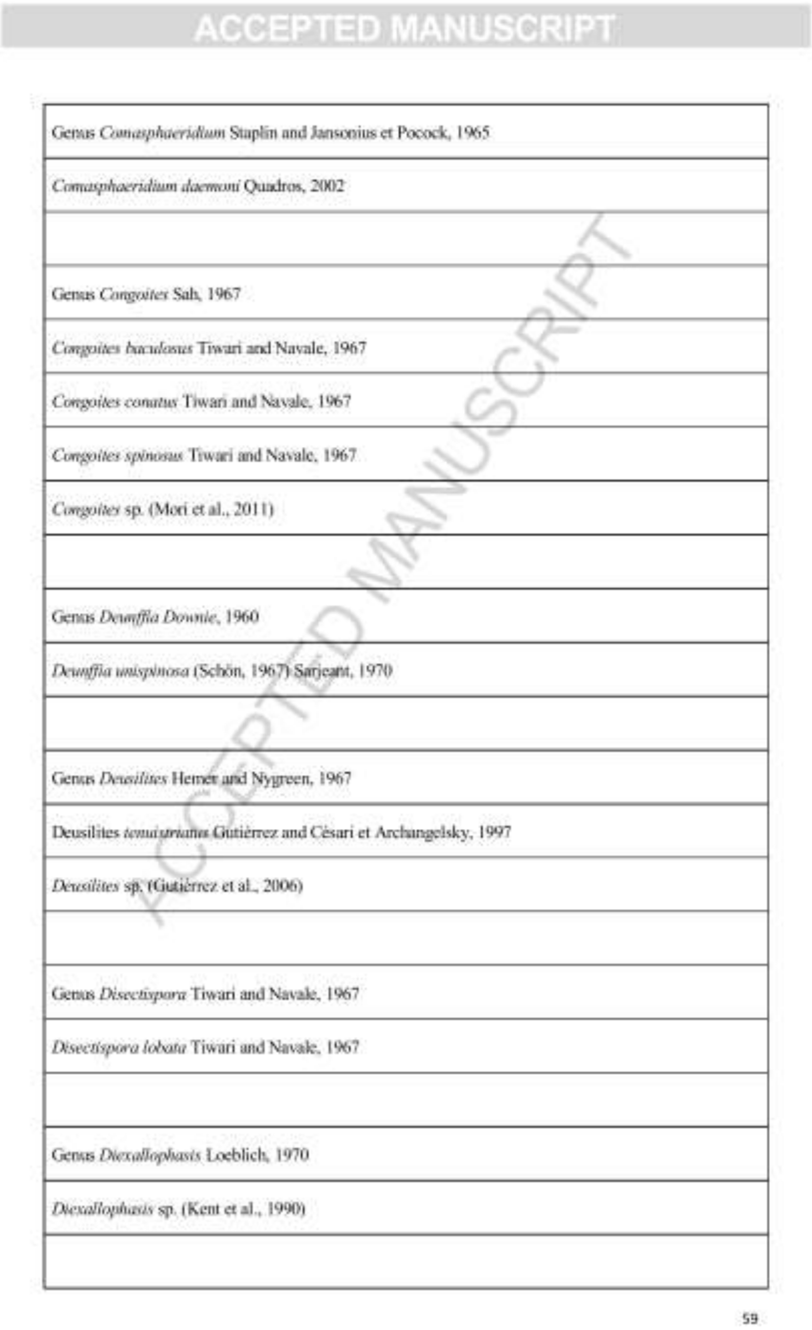

Genus *Comasphaeridium* Staplin and Jansonius et Pocock, 1965
Comasphaeridium daemoni Quadros, 2002
Genus *Congoites* Sah, 1967
Congoites baculosus Tiwari and Navale, 1967
Congoites conatus Tiwari and Navale, 1967
Congoites spinosus Tiwari and Navale, 1967
Congoites sp. (Mori et al., 2011)
Genus *Deunffia Downie*, 1960
Deunffia unispinosa (Schön, 1967) Sarjeant, 1970
Genus *Deusilites* Hemer and Nygreen, 1967
Deusilites *tenuistriatus* Gutièrrez and Cèsari et Archangelsky, 1997
Deusilites sp. (Gutièrrez et al., 2006)
Genus *Disectispora* Tiwari and Navale, 1967
Disectispora lobata Tiwari and Navale, 1967
Genus *Diexallophasis* Loeblich, 1970
Diexallophasis sp. (Kent et al., 1990)

Genus *Foveofusa* Lele and Chandra, 1972
Foveofusa attenuata Lele and Chandra, 1972
Foveofusa cylindrica Lele and Chandra, 1972
Foveofusa mutabilis Lele and Chandra, 1972
Foveofusa obese Lele and Chandra, 1972
Foveofusa perforata Lele and Chandra, 1972
Foveofusa pumila Lele and Chandra, 1972
Genus *Globulaesphaeridium* Tiwari and Moiz, 1971
Globulaesphaeridium densum Tiwari and Moiz, 1971
Genus *Gorgonisphaeridium* Staplin and Jansonius et Pocock, 1965
Gorgonisphaeridium sp. (Pérez Loinaze et al., 2010)
Genus *Gondisphaeridium* Tiwari and Moiz, 1971
Gondisphaeridium leve Tiwari and Moiz, 1971
Genus *Greinervillites* Bose and Kar, 1967
Greinervillites sp. (Tripathi, 2001)
Genus *Haplocystia* Segroves, 1967
Haplocystia pellucida Segroves, 1967

Genus *Hystrichosphaeridium* Deflandre, 1937
Hystrichosphaeridium leonardianum Tasch, 1963
Hystrichosphaeridium equispinosum Tasch, 1963
Hystrichosphaeridium sp. (Wilson, 1960)
Genus *Inaperturopollenites* Pflug and Thomson, 1953
Inaperturopollenites nebulosus Balme, 1970
Genus *Inderites Abramova* and Martchenko, 1964
Inderites bulbifera Abramova and Martchenko, 1964
Inderites compacta Abramova and Martchenko, 1964
Inderites crassus Dyupina, 1970
Inderites elegans Dyupina, 1970
Inderites flexuosus Dyupina, 1970
Inderites microreticulatus Dyupina, 1970
Inderites robusta Abramova and Martchenko, 1964
Inderites scrobiculatus Dyupina, 1970
Genus *Kagulubeites* Bose and Maheshwari, 1968
Kagulubeites verrucosus Bose and Maheshwari, 1968
Kagulubeites sp. (Banerjee and D'Rozario, 1988; Banerjee and D'Rozario, 1990)

Genus *Leiofusa* Eisenack, 1938
Leiofusa punctalirella Loeblich, 1970
Leiofusa stassfurtensis Schön, 1967
Leiofusa jurassica (Schön, 1967) Sarjeant, 1970
Leiofusa spp. (Foster, 1974)
Genus *Leiosphaeridium* Staplin, 1961
Leiosphaeridium belloyense Jansonius, 1962
Genus *Leiosphaeridia* (Eisenack, 1958) Downie and Sarjeant, 1963
Leiosphaeridia baltica Eisenack, 1958
Leiosphaeridia changxingensis Ouyang Shu and Utting, 1990
Leiosphaeridia ghoshii (Lele, 1979) Fensome et al., 1990
Leiosphaeridia indica Lele and Chandra, 1972
Leiosphaeridia minutissima (Naumova, 1949) Jankauskas, 1989
Leiosphaeridia schopfii Jacobson, 1982
Leiosphaeridia shepeleva (Lele, 1979) Fensome et al., 1990
Leiosphaeridia tenuissima Eisenack, 1958
Leiosphaeridia umariensis Lele and Chandra, 1972
Leiosphaeridia sp.1 (Stephenson et al., 2008)
Leiosphaeridia sp.2 (Stephenson et al., 2008)

Leiosphaeridia sp. (Beri et al., 2006; Beri et al., 2010; El-Nakhal et al., 2002; Gutièrrez et al., 2005; Kent et al., 1990; Iannuzzi et al., 2006; Lindström, 1995 a; Mautino et al., 1998; Mori et al., 2011; Segroves, 1967; Tripathi, 2001)
Leiosphaeridia spp. (Gilby and Foster, 1988; Li et al., 2004; Lindstrm, 1995 b)
Leiosphaeridia sp. A (Backhouse, 1991)
Leiosphaeridia sp. B (Lindström, 1996; Lindström, 2005)
Genus *Lophosphaeridium*(Timofeev, 1959) Downie, 1963
Lophosphaeridium spp. (Gilby and Foster, 1988; Lindstrm, 1995 b)
Lophosphaeridium sp. (Utting and S-petrole, 1978)
Genus *Maculatasporites* Tiwari, 1964
Maculatasporites amplus Segroves, 1967
Maculatasporites delicates Foster, 1975
Maculatasporites gondwanensis Tiwari, 1964
Maculatasporites gravidus Playford and Rigby, 2011
Maculatasporites indicus Tiwari, 1964
Maculatasporites karanpurensis Lele and Kulkarni, 1969
Maculatasporites minimus Segroves, 1967
Maculatasporites zairensis Kar and Bose, 1976
Maculatasporites sp. (Cazzulo-Klepzig et al., 2007; Hankel, 1992; Stephen, 1993)
Maculatasporites spp. (Foster and Waterhouse, 1988; Mangerud, 1994)
Maculatasporites sp A. (Backhouse, 1991)

Genus *Mehlisphaeridium* Segroves, 1967
Mehlisphaeridium fibratum Segroves, 1967
Mehlisphaeridium regulare Anderson, 1977
Mehlisphaeridium sp. (Lindström, 1995 a; Stephen, 1993)
Mehlisphaeridium sp. A (Lindström, 1996)
Genus *Micrhystridium* (Deflandre, 1937) Sarjeant and Stancliffe, 1994
Micrhystridium albertensis Staplin, 1961
Micrhystridium bistchoensis Staplin, 1961
Micrhystridium breve Jansonias, 1962
Micrhystridium circulum Schön, 1967
Micrhystridium densispinum Valensi, 1953
Micrhystridium fragile Deflandre, 1947
Micrhystridium inconspicuum (Deflandre, 1935) Deflandre, 1937
Micrhystridium karamurzae Sarjeant, 1970
Micrhystridium keratoides Spode, 1964
Micrhystridium microspinosum Schaarschmidt, 1963
Micrhystridium pakistante Sarjeant, 1970
Micrhystridium parvispinum Deflandre, 1946
Micrhystridium piliferum Deflandre, 1937

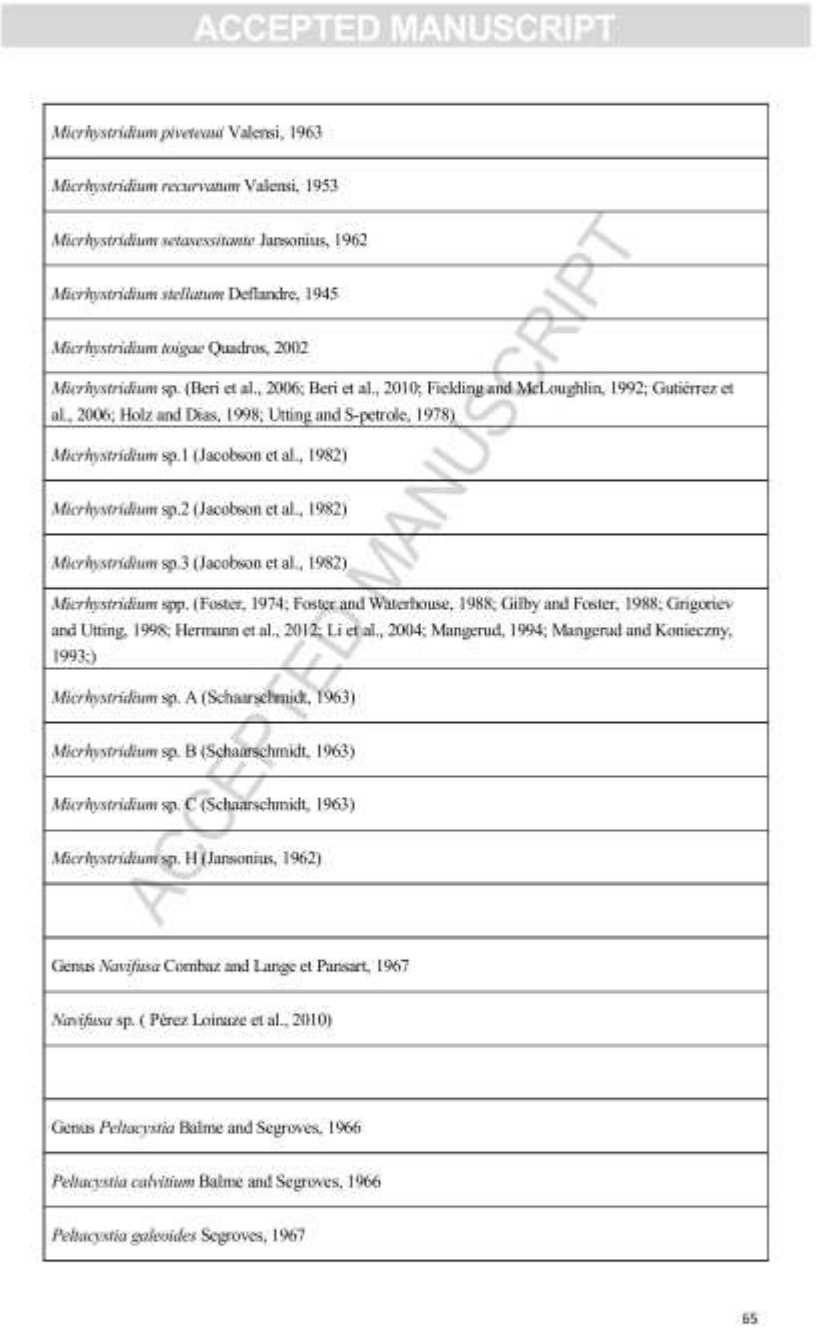

Micrhystridium piveteaui Valensi, 1963
Micrhystridium recurvatum Valensi, 1953
Micrhystridium setasessitante Jansonius, 1962
Micrhystridium stellatum Deflandre, 1945
Micrhystridium toigae Quadros, 2002
Micrhystridium sp. (Beri et al., 2006; Beri et al., 2010; Fielding and McLoughlin, 1992; Gutiérrez et al., 2006; Holz and Dias, 1998; Utting and S-petrole, 1978)
Micrhystridium sp.1 (Jacobson et al., 1982)
Micrhystridium sp.2 (Jacobson et al., 1982)
Micrhystridium sp.3 (Jacobson et al., 1982)
Micrhystridium spp. (Foster, 1974; Foster and Waterhouse, 1988; Gilby and Foster, 1988; Grigoriev and Utting, 1998; Hermann et al., 2012; Li et al., 2004; Mangerud, 1994; Mangerud and Konieczny, 1993;)
Micrhystridium sp. A (Schaarschmidt, 1963)
Micrhystridium sp. B (Schaarschmidt, 1963)
Micrhystridium sp. C (Schaarschmidt, 1963)
Micrhystridium sp. H (Jansonius, 1962)
Genus *Navifusa* Combaz and Lange et Parsart, 1967
Navifusa sp. (Pérez Loinaze et al., 2010)
Genus *Peltacystia* Balme and Segroves, 1966
Peltacystia calvitium Balme and Segroves, 1966
Peltacystia galeoides Segroves, 1967

Peltacystia monilis Balme and Segroves, 1966
Peltacystia venosa Balme and Segroves, 1966
Peltacystia sp. (Stephen, 1993)
Genus *Pilasporites* Balme and Hennelly, 1956
Pilasporites calculus Balme and Hennelly, 1956
Pilasporites plurigenus Balme and Hennelly, 1956
Pilasporites sp. (Banerjee and D'Rozario, 1990; Gutiérrez et al., 2006; Holz and Dias, 1998; Gutiérrez et al., 2006)
Pilasporites sp. B (Beri et al., 2006; Beri et al., 2010)
Genus *Polyedryxium* Deunff, 1954
Polyedryxium deflandrei Deunff, 1954
Polyedryxium kraeuselianum Schaarschmidt, 1963
Polyedryxium sp. (Sarjeant et al., 1970; Schaarschmidt, 1963)
Genus *Psiloschizosporis* Jain, 1968
Psiloschizosporis scissus (Balme and Henn, 1956) Ouyang, 1985
Genus *Pyramidosporites* Segroves, 1967
Pyramidosporites cyathodes Segroves, 1967
Pyramidosporites racemosus Balme, 1970

Genus *Pterospermopsis* Wetzel, 1952
Pterospermopsis triangularis Horowitz, 1973
Genus *Protoleiosphaeridium* Timofeev, 1959
Protoleiosphaeridium conglutinatum Timofeev, 1959
Genus *Quadrisporites* Hennelly, 1959
Quadrisporites horridus(Hennelly, 1959) Potonié and Lele, 1961
Quadrisporites lobatus (Tiwari and Navale, 1967) Ybert, 1975
Quadrisporites sp. (Segroves, 1967)
Quadrisporites spp. (Cazzulo-Klepzig et al., 2007)
Genus *Schizosporis* (Cookson and Dettman, 1959) Pierce, 1976
Schizosporis reticulatus Cookson and Dettman, 1959
Schizosporis dejerseyi Segroves, 1967
Schizosporis scissus (Balme and Hennelly, 1956) Hart, 1965
Schizosporis sp. (Shu, 1985; Shu and Utting, 1990)
Genus *Solisphaeridium* Staplin and Jansonius et Pocock, 1965
Solisphaeridium rossignoli Glikson, 1966
Solisphaeridium solidum Ouyang and Li, 1980
Solisphaeridium spinulatum Ouyang, 1985

Genus *Spongocystia* Segroves, 1967
Spongocystia eraduica Segroves, 1967
Spongocystia sp. (Fielding and McLoughlin, 1992; Stephen, 1993)
Genus *Spheripollenites* Couper, 1958
Spheripollenites scabratus Couper, 1958
Spheripollenites scissus (Balme and Hennelly, 1956) Jansonius, 1962
Spheripollenites sp. (Segroves, 1967)
Genus *Tessellaesphaera* Foster, 1979
Tessellaesphaera tessellata Foster, 1979
Genus *Tetraporina* Naumova, 1939
Tetraporina antiqua Naumova, 1950
Tetraporina gigantea (Bose and Maheshwari, 1968) Backhouse, 1991
Tetraporina horologia (Staplin, 1960) Playford, 1963
Tetraporina punctata (Tiwari and Navale, 1967) Kar and Bose, 1976
Tetraporina simplex Anderson, 1977
Tetraporina superba Anderson, 1977
Tetraporina tetragona Anderson, 1977
Tetraporina sp. (Banerjee and D'Rozario, 1988; Cazzulo-Klepzig et al., 2007; Gutiérrez et al., 2006; Iannuzzi et al., 2006; Kent et al., 1990; Segroves, 1967)

Tetraporina sp. A (Backhouse, 1991; Gilby and Foster, 1988; Lindstrm, 1995 b; Stolle et al. 2011)
Genus *Tunisphaeridium* Deunff and Evitt, 1968
Tunisphaeridium sp. A (Li et al., 2004)
Genus *Ulanisphaeridium* McMinn, 1982
Ulanisphaeridium berryense McMinn, 1982
Ulanisphaeridium omanensis Stephenson and Osterloff et Filatoff, 2003
Ulanisphaeridium sp. (Gorter et al., 2008)
Genus *Unellium* Rauscher, 1969
Unellium phosphoriensis Jacobson, 1982
Unellium spp. (Mangerud and Konieczny, 1993)
Genus *Veryhachium* (Deunff, 1954) Sarjeant and Stancliffe, 1994
Veryhachium brevispinum Horowitz, 1972
Veryhachium conispinosum Schaarschmidt, 1963
Veryhachium cylindricum Schaarschmidt, 1963
Veryhachium europaeum Stockmans and Willière, 1960
Veryhachium flagelliferum Wall, 1963
Veryhachium formosum Stockmans and Willière, 1960
Veryhachium hyalodermum (Cookson, 1955) Schaarschmidt, 1963
Veryhachium irregulare Jekhowsky, 1961

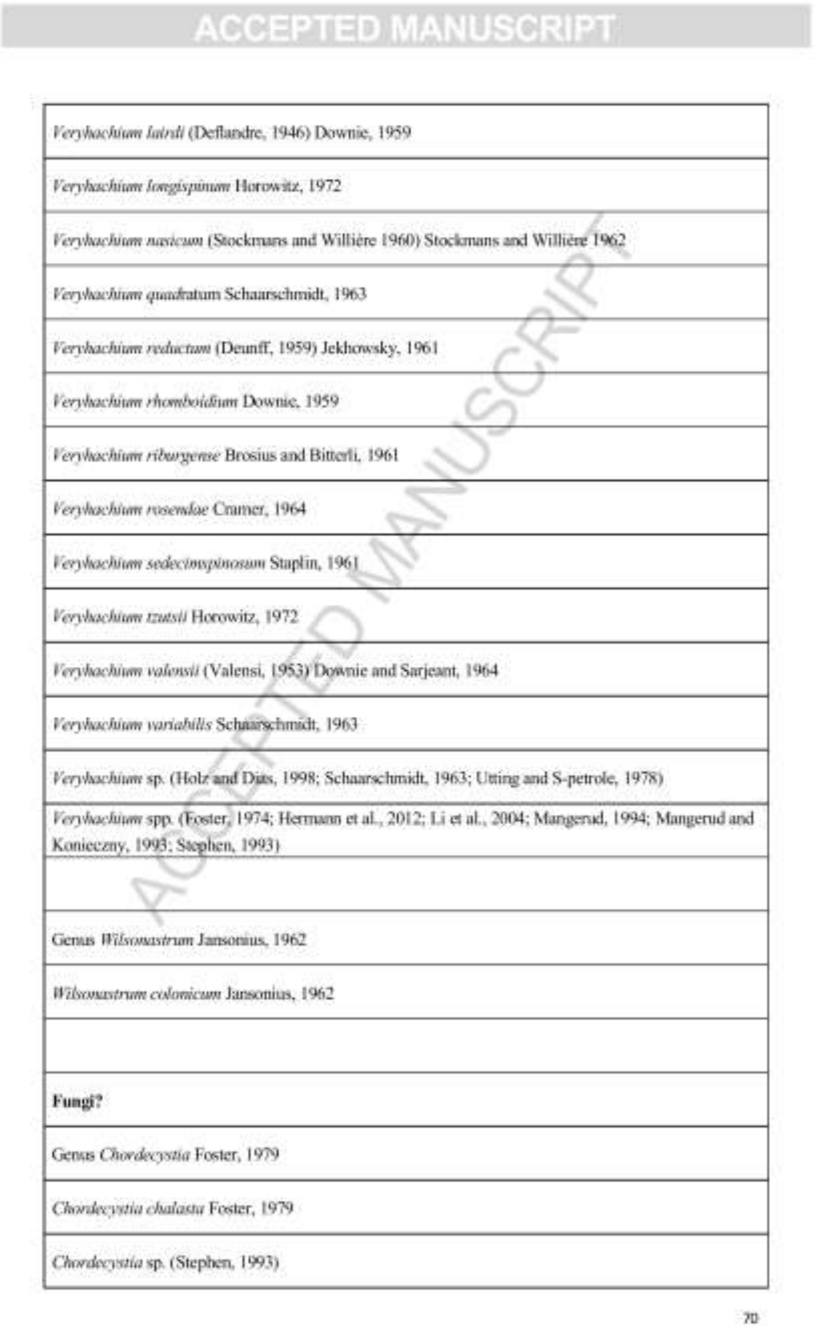

Veryhachium lairdi (Deflandre, 1946) Downie, 1959
Veryhachium longispinum Horowitz, 1972
Veryhachium nasicum (Stockmans and Willière 1960) Stockmans and Willière 1962
Veryhachium quadratum Schaarschmidt, 1963
Veryhachium reductum (Deunff, 1959) Jekhowsky, 1961
Veryhachium rhomboidium Downie, 1959
Veryhachium riburgense Brosius and Bitterli, 1961
Veryhachium rosendae Cramer, 1964
Veryhachium sedecimspinosum Staplin, 1961
Veryhachium tzutsii Horowitz, 1972
Veryhachium valensii (Valensi, 1953) Downie and Sarjeant, 1964
Veryhachium variabilis Schaarschmidt, 1963
Veryhachium sp. (Holz and Dias, 1998; Schaarschmidt, 1963; Utting and S-petrole, 1978)
Veryhachium spp. (Foster, 1974; Hermann et al., 2012; Li et al., 2004; Mangerud, 1994; Mangerud and Konieczny, 1993; Stephen, 1993)
Genus *Wilsonastrum* Jansonius, 1962
Wilsonastrum colonicum Jansonius, 1962
Fungi?
Genus *Chordecystia* Foster, 1979
Chordecystia chalasta Foster, 1979
Chordecystia sp. (Stephen, 1993)

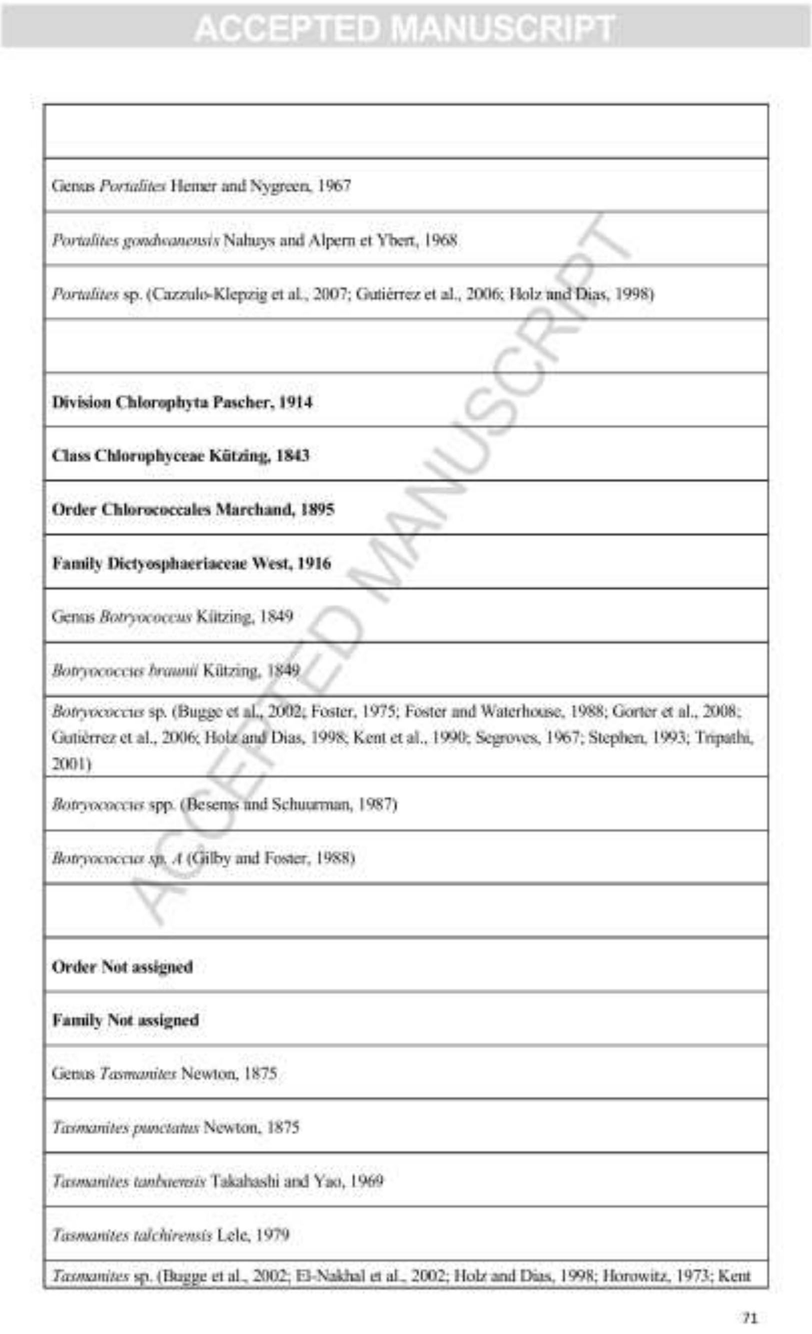

Genus *Portalites* Hemer and Nygreen, 1967
Portalites gondwanensis Nahuys and Alpern et Ybert, 1968
Portalites sp. (Cazzulo-Klepzig et al., 2007; Gutiérrez et al., 2006; Holz and Dias, 1998)
Division Chlorophyta Pascher, 1914
Class Chlorophyceae Kützing, 1843
Order Chlorococcales Marchand, 1895
Family Dictyosphaeriaceae West, 1916
Genus *Botryococcus* Kützing, 1849
Botryococcus braunii Kützing, 1849
Botryococcus sp. (Bugge et al., 2002; Foster, 1975; Foster and Waterhouse, 1988; Gorter et al., 2008; Gutièrrez et al., 2006; Holz and Dias, 1998; Kent et al., 1990; Segroves, 1967; Stephen, 1993; Tripathi, 2001)
Botryococcus spp. (Besems and Schuurman, 1987)
Botryococcus sp. A (Gilby and Foster, 1988)
Order Not assigned
Family Not assigned
Genus *Tasmanites* Newton, 1875
Tasmanites punctatus Newton, 1875
Tasmanites tanbaensis Takahashi and Yao, 1969
Tasmanites talchirensis Lele, 1979
Tasmanites sp. (Bugge et al., 2002; El-Nakhal et al., 2002; Holz and Dias, 1998; Horowitz, 1973; Kent

et al., 1990; Sarjeant et al., 1970; Shu, 1985; Souza and Callegari, 2010; Tasch, 1963)
Tasmanites spp. (Mangerud, 1994; Quadros, 2002)
Tasmanites sp. A (Lindstrm, 1995 b)
Class Zygnematophyceae Round, 1971
Order Zygnematales Kützing, 1898
Family Not assigned
Genus *Reduviasporonites* (Wilson, 1962) Foster, 2002
Reduviasporonites catenulatus Wilson, 1962
Reduviasporonites chalastus (Foster, 1979) Elsik, 1999
Reduviasporonites stoschianus (Balme, 1980) Elsik, 1999
Reduviasporonites sp. (Eshet et al., 1995; Visscher et al., 1996; Looy et al., 2001; Steiner et al., 2003; Sandler et al., 2006; Sephton et al., 2009)
Reduviasporonites sp. B (Mangerud, 1994; Stolle et al. 2011)
Reduviasporonites spp. (Li et al., 2004)
Division Prasinophyta Christensen, 1962
Class Prasinophyceae Christensen, 1962
Order Not assigned
Family Pterosphaeridiaceae Mädler, 1963
Genus *Cymatiosphaera* Wetzel, 1933
Cymatiosphaera gondwanensis (Tiwari, 1965) Backhouse, 1991
Cymatiosphaera sp. (Dypvik et al., 2001; Grigoriev and Utting, 1998; Mautino et al., 1998; Schaarschmidt, 1963; Utting and S-petrole, 1978)

Cymatiosphaera spp. (Li et al., 2004; Mangerud, 1994)
Cymatiosphaera sp. A (Backhouse, 1991)
Genus *Dictyotidium* (Eisenack, 1955) Staplin, 1961
Dictyotidium souzae Quadros, 2002
Dictyotidium reticulatum Schulz, 1965
Dictyotidium sp. A (Lindstrm, 1995 b)
Dictyotidium sp. (Kent et al., 1990; McLoughlin et al., 1997)
Dictyotidium spp. (Gilby and Foster, 1988; Stolle, 2007)

Highlights

1. We review the Permian phytoplankton, based on about 100 publications.

2. We observe relatively high phytoplankton diversities in the Early and latest Permian.

3. Most taxa are related to the acritarchs.

4. Some other taxa are probably belonging to the green algae or to the fungi.

5. The most common genera recorded in Permian are the *Micrhystridium* and *Veryhachium*.

Manuscript 2: (Section 2.3.3)

Submitted to Review of Palaeobotany and Palynology. (revised and under corrections)

Palynology and palynofacies of the Upper Permian to Lower Triassic of Shangsi (Sichuan, China)

Yong Lei[1,2], Thomas Servais[2], Jun Shen[1], Nicolas Tribovillard[2], Taniel Danelian[2], Qinglai Feng[1*]

[1] State Key Laboratory of Geological Processes and Mineral Resources, China University of Geosciences, Wuhan, China
[2] UMR 8217 Géosystèmes, CNRS-Université Lille1, Cité Scientifique, F-59655 Villeneuve d'Ascq, France
***Corresponding author**, E-mail: qinglaifeng@cug.edu.cn
Fax: +86-027-67883002; Tel: +86-027-67883006
Yong Lei, E-mail: leiyongdida@163.com; Tel: +86-13485387952
Thomas Servais, E-mail: thomas.servais@univ-lille1.fr;
Fax: +33-320436900; Tel: +33-320337220
Jun Shen, E-mail: shenjun_2009@163.com; Tel: +86-18062435228
Nicolas Tribovillard, E-mail: Nicolas.Tribovillard@univ-lille1.fr
Fax. + 33-320434910; Tel. +33-320434100
Taniel Danelian, E-mail: Taniel.Danelian@univ-lille1.fr
Fax. +33-320434910; Tel. +33-320336108

Abstract. The palynology, palynofacies and geochemistry of the Upper Permian to Lower Triassic sequence of the Shangsi section, northern Sichuan province, China, were analyzed to determine their petroleum source-rock potential and depositional environment. Three palynological zones are recognized, in ascending order the *Dictyotidium* (Wuqiapingian), the *Leiosphaeridia –Micrhystridium –Veryhachium* (Changxingian) and the *Pteruchipollenites –Leiotriletes* (Induan) assemblage zones. Five palynofacies types are recognized and interpreted in terms of depositional environments. Two main depositional intervals are recognized. The first interval (beds 15 to 22) is dominated by amorphous organic matter (AOM) and acritarchs, with moderate or high total organic carbon (TOC) values, indicating offshore and shallow–deep marine, dysoxic –anoxic depositional environments. The second interval (beds 23 to 29) is dominated by terrestrial components with low TOC values, clearly indicating deltaic–nearshore and shallow marine, oxic depositional environments. The former interval has a good petroleum potential, but the latter does not.

Keywords: acritarchs, Permian-Triassic, hydrocarbon-source potential, depositional environment

Introduction

Palynological investigations in the Late Permian are not common. Most of the existing published palynological studies focus on the taxonomy and biostratigraphy of spores and pollen grains, which are both usually abundant and diverse in Permian palynological assemblages. These plant-derived microfossils, that are much larger in size than the phytoplankton in the same assemblages, are easier to observe and to describe (in particular with the light microscope). As a result, numerous spores and pollen grains have been documented (e.g. Ouyang, 1982; 1986; Ouyang and Utting, 1990; Hou and Song, 1995; Ouyang and Hou, 1999a, b; Yang, 2002; Peng et al., 2006; Ouyang and Zhu, 2007; Zhang et al., 2007). However, studies on Permian acritarchs have generally been neglected (Lei et al., accepted).

Several authors suggested that the palaeoclimate was different between North China and South China during the Late Permian to Early Triassic interval. For example Ouyang (1982, 1986) summarized the work on Late Permian and Early Triassic palynological assemblages in South and North China and suggested that, in ascending order, the *Patellisporites meishanensis –Macrotorispora gigantean* (Late Permian), the *Yunnanospora radiate –Gardenasporites* sp. (Late Permian), and the *Aratrisporites –Lundbladispora* (Early Triassic) assemblage zones indicated a humid and warm climate in South China, whereas in North China the *Patellisporites –Nuskoisporites* (Late Permian), *Lueckisporites –Jugasporites* (Late Permian) and *Aratrisporites –Lundbladispora –Fulsaesporites –Scutasporites* (Early Triassic) assemblage zones reflected a dry climate.

In China, four papers have described acritarchs from the latest Permian Changhsingian Stage (Ouyang, 1982; 1986; Ouyang and Utting, 1990; Li et al. 2004a), documenting the presence of 13 genera of organic-walled microfossils of unknown biological origin (acritarchs and related forms): *Archaeodinium, Baltisphaeridium*, *Cymatiosphaera*, *Dictyotidium*, *Leiosphaeridia*, *Micrhystridium*, *Psiloschizosporis*, *Veryhachium*, *Reduviasporonites*, *Schizosporis*, *Solisphaeridium*, *Tasmanites* and *Tunisphaeridium*. Ouyang and Utting (1990) mentioned the presence of a *Leiosphaeridia changxingensis –Micrhystridium stellatum* Assemblage Zone and described a new species (*Leiosphaeridia changxingensis*) from the Meishan section, Zhejiang Province, that serves as the Global Boundary Stratotype Section and Point (GSSP) for the Permian-Triassic Boundary (PTB).

The concept of palynofacies studies has evolved during the last few decades. First introduced by Combaz (1964), palynofacies studies correspond to the analyses of the distribution in a sediment or a sedimentary rock of all variants of acid–resistant microscopic particulate organic matter. Palynofacies studies are especially used to understand depositional environment and hydrocarbon source potential. Analyzed parameters include the type, origin, size, abundance, and condition (color, shape, degradation) of the particles (Waterhouse, 1999). The particles of organic matter are considered as sedimentary components that reflect the original conditions in the source area and the depositional environments (Carvalho et al., 2006). The different palynofacies data allow palaeoenvironmental interpretations regarding palaeoceanography, palaeogeography, bottom–water oxygenation, climate change, and terrestrial vegetation change (Tyson, 1995). Palynofacies studies can also be used to stratigraphically define sedimentary sequences (Wood and Gorin, 1998).

A huge oolitic beach has been described from the Feixianguan Formation in the northern Sichuan basin, South China. More than 7200 km^2 of bioherm–platform edge bank facies have been discovered with more than $6000\times10^8 m^3$ of gas to be explored in this area. These discoveries indicate an enormous exploration potential (Hong et al., 2008). It is considered that organic matter is fairly rare in the Feixianguan Formation, so that the gas only comes from the Upper Permian (Chen, 2007).

The objectives of the present study are to identify and describe the composition of the palynological assemblages and the palynofacies types of the Shangsi section, in order to determine its hydrocarbon-source potential and its depositional environment.

1. Geologic setting

The Shangsi section is located near Guangyuan City, northern Sichuan Province, China (Fig. 1-A and Fig. 1-B). It belongs to the northwestern corner of the Upper Yangtze block (Fig. 1-C). This area lies on the southern flank of the Longmenshan Indosinian folded zone of the Qinling folded system (Lai et al., 1996). The Shangsi section comprises, in ascending order, the Maokou Formation (Guadalupian), the Wujiaping Formation (Wuchiapingian), the Dalong Formation (Wuchiapingian to Changhsingian), and the Feixianguan Formation (Induan). The geology of the Shangsi section was first described by Li et al. (1986). The bed numbers of this latter study are also used herein. The uppermost Wuchiapingian (beds 15 to 16) are dominated by an alternation of mixed carbonate-siliceous rocks and siliceous limestones with a few mudstone intervals. Beds 17 to 22 comprise an alternation of carbonate-rich siliceous rocks and siliceous limestone with a few mudstone intercalations, containing radiolarians, bivalves, brachiopods and ammonites. Beds 23 to 29 comprise siliceous mudstone and calcareous mudstone with few claystone, containing abundant ammonites (Fig. 2). The facies of this section changed dramatically, from basinal facies (Dalong Formation) to more proximal facies (Feixianguan Formation) (Li et al., 1986). There is a dispute about the PTB in the Shangsi section. In accordance with the first occurrence of *Hindeodus parvus*, the PTB has to be placed in bed 30, over 4 meters above the mass extinction level (Li et al., 1986; Wignall et al., 1995; Lai et al., 1996; Nicoll et al., 2002; Jiang et al., 2011). However, Jiang et al. (2011) suggested that the PTB is placed 22 cm above the base of bed 28, based on hindeodid and gondolellid conodont taxa (Fig. 3). Recently, based on the U-Pb ages, an absolute age (252.28±0.13 Ma) has been attributed to the claystone of bed 27 by Shen et al. (2011).

2. Material and methods

141 samples were collected from the Upper Permian Dalong Formation and the Lower Triassic Feixianguan Formation, Shangsi section, Sichuan Province, southwest China. All the samples were analyzed for palynological and palynofacies studies. Most of these samples were also geochemically analyzed, in particular for major (125 samples) and trace elements (119 samples), and for total organic carbon (TOC) composition (101 samples).

2.1. Palynological and palynofacies analysis

Fifty grams of each of the 141 palynological samples were prepared using standard palynological methods. After treatment with hydrochloric (33%) and hydrofluoric acid (40%), the organic material was subsequently concentrated by treatment with zinc bromide solution (S.G. 2.2). Samples were neither oxidized nor sieved. *Lycopodium* spores were added during processing to allow calculation of absolute particle abundances, following the procedure of Tyson and Follows (2000). Residues were studied with the use of light and scanning electron microscopy. Palynological slides are stored in the China University of Geosciences (Wuhan).

To assess palynofacies components, particles were divided into four types, including palynomorphs (spores, pollen grains and acritarchs), phytoclasts (wood, leaf cuticles, and other vascular plant tissues), zooclasts (foraminifera linings, etc.), and unstructured organic matter (amorphous organic matter or AOM), following the subdivision of Tyson (1995). For each sample, 300 particles were counted in transmitted light (including *Lycopodium* spores and amorphous organic matter). Spore and pollen grains were identified at the generic level, whereas acritarchs were identified at the specific level.

2.2. Major and trace element analysis

119 samples from the Shangsi section were prepared for chemical analyses. Visible veins and weathered surfaces were removed, before the samples were pulverized to ~200 mesh size in an agate mortar. Major element abundances were determined by wavelength–dispersive X–ray fluorescence (XRF) analysis on fused glass beads using a XRF–1800 apparatus at the Key Laboratory of Biogeology and Environmental Geology of the Ministry of Education, China University of Geosciences (Wuhan).

Trace elements and REEs were measured using an Agilent 7500a ICP-MS (Inductively Coupled Plasma Mass Spectrometer) at the State Key Laboratory of Geological Processes and Mineral Resources, China University of Geosciences (Wuhan). About 50 mg of powder from each sample was weighed into a Teflon bomb and then moistened with a few drops of ultra–pure water before addition of 1 ml HNO_3 and 1 ml HF. The sealed bomb was heated at 190ºC in an oven for more than 48 hours. After cooling, the bomb was opened and evaporated at 115ºC to incipient dryness, then 1 ml HNO_3 was added and the sample was dried again. The resultant salt was re–dissolved with 3 ml 30% HNO_3 before it was again sealed and heated in the bomb at 190ºC for 12 hours. The final solution was transferred to a polyethylene bottle and diluted in 2% HNO_3 to about 80 ml for ICP–MS analysis. Analysis of the international rock standards BHVO–2 and BCR–2 indicated that the analytical precision is mostly better than 5%, according to the RSD.

2.3. Total organic carbon (TOC) analysis

For the analyses of the total organic carbon (TOC) composition of 101 samples, the C and S elemental concentrations were measured using an Eltra 2000 C–S analyzer at the University of Cincinnati. Data quality was monitored via multiple analyses of the USGS SDO–1 standard, yielding an analytical precision (2σ) of ±2.5% of reported values for C and ±5% for S. An aliquot of each sample was digested in 2N HCl at 50°C for 6 hours to dissolve carbonate minerals, and the residue was analyzed for TOC and non–acid–volatile sulfur (NAVS); total inorganic carbon (TIC) and acid–volatile sulfur (AVS) were obtained by difference.

3. Results and interpretation

3.1. Palynological Assemblages

This study indicates that diverse and abundant palynomorphs occur in the Upper Permian Dalong Formation and in the Lower Triassic Feixianguan Formation of the Shangsi section (Fig. 2). After qualitative and quantitative analysis, three palynological assemblage zones are identified. These assemblage zones can be correlated and compared with the conodont zones and the palynological assemblages of the Meishan section (Fig. 3), based on the investigations of Li et al. (1986), Jiang et al. (2007; 2011) and Zhang et al. (2007; 2009). Below, the palynological assemblages of the Shangsi section are summarized in ascending order:

(1) The *Dictyotidium* Assemblage Zone occurs in beds 15 to 17, corresponding to the lower part of the Dalong Formation and the *Neogondolella orienta* Conodont Biozone (Wuchiapingian) (Li et al., 1986) (Fig. 2). The palynological assemblage is very monotonous, of low diversity, and only comprises one large thick–walled acritarch, *Dictyotidium reticulatum*.

(2) The *Leiosphaeridia –Micrhystridium –Veryhachium* Assemblage Zone occurs in beds 20 to 25, in the upper part of the Dalong Formation, corresponding to the *Neogondolella yini* and *Neogondolella meishanensis* conodont Biozone (Changhsingian), (Jiang et al., 2011) (Fig. 2). This assemblage records the highest diversity and contains many acritarch species, including the following: *Dictyotidium reticulatum*, *Dictyotidium* sp., *Leiofusa* sp., *Leiosphaeridia microgranifera*, *Leiosphaeridia minutissima*, *Micrhystridium breve*, *Micrhystridium fragile*, *Micrhystridium pentagonale*, *Micrhystridium stellatum*, *Reduviasporonites catenulatus*, *Reduviasporonites chalastus*, *Schizosporis scissus*, *Schizosporis* sp., *Veryhachium cylindricum*, *Veryhachium hyalodermum*, *Veryhachium nasicum*, *Veryhachium quadratum*, *Veryhachium sedecimspinosum*, *Veryhachium* sp. *Leiotriletes*, *Lycopodiacidites* and *Waltzispora*. The genus *Leiosphaeridia* (with an average occurrence of over 67%) is the most common taxon in this assemblage, followed by the genera *Micrhystridium* (14.9%) and *Veryhachium* (14.8%).

(3) The *Pteruchipollenites –Leiotriletes* Assemblage Zone occurs in beds 26 and 29, corresponding to the lower part of the Feixianguan Formation (Induan), dated to belong to the *Neogondolella taylorae* or *Hindeodus changxingensis* and *Hindeodus parvus* conodont biozones (Jiang et al., 2011) (Fig. 2 and Fig. 3). This assemblage zone includes the following taxa: *Lycopodiacidites*, *Waltzispora*, *Indotriradites*, *Leiotriletes*, *Cycadopites*, *Tripartites*, *Propterisispora*, *Lueckisporites*, *Pteruchipollenites*, *Alisporites*, *Gardenasporites*, *Vitreisporites*, *Protohaploxypinus*, *Cordaitina*, *Baltisphaeridium* sp., *Leiosphaeridia microgranifera*, *Micrhystridium breve*, *Veryhachium hyalodermum*, *Reduviasporonites catenulatus* and *Reduviasporonites chalastus*. The percentage of spore and pollen grains in this zone is relatively high (over 86% of all palynomorphs in average), with the spores being the most abundant (43.7%), and pollen slightly less frequent (42.6%). The taxa *Pteruchipollenites* (18.4%) and *Leiotriletes* (14.1%) dominate in this assemblage. Acritarchs are generally rare, only several species occur in a few samples of the lower part of bed 28. Some authors suggested that the enigmatic taxon *Reduviasporonites* is a fungal spore, interpreting the frequent abundance of this microfossil as a fungal ‘spike’ just below the PTB (Eshet et al., 1995; Visscher et al., 1996; Looy et al., 2001; Steiner et al., 2003; Sandler et al., 2006; Sephton et al., 2009; Visscher et al., 2011). However, other authors (Afonin et al., 2001; Foster et al., 2002; Ouyang and Zhu, 2007) considered that *Reduviasporonites* is most likely of algal origin. In the present study, *Reduviasporonites* is recovered in seven samples with relatively low percentages (no more than 14% in every sample) (Fig. 2). A ‘spike’ of *Reduviasporonites* does therefore not occur in the section analyzed in this study.

3.2. Palynofacies and total organic carbon (TOC)

In the Shangsi section most samples show a clear dominance of amorphous organic matter (AOM) in the palynofacies samples. Palynomorphs are generally common, followed by phytoclasts and zooclasts. The varying character and changing distribution of the various palynological constituents are here classed into five palynofacies types and interpreted in terms of depositional environment. These are illustrated in figures 4 and 5, together with the concentrations of the different types of palynological organic matter. The values of TOC in the Shangsi section are generally high, ranging from 0.18% to 14% (Fig. 5). TOC values normally correlate well with the relative abundance of AOM in the sediment (Tyson, 1995). In the Shangsi section the TOC values show a positive correlation with the siliciclastic deposits. In the calcareous mudstones and limestones the average level is lower than that in siliciclastic lithologies (Fig. 5). It is therefore concluded that the TOC values in the Dalong Formation are much higher than those in the Feixianguan Formation.

Palynofacies type A, present in bed 15 and up to the lower part of bed 17, is dominated by an alternation of carbonate and siliceous rocks and siliceous limestones with a few mudstone intervals. It is clearly dominated by AOM (average of 57.5% in all organic types). Palynomorphs are common (21%), but they belong to only one acritarchs genus, *Dictyotidium*. The percentage of phytoclasts is moderate (19.5%). A few foraminiferal linings occur in several samples. The TOC values of this palynofacies type are high, ranging from 0.33% to 12.03%, with an average value of 6.12%. It is the highest average value observed for all the five types, showing that it has an excellent organic matter accumulation. According to the classification of kerogens, this palynofacies type is close to the kerogens that are classified as Type Ⅰ–Type Ⅱ kerogen using to Rock Eval parameters (Tyson, 1987, 1995; Carvalho et al., 2001) and has very good petroleum potential (oil prone).

Palynofacies type B, present in the upper part of bed 17 up to bed 19, is dominated by carbonate-siliceous rocks and mud–siliceous limestones with a few mudstones and limestones. It shows some difference with palynofacies type A, as it contains large amounts of the well–preserved brown opaque AOM (over 94%) in all samples, which is irregular and sponge like. According to the character of AOM, it is derived from phytoplankton or bacteria (Tyson, 1995; Carvalho et al., 2006; Ercegovac and Kostic, 2006). In addition, some foraminiferal linings (about 6%) occur in many samples. But palynomorphs and phytoclasts are absent in all samples from this palynofacies type. The TOC values change dramatically, ranging from the highest (14%) to the lowest (0.18%) levels. Their mean value is 3.73%, which is much lower than that in palynofacies type A. Similar to palynofacies type A, it could be classified as Type Ⅰ–Type Ⅱ kerogen (Tyson, 1987; 1995; Carvalho et al., 2001) and has also good petroleum potential.

Palynofacies type C (in the beds 20 to 25) is dominated by mud–siliceous limestones with a few mudstones and clays. In general, the amount of palynomorphs (about 58.4%) is the highest for all palynofacies types described in the sequence, while the brown opaque AOM (40.5%) is less abundant. Similar to palynofacies types A and B, a few foraminiferal linings occur in most samples of palynofacies type C. In addition, no terrestrial components are present. The palynomorphs are composed of a few genera of small, but well–preserved and thin–walled acritarchs, such as *Leiosphaeridia*, *Micrhystridium*, *Veryhachium* and others. The TOC values in the 44 samples range from 0.18% to 3.72%, with mean values of only 0.67%, much lower than that in palynofacies types A and B. Palynofacies type C is close to the kerogen types classified as Type Ⅰ–Type Ⅱ kerogen based on the Rock Eval data (Tyson, 1987; 1995; Carvalho et al., 2001), and has good petroleum potential.

Palynofacies type D is dominated by limestones (bed 26) and calcareous mudstones (the lower part of bed 28) with a clay interval (bed 27). Similar to palynofacies type C the palynomorphs are the most common component (41.5%), with two–thirds of them being spore and pollen grains, only one–third of them are small acritarchs, dominated by the genus *Micrhystridium*. The AOM is less abundant (29.3%), and the phytoclasts (29.1%) become common again after they disappeared in the sequence. Foraminiferal linings only occur in one sample of this type. The TOC values in 5 samples range from 0.21% to 0.30%, with the lowest mean value (only 0.25%) of all five palynofacies types. Although palynofacies type D could be classified as Type Ⅱ kerogen (Tyson, 1987; 1995; Carvalho et al., 2001) it does not have a good petroleum potential.

Palynofacies type E (in the upper part of bed 28 to bed 29) is dominated by calcareous mudstones. It contains only terrestrial components. The palynomorphs are the most common component (38.2%), represented by well–preserved spore and pollen grains. Phytoclasts are less abundant (33%), they are small, well–sorted, rounded and opaque. The other frequent component is the AOM (28.8%), that is rounded, or sharp to diffuse in outline. According to the character of the AOM, it appears to be formed by degraded terrestrial components (Tyson, 1995; Carvalho et al., 2006; Ercegovac and Kostic, 2006). Marine organic walled phytoplankton and foraminiferal linings are absent in this palynofacies type. The TOC values are generally low, except in two samples with 1.97% and 2.45%. The mean value is only 0.47%, a little higher than that in palynofacies type D. Thus, palynofacies type E could be classified as Type Ⅲ–Type Ⅱ kerogen (Tyson, 1987; 1995; Carvalho et al., 2001) and does not have a good petroleum potential.

3.3. Major and trace element concentrations

Concentrations of Al are rarely influenced by biogenic or diagenetic processes and, thus are commonly used to assess the amount of terrigenous material in modern marine sediments, sediment trap material, and ancient sedimentary rocks (Walsh et al., 1988; Murray et al., 1992; Saito et al., 1992; Murray and Leinen, 1996). Cross-plots reveal whether major/trace elements were supplied with the land-derived aluminosilicate fraction of the sediments. In the Shangsi Section, from the *r* values of these plots (Table 1), the results show that (1) Th, K and Ti concentrations are strongly correlated with Al ($0.90<r<0.97$); (2) Pb, Zr and Fe are less tightly correlated with Al ($0.84<r<0.85$); (3) Ba, Co, Cr, Cu, Mo, Ni, U, V, Zn, Si, Mn and Na are poorly to not correlated with Al ($r<0.70$); (4) Sr and Ca are negatively correlated to Al. However, it is out of the scope of the present paper to discuss in depth inorganic geochemistry, (see Shen et al., unpublished). The concentrations of Al are shown in Figure 5, indicating that, the Feixianguan Formation contains an abundant terrestrial fraction, but the Dalong Formation contains only a relatively reduced clastic fraction.

Redox sensitive trace elements concentrations or ratios have long been used as palaeoredox proxies (Brumsack, 1980; Wignall and Myers, 1988; Dean et al., 1999; Riquier et al., 2006; Tribovillard et al., 2006; Algeo and Tribovillard, 2009). Hatch and Leventhal (1992) and Jones and Manning (1994) considered that the degree of pyritisation (DOP), as well as the V/Cr, U/Th, Ni/Co and V/(V+Ni) ratios are reliable tracers for palaeoredox conditions, subsequently frequently used by many authors (e.g., Wilkin et al., 1996, 1997; Joachimski et al., 2001; Lyons et al., 2003;

Algeo and Maynard, 2004; Riquier et al., 2006). In the present study, the concentrations of Co, Cr, Ni, Th, U and V are shown in Figure 5 and V/Cr, U/Th, Ni/Co and V/(V+Ni) ratios have been calculated and illustrated in Figure 6. The correlations between these element ratio values and redox conditions are shown in Table 2. The results show that:

(1) the concentrations of Co and Th are high in the Feixianguan Formation, influenced by the high abundance of terrestrial components, to be compared to the concentrations of Cr, Ni, V and U in lower parts of the Dalong Formation (Fig. 5);

(2) based on the cross-plots of some redox indices, such as V/Cr, U/Th, Ni/Co and V/(V+Ni), palynofacies type A and type B correspond to a dysoxic–anoxic environment of deposition (Fig. 6), although the result of cross-plotting V/Cr vs. Ni/Co do not support this conclusion for palynofacies type B;

(3) according to the cross-plots of V/Cr vs. U/Th and V/(V+Ni) vs. U/Th, the lower part of palynofacies type C (beds 20 to 21) corresponds to a dysoxic–anoxic environment, but the Ni/Co ratio indicates oxic conditions. In addition, the upper part of palynofacies type C (beds 22 to 25) corresponds to an oxic–dysoxic environment uniformly;

(4) palynofacies types D and E clearly indicate oxic environmental conditions, although the V/(V+Ni) ratio shows anoxic environments. These results are shown in Figure 6, which indicates that beds 15 to 21 correspond to the most oxygen-poor conditions, while beds 26 to 29 have been deposited under the most oxygen-rich conditions.

4. Discussion

In general, the high percentage of AOM indicates reducing conditions and dysoxic–anoxic environments (Batten, 1983; Tyson, 1987). In the Shangsi section, most samples show high percentages of AOM, especially in palynofacies type A and type B. According to the above results, the interval between beds 15 to 21 represents a dysoxic–anoxic environment, beds 22 to 25 an oxic–dysoxic environment and beds 26 to 29 an oxic environment (Fig. 5). The environmental interpretation of the palynofacies types is as follows.

Palynofacies type A: the AOM –palynomorph –phytoclast ternary plot of Tyson (1995) suggests that this type was deposited in an offshore marine environment with low terrestrial components (Fig. 7). Similar conclusions can be obtained from the fossil record and the geochemical results. The concentrations of Al in this palynofacies type are generally low (Fig. 5). This also suggests that the deposits are distant from any significant input of terrigenous material. There are a few radiolarian and many foraminiferal linings in beds 15 to 16 (Fig. 4). Based on the fossil records and lithology, Li et al. (1986) considered that these beds were deposited in platform-margin slope facies (Fig. 5). According to the cross-plots of redox indices, the palynofacies type A indicate dysoxic–anoxic environments.

Palynofacies type B has abundant AOM. Many authors suggested that the abundance of AOM indicates the deposition in dysoxic–anoxic conditions during periods of sluggish circulation (Tyson, 1995; Al-Ameri et al., 1999; Filipiak, 2002; Schiøler et al., 2002; Carvalho et al., 2006; Blažeković Smojić et al., 2009). Li et al. (1986) concluded that beds 17 to 19 have been deposited under deep water conditions, as indicated by the basinal facies (Fig. 5). Moreover, radiolarian-rich samples occur in bed 18 with low concentrations of Al. In addition, the geochemical results show that this palynofacies type corresponds to a dysoxic–anoxic environment (Figs. 5 and 6). It can be suggested that these sediments were deposited under offshore basin conditions and dysoxic–anoxic oxygenation conditions.

Palynofacies type C: The AOM –palynomorphs –phytoclasts ternary plot and the spore –pollen –microplankton ternary plot (Tyson, 1995) suggest that this palynofacies type was deposited in offshore environments with low levels of terrestrial components, similarly to palynofacies type A (Fig. 7). Some authors (Jacobson, 1979; Vecoli, 2000; Courtinat and Malartre, 2003) considered that a dominance of the leiosphaerid acritarch class corresponds to a nearshore, shallow marine environment; the baltisphaerid –veryhachid –*Polygonium* class reflects, however an open marine environment; whereas the high abundance of *Micrhystridium* indicates restricted marine conditions. Li et al. (2004a) described the Late Permian acritarch assemblages from the Meishan section, dominated by the *Micrhystridium –Veryhachium* complex, and suggested that these assemblages are typical of offshore environments. Subsequently, Yan and Li (2010) considered that the *Leiosphaeridia –Baltisphaeridium –Polygonium –Micrhystridium* association corresponds to deeper marine environment. The palynomorphs of this palynofacies type are similar to those of the Meishan section, with low diversity but a high abundance of acritarchs, dominated by *Leiosphaeridia*, *Micrhystridium* and *Veryhachium* being less common. Beds 19 to 21 are dominated by foraminiferal linings and no radiolarians are present (Fig. 4), in contrast to the abundance of radiolarians and the absence of foraminiferal linings in beds 22 to 25. From Li et al. (1986) sea-level curve, it appears that the sea level rose from beds 22 to 25, then it declined from beds 19 to 21**,** based on the fossil records and lithology, although both of the two parts were deposited in basinal environment (Fig. 5). Similar to palynofacies type A and B, the low concentrations of Al suggest that the deposits are too distant for any significant terrigenous input in beds 19 to 23. However, the concentrations of Al are much higher than those in beds 24 to 29.

Palynofacies type D: The AOM –palynomorphs –phytoclasts ternary plot and the spore –pollen –microplankton ternary plot (Fig. 7) and the high concentrations of Al (Fig. 5) suggest that palynofacies type D was deposited in shallow marine and nearshore environments with a high abundance of terrestrial components (Tyson, 1995; Carvalho et al., 2006). According to the sea-level curve (Fig. 5), the sea level declined dramatically from bed 25, but it rose again after bed 27 with a reduced input of terrestrial palynoclasts (compare to Pross et al., 2006). There is a temporary peak of acritarchs in bed 25, not only in terms of abundance but also diversity. A possible interpretation is that the metazoan animals that fed on acritarchs or algae strongly decreased during the latest Permian (Jin et al., 2000; Yin et al., 2007). However, there are only several acritarchs species with low abundance in bed 28. Moreover, only a few *Micrhystridium* are present in some samples, indicating restricted marine conditions (Vecoli, 2000; Li et al., 2004b; Ercegovac and Kostic, 2006).

Palynofacies type E was deposited in deltaic to nearshore environments with a high abundance of terrestrial components (Fig. 7). The sea level in this palynofacies type appears a little higher than that in palynofacies type D (Fig. 5). There are lower abundances of terrestrial components in palynofacies type E than that in type D (compare Pross et al., 2006). According to the cross-plots of redox indices (Figs. 5 and 6), palynofacies type E indicates an oxic environment.

5. Conclusions

(1) Three palynological assemblage zones are identified. These are in ascending order: the *Dictyotidium* Assemblage Zone (Wuqiapingian), the *Leiosphaeridia –Micrhystridium –Veryhachium* Assemblage Zone (Changxingian), and the *Pteruchipollenites –Leiotriletes*

Assemblage Zone (Induan). It is important to note that an abundance 'spike' of *Reduviasporonites* is not observed at the PTB of the Shangsi section. This enigmatic taxon, considered by several authors as a fungal spore, occurs in seven samples with relatively low percentages.

(2) From the varying character and distribution of the palynological constituents in the sediments of the analyzed succession, five palynofacies types can be identified, which relate to the different depositional environments (Table 3). Beds 15 to 21 have a high petroleum potential.

Acknowledgments

We wish to express sincere thanks to Mr. Qing Hu, Lei Zhang, Guichun Liu, Yu Xiang and Miss Guozhen Xu and Xiaomei Nie for their help in field work. We thank Carys Bennett (Université de Lille1, University of Leicester) for linguistic improvements and the correction of the text. This work was supported by the National Science Foundation of China (NSFC) project no. 40839903, 40921062, the Chinese 973 (2011CB808800) and 111 programs (B08030) and by grants of the University of Lille1 ("Allocation Présidentielle" and "Bonus Qualité Recherche") and the Conseil Régional du Nord (France).

References

Afonin, S., Barinova, S., Krassilov, V., 2001. A bloom of *Tympanicysta* Balme (green algae of zygnematalean affinities) at the Permian-Triassic boundary. Geodiversitas 23, 481-487.

Al-Ameri, T.K., Al-Musawi, F.S., Batten, D.J., 1999. Palynofacies indications of depositional environments and source potential for hydrocarbons: uppermost Jurassic-basal Cretaceous Sulaiy Formation, southern Iraq. Cretaceous Research 20, 359-363.

Algeo, T.J., Tribovillard, N., 2009. Environmental analysis of paleoceanographic systems based on molybdenum-uranium covariation. Chemical Geology 268, 211-225.

Algeo, T.J., Maynard, J.B., 2004. Trace-element behavior and redox facies in core shales of Upper Pennsylvanian Kansas-type cyclothems. Chemical Geology 206, 289-318.

Batten, D.J., 1983. Identification of amorphous sedimentary organic matter by transmitted light microscopy. Geological Society, London, Special Publications 12, 275.

Blažeković Smojić, S., Smajlović, J., Koch, G., Bulić, J., Trutin, M., Oreški, E., Alajbeg, A., Veseli, V., 2009. Source potential and palynofacies of Late Jurassic "Lemeš facies", Croatia. Organic Geochemistry 40, 833-845.

Brumsack, H.J., 1980. Geochemistry of Cretaceous black shales from the Atlantic Pcean (DSDP Legs 11, 14, 36 and 41). Chemical Geology 31, 1-25.

Carvalho, M.A., 2001. Paleoenvironmental reconstruction based on palynology and palynofacies analyses of the Aptian-Albian in the Sergipe Basin, northeastern Brazil. Universität Heidelberg, 1-150. (Unpublished Thesis).

Carvalho, M.A., Mendonça Filho, J.G., Menezes, T.R., 2006. Palynofacies and sequence stratigraphy of the Aptian-Albian of the Sergipe Basin, Brazil. Sedimentary Geology 192, 57-74.

Combaz, A., 1964. Les palynofaciès. Revue de Micropaléontologie 7, 205-218.

Courtinat, B., Malartre, F., 2003. Palynofacies variations in a carbonate ramp system environment (Upper Muschelkalk, NE France). Bulletin de la Société Géologique de France 174, 595-601.

Chen, Z.Q., 2007. Discussion on gas exploration of Feixianguan Formation in the Lower Triassic of Sichuan Basin. Acta Petrolei Sinica 28, 12-26 (In Chinese and English summary).

Dean, W.E., Piper, D.Z., Peterson, L.C., 1999. Molybdenum accumulation in Cariaco basin sediment over the past 24 ky: A record of water-column anoxia and climate. Geology 27, 507.

Ercegovac, M., Kostic, A., 2006. Organic facies and palynofacies: Nomenclature, classification and applicability for petroleum source rock evaluation. International Journal of Coal Geology 68, 70-78.

Eshet, Y., Rampino, M.R., Visscher, H., 1995. Fungal event and palynological record of ecological crisis and recovery across the Permian-Triassic boundary. Geology 23, 967-970.

Filipiak, P., 2002. Palynofacies around the Frasnian/Famennian boundary in the Holy Cross Mountains, southern Poland. Palaeogeography, Palaeoclimatology, Palaeoecology 181, 313-324.

Foster, C.B., Stephenson, M.H., Marshall, C., Logan, G.A., Greenwood, P.F., 2002. A revision of *Reduviasporonites* Wilson 1962: description, illustration, comparison and biological affinities. Palynology 26, 35-58.

Hatch, J.R., Leventhal, J.S., 1992. Relationship between inferred redox potential of the depositional environment and geochemistry of the Upper Pennsylvanian (Missourian) Stark Shale Member of the Dennis Limestone, Wabaunsee County, Kansas, USA. Chemical Geology 99, 65-82.

Hong, H.T., Wang, Y. G., Yang, T.Q., Wen, Y.C., Xia, M.L., 2008. Sedimentary facies of Changxing Formation and distribution of organic reef gas reservoirs in northern Sichuan basin. Natural Gas Industry 28, 38-41 (In Chinese and English summary).

Hou, J.P., Song, P., 1995. Late early Permian and Late Permian spore-pollen assemblages of Meishan, Changxing county, Zhejiang Province 25, 168–187 (In Chinese and English summary).

Jacobson, S.R., 1979. Acritarchs as paleoenvironmental indicators in Middle and Upper Ordovician rocks from Kentucky, Ohio and New York. Journal of Paleontology 53, 1197-1212.

Jiang, H.S., Lai, X.L., Luo, G.M., Aldridge, R.J., Zhang, K.X., Wignall, P.B., 2007. Restudy of conodont zonation and evolution across the P/T boundary at Meishan section, Changxing, Zhejiang, China. Global and Planetary Change 55, 39-55.

Jiang, H.S., Lai, X.L., Yan, C.B., Aldridge, R.J., Wignall, P.B., Sun, Y.D., 2011. Revised conodont zonation and conodont evolution across the Permian–Triassic boundary at the Shangsi section, Guangyuan, Sichuan, South China. Global and Planetary Change 77, 103-115.

Jin, Y.G., Wang, Y., Wang, W., Shang, Q.H., Cao, C.Q., Erwin, D.H., 2000. Pattern of marine mass extinction near the Permian-Triassic boundary in South China. Science 289, 432-436.

Joachimski, M.M., Ostertag-Henning, C., Pancost, R.D., Strauss, H., Freeman, K.H., Littke, R., Sinninghe Damste, J.S., Racki, G., 2001. Water column anoxia, enhanced productivity and concomitant changes in δ^{13}C andδ^{34}S across the Frasnian-Famennian boundary (Kowala--Holy Cross Mountains/Poland). Chemical Geology 175, 109-131.

Jones, B., Manning, D.A.C., 1994. Comparison of geochemical indices used for the interpretation of palaeoredox conditions in ancient mudstones. Chemical Geology 111, 111-129.

Lai, X. L., Yang, F. Q., Hallam, A., Wignall, P. 1996. The Shangsi section, candidate of the Global Stratotype section and point of the Permian-Triassic boundary. In: Yin, H. F. (Ed.), The Palaeozoic-Mesozoic Boundary. Candidates of Global Stratotype Section and Point of the

Permian-Triassic Boundary. China University of Geosciences Press, Wuhan, 113-124 .

Lei, Y., Servais, T., Feng, Q.L. The diversity of the Permian phytoplankton. Review of Palaeobotany and Palynology (accepted for publication).

Li, J., Cao, C.Q., Servais, T., Zhu, Y., 2004a. Later Permian acritarchs from Meishan (SE China) in the context of Permian palaeobiogeography and palaeoecology. Neues Jahrbuch für Geologie und Paläontologie, Monatshefte, 427-448.

Li, J., Servais, T., Yan, K., Zhu, H.C., 2004b. A nearshore-offshore trend in acritarch distribution from the Early-Middle Ordovician of the Yangtze Platform, South China. Review of Palaeobotany and Palynology 130, 141-161.

Li, Z.S., Zhan, L.P., Zhu, X.F., Zhang, J.H., Jin, R.G., Liu, G.F., Sheng, H.B., Shen, G.M., Dai, J.Y., Huang, H.Q., Xie, L.C., Yan, Z., 1986. Mass extinction and geological events between Palaeozoic and Mesozoic era. Acta Geologica Sinica 60, 1-15 (In chinese with English abstract)

Looy, C.V., Twitchett, R.J., Dilcher, D.L., Van Konijnenburg-Van Cittert, J.H.A., Visscher, H., 2001. Life in the end-Permian dead zone. Proceedings of the National Academy of Sciences of the United States of America 98, 7879.

Lyons, T.W., Werne, J.P., Hollander, D.J., Murray, R., 2003. Contrasting sulfur geochemistry and Fe/Al and Mo/Al ratios across the last oxic-to-anoxic transition in the Cariaco Basin, Venezuela. Chemical Geology 195, 131-157.

Murray, R.W., Leinen, M., 1996. Scavenged excess aluminum and its relationship to bulk titanium in biogenic sediment from the central equatorial Pacific Ocean. Geochimica et Cosmochimica Acta 60, 3869-3878.

Murray, R.W., Buchholtz ten Brink, M.R., Gerlach, D.C., Russ III, G.P., Jones, D.L., 1992. Interoceanic variation in the rare earth, major, and trace element depositional chemistry of chert: perspectives gained from the DSDP and ODP record. Geochimica et Cosmochimica Acta 56, 1897-1913.

Nicoll, R.S., Metcalfe, I., Cheng-Yuan, W., 2002. New species of the conodont genus *Hindeodus* and the conodont biostratigraphy of the Permian-Triassic boundary interval. Journal of Asian Earth Sciences 20, 609-631.

Nie, X.M., Lei, Y., Feng, Q.L., Xiang, Y., 2012. Development laws of Changhsingian radiolarian fauna at the Shangsi Section of Sichuan Province and its control factors. Geological Review-(In Chinese and English summary, in press).

Ouyang, S., 1982. Upper Permian and Lower Triassic palynomorphs from eastern Yunnan, China. Canadian Journal of Earth Sciences 19, 68-80.

Ouyang, S., 1986. Palynology of Upper Permian and Lower Triassic strata of Fuyuan district, Eastern Yunan. Palaeontologia sinica 169, pp. 1-122 (In Chinese).

Ouyang, S., Hou J.P., 1999a. On characteristics of the Cathaysian palynoflora. Acta Palaeontologica Sinica 38, 262–283 (In Chinese and English summary).

Ouyang, S., Hou J.P., 1999b. On the relationship between the Cathaysia flora and Angara flora based on palynological data. Acta Micropalaeontologica Sinica 16, 351–368 (In Chinese and English summary).

Ouyang, S., Utting, J., 1990. Palynology of Upper Permian and Lower Triassic rocks, Meishan, Changxing County, Zhejiang Province, China. Review of Palaeobotany and Palynology 66, 65-103.

Ouyang, S., Zhu, H.C., 2007. Query the assumption of “end-Permian fungal spike event”, with special reference to the Permo-Triassic transitional palynofloras. Acta Palaeontologica Sinica 46, 394–410 (In Chinese and English summary).

Peng, Y.Q., Yu, J.X., Gao, Y.Q., Yang, F.Q., 2006. Palynological assemblages of non-marine rocks at the Permian-Triassic boundary, western Guizhou and eastern Yunnan, South China. Journal of Asian Earth Sciences 28, 291-305.

Pross, J., Link, E., Ruf, M., Aigner, T., 2006. Delineating sequence stratigraphic patterns in deeper ramp carbonates: quantitative palynofacies data from the Upper Jurassic (Kimmeridgian) of Southwest Germany. Journal of Sedimentary Research 76, 524-538.

Riquier, L., Tribovillard, N., Averbuch, O., Devleeschouwer, X., Riboulleau, A., 2006. The Late Frasnian Kellwasser horizons of the Harz Mountains (Germany): two oxygen-deficient periods resulting from different mechanisms. Chemical Geology 233, 137-155.

Saito, C., Noriki, S., Tsunogai, S., 1992. Particulate flux of A1, a component of land origin, in the western North Pacific. Deep Sea Research Part A. Oceanographic Research Papers 39, 1315-1327.

Sandler, A., Eshet, Y., Schilman, B., 2006. Evidence for a fungal event, methane-hydrate release and soil erosion at the Permian-Triassic boundary in southern Israel. Palaeogeography, Palaeoclimatology, Palaeoecology 242, 68-89.

Schiøler, P., Crampton, J.S., Laird, M.G., 2002. Palynofacies and sea-level changes in the Middle Coniacian-Late Campanian (Late Cretaceous) of the East Coast Basin, New Zealand. Palaeogeography, Palaeoclimatology, Palaeoecology 188, 101-125.

Sephton, M.A., Visscher, H., Looy, C.V., Verchovsky, A.B., Watson, J.S., 2009. Chemical constitution of a Permian-Triassic disaster species. Geology 37, 875-878.

Shen, S. Z., Crowley, J. L., Wang, Y., Bowring, S. A., Erwin, D. H., Sadler, P. M., Cao, C. Q., Rothman, D. H., Henderson, C. M., Ramezani, J., 2011. Calibrating the end-Permian mass extinction. Science 334, 1367-1372.

Steiner, M.B., Eshet, Y., Rampino, M.R., Schwindt, D.M., 2003. Fungal abundance spike and the Permian-Triassic boundary in the Karoo Supergroup (South Africa). Palaeogeography, Palaeoclimatology, Palaeoecology 194, 405-414.

Tribovillard, N., Algeo, T.J., Lyons, T., Riboulleau, A., 2006. Trace metals as paleoredox and paleoproductivity proxies: An update. Chemical Geology 232, 12-32.

Tyson, R.V., 1987. The genesis and palynofacies characteristics of marine petroleum source rocks. Geological Society, London, Special Publications 26, 47.

Tyson, R.V., 1995. Sedimentary Organic Matter: Organic Facies and Palynofacies. Chapman and Hall, New York, pp. 1-615.

Tyson, R.V., Follows, B., 2000. Palynofacies prediction of distance from sediment source: A case study from the Upper Cretaceous of the Pyrenees. Geology 28, 569.

Vecoli, M., 2000. Palaeoenvironmental interpretation of microphytoplankton diversity trends in the Cambrian-Ordovician of the northern Sahara Platform. Palaeogeography, Palaeoclimatology, Palaeoecology 160, 329-346.

Visscher, H., Brinkhuis, H., Dilcher, D., Elsik, W., Eshet, Y., Looy, C., Rampino, M., Traverse, A., 1996. The terminal Paleozoic fungal event: evidence of terrestrial ecosystem destabilization and collapse. Proceedings of the National Academy of Sciences of the United States of America 93, 2155.

Visscher, H., Sephton, M.A., Looy, C.V., 2011. Fungal virulence at the time of the end-Permian biosphere crisis? Geology 39, 883.

Walsh, I., Dymond, J., Collier, R., 1988. Rates of recycling of biogenic components of settling particles in the ocean derived from sediment trap experiments. Deep Sea Research Part A. Oceanographic Research Papers 35, 43-58.

Waterhouse, H.K., 1999. Orbital forcing of palynofacies in the Jurassic of France and the United Kingdom. Geology 27, 511-514.

Wignall, P.B., Myers, K.J., 1988. Interpreting benthic oxygen levels in mudrocks: a new approach. Geology 16, 452.

Wignall, P.B., Hallam, A., Lai, X.L., Yang, F.Q., 1995. Palaeoenvironmental changes across the Permian/Triassic boundary at Shangsi (N. Sichuan, China). Historical Biology 10, 175-189.

Wilkin, R.T., Barnes, H.L., Brantley, S.L., 1996. The size distribution of framboidal pyrite in modern sediments: An indicator of redox conditions. Geochimica et Cosmochimica Acta 60, 3897-3912.

Wilkin, R.T., Arthur, M.A., Dean, W.E., 1997. History of water-column anoxia in the Black Sea indicated by pyrite framboid size distributions. Earth and Planetary Science Letters 148, 517-525.

Wood, S.E., Gorin, G.E., 1998. Sedimentary organic matter in distal clinoforms of Miocene slope sediments; Site 903 of ODP Leg 150, offshore New Jersey (USA). Journal of Sedimentary Research 68, 856.

Xie, S.C., Pancost, R.D., Wang, Y.B., Yang, H., Wignall, P.B., Luo, G.M., Jia, C.L., Chen, L., 2010. Cyanobacterial blooms tied to volcanism during the 5 my Permo-Triassic biotic crisis. Geology 38, 447.

Yan, K., Li, J., 2010. The palaeoenvironmental implication of Early-Middle Ordovician acritarch communities from South China. Chinese Science Bulletin 55, 957-964.

Yang X.Y., 2002. Late Permian spores and pollen thermal alteration index and organic matter types from the Longtan Formation in Southern Jiangsu. Acta Micropalaeontologica Sinica 19, 309–315 (In Chinese and English summary).

Yin, H.F., Feng, Q.L. Lai, X.L., Baud, A., Tong, J.N., 2007. The protracted Permo-Triassic crisis and multi-episode extinction around the Permian-Triassic boundary. Global and Planetary Change 55, 1-20.

Zhang, K.X., Tong, J.N., Shi, G., Lai, X.L., Yu, J.X., He, W.H., Peng, Y.Q., Jin, Y.L., 2007. Early Triassic conodont-palynological biostratigraphy of the Meishan D Section in Changxing, Zhejiang Province, South China. Palaeogeography, Palaeoclimatology, Palaeoecology 252, 4-23.

Zhang K.X., Lai X.L., Tong J.N., Jiang H.S., 2009. Progresses on study of conodont sequence for the GSSP section at Meishan, Changxing, Zhejiang Province, South China. Acta Palaeontologica Sinica 48, 474–486 (In Chinese and English summary).

Figure captions

Figure 1: Location map of the Shangsi section (A and B); End Permian paleogeography in South China (C) (revised from Xie et al, 2010).

Figure 2: Palynological assemblages of the Shangsi section. Each bar is 10 µm. St.: Stage age; Fo.: Formation; Lith.: Lithology; C. Z.: Conodont Zone; P. a.: Palynological assemblages; Sa.: Samples;

Figure 3: Conodont zones and palynological assemblages zones at Meishan and Shangsi. Compiled mainly from Li et al.(1986), Ouyang and Utting (1990), Jiang et al. (2007, 2011) Zhang et al. (2007, 2009). H.: *Hindeodus*; I.: *Isarcicella*; N.: *Neogondolella*; ch.: *changxingensis*; la.: *latidentatus*; lo.: *longicuspidata*; me.: *meishanensis*; pr.: *praeparvus*; st.: *staeschei.*

Figure 4: Concentrations of organic matter and the palynofacies types in the Shangsi section. The concentrations of radiolarian are adapted from Nie et al. (in press). St.: Stage age; Fo.: Formation; Lith.: Lithology; C. Z.: Conodont Zone; P. a.: Palynological assemblages; *Dic*.: *Dictyotidium*; *Lei*.: *Leiosphaeridia*; *Ver*.: *Veryhachium*; *Mic*.: *Micrhystridium*; Phy.: Phytoclasts; For.: foraminiferal linings; Rad.: radiolarian.

Figure 5: Concentrations of TOC and selected major and trace elements, sea-level changes and the results of redox conditions in the Shangsi section. St.: Stage; Fo.: Formation; Lith.: Lithology; C. Z.: Conodont Zone; P. t.: Palynofacies types; sea-level changes compiled mainly from Li et al. (1986).

Figure 6: Crossplot of redox indices in five palynofacies types, revised from Riquier et al. (2006). V/Cr vs. U/Th, Ni/Co vs. U/Th, V/(V+Ni) vs. U/Th and V/Cr vs. Ni/Co. C1: bed 20 to bed 21; C2 : bed 22 to bed 25.

Figure 7: AOM –Palynomorphs –Phytoclasts ternary plot and the Spore –Pollen –Microplankton ternary plot in Shangsi section, based on Tyson (1995).

Table captions

Table 1. Correlation coefficients (r) between Al and selected major and trace elements and level of significance of correlations (p).

Table 2. Correlations between trace-element ratio values and redox zones. a: ranges for V/Cr, U/Th and Ni/Co are from Jones and Manning (1994); b: ranges for V/(V+Ni) are from Hatch and Leventhal (1992).

Table 3. Depositional environments of the palynofacies types A-E.

Figure 1:

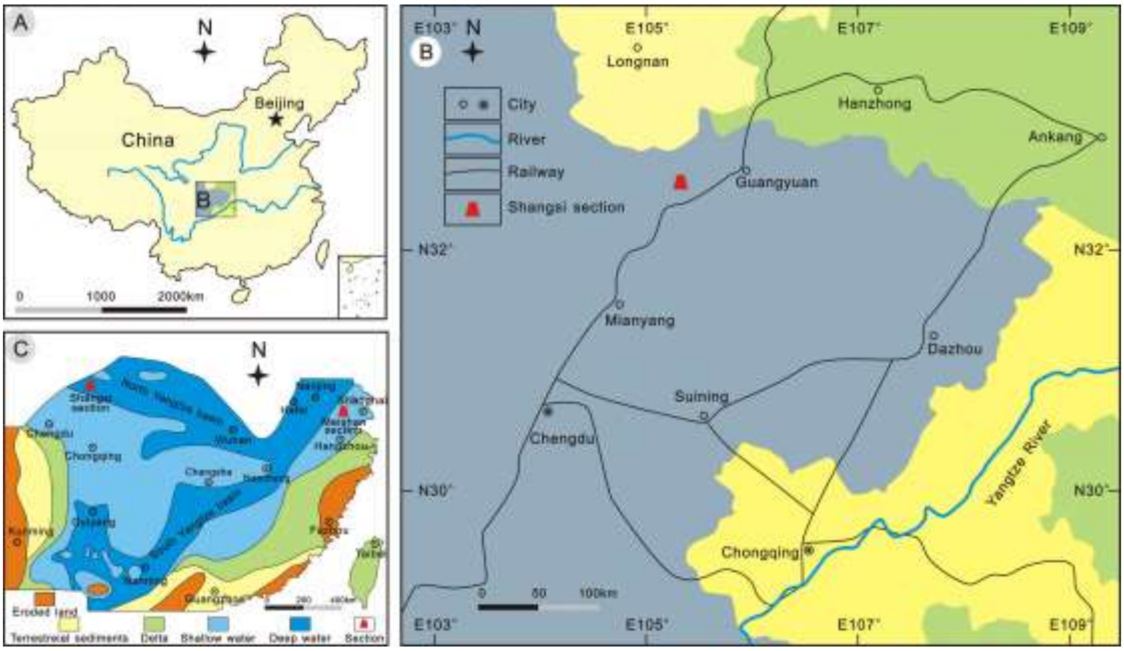
A
N
Beijing
China
B
0
1000
2000km
B
N
E103°
E105°
E107°
E109°
Longnan
City
River
Railway
Shangsi section
Hanzhong
Ankang
Guangyuan
N32°
Mianyang
Dazhou
Suining
Chengdu
N30°
Yangtze River
Chongqing
0
50
100km
C
N
Shangsi section
North Yangtze basin
Nanjing
Hefei
Shanghai
Meishan section
Hangzhou
Chengdu
Chongqing
Wuhan
Changsha
Nanchang
Guiyang
Kunming
South Yangtze basin
Fuzhou
Taibei
Nanning
Guangzhou
0
200
400km
Eroded land
Terrestrial sediments
Delta
Shallow water
Deep water
Section

Figure 2:

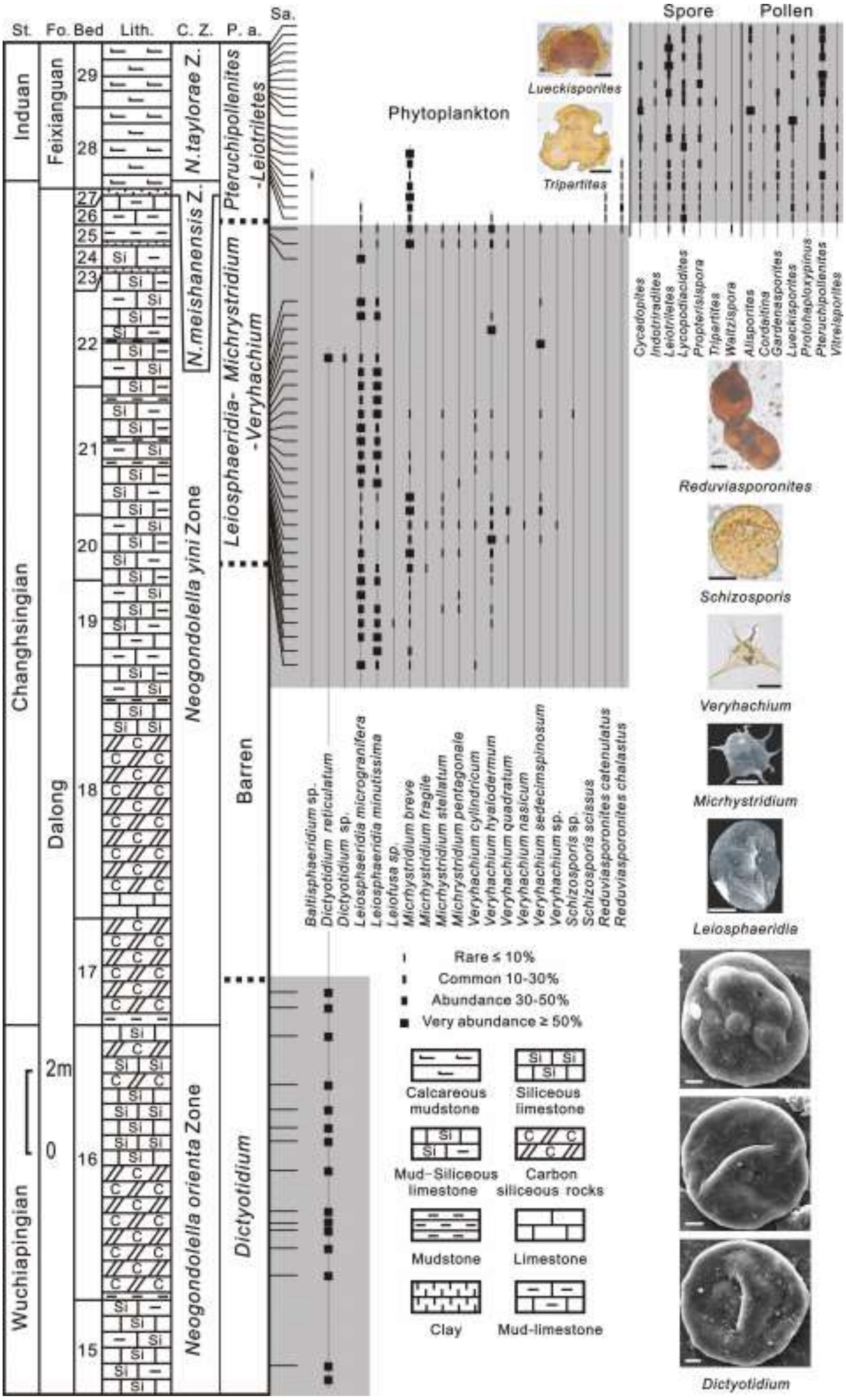
St.
Fo.
Bed
Lith.
C. Z.
P. a.
Sa.
Induan
Changhsingian
Wuchiapingian
Feixianguan
Dalong
29
28
27
26
25
24
23
22
21
20
19
18
17
16
15
2m
0
N.taylorae Z.
N.meishanensis Z.
Neogondolella yini Zone
Neogondolella orienta Zone
Pteruchipollenites -Leiotriletes
Leiosphaeridia- Michrystridium -Veryhachium
Barren
Dictyotidium
Phytoplankton
Spore
Pollen
Lueckisporites
Tripartites
Reduviasporonites
Schizosporis
Veryhachium
Micrhystridium
Leiosphaeridia
Dictyotidium
Baltisphaeridium sp.
Dictyotidium reticulatum
Dictyotidium sp.
Leiosphaeridia microgranifera
Leiosphaeridia minutissima
Leiofusa sp.
Micrhystridium breve
Micrhystridium fragile
Michrystridium stellatum
Michrystridium pentagonale
Veryhachium cylindricum
Veryhachium hyalodermum
Veryhachium quadratum
Veryhachium nasicum
Veryhachium sedecimspinosum
Veryhachium sp.
Schizosporis sp.
Schizosporis scissus
Reduviasporonites catenulatus
Reduviasporonites chalastus
Cycadopites
Indotriradites
Leiotriletes
Lycopodiacidites
Propterisispora
Tripartites
Waltzispora
Alisporites
Cordaitina
Gardenasporites
Lueckisporites
Protohaploxypinus
Pteruchipollenites
Vitreisporites
Rare ≤ 10%
Common 10-30%
Abundance 30-50%
Very abundance ≥ 50%
Calcareous mudstone
Siliceous limestone
Mud-Siliceous limestone
Carbon siliceous rocks
Mudstone
Limestone
Clay
Mud-limestone
Si
C

Figure 3:

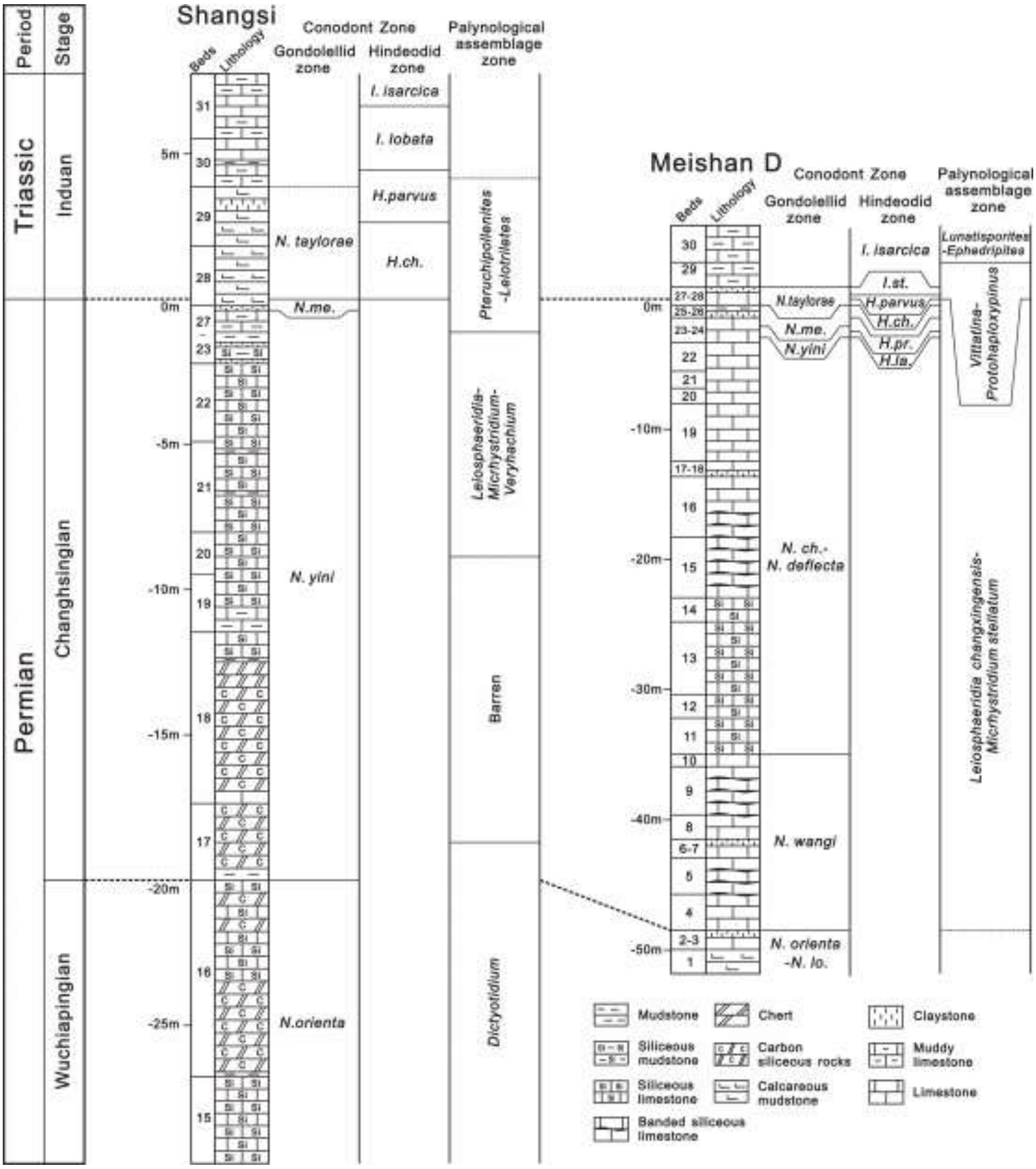
Period
Stage
Triassic
Induan
Permian
Changhsingian
Wuchiapingian
Shangsi
Beds
Lithology
Conodont Zone
Gondolellid zone
Hindeodid zone
Palynological assemblage zone
5m
0m
-5m
-10m
-15m
-20m
-25m
31
30
29
28
27
23
22
21
20
19
18
17
16
15
I. isarcica
I. lobata
H.parvus
H.ch.
N. taylorae
N.me.
N. yini
N.orienta
Pteruchipollenites -Lelotriletes
Leiospheeridia-Micrhystridium-Veryhachium
Barren
Dictyotidium
Meishan D
Beds
Lithology
Conodont Zone
Gondolellid zone
Hindeodid zone
Palynological assemblage zone
0m
-10m
-20m
-30m
-40m
-50m
30
29
27-28
25-26
23-24
22
21
20
19
17-18
16
15
14
13
12
11
10
9
8
6-7
5
4
2-3
1
I. isarcica
Lunatisporites -Ephedripites
I.st.
N.taylorae
H.parvus
H.ch.
N.me.
H.pr.
N.yini
H.la.
Vittatina-Protohaploxypinus
N. ch.-N. deflecta
N. wangi
N. orienta -N. lo.
Leiospheeridia changxingensis-Micrhystridium stellatum
Mudstone
Chert
Claystone
Siliceous mudstone
Carbon siliceous rocks
Muddy limestone
Siliceous limestone
Calcareous mudstone
Limestone
Banded siliceous limestone

Figure 4:

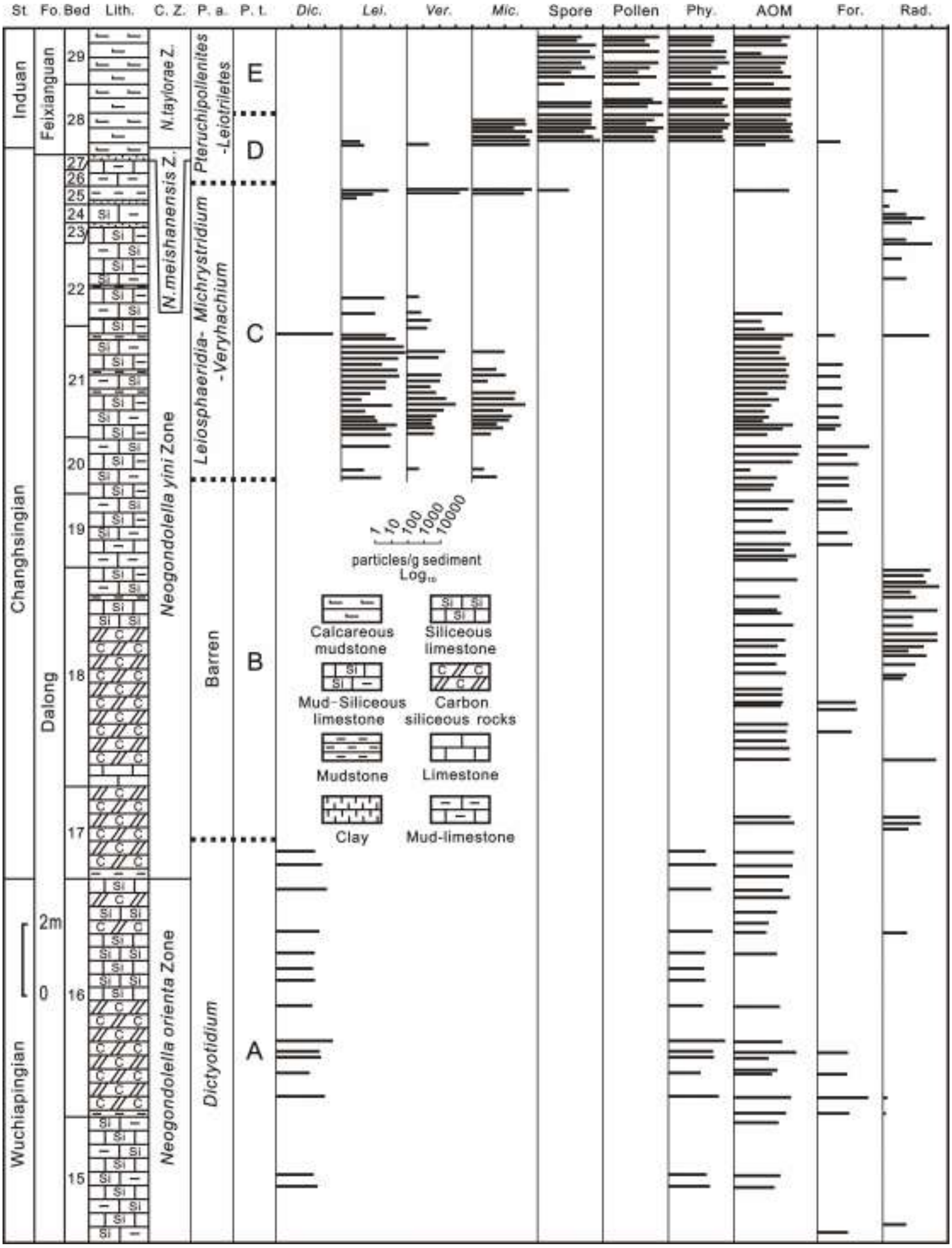
St.
Fo.
Bed
Lith.
C. Z.
P. a.
P. t.
Dic.
Lei.
Ver.
Mic.
Spore
Pollen
Phy.
AOM
For.
Rad.
Induan
Changhsingian
Wuchiapingian
Feixianguan
Dalong
2m
0
29
28
27
26
25
24
23
22
21
20
19
18
17
16
15
N.taylorae Z.
N.meishanensis Z.
Neogondolella yini Zone
Neogondolella orienta Zone
Pteruchipollenites -Leiotriletes
Leiosphaeridia- Michrystridium -Veryhachium
Barren
Dictyotidium
E
D
C
B
A
1
10
100
1000
10000
particles/g sediment
Log₁₀
Calcareous mudstone
Siliceous limestone
Mud-Siliceous limestone
Carbon siliceous rocks
Mudstone
Limestone
Clay
Mud-limestone
Si
C

Figure 5:

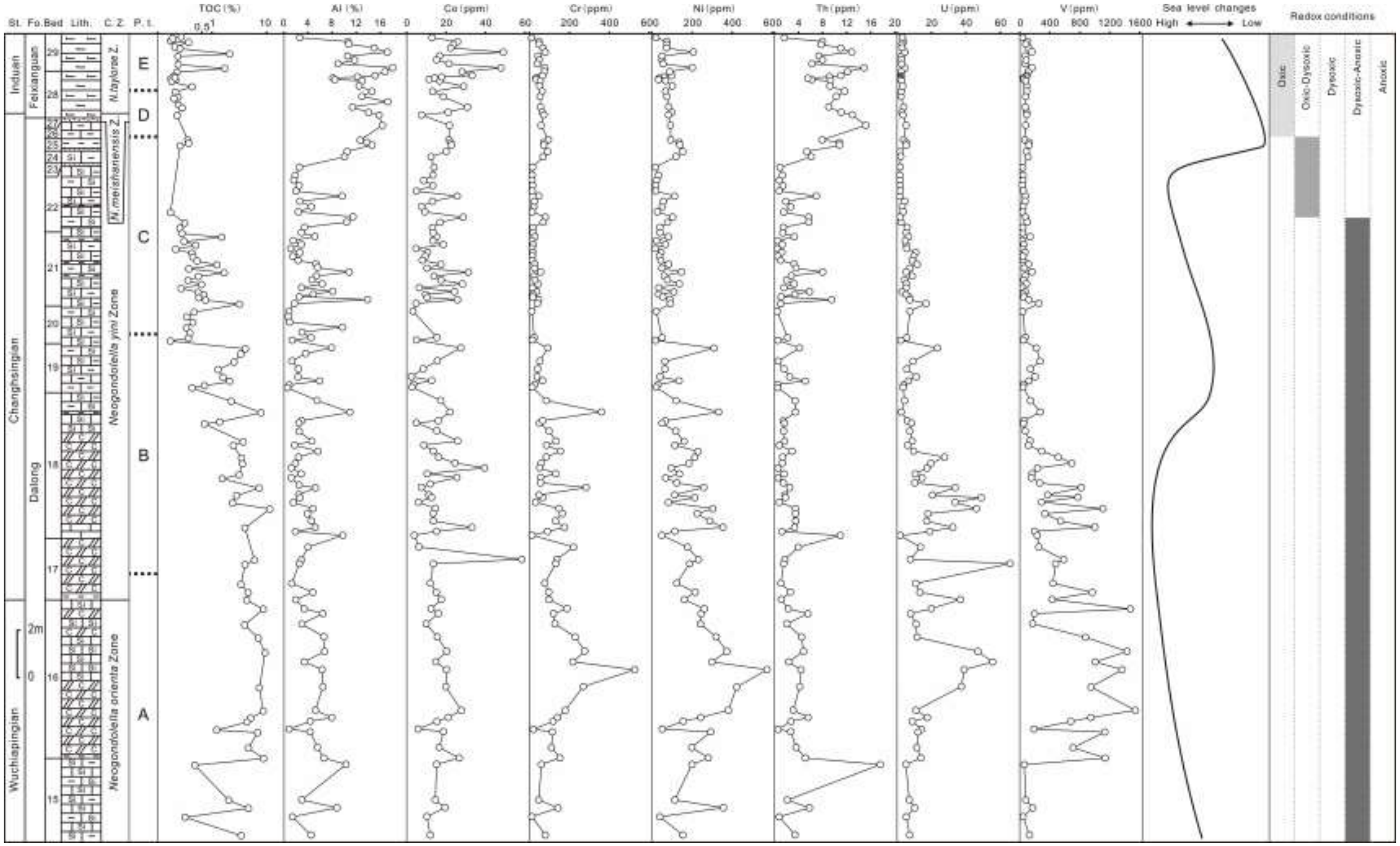
St.
Fo.
Bed
Lith.
C.Z.
P. I.
TOC (%)
0.5
1
10
Al (%)
0
4
8
12
16
Co (ppm)
0
20
40
60
Cr (ppm)
200
400
600
Ni (ppm)
200
400
600
Th (ppm)
4
8
12
16
20
U (ppm)
20
40
60
V (ppm)
0
400
800
1200
1600
Sea level changes
High
Low
Redox conditions
Oxic
Oxic-Dysoxic
Dysoxic
Dysoxic-Anoxic
Anoxic
Induan
Feixianguan
Changhsingian
Dalong
Wuchiapingian
29
28
27
26
25
24
23
22
21
20
19
18
17
16
15
Si
N.taylorae Z.
N.meishanensis Z.
Neogondolella yini Zone
Neogondolella orienta Zone
E
D
C
B
A
2m
0

Figure 6:

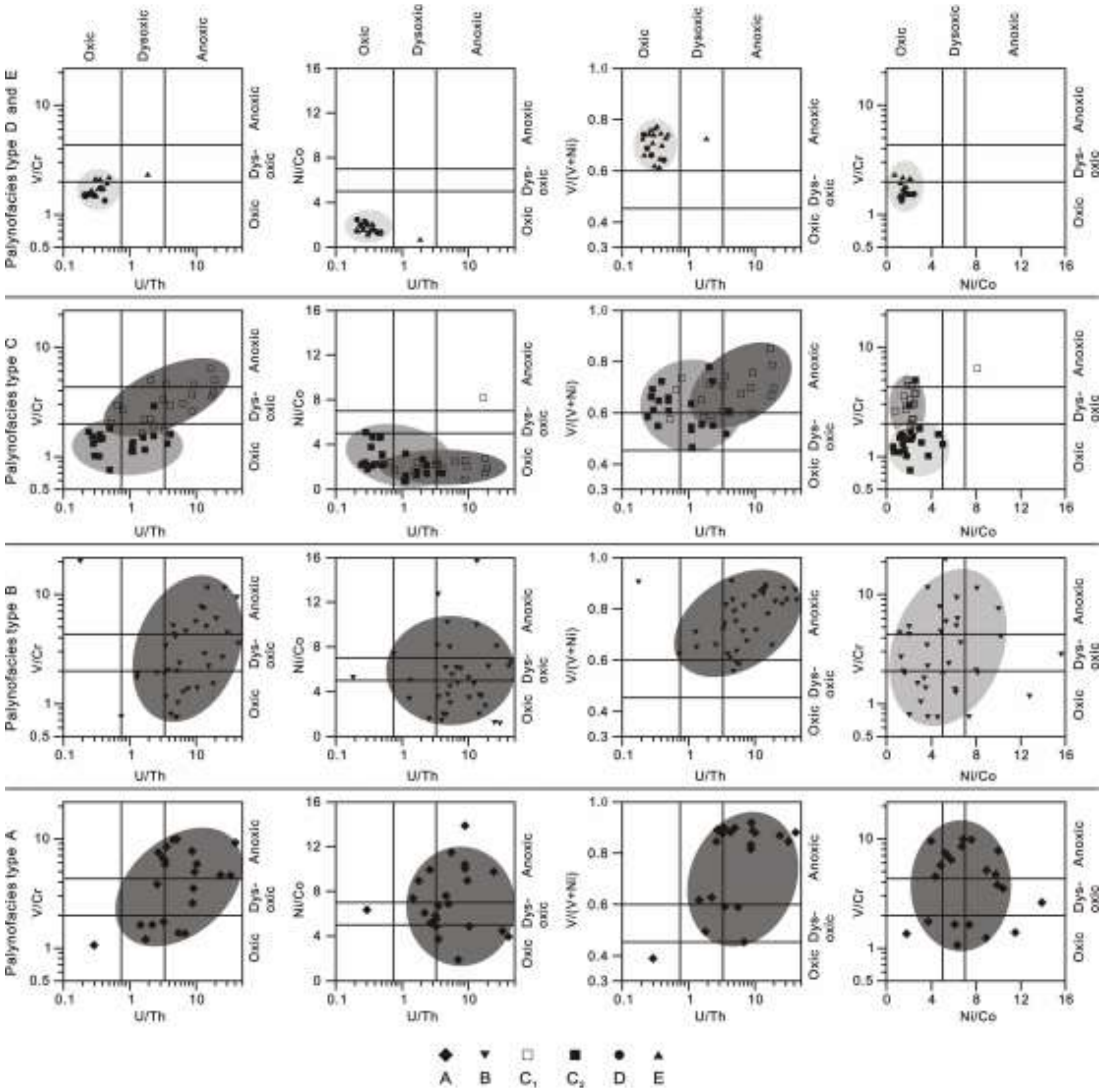
Palynofacies type D and E
Palynofacies type C
Palynofacies type B
Palynofacies type A
Oxic
Dysoxic
Anoxic
Dys-oxic
V/Cr
Ni/Co
V/(V+Ni)
U/Th
Ni/Co
0.1
1
10
0.5
0
4
8
12
16
0.3
0.4
0.6
0.8
1.0
A
B
C₁
C₂
D
E

Figure 7:

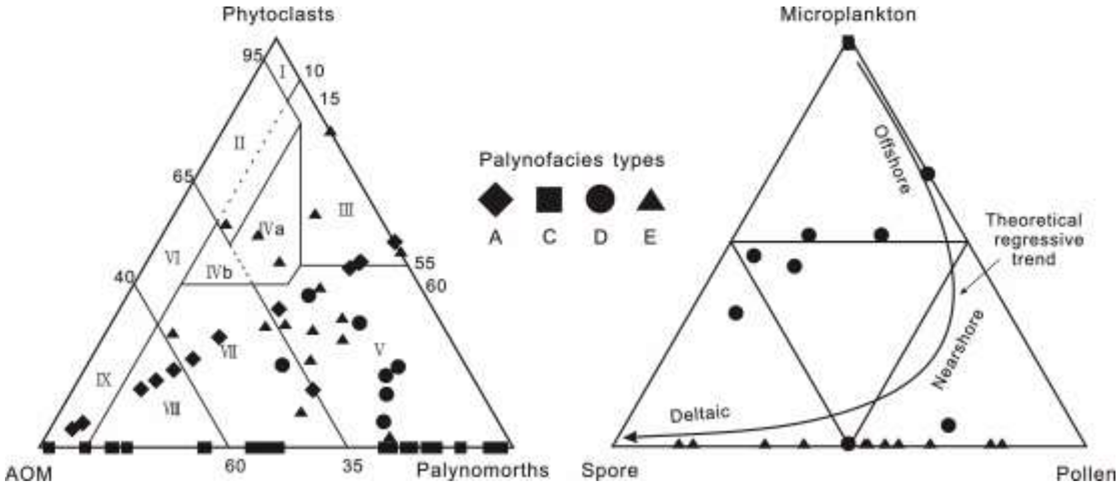

Table 1:

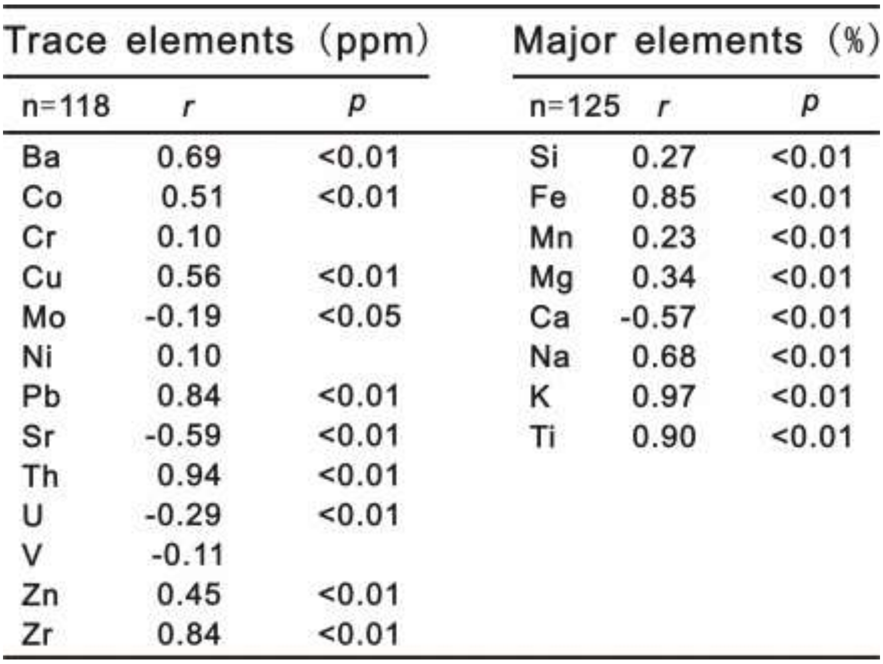

Trace elements (ppm)			Major elements (%)		
n=118	*r*	*p*	n=125	*r*	*p*
Ba	0.69	<0.01	Si	0.27	<0.01
Co	0.51	<0.01	Fe	0.85	<0.01
Cr	0.10		Mn	0.23	<0.01
Cu	0.56	<0.01	Mg	0.34	<0.01
Mo	-0.19	<0.05	Ca	-0.57	<0.01
Ni	0.10		Na	0.68	<0.01
Pb	0.84	<0.01	K	0.97	<0.01
Sr	-0.59	<0.01	Ti	0.90	<0.01
Th	0.94	<0.01			
U	-0.29	<0.01			
V	-0.11				
Zn	0.45	<0.01			
Zr	0.84	<0.01			

Table 2:

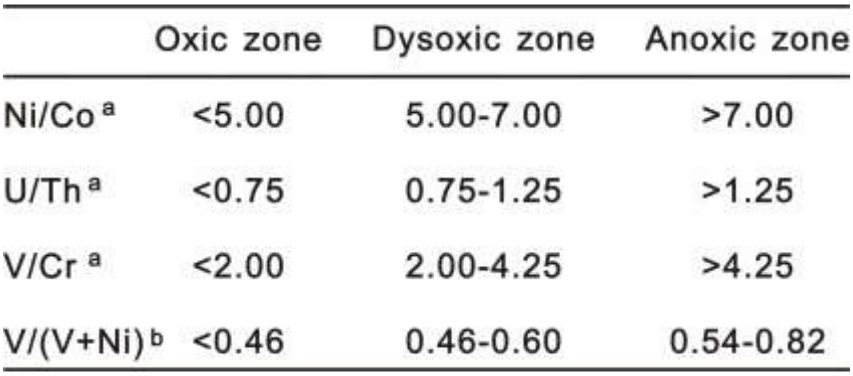

	Oxic zone	Dysoxic zone	Anoxic zone
Ni/Co[a]	<5.00	5.00-7.00	>7.00
U/Th[a]	<0.75	0.75-1.25	>1.25
V/Cr[a]	<2.00	2.00-4.25	>4.25
V/(V+Ni)[b]	<0.46	0.46-0.60	0.54-0.82

Table 3:

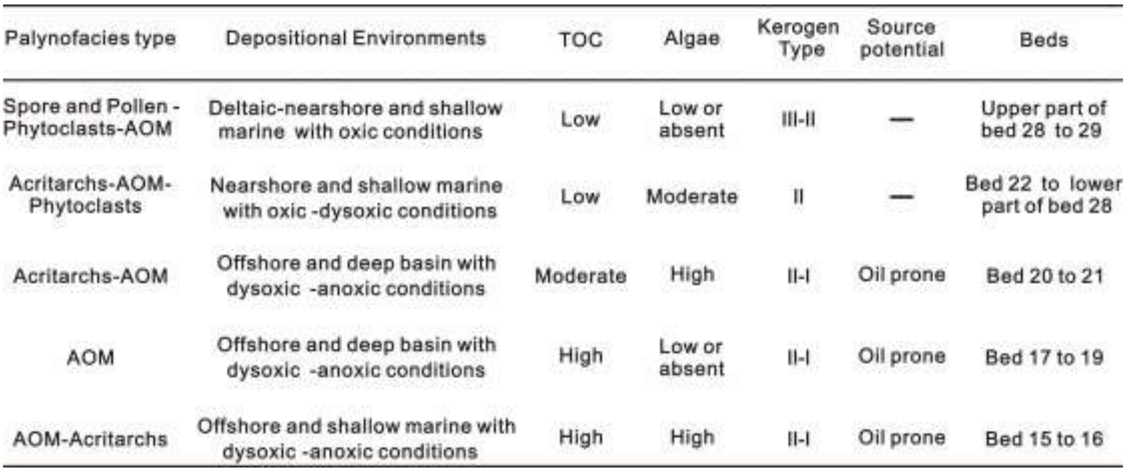

Palynofacies type	Depositional Environments	TOC	Algae	Kerogen Type	Source potential	Beds
Spore and Pollen - Phytoclasts-AOM	Deltaic-nearshore and shallow marine with oxic conditions	Low	Low or absent	III-II	—	Upper part of bed 28 to 29
Acritarchs-AOM-Phytoclasts	Nearshore and shallow marine with oxic -dysoxic conditions	Low	Moderate	II	—	Bed 22 to lower part of bed 28
Acritarchs-AOM	Offshore and deep basin with dysoxic -anoxic conditions	Moderate	High	II-I	Oil prone	Bed 20 to 21
AOM	Offshore and deep basin with dysoxic -anoxic conditions	High	Low or absent	II-I	Oil prone	Bed 17 to 19
AOM-Acritarchs	Offshore and shallow marine with dysoxic -anoxic conditions	High	High	II-I	Oil prone	Bed 15 to 16

Paper 3: (Section 3)

Lei, Y., Servais, T., Feng, Q.L., He, W.H. The spatial (nearshore-offshore) distribution of latest Permian phytoplankton from the Yangtze Block, South China. Palaeogeography, Palaeoclimatology, Palaeoecology. 2012. (363-364): 151-162.

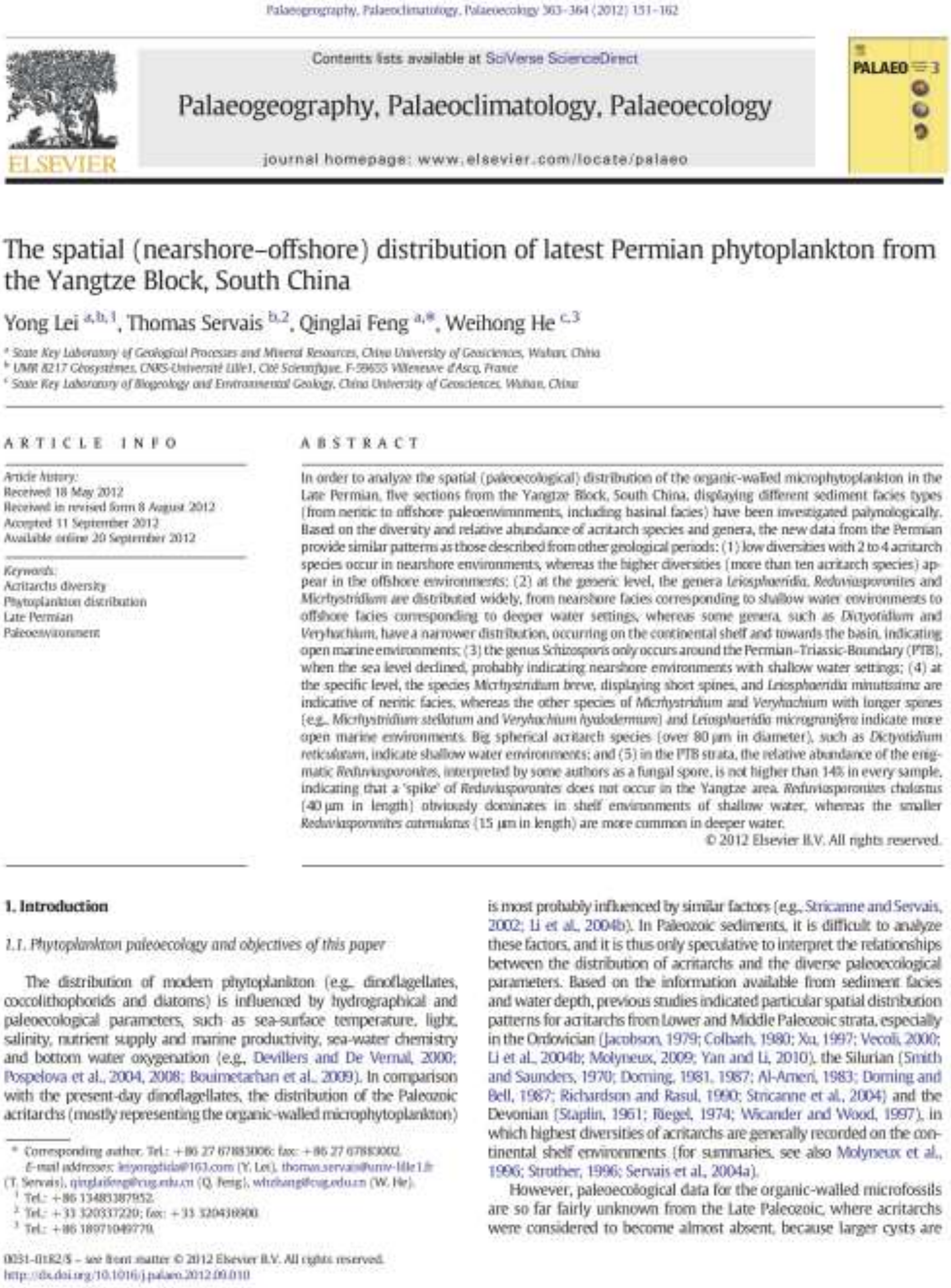

Palaeogeography, Palaeoclimatology, Palaeoecology 363–364 (2012) 151–162

Contents lists available at SciVerse ScienceDirect

Palaeogeography, Palaeoclimatology, Palaeoecology

journal homepage: www.elsevier.com/locate/palaeo

The spatial (nearshore–offshore) distribution of latest Permian phytoplankton from the Yangtze Block, South China

Yong Lei [a,b,1], Thomas Servais [b,2], Qinglai Feng [a,*], Weihong He [c,3]

[a] State Key Laboratory of Geological Processes and Mineral Resources, China University of Geosciences, Wuhan, China
[b] UMR 8217 Géosystèmes, CNRS-Université Lille1, Cité Scientifique, F-59655 Villeneuve d'Ascq, France
[c] State Key Laboratory of Biogeology and Environmental Geology, China University of Geosciences, Wuhan, China

ARTICLE INFO

Article history:
Received 18 May 2012
Received in revised form 8 August 2012
Accepted 11 September 2012
Available online 20 September 2012

Keywords:
Acritarchs diversity
Phytoplankton distribution
Late Permian
Paleoenvironment

ABSTRACT

In order to analyze the spatial (paleoecological) distribution of the organic-walled microphytoplankton in the Late Permian, five sections from the Yangtze Block, South China, displaying different sediment facies types (from neritic to offshore paleoenvironments, including basinal facies) have been investigated palynologically. Based on the diversity and relative abundance of acritarch species and genera, the new data from the Permian provide similar patterns as those described from other geological periods: (1) low diversities with 2 to 4 acritarch species occur in nearshore environments, whereas the higher diversities (more than ten acritarch species) appear in the offshore environments; (2) at the generic level, the genera *Leiosphaeridia*, *Reduviasporonites* and *Micrhystridium* are distributed widely, from nearshore facies corresponding to shallow water environments to offshore facies corresponding to deeper water settings, whereas some genera, such as *Dictyotidium* and *Veryhachium*, have a narrower distribution, occurring on the continental shelf and towards the basin, indicating open marine environments; (3) the genus *Schizosporis* only occurs around the Permian–Triassic-Boundary (PTB), when the sea level declined, probably indicating nearshore environments with shallow water settings; (4) at the specific level, the species *Micrhystridium breve*, displaying short spines, and *Leiosphaeridia minutissima* are indicative of neritic facies, whereas the other species of *Micrhystridium* and *Veryhachium* with longer spines (e.g., *Micrhystridium stellatum* and *Veryhachium hyalodermum*) and *Leiosphaeridia microgranifera* indicate more open marine environments. Big spherical acritarch species (over 80 μm in diameter), such as *Dictyotidium reticulatum*, indicate shallow water environments; and (5) in the PTB strata, the relative abundance of the enigmatic *Reduviasporonites*, interpreted by some authors as a fungal spore, is not higher than 14% in every sample, indicating that a 'spike' of *Reduviasporonites* does not occur in the Yangtze area. *Reduviasporonites chalastus* (40 μm in length) obviously dominates in shelf environments of shallow water, whereas the smaller *Reduviasporonites catenulatus* (15 μm in length) are more common in deeper water.

1. Introduction

1.1. Phytoplankton paleoecology and objectives of this paper

The distribution of modern phytoplankton (e.g., dinoflagellates, coccolithophorids and diatoms) is influenced by hydrographical and paleoecological parameters, such as sea-surface temperature, light, salinity, nutrient supply and marine productivity, sea-water chemistry and bottom water oxygenation (e.g., Devillers and De Vernal, 2000; Pospelova et al., 2004, 2008; Bouimetarhan et al., 2009). In comparison with the present-day dinoflagellates, the distribution of the Paleozoic acritarchs (mostly representing the organic-walled microphytoplankton) is most probably influenced by similar factors (e.g., Stricanne and Servais, 2002; Li et al., 2004b). In Paleozoic sediments, it is difficult to analyze these factors, and it is thus only speculative to interpret the relationships between the distribution of acritarchs and the diverse paleoecological parameters. Based on the information available from sediment facies and water depth, previous studies indicated particular spatial distribution patterns for acritarchs from Lower and Middle Paleozoic strata, especially in the Ordovician (Jacobson, 1979; Colbath, 1980; Xu, 1997; Vecoli, 2000; Li et al., 2004b; Molyneux, 2009; Yan and Li, 2010), the Silurian (Smith and Saunders, 1970; Dorning, 1981, 1987; Al-Ameri, 1983; Dorning and Bell, 1987; Richardson and Rasul, 1990; Stricanne et al., 2004) and the Devonian (Staplin, 1961; Riegel, 1974; Wicander and Wood, 1997), in which highest diversities of acritarchs are generally recorded on the continental shelf environments (for summaries, see also Molyneux et al., 1996; Strother, 1996; Servais et al., 2004a).

However, paleoecological data for the organic-walled microfossils are so far fairly unknown from the Late Paleozoic, where acritarchs were considered to become almost absent, because larger cysts are

---

[*] Corresponding author. Tel.: +86 27 67883006; fax: +86 27 67883002.
E-mail addresses: leiyongfida@163.com (Y. Lei), thomas.servais@univ-lille1.fr (T. Servais), qinglaifeng@cug.edu.cn (Q. Feng), whzhang@cug.edu.cn (W. He).
[1] Tel.: +86 13483387952.
[2] Tel.: +33 320337220; fax: +33 320436900.
[3] Tel.: +86 18971049779.

0031-0182/$ – see front matter © 2012 Elsevier B.V. All rights reserved.
http://dx.doi.org/10.1016/j.palaeo.2012.09.010

no longer observed in the fossil record. Riegel (1996, 2008), for example, named this Late Paleozoic interval with a virtual absence of organic-walled phytoplankton (after the Late Devonian acritarch 'extinction' and before the appearance of dinoflagellate cysts in the Triassic) the 'Phytoplankton Blackout'. However, although larger cysts appear to be virtually absent, numerous organic-walled microphytoplankton morphotypes exist during the Carboniferous and Permian. Mullins and Servais (2008) reviewed the diversity of the Carboniferous phytoplankton, and noted that phytoplankton diversity was still high in the earliest Carboniferous, but declined significantly from the Tournaisian to the Serpukhovian. Phytoplankton diversity in the Late Carboniferous was generally very low, with typically only 1–3 species being documented in each assemblage (Mullins and Servais, 2008). Regarding the Permian, Lei et al. (accepted for publication) reviewed the diversity of the phytoplankton of this geological period, based on a detailed literature revision of more than 100 publications focused on Permian phytoplanktonic studies. These authors pointed out that the phytoplankton diversities are much higher than previously assumed, with highest diversities in the Early Permian and the latest Permian, where over 30 phytoplankton genera have been reported.

The main objective of the present study is to understand the spatial distribution of the phytoplankton in the latest Permian, including the analyses of the diversity at the generic and specific levels, and of the relative abundance of the different taxa. The Yangtze Block, South China, represents an ideal key-area for such a study, because a detailed investigation of the phytoplankton from different facies (from neritic to offshore paleoenvironments including basinal facies) is possible due to the presence of well preserved assemblages from the same age interval.

1.2. Review of previous investigations on Precambrian and Paleozoic phytoplankton paleoecology

In the Neoproterozoic paleoecological studies on the organic-walled microfossils remain rare. However, Butterfield and Chandler (1992) recognized five phytoplankton zones from the Agu Bay Formation, Baffin Island, Arctic Canada, which were interpreted as corresponding to restricted nearshore to basinal environments. The authors concluded that: (1) in the nearshore restricted environments, the fossils are dominated by autochthonous filaments and small spheroids with low diversities; (2) in the nearshore unrestricted environments, the filaments and large acritarchs (>50 μm in diameter) are abundant with moderate to high diversities; (3) in the middle part of the shelf, corresponding to moderately deep environments (lower photic zone), moderately diverse assemblages of spherical acritarchs are present without substantially ornamented forms; (4) in the middle to outer shelf deep water environments (subphotic zone), a low taxonomic diversity is observed in assemblages dominated by moderately large to small spheroids (<50 μm in diameter); and (5) in the slope to basinal, turbiditic dominated environments, corresponding to deeper water settings, acritarchs are abundant, but generally of very low taxonomic diversity.

In the Cambrian and Ordovician, paleoecological interpretations are more abundant. Vecoli (2000) noted that the phytoplankton diversity and abundance from successions of the North Sahara Platform allow the proposal of several classes indicating different paleoenvironments. Vecoli (2000) concluded that the high dominance of the leiosphaerid–Netromorphitae and *Veryhachium* classes in low-diversity assemblages can be related to nearshore, shallow-marine conditions; the Polygonium–*Micrhystridium* class corresponds to low-diversity assemblages and seems generally indicative of restricted marine conditions.

Seven studies investigated the distribution of the organic-walled phytoplankton from Ordovician strata. In the Middle and Upper Ordovician of the Midcontinent, USA, Jacobson (1979) considered that a dominance of the "leiosphaerid class" corresponds to a nearshore, shallow marine environment; the "peteinosphaerid–*Dicommopalla* class" corresponds to a shoal environment; and the "baltisphaerid–veryhachid–*Polygonium*" class reflected an open marine environment. In the Upper Ordovician, Colbath (1980) identified two phytoplankton communities, and proposed a model of changing water masses to explain the abundance fluctuations from a core of the Eden Shale, Indiana, USA. In the Lower Ordovician of China, Xu (1997) noted that abundant acritarchs from the Dawan Formation, Yangtze Platform, South China, including *Striatotheca*, *Coryphidium*, *Pirea*, *Acanthodiacrodium*, *Dasydiacrodium* and *Arbusculidium filamentosum*, indicated a deep-water environment. The so far the most detailed study from the Lower–Middle Ordovician of the Yangtze Platform, South China, is that from Li et al. (2004b), who reported a continuous nearshore to offshore trend in acritarch distribution. The investigations of a selection of sections ranging from inshore to offshore settings indicated that the nearshore environments show low diversity assemblages with about 10 acritarch species, whereas the offshore shelf environments reflect higher diversities with about 40 species. In the same area, Yan and Li (2010) divided ten acritarch assemblages by using cluster and principal component analysis. They suggested that the acritarch assemblages and their distributions are controlled by environmental changes. In addition, they concluded that the *Stelliferidium* assemblage occurs in the inner shelf environments; the *Baltisphaeridium*–*Leiosphaeridia* assemblage, *Baltisphaeridium*–*Peteinosphaeridium* assemblage, *Cymatiogalea* assemblage, *Polygonium* assemblage and *Stelliferidium*–*Leiosphaeridia* assemblage indicated outer shelf environments, and the *Baltisphaeridium* assemblage, *Leiosphaeridia* assemblage, *Peteinosphaeridium* assemblage and *Rhopaliophora* assemblage inhabited the deep water shale basin environments.

Another detailed study of the paleoecology of Ordovician acritarchs from South China is that of Tongiorgi et al. (2003). These authors attempted to understand the compositional fluctuations of acritarch assemblages by using an interpretative model integrating the inshore–offshore trend and climate (temperature) through time. The model predicts that phytoplankton diversity increases from cold, proximate habitats, towards warmer, distal environments.

In the Early Ordovician (the Skiddaw Group, northern England), Molyneux (2009) concluded that in deep-water settings acritarch diversity parallels sea-level changes, with high diversities occurring during lowstands and low diversity during highstands. Molyneux (2009) also suggested that high acritarch diversities occur in offshore settings, and that low diversities are present in nearshore and basinal settings.

In Silurian strata, seven papers reported the spatial distribution of phytoplankton. Smith and Saunders (1970) summarized the relationship between acritarch distribution and sedimentary facies in a series of Silurian clastics representing several major depositional environments. They suggested that (1) the acritarchs are confined to depositional areas continuously or intermittently open to marine waters and do not occur in the fluvial deposits; (2) the degree of preservation reflects the depositional environment: forms from deeper open marine sediments are generally well preserved, while those in nearshore and transitional facies are usually fragmentary and degraded; and (3) acritarch distribution patterns are in part controlled by directions of prevailing currents. In the Welsh Borderland and Wales, United Kingdom, four studies analyzed acritarch distribution in some detail (Dorning, 1981, 1987; Dorning and Bell, 1987; Richardson and Rasul, 1990). Three acritarch assemblages (nearshore, offshore and deep water) were recognized by Dorning (1981). He concluded that 5–15 species were found in the nearshore assemblages; generally 25–60 species in offshore shelf assemblages; only 2–15 species in deep water assemblages. Subsequently, Dorning (1987) and Dorning and Bell (1987) recognized four acritarchs assemblages, including the *Leiosphaeridia wenlockia* Assemblage, the *Leiofusa tumida* Assemblage, the *Micrhystridium intonsurans* Assemblage and the *Salopidium granuliferum* Assemblage, which were attributed to reef limestone, shallow shelf carbonates, open shelf carbonates and deeper shelf environments, respectively. Richardson and Rasul (1990) considered that in their investigations acritarch, chitinozoan, and scolecodont associations indicated marine facies, while sporomorphs, micrhystrids and tasmanitids present environments near the shoreline. In the Rhadames Basin, Libya, Al-Ameri (1983) analyzed the acid-resistant microfossils and used them to determinate different paleoenvironments. He suggested that the tasmanitids may indicate a lagoonal environment, and that the peak of the acritarch species *Veryhachium lairdi* occurs in the transitional boundary between intermediate and lagoonal settings. Stricanne et al. (2004) analyzed both qualitatively and quantitatively the acritarch distribution along an inshore–offshore transect in the Ludlow of the Silurian of Gotland, Sweden. They noted paleoecological changes at three different levels: a suprageneric level (acanthomorphic acritarchs increase towards the shelf but sphaeromorphs decrease), a generic level (the acritarchs *Micrhystridium* and *Dilatisphaera* are abundant in the proximal facies, while *Evittia*, *Percultisphaera* and Oppilatala are common in distal environments), and a specific level (*Micrhystridium* morphotypes tend to present longer and more complex processes towards the shelf).

Three papers investigated the distribution of phytoplankton in the Devonian. Based on studies from Alberta, Canada, Staplin (1961) was the first who 50 years ago already noted acritarch abundance changes in relation to the distance from reefs. Spherical forms were considered widespread, the thin-spined species are widespread but more common near the reefs, while the thick-spined and polyhedral forms were considered only abundant in off-reef strata. In the Lower and Middle Devonian rocks of western Germany, Riegel (1974) reported that the neritic facies is connected with poor phytoplankton assemblages, whereas the pelagic facies generally produced abundant and diversified phytoplankton. In the Rapid Member of the Cedar Valley Formation, Iowa, Wicander and Wood (1997) investigated the fluctuations in the microphytoplankton and analyzed the relative percentage of palynomorphs in the microphytoplankton/spore assemblages. They suggested that the dominance of microphytoplankton compared to spores reflects an inshore–offshore trend, with higher abundances of acritarchs indicating normal-marine near to offshore environments.

Few studies discuss acritarch paleoecology in post-Paleozoic strata. In the Jurassic of England and South Wales, Wall (1965) concluded that acritarch distribution was controlled by environmental changes: in the inshore settings with enclosed environments, the assemblages were composed of acanthomorphic acritarchs (*Micrhystridium* and *Baltisphaeridium*), whereas in the open sea the assemblages were dominated by the taxa *Veryhachium*, *Leiofusa*, *Metaleiofusa* and *Domasia*.

2. Geological setting of the Yangtze Platform at latest Permian

For the present study, five geological sections have been analyzed. They are all located in southern China, corresponding to the Yangtze Block, and are located in the Guizhou, Zhejiang, Sichuan, Hubei and Guangxi Provinces (Fig. 1). The sections correspond to different paleogeographical and paleoenvironmental settings, from near-shore shallow-water to deeper water and slope environments (Figs. 2, 3), and they all cover the Latest Permian to Earliest Triassic interval, including the Permian–Triassic boundary (PTB) (Fig. 4).

2.1. Zhongzhai section

The Zhongzhai section (26°09.110N and 105°17.113E) is located approximately 150 km WSW of Guiyang and 25 km SW of Liuzhi County, in the western Guizhou Province (Fig. 1) (Metcalfe and Nicoll, 2007). It is located in the terrestrial to neritic transitional facies in the west of the Yangtze Block (Figs. 2, 3) (Peng et al., 2005; Metcalfe and Nicoll, 2007; He et al., 2008). This section comprises the uppermost Longtan Formation (bed 1 to bed 27) and the lowermost Yelang Formation (bed 28 to bed 37) (Fig. 4). The Longtan Formation displays brownish sandstones and mudstones with a few limestone intervals, containing brachiopods, bivalves, gastropods,

Fig. 1. Location of the five investigated sections from the Yangtze Block, South China (Zhongzhai, Meishan, Shangsi, Xiakou and Dongpan sections).

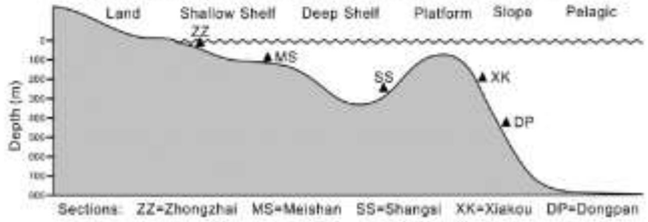

Fig. 2. Estimated water depth and sedimentary facies during the PTB of the five investigated sections from the Yangtze Block, South China (Zhongzhai, Meishan, Shangsi, Xiakou and Dongpan sections).

ostracods and cephalopods (He et al., 2008). The lowermost Yelang Formation comprises yellowish green or purplish red silty calcareous mudstones, and a few limestones and claystones at the base of the formation, containing lingulid brachiopods and abundant bivalves (Gao et al., 2009; He et al., 2008). According to the conodont biozonation, Metcalfe and Nicoll (2007) suggested that the PTB at the Zhongzhai section is located in bed 30. In addition, based on the U–Pb dates, the absolute age determination from the claystone of bed 29 by Shen et al. (2011b) indicated an age of 252.24 ± 0.13 Ma.

2.2. *Meishan section*

The Meishan section (31°03 N and 119°54E) is located about 25 km northwest of the Changxing County, in the Zhejiang Province (Fig. 1). This section has been accepted as the Global Stratotype Section and Point (GSSP) for the PTB in 2001, with the boundary marked by the first appearance datum (FAD) of *Hindeodus parvus*, at the base of bed 27c in Section D (Yin et al., 2001; Jiang et al., 2007; Zhang et al., 2007). This stratotype section is located in an intra-platform depression between the uplift and the platform, mostly in the range of 30 to 60 m depth during the PTB (Yin et al., 2001) (Figs. 2 and 3). The Meishan section displays the Changxing Formation (bed 22 to bed 24) and the Yinkeng Formation (bed 25 to bed 30). The uppermost Changxing Formation comprises limestones with a few mudstones. The lowermost Yinkeng Formation is dominated by muddy limestones and limestones with a few mudstone and claystone intervals (Fig. 4). Based on the U–Pb dates, the absolute age determined from the claystones of bed 25 and bed 28 by Shen et al. (2011b) indicated an age of 252.28 ± 0.08 Ma and 252.10 ± 0.06 Ma, respectively.

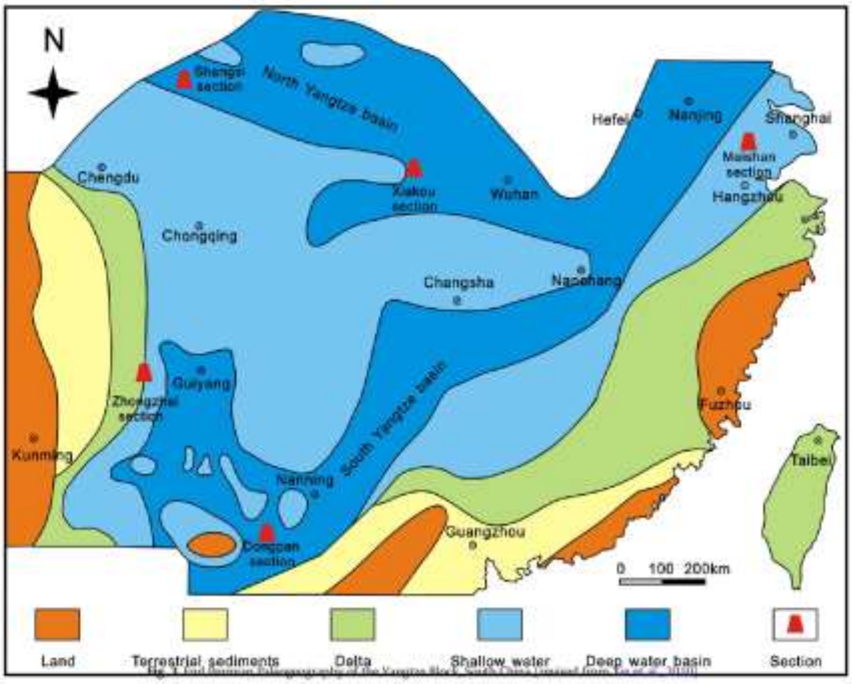

Fig. 1. End Permian Palaeogeography of the Yangtze Block, South China (revised from [illegible] et al., 2010).

Y. Lei et al. / Palaeogeography, Palaeoclimatology, Palaeoecology 363–364 (2012) 151–162 155

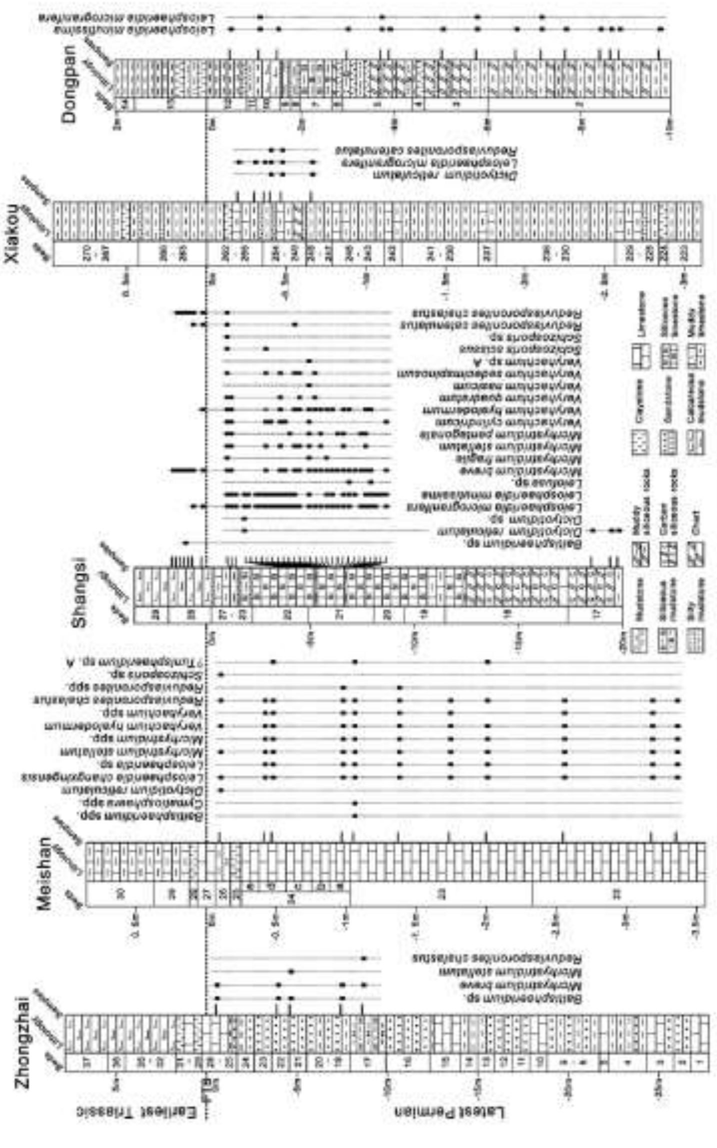

Fig. 4. Stratigraphical sequences, biostratigraphy and phytoplankton distribution in the five investigated sections.

Table 1
Relative abundances (in percentages) of individual acritarch species in all investigated samples from the five analyzed sections.

Species/samples (%)	Shangsi section	TS28b-10	TS28b-11	TS28b-13	TS28b-14	TS28a-16	TS28a-17	TS28a-18	ps-25e	ps-25c	ps-25a	ss293-6	ss293-3	ss292-12	ss292-6	ss292-4	ss292-2	ss292-1	ss291-7	ss291-6	ss291-5
Baltisphaeridium sp.				7.0																	
Dictyotidium reticulatum																65.4					
Dictyotidium sp.																10.9					
Leiofusa sp.																					
Leiosphaeridia microgranifera							0.8	1.1	8.4	3.0	100.0	72.9	62.8			11.6	42.1	33.3	29.6	40.5	28.3
Leiosphaeridia minutissima									2.5	0.4		26.3	32.9			12.1	57.9	66.5	70.4	57.6	70.4
Micrhystridium breve		100.0	99.1	88.0	97.8	94.3	72.4	72.3	43.9	50.7										0.2	
Micrhystridium fragile									1.2	0.0											
Micrhystridium pentagonale									2.3	0.4											
Micrhystridium stellatum									3.2	0.5										0.4	
Reduviasporonites catenulatus						1.8	6.4	3.5													
Reduviasporonites chalastus			0.9	5.0	2.2	3.8	20.4	22.1	1.2												
Schizosporis sp.									0.7											0.1	
Schizosporis scissus									0.5												
Veryhachium cylindricum									1.2	7.9										0.3	1.3
Veryhachium hyalodermum								1.0	30.9	25.2			4.3	100.0						0.4	
Veryhachium nasicum									2.3	5.9											
Veryhachium quadratum																					
Veryhachium sedecimspinosum									1.7			0.8			100.0					0.5	
Veryhachium sp. A																					

Species/samples (%)	Zhongzhai section	ZZ-27-6	ZZ-22-3	ZZ-22-2	ZZ-20-1	ZZ-10-3	Average	Xiakou section	257-2	250	254-2	254-1	252	248-2	Average	Dongpan section
Baltisphaeridium sp.		42.6	25.3	85.7	25.0		35.7									
Dictyotidium reticulatum												37.0	34.2	42.9	19.0	
Leiosphaeridia microgranifera									100.0	100.0	100.0	46.9	41.9	57.1	74.3	
Leiosphaeridia minutissima																
Micrhystridium breve		57.4	74.7		75.0	85.7	58.6									
Micrhystridium stellatum				14.3			2.9									
Reduviasporonites catenulatus												16.1	23.8		6.7	
Reduviasporonites chalastus						14.3			2.9							
Schizosporis sp.																
Veryhachium hyalodermum																

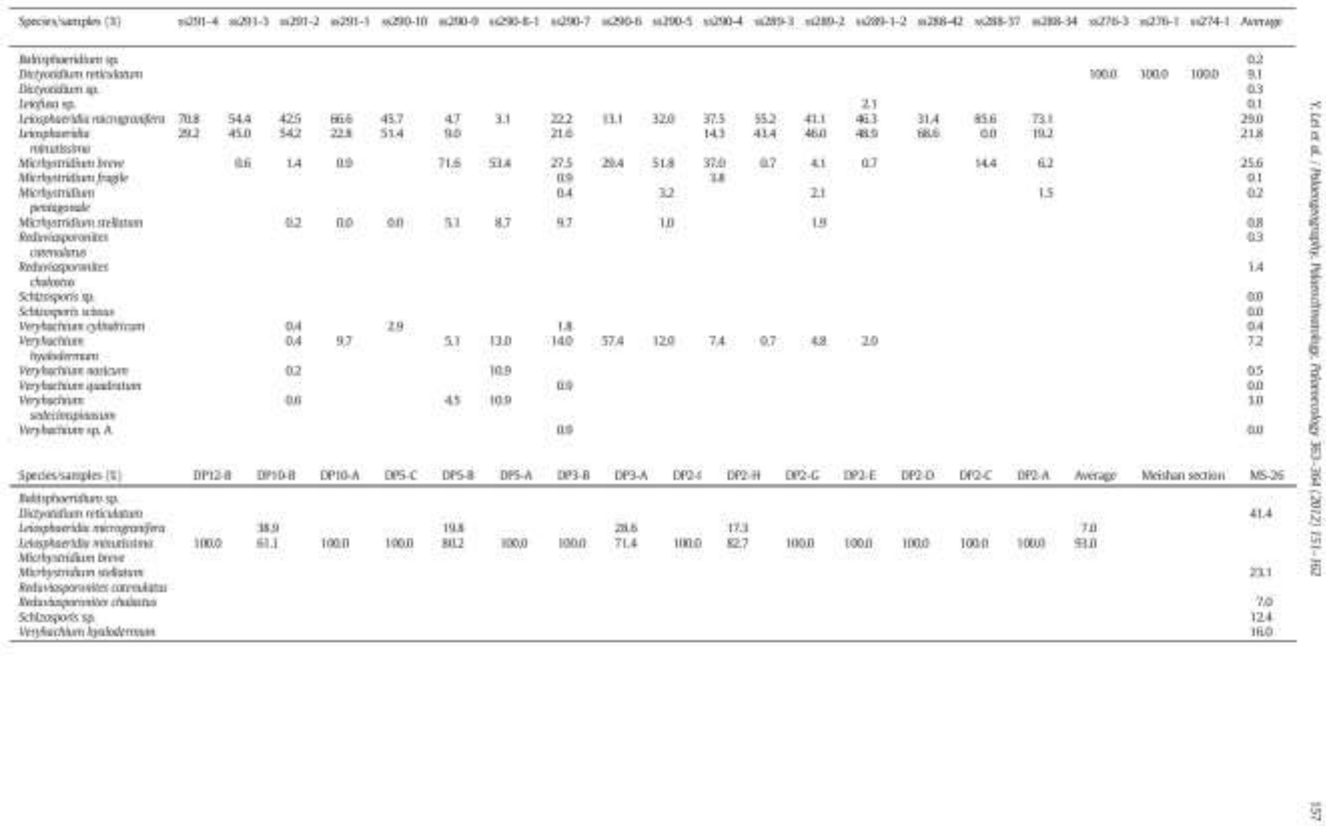

Species/samples (%)	ss291-4	ss291-3	ss291-2	ss291-1	ss290-10	ss290-9	ss290-8-1	ss290-7	ss290-6	ss290-5	ss290-4	ss289-3	ss289-2	ss289-1-2	ss288-42	ss288-37	ss288-34	ss276-3	ss276-1	ss274-1	Average
Baltisphaeridium sp.																					0.2
Dictyotidium reticulatum																		100.0	100.0	100.0	9.1
Dictyotidium sp.																					0.3
Leiofusa sp.														2.1							0.1
Leiosphaeridia microgranifera	70.8	54.4	42.5	66.6	45.7	4.7	3.1	22.2	13.1	32.0	37.5	55.2	41.1	46.3	31.4	85.6	73.1				29.0
Leiosphaeridia minutissima	29.2	45.0	54.2	22.8	51.4	9.0		21.6			14.3	43.4	46.0	48.9	68.6	0.0	19.2				21.8
Micrhystridium breve		0.6	1.4	0.9		71.6	53.4	27.5	29.4	51.8	37.0	0.7	4.1	0.7		14.4	6.2				25.6
Micrhystridium fragile								0.9			3.8										0.1
Micrhystridium pentagonale								0.4		3.2			2.1				1.5				0.2
Micrhystridium stellatum			0.2	0.0	0.0	5.1	8.7	9.7		1.0			1.9								0.8
Reduviasporonites catenulatus																					0.3
Reduviasporonites chalastus																					1.4
Schizosporis sp.																					0.0
Schizosporis scissus																					0.0
Veryhachium cylindricum			0.4		2.9			1.8													0.4
Veryhachium hyalodermum			0.4	9.7		5.1	13.0	14.0	57.4	12.0	7.4	0.7	4.8	2.0							7.2
Veryhachium nasicum			0.2				10.9														0.5
Veryhachium quadratum								0.9													0.0
Veryhachium sedecimspinosum			0.6			4.5	10.9														3.0
Veryhachium sp. A								0.9													0.0

Species/samples (%)	DP12-B	DP10-B	DP10-A	DP5-C	DP5-B	DP5-A	DP3-B	DP3-A	DP2-I	DP2-H	DP2-G	DP2-E	DP2-D	DP2-C	DP2-A	Average	Meishan section	MS-26
Baltisphaeridium sp.																		
Dictyotidium reticulatum																		41.4
Leiosphaeridia microgranifera		38.9			19.8			28.6		17.3						7.0		
Leiosphaeridia minutissima	100.0	61.1	100.0	100.0	80.2	100.0	100.0	71.4	100.0	82.7	100.0	100.0	100.0	100.0	100.0	93.0		
Micrhystridium breve																		
Micrhystridium stellatum																		23.1
Reduviasporonites catenulatus																		
Reduviasporonites chalastus																		7.0
Schizosporis sp.																		12.4
Veryhachium hyalodermum																		16.0

2.3. *Shangsi section*

The Shangsi section is located near Guangyuan city in the northern Sichuan Province, in the northwestern margin of the Upper Yangtze Block (Figs. 1 and 3) (Wignall et al., 1995; Lai et al., 1996). The Shangsi section comprises the Dalong Formation (Wuchiapingian to Changhsingian) and the Feixianguan Formation (Induan). The geology of the Shangsi section was first described in detail by Li et al. (1986). The beds 17 to 22 comprise an alternation of carbonaceous and siliceous rocks and siliceous limestones with a few mudstone intervals, containing radiolarians, bivalves, brachiopods and ammonites. Beds 23 to 29 comprise siliceous mudstones and calcareous mudstones with few claystones, containing abundant ammonites (Fig. 4). The facies of this section changed dramatically from a basinal (Dalong Formation) to a neritic environment (Feixianguan Formation) (Li et al., 1986). The precise location of the PTB in the Shangsi section is still debated. According to the first occurrence of *Hindeodus parvus*, the PTB has to be placed within bed 30, over 4 m above the mass extinction level (Li et al., 1986; Wignall et al., 1995; Lai et al., 1996; Nicoll et al., 2002; Jiang et al., 2011). However, Jiang et al. (2011) suggested that the PTB is placed 22 cm above the base of bed 28, based on hindeodid and gondolellid conodont taxa. Recently, new U–Pb data indicate an absolute age of 252.28 ± 0.13 Ma, determined from the claystone of bed 27 (in the present paper) by Shen et al. (2011b).

2.4. *Xiakou section*

The Xiakou section (31°06.874N and 110°48.221E) is located near Xiakou town, in Xingshan County, Yichang city, Hubei Province (Fig. 1). This area corresponds to the north of the central Yangtze Block (Wang and Xia, 2004) (Fig. 3). The section includes the Changxing and Daye formations. The uppermost Changxing Formation (bed 223 to bed 256) is composed of thin-bedded mudstones and muddy limestones. The lowermost Daye Formation (bed 257 to bed 270) is dominated by mudstones with a few claystones (Fig. 4). Both formations indicate an open continental-shelf sedimentary environment (Wang, 1998; Wang and Xia, 2004) (Fig. 2). According to the new conodont zonation, the PTB is placed in bed 262 (Shen et al., in press), rather than in bed 266 (Wang and Xia, 2004; Hong et al., 2008, 2011).

2.5. *Dongpan section*

The Dongpan section (22° 16.196N and 107° 41.505E) (Shen et al., 2011a), is situated 80 km southwest of Nanning, Guangxi Province, in the southern part of the Yangtze Block (He et al., 2007b) (Figs. 1, 3). This section comprises the Dalong (beds 2 to 12) and Luolou Formations (beds 13 to 14) (Fig. 4). According to Feng et al. (2007), beds 2 to 8 are mainly composed of bedded siliceous rocks, muddy siliceous rocks and mudstones, containing bivalves, brachiopods, gastropods, ostracods, and radiolarians. Beds 9 to 14 are dominated by mudstones and silty mudstones with thin intercalations of claystones, containing a few ammonoids, foraminifers, and radiolarians. Feng et al. (2007) considered that the Dalong Formation was deposited in slope to basin environments (Fig. 2). In addition, based on the abundance of the deepwater radiolarian *Albaillella*, bed 5 indicates a water depth of nearly 500 m (He et al., 2005). According to the distribution of the bivalves and ammonoids, He et al. (2005, 2007a,b) and Feng et al. (2007), suggested that the PTB in the Dongpan section should be located between bed 12 and bed 13.

3. Materials and methods

270 samples have been collected from the five sections (45 samples from the Zhongzhai section; 141 samples from the Shangsi section; 60 samples from the Xiakou; 23 samples from the Dongpan section; one sample from the Meishan section). All the samples were analyzed for palynological studies.

Fifty grams of each sample were prepared following standard palynological techniques. After treatment with hydrochloric acid (33%) and hydrofluoric acid (40%), the samples have been subsequently concentrated with zinc bromide solution (S.G. 2.2). Known amounts of *Lycopodium* spores were added during the process in order to allow calculation of absolute particle abundances, following standard counting techniques (Tyson and Follows, 2000). The samples were neither oxidized nor sieved. The residue was studied using light microscopy and scanning electron microscopy. The phytoplankton taxa were determined at the generic and the specific level. All palynological slides are stored in the collections of the China University of Geosciences (Wuhan).

4. Results

The present investigation indicates that diverse and abundant phytoplankton occurs in different paleoenvironmental settings from the latest Permian of the Yangtze Block, South China (Fig. 4). The relative abundance of the phytoplankton species in each of the sections is presented in Table 1.

In the Shangsi section, about 20 species corresponding to 8 genera have been recorded in the 37 samples investigated. They include *Baltisphaeridium* sp., *Dictyotidium reticulatum*, *Dictyotidium* sp., *Leiofusa* sp., *Leiosphaeridia microgranifera*, *Leiosphaeridia minutissima*, *Micrhystridium breve*, *Micrhystridium fragile*, *Micrhystridium pentagonale*, *Micrhystridium stellatum*, *Reduviasporonites catenulatus*, *Reduviasporonites chalastus*, *Schizosporis scissus*, *Schizosporis* sp., *Veryhachium cylindricum*, *Veryhachium hyalodermum*, *Veryhachium nasicum*, *Veryhachium quadratum*, *Veryhachium sedecimspinosum* and *Veryhachium* sp. A. As indicated in Table 1, the genus *Leiosphaeridia* (50.8%) is the most common, followed by *Micrhystridium* (26.8%) and *Veryhachium* (11.1%). At the species level, the acritarchs of the Shangsi section are clearly dominated by *L. microgranifera*, *L. minutissima* and *M. breve*. *D. reticulatum* and *V. hyalodermum* are also common.

In the Meishan section, Ouyang and Utting (1990) and Li et al. (2004a) reported nine phytoplankton genera (*Baltisphaeridium*, *Cymatiosphaera*, *Dictyotidium*, *Leiosphaeridia*, *Micrhystridium*, *Veryhachium*, *Reduviasporonites*, *Schizosporis* and ?*Tunisphaeridium*). In the present study, five phytoplankton species occur in bed 26, including *Dictyotidium reticulatum* (41.4%), *Micrhystridium stellatum* (23.1%), *Veryhachium hyalodermum* (16.0%), *Reduviasporonites chalastus* (7.0%) and *Schizosporis* sp. (12.4%).

In the Zhongzhai and Xiakou sections, only a few species occur in several samples, including *Baltisphaeridium* sp., *Dictyotidium reticulatum*, *Leiosphaeridia microgranifera*, *Micrhystridium breve*, *Micrhystridium stellatum*, *Reduviasporonites catenulatus* and *Reduviasporonites chalastus*. Interestingly, *M. breve* (58.6%) is the most common species in the Zhongzhai section, whereas *L. microgranifera* (74.3%) is clearly dominant in the Xiakou section. In the Dongpan section, only two species of *Leiosphaeridia* are found, however, they are abundantly present in fifteen samples (Fig. 4).

5. Discussion

5.1. *Phytoplankton distribution changes in the latest Permian of the Yangtze Block, south China*

Similar to previous studies on acritarch paleoecology from the Paleozoic, the phytoplankton distribution changes from the nearshore–offshore transect of the Yangtze Block are here interpreted in relation to the changing paleoecology. The paleoecological distribution is analyzed in terms of diversity (at the generic and specific level) and of relative abundance.

5.2. Spatial distribution of phytoplankton in terms of diversity of taxa

Previous studies (Figs. 2 and 3) indicated that in the western part of the Yangtze Block the Zhongzhai section is located in the terrestrial to neritic transitional facies (Peng et al., 2005; Metcalfe and Nicoll, 2007; He et al., 2008), while in the southern part of the Yangtze Block, according to He et al. (2005) and Feng et al. (2007), the Dongpan section was deposited in slope to basinal environments. In addition, based on the abundance of the deepwater radiolarian *Albaillella*, bed 5 was interpreted as indicating water depths of about 500 m (He et al., 2005). In the eastern part of the Yangtze Block, the Meishan section is located in an intra-platform depression between the uplift and the platform (Yin et al., 2001), whereas in the northern part of the Yangtze Block the Shangsi section was deposited in deep-water with offshore settings during the latest Permian (Li et al., 1986). Finally, the Xiakou section was deposited in open continental-shelf with offshore settings (Wang, 1998; Wang and Xia, 2004).

In order to understand the different paleoenvironments more easily and to interpret the spatial distribution of the phytoplankton taxa, the five sections have been tentatively placed in a nearshore–offshore transect in Figs. 5 and 6.

Both the nearshore environments of the Zhongzhai section and the basinal facies of the Dongpan section indicate low diversities of only 2 to 4 acritarch species distributed in 1 to 3 genera (Fig. 5). However, in the offshore environments, the platform (Meishan section) and the basinal (Shangsi section) facies show much higher phytoplankton diversities with up to 20 acritarch species in up to 9 genera (Fig. 5). In addition, far from the shore and thus from terrestrial input, the offshore settings in deeper water environments (Xiakou section) show a very low diversity of phytoplankton.

The present investigation thus confirms the distribution trends that have been reported in previous studies (Riegel, 1974; Dorning, 1981; Butterfield and Chandler, 1992; Wicander and Wood, 1997; Vecoli, 2000; Li et al., 2004b). For example, Dorning (1981) and Li et al. (2004b) counted only about 10 acritarch species in nearshore environments, but generally 25 to 60 species in offshore settings. These numbers have to be placed in the context of a much higher diversity in the Ordovician and Silurian, with over 400 acritarch species being reported in the different Ordovician periods (Servais et al., 2008), for example, whereas no more than 100 acritarch species in about 40 genera were documented for the entire Late Permian (Lei et al., accepted for publication).

At a qualitative level, it is interesting to analyze the distribution of several individual taxa. At the generic level, for example, some genera appear occasionally, such as *Cymatiosphaera*, *Leiofusa* and ? *Tunisphaeridium*. Other genera, such as *Leiosphaeridia*, *Reduviasporonites* and *Micrhystridium*, are distributed more widely, from the nearshore environments with shallow water settings to offshore environments in deeper water. The genera *Dictyotidium* and *Veryhachium* have narrower distributions, as they occur on the shelf and towards the basin, indicating an open marine environment. The genus *Schizosporis* only occurs around the PTB of the Shangsi and Meishan sections (Fig. 4) in levels when the sea level declined, probably indicating nearshore settings with shallower waters.

5.3. Spatial distribution of phytoplankton at the level of relative abundance of species

In Permian strata, the species of *Micrhystridium* and *Veryhachium* were reported most frequently (Servais et al., 2007; Lei et al., accepted for publication). In the present study, over ten species of these two genera were reported, representing nearly one half of all species occurring in the Late Permian of southern China. Interestingly, the species *Micrhystridium breve* (displaying short spines) is obviously dominant in the Zhongzhai section and around the PTB of the Shangsi section (Figs. 4 and 6), indicating neritic facies, whereas the

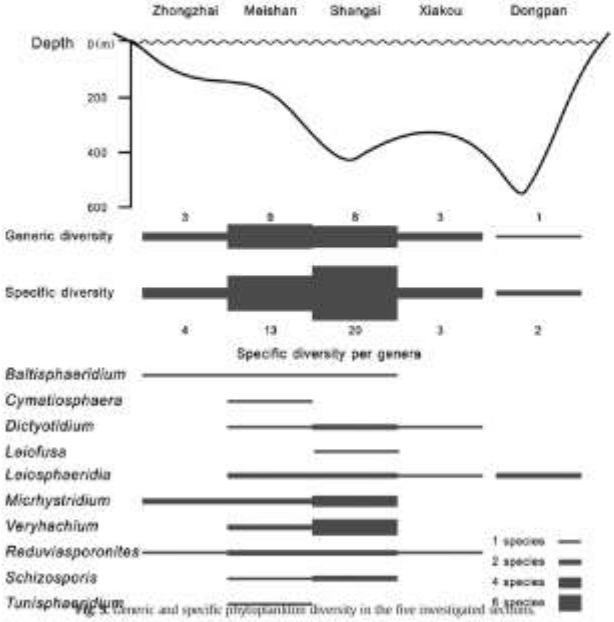

Fig. 5. Generic and specific phytoplankton diversity in the five investigated sections.

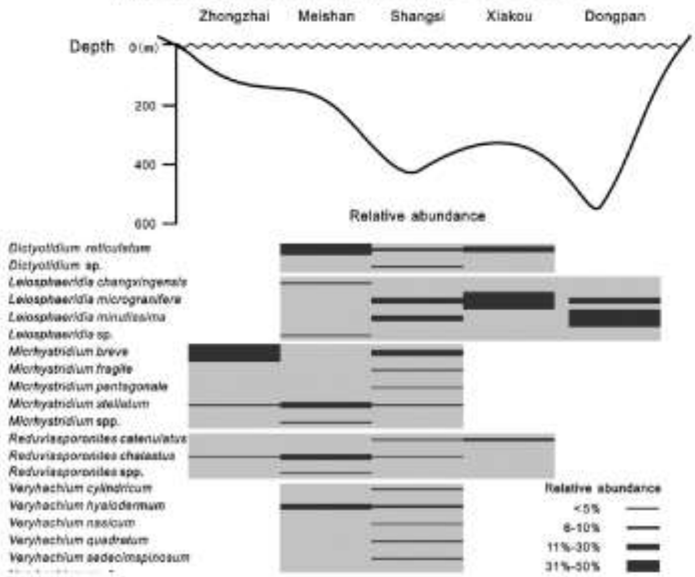

Fig. 6. Relative abundance of phytoplankton species in the five investigated sections.

other species of *Micrhystridium* and *Veryhachium* with longer spines (e.g. *Micrhystridium stellatum* and *Veryhachium hyalodermum*) are generally common in the Meishan and Shangsi sections (Figs. 4 and 6), showing a clearly open marine environment. This observation is thus similar to the results of other authors (Wall, 1965; Jacobson, 1979; Al-Ameri, 1983; Dorning, 1987; Richardson and Rasul, 1990; Vecoli, 2000; Li et al., 2004a; Stricanne et al., 2004; Servais et al., 2007) and in particular with the study of Stricanne et al. (2004), who observed a change in the relative abundance of long and short spined micrhystrids in the nearshore–offshore transect of the Silurian of Gotland. Such changes in the morphology (length) of phytoplankton (dinoflagellates) have been documented in detail and related to salinity and temperature fluctuations (e.g., Mertens et al., 2009, and references therein). Such morphology changes have also been interpreted concerning some acritarch taxa (Servais et al., 2004b).

For the spherical acritarchs, Dorning (1981) indicated higher proportions in nearshore environments and in the basinal facies in the Silurian. In the latest Precambrian, Butterfield and Chandler (1992) suggested that the small spheroids dominated in the nearshore settings and in the outer shelf environment, whereas larger spherical acritarchs with no substantial ornamentation were more common in the middle part of the shelf. Similarly, Yan and Li (2010) concluded that the *Leiosphaeridia* assemblage of the Lower–Middle Ordovician in South China inhabited the deep water shale basin environments. In the present study, the small spherical acritarchs *Leiosphaeridia* clearly dominate in the open marine environments, from the shelf to the basinal settings (Dongpan section, Shangsi section and Xiakou section) (Figs. 4 and 6). The species *Leiosphaeridia microgranifera* that is characterized by a granulose vesicle wall is also common in offshore environments. On the other hand, the species *Leiosphaeridia minutissima* with smooth vesicles generally occurs more frequently in the nearshore settings of the Dongpan section (Figs. 4 and 6). In addition, the big spherical species (over 80 μm in diameter) *Dictyotidium reticulatum* (considered by some authors as a prasinophyte) is abundant in bed 22 of the Shangsi section and in bed 26 of the Meishan section when the sea level declined, indicating shallow water environments (Figs. 4 and 6).

It is particularly interesting to analyze the spatial distribution of the genus *Reduviasporonites*, which is a taxon considered by some authors as a fungal spore and indicating a 'fungal spike' leading to the mass extinction of the PTB (e.g., Visscher et al., 1996). Previous studies show that the 'spike' of *Reduviasporonites* occurs at shallow marine environments of the PTB (Eshet et al., 1995; Visscher et al., 1996; Looy et al., 2001; Steiner et al., 2003; Sandler et al., 2006). Indeed, around the PTB strata, the relative abundances of *Reduviasporonites* are much higher than that in other strata, but they are never more abundant than 14%, which clearly indicates that a 'spike' does not occur in South China, at least in the present study. Interestingly, the species *Reduviasporonites chalastus* displaying big vesicles (40 μm in length) obviously dominates in shelf environments of shallower water (Meishan section and Zhongzhai section), whereas the species *Reduviasporonites catenulatus* with smaller vesicles (15 μm in length) is more common in deeper water environments of the Shangsi and Xiakou sections (Figs. 4 and 6).

6. Conclusions

The quantitative palynological investigations of five sections (from neritic to offshore, including basinal facies) in the latest Permian of the Yangtze Block, southern China, allows an interpretation of the spatial distribution of the phytoplankton integrating both the diversity of species and genera and the relative abundance of species. The present investigation provides the following information:

(1) low acritarch diversities of 2 to 4 acritarch species occur in the nearshore environments, whereas the higher diversities of up to 20 acritarch species appear in the offshore environment.

(2) at the generic level, the genera *Leiosphaeridia*, *Reduviasporonites* and *Micrhystridium* are distributed widely, from nearshore settings in shallow water to offshore settings in deeper water. The genera *Dictyotidium* and *Veryhachium* have narrower distributions, occurring on the shelf and towards the basin, indicating open marine environments. The genus *Schizosporis* only occurs around the PTB, when the sea level declined, probably indicating nearshore settings in shallow water.

(3) at the specific level the species *Micrhystridium breve* displaying short spines indicates neritic facies, whereas the other species of *Micrhystridium* and *Veryhachium* with longer spines (e.g. *Micrhystridium stellatum* and *Veryhachium hyalodermum*) are indicative of more open marine environments.

(4) for the spherical acritarchs, the small spherical *Leiosphaeridia* clearly indicate deeper water. The species *Leiosphaeridia microgranifera* with granulose walls is more common in offshore settings while *Leiosphaeridia minutissima* with smooth walls generally occurs in nearshore settings. In addition, the big spherical (over 80 μm in diameter) acritarch species *Dictyotidium reticulatum* indicates shallow water settings.

(5) in the PTB strata, the relative abundance of *Reduviasporonites* is never higher than 14%, which indicates that a 'spike' does not occur. In addition, the larger species *Reduviasporonites chalastus* obviously dominates in shelf environments of shallow water, whereas the smaller *Reduviasporonites catenulatus* are more common in deeper waters.

Acknowledgments

We wish to express sincere thanks to Mr. Qing Hu, Lei Zhang, Guichun Liu, Jun Shen, Yu Xiang and Miss Guozhen Xu and Xiaomei Nie for their help in field work. We acknowledge the remarks and suggestions of two anonymous referees who greatly approved the final version of the paper. This work was supported by the National Science Foundation of China (NSFC) projects no. 40839903, 40921062, the Chinese 973 (2011CB808800) and 111 (B08030) programs, the Ministry of Education of China (NCET-10-0712), and the Fundamental Funds for the Central Universities, as well as by grants of the University of Lille 1 ("Allocation Présidentielle" and "Bonus Qualité Recherche") and the Conseil Régional du Nord (France).

Appendix A. Supplementary data

Supplementary data associated with this article can be found in the online version, at http://dx.doi.org/10.1016/j.palaeo.2012.09.010. These data include Google maps of the most important areas described in this article.

References

Al-Ameri, T.K., 1983. Acid-resistant microfossils used in the determination of Palaeozoic palaeoenvironments in Libya. Palaeogeography, Palaeoclimatology, Palaeoecology 44, 103–116.
Bouimetarhan, I., Marret, F., Dupont, L., Zonneveld, K., 2009. Dinoflagellate cyst distribution in marine surface sediments off West Africa (17–6 N) in relation to sea-surface conditions, freshwater input and seasonal coastal upwelling. Marine Micropaleontology 71, 113–130.
Butterfield, N.J., Chandler, F.W., 1992. Paleoenvironmental distribution of Proterozoic microfossils, with an example from the Agu Bay Formation, Baffin Island. Palaeontology 35, 943–957.
Colbath, G.K., 1980. Abundance fluctuations in Upper Ordovician organic-walled microplankton from Indiana. Micropaleontology 26, 97–102.
Devillers, R., De Vernal, A., 2000. Distribution of dinoflagellate cysts in surface sediments of the northern North Atlantic in relation to nutrient content and productivity in surface waters. Marine Geology 166, 103–124.
Dorning, K., 1981. Silurian acritarch distribution in the Ludlovian shelf sea of South Wales and the Welsh Borderland. In: Neale, J.W., Brasier, M.D. (Eds.), Microfossils from Recent and Fossil Shelf Seas. Ellis Horwood, Chichester, England, pp. 31–36.
Dorning, K., 1987. The organic palaeontology of Palaeozoic carbonate environments. Micropalaeontology of carbonate environments. In: Hart, M.B. (Ed.), Micropalaeontology of Carbonate Environments. Ellis Horwood, Chichester, England, pp. 256–265.
Dorning, K., Bell, D., 1987. The Silurian carbonate shelf microflora: acritarch distribution in the Much Wenlock Limestone Formation. In: Hart, M.B. (Ed.), Micropalaeontology of Carbonate Environments. Ellis Horwood, Chichester, England, pp. 266–287.
Eshet, Y., Rampino, M.R., Visscher, H., 1995. Fungal event and palynological record of ecological crisis and recovery across the Permian–Triassic boundary. Geology 23, 967–970.
Feng, Q.L., He, W.H., Gu, S.Z., Meng, Y.Y., Jin, Y.X., Zhang, F., 2007. Radiolarian evolution during the latest Permian in South China. Global and Planetary Change 55, 177–192.
Gao, Y.Q., Shi, G.R., Peng, Y.Q., 2009. A new bivalve fauna from the Permian–Triassic boundary section of southwestern China. Australasian Journal of Paleontology 33, 33–47.
He, W.H., Shen, S.Z., Feng, Q.L., Gu, S.Z., 2005. A late Changhsingian (Late Permian) deepwater brachiopod fauna from the Talung Formation at the Dongpan section, southern Guangxi, South China. Journal of Paleontology 79, 927–938.
He, W.H., Feng, Q.L., Weldon, E.A., Gu, S.Z., Meng, Y.Y., Zhang, F., Wu, S.B., 2007a. A Late Permian to early Triassic bivalve fauna from the Dongpan Section, southern Guangxi, South China. Journal of Paleontology 81, 1009–1019.
He, W.H., Shi, G.R., Feng, Q.L., Campi, M.J., Gu, S.Z., Bu, J.Z., Peng, Y.Q., Meng, Y.Y., 2007b. Brachiopod miniaturization and its possible causes during the Permian–Triassic crisis in deep water environments, South China. Palaeogeography, Palaeoclimatology, Palaeoecology 252, 145–163.
He, W.H., Shi, G.R., Gao, Y.Q., Peng, Y.Q., Zhang, Y., 2008. A new Early Triassic microgastropod fauna from the Zhongzhai Section, Guizhou, southwestern China. Proceedings of the Royal Society of Victoria 120, 157–166.
Hong, H.L., Zhang, N., Li, Z.H., Xue, H., Xia, W., Yu, N., 2008. Clay mineralogy across the PT boundary of the Xiakou section, China: evidence of clay provenance and environment. Clays and Clay Minerals 56, 131–143.
Hong, H.L., Xie, S.C., Lai, X.L., 2011. Volcanism in association with the prelude to mass extinction and environment change across the Permian–Triassic boundary (PTB), southern China. Clays and Clay Minerals 59, 478–489.
Jacobson, S.R., 1979. Acritarchs as paleoenvironmental indicators in Middle and Upper Ordovician rocks from Kentucky, Ohio and New York. Journal of Paleontology 53, 1197–1212.
Jiang, H.S., Lai, X.L., Luo, G.M., Aldridge, R., Zhang, K.X., Wignall, P.B., 2007. Restudy of conodont zonation and evolution across the P/T boundary at Meishan section, Changxing, Zhejiang, China. Global and Planetary Change 55, 39–55.
Jiang, H.S., Lai, X.L., Yan, C.B., Aldridge, R., Wignall, P.B., Sun, Y.D., 2011. Revised conodont zonation and conodont evolution across the Permian–Triassic boundary at the Shangsi section, Guangyuan, Sichuan, South China. Global and Planetary Change 77, 103–115.
Lai, X.L., Yang, F.Q., Hallam, A., Wignall, P., 1996. The Shangsi section, candidate of the Global Stratotype section and point of the Permian–Triassic boundary. In: Yin, H.F. (Ed.), The Palaeozoic–Mesozoic Boundary. Candidates of Global Stratotype Section and Point of the Permian–Triassic Boundary. China University of Geosciences Press, Wuhan, pp. 113–124.
Lei, Y., Servais, T., Feng, Q.L., accepted for publication. The diversity of the Permian phytoplankton. Review of Palaeobotany and Palynology.
Li, Z.S., Zhan, L.P., Zhu, X.F., Zhang, J.H., Jin, R.G., Liu, G.F., Sheng, H.B., Shen, G.M., Dai, J.Y., Huang, H.Q., Xie, L.C., Yan, Z., 1986. Mass extinction and geological events between Palaeozoic and Mesozoic era. Acta Geologica Sinica 60, 1–15.
Li, J., Cao, C., Servais, T., Zhu, Y., 2004a. Later Permian acritarchs from Meishan (SE China) in the context of Permian palaeobiogeography and palaeoecology. Neues Jahrbuch für Geologie und Paläontologie, Monatshefte, pp. 427–448.
Li, J., Servais, T., Yan, K., Zhu, H., 2004b. A nearshore–offshore trend in acritarch distribution from the Early–Middle Ordovician of the Yangtze Platform, South China. Review of Palaeobotany and Palynology 130, 141–161.
Looy, C.V., Twitchett, R.J., Dilcher, D.L., Van Konijnenburg-Van Cittert, J.H.A., Visscher, H., 2001. Life in the end-Permian dead zone. Proceedings of the National Academy of Sciences of the United States of America 98, 7879.
Mertens, K.N., Ribeiro, S., Bouimetarhan, I., Caner, H., Combourieu-Nebout, N., Dale, B., De Vernal, A., Ellegaard, M., Filipova, M., Godhe, A., Goubert, E., Grøsfjeld, K., Holzwarth, U., Kotthoff, U., Leroy, S.A.G., Londeix, L., Marret, F., Matsuoka, K., Mudie, P.J., Naudts, L., Peña-Manjarrez, J.L., Persson, A., Popescu, S.-M., Pospelova, V., Sangiorgi, F., Van De Meer, M.T.J., Vink, A., Zonneveld, K.A.F., Vercauteren, D., Vlassenbroeck, J., Louwye, S., 2009. Process length variation in cysts of a dinoflagellate, Lingulodinium machaerophorum, in surface sediments: investigating its potential as salinity proxy. Marine Micropaleontology 70, 54–69.
Metcalfe, I., Nicoll, R.S., 2007. Conodont biostratigraphic control on transitional marine to non-marine Permian–Triassic boundary sequences in Yunnan-Guizhou, China. Palaeogeography, Palaeoclimatology, Palaeoecology 252, 56–65.
Molyneux, S.G., 2009. Acritarch (marine microphytoplankton) diversity in an Early Ordovician deep-water setting (the Skiddaw Group, northern England): implications for the relationship between sea-level change and phytoplankton diversity. Palaeogeography, Palaeoclimatology, Palaeoecology 275, 59–76.
Molyneux, S.G., Le Hérissé, A., Wicander, R., 1996. Paleozoic phytoplankton. In: Jansonius, J., McGregor, D.C. (Eds.), Palynology: Principles and Applications, American Association of Stratigraphic Palynologists Foundation, pp. 493–529.
Mullins, G.L., Servais, T., 2008. The diversity of the Carboniferous phytoplankton. Review of Palaeobotany and Palynology 149, 29–49.
Nicoll, R.S., Metcalfe, I., Cheng-Yuan, W., 2002. New species of the conodont genus Hindeodus and the conodont biostratigraphy of the Permian–Triassic boundary interval. Journal of Asian Earth Sciences 20, 609–631.

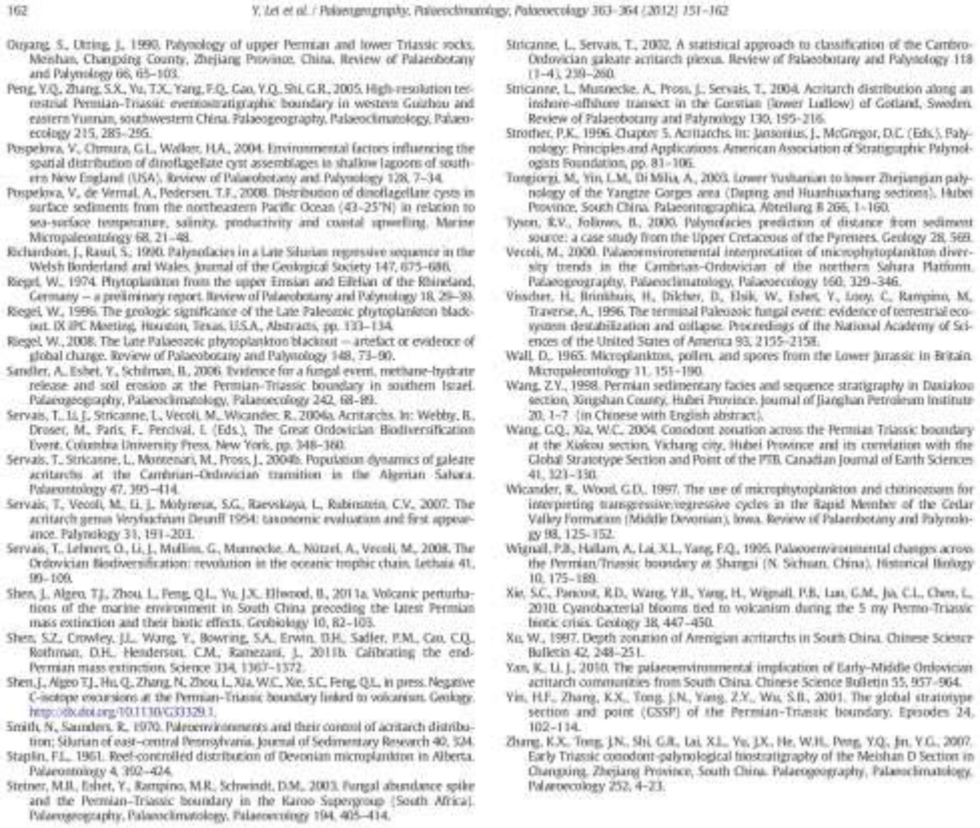

Ouyang, S., Utting, J., 1990. Palynology of upper Permian and lower Triassic rocks, Meishan, Changxing County, Zhejiang Province, China. Review of Palaeobotany and Palynology 66, 65–103.

Peng, Y.Q., Zhang, S.X., Yu, T.X., Yang, F.Q., Gao, Y.Q., Shi, G.R., 2005. High-resolution terrestrial Permian–Triassic eventostratigraphic boundary in western Guizhou and eastern Yunnan, southwestern China. Palaeogeography, Palaeoclimatology, Palaeoecology 215, 285–295.

Pospelova, V., Chmura, G.L., Walker, H.A., 2004. Environmental factors influencing the spatial distribution of dinoflagellate cyst assemblages in shallow lagoons of southern New England (USA). Review of Palaeobotany and Palynology 128, 7–34.

Pospelova, V., de Vernal, A., Pedersen, T.F., 2008. Distribution of dinoflagellate cysts in surface sediments from the northeastern Pacific Ocean (43–25°N) in relation to sea-surface temperature, salinity, productivity and coastal upwelling. Marine Micropaleontology 68, 21–48.

Richardson, J., Rasul, S., 1990. Palynofacies in a Late Silurian regressive sequence in the Welsh Borderland and Wales. Journal of the Geological Society 147, 675–686.

Riegel, W., 1974. Phytoplankton from the upper Emsian and Eifelian of the Rhineland, Germany – a preliminary report. Review of Palaeobotany and Palynology 18, 29–39.

Riegel, W., 1996. The geologic significance of the Late Paleozoic phytoplankton blackout. IX IPC Meeting, Houston, Texas, U.S.A., Abstracts, pp. 133–134.

Riegel, W., 2008. The Late Palaeozoic phytoplankton blackout — artefact or evidence of global change. Review of Palaeobotany and Palynology 148, 73–90.

Sandler, A., Eshet, Y., Schilman, B., 2006. Evidence for a fungal event, methane-hydrate release and soil erosion at the Permian–Triassic boundary in southern Israel. Palaeogeography, Palaeoclimatology, Palaeoecology 242, 68–89.

Servais, T., Li, J., Stricanne, L., Vecoli, M., Wicander, R., 2004a. Acritarchs. In: Webby, B., Droser, M., Paris, F., Percival, I. (Eds.), The Great Ordovician Biodiversification Event. Columbia University Press, New York, pp. 348–360.

Servais, T., Stricanne, L., Montenari, M., Pross, J., 2004b. Population dynamics of galeate acritarchs at the Cambrian–Ordovician transition in the Algerian Sahara. Palaeontology 47, 395–414.

Servais, T., Vecoli, M., Li, J., Molyneux, S.G., Raevskaya, L., Rubinstein, C.V., 2007. The acritarch genus *Veryhachium* Deunff 1954: taxonomic evaluation and first appearance. Palynology 31, 191–203.

Servais, T., Lehnert, O., Li, J., Mullins, G., Munnecke, A., Nützel, A., Vecoli, M., 2008. The Ordovician Biodiversification: revolution in the oceanic trophic chain. Lethaia 41, 99–109.

Shen, J., Algeo, T.J., Zhou, L., Feng, Q.L., Yu, J.X., Ellwood, B., 2011a. Volcanic perturbations of the marine environment in South China preceding the latest Permian mass extinction and their biotic effects. Geobiology 10, 82–103.

Shen, S.Z., Crowley, J.L., Wang, Y., Bowring, S.A., Erwin, D.H., Sadler, P.M., Cao, C.Q., Rothman, D.H., Henderson, C.M., Ramezani, J., 2011b. Calibrating the end-Permian mass extinction. Science 334, 1367–1372.

Shen, J., Algeo T.J., Hu, Q., Zhang, N., Zhou, L., Xia, W.C., Xie, S.C., Feng, Q.L., in press. Negative C-isotope excursions at the Permian–Triassic boundary linked to volcanism. Geology. http://dx.doi.org/10.1130/G33329.1.

Smith, N., Saunders, R., 1970. Paleoenvironments and their control of acritarch distribution; Silurian of east–central Pennsylvania. Journal of Sedimentary Research 40, 324.

Staplin, F.L., 1961. Reef-controlled distribution of Devonian microplankton in Alberta. Palaeontology 4, 392–424.

Steiner, M.B., Eshet, Y., Rampino, M.R., Schwindt, D.M., 2003. Fungal abundance spike and the Permian–Triassic boundary in the Karoo Supergroup (South Africa). Palaeogeography, Palaeoclimatology, Palaeoecology 194, 405–414.

Stricanne, L., Servais, T., 2002. A statistical approach to classification of the Cambro-Ordovician galeate acritarch plexus. Review of Palaeobotany and Palynology 118 (1–4), 239–260.

Stricanne, L., Munnecke, A., Pross, J., Servais, T., 2004. Acritarch distribution along an inshore–offshore transect in the Gorstian (lower Ludlow) of Gotland, Sweden. Review of Palaeobotany and Palynology 130, 195–216.

Strother, P.K., 1996. Chapter 5. Acritarchs. In: Jansonius, J., McGregor, D.C. (Eds.), Palynology: Principles and Applications. American Association of Stratigraphic Palynologists Foundation, pp. 81–106.

Tongiorgi, M., Yin, L.M., Di Milia, A., 2003. Lower Yushanian to lower Zhejiangian palynology of the Yangtze Gorges area (Daping and Huanghuachang sections), Hubei Province, South China. Palaeontographica, Abteilung B 266, 1–160.

Tyson, R.V., Follows, B., 2000. Palynofacies prediction of distance from sediment source: a case study from the Upper Cretaceous of the Pyrenees. Geology 28, 569.

Vecoli, M., 2000. Palaeoenvironmental interpretation of microphytoplankton diversity trends in the Cambrian–Ordovician of the northern Sahara Platform. Palaeogeography, Palaeoclimatology, Palaeoecology 160, 329–346.

Visscher, H., Brinkhuis, H., Dilcher, D., Elsik, W., Eshet, Y., Looy, C., Rampino, M., Traverse, A., 1996. The terminal Paleozoic fungal event: evidence of terrestrial ecosystem destabilization and collapse. Proceedings of the National Academy of Sciences of the United States of America 93, 2155–2158.

Wall, D., 1965. Microplankton, pollen, and spores from the Lower Jurassic in Britain. Micropaleontology 11, 151–190.

Wang, Z.Y., 1998. Permian sedimentary facies and sequence stratigraphy in Daxiakou section, Xingshan County, Hubei Province. Journal of Jianghan Petroleum Institute 20, 1–7 (in Chinese with English abstract).

Wang, G.Q., Xia, W.C., 2004. Conodont zonation across the Permian Triassic boundary at the Xiakou section, Yichang city, Hubei Province and its correlation with the Global Stratotype Section and Point of the PTB. Canadian Journal of Earth Sciences 41, 323–330.

Wicander, R., Wood, G.D., 1997. The use of microphytoplankton and chitinozoans for interpreting transgressive/regressive cycles in the Rapid Member of the Cedar Valley Formation (Middle Devonian), Iowa. Review of Palaeobotany and Palynology 98, 125–152.

Wignall, P.B., Hallam, A., Lai, X.L., Yang, F.Q., 1995. Palaeoenvironmental changes across the Permian/Triassic boundary at Shangsi (N. Sichuan, China). Historical Biology 10, 175–189.

Xie, S.C., Pancost, R.D., Wang, Y.B., Yang, H., Wignall, P.B., Luo, G.M., Jia, C.L., Chen, L., 2010. Cyanobacterial blooms tied to volcanism during the 5 my Permo-Triassic biotic crisis. Geology 38, 447–450.

Xu, W., 1997. Depth zonation of Arenigian acritarchs in South China. Chinese Science Bulletin 42, 248–251.

Yan, K., Li, J., 2010. The palaeoenvironmental implication of Early–Middle Ordovician acritarch communities from South China. Chinese Science Bulletin 55, 957–964.

Yin, H.F., Zhang, K.X., Tong, J.N., Yang, Z.Y., Wu, S.B., 2001. The global stratotype section and point (GSSP) of the Permian–Triassic boundary. Episodes 24, 102–114.

Zhang, K.X., Tong, J.N., Shi, G.R., Lai, X.L., Yu, J.X., He, W.H., Peng, Y.Q., Jin, Y.C., 2007. Early Triassic conodont-palynological biostratigraphy of the Meishan D Section in Changxing, Zhejiang Province, South China. Palaeogeography, Palaeoclimatology, Palaeoecology 252, 4–23.

Manuscript 4: (Section 4)

To be submitted to Palaeogeography, Palaeoclimatology, Palaeoecology

Phytoplankton community changes during the Permian-Triassic boundary in South China - one of the possible mechanisms for the mass extinction

Yong Lei[1,2], Thomas Servais[2], Qinglai Feng[1*], Jun Shen[1], Shucheng Xie[1], Wenfeng Zhou[1]

[1] State Key Laboratory of Geological Processes and Mineral Resources, China University of Geosciences, Wuhan, China
[2] UMR 8217 Géosystèmes, CNRS-Université Lille1, Cité Scientifique, F-59655 Villeneuve d'Ascq, France
***Corresponding author**, E-mail: qinglaifeng@cug.edu.cn
Fax: +86-027-67883002; Tel: +86-027-67883006
Yong Lei, E-mail: leiyongdida@163.com; Tel: +86-13485387952
Thomas Servais, E-mail: thomas.servais@univ-lille1.fr;
Fax: +33-320436900; Tel: +33-320337220
Jun Shen, E-mail: shenjun_2009@163.com; Tel: +86-18062435228
Shucheng Xie, E-mail: xiecug@163.com; Tel:+86-13554116626
Wenfeng Zhou, E-mail: wenfeng4000@126.com; Tel:+86-18907145343

Abstract.

The end-Permian marine ecosystem changed dramatically. Large-scale volcanic eruptions, sea-level drop and intense terrigenous inputs, high sea-water temperatures and high inorganic nutrient concentrations promoted widespread cyanobacterial blooms, as recorded by lipid biomarkers and microbialites. These cyanobacterial blooms changed the marine ecosystems by increased light attenuation, depleted the water of oxygen and poisoned metazoan life. Here we document that diverse and abundant organic-wall phytoplankton (acritarchs) occurred before the metazoan mass extinction. However, in South China, the acritarchs communities continuously decreased in diversity and abundance synchronously along with cyanobacterial proliferations and metazoan mass extinctions towards the Permian-Triassic boundary (PTB). Our analyses shows that the decreasing organic-walled phytoplankton (acritarchs) diversity correlates with the decreasing diversity of marine invertebrates. We suggest that if the end Permian mass extinction was triggered by the large-scale volcanic eruptions, and was caused by the ocean anoxia, food deficiency and high temperature directly, the cyanobacterial blooms would have enhanced the ocean anoxia and food deficiency during the PTB. The relationships between the mass extinction, the diversity and abundance of the phytoplankton, and the cyanobacterial blooms are more complex than that we previously thought.

Keywords: acritarchs; cyanobacterial blooms; end-Permian mass extinction; Yangtze Block

1 Introduction

The end-Permian extinction event (252 Ma ago) was the greatest mass extinction in the history of the Earth, with over 96% of marine species getting extinct (Erwin 1990; Erwin et al., 2002). Many authors try to explain the causes of the mass extinction and linked it with environmental catastrophes, such as ocean anoxia (Wignall and Twitchett, 1996; Isozaki, 1997; Kump et al., 2005), Siberian trap volcanism (Reichow et al., 2002, 2009; Kamo et al., 2003; Renne et al., 1995), expansion of oceanic oxygen-minimum zone (Algeo et al., 2011), but the causes remain controversial. On the other hand, most studies documented in detail the extinction of marine metazoans (e.g. Raup and Sepkoski Jr, 1982; Shen and Shi, 1996, 2002; Jin et al., 2000; Villier and Korn, 2004; Alroy, 2008; Song et al., 2009), but did ignore the changes of primary producers in marine environments at the Permian to Triassic boundary (PTB). Only the possible presence of a “fungal spike” was presented as a probable cause of the extinction, but was subsequently largely debated (Eshet et al., 1995; Visscher et al., 1996, 2011; Afonin et al., 2001; Foster et al., 2002; Sephton et al., 2009). Recently, a series of papers analyzed the cyanobacterial changes during the Permian-Triassic boundary interval in South China (Grice et al., 2005; Xie et al., 2005, 2007, 2010; Cao et al., 2009; Chen et al., 2011;). For instance, Xie et al. (2010) pointed out that widespread cyanobacterial mats occurred during a 5 my Permo-Triassic biotic crisis in this area.

Cyanobacteria occurred on Earth probably 3.5 billion years ago (e.g. Schopf, 1993). They are one of the most diverse groups of photosynthetic and N_2-fixing microorganism in modern oceans (e.g. Capone et al., 1997; Wiegand and Pflugmacher, 2005). However, cyanobacterial blooms are also considered to cause problems to other phytoplanktonic organisms and animals in both marine and freshwater systems (e.g. Briand et al., 2003; Wiegand and Pflugmacher, 2005). Most cyanobacterial species can colonize different depths in the water column by regulating their buoyancy (the possession of gas vesicles) (e.g. Walsby et al., 2001; Briand et al., 2003). Cyanobacterial blooms increase light attenuation (e.g. Phlips and Badylak, 1996; Phlips et al., 1999), which reduces the distribution of other primary producers and metazoans, such as diatoms, sea grass beds and coral communities (e.g. Hall et al., 1999; O’Neil et al., 2012).

For the predators, several bloom-forming cyanobacteria are toxic, including hepatotoxins (microcystins, nodularins and cylindrospermopsins), neurotoxins (anatoxins and saxitoxins) and dermatotoxins/ irritant toxins (lyngbyatoxin A, aplysiatoxins and lipopolysaccharides), as their toxicological target (e.g. Briand et al., 2003). These toxic compounds, as the secondary metabolites produced by cyanobacteria, are dangerous for zooplankton (e.g. copepods), causing increased mortality and reduced reproductive output (e.g. DeMott et al., 1991; Engström-Öst et al., 2002; Golubic et al., 2010). The toxicity is likely to be transferred and concentrated up in mussels, crustaceans and fish and on the entire food web (e.g. Endean et al., 1993; Engström-Öst et al., 2002; Wiegand and Pflugmacher, 2005; Golubic et al., 2010; Karlson and Mozūraitis, 2011).

Moreover, non-toxic cyanobacterial blooms may also damage the environment, and may even lead to the death of fishes and other animals (e.g. Stal et al., 2003). Sedimentary and grazing losses of cyanobacterial blooms are generally small (e.g. filamentous species occur on the marine surface layer), but most of these organic matters are decomposed in the surface layer and deplete the water of O_2 (e.g. Heiskanen and Kononen, 1994; Sellner et al., 1994; Vahtera et al., 2007; FerrÃo-Filho et al., 2001).

The cyanobacterial blooms were possibly initiated by increased availability of nutrients (e.g. phosphorus and iron) (e.g. Bianchi et al., 2000; Boyd et al., 2004), and favoured by high water temperature (e.g. Kanoshina et al., 2003; O'Neil et al., 2012; Posch et al., 2012). Interestingly, these environmental conditions (high inorganic nutrient concentrations and high temperature) exactly happened during the PTB by enhanced chemical weathering, intense terrestrial input and large-scale volcanic eruption (Sheldon, 2006; Algeo and Twitchett, 2010; Joachimski et al., 2012; Sun et al, 2012). Indeed, widespread cyanobacteria occurred in South China from shallow platform to deep sea settings during the PTB strata (Figure 1), recorded by calci-microbialite and biomarker data (Lehrmann, 1999; Wang et al., 2005; Xie et al., 2005, 2010). Although Xie et al. (2005; 2007) analyzed the cause of the enhanced cyanobacterial population, the relationship between the mass extinction and the widespread cyanobacteria remain unclear.

Surprisingly, the evolution of the organic-walled microphytoplankton during the PTB strata, represented by the acritarchs, remains greatly unknown, although the organic-walled fraction of the microphytoplankton is the most common in Palaeozoic strata (Munnecke and Servais, 2008). More recently, Lei et al. (in press) reviewed the diversity of the Permian phytoplankton at a global scale, and noted that over 30 genera of phytoplankton have been recorded in the latest Permian strata (Changhsingian), and almost 30 species of phytoplankton have been documented from the Yangtze Block, South China (e.g. Li et al., 2004a; Ouyang and Utting, 1990). Lei et al. (2012) also investigated the inshore-offshore distribution of the end Permian phytoplankton in this area, indicating that the distribution patterns were similar to those of other Palaeozoic periods or to that of modern dinoflagellates. Nevertheless,, the phytoplankton community changes remain unclear. In the present study, we try to understand the phytoplankton community succession (including cyanobacteria and acritarchs) and to analyze the relationships between the phytoplankton community changes and the mass extinction at the PTB in South China.

2 Geological setting

Seven geological sections, located in the Yangtze Block of southern China (Fig. 1), have been analyzed for the present study. Five of these sections have already been described in detail by Lei et al. (2012) and the reader is referred to this latter study for details on the geological setting and the palynological content (including the organic-welled phytoplankton). The two other sections are presented below.

2.1 Liangfengya section

The Liangfengya section is located in Shandong Village, Zhongliang Mountain area, Chongqing City. This section comprises the Changxing Formation (bed 4 and below) and the Feixianguan Formation (beds 5 to 22). The geology of the Liangfengya section was described in detail by Wu et al. (1988). The beds 1 to 4 are dominated by limestones, with a few volcanic ash intervals. The beds 5 to 22 are dominated by mud-limestones with a few shales and volcanic ashes, containing conodont, brachiopods and ammonites. The facies of this section is interpreted as being located in intra-platform environments (Xia Wenchen, unpublished data). According to the conodont zone, the PTB is placed in bed 6. The three conodont biozones recovered in the Liangfengya section are the *Clarkina yini* Zone (beds 1 to 4), the *Clarkina microcuspidata* Zone (beds 5 to 6-a) and the *Hindeodus parvus* Zone (beds 6-b to 22), in ascending order (Xia Wenchen, unpublished data).

2.2 Ganxi section

The Ganxi section (N30°07.4′, E109°26.8′) is located near Enshi City, Hubei Province. The uppermost Dalong Formation (Beds 220-233.3, 2.5 m) comprises mudstones with a few limestones. The Yinkeng Formation (over 100 m) is dominated by limestones with a few mudstone and volcanic ash intervals. According to the conodont zonation, the PTB is placed in bed 238 (Mutwakil et al., 2006). The three conodont biozones at the Ganxi section are the *Clarkina yini* Zone (beds 220-233.3), the *Clarkina meishanensis* Zone (beds 233.4-237) and the *Hindeodus parvus* Zone (beds 238), in ascending order (Mutwakil et al., 2006; Yin et al., under review).

3 Materials and methods

Palynological analysis

Similarly to the previously analyzed sections (Lei et al., 2012), 106 samples have been collected from the two sections around the Permian-Triassic boundary (29 samples from the Liangfengya section; 77 samples from the Ganxi section). All the samples were analyzed for palynological studies.

Fifty grams of each sample were prepared following standard palynological techniques. One *Lycopodium* spore was added in each of the samples before processing in order to allow calculation of absolute particle abundances, following standard counting techniques (Tyson and Follows, 2000). All samples were treated successively with 34% HCl and 40% HF for the respective removal of carbonates and silicates. The residues have subsequently been concentrated with zinc bromide solution (S.G. 2.1). The residues were neither oxidized nor sieved. The residue was studied using light microscopy and scanning electron microscopy. For each sample, 300 particles were counted in transmitted light (including *Lycopodium* spores and acritarchs). The acritarch taxa were determined at the specific level. All palynological residues are stored in the collections of the China University of Geosciences (Wuhan).

4 Results

4.1 Acritarchs from the Ganxi and Liangfengya sections

In the Ganxi section, the present investigation indicates that only one spherical acritarchs (*Leiosphaeridia minutissima*) has been recorded rarely in the 10 samples (Table 1) from the end Permian to the Early Triassic (only 4 samples are shown in Fig. 2).

In the Liangfengya section, about 8 species attributed to 3 genera have been recorded in the 7 samples investigated, including *Leiosphaeridia micrograniféra*, *Leiosphaeridia minutissima*, *Micrhystridium breve*, *Micrhystridium pentagonale*, *Micrhystridium stellatum*, *Veryhachium hyalodermum*, *Veryhachium quadratum*, *Veryhachium sedecimspinosum*. Diverse and abundant acritarchs occur in the end Permian strata of the Liangfengya section (Fig. 2, Table 1). Interestingly, similarly to the Ganxi section, only *Leiosphaeridia minutissima* occurs in the earliest Triassic.

4.2 Acritarch communities at the Permian-Triassic boundary in South China

The acritarchs are here plotted against the conodont biozones, rather than the the sedimentary beds (Lei et al., 2012; Fig. 2). Based on the diversity of acritarchs throughout the differents sections, we can identify three different stages of acritarchs communities (Stage I to III) around the PTB in South China (Figure 2) and compare them with the diversity drop of metazoans leading to the mass extinction in the Meishan section (Jin et al., 2000). Some of the acritarchs species from the Late Permian of China are illustrated in Figure 3.

Diverse (28 species attributed to 10 genera, Figure 2) and abundant acritarchs occur in Stage I, corresponding to the *Clarkina changxingensis* and *Clarkina yini* conodont Biozone. A moderately rich acritarch community (11 species attributed to 7 genera, Figure 2) is present in Stage II at the PTB transition, corresponding to the *Clarkina meishanensis*, *Hindeodus changxingensis*, *Clarkina taylorae* and *Hindeodus parvus* conodont biozones. Only a single species (*Leiosphaeridia minutissima*) has been recorded in Stage III indicating possible low biomass, corresponding to the *Isarcicella staeschei* and *Isarcicella isarcica* conodont biozones.

5 Discussion

5.1 The cyanobacterial proliferation

Two genera of filamentous cyanobacteria (*Lyngbya* and *Trichodesmium*) and one coccoid cyanobacteria *Synechococcus* are the most conspicuous marine cyanobacterial bloom formers in modern oceans (O'Neil et al., 2012). The filamentous cyanobacteria as N_2 fixers can form dense surface blooms utilizing their buoyancy (the possession of gas vesicles) (Walsby et al., 2001; Briand et al., 2003). Generally, the genus *Lyngbya* more likely grows attached to seagrasses, macroalgae, corals and sediments (O'Neil et al., 2012). However, *Trichodesmium* forms blooms distributed in pelagic environments with tropical and subtropical oceans (O'Neil et al., 2012), whereas *Synechococcus* is a cosmopolitan open ocean cyanobacterial bloom former (Zwirglmaier et al., 2008). Nevertheless, all of these cyanobacteria only are promoted by high temperatures (even 30^{o}C) and high concentrations of inorganic nutrients (e.g. P and Fe) (O'Neil et al., 2012). Blooms of these cyanobacteria increase the light attenuation (Phlips and Badylak, 1996; Phlips et al., 1999), which has negative impacts on distributions of other phytoplankton groups, seagrass and coral communities (Hall et al., 1999; O'Neil et al., 2012).

Generally, two kinds of cyanobacteria-like microfossils occurred in the calci-microbialites in the PTB strata, including filamentous microfossils (*Renalcis* or *Epiphyton* and *Rivularia*) and coccoid microfossils (Lehrmann, 1999; Wang et al., 2005; Jiang et al., 2008). These cyanobacterial blooms occurred immediately after the end-Permian mass extinction as calci-microbialites in shallow water, South China (Xie et al., 2010; Fig. 1). Kershaw et al. (2007) suggested that the calci-microbialites have a wide geographic distribution but mostly existed within the Tethys Ocean in the earliest Triassic (Figure 1). Moreover, the cyanobacterial blooms, evaluated using biomarkers (2-methylhopane), occurred immediately following the end-Permian faunal extinction in deep water sediments of the Meishan section (Xie et al., 2005, 2010) and the Shangsi section (Zhou et al., in prepare, beds 28 to 33; Fig. 2).

Joachimski et al. (2012) pointed out that the climate changed with a warming immediately after the end-Permian mass extinction (bed 27 in Meishan and bed 28 in Shangsi; Fig. 2), documented by the oxygen isotope records of conodont apatite. In the same time, the inorganic nutrients (e.g. Fe and P) increased dramatically by large-scale volcanic eruptions and the intense weathering (Sheldon, 2006; Algeo and Twitchett, 2010; Joachimski et al., 2012). Those environmental conditions probably promoted the cyanobacterial proliferation and decreased the abundance and diversity of the other phytoplankton groups, seagrass and corals communities.

5.2 The decreasing diversity of acritarch communities

The diversity of the acritarchs was clearly reduced from Stage I to Stage II, possibly due to a sea-level drop (Figure 2). Many offshore sections changed to near-shore environments, where low diversities of acritarchs occurred (e.g. Li et al., 2004b; Lei et al., 2012). However, the acritarch diversity did not increase with the sea-level rise between Stage II and Stage III, possibly due to a cyanobacterial proliferation (e.g. high temperature and the light attenuation; see above).

Generally, the abundance of the acritarchs decreased from Stage I to Stage III (Fig. 2). On the contrary, the acritarch biomass increased obviously in the beds after and close to the volcanic ashes (e.g. bed 26 in Meishan; beds 25 and 28 in Shangsi; bed 1 in Liangfengya; Fig. 2), the volcanic eruption being considered as fertilizing the marine ecosystems (Algeo and Twitchett, 2010; Ayris and Delmelle, 2012; Lindenthal et al., 2012). These beds contain abundant inorganic nutrients (e.g. Fe), which probably initiated the blooms of phytoplankton in the surface ocean (Abraham et al., 2000; Duggen et al., 2010; Olgun et al., 2011). However, these stimulating phenomena did apparently not occur in Stage III (e.g. bed 29 in Meishan and bed 30 in Shangsi), maybe due to other environmental changes (e.g. high temperature and the light attenuation). On the other hand, the controversial taxa *Reduviasporonites* (interpretes by some authors as a fungal spore, but not by other authors) is present in some samples with relatively low percentages (never more than 14%). A 'spike' of *Reduviasporonites* (over 90% in sample, as documented elsewhere, see Eshet et al., 1995; Visscher et al., 1996, 2011; Looy et al., 2001; Steiner et al., 2003; Sandler et al., 2006; Sephton et al., 2009) does therefore not occur in any of the sections analyzed in South China. Indeed, *Reduviasporonites* most probably increased in abundance after the volcanic ashes and decreased in Stage III, as did most of all other acritarchs species.

5.3 The possible relationship between the phytoplankton community changes and the mass extinction

Before the mass extinction, diverse and abundant acritarchs and metazoans are documented from South China (Jin et al., 2000; Fig. 2). However, the diversity of the metazoan decreased dramatically along with the large-scale volcanic eruptions and ocean anoxia (Renne et al., 1995; Wignall and Twitchett, 1996; Isozaki, 1997; Reichow et al., 2002, 2009; Kamo et al., 2003; Kump et al., 2005). In the same time, the cyanobacterial blooms occurred immediately in the shallow waters in form of calci-microbialites (Xie et al., 2010), which were dominated by the microgastropods, bivalves and ostracodes (Lehrmann, 1999; Wang et al., 2005).

Sun et al. (2012) pointed out that the high temperatures played an important role for the end-Smithian crisis, which drove most Early Triassic plants and animals out of the equatorial terrestrial ecosystems. They also noticed that the temperature of the sea water in the end Permian (about 25°C; bed 26 in Meishan) was not much higher as that in the end-Smithian (about 40°C; Joachimski et al., 2012; Sun et al., 2012). However, this temperature already stimulated the cyanobacterial proliferation at a worldwide level at the end Permian (Kershaw et al., 2007; Xie et al., 2010). And these cyanobacteria blooms maybe a major cause of the end Permian mass extinction.

In modern oceans, cyanobacteria are a poor-quality food for metazoans, caused by their toxicity and nutritional inadequacy (Hairston et al., 2007; Nascimento et al., 2009). FerrÃo-Filho et al. (2001), through feeding experiments, proved that even the non-toxic cyanobacterium *Synechococcus elongatus* supported poor growth in *Moinodaphnia macleayi* (zooplankton). However, the nutritional deficiency was overcome when *Synechococcus* was mixed with a few other green algae. Moreover, different species of metazoans have different physiological capacities to tolerate (or not) the cyanobacteria. These phenomena have been proved in zooplankton, bivalves and gastropods (FerrÃo-Filho et al., 2001; Lance et al., 2010; Wiegand and Pflugmacher, 2005). Furthermore, Limén and Ólafsson (2002) showed that when the macrofauna (bivalves) and the meiofauna (ostracods) live in low energy systems (food-limitation) together, the abundance and diversity of macrofauna decreases, but the meiofauna still growth abundatntly. Limén and Ólafsson (2002) proved that the small size primary consumers have better access to the food available in the interference competition.

These results can be discussed in the frame of the end Permian extinction, with marine ecosystems being balanced before the dramatic changes (diverse and abundant metazoan and phytoplankton; Fig. 2). However, this balance was destroyed by drastic environmental changes (e.g. large-scale volcanic eruptions, sea-level changes and high temperatures) (Renne et al., 1995; Reichow et al., 2002, 2009; Kamo et al., 2003; Joachimski et al., 2012; Sun et al., 2012), which possibly promoted the cyanobacterial blooms that rapidly spread all over the world (Kershaw et al., 2007; Xie et al., 2010). The cyanobacterial proliferation would have poisoned the metazoans, accelerate the ocean anoxia and reduce the abundance and diversity of other primary producers (see above). Most species of the metazoans become extinct in the deteriorating environment during Stage II (anoxic and food-limitation system; Fig. 2), only some primary consumers grew well, probably those with small sizes or/and insensitive to the cyanobacterial toxin (He et al., 2010; Algeo et al., 2011; Song et al., 2011; Chen and Benton, 2012).

Along with the rising temperatures and intense inorganic nutrients (Fe and P), the cyanobacterial blooms proliferated in offshore environments and deeper waters (bed 28 in Shangsi and bed 29 in Meishan), and the acritarchs (high quality food for metazoan) became rare (Fig. 2). Many species of primary consumers which survived in the end Permian mass extinction, became extinct during the earliest Triassic, probably due to the deteriorated environment (high temperature, ocean anoxia and food deficiency). Only a few disaster taxa dominated in the ocean (e.g. the bivalve *Claraia*) (Chen and Benton, 2012).

6 Conclusions

(1) The acritarch communities continuously decreased in diversity and abundance toward the PTB along with a cyanobacterial proliferation. The acritarchs being interpreted as the cysts of organic-walled microphytoplankton therefore indicate an indirect evidence of the presence (and decrease) of the cyst-forming phytoplankton.

(2) If the end Permian mass extinction was triggered by large-scale volcanic eruptions and was caused by general ocean anoxia, food deficiency and high temperatures, we consider that cyanobacterial blooms, promoted by the high temperatures and intense inorganic nutrients, probably enhanced the ocean anoxia and food deficiency during the PTB.

Nevertheless, the relationships between the mass extinction, phytoplankton diversity and abundance, and cyanobacterial blooms are more complex than that we previously thought.

Acknowledgements

This is part of a co-tutorial PhD investigation of the first author, between the University of Lille 1 and the China University of Geosciences (Wuhan). This co-tutorial study benefited from the support of the University of Lille 1 and of the Regional Council of Nord- Pas- de- Calais (France).

References

Abraham, E.R., Law, C.S., Boyd, P.W., Lavender, S.J., Maldonado, M.T., Bowie, A.R., 2000. Importance of stirring in the development of an iron-fertilized phytoplankton bloom. Nature 407, 727-730.

Afonin, S., Barinova, S., Krassilov, V., 2001. A bloom of *Tympanicysta* Balme (green algae of zygnematalean affinities) at the Permian-Triassic boundary. Geodiversitas 23, 481-487.

Algeo, T.J., Twitchett, R.J., 2010. Anomalous Early Triassic sediment fluxes due to elevated weathering rates and their biological consequences. Geology 38, 1023-1026.

Algeo, T.J., Chen, Z.Q., Fraiser, M.L., Twitchett, R.J., 2011. Terrestrial–marine teleconnections in the collapse and rebuilding of Early Triassic marine ecosystems. Palaeogeography, Palaeoclimatology, Palaeoecology 308, 1-11.

Alroy, J., 2008. Dynamics of origination and extinction in the marine fossil record. Proceedings of the National Academy of Sciences 105, 11536-11542.

Ayris, P., Delmelle, P., 2012. Volcanic and atmospheric controls on ash iron solubility: A review. Physics and Chemistry of the Earth, Parts A/B/C 45–46, 103-112.

Bianchi, T.S., Engelhaupt, E., Westman, P., Andren, T., Rolff, C., Elmgren, R., 2000. Cyanobacterial blooms in the Baltic Sea: Natural or human-induced? Limnology and Oceanography, 716-726.

Boyd, P.W., Law, C.S., Wong, C., Nojiri, Y., Tsuda, A., Levasseur, M., Takeda, S., Rivkin, R., Harrison, P.J., Strzepek, R., 2004. The decline and fate of an iron-induced subarctic phytoplankton bloom. Nature 428, 549-553.

Briand, J.F., Jacquet, S., Bernard, C., Humbert, J.F., 2003. Health hazards for terrestrial vertebrates from toxic cyanobacteria in surface water ecosystems. Veterinary research 34, 361-377.

Cao, C.Q., Love, G.D., Hays, L.E., Wang, W., Shen, S.Z., Summons, R.E., 2009. Biogeochemical evidence for euxinic oceans and ecological disturbance presaging the end-Permian mass extinction event. Earth and Planetary Science Letters 281, 188-201.

Capone, D.G., Zehr, J.P., Paerl, H.W., Bergman, B., Carpenter, E.J., 1997. *Trichodesmium*, a globally significant marine cyanobacterium. science 276, 1221-1229.

Chen, L., Wang, Y.B., Xie, S.C., Kershaw, S., Dong, M., Yang, H., Liu, H., Algeo, T.J., 2011. Molecular records of microbialites following the end-Permian mass extinction in Chongyang, Hubei Province, South China. Palaeogeography, Palaeoclimatology, Palaeoecology 308, 151-159.

Chen, Z.Q., Benton, M.J., 2012. The timing and pattern of biotic recovery following the end-Permian mass extinction. Nature Geoscience 5, 375-383.

DeMott, W.R., Zhang, Q.X., Carmichael, W.W., 1991. Effects of toxic cyanobacteria and purified toxins on the survival and feeding of a copepod and three species of Daphnia. Limnology and

Oceanography, 1346-1357.

Duggen, S., Olgun, N., Croot, P., Hoffmann, L.J., Dietze, H., Delmelle, P., Teschner, C., 2010. The role of airborne volcanic ash for the surface ocean biogeochemical iron-cycle: a review. Biogeosciences 7, 827-844.

Engström-Öst, J., Lehtiniemi, M., Green, S., Kozlowsky-Suzuki, B., Viitasalo, M., 2002. Does cyanobacterial toxin accumulate in mysid shrimps and fish via copepods? Journal of Experimental Marine Biology and Ecology 276, 95-107.

Erwin, D.H., 1990. The end-Permian mass extinction. Annual review of ecology and systematics 21, 69-91.

Erwin, D.H., Bowring, S.A., Yugan, J., 2002. End-Permian mass extinctions: a review. Catastrophic events and mass extinctions: impacts and beyond 356, 363-383.

Eshet, Y., Rampino, M.R., Visscher, H., 1995. Fungal event and palynological record of ecological crisis and recovery across the Permian-Triassic boundary. Geology 23, 967-970.

Feng, Q.L., Gu, S.Z., 2002. Uppermost Changxingian (Permian) radiolarian fauna from southern Guizhou, southwestern China. Journal of Paleontology 76, 797-809.

Feng, Q.L., He, W.H., Gu, S.Z., Meng, Y.Y., Jin, Y.X., Zhang, F., 2007. Radiolarian evolution during the latest Permian in South China. Global and Planetary Change 55, 177-192.

FerrÃo-Filho, A.S., Azevedo, S.M.F.O., DeMott, W.R., 2001. Effects of toxic and non-toxic cyanobacteria on the life history of tropical and temperate cladocerans. Freshwater Biology 45, 1-19.

Foster, C.B., Stephenson, M.H., Marshall, C., Logan, G.A., Greenwood, P.F., 2002. A revision of *Reduviasporonites* Wilson 1962: description, illustration, comparison and biological affinities. Palynology 26, 35-58.

Golubic, S., Abed, R.M.M., Palińska, K., Pauillac, S., Chinain, M., Laurent, D., 2010. Marine toxic cyanobacteria: Diversity, environmental responses and hazards. Toxicon 56, 836-841.

Grice, K., Cao, C.Q., Love, G.D., Boettcher, M.E., Twitchett, R.J., Grosjean, E., Summons, R.E., Turgeon, S.C., Dunning, W., Jin, Y.G., 2005. Photic zone euxinia during the Permian-Triassic superanoxic event. science 307, 706-709.

Hairston, N., Holtmeier, C., Lampert, W., Weider, L., Post, D., Fischer, J., Caceres, C., Fox, J., Gaedke, U., 2007. Natural selection for grazer resistance to toxic cyanobacteria: evolution of phenotypic plasticity? Evolution 55, 2203-2214.

Hall, M.O., Durako, M.J., Fourqurean, J.W., Zieman, J.C., 1999. Decadal changes in seagrass distribution and abundance in Florida Bay. Estuaries and Coasts 22, 445-459.

He, W.H., Shen, S.Z., Feng, Q.L., Gu, S.Z., 2005. A late Changhsingian (Late Permian) deepwater brachiopod fauna from the Talung Formation at the Dongpan section, southern Guangxi, South China. Journal of Paleontology 79, 927-938.

He, W.H., Feng, Q.L., Weldon, E.A., Gu, S.Z., Meng, Y.Y., Zhang, F., Wu, S.B., 2007a. A late Permian to early Triassic bivalve fauna from the Dongpan Section, southern Guangxi, South China. Journal of Paleontology 81, 1009-1019.

He, W.H., Shi, G.R., Feng, Q.L., Campi, M.J., Gu, S.Z., Bu, J.Z., Peng, Y.Q., Meng, Y.Y., 2007b. Brachiopod miniaturization and its possible causes during the Permian–Triassic crisis in deep water environments, South China. Palaeogeography, Palaeoclimatology, Palaeoecology 252, 145-163.

He, W.H., Shi, G.R., Gao, Y.Q., Peng, Y.Q., Zhang, Y., 2008. A new Early Triassic microgastropod fauna from the Zhongzhai Section, Guizhou, southwestern China. Proceedings of the Royal Society of Victoria 120, 157-166.

He, W.H., Twitchett, R.J., Zhang, Y., Shi, G.R., Feng, Q.L., Yu, J.X., Wu, S.B., Peng, X.F., 2010. Controls on body size during the Late Permian mass extinction event. Geobiology 8, 391-402.

Heiskanen, A.S., Kononen, K., 1994. Sedimentation of vernal and late summer phytoplankton communities in the coastal Baltic Sea. Archiv fur Hydrobiologie. Stuttgart 131, 175-198.

Jiang, H.S., Lai, X.L., Yan, C.B., Aldridge, R., Wignall, P.B., Sun, Y.D., 2011. Revised conodont zonation and conodont evolution across the Permian–Triassic boundary at the Shangsi section, Guangyuan, Sichuan, South China. Global and Planetary Change 77, 103-115.

Jiang, H.X., Wu, Y.S., Cai, C.F., 2008. Filamentous cyanobacteria fossils and their significance in the Permian-Triassic boundary section at Laolongdong, Chongqing. Chinese Science Bulletin 53, 1871-1879.

Jin, Y.G., Wang, Y., Wang, W., Shang, Q.H., Cao, C.Q., Erwin, D.H., 2000. Pattern of marine mass extinction near the Permian-Triassic boundary in South China. science 289, 432-436.

Joachimski, M.M., Lai, X.L., Shen, S.Z., Jiang, H.S., Luo, G.M., Chen, B., Chen, J., Sun, Y.D., 2012. Climate warming in the latest Permian and the Permian–Triassic mass extinction. Geology 40, 195-198.

Kamo, S.L., Czamanske, G.K., Amelin, Y., Fedorenko, V.A., Davis, D., Trofimov, V., 2003. Rapid eruption of Siberian flood-volcanic rocks and evidence for coincidence with the Permian–Triassic boundary and mass extinction at 251 Ma. Earth and Planetary Science Letters 214, 75-91.

Kanoshina, I., Lips, U., Leppänen, J.M., 2003. The influence of weather conditions (temperature and wind) on cyanobacterial bloom development in the Gulf of Finland (Baltic Sea). Harmful algae 2, 29-41.

Karlson, A.M.L., Mozūraitis, R., 2011. Deposit-feeders accumulate the cyanobacterial toxin nodularin. Harmful algae 12, 77-81.

Kershaw, S., Li, Y., Crasquin-Soleau, S., Feng, Q.L., Mu, X.N., Collin, P.Y., Reynolds, A., Guo, L., 2007. Earliest Triassic microbialites in the South China block and other areas: Controls on their growth and distribution. Facies 53, 409-425.

Kump, L., Pavlov, A., Arthur, M., 2005. Massive release of hydrogen sulfide to the surface ocean and atmosphere during intervals of oceanic anoxia. Geology 33, 397.

Lance, E., Brient, L., Carpentier, A., Acou, A., Marion, L., Bormans, M., Gérard, C., 2010. Impact of toxic cyanobacteria on gastropods and microcystin accumulation in a eutrophic lake (Grand-Lieu, France) with special reference to Physa (= Physella) acuta. Science of the total environment 408, 3560-3568.

Lehrmann, D.J., 1999. Early Triassic calcimicrobial mounds and biostromes of the Nanpanjiang basin, south China. Geology 27, 359-362.

Lei, Y., Servais, T., Feng, Q.L., He, W.H., 2012. The spatial (nearshore-offshore) distribution of latest Permian phytoplankton from the Yangtze Block, South China. Palaeogeography, Palaeoclimatology, Palaeoecology 363-364, 151-162.

Li, J., Cao, C.Q., Servais, T., Zhu, Y.H., 2004a. Later Permian acritarchs from Meishan (SE China) in the context of Permian palaeobiogeography and palaeoecology. Neues Jahrbuch für Geologie und Paläontologie, Monatshefte, 427-448.

Li, J., Servais, T., Yan, K., Zhu, H.C., 2004b. A nearshore-offshore trend in acritarch distribution from the Early-Middle Ordovician of the Yangtze Platform, South China. Review of Palaeobotany and Palynology 130, 141-161.

Li, Z.S., Zhan, L.P., Zhu, X.F., Zhang, J.H., Jin, R.G., Liu, G.F., Sheng, H.B., Shen, G.M., Dai, J.Y., Huang, H.Q., Xie, L.C., Yan, Z., 1986. Mass extinction and geological events between Palaeozoic and Mesozoic era. Acta Geologica Sinica 60, 1-15.

Limén, H., Ólafsson, E., 2002. Ostracod species-specific utilisation of sediment detritus and newly settled cyanobacteria, Aphanizomenon sp., in the Baltic Sea: evidence from stable carbon isotopes. Marine Biology 140, 733-738.

Lindenthal, A., Langmann, B., Paetsch, J., Lorkowski, I., Hort, M., 2012. The ocean response to volcanic iron fertilisation after the eruption of Kasatochi volcano: a regional scale biogeochemical ocean model study. Biogeosciences Discuss 9, 9233-9257.

Looy, C.V., Twitchett, R.J., Dilcher, D.L., Van Konijnenburg-Van Cittert, J.H.A., Visscher, H., 2001. Life in the end-Permian dead zone. Proceedings of the National Academy of Sciences of the United States of America 98, 7879.

Munnecke, A., Servais, T., 2008. Palaeozoic calcareous plankton: evidence from the Silurian of Gotland. Lethaia 41, 185-194.

Mutwakil, N., Xia, W.C., Zhang, N., 2006. Late Permian (Changhsingian) conodont biozonation and the basal boundary, Ganxi section, western Hubei Province, south China. Canadian Journal of Earth Sciences 43, 121-133.

Nascimento, F.J.A., Karlson, A.M.L., Näslund, J., Gorokhova, E., 2009. Settling cyanobacterial blooms do not improve growth conditions for soft bottom meiofauna. Journal of Experimental Marine Biology and Ecology 368, 138-146.

O’Neil, J.M., Davis, T.W., Burford, M.A., Gobler, C.J., 2012. The rise of harmful cyanobacteria blooms: The potential roles of eutrophication and climate change. Harmful algae 14, 313-334.

Olgun, N., Duggen, S., Croot, P.L., Delmelle, P., Dietze, H., Schacht, U., Óskarsson, N., Siebe, C., Auer, A., Garbe-Schönberg, D., 2011. Surface ocean iron fertilization: The role of airborne volcanic ash from subduction zone and hot spot volcanoes and related iron fluxes into the Pacific Ocean. Global Biogeochemical Cycles 25, GB4001.

Ouyang, S., Utting, J., 1990. Palynology of upper Permian and lower Triassic rocks, Meishan, Changxing County, Zhejiang Province, China. Review of Palaeobotany and Palynology 66, 65-103.

Phlips, E.J., Badylak, S., 1996. Spatial variability in phytoplankton standing crop and composition in a shallow inner-shelf lagoon, Florida Bay, Florida. Bulletin of Marine Science 58, 203-216.

Phlips, E.J., Badylak, S., Lynch, T.C., 1999. Blooms of the picoplanktonic cyanobacterium Synechococcus in Florida Bay, a subtropical inner-shelf lagoon. Limnology and Oceanography, 1166-1175.

Posch, T., Koster, O., Salcher, M.M., Pernthaler, J., 2012. Harmful filamentous cyanobacteria favoured by reduced water turnover with lake warming. Nature Clim. Change advance online publication.

Raup, D.M., Sepkoski Jr, J.J., 1982. Mass extinctions in the marine fossil record. science 215, 1501-1503.

Reichow, M.K., Saunders, A.D., White, R.V., Pringle, M.S., Al'Mukhamedov, A.I., Medvedev, A.I., Kirda, N.P., 2002. 40Ar/39Ar dates from the West Siberian Basin: Siberian flood basalt province doubled. science 296, 1846-1849.

Reichow, M.K., Pringle, M.S., Al'Mukhamedov, A.I., Allen, M.B., Andreichev, V.L., Buslov, M.M., Davies, C.E., Fedoseev, G.S., Fitton, J.G., Inger, S., Medvedev, A.Y., Mitchell, C., Puchkov, V.N., Safonova, I.Y., Scott, R.A., Saunders, A.D., 2009. The timing and extent of the eruption of the Siberian Traps large igneous province: Implications for the end-Permian environmental crisis. Earth and Planetary Science Letters 277, 9-20.

Renne, P.R., Black, M.T., Zichao, Z., Richards, M.A., Basu, A.R., 1995. Synchrony and causal relations between Permian-Triassic boundary crises and Siberian flood volcanism. science 269, 1413.

Sandler, A., Eshet, Y., Schilman, B., 2006. Evidence for a fungal event, methane-hydrate release and soil erosion at the Permian-Triassic boundary in southern Israel. Palaeogeography, Palaeoclimatology, Palaeoecology 242, 68-89.

Schopf, J.W., 1993. Microfossils of the Early Archean Apex chert: new evidence of the antiquity of life. science 260, 640-646.

Sellner, K., Olson, M., Kononen, K., 1994. Copepod grazing in a summer cyanobacteria bloom in the Gulf of Finland. Hydrobiologia 292, 249-254.

Sephton, M.A., Visscher, H., Looy, C.V., Verchovsky, A.B., Watson, J.S., 2009. Chemical constitution of a Permian-Triassic disaster species. Geology 37, 875-878.

Sheldon, N.D., 2006. Abrupt chemical weathering increase across the Permian–Triassic boundary. Palaeogeography, Palaeoclimatology, Palaeoecology 231, 315-321.

Shen, J., Algeo, T.J., Zhou, L., Feng, Q.L., Yu, J.X., Ellwood, B., 2012. Volcanic perturbations of the marine environment in South China preceding the latest Permian mass extinction and their biotic effects. Geobiology 10, 82-103.

Shen, S.Z., Shi, G.R., 1996. Diversity and extinction patterns of Permian Brachiopoda of South China. Historical Biology 12, 93-110.

Shen, S.Z., Shi, G.R., 2002. Paleobiogeographical extinction patterns of Permian brachiopods in the Asian–western Pacific region. Paleobiology 28, 449-463.

Shen, S.Z., Crowley, J.L., Wang, Y., Bowring, S.A., Erwin, D.H., Sadler, P.M., Cao, C.Q., Rothman, D.H., Henderson, C.M., Ramezani, J., 2011. Calibrating the end-Permian mass extinction. science 334, 1367-1372.

Song, H.J., Tong, J.N., Chen, Z.Q., Yang, H., Wang, Y.B., 2009. End-Permian mass extinction of foraminifers in the Nanpanjiang Basin, South China. Journal of Paleontology 83, 718-738.

Song, H.J., Tong, J.N., Chen, Z.Q., 2011. Evolutionary dynamics of the Permian–Triassic foraminifer size: Evidence for Lilliput effect in the end-Permian mass extinction and its aftermath. Palaeogeography, Palaeoclimatology, Palaeoecology 308, 98-110.

Stal, L.J., Albertano, P., Bergman, B., Bröckel, K.v., Gallon, J.R., Hayes, P.K., Sivonen, K., Walsby, A.E., 2003. BASIC: Baltic Sea cyanobacteria. An investigation of the structure and dynamics of water blooms of cyanobacteria in the Baltic Sea—responses to a changing environment. Continental Shelf Research 23, 1695-1714.

Steiner, M.B., Eshet, Y., Rampino, M.R., Schwindt, D.M., 2003. Fungal abundance spike and the Permian-Triassic boundary in the Karoo Supergroup (South Africa). Palaeogeography, Palaeoclimatology, Palaeoecology 194, 405-414.

Sun, Y.D., Joachimski, M.M., Wignall, P.B., Yan, C.B., Chen, Y.L., Jiang, H.S., Wang, L.N., Lai, X.L., 2012. Lethally Hot Temperatures During the Early Triassic Greenhouse. science 338, 366-370.

Tyson, R.V., Follows, B., 2000. Palynofacies prediction of distance from sediment source: A case study from the Upper Cretaceous of the Pyrenees. Geology 28, 569.

Vahtera, E., Conley, D.J., Gustafsson, B.G., Kuosa, H., Pitkänen, H., Savchuk, O.P., Tamminen, T., Viitasalo, M., Voss, M., Wasmund, N., 2007. Internal ecosystem feedbacks enhance nitrogen-fixing cyanobacteria blooms and complicate management in the Baltic Sea. AMBIO: A journal of the Human Environment 36, 186-194.

Villier, L., Korn, D., 2004. Morphological Disparity of Ammonoids and the Mark of Permian Mass Extinctions. science 306, 264-266.

Visscher, H., Brinkhuis, H., Dilcher, D., Elsik, W., Eshet, Y., Looy, C., Rampino, M., Traverse, A., 1996. The terminal Paleozoic fungal event: evidence of terrestrial ecosystem destabilization and collapse. Proceedings of the National Academy of Sciences of the United States of America 93, 2155-2158.

Visscher, H., Sephton, M.A., Looy, C.V., 2011. Fungal virulence at the time of the end-Permian biosphere crisis? Geology 39, 883-886.

Walsby, A., Dubinsky, Z., Kromkamp, J., Lehmann, C., Schanz, F., 2001. The effects of diel changes in photosynthetic coefficients and depth of Planktothrix rubescens on the daily integral of photosynthesis in Lake Zürich. Aquatic Sciences-Research Across Boundaries 63, 326-349.

Wang, Y.B., Tong, J.N., Wang, J.S., Zhou, X.G., 2005. Calcimicrobialite after end-Permian mass extinction in South China and its palaeoenvironmental significance. Chinese Science Bulletin 50, 665-671.

Wiegand, C., Pflugmacher, S., 2005. Ecotoxicological effects of selected cyanobacterial secondary metabolites a short review. Toxicology and Applied Pharmacology 203, 201-218.

Wignall, P., Twitchett, R., 1996. Oceanic anoxia and the end Permian mass extinction. science 272, 1155-1158.

Wu, S.B., Li, Q., Wang, W.W., 1988. Characteristics of stratigrphical and faunal changes near the Permo-Triassic boundary in the huayungshan area, Sichuan Province. Geoscience 2, 375-385.

Xie, S.C., Pancost, R.D., Yin, H.F., Wang, H.M., Evershed, R.P., 2005. Two episodes of microbial change coupled with Permo/Triassic faunal mass extinction. Nature 434, 494-497.

Xie, S.C., Pancost, R.D., Huang, J.H., Wignall, P.B., Yu, J.X., Tang, X.Y., Chen, L., Huang, X.Y., Lai, X.L., 2007. Changes in the global carbon cycle occurred as two episodes during the Permian-Triassic crisis. Geology 35, 1083-1086.

Xie, S.C., Pancost, R.D., Wang, Y.B., Yang, H., Wignall, P.B., Luo, G.M., Jia, C.L., Chen, L., 2010. Cyanobacterial blooms tied to volcanism during the 5 my Permo-Triassic biotic crisis. Geology 38, 447-450.

Yin, H.F., Zhang, K.X., Tong, J.N., Yang, Z.Y., Wu, S.B., 2001. The global stratotype section and point (GSSP) of the Permian-Triassic boundary. Episodes 24, 102-114.

Zhang, K.X., Lai, X.L., Tong, J.N., Jiang, H.S., 2009. Progresses on study of conodont sequence for the GSSP section at Meishan, Changxing, Zhejiang Province, South China. Acta Palaeontologica Sinica 48, 474-486.

Ziegler, A.M., Hulver, M.L., Rowley, D.B., 1996. Permian world topography and climate. In:

Martini, I. P. (ed.). Late glacial and postglacial environmental changes-Quaternary, Carboniferous-Permian and Proterozoic, 111-146.

Zwirglmaier, K., Jardillier, L., Ostrowski, M., Mazard, S., Garczarek, L., Vaulot, D., Not, F., Massana, R., Ulloa, O., Scanlan, D.J., 2008. Global phylogeography of marine Synechococcus and Prochlorococcus reveals a distinct partitioning of lineages among oceanic biomes. Environmental microbiology 10, 147-161.

Figure captions

Fig. 1: Latest Permian paleogeography of the world (A, modified after Ziegler et al., 1997) and south China (B, modified after Feng and Gu, 2002). The distribution of calci-microbialites and Late Permian acritarchs are from Kershaw et al. (2007);Jiang et al. (2008); Xie et al. (2010); and Lei et al. (in press).

Fig. 2: The Permian-Triassic Boundary sequence of south China. The data are provided for each conodont zone. MS: Meishan; ZZ: Zhongzhai; SS: Shangsi; LFY: Liangfengya; XK: Xiakou; GX: Ganxi; DP: Dongpan. ME: mass extinction. *I. is.*: *Isarcicella isarcica*; *I. s.*: *Isarcicella staeschei*; *H. p.*: *Hindeodus parvus*; *C. t.*: *Clarkina taylorae*; *H. c.*: *Hindeodus changxingensis*; *C. m.*: *Clarkina meishanensis*; *C.y.*: *Clarkina yini*; *C. ch.*: *Clarkina changxingensis*. The original references are as follows: Meishan section, Yin et al. (2001); conodont zones, Zhang et al. (2009); sequences, Yin et al. (in press); diversity of animals, Jin et al. (2000); C_{31} 2-MHP, Xie et al. (2010); estimated water temperatures, Joachimski et al. (2012); absolute ages, Shen et al. (2011). The information of beds and conodont zones in other sections are modified respectively from (Li et al., 1986; He et al., 2005, 2007a, b, 2008; Feng et al., 2007; Jiang et al., 2011; Shen et al., 2012). The data of acritarchs shown in Table 1 based on Lei et al., 2012, except for the new data of the Liangfengya and Ganxi sections. The data of C_{31} 2-MHP in the Shangsi section are from Xie et al. (unpublished data)

Fig. 3: Selected microphotographs of acritarchs species of the Permian-Triassic boundary interval of south China. 1-2: *Veryhachium hyalodermum*; 3-5: *Veryhachium sedecimspinosum*; 6-9: *Michrystridium stellatum*; 10-11: *Michrystridium breve*; 12: *Schizosporis* sp.; 13-15: *Leiosphaeridia minutissima*; 16-17: *Leiosphaeridia micrograniferа*; 18-20: *Dictyotidium reticulatum*. The bar is 25 μm for 18-20, and 15 μm for 10-12, and 10 μm for the rest.

Table captions

Table 1: The concentrations of acritarch during the Permian to Triassic boundary, south China (particles/g).

Fig. 1

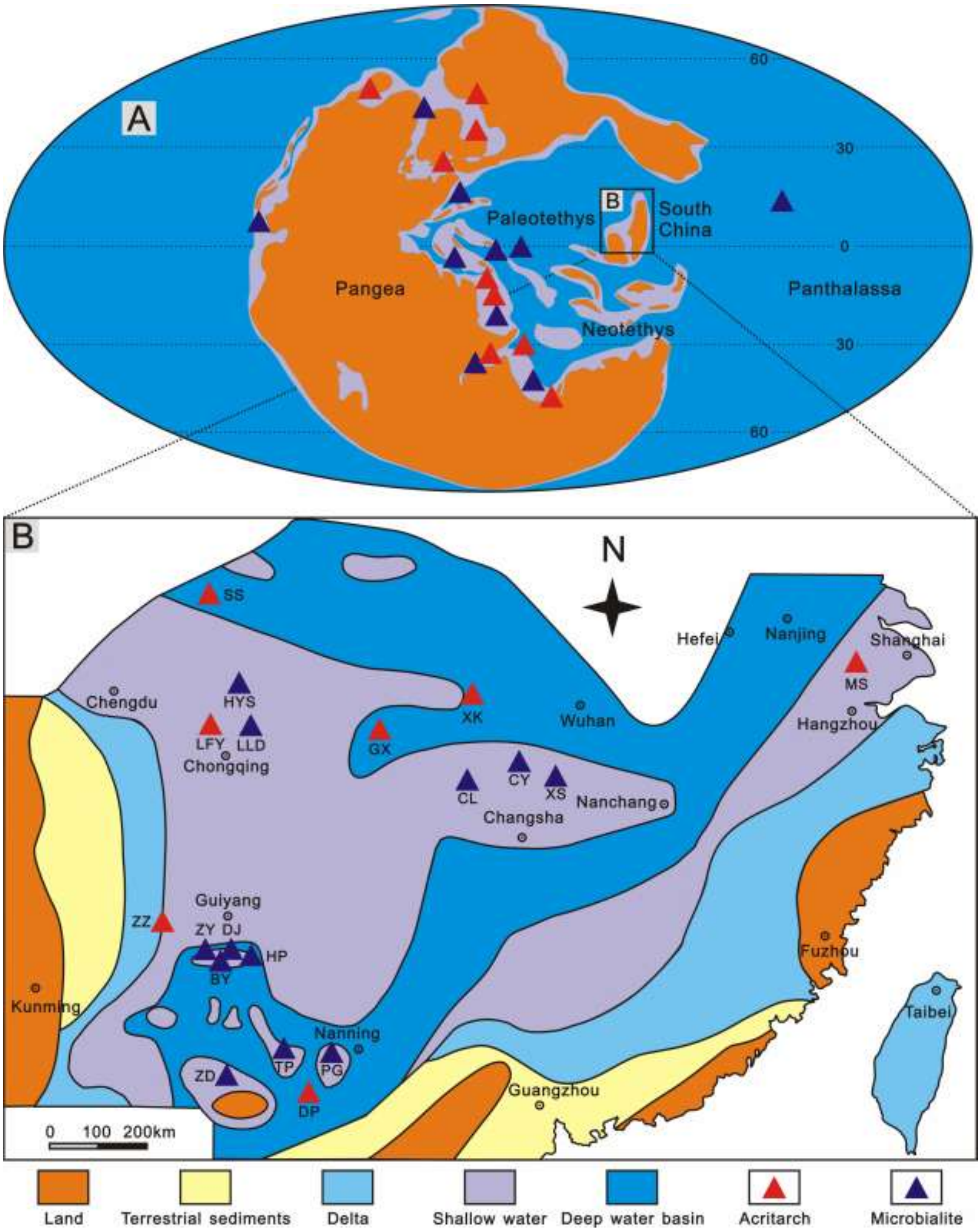
A
60
30
0
30
60
B
South China
Paleotethys
Pangea
Panthalassa
Neotethys
B
N
SS
Hefei
Nanjing
Shanghai
MS
Hangzhou
Chengdu
HYS
LFY
LLD
Chongqing
XK
GX
Wuhan
CY
CL
XS
Nanchang
Changsha
Guiyang
ZZ
ZY
DJ
HP
BY
Fuzhou
Kunming
Taibei
Nanning
TP
PG
ZD
DP
Guangzhou
0 100 200km
Land
Terrestrial sediments
Delta
Shallow water
Deep water basin
Acritarch
Microbialite

Fig. 2

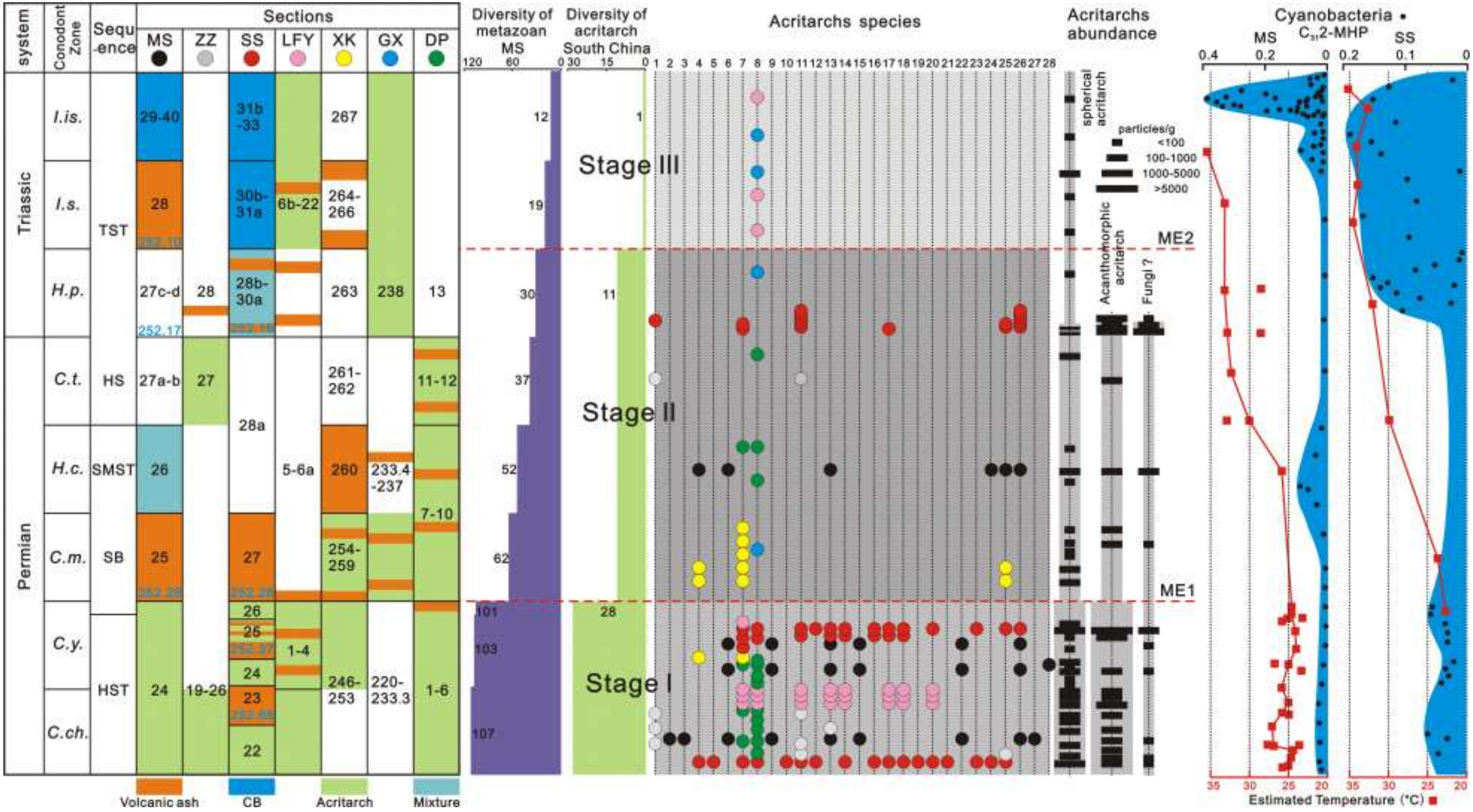
system
Conodont Zone
Sequ-ence
Sections
MS
ZZ
SS
LFY
XK
GX
DP
Triassic
Permian
I.is.
I.s.
H.p.
C.t.
H.c.
C.m.
C.y.
C.ch.
TST
HS
SMST
SB
HST
29-40
31b-33
267
28
30b-31a
6b-22
264-266
252.10
27c-d
28
28b-30a
263
238
13
252.17
252.16
27a-b
27
261-262
11-12
28a
26
5-6a
260
233.4-237
7-10
25
27
254-259
252.28
26
25
1-4
24
24
19-26
246-253
220-233.3
1-6
23
22
Volcanic ash
CB
Acritarch
Mixture
Diversity of metazoan MS
120
60
0
12
19
30
37
52
62
101
103
107
Diversity of acritarch South China
30
15
0
1
11
28
Stage III
Stage II
Stage I
Acritarchs species
1 2 3 4 5 6 7 8 9 10 11 12 13 14 15 16 17 18 19 20 21 22 23 24 25 26 27 28
ME2
ME1
Acritarchs abundance
spherical acritarch
particles/g
<100
100-1000
1000-5000
>5000
Acanthomorphic acritarch
Fungi ?
Cyanobacteria •
MS
C_{31}2-MHP
SS
0.4
0.2
0
0.2
0.1
0
35
30
25
20
35
30
25
20
Estimated Temperature (°C) ■

Fig. 3

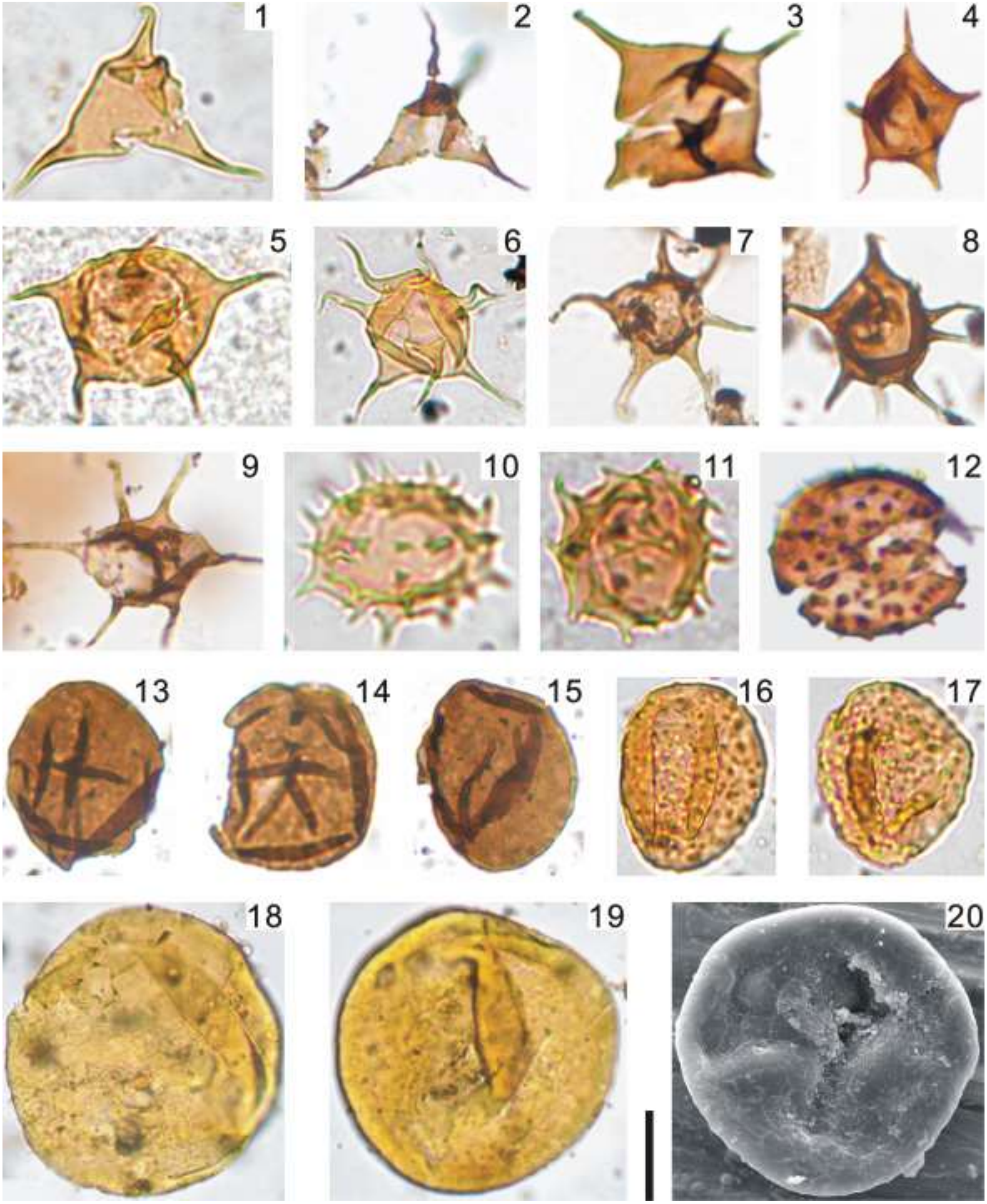

Table 1

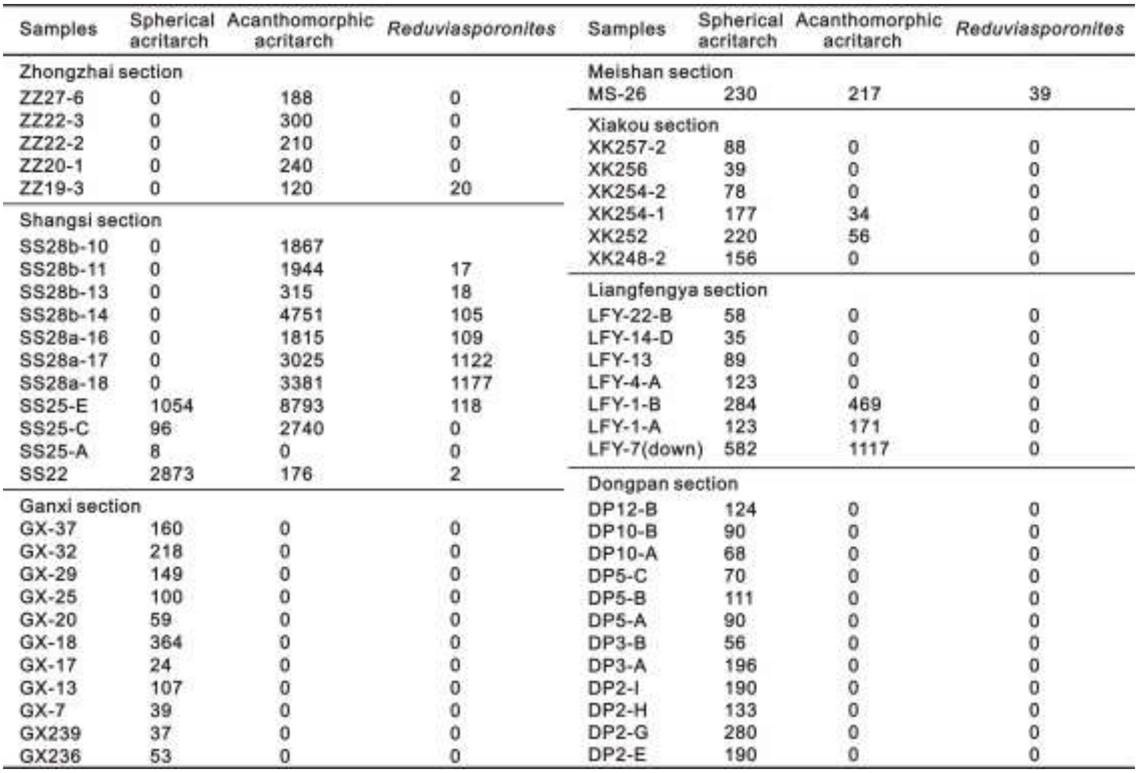

Samples	Spherical acritarch	Acanthomorphic acritarch	*Reduviasporonites*
Zhongzhai section			
ZZ27-6	0	188	0
ZZ22-3	0	300	0
ZZ22-2	0	210	0
ZZ20-1	0	240	0
ZZ19-3	0	120	20
Shangsi section			
SS28b-10	0	1867	
SS28b-11	0	1944	17
SS28b-13	0	315	18
SS28b-14	0	4751	105
SS28a-16	0	1815	109
SS28a-17	0	3025	1122
SS28a-18	0	3381	1177
SS25-E	1054	8793	118
SS25-C	96	2740	0
SS25-A	8	0	0
SS22	2873	176	2
Ganxi section			
GX-37	160	0	0
GX-32	218	0	0
GX-29	149	0	0
GX-25	100	0	0
GX-20	59	0	0
GX-18	364	0	0
GX-17	24	0	0
GX-13	107	0	0
GX-7	39	0	0
GX239	37	0	0
GX236	53	0	0
Meishan section			
MS-26	230	217	39
Xiakou section			
XK257-2	88	0	0
XK256	39	0	0
XK254-2	78	0	0
XK254-1	177	34	0
XK252	220	56	0
XK248-2	156	0	0
Liangfengya section			
LFY-22-B	58	0	0
LFY-14-D	35	0	0
LFY-13	89	0	0
LFY-4-A	123	0	0
LFY-1-B	284	469	0
LFY-1-A	123	171	0
LFY-7(down)	582	1117	0
Dongpan section			
DP12-B	124	0	0
DP10-B	90	0	0
DP10-A	68	0	0
DP5-C	70	0	0
DP5-B	111	0	0
DP5-A	90	0	0
DP3-B	56	0	0
DP3-A	196	0	0
DP2-I	190	0	0
DP2-H	133	0	0
DP2-G	280	0	0
DP2-E	190	0	0

Paper 5: (Section 5)
Accepted for publication in Palynology

Latest Permian acritarchs from South China and the *Micrhystridium*/*Veryhachium* complex revisited

Yong Lei [1, 2, *], Thomas Servais [2], Qinglai Feng [1], Weihong He [3]

[1] State Key Laboratory of Geological Process and Mineral Resources, China University of Geosciences, Wuhan, Hubei, China
[2] UMR 8217 Géosystèmes, CNRS-Université Lille1, Cité Scientifique, F-59655 Villeneuve d'Ascq, France
[3] State Key Laboratory of Biogeology and Environmental Geology, China University of Geosciences, Wuhan, China
*Corresponding author, E-mail: leiyongdida@163.com;
Tel: +86-13485387952
Thomas Servais, thomas.servais@univ-lille1.fr;
Fax: +33-320436900; Tel: +33-320337220
Qinglai Feng, qinglaifeng@cug.edu.cn; Tel: +86-027-67883006
Weihong He, whzhang@cug.edu.cn; Tel: +86-18971049779

Abstract. Diverse and well-preserved latest Permian phytoplankton assemblages are described from four sections of the Yangtze Block (South China) from the localities Zhongzhai (Guizhou Province), Shangsi (Sichuan Province), Xiakou (Hubei Province) and Dongpan (Guangxi Province). Most of the species have been reported previously from other Late Permian sections worldwide. The South Chinese phytoplankton taxa are generally very small in size, usually displaying diameters of about 20 µm, and commonly include the genera *Micrhystridium*, *Veryhachium* and *Leiosphaeridia*. However, lager taxa with vesicles often exceeding 80µm in diameter, such as *Dictyotidium*, are also abundant in the Shangsi section.

Due to the presence of large populations of *Micrhystridium* and *Veryhachium*, a simple classification scheme for the *Micrhystridium*/*Veryhachium* complex is proposed, based on the geometrical shape of the vesicle. We propose dividing the complex into five groups: the *Veryhachium cylindricum* group, representing all ellipsoidal specimens; the *Veryhachium trispinosum* group, all with triangular shape vesicles; the *Veryhachium lairdii* group, all with rectangular forms; the *Micrhystridium pentagonale* group, all with pentagonal specimens; and the *Micrhystridium breve* group, with includes all spherical forms.

Keywords: phytoplankton, *Micrhystridium*/*Veryhachium* complex, Late Permian, Yangtze Block

1. Introduction

The group Acritarcha was created by Evitt (1963) as an informal grouping of all organic-walled microfossils with unknown or uncertain biological affinities (Servais 1996; Strother 1996). They first appear in the Proterozoic and reached maximum diversity during the early and middle Paleozoic, especially during the Ordovician and Early Devonian (Strother 1996; Servais et al. 2004, 2008). However, acritarch diversity dropped dramatically in the Late Paleozoic, particularly between the Late Devonian and Carboniferous, with very low diversities in the Carboniferous and Permian, leading to almost a complete absence of organic-walled microplankton, that was named by Riegel (1996, 2008) the 'Phytoplankton Blackout'. Servais et al. (2006) questioned the existence of a 'phytoplankton blackout,' because the absence of resting cysts in the fossil record does not necessarily imply the absence of phytoplanktonic cyst-building organisms in the Late Palaeozoic oceans. Subsequently, Mullins and Servais (2008) reviewed the diversity of the Carboniferous phytoplankton, and noted that phytoplankton diversity was still high in the earliest Carboniferous, but declined significantly from the Tournaisian to the Serpukhovian. Phytoplankton diversity in the Late Carboniferous was generally very low, with typically only one to three species being documented in each assemblage (Mullins and Servais 2008). Subsequently, Lei et al. (accepted for publication) similarly reviewed the diversity of the phytoplankton of the Permian, and pointed out that phytoplankton diversities were much more important than previously assumed, with highest diversities in the Early Permian and the latest Permian, where more than 30 phytoplankton genera have been reported.

Chinese acritarch studies, like elsewhere also focused mainly on the Early and Middle Paleozoic, with only a few studies in the Permian (Li et al. 2002, 2004). In the Late Permian of South China, most palynological investigations were focused on the taxonomy and biostratigraphy of spores and pollen grains. Only four papers published so far (Ouyang 1982, 1986; Ouyang and Utting 1990; Li et al. 2004) have described acritarchs from the Permian-Triassic boundary (PTB), documenting the presence of 13 genera of acritarchs and related forms: *Archaeodinium, Baltisphaeridium*, *Cymatiosphaera*, *Dictyotidium*, *Leiosphaeridia*, *Micrhystridium*, *Psiloschizosporis*, *Veryhachium*, *Reduviasporonites*, *Schizosporis*, *Solisphaeridium*, *Tasmanites* and *Tunisphaeridium*. In these studies, the small taxa (diameter ca. 20 μm, such as *Micrhystridium*, *Veryhachium* and some species of *Leiosphaeridia*) are the most common.

This paper will document the Late Permian acritarch populations from four sections of the Yangtze Block, South China, with a special focus on the dominant group of taxa belonging to the *Micrhystridium*/*Veryhachium* complex, for which we propose a simple classification scheme of five informal groups.

2. Geology setting

The Yangtze Block, South China, displays numerous continuous sections of Upper Permian and Lower Triassic sediments from different paleoenvironments, ranging from nearshore to platform and slope setting (Figure 1-C). For the present study, four sections have been investigated in the Guizhou, Sichuan, Hubei, Guangxi province (Figure 1-A, B). For each of these sections, the reader is referred to the corresponding geological and paleontological studies published.

2.1. Zhongzhai section

The Zhongzhai section (26°09.110N and 105°17.113E) is located about 5 km north of the Zhongzhai Village, near Langdai Town, Liuzhi County, Guizhou Province (He et al. 2008). The section is located in the western Yangtze Block (Figure 1) and it includes the uppermost Longtan Formation (beds 1 to 27) and the lowermost Yelang Formation (beds 28 to 37) that are investigated in this study. The Longtan Formation is mainly composed of brownish sandstones and mudstones with a few limestone intervals. The lowermost Yelang Formation is dominated by yellowish green or purplish red silty calcareous mudstones, and a few limestones and claystones at its base. According to the conodont zonation, Metcalfe and Nicoll (2007) considered that the Permian-Triassic boundary (PTB) at the Zhongzhai section is located in bed 28 (Figure 2). Recently, based on the U-Pb dates, the absolute age determination from the claystone of bed 29 by Shen et al. (2011), indicated an age of 252.24 ±0.13 Ma.

2.2. Shangsi section

The Shangsi section is located near Guangyuan city in the northern part of Sichuan Province, and belongs to the northwestern corner of the Yangtze Block (Lai et al. 1996) (Figure 1). Both the Dalong (upper Wuchiapingian to Changhsingian) and the Feixianguan formations (Induan) are exposed here. The geology of the Shangsi section was first described by Li et al. (1986). The interval from beds 17 to 22 is dominated by an alternation of carbonaceous-siliceous rocks and siliceous limestone with a few mudstone intervals. The interval from beds 23 to 29 is mainly composed of siliceous mudstones and calcareous mudstones with few claystone. Recently, Jiang et al. (2011) suggested that the PTB be placed 22 cm above the base of bed 28, based on hindeodid and gondolellid conodont taxa. Similarly to the Zhongzhai section, an absolute age (252.28 ±0.13 Ma) was determinated from the claystones of bed 27 by Shen et al. (2011).

2.3. Xiakou section

The Xiakou section (31°06.874 N and 111°48.221E) is situated near the town of Xiakou, in Xingshan County, Yichang city, Hubei Province. It is located in the north of the Yangtze Block (Wang and Xia 2004) (Figure 1) and comprises the uppermost Changxing Formation (beds 223 to 256), which is dominated by mudstones and muddy limestones, and the lowermost Daye

Formation (beds 257 to 270), which is dominated by mudstones with a few claystones. According to the new conodont biozonation, the PTB is placed in bed 262 (Shen et al. 2012a), rather than in bed 266 (Wang and Xia 2004; Hong et al. 2008, 2011).

2.4. Dongpan section

The Dongpan section, located at 22°16.196 N and 107°41.505 E (Shen et al. 2012b), is situated 80 km southwest of Nanning, Guangxi Province, in the southern portion of the Yangtze Block (He et al. 2007b) (Figure 1). Here, the Dalong Formation (beds 2 to 12) and the Luolou Formation (beds 13 to 14) are exposed. The interval from beds 2 to 8 is mainly composed of bedded siliceous rocks, muddy siliceous rocks and mudstones. The interval from beds 9 to 14 is dominated by mudstones and silty mudstones with thin intercalations of claystones (Feng et al. 2007). According to He et al. (2005, 2007a, b) and Feng et al. (2007), beds 2 to 12 are considered to be Late Changhsingian in age and bed 13 is considered to be Early Induan in age.

3. Material and methods

Two hundred sixty nine samples have been collected from these four sections (45 samples from the Zhongzhai section; 141 samples from Shangsi; 60 samples from Xiakou; 23 samples from Dongpan). All of the samples were processed for palynological analysis.

Fifty grams of each sample were prepared according to standard palynological methods. After treatment with hydrochloric acid (33%) and hydrofluoric acid (40%), the samples were concentrated by treatment with zinc bromide solution (S.G. 2.2). The samples were not oxidized or sieved. The residue was studied using light microscopy and scanning electron microscopy (SEM). All residues are stored in the collections of the China University of Geosciences (Wuhan).

4. Palynological results

The present investigation indicates that diverse and abundant phytoplankton occur in the latest Permian of the Yangtze Block, South China, from the four different sections investigated herein (Figure 2). The highest diversity is observed in the Shangsi section, with twenty species and eight genera recorded in 37 samples, including *Baltisphaeridium* sp., *Dictyotidium reticulatum*, *D.* sp., *Leiofusa* sp., *Leiosphaeridia microgranifera*, *L. minutissima*, *Micrhystridium breve*, *M. fragile*, *M. pentagonale*, *M. stellatum*, *Reduviasporonites catenulatus*, *R. chalastus*, *Schizosporis scissus*, *S.* sp., *Veryhachium cylindricum*, *V. hyalodermum*, *V. nasicum*, *V. quadratum*, *V. sedecimspinosum* and *V.* sp.

In the Zhongzhai and Xiakou sections, only a few species occur in several samples, including *Baltisphaeridium* sp., *Dictyotidium reticulatum*, *Leiosphaeridia micrograntfera*, *Micrhystridium pentagonale*, *M. stellatum*, *Reduviasporonites catenulatus* and *R. chalastus*. In addition, only two species of *Leiosphaeridia* occur in the Dongpan section. However, they are abundant in 15 samples (Figure 2). The palynofacies changes in the Shangsi section is described in a separate paper (Lei et al. submitted), and the paleoenvironmental distribution of the different microphytoplankton taxa has been interpreted by Lei et al. (2012). The present paper describes the systematical paleontology of the investigated assemblages, with a special focus on the *Micrhystridium*/*Veryhachium* complex.

5. The *Micrhystridium*/*Veryhachium* complex revisited

The genera *Micrhystridium* Deflandre 1937 and *Veryhachium* Deunff 1954 are among the most widely recorded acritarch genera throughout the entire Phanerozoic. Fensome et al. (1990) listed more than 200 species of them respectively. With a wide range of diagnoses, they became typical 'waste-basket' genera, similar to other genera, such as *Baltisphaeridium* (Eisenack 1958) Eisenack 1969, *Multiplicisphaeridium* Staplin 1961, and *Polygonium* Vavrdová 1966 (Servais et al. 2007). Many palynologists described new species of small spherical acanthomorth acritarchs and placed them in *Micrhystridium* whereas numerous new small polygonal acritarch species were attributed to *Veryhachium*. However, because the interspecific variability is very great, it is commonly difficult, if not impossible, to distinguish the different species, as well as differentiating the two genera. These genera and their species thus form a large plexus with a continuum of intermediate morphotypes.

Generally, the Permian specimens attributed to *Micrhystridium* display a spherical or oval vesicle, bearing many proximally open spines with closed tips, most often simple, and rarely branching. The vesicle diameter is usually less than 20 µm (larger species were usually attributed to the genera *Baltisphaeridium* and/or *Multiplicisphaeridium*). On the other hand, *Veryhachium* embraces all smaller acritarchs with polygonal body outlines and less than eight spines.

In the Permian, the two genera *Micrhystridium* and *Veryhachium* are very frequent. According to a recent literature search, 27 species of *Micrhystridium* were recorded 55 times in 26 publications, whereas 22 species of *Veryhachium* were documented 46 times (Lei et al. accepted for publication). At the species level, *Micrhystridium breve*, *M. stellatum* and *Veryhachium reductum* are the most frequently reported species of the *Micrhystridium*/*Veryhachium* complex (Lei et al. accepted for publication).

The genera *Micrhystridium* and *Veryhachium* have a complex taxonomical history and both have been revised and reviewed by many authors (see Sarjeant and Stancliffe 1994; Servais et al. 2007). The taxonomy is still being debated, and it remains difficult to identify some of the individual species. This problem of identification was noted very early, and some authors used the term *Micrhystridium*/*Veryhachium* complex several decades ago (e.g., Wall and Downie 1963; Visscher and Brugman 1981; Sarjeant and Stancliffe 1994; Eshet et al. 1995; Li et al. 2004; Van de Schootbrugge et al. 2005; Riegel 2008).

It is not the objective of this paper to fully review the classification scheme of the two genera, or to emend their diagnose which have been modified several times already. A full revision, including population analyses with biometrical studies, of all described taxa of the genera

Micrhystridium and *Veryhachium,* is necessary in order to understand the taxonomy of these taxa and to provide synonomical lists. Our objective is to propose a simple classification scheme that can easily be used for the analyses of latest Permian phytoplankton assemblages, especially by all palynologists that do not describe the acritarch taxonomy in detail. However, the simplified classification scheme presented here has not the intention to consider all previously described taxa as synonyms.

In the present study of Late Permian phytoplankton assemblages from South China, ten morphotypes within the *Micrhystridium*/*Veryhachium* complex are recognized and are here tentatively attributed to formerly described species. However, interspecific and intergeneric variability is large and it is difficult to draw clear lines between the previously and formally described species. For identifying this complex more easily, we propose to divide them into five informal categories, which are based on the geometrical shape of the vesicle and do not take into account the morphologies of the spines (or appendices) (Figure 3).

Servais et al. (2007) revised the oldest morphotypes of *Veryhachium* that first appeared in the Ordovician and, following the informal usage of several authors, proposed two informal groups for the genus *Veryhachium* in order to facilitate their classification: the *Veryhachium trispinosum* group was proposed for triangular specimens, and the *Veryhachium lairdii* group for rectangular forms.

Compared to the Ordovician, the Permian morphotypes of *Veryhachium* are even more variable and include morphological transients that range into the genus *Micrhystridium*. Therefore, we continue the reasoning of Servais et al. (2007) and propose three additional informal groupings to facilitate the classification of these morphotypes in the Late Paleozoic. The informal *Veryhachium cylindricum* group is here proposed to include all ellipsoidal specimens of *Veryhachium*, whereas two informal groups for *Micrhystridium* are proposed. These correspond to the *Micrhystridium pentagonale* group for all pentagonal and hexagonal specimens, and the *Micrhystridium breve* group for all spherical specimens.

In our study, the *Veryhachium cylindricum* group includes the previously described species *Veryhachium cylindricum* (Table 1). The *Veryhachium trispinosum* group includes all triangular specimens, among them *Veryhachium hyalodermum* and *Veryhachium* sp. The *Veryhachium lairdii* group includes all morphotypes with rectangular or square vesicles, such as *Veryhachium nasicum*, *V. quadratum* and *V. sedecimspinosum*. The *Micrhystridium pentagonale* group includes the two species *Micrhystridium pentagonale* and *M. stellatum*, whereas the *Micrhystridium breve* group includes both *Micrhystridium fragile* and *M. breve*. It is clear that this proposal is a tentative classification into an informal subgeneric scheme, and other geometrical shape-like groupings could be added if necessary. The idealized line drawings of Figure 3 illustrate that all vesicle shapes from triangular to square, pentagonal to polygonal, round and ellipsoidal, may exist, and the microphotographs of Plate 2 show that morphotypes with such vesicles shapes are actually present in the Permian assemblages. It is obvious that these specimens belong to a

Micrhystridium/*Veryhachium* complex and that the determination at the specific level becomes problematical when dealing with larger populations, as those recorded from the Chinese Permian.

The objective of this tentative classification into informal groupings is simply to propose a rapid classification scheme of the *Micrhystridium*/*Veryhachium* complex. We do not know if these morphotypes actually represent the cysts of a single biological species or of a greater number of taxa. It is beyond the scope of this paper to answer that question. However, future research, such as analysis of the biomarkers or biochemistry of the vesicle walls would help facilitate a better understanding of the generic relationship of the different taxa. Interestingly, Grice et al. (2005) and Hays et al. (2011) analyzed the biomarker of sediments from Greenland at the Permian-Triassic boundary, and suggested that the C33 *n*-alkylcyclohexane maybe a potential biomarker for the *Micrhystridium*/*Veryhachium* complex. So far, these data result from the analyses of both *Micrhystridium* and *Veryhachium*. Future research of separated *Micrhystridium* and *Veryhachium* populations may provide more precise interpretations.

6. Systematic paleontology

Acritarchs are, by definition (Evitt 1963; see also Servais 1996) organic-walled microfossils of unknown biological affinities. Several authors have suggested, mostly based on morphological comparisons with extant phytoplankton, biological relationships with various microalgal groups. According to various authors (e.g. Colbath and Grenfell 1995; Le Hérissé et al., 2009), the genera *Dictyotidium*, *Leiosphaeridia* and *Schizosporis* could be related to the green algae (Prasinophyceae and Zygnematophyceae). We follow this suggestion, without providing arguments for or against this interpretation. In addition, the animated debate of whether *Reduviasporonites* is of algal origin or a fungal spore continues (Eshet et al. 1995; Visscher et al. 1996, 2011; Afonin et al. 2001; Foster et al. 2002; Sephton et al. 2009). We do not discuss herein the biological affinity of *Reduviasporonites*, and tentatively place it in the acritarchs. All acritarchs are classified as 'Incertae sedis' and listed in alphabetical order.

Algae
Division Chlorophyta Pascher 1914
Class Prasinophyceae Christensen 1962
Order Not assigned
Family Pterosphaeridiaceae Mädler 1963
Genus *Dictyotidium* Eisenack 1955 emend. Staplin 1961
Type species. *Dictyotidium dietyotum* (Eisenack 1938) Eisenack 1955

Dictyotidium reticulatum Schulz 1965
Plate 1, figures 1-12
Dictyotidium reticulatum Schulz 1965, p. 278, pl. 23, figs. 12-14

Description. The vesicle is spherical to subspherical, and covered by a reticulate ornamentation. The ornamentation includes irregular and interconnected fields, with four to six ridges. The width of each ridge is ca. 4-10 μm. The wall is approximately 2-5 μm thick and usually folded. Folds are straight or slightly sinuous. The wall occasionally splits open.
Dimensions. Vesicle diameter 52(76)110 μm, 45 specimens measured.
Remarks. In Permian strata, the morphology and size of *Dictyotidium reticulatum* are comparable to those of *Leiosphaeridia changxingesis* Ouyang & Utting 1990. However, the surface of the two species is very different. The former is covered by an ornamentation of irregular ridges, whereas the latter is nearly laevigate to slightly scabrate, or punctuate with locally developed ridges.
Previous records. Permian, China (Ouyang and Utting 1990); Norway (Mangerud 1994); Triassic, Germany (Schulz 1965); Spain (Besems 1981).
Stratigraphic occurrence. Abundant in beds 15 to 22 of the Shangsi section, and present in the Xiakou section.

Dictyotidium sp.
Plate 3, figures 11-12
Description. The vesicle is spherical. The surface of the vesicle is covered by irregular and interconnected fields, four to six-sided with ridges commonly 2-4 μm long, the fields are mostly hollow.
Dimensions. Vesicle diameter 30(36)42 μm, 5 specimens measured.
Remarks. The vesicle of this species is nearly spherical in shape, and generally not folded. The fields are much smaller than those of *Dictyotidium reticulatum*.
Stratigraphic occurrence. Present in bed 22 of the Shangsi section.

Genus *Leiosphaeridia* Eisenack 1958 emend. Downie & Sarjeant 1963
Type species. *Leiosphaeridia baltica* Eisenack 1958

Leiosphaeridia micrograntifera (Staplin 1961) Downie & Sarjeant 1963
Plate 3, figures 19-21
Protoleiosphaeridium micrograntifera Staplin 1961, p. 405, pl. 48, fig. 4
Leiosphaeridia micrograntifera (Staplin 1961) Downie & Sarjeant 1963, p.124

Description. The vesicle is ellipsoidal to spherical in outline, commonly folded, with a dense granulose wall. The granules are rounded, clearly separated, and about 0.5 μm in diameter.
Dimensions. Vesicle diameter 25(32)40 μm, 14 specimens measured.
Remarks. This species is similar to *Leiosphaeridia granulosa* Staplin 1961. However, the vesicle of the former is much larger and the granules are much smaller (0.5 μm in diameter) than that on

the latter (1 μm diameter).

Previous records. Lower Silurian, Pennsylvania (Johnson 1985); Upper Devonian, Canada (Staplin 1961)

Stratigraphic occurrence. Abundant in the Shangsi and Xiakou sections.

Leiosphaeridia minutissima (Naumova 1949) Jankauskas 1989
Plate 3, figures 13-18
Leiosphaeridia minutissima Naumova 1949, p. 52-53, pl. 1, figs. 1-2, pl. 2, figs. 1-2
Leiosphaeridia minutissima (Naumova 1949) Jankauskas 1989, p. 79-80, pl. 9, figs. 1-4, 11

Description. The vesicle is spherical to subspherical, smooth, single layered, always folded with the folds being straight or slightly sinuous.

Dimensions. Vesicle diameter 25(31)40 μm, 23 specimens measured.

Remarks. The outline of this species is similar to that of *Leiosphaeridia microgranifera*, and both of them are generally folded. However, the surfaces of the two species are usually very different. *L. minutissima* has a smooth vesicle wall, whereas *L. microgranifera* displays dense granules.

Previous records. Neoproterozoic, Canada (Butterfield and Chandler 1992); Congo (Gaucher and Germs 2006); Czech Republic (Vavrdová 2008); India (Bhat et al. 2009); Russia (Maslov 2004; Stanevich et al. 2007; Vorob'eva et al. 2009); Ediacaran, Poland (Moczydlowska 2008); Ukraine (Leonov and Ragozina 2007); Uruguay (Gaucher et al. 2008); Cambrian, Czech Republic (Konzalová 1995; Steiner and Fatka 1996); Russia (Naumova 1949)

Stratigraphic occurrence. Abundant in the Shangsi and Dongpan sections.

Class Zygnematophyceae Round 1971
Order Zygnematales Borge & Pascher 1913
Family Zygnemataceae Kützing 1843
Genus *Schizosporis* Cookson and Dettmann 1959 emend. Pierce 1976
Type species. *Schizosporis reticulatus* Cookson & Dettmann 1959

Schizosporis scissus (Balme & Hennelly 1956) Hart 1965
Plate 3, figures 8-10
Laevigatosporites scissus Balme & Hennelly 1956, p. 56, pl.1, figs. 6-9
Spheripollenites scissus (Balme & Hennelly 1956) Jansonius 1962, p. 82, pl. 16, fig. 8
Schizosporis scissus (Balme & Hennelly 1956) Hart 1965, p. 14

Description. The vesicle is subspherical. The laevigate wall is 0.5-1um thick, and occasionally splits open or into two halves.

Dimensions. Vesicle diameter 25(36)45 μm, 5 specimens measured.

Remarks. The wall of this species is much thicker than that of other taxa, such as *Micrhystridium*, *Veryhachium*, *Leiosphaeridia* and other genera, but it is much smaller and thinner than that of *Dictyotidium*. Generally, the vesicle splits into two halves and is not folded.

Previous records. Permian, Antarctica (Balme and Playford 1967; Farabee et al. 1991); Australia (Balme and Hennelly 1956; Segroves 1967); Pakistan (Balme 1970); Triassic, Canada (Jansonius 1962)

Stratigraphic occurrence. Recorded from beds 22 and 25, Shangsi section.

Schizosporis sp.

Plate 3, figures 1-7

Description. The vesicle is spherical. Wall occasionally splits open or into two halves. Dense short spines (ca. 0.5 µm long) present along the surface of the vesicle, well-distributed, simple, hollow and acuminate, closed distally.

Dimensions. Vesicle diameter 20(23)25 µm, 8 specimens measured.

Remarks. Similar to *Schizosporis scissus*, the wall of *Schizosporis* sp. splits open. Compared with *Leiosphaeridia micrograniferа*, it has a similar vesicle (wall thickness and the dense spines). However, whereas *L. microgranifera* has a generally ellipsoidal and folded vesicle, that of *Schizosporis* sp. is spherical and rarely folded.

Stratigraphic occurrence. Present in bed 25, Shangsi section.

Group Acritarcha Evitt 1963

Genus *Gorgonisphaeridium* Staplin and Jansonius & Pocock 1965

Type species. *Gorgonisphaeridium winslowiae* Staplin and Jansonius & Pocock 1965

Gorgonisphaeridium sp.

Plate 2, figure 20

Description. The thin and single layered vesicle is spherical to subspherical, and covered by dense short spines that are not pointed.

Dimensions. Vesicle diameter 25(35)42 µm, process length 2-4 µm, 4 specimens measured.

Remarks. This species is very different from *Micrhystridium* and *Veryhachium*, because of the spines and the general outline. The vesicle is clearly much larger than those of *Micrhystridium*, with dense spines on the surface of the vesicle that are solid and not pointed.

Stratigraphic occurrence. Occurs in Zhongzhai and Shangsi sections.

Genus *Leiofusa* Eisenack 1938

Type species. *Leiofusa fusiformis* Eisenack 1938

Leiofusa sp.

Plate 2, figure 13

Description. The central body is elliptical. The thin wall is laevigate. Two long spines are present at both ends of the central body.

Dimensions. Vesicle diameter 35 µm, spine length 17-20 µm, 1 specimen measured.

Remarks. The central body is much bigger than that of *Micrhystridium* and *Veryhachium*, but the spines are similar. As only one specimen is recorded, it is left in open nomenclature.

Stratigraphic occurrence. Present in bed 21, Shangsi section.

Genus *Micrhystridium* Deflandre 1937 emend. Sarjeant & Stancliffe 1994

Type species. *Micrhystridium inconspicuum* (Deflandre 1935) Deflandre 1937

Micrhystridium breve Jansonius 1962
Plate 2, figures 21-25
Micrhystridium breve Jansonius 1962, p. 85, pl. 16, figs. 62, 63, 66

Description. The vesicle is ellipsoidal to spherical in outline. The wall is single layered and thin. About 20-40 processes are present along the surface of the vesicle, they are simple, hollow and acuminate, closed distally. Vesicle and process surfaces are laevigate.

Dimensions. Vesicle diameter 15(17)21 µm, process length 2-5 µm, 23 specimens measured.

Remarks. Sarjeant et al. (1970) suggested that *Micrhystridium breve* and *M. recurvatum* forma *brecispinosa* Valensi 1953 are possibly the same species. Because of its numerous, short spines it is easily recognized.

Previous records. In Permian, Pakistan (Sarjeant et al. 1970); Canada (Utting 1978); Australia (McMinn 1982); USA (Jacobson et al. 1982); Brazil (Quadros 2002); In Triassic, Canada (Jansonius 1962; Utting et al. 2004; Utting et al. 2005; Zonneveld et al. 2010); Siberia (Ilyina and Egorov 2008); Cretaceous, Canada (Collom and Hills 1999).

Stratigraphic occurrence. Abundant in beds 20 to 28, Shangsi section.

Micrhystridium fragile Deflandre 1947
Plate 2, figure 18
Micrhystridium fragile Deflandre 1947, p. 8, fig. 13-18

Description. The vesicle is spherical to subspherical, with a thin wall covered by tiny spines that are pointed and generally flexible. Most of these spines are longer than the diameter of the central body.

Dimensions. Vesicle diameter 9(11)12 µm, process length 11-15 µm, 4 specimens measured.

Remarks. The vesicle of this species is the smallest in our samples, only about 10 µm in diameter. The spines are more flexible than those of other species of *Micrhystridium*.

Previous records. Permian, Uruguay (Mautino et al. 1998); England (Sarjeant 1962); Triassic, England (Van de Schootbrugge et al. 2007); Jurassic, England (Wall 1965; Porter 1988; Stancliffe 1990); Israel (Sarjeant 1962)

Stratigraphic occurrence. Recorded from beds 21 to 25, Shangsi section.

Micrhystridium pentagonale Stockmans & Willière 1963
Plate 2, figures 11-12
Micrhystridium pentagonale Stockmans & Willière 1963, p. 470-471, pl. 3, fig. 32

Description. The thin-walled vesicle is pentagonal in outline. Five prominent spines are present along each corner. The other one to four spines arise from the central area of the vesicle. All spines are pointed.

Dimensions. Vesicle diameter 12(14)17 µm, process length 4-10 µm, 15 specimens measured.

Remarks. The outline of the vesicle is similar to that of *Micrhystridium stellatum*, but it has a more pentagonal shape. Moreover, the spines of the former are much shorter.

Previous records. Carboniferous, Turkey (Higgs et al. 2002); Silurian, Belgium (Stockmans and Willière 1963)

Stratigraphic occurrence. Present in beds 21 to 25 of the Shangsi and Zhongzhai sections.

Micrhystridium stellatum Deflandre 1945
Plate 2, figure 19
Micrhystridium stellatum Deflandre 1945, p. 65, pl. 3, figs. 16-19

Description. The vesicle is polyangular in outline. The thin wall is single layered. About 8 to 12 strong but simple processes are present around the vesicle, they are relatively long, tapering, with sharp points and hollow.

Dimensions. Vesicle diameter 13(16)18 µm, process length 6-15 µm, 15 specimens measured.

Remarks. Common in Permian strata, the species can easily be distinguished because of its polyangular vesicle and the long spines.

Previous records. Ordovician, USA (Eley and Legault 1988); Silurian, England (Dorning 1981); France (Deflandre 1945); Sweden (Gelsthorpe 2004; Stricanne et al. 2006); Devonian, Libya (Moreau-Benoit 1984); Poland (Filipiak 2009); Carboniferous, China (Gao 1986); Turkey (Higgs et al. 2002); Permian, Britain (Wall and Downie 1963); China (Ouyang and Utting 1990); Germany (Schaarschmidt 1963); Israel (Horowitz 1973); Triassic, England (Van de Schootbrugge et al. 2007);

Stratigraphic occurrence. Common in the beds 21 to 28, Shangsi section, and present in the Zhongzhai section.

Genus *Reduviasporonites* Wilson 1962 emend. Foster et al. 2002

Type species. *Reduviasporonites catenulatus* Wilson 1962

Remarks. *Reduviasporonites* has been considered by several authors as a fungal spore. However, several authors (e.g. Afonin et al. 2001; Foster et al. 2002) questioned a fungal affinity, and suggested that it is a green algae. Because the biological affinity is so far unknown, we place it here within the acritarchs. Interestingly, many authors pointed out that the 'spike' of *Reduviasporonites* occurs at the PTB (e.g. Eshet et al. 1995; Visscher et al. 1996). Indeed, around the PTB strata of South China, the relative abundances of *Reduviasporonites* is much higher than that in other strata, but they are never more abundant than 14% of an assemblage, which clearly indicates that a 'spike' does not occur in the present study.

Reduviasporonites catenulatus Wilson 1962, p. 94-95, pl. 1, figs. 1-6

Plate 4, figures 12-17

Description. The vesicle is circular or oval in outline, sometimes folded, wall laevigate. Many cells connect together usually like a chain, but sometimes they are present as pairs of cells or as a single cell. The length/width ratio of the vesicle between 1:1 and 2:1.

Dimensions. Vesicle diameter 8(15)20 μm, 17 specimens measured.

Remarks. Foster et al. (2002) described them in detail indicating that many characteristics are the same between *Reduviasporonites catenulatus* and *Reduviasporonites chalastus*. We simply distinguish them on the basis that the former is much smaller than the latter.

Previous records. Permian, Australia (Foster et al. 2002); USA (Wilson 1962; Elsik 1999); Cretaceous, Canada (Kalgutkar and Braman 2008);

Stratigraphic occurrence. Common in the Shangsi section, and present in the Xiakou section.

Reduviasporonites chalastus (Foster 1979) Elsik 1999

Plate 4, figures 1-11, 18-23

Chordecystia chalasta Foster 1979, p. 109-110, pl. 41, figs. 3-9

? *Brazilea helbyi* forma *gregata* Foster 1979, p. 112, pl. 41, figs. 1-2

Tympanicysta stoschiana Balme 1979, p. 22-24, pl. 1, figs. 3-7

Tympanicysta stoschiana Afonin et al. 2001, p. 484-486, figs. 1, 2A-C, E, F

Reduviasporonites stoschianus (Balme 1979) Elsik 1999, p. 40, pl. 1, figs. 1-24.

? *Reduviasporonites stoschianus* (Balme 1979) Elsik 1999, Wood & Elsik 1999, p. 46-48, pl. 1, figs. 1-9, pl. 2, figs. 1-7

Description. The vesicle is subcircular or subrectangular, sometimes folded, smooth. Many cells connect together, usually forming a chain, but sometimes they are present as pairs of cells or isolated as a single cell. The length/width ratio of the vesicle varies between 2:1 and 6:1.

Dimensions. Vesicle diameter 15(36)65 μm, 19 specimens measured.

Remarks. The species is distinguished thanks to the characteristic chain forming cells, the vesicle being much larger than those of *Reduviasporonites catenulatus*.

Previous records. Permian, Australia (Foster 1979; Foster et al. 2002); China (Ouyang and Utting 1990); Denmark (Balme 1979); Iraq (Stolle 2007); Kenya (Hankel 1992); Paraguay (Pérez Loinaze et al. 2010); Peru (Wood and Elsik 1999); Russia (Afonin et al. 2001); Turkey (Stolle 2010); USA (Elsik 1999);

Stratigraphic occurrence. Common in the Shangsi and Zhongzai sections.

Genus *Veryhachium* Deunff 1954 emend. Sarjeant & Stancliffe 1994

Type species. *Veryhachium trisulcum* (Deunff 1954) Deunff 1959

Veryhachium cylindricum Schaarschmidt 1963

Plate 2, figures 14,15

Veryhachium cylindricum Schaarschmidt 1963, p. 64, pl. 18, figs. 8-10

Description. The vesicle is ellipsoidal in outline. The thin wall is single layered. Six prominent but simple processes are present around the vesicle, they are proximally wide (about 5 μm in width), and the tips are acuminate, and closed distally.

Dimensions. Vesicle diameter 15(18)22 μm, process length 8-12 μm, 13 specimens measured.

Remarks. This species is easily recognizable, because of its six spines that are arranged symmetrically around the vesicle. Two of them prolong the long axis of the vesicle, and the other four spines are displayed symmetrically around the short axis of the vesicle.

Previous records. Permian, Germany (Schaarschmidt 1963)

Stratigraphic occurrence. Recorded from beds 21 to 25, Shangsi section.

Veryhachium hyalodermum (Cookson 1956) Schaarschmidt 1963

Plate 2, figures 1-4

Veryhachium hyalodermum Cookson 1956, p. 188-189, pl. 1, figs. 12-16

Veryhachium hyalodermum (Cookson 1956) Schaarschmidt 1963, p. 62-63

Description. The vesicle is triangular in outline, with four processes. Three processes are present along each angle of the vesicle, and another process is attached on the central body. The processes are simple, long, and distally closed. The thin wall is single layered.

Dimensions. Vesicle diameter 10(12)14 μm, process length 9-15 μm, 25 specimens measured.

Remarks. Many species of *Veryhachium* with four spines or a triangular vesicles have been described, such as *V. ceratioides* Stockmans & Willière 1962, *V. europaeum* Stockmans & Willière 1960, *V. leonense* Cramer 1964 and others. It is indeed difficult to distinguish *V. hyalodermum* and *V. europaeum* solely by their vesicle outline. However, the spines of the former are obviously much longer than those of the latter.

Previous records. Permian, China (Ouyang and Utting 1990); Germany (Schaarschmidt 1963); Israel (Horowitz 1974); South Africa (Horowitz 1990); Eocene, Australia (Cookson 1956)

Stratigraphic occurrence. Common in beds 21 to 28, Shangsi section.

Veryhachium nasicum (Stockmans & Willière 1960) Stockmans & Willière 1962
Plate 2, figures 5-8
Stellinium nasicum Stockmans & Willière 1960, p. 3, pl. 1, fig. 3
Veryhachium nasicum (Stockmans & Willière 1960) Stockmans & Willière 1962, p. 52

Description. The vesicle is rectangular in outline, with five processes. Four of these processes are present at each corner of the vesicle, and another process arises from the central body; the processes are simple, short, and distally closed. The thin wall is single layered.

Dimensions. Vesicle diameter 17(19)22 µm, process length 5-9 µm, 21 specimens measured.

Remarks. There are many species of *Veryhachium* with rectangular vesicle and Servais et al. (2007) attributes them to the *Veryhachium lairdii* group. *V. nasicum* is easily recognized with its characteristic four spines present at each corner, and a further attached on the surface of the vesicle.

Previous records. Devonian, Belgium (Stockmans and Willière 1960); China (Gao 1986); Libya (Moreau-Benoit 1984); Carboniferous, Russia (Marhoumi and Rauscher 1984); Permian, Germany (Schaarschmidt 1963)

Stratigraphic occurrence. Common in beds 21 to 25, Shangsi section.

Veryhachium quadratum Schaarschmidt 1963
Plate 2, figure 17
Veryhachium quadratum Schaarschmidt 1963, p. 63, pl. 17, figs. 8-10.

Description. The vesicle is polyangular in outline. The thin wall is single layered, with about 5 to 8 short spines, that are 2 µm wide at their base and 1-2 µm long.

Dimensions. Vesicle diameter about 20 µm, process length 1-2 µm, 1 specimen measured.

Remarks. This species is very different from the other species of *Veryhachium*, because of its very short spines, generally only 1-2 µm in length.

Previous records. Permian, Germany (Schaarschmidt 1963)

Stratigraphic occurrence. Present in bed 21, Shangsi section.

Veryhachium sedecimspinosum Staplin 1961
Plate 2, figures 9-10
Veryhachium sedecimspinosum Staplin 1961, p. 414, pl. 49, figs. 9-11

Description. The thin wall is single layered, and the outline is rectangular, with five to eight processes. Four of these processes arise from each corner of the vesicle, and the other processes (2 to 4 in number) arise from the central body. All of the processes are simple, short, and distally closed.

Dimensions. Vesicle diameter 15(16)17 μm, process length 7-13 μm, 4 specimens measured.

Remarks. Similar to *Veryhachium nasicum*, the rectangular vesicle of *V. sedecimspinosum* has four spines that arise from each corner. However, there are more (generally two to four) additional spines attached on the surface of the vesicle.

Previous records. Devonian, Canada (Staplin 1961); Permian, Germany (Schaarschmidt 1963)

Stratigraphic occurrence. Common in the Shangsi section.

Veryhachium sp.

Plate 2, figure 16

Description. The vesicle is triangular with a smooth wall. Three short spines are present at each of the angles. One or two short additional spines arise from the central body.

Dimensions. Vesicle diameter 25 μm, process length about 5 μm, 1 specimen measured.

Remarks. Similar to *Veryhachium hyalodermum*, *Veryhachium* sp. has a triangular vesicle, but it is much larger than the latter, and the spines are much shorter. Because only one specimen has been recovered, the species is left in open nomenclature.

Stratigraphic occurrence. Present in bed 21, Shangsi section.

Acknowledgments

We express sincere thanks to Mr. Hu Qing, Zhang Lei, Liu Guichun, Shen Jun, Xiang Yu and Miss Xu Guozhen and Nie Xiaomei for their help in field work. We acknowledge the two referees (Reed Wicander, Central Michigan University, USA, and Clinton Foster, Australian Geological Survey) for detailed review and their helpful comments, and the editor of the journal Jim Riding (British Geological Survey) for his help and advice. This work was supported by National Science Foundation of China (NSFC) project no. 40839903, 40921062, the Chinese 973 (2011CB808800), and 111 programmes (B08030), and the Ministry of Education of China (NCET-10-0712), and the Fundamental Funds for the Central Universities, and by grants of the University of Lille1 ("Allocation Présidentielle" and "Bonus Qualité Recherche") and the Conseil Régional du Nord (France).

References

Afonin S.A., Barinova S.S., Krassilov V.A. 2001. A bloom of *Tympanicysta* Balme (green algae of zygnematalean affinities) at the Permian-Triassic boundary. *Geodiversitas*, 23(4): 481-487.

Balme B.E. 1970. Palynology of Permian and Triassic strata in the Salt range and Surghar range, West Pakistan. *Special Publication-University of Kansas, Department of Geology*, 4: 305-453.

Balme B.E. 1979. Palynology of Permian-Triassic boundary beds at Kap Stosch, East Greenland. *Meddelelser om Grønland*, 200(6): 1-37.

Balme B.E., Hennelly J.P.F. 1956. Monolete, monocolpate, and alete sporomorphs from Australian Permian sediments. *Australian Journal of Botany*, 4(1): 54-67.

Balme B.E., Playford G. 1967. Late Permian plant microfossils from the Prince Charles Mountains, Antarctica. *Revue de Micropaléontologie*, 10(3): 179-192.

Besems R.E. 1981. Aspects of middle and late Triassic palynology. 2. Preliminary palynological data from the Hornos-Siles Formation of the Prebetic Zone, NE province of Jaen (Southeastern Spain). *Review of Palaeobotany and Palynology*, 32(4): 389-400.

Bhat G.M., Ram G., Koul S. 2009. Potential for oil and gas in the Proterozoic carbonates (Sirban Limestone) of Jammu, northern India. *Geological Society, London, Special Publications*, 326(1): 245-254.

Borge O., Pascher A. 1913. Zygnemales. In: Pascher, A. (Ed.). Die Süßwasserflora Deutschlands, Österreichs und der Schweiz, 9: 51 p.

Butterfield N.J., Chandler F.W. 1992. Paleoenvironmental distribution of Proterozoic microfossils, with an example from the Agu Bay Formation, Baffin Island. *Palaeontology*, 35(4): 943-957.

Christensen K. 1962. Alger. In: Bocher, T.W., Lange, M., Sorensen, T., editors. Botanik, 2. Copenhagen. 178 p.

Colbath G.K., Grenfell H.R. 1995. Review of biological affinities of Paleozoic acid-resistant, organic-walled eukaryotic algal microfossils (including "acritarchs"). *Review of Palaeobotany and Palynology*, 86(3-4): 287-314.

Collom C.J., Hills L.V. 1999. Geological Survey of Canada, Open File 3833. *Natural Resources Canada*. 37 p.

Cookson I.C. 1956. Additional Microplankton from Australian Late Mesozoic and Tertiary Sediments. *Marine and Freshwater Research*, 7(1): 183-191.

Cookson I.C., Dettmann M.E. 1959. On *Schizosporis*, a new form genus from Australian Cretaceous deposits. *Micropaleontology*, 5(2): 213-216.

Cramer F.H. 1964. Microplankton from three Palaeozoic formations in the Province of León, NW Spain. *Leidse Geologische Mededelingen*, 30: 253-361.

Deflandre G. 1935. Considérations biologiques sur les microorganismes d'origine planctonique conservés dans les silex de la craie. *Bulletin biologique de la France et de la Belgique*, 69: 213-244.

Deflandre G. 1937. Microfossiles des silex crétacés: Flagellés incertae sedis, Hystrichosphaeridés, Sarcodinés, organismes divers. *Annales de paléontologie*, 26: 51-103.

Deflandre G. 1945. Microfossiles des calcaires siluriens de la Montagne Noire. *Annales de Paléontologie*, 31: 41-75.

Deflandre G. 1947. Le probléme des Hystrichosphères. *Bulletin de l'Institut océanographique (Monaco)*, 23 p.

Deunff J. 1954. *Veryhachium*, genre nouveau d'Hystrichosphères du Primaire. *Compte Rendu Sommaire des Séances de la Société géologique de France*, 13: 305-306.

Deunff J. 1959. Microorganismes planctoniques du Primaire armoricain: Ordovicien du Veryhac'h (presqu'île de Crozon). *Bulletin de la Société géologique et minéralogique de Bretagne*, 2: 1-41.

Dorning K.J. 1981. Silurian acritarchs from the type Wenlock and Ludlow of Shropshire, England. *Review of Palaeobotany and Palynology*, 34(2): 175-203.

Downie C., Sarjeant W.A.S. 1963. On the interpretation and status of some hystrichosphere genera. *Palaeontology*, 6(1): 83-96.

Eisenack A. 1938. Hystrichosphäerideen und verwandte Formen im baltischen Silur. *Zeitschrift für Geschiebeforschung und Flachlandgeologie*, 14(1): 1-30.

Eisenack A. 1955. Chitinozoen, Hystrichosphären und andere Mikrofossilien aus dem Beyrichia-Kalk. *Senckenbergiana Lethaea*, 36(1-2): 157-188.

Eisenack A. 1958. Mikroplankton aus dem norddeutschen Apt, nebst einigen Bemerkungen über fossile Dinoflagellaten. *Neues Jahrbuch für Geologie und Paläontologie, Abhandlungen*, 39(5-6): 389-405.

Eisenack A. 1969. Zur systematik einiger paläozoischer Hystrichosphären (Acritarcha) des baltischen Gebietes. *Neues Jahrbuch für Geologie und Paläontologie, Abhandlungen*, 133(3): 245-266.

Eley B.E., Legault J.A. 1988. Palymorphs from the Manitoulin Formation (Early Llandovery) of southern Ontario. *Palynology*, 12(1): 49-63.

Elsik W.C. 1999. *Reduviasporonites* Wilson 1962: Synonymy of the fungal organism involved in the late Permian crisis. *Palynology*: 37-41.

Eshet Y., Rampino M.R., Visscher H. 1995. Fungal event and palynological record of ecological crisis and recovery across the Permian-Triassic boundary. *Geology*, 23(11): 967-970.

Evitt W.R. 1963. A discussion and proposals concerning fossil dinoflagellates, hystrichospheres, and acritarchs, II. *Proceedings of the National Academy of Sciences of the United States of America*, 49(3): 298-302.

Farabee M.J., Taylor E.L., Taylor T.N. 1991. Late Permian palynomorphs from the Buckley Formation, central transantarctic mountains, Antarctica. *Review of Palaeobotany and Palynology*, 69(4): 353-368.

Feng Q.L., Gu S.Z. 2002. Uppermost Changxingian (Permian) radiolarian fauna from southern Guizhou, southwestern China. *Journal of Paleontology*, 76(5): 797-809.

Feng Q.L., He W.H., Gu S.Z., Meng Y.Y., Jin Y.X., Zhang F. 2007. Radiolarian evolution during the latest Permian in South China. *Global and Planetary Change*, 55(1-3): 177-192.

Fensome R.A., Williams G.L., Sedley Barss M., Freeman J.M., Hill J.M. 1990. Acritarchs and fossil Prasinophytes: An index to genera, species and intraspecific taxa. *American Association of Stratigraphic Palynologists Foundation*, 25: 1-771.

Filipiak P. 2009. Lower Famennian phytoplankton from the Holy Cross Mountains, Central Poland. *Review of Palaeobotany and Palynology*, 157(3-4): 326-338.

Foster C.B. 1979. Permian plant microfossils of the Blair Athol Coal Measures, Baralaba Coal Measures, and basal Rewan Formation of Queensland. *Geological Survey of Queensland Publications*, (372): 244 p.

Foster C.B., Stephenson M.H., Marshall C., Logan G.A., Greenwood P.F. 2002. A revision of *Reduviasporonites* Wilson 1962: description, illustration, comparison and biological affinities. *Palynology*, 26(1): 35-58.

Gao L.D. 1986. Late Devonian and Early Carboniferous acritarchs from Nyalam county, Xizang (Tibet), China. *Review of Palaeobotany and Palynology*, 47(1-2): 17-30.

Gaucher C., Blanco G., Chiglino, L., Poiré D., Germs G.J.B. 2008. Acritarchs of Las Ventanas Formation (Ediacaran, Uruguay): Implications for the timing of coeval rifting and glacial events in western Gondwana. *Gondwana Research*, 13(4): 488-501.

Gaucher C., Germs G.J.B. 2006. Recent advances in South African Neoproterozoic-Early Palaeozoic biostratigraphy: correlation of the Cango Caves and Gamtoos Groups and acritarchs of the Sardinia Bay Formation, Saldania Belt. *South African Journal of Geology*, 109(1-2): 193-214.

Gelsthorpe D.N. 2004. Microplankton changes through the early Silurian Ireviken extinction event on Gotland, Sweden. *Review of Palaeobotany and Palynology*, 130(1-4): 89-103.

Grice K., Twitchett R.J., Alexander R., Foster C.B., Looy C.V. 2005. A potential biomarker for the Permian-Triassic ecological crisis. *Earth and Planetary Science Letters*, 236(1-2): 315-321.

Hankel O. 1992. Late Permian to early Triassic microfloral assemblages from the Maji y a Chumvi Formation, Kenya. *Review of Palaeobotany and Palynology*, 72(1-2): 129-147.

Hart G.F. 1965. The systematics and distribution of Permian miospores. *Witwatersrand University Press, Johannesburg, South Africa*, 252 p.

Hays L.E., Grice K., Foster C.B., Summons R.E. 2011. Biomarker and isotopic trends in a Permian-Triassic sedimentary section at Kap Stosch, Greenland. *Organic Geochemistry*, 43: 67-82.

He W.H., Feng Q.L., Weldon E.A., Gu S.Z., Meng Y.Y., Zhang F., Wu S.B. 2007a. A late Permian to early Triassic bivalve fauna from the Dongpan Section, southern Guangxi, South China. *Journal of Paleontology*, 81(5): 1009-1019.

He W.H., Shen S.Z., Feng Q.L., Gu S.Z. 2005. A late Changhsingian (Late Permian) deepwater brachiopod fauna from the Talung Formation at the Dongpan section, southern Guangxi, South China. *Journal of Paleontology*, 79(5): 927-938.

He W.H., Shi G.R., Feng Q.L., Campi M.J., Gu S.Z., Bu J.Z., Peng Y.Q., Meng Y.Y. 2007b. Brachiopod miniaturization and its possible causes during the Permian-Triassic crisis in deep water environments, South China. *Palaeogeography, Palaeoclimatology, Palaeoecology*, 252(1): 145-163.

He W.H., Shi G.R., Gao Y.Q., Peng Y.Q., Zhang Y. 2008. A new Early Triassic microgastropod fauna from the Zhongzhai Section, Guizhou, southwestern China. *Proceedings of the Royal Society of Victoria*, 120(1): 157-166.

Higgs K.T., Finucane D., Tunbridge I.P. 2002. Late Devonian and early Carboniferous microfloras from the HakkarI Province of southeastern Turkey. *Review of Palaeobotany and Palynology*, 118(1-4): 141-156.

Hong H.L., Xie S.C., Lai X.L. 2011. Volcanism in association with the prelude to mass extinction and environment change across the Permian-Triassic boundary (PTB), southern China. *Clays and Clay Minerals*, 59(5): 478-489.

Hong H.L., Zhang N., Li Z.H., Xue H., Xia W., Yu N. 2008. Clay mineralogy across the PT boundary of the Xiakou section, China: Evidence of clay provenance and environment. *Clays and Clay Minerals*, 56(2): 131-143.

Horowitz A. 1973. Late Permian palynomorphs from southern Israel. *Pollen et Spores*, 15(2): 315-341.

Horowitz A. 1974. Espéces du genre *Veryhachium* du Permo-Trias du Sud d'Israel. *Revue de Micropaléontologie*, 17(2): 75-80.

Horowitz A. 1990. Palynology and paleoenvironment of uranium deposits in the Permian Beaufort Group, South Africa. *Ore Geology Reviews*, 5(5-6): 537-540.

Ilyina N.V., Egorov A.Y. 2008. The Upper Triassic of northern Middle Siberia: stratigraphy and palynology. *Polar Research*, 27(3): 372-392.

Jacobson S.R., Wardlaw B.R., Saxton J.D. 1982. Acritarchs from the Phosphoria and Park City Formations (Permian, Northeastern Utah). *Journal of Paleontology*, 56(2): 449-458.

Jankauskas T.V. 1989. Mikrofossilii dokembriia SSSR. Nauka, Leningrad, 1-188.

Jansonius J. 1962. Palynology of Permian and Triassic sediments, Peace River area, western Canada. *Palaeontographica Abteilung B*, 110(1-4): 35-98.

Jiang H.S., Lai X.L., Yan C.B., Aldridge R., Wignall P.B., Sun Y.D. 2011. Revised conodont zonation and conodont evolution across the Permian-Triassic boundary at the Shangsi section, Guangyuan, Sichuan, South China. *Global and Planetary Change*, 77(3-4): 103-115.

Johnson N.G. 1985. Early Silurian palynomorphs from the Tuscarora Formation in central Pennsylvania and their paleobotanical and geological significance. *Review of Palaeobotany and Palynology*, 45(3-4): 307-359.

Kalgutkar R.M., Braman D.R. 2008. Santonian To ?Earliest Campanian (Late Cretaceous) Fungi from the Milk River Formation, Southern Alberta, Canada. *Palynology*, 32(1): 39.

Konzalová O.F.M. 1995. Microfossils of the Paseky Shale (Lower Cambrian, Czech Republic). *Journal of the Czech Geological Society*, 40(4): 55-66.

Kützing F.T. 1843. Phycologia generalis. *Brockhouse, Leipzig*, 458 p.

Lai X.L., Yang F.Q., Hallam A., Wignall P. 1996. The Shangsi section, candidate of the Global Stratotype Section and Point of the Permian-Triassic boundary. In: Yin, H. F. (Ed.), The Palaeozoic-Mesozoic Boundary. Candidates of Global Stratotype Section and Point of the Permian-Triassic Boundary. *China University of Geosciences Press, Wuhan*, p. 113-124.

Le Herisse A., Dorning K.J., Mullins G.L., Wicander R. 2009. Global patterns of organic-walled phytoplankton biodiversity during the Late Silurian to Earliest Devonian. *Palynology*, 33(1): 25-75.

Lei Y., Servais T., Feng Q.L. The diversity of the Permian phytoplankton. Review of Palaeobotany and Palynology, (accepted for publication).

Lei Y., Servais T., Feng Q.L., He W.H. 2012. The spatial (nearshore-offshore) distribution of latest Permian phytoplankton from the Yangtze Block, South China. *Palaeogeography, Palaeoclimatology, Palaeoecology*, 363-364: 151-162.

Lei Y., Servais T., Shen J., Tribovillard N., Danelian T., Feng Q.L. Palynology and palynofacies of the Upper Permian to Lower Triassic of Shangsi (Sichuan, China)(submitted).

Leonov M.V., Ragozina A.L. 2007. Upper Vendian assemblages of carbonaceous micro-and macrofossils in the White Sea Region: systematic and biostratigraphic aspects. *Geological Society, London, Special Publications*, 286(1): 269-275.

Li J., Servais T., Brocke R. 2002. Chinese Paleozoic acritarch research: review and perspectives. *Review of Palaeobotany and Palynology*, 118(1-4): 181-193.

Li J., Cao C.Q., Servais T., Zhu Y.H. 2004. Later Permian acritarchs from Meishan (SE China) in the context of Permian palaeobiogeography and palaeoecology. *Neues Jahrbuch für Geologie und Paläontologie, Monatshefte*: 427-448.

Li Z.S., Zhan L.P., Zhu X.F., Zhang J.H., Jin R.G., Liu G.F., Sheng H.B., Shen G.M., Dai J.Y., Huang H.Q., Xie L.C., Yan Z. 1986. Mass extinction and geological events between Palaeozoic and Mesozoic era. *Acta Geologica Sinica*, 60: 1-15.

Mädler K. 1963. Die figurierten organischen Bestandteile der Posidonienschiefer. *Geologisches Jahrbuch Beihefte*, 58: 287-406.

Mangerud G. 1994. Palynostratigraphy of the Permian and lowermost Triassic succession, Finnmark Platform, Barents Sea. *Review of Palaeobotany and Palynology*, 82(3-4): 317-349.

Marhoumi R., Rauscher R. 1984. Un plancton Dévonien de la Méseta orientale au Maroc. *Review of Palaeobotany and Palynology*, 43(1-3): 237-253.

Maslov A.V. 2004. Riphean and Vendian sedimentary sequences of the Timanides and Uralides, the eastern periphery of the East European Craton. *Geological Society, London, Memoirs*, 30(1): 19-35.

Mautino L.R., Vergel M.D.M., Anzótegui L.M. 1998. Palinologia de la Formacion Melo (Permico inferior) en Arroyo Seco, Departamento Rivera, Uruguay, Parte V: Granos de polen, acritarcas E Incertae sedis. *Ameghiniana*, 35(3): 299-314.

McMinn A. 1982. Late Permian acritarchs from the northern Sydney Basin. *Journal and*

Proceedings of the Royal Society of New South Wales, 115: 79-86.

Metcalfe I., Nicoll R.S. 2007. Conodont biostratigraphic control on transitional marine to non-marine Permian-Triassic boundary sequences in Yunnan-Guizhou, China. *Palaeogeography, Palaeoclimatology, Palaeoecology*, 252(1-2): 56-65.

Moczydłowska M. 2008. The Ediacaran microbiota and the survival of Snowball Earth conditions. *Precambrian Research*, 167(1-2): 1-15.

Moreau-Benoit A. 1984. Acritarches et chitinozoaires du Dévonien moyen et supérieur de Libye occidentale. *Review of Palaeobotany and Palynology*, 43(1-3): 187-216.

Mullins G.L., Servais T. 2008. The diversity of the Carboniferous phytoplankton. *Review of Palaeobotany and Palynology*, 149(1-2): 29-49.

Naumova S.N. 1949. Spores of the Lower Cambrian. *Izvestiya Akademiya Nauk SSSR, Seriya Geologicheskaya*, 4: 49-56.

Ouyang S. 1982. Upper Permian and Lower Triassic palynomorphs from eastern Yunnan, China. *Canadian Journal of Earth Sciences*, 19(1): 68-80.

Ouyang S. 1986. Palynology of Upper Permian and Lower Triassic strata of Fuyuan district, Eastern Yunan. *Palaeontologia sinica*, 169(9): 1-122.

Ouyang S., Utting J. 1990. Palynology of upper Permian and lower Triassic rocks, Meishan, Changxing County, Zhejiang Province, China. *Review of Palaeobotany and Palynology*, 66(1-2): 65-103.

Pascher A. 1914. Über Flagellaten und Algen. *Berichte der Deutschen botanischen Gesellschaft*, 32: 136-160.

Pérez Loinaze V.S., Césari S.N., López Gamundí O., Buatois L. 2010. Palynology of the Permian San Miguel Formation (Western Paraná Basin, Paraguay): Gondwanan biostratigraphic correlations. *Geologica Acta*, 8(4): 483-493.

Pierce S.T. 1976. Morphology of *Schizosporis reticulatus* Cookson and Dettmann 1959. *Geoscience and Man*, 15(1): 25-33.

Porter R. 1988. Palynological evidence for Jurassic microplankton provinces in Great Britain. *Review of Palaeobotany and Palynology*, 56(1-2): 21-39.

Quadros L.P. 2002. Acritarcos e tasmanites do Permo-Carbonífero da bacia do Paraná. *Revista do Instituto Geológico*, 23(1): 39-50.

Riegel W. 1996. The geologic significance of the Late Paleozoic phytoplankton blackout. *IX IPC Meeting, Houston,Texas, U.S.A*., Abstracts, p. 133-134.

Riegel W. 2008. The Late Palaeozoic phytoplankton blackout -Artefact or evidence of global change. *Review of Palaeobotany and Palynology*, 148(2-4): 73-90.

Round F.E. 1971. The taxonomy of the Chlorophyta. II. *British Phycological Journal*, 6(2): 235-264.

Sarjeant W.A.S. 1962. Microplankton from the Ampthill Clay of Melton, South Yorkshire. *Palaeontology*, 5(3): 478-497.

Sarjeant W.A.S., Kummel B., Teichert C. 1970. Acritarchs and tasmanitids from the Chhidru Formation, uppermost Permian of West Pakistan. Stratigraphical Boundary Problems: Permian and Triassic of West Pakistan. *University of Kansas, Department of Geology, Special Publication*, 4: 277-304.

Sarjeant W.A.S., Stancliffe R.P.W. 1994. The *Micrhystridium* and *Veryhachium* complexes (Acritarcha: Acanthomorphitae and Polygonomorphitae); a taxonomic reconsideration. *Micropaleontology*, 40(1): 1-77.

Schaarschmidt F. 1963. Sporen und Hystrichosphaerideen aus dem Zechstein von Büdingen in der Wetterau. *Palaeontographica Abteilung B*, 113(1-4): 38-91.

Schulz E. 1965. *Sporae dispersae* aus der Trias von Thüringen. *Abhandlungen des ZGI*, 1: 257-287.

Segroves K.L. 1967. Cutinized microfossils of probable nonvascular origin from the Permian of Western Australia. *Micropaleontology*, 13(3): 289-305.

Sephton M.A., Visscher H., Looy C.V., Verchovsky A.B., Watson J.S. 2009. Chemical constitution of a Permian-Triassic disaster species. *Geology*, 37(10): 875-878.

Servais T. 1996. Some considerations on acritarch classification. *Review of Palaeobotany and Palynology*, 93(1-4): 9-22.

Servais T., Lehnert O., Li J., Mullins G.L., Munnecke A., Nützel A., Vecoli M. 2008. The Ordovician Biodiversification: revolution in the oceanic trophic chain. *Lethaia*, 41(2): 99-109.

Servais T., Nützel A., Mullins G.L. 2006. Was there a phytoplankton blackout in the late Paleozoic? *Palynology*, 30: 228.

Servais T., Li J., Stricanne L., Vecoli M., Wicander R. 2004. Acritarchs. In: Webby B.D., Droser M.L., Paris F., Percival I.G. (Eds.), The Great Ordovician Biodiversification Event. Columbia University Press, New York, p. 348-360.

Servais T., Vecoli M., Li J., Molyneux S.G., Raevskaya E.G., Rubinstein C., Claudia V. 2007. The acritarch genus *Veryhachium* Deunff 1954: taxonomic evaluation and first appearance. *Palynology*, 31(1): 191-203.

Shen J., Algeo T.J., Hu Q., Zhang N., Zhou L., Xia W.C., Xie S.C., Feng Q.L. 2012a. Negative C-isotope excursions at the Permian-Triassic boundary linked to volcanism. *Geology*, 40: 963-966.

Shen J., Algeo T.J., Zhou L., Feng Q.L., Yu J.X., Ellwood B. 2012b. Volcanic perturbations of the marine environment in South China preceding the latest Permian mass extinction and their biotic effects. *Geobiology*, 10(1): 82-103.

Shen S.Z., Crowley J.L., Wang Y., Bowring S.A., Erwin D.H., Sadler P.M., Cao C.Q., Rothman D.H., Henderson C.M., Ramezani J. 2011. Calibrating the end-Permian mass extinction. *Science*, 334(6061): 1367-1372.

Stancliffe R.P.W. 1990. Acritarchs and other non-Dinophycean marine Palynomorphs from the

Oxfordian (Upper Jurassic) of Skye, Western Scotland and Dorset, Southern England. *Palynology*, 14(1): 175-192.

Stanevich A.M., Maksimova E.N., Kornilova T.A., Mazukabzov A.M., Gladkochub D.P. 2007. Microfossils of the late Proterozoic Debengdinskaya Formation of the Olenekskiy uplift. *Bulletin of the Томск Polytechnic University*, 311(1): 9-14.

Staplin F.L. 1961. Reef-controlled distribution of Devonian microplankton in Alberta. *Palaeontology*, 4(3): 392-424.

Staplin F.L., Jansonius J., Pocock S.A.J. 1965. Evaluation of some acritarchous hystrichosphere genera. *Neues Jahrbuch für Geologie und Paläontologie, Abhandlungen*, 123(2): 167-201.

Steiner M., Fatka O. 1996. Lower Cambrian tubular micro-to macrofossils from the Paseky Shale of the Barrandian area (Czech Republic). *Paläntologische Zeitschrift*, 70(3): 275-299.

Stockmans F., Willière Y. 1960. Hystrichosphères du Dévonien belge (Sondage de l'Asile d'aliенés à Tournai). *Senckenbergiana Lethaea*, 41: 1-11.

Stockmans F., Willière Y. 1962. Hystrichosphères du Dévonien belge (Sondage de l'Asile d'alienés à Tournai). *Bulletin de la Société belge de géologie, de paléontologie et d'hydrologie*, 71: 41-77.

Stockmans F., Willière Y. 1963. Les Hystrichosphères ou mieux les Acritarches du Silurien Belge. Sondage de la Brasserie Lust à Courtrai (Kortrijk). *Bulletin de la Société belge de Géologie, de paléontologie et d' hydrologie*, 71(3): 450-481.

Stolle E. 2007. Regional Permian palynological correlations: Southeast Turkey-Northern Iraq. *Comunicações Geológicas*, 94: 125-143.

Stolle E. 2010. Recognition of southern Gondwanan palynomorphs at Gondwana's northern margin and biostratigraphic correlation of Permian strata from SE Turkey and Australia. *Geological Journal*, 45(2-3): 336-349.

Stricanne L., Munnecke A., Pross J. 2006. Assessing mechanisms of environmental change: Palynological signals across the Late Ludlow (Silurian) positive isotope excursion ($\delta^{13}C$, $\delta^{18}O$) on Gotland, Sweden. *Palaeogeography, Palaeoclimatology, Palaeoecology*, 230(1-2): 1-31.

Strother P.K. 1996. Chapter 5. Acritarchs. In: Jansonius, J., McGregor, D.C. (eds.), Palynology: Principles and Applications. *American Association of Stratigraphic Palynologists Foundation*, p. 81-106.

Utting J. 1978. Geological Survey of Canada, Open File 593. Natural Resources Canada. *Natural Resources Canada*, 17 p.

Utting J., Spina A., Jansonius J., McGregor D.C., Marshall J.E.A. 2004. Reworked miospores in the Upper Paleozoic and Lower Triassic of the northern circum-polar area and selected localities. *Palynology*, 28(1): 75.

Utting J., Zonneveld J.P., MacNaughton R.B., Fallas K.M., Deunff J. 2005. Palynostratigraphy, lithostratigraphy and thermal maturity of the Lower Triassic Toad and Grayling, and Montney formations of western Canada, and comparisons with coeval rocks of the Sverdrup Basin, Nunavut. *Bulletin of Canadian Petroleum Geology*, 53(1): 5-24.

Valensi L. 1953. Microfossiles des silex du Jurassique moyen: Remarques pétrographiques. *Mémoire de la Société géologique de France*, 32(4): 1-100.

Van de Schootbrugge B., Bailey T.R., Rosenthal Y., Katz M.E., Wright J.D., Miller K.G., Feist-Burkhardt S., Falkowski P.G. 2005. Early Jurassic climate change and the radiation of organic-walled phytoplankton in the Tethys Ocean. *Paleobiology*, 31(1): 73-97.

Van de Schootbrugge B., Tremolada F., Rosenthal Y., Bailey T.R., Feist-Burkhardt S., Brinkhuis H., Pross J., Kent D.V., Falkowski P.G. 2007. End-Triassic calcification crisis and blooms of organic-walled 'disaster species'. *Palaeogeography, Palaeoclimatology, Palaeoecology*, 244(1-4): 126-141.

Vavrdová M. 1966. Palaeozoic microplankton from central Bohemia. *Casopis pro mineralogii a geologii*, 11(4): 409-414.

Vavrdová M. 2008. Proterozoic acritarchs from the Precambrian-Cambrian transition in southern Moravia (Mìnín-1 borehole, Czech Republic). *Bulletin of Geosciences*, 83(1): 85-92.

Visscher H., Brinkhuis H., Dilcher D.L., Elsik W.C., Eshet Y., Looy C.V., Rampino M.R., Traverse A. 1996. The terminal Paleozoic fungal event: evidence of terrestrial ecosystem destabilization and collapse. *Proceedings of the National Academy of Sciences of the United States of America*, 93(5): 2155-2158.

Visscher H., Brugman W.A. 1981. Ranges of selected palynomorphs in the Alpine Triassic of Europe. *Review of Palaeobotany and Palynology*, 34(1): 115-128.

Visscher H., Sephton M.A., Looy C.V. 2011. Fungal virulence at the time of the end-Permian biosphere crisis? *Geology*, 39(9): 883-886.

Vorob'eva N.G., Sergeev V.N., Knoll A.H. 2009. Neoproterozoic Microfossils from the Northeastern Margin of the East European Platform. *Journal of Paleontology*, 83(2): 161-196.

Wall D. 1965. Microplankton, pollen, and spores from the Lower Jurassic in Britain. *Micropaleontology*, 11(2): 151-190.

Wall D., Downie C. 1963. Permian hystrichospheres from Britain. *Palaeontology*, 5(4): 770-784.

Wang G.Q., Xia W.C. 2004. Conodont zonation across the Permian Triassic boundary at the Xiakou section, Yichang city, Hubei Province and its correlation with the Global Stratotype Section and Point of the PTB. *Canadian Journal of Earth Sciences*, 41(3): 323-330.

Wilson L.R. 1962. A Permian fungus spore type from the Flowerpot Formation of Oklahoma. *Oklahoma Geology Notes*, 22(4): 91-96.

Wood G.D., Elsik W.C. 1999. Paleoecologic and stratigraphic importance of the fungus *Reduviasporonites stoschianus* from the 'Early-Middle' Pennsylvanian of the Copacabana Formation, Peru. *Palynology*, 23: 43-53.

Zonneveld J.P., Beatty T.W., MacNaughton R.B., Pemberton S.G., Utting J., Henderson C.M. 2010. Sedimentology and ichnology of the Lower Triassic Montney Formation in the

Pedigree-Ring/Border-Kahntah River area, northwestern Alberta and northeastern British Columbia. *Bulletin of Canadian Petroleum Geology*, 58(2): 115-140.

Figure captions:

Figure 1: Location of four sections in South China (Zhongzhai section, Shangsi section, Xiakou section and Dongpan section) (A and B), and latest Permian paleogeography of South China (C, modified after Feng and Gu 2002).

Figure 2: Phytoplankton distribution in the four investigated sections.

Figure 3: Idealized line drawings allowing the proposal of a simplified classification scheme of the *Micrhystridium*/*Veryhachium* complex.

Plate 1: Phytoplankton fossils from the latest Permian, South China. Each bar is 10μm. Figures 1-9 were taken using SEM; figures 10-12 were taken using the transmitted light microscope.1-12: *Dictyotidium reticulatum*. All specimens are from Shangsi section/SS292-4.

Plate 2: Phytoplankton fossils from the latest Permian, South China. Each bar is 10μm. All figures were taken using the transmitted light microscope. 1-4: *Veryhachium hyalodermum*; 5-8: *Veryhachium nasicum*; 9-10: *Veryhachium sedecimspinosum*; 11-12: *Michrystridium pentagonale*; 13: *Leiofusa* sp.; 14-15 *Veryhachium cylindricum*; 16: *Veryhachium* sp.; 17: *Veryhachium quadratum*; 18: *Michrystridium fragile*; 19: *Michrystridium stellatum*; 20: *Baltisphaeridium* sp.; 21-25: *Michrystridium breve*. The informations of section/sample numbers for all specimens are following. 1-12: Shangsi section/SS25-E; 13: Shangsi section/SS289-1-2; 14-15,17: Shangsi section/SS290-7; 16: Shangsi section/SS291-6; 18: Shangsi section/SS290-4; 19,21-25: Shangsi section/TS28-18; 20:Zhongzhai section/ZZ22-2.

Plate 3: Phytoplankton fossils from the latest Permian, South China. Each bar is 10μm. Figures 11-12 were taken using scanning electron microscopy (SEM); figures 1-10 and 13-21 were taken using the transmitted light microscope.1-7: *Schizosporis* sp.; 8-10: *Schizosporis scissus*; 11-12: *Dictyotidium* sp.; 13-18: *Leiosphaeridia minutissima*; 19-21: *Leiosphaeridia micrugranifera*. The informations of section/sample numbers for all specimens are following. 1-10: Shangsi section/SS25-E; 11-12: Shangsi section/SS292-4; 13-14:Dongpan section/DP2-G; 15-16: Dongpan section/DP3-A; 17: Dongpan section/DP5-B; 18: Shangsi section/SS290-8-1; 19-21: Shangsi section/SS291-2.

Plate 4: Phytoplankton fossils from the latest Permian, South China. Each bar is 10μm. All figures were taken using the transmitted light microscope. 1-11,18-23: *Reduviasporonites chalastus*; 12-17: *Reduviasporonites catenulatus*. The informations of section/sample numbers for all specimens are following. 1-6, 11, 14, 23: Shangsi section/TS28-17; 12-13: Xiakou section/XK254-1; 16-17: Zhongzhai section/ZZ19-3; 7-10, 15, 18-22: Shangsi section/ TS28-18.

Table 1: South Chinese species of the *Micrhystridium*/*Veryhachium* complex recorded in the present study and their attribution to five informal groups, based on their general central body

outline.

Figure 1:

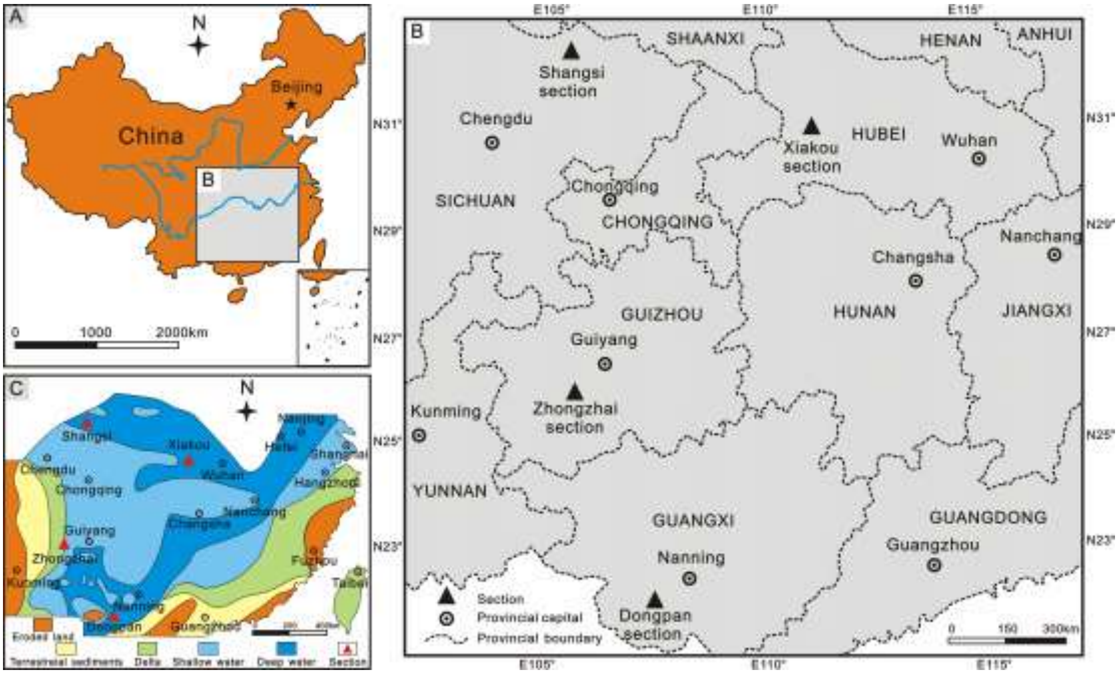

Figure 2:

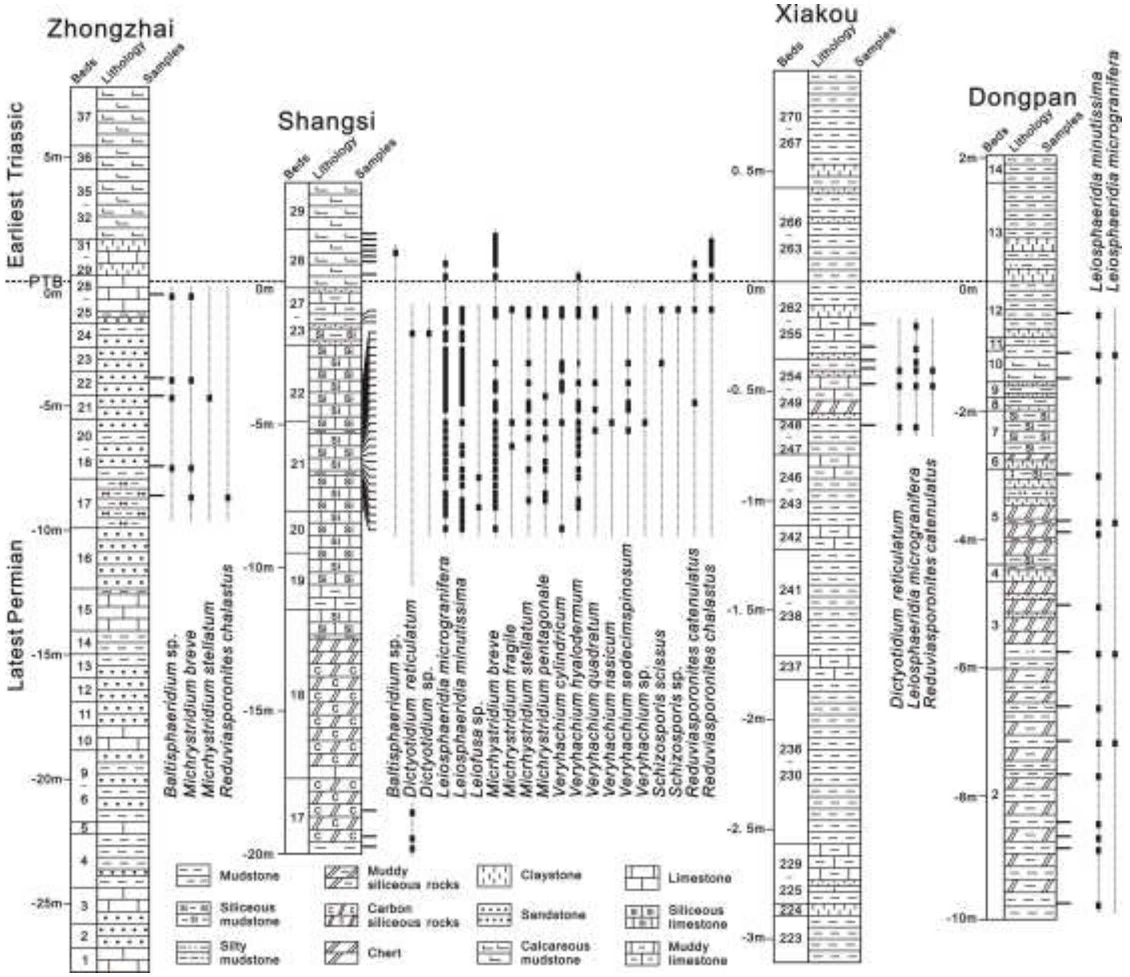
Zhongzhai
Shangsi
Xiakou
Dongpan
Beds
Lithology
Samples
Earliest Triassic
Latest Permian
PTB
0m
5m
-5m
-10m
-15m
-20m
-25m
0. 5m
-0. 5m
-1m
-1. 5m
-2m
-2. 5m
-3m
2m
-2m
-4m
-6m
-8m
-10m
Baltisphaeridium sp.
Michrystridium breve
Michrystridium stellatum
Reduviasporonites chalastus
Baltisphaeridium sp.
Dictyotidium reticulatum
Dictyotidium sp.
Leiosphaeridia microgranifera
Leiosphaeridia minutissima
Leiofusa sp.
Michrystridium breve
Michrystridium fragile
Michrystridium stellatum
Michrystridium pentagonale
Veryhachium cylindricum
Veryhachium hyalodermum
Veryhachium quadratum
Veryhachium nasicum
Veryhachium sedecimspinosum
Veryhachium sp.
Schizosporis scissus
Schizosporis sp.
Reduviasporonites catenulatus
Reduviasporonites chalastus
Dictyotidium reticulatum
Leiosphaeridia microgranifera
Reduviasporonites catenulatus
Leiosphaeridia minutissima
Leiosphaeridia microgranifera
Mudstone
Siliceous mudstone
Silty mudstone
Muddy siliceous rocks
Carbon siliceous rocks
Chert
Claystone
Sandstone
Calcareous mudstone
Limestone
Siliceous limestone
Muddy limestone

Figure 3:

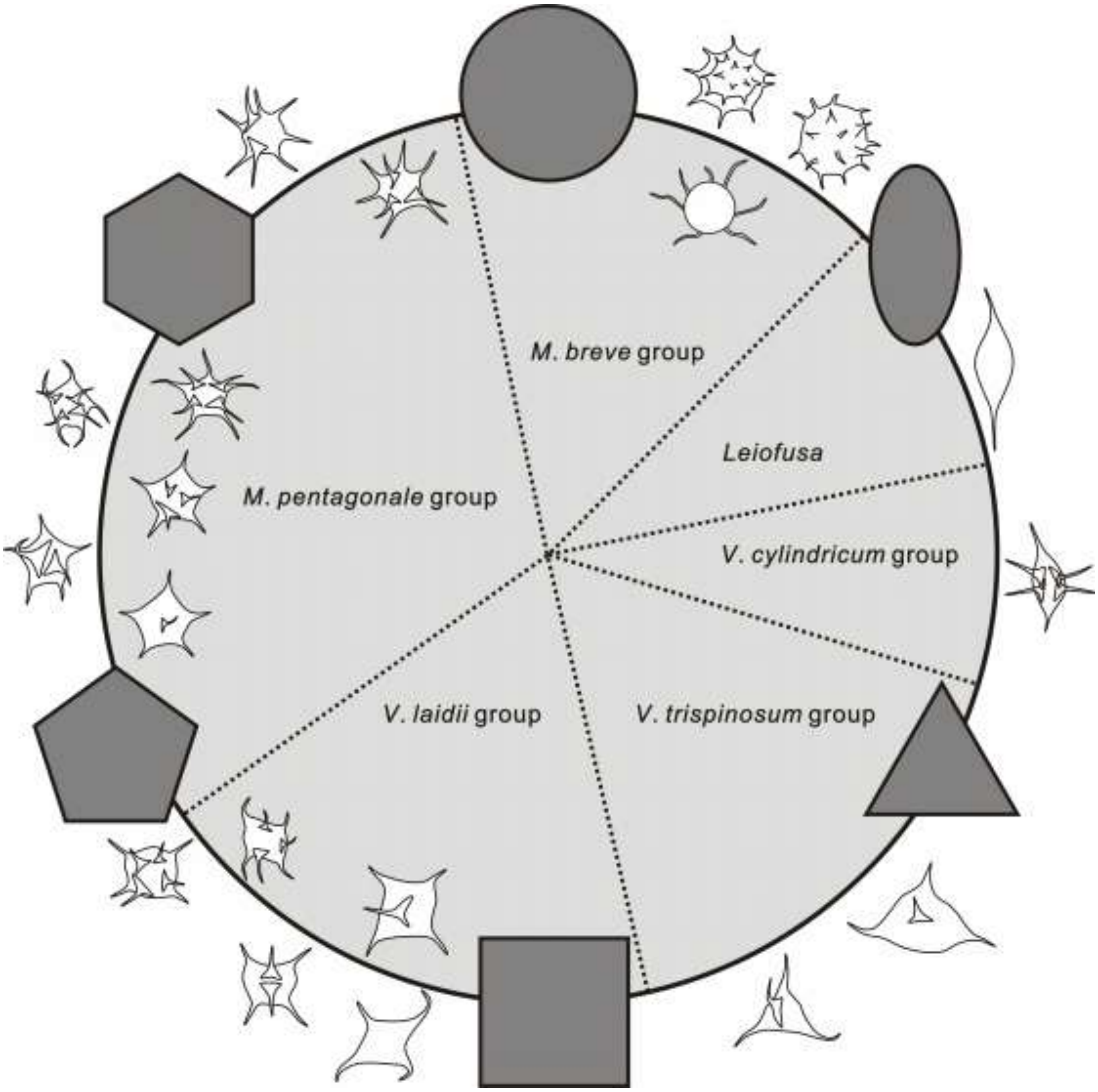

Table 1:

Group name	Shape of the vesicle	Include in this paper
V. cylindricum group	ellipsoidal	*V. cylindricum*
V. trispinosum group	triangular	*V. hyalodermum* *V.* sp.
V. laidii group	rectangular	*V. nasicum* *V. quadratum* *V. sedecimspinosum*
M. pentagonale group	pentagonal & hexagonal	*M. pentagonale* *M. stellatum*
M. breve group	spherical	*M. fragile* *M. breve*

Manuscript 6:
Submitted to Palaios

Volcanic Effects on Microplankton during the Permian-Triassic Transition (Shangsi and Xinmin, South China)

JUN SHEN[1, 2], **YONG LEI**[1, 3], THOMAS J. ALGEO[2], QINGLAI FENG[1,*], THOMAS SERVAIS[3], JIANXIN YU[4], and LIAN ZHOU[1]

[1] State Key Laboratory of Geological Processes and Mineral Resources, China University of Geosciences, Wuhan, Hubei, 430074, P.R. China

[2] Department of Geology, University of Cincinnati, Cincinnati, Ohio 45221-0013, U.S.A.

[3] UMR 8217 Géosystèmes, CNRS-Université Lille1, Cité Scientifique, F-59655 Villeneuve d'Ascq, France

[4] State Key Laboratory of Biology and Environmental Geology, China University of Geosciences, Wuhan, Hubei, 430074, P.R. China

ABSTRACT

The end-Permian mass extinction, the most severe biocrisis in Earth history, has been attributed to major flood basalt volcanism, but direct evidence of volcanic effects on contemporaneous marine biotas is scarce. In this study, we examined the relationship of two components of the microplankton community (acritarchs and radiolarians) to volcanic ash deposits in two deepwater sections from South China (Shangsi and Xinmin). In these sections, each eruptive event was recorded as a 'volcanic couplet' consisting of a pale, 0.1-3.0-cm-thick bentonite (altered volcanic ash) overlain by a dark, 0.1-1.0-cm-thick, organic-rich mudstone layer. Acritarchs were found in peak abundance in the mudstone overlying each ash layer but were otherwise present in only low concentrations in the background sediment. In contrast, radiolarians were rare in the volcanic couplets but frequently abundant in the background intervals. The thickest volcanic ash layers in both sections are found immediately below and above the latest Permian mass extinction (LPME) horizon. At this level, radiolarians underwent a major regional extinction but acritarchs reached their peak abundance, confirming their role as a 'disaster taxon'. Above the LPME, long-spined and small spherical acritarchs declined more rapidly than short-spined forms. The preference of the short-spined acritarchs for neritic inner-shelf facies may indicate that such areas served as biotic refugia during intervals of extreme environmental stress. We infer that volcanic eruptions during the Permian-Triassic transition had both positive effects (increased nutrient supply) and negative effects (metal toxicity, lowered seawater pH, increased turbidity) on marine microplankton communities, the importance of which varied both spatially and temporally.

Keywords: acritarch; radiolarian; South China; volcanic ash; mass extinction; end-Permian

INTRODUCTION

The end-Permian mass extinction at 252.28 Ma (Shen et al., 2011) was the largest biocrisis in Earth history, during which ~90% of marine and ~70% terrestrial species disappeared (Erwin, 1994; Erwin et al., 2002; Alroy, 2010). It has been linked to the Siberian Traps based on age correlation (Campbell et al., 1992; Renne et al., 1995; Reichow et al., 2009; Korte and Kozur, 2010), although the mechanisms by which these volcanic eruptions might have produced mass mortality remain under debate. Marine and terrestrial ecosystems are thought to have been stressed by a combination of global warming, acid rainfall, and changes in weathering rates and fluxes (Wignall, 2007; Algeo and Twitchett, 2010; Algeo et al., 2011a; Sobolev et al., 2011; Brand et al., 2012; Iacono-Marziano et al., 2012; Ogden and Sleep, 2012; Romano et al., 2012; Sun et al., 2012). Despite the coincidence of the main mass extinction of marine invertebrates with thin volcanic ash layers at Meishan D (Jin et al., 2000; Yin et al., 2001), the relationship of volcanism to changes in the marine microplankton community has received only limited attention to date (Isozaki et al., 2007; Shen et al., 2012a).

Volcanic ash/tuff layers are widely present around the Permian-Triassic boundary (PTB) in both shallow- and deep-water areas of the South China craton (Yang et al., 1991; Yin et al., 1992). In shallow-water sections, volcanic activity may have been associated with a proliferation of microbialites (Xie et al., 2010). In deep-water sections, volcanic activity has been linked to changes in marine redox conditions (Shen et al., 2012a, 2012b) and carbon cycle perturbations (Shen et al., 2012c). The source of these ash deposits has been a matter of debate, with some workers favoring continent-margin subduction-zone volcanism (Yin et al., 1992; Yang et al., 2012) and others favoring flood basalt volcanism (Xu et al., 2007) or, more specifically, the early, highly felsic eruptions of the Siberian Traps large igneous province (Shen et al., 2012c; Zhao et al., 2013). In this study, we generated paleontologic and geochemical data for two deepwater sections in South China (Shangsi and Xinmin) in order to investigate the relationship between volcanism and changes in the composition of the marine microplankton community during the Permian-Triassic transition.

MICROPLANKTON OF PERMIAN-TRIASSIC TRANSITION

Acritarchs

An acritarch is any small organic fossil that does not have a known biological affinity (Javaux et al., 2010). Many types are considered to be the resting cysts of eukaryotic marine algae, although some may be derived from archaea, bacteria, or metazoans. The group is thus polyphyletic, a condition reflected in the origin of their name, which can be translated to mean "confused origin". Acritarch diversity has varied tremendously through time, probably in relation to changes in plankton communities, nutrients, seawater chemistry, or atmospheric $p\text{CO}_2$ (see recent discussions in Riegel, 2008, and Strother, 2008). Acritarchs are closely associated with some major crises in Earth history, including the Triassic-Jurassic boundary crisis (van de Schootbrugge et al., 2007), and hence are considered to be 'disaster taxa'. Paleozoic acritarchs may be the remains of an important group of primary producers, predating modern oceanic primary producers such as dinoflagellates and diatoms, which diversified only in the Mesozoic (Katz et al., 2004; Munnecke and Servais, 2008). Because so few acritarchs are known from the Recent, modern marine dinoflagellates have been used as ecological analogs for ancient acritarchs (Strother, 2008).

The most common acritarch genera during the Late Permian to Early Triassic were *Dictyotidium, Leiosphaeridia, Veryhachium,* and *Micrhystridium*, representing four different morphological types. Spineless acritarchs had a smooth spherical shape and were either big spherical forms such as *Dictyotidium*, which could exceed 80 μm in diameter, or small spherical forms such as *Leiosphaeridia*, which were generally 20-30 μm in diameter. Acritarchs with spines were either long-spined, such as *Veryhachium* and some species of *Micrhystridium*, or short-spined, as were other species of *Micrhystridium*. All of the spineless forms were of relatively small diameter (<20 μm).

Acritarch diversity declined sharply at the time of the end-Permian crisis (Fig. 1). About 30 genera of acritarchs were present in the Changhsingian (Late Permian), ten genera between the LPME and the PTB, and seven genera in the Griesbachian (earliest Triassic; Ouyang and Utting, 1990; Li et al., 2004; Lei et al., 2012). Big spherical forms were the most strongly affected by the biocrisis; they declined abruptly at the LPME and went extinct at the PTB. Small spherical and long-spined forms also show a large decline at the LPME but survived into the Early Triassic. The short-spined forms, although relatively less diverse during the Late Permian, show the smallest decline during the P-Tr crisis interval (Fig. 1; Lei et al., 2012, 2013).

Radiolarians

Radiolarians are single-celled, eukaryotic marine zooplankton (Itaki, 2003). They are most abundant in the upper few hundred meters of the open ocean, although some species can be found at greater depths (Itaki, 2003). As with many types of zooplankton, they migrate diurnally through the water column, rising toward the surface at night in order to feed on phytoplankton and sinking below the photic zone during the day as a predator avoidance strategy. The siliceous skeletons of radiolarians commonly accumulate in large quantities in deep-ocean areas, producing radiolarian oozes in areas below the calcite compensation depth (CCD), where calcareous skeletons are completely dissolved (Thurman and Trujillo, 2004).

Deep-water sediments of Permo-Triassic age are commonly rich in radiolarians (Feng et al., 2000, 2007; Sano et al., 2010), which are useful for biostratigraphic correlation of facies lacking calcareous and phosphatic microfossils (Xia et al., 2004). Four orders of radiolarians are known from the Late Permian: Spumellaria, Entactinaria, Latentifistularia, and Albaillellaria. The relative depth preferences of these orders have been determined from their distributions in marine sediments of that age: spumellarians and entactinarians generally lived in shallower water, whereas latentifistularians and especially albaillellarians preferred deeper-water environments (Kozur, 1993; Feng and Algeo, 2013).

Radiolarians were strongly affected by the end-Permian crisis, with one order (Albaillellaria) going completely extinct at the LPME (Feng et al., 2000, 2007; Shen et al., 2012a; Feng and Algeo, 2013). Latentifistularians almost disappeared at the same time, and their diversity and abundance remained very low through the mid-Induan. The radiolarian orders preferring shallower waters (entactinarians and spumellarians) fared relatively better, with only moderate decreases in diversity and abundance at the LPME and with a stronger recovery in the mid-Induan. Radiolarians that survived the PTB crisis interval underwent a major radiation in the Anisian, or early Middle Triassic (Fig.1; see reviews by Feng et al., 2000, 2007).

STUDY SECTIONS

During the Permo-Triassic, the South China craton was a small (~3×10^8 km^2) peri-equatorial landmass located in the eastern part of the Paleotethys Ocean (Fig. 2A; Yang et al., 1987). The central part of the craton was a large area of shallow-marine carbonate facies known as the Yangtze Platform. West of this platform (equivalent to present-day north) was a carbonate ramp that descended toward the Qinling Sea, an arm of the Paleotethys. East of the Yangtze Platform (equivalent to present-day south) was the deepwater Nanpanjiang Basin, in which mainly siliceous and argillaceous sediments accumulated in the basinal facies. Sedimentation was essentially continuous in this basin during the Late Permian and Early Triassic, yielding an unbroken record of oceanic conditions throughout the crisis interval (Farabegoli and Perri, 2012; Yin et al., in review).

The Shangsi section is located on the southwestern margin of the Yangtze Platform (Fig. 2B). It has yielded one of the most detailed records of events during the Permian-Triassic mass extinction and was proposed as a candidate for the global stratotype section and point (GSSP) of the PTB (Lai et al., 1996). This section has been the subject of numerous biostratigraphic studies (Li et al., 1986; Lai et al., 1996; Nicoll et al., 2002; Jiang et al., 2011), providing a detailed framework for further research. The PTB was placed 22 cm above the base of Bed 28a by Jiang et al. (2011). The present study investigated the interval from 1.2 m below to 0.5 m above the PTB, representing the upper *Clarkina yini* Zone, the *C. meishanensis* Zone, and the lower *Hindeodus parvus* Zone. Based on our correlation of Shangsi to the Meishan D GSSP and recent radiometric dating of the both sections by Shen et al. (2011), we estimate the durations of the study intervals below and above the PTB to be ~0.5 Myr and 0.01 Myr, respectively.

The Xinmin section is located in the southern part of the South China craton (Fig. 2B). There, the Upper Permian Dalong Formation consists of argillaceous limestone, mudstone, and black shale and is highly fossiliferous. In contrast, the uppermost Permian to Lower Triassic Daye Formation consists of yellow mudstone containing few fossils. The PTB was placed 15 cm above the base of Bed 6 on the basis of correlations of conodont and carbon isotope profiles to the Meishan D GSSP (Shen et al., 2012b, 2012c). The present study investigated the interval from 1.8 m below to 0.4 m above the PTB, representing the upper *Clarkina yini* Zone, the *C. meishanensis* Zone, and the lower *Hindeodus parvus* Zone. Based on the timescale of Shen et al. (2011), we estimate the durations of the study intervals below and above the PTB to be ~0.3 Myr and 0.01 Myr, respectively. Environmental conditions during deposition of the Xinmin section were considered in detail by Shen et al. (2012b, 2012c).

Many volcanic ash layers are present in the two study sections, and they show an increase in frequency and thickness close to the PTB (Shen et al., 2012b, 2012c). Each ash layer is pale in color, soft in consistency, from 1 mm to <10 cm in thickness, and fossil free. The ash layers form the lower half of 'volcanic couplets' in the study sections, the upper half of which consists of thin (1 mm to few cm) laminated black mudstone layers with TOC concentrations up to 0.8%. These couplets are enclosed in background sediments consisting of deep-water deposits of calcareous mudstone at Shangsi and mixed calcareous and siliceous mudstones at Xinmin. The Shangsi section contains about six volcanic couplets and the Xinmin section about nine within the narrow study intervals bracketing the PTB (Figs. 3-4). In contrast, the much thinner Meishan D GSSP section contains only two couplets within the correlative interval, i.e., the volcanic ash layers of Beds 25 and 28 and their overlying black mudstone layers (Yin et al., 2001).

METHODS AND MATERIALS

Petrographic analysis

Fifty grams of each sample were processed using standard palynological methods (Albani et al., 2006) for acritarch analysis. Each sample was spiked with a known number of *Lycopodium* spores, and the mixture was then treated with hydrochloric acid (36.5%) and hydrofluoric acid (40%). The residue was concentrated using zinc bromide solution (S.G. 2.2). Neither oxidative nor alkali treatments were applied. We determined the concentrations of acritarch by measuring the frequency ratio of the components to *Lycopodium* spores in the concentrated residues using light microscopy and scanning electron microscopy (Tyson and Follows, 2000). Acritarch abundance was calculated from the ratio of the components of interest to the *Lycopodium* spores that had been added in the previous step. The concentration data shown in this study represent the abundance of each component per gram of sample.

The technique of Pessagno and Newport (1972) was used to analyze radiolarians in this study. One hundred grams of each sample were placed in dilute (3%) hydrofluoric acid for eight hours and then rinsed. After repetition of this process for two weeks, the residues were sieved (0.054 mm) and dried. Specimens were recovered from the dry residue with a fine brush under a microscope for taxonomic identification. Specimens were counted as whole fossils when the shell was at least three-quarters preserved. Two large and/or three small siliceous shell fragments were also counted as one individual. The best-preserved specimens were mounted on stubs and photographed with a scanning electronic microscope (SEM) for more precise determinations. Sample diversity was calculated on the basis of SEM analysis. The concentration data shown in this study represent the abundance of each component per gram of sample.

Geochemical analyses

Samples for geochemical analysis were trimmed to remove visible veins and weathered surfaces and pulverized to ~200 mesh size in an agate mortar. Major element abundances were determined by wavelength-dispersive X-ray fluorescence (XRF) analysis of fused glass beads using a XRF-1800 at the State Key Laboratory of Biogeology and Environmental Geology, China University of Geosciences (Wuhan). Trace elements and REEs were measured by Agilent 7500a inductively coupled plasma mass spectrometry (ICP-MS) at the State Key Laboratory of Geological Processes and Mineral Resources, China University of Geosciences (Wuhan). C and S elemental concentrations were measured using an Eltra 2000 C-S analyzer at the University of Cincinnati. Data quality was monitored via multiple analyses of USGS SDO-1 standard, yielding an analytical precision (2σ) of ±2.5% of reported values for C and ±5% for S.

RESULTS

Biota in Shangsi section

Although large spherical acritarchs (mainly *Dictyotidium*) are abundant in Wujiapingian and early Changhsingian strata at Shangsi, they were not recovered from the 1.7-m-thick study section bracketing the Permian-Triassic boundary (Lei et al., 2012). Only three types of acritarch were recovered from this interval: (1) small spherical forms, (2) long-spined forms, and (3) short-spined forms. The most abundant small spherical genus is *Leiosphaeridia*, the compressed vesicles of which are ~30 μm in diameter and have a dense granulose wall (Fig. 5a-e). The most abundant long-spined species are *Veryhachium hyalodermum* and *Micrhystridium stellatum*, which have ~20-μm-diameter polyangular vesicles with 8 to 12 simple spines or 'processes' (Fig. 5f-h). Despite being relatively long (6-15 μm) and hollow, the spines must have been strong as they are almost always preserved intact. The most abundant short-spined species is *Micrhystridium breve* (Fig. 5i-l). Its vesicles are <20 μm in diameter, ellipsoidal to spherical in outline, and covered with from 20 to 40 spines, each of which is 2 to 5 μm long, hollow, and acuminate (sharp-pointed).

The stratigraphic distributions of all three types of acritarchs are similar. Both small spherical and long-spined forms show increased abundances in the upper part of Bed 25 (just below the LPME) and at the base of Bed 28 (around the PTB; Fig. 6A-B). Lower concentrations of acritarchs were recovered between the LPME and the PTB, an interval equivalent to the *Clarkina meishanensis* conodont Zone (Yin et al., 2001). Short-spined forms show a similar distribution to the other two types below the PTB, but above the PTB their range extends ~30 cm higher within Bed 28 than those of the small spherical and long-spined forms (Fig. 6C). The total mass of acritarchs closely reflects the stratigraphic distribution of the three main types (Figs. 6D). The three types of acritarchs have similar abundances below Bed 28 and, thus, contribute more-or-less equally to total acritarch mass, but short-spined forms are completely dominant within Bed 28 (Fig. 6A-C, 7A).

Radiolarians in the Shangsi section are mainly of the spherical variety (Fig. 5m), belonging to the order Spumellaria. They were abundant during deposition of much of the Upper Permian Dalong Formation but declined toward the LPME. In the study interval, radiolarian abundance decreases rapidly in the upper part of Bed 24 and falls to zero in Bed 25 (Fig. 7B). A small number of radiolarians are found in Bed 26, just below the main extinction horizon, but they disappeared entirely during the LPME.

Total organic carbon (TOC) at Shangsi is low (0.2-0.5%), with the highest concentrations generally in the black mudstone portions of volcanic couplets (Fig. 7C). TOC shows modest positive covariation with acritarch concentration (Fig. 7A), with all intervals containing large concentrations of acritarchs also showing relative TOC enrichment (although the converse is not true). On the other hand, TOC shows no relationship to radiolarian concentrations (Fig. 7B).

Volcanic ash layers in Shangsi section

Six volcanic ash layers are found within the 1.7-m-thick study interval at Shangsi. They can be recognized easily in the field on the basis of color, consistency, and other characteristics (Fig. 3). The ash layers are also geochemically distinct, exhibiting higher Al concentrations (>8%) than the background sediment (Fig. 7D). The background sediment exhibits an increase in Al concentrations from <6% below Bed 25 to >6% in Beds 25-28, which may indicate that ash is present in significant amounts throughout the boundary interval—even within beds that are not obviously of volcanic origin. The background sediments show Pb/Al ratios similar to PAAS (i.e., 2-4 ppm/%; Taylor and McLennan, 1985; McLennan, 2001), but the black mudstone portions of volcanic couplets show 2-3X enrichment of Pb relative to these background values (Fig. 7E).

Biota in Xinmin section

Acritarchs at Xinmin are represented mainly by *Leiosphaeridia* (in Beds 1-3) and *Micrhystridium* (in Beds 4-6) (J. Yu, unpubl. data). They are relatively abundant below the middle of Bed 5 (Fig. 8A), where their concentrations are roughly an order of magnitude lower than in the Shangsi section (Fig. 7A). In the upper half of Bed 5, acritarch abundance falls to low values in the volcanic ash layers but increases somewhat in the black mudstones, relative to concentrations in background sediments lower in the section (Fig. 8A). In Bed 6, acritarch abundance falls sharply in the black mudstone portions of volcanic couplets.

Radiolarians at Xinmin were also dominated by spumellarians, with very rare albaillellarians (Fig. 8B; Xiang et al., 2013). Radiolarian abundance below the LPME is somewhat greater at this locale compared to Shangsi (Fig. 7B). As at Shangsi, radiolarian abundance falls sharply as the LPME horizon is approached and is effectively zero above the LPME (Fig. 8B).

TOC concentrations are generally low at Xinmin (0-0.8%), with the highest values found in the black mudstone portions of volcanic couplets (Fig. 8C). TOC appears to show weak positive covariation to acritarch and radiolarian abundances below the LPME, and somewhat stronger positive covariation with acritarch abundance in the volcanic couplets around the LPME and PTB (i.e., upper half of Bed 5 and Bed 6). However, these relationships could not be rigorously tested owing to measurement of fossil concentrations and TOC values on different suites of samples. See Shen et al. (2012b, 2012c) for a more detailed examination of the geochemistry of the Xinmin section.

Volcanic ash layers in Xinmin section

Volcanic ash layers were preserved well in the Xinmin section because of its relatively deep environment (Shen et al., 2012b). They can be recognized easily in the field based on color, consistency, and other characteristics (Fig. 4). Nine ash layers are present in the 2.2-m-thick study interval (Fig. 8), although additional ash layers, generally at wider stratigraphic spacing, are present above and below this interval. The ash layers are geochemically distinct, having Al concentrations (>8%) higher than in the background calcareous mudstones (Fig. 8D; Shen et al., 2012b). The background sediments exhibit Pb/Al and Cd/Al ratios similar to PAAS (i.e., ~2-4 ppm/% for Pb/Al and 1-2 ppm/% for Cd/Al; Taylor and McLennan, 1985; McLennan, 2001), but the black mudstone portions of volcanic couplets show enrichment of Pb and Cd by a factor of ~2-4X relative to background values (Fig. 8E).

DISCUSSION

General environmental controls on acritarchs and radiolarians

The distribution of phytoplankton in the modern ocean is influenced mainly by light, nutrients, and temperature (Thurman and Trujillo, 2004; Bouimetarhan et al., 2009). Photosynthetic primary producers are limited to the euphotic zone (~<100 m water depth) and frequently concentrated at much shallower depths (<10 m). Within the euphotic zone, phytoplankton abundance is often determined by the concentrations of major nutrients such as P and N, which are generally high within upwelling zones and low to moderate elsewhere. However, micronutrients such as Fe can be biolimiting in high-nutrient low-chlorophyll (HNLC) regions (Martin and Fitzwater, 1988), as shown by iron fertilization experiments (reviewed by Duggen et al., 2010). In most areas, modest increases in surface-water temperatures stimulate phytoplankton growth (Eppley, 1972; Nona et al., 2000). If, as generally believed, Paleozoic acritarchs were important primary producers, then they would have been subject to a similar set of influences as modern marine phytoplankton.

Environmental influences on Permian-Triassic acritarchs were considered by Lei et al. (2012). Based on studies in several areas of South China, they demonstrated that acritarchs were most abundant and diverse in shelf and upper-slope settings (Fig. 9). However, they noted a strong onshore-offshore gradient among the different types of acritarchs. Short-spined forms were relatively most abundant in neritic nearshore facies, but were also present in deep-shelf facies. Long-spined forms were present in nearshore facies but relatively more abundant in shallow- to deep-shelf settings. The small spherical species *Leiosphaeridia* was very rare in nearshore and shallow-shelf facies and showed an abundance peak in upper-slope settings (Fig. 9). As with modern plankton, this distribution reflects an optimization of different taxa to local environmental conditions, although the exact nature of the environmental controls remains uncertain (Servais et al., 2004; Lei et al., 2012).

The distribution of radiolarians in the modern open ocean is controlled by temperature, salinity, and water depth (Empson-Morin, 1984; Anderson et al., 1989; Matsuoka and Anderson, 1992; Kling and Boltovskoy, 1995). Optimum growth and longevity are observed at moderately warm temperatures (close to 28°C), and temperatures higher than 35°C and lower than 15°C inhibit radiolarian reproduction (Anderson et al., 1989; Matsuoka and Anderson, 1992). Temperature is probably the dominant control on the latitudinal distribution of radiolarians (Empson-Morin, 1984; Abelmann and Gowing, 1997). Radiolarians favor normal-marine salinities (Anderson et al., 1989) and do not generally thrive in reduced-salinity, estuarine environments (Moore, 1978; Kling, 1976; Abelmann and Gowing, 1997). Most species of radiolarians exhibit specific depth preferences, resulting in vertically stratified distributions in oceanic systems (Funnell, 1967; Kling and Boltovskoy, 1995).

Radiolarians from the Permian-Triassic transition interval are recovered mainly from slope and open oceanic settings (Feng et al., 2000, 2007; Sashida et al., 2000; Xia et al., 2004; De Wever et al., 2006; Sano et al., 2010). Low-latitude regions such as South China exhibit significantly greater diversity and abundance of radiolarians than high-latitude regions such as Russia (Vishnevskaya, 1997; Feng and Gu, 2002; He et al., 2005; Feng et al., 2007), probably due to latitude-related temperature variation as in the modern ocean (Abelmann and Gowing, 1997). The water-depth dependence of Permian-Triassic radiolarian communities has also been demonstrated (Fig. 9; Kozur et al., 1993; Feng and Algeo, 2013). Only orders favoring relatively shallow-water conditions (e.g., the Spumellaria and Entactinaria) were recovered from shallower marine sections such as Meishan (He et al., 2005), whereas all radiolarian orders were recovered from some deeper marine sections such as Dongpan (Feng et al., 2007; Shen et al., 2012a; Xiang et al., 2013). This pattern demonstrates that certain orders (e.g., the Latentifistularia and Albaillelaria) favored relatively deeper water habitats (Feng et al., 2007; Feng and Algeo, 2013).

Relationship of microplankton to volcanic ash layers in study sections

Acritarch and radiolarian concentrations vary in a quasi-systematic manner in relation to the volcanic couplets identified in the two study sections. Below the LPME horizon, acritarchs are found at low concentrations in the background sediments and at peak abundance in the black mudstone layers of volcanic couplets (Figs. 7A, 8A). In contrast, radiolarians are relatively abundant in the background sediments but generally absent in the black mudstone layers (Figs. 7B, 8B). Thus, acritarch and radiolarian concentrations are broadly anti-correlated. Acritarchs show no change in distribution pattern at and above the LPME, but radiolarians disappear almost completely from the study sections at this level.

We infer that these relationships represent control of contemporaneous microplankton community composition by volcanically induced marine environmental changes. Other than the presence of the thin volcanic couplets at decimeter intervals, each study section is of nearly uniform lithology and without evidence of changes in depositional facies or water depth that might have influenced microplanktic organisms (Li et al., 1986; Wignall et al., 1995; Jiang et al., 2011). Therefore, we consider below what types of effects volcanism might have had on Permian-Triassic microplankton communities.

Short-term volcanic effects on microplankton

Volcanic ash is fine-grained tephra that is produced and dispersed through the atmosphere during volcanic eruptions; it has particle diameters ranging from submicron to less than two millimeters (Horwell, 2007). Volcanic ash produced by large explosive eruptions can be dispersed thousands of kilometers away from the volcanic source and, thus, can potentially influence large areas of the ocean (cf. Duggen et al., 2010). Ash that settles in the ocean undergoes reactions with seawater and is eventually deposited and preserved in the form of bentonites (volcanic clay layers; e.g., Huff et al., 1992).

When ash is deposited on the ocean, gases and metals can be released to seawater, perturbing surface-water chemistry and biogeochemical cycles (Jones and Gislason, 2008). The deposition of volcanic ash may enhance marine plankton productivity by providing nutrients such as Fe (Frogner Kockum et al., 2006). Bio-available iron salts absorbed on the surface of ash can be released rapidly on contact with seawater (Jones and Gislason, 2008; Duggen et al., 2010; Olgun et al., 2011; Ayris and Delmelle, 2012). Addition of fine particulate iron to seawater can trigger a phytoplankton bloom at short timescales, i.e., days to weeks (Hamme et al., 2010; Lindenthal et al., 2012). Such a bloom resulted from the eruption of Kasatochi in the Aleutian Islands in 2008, covering an area of ~10^6 km^2 in the northeastern Pacific Ocean with fine ash (Langmann et al., 2010a, 2010b). Ash from Alaskan eruptions, including the 1912 Katmai event, are also thought to have triggered lacustrine phytoplankton blooms, as inferred from historical records of salmon catches (Eicher and Rounsefell, 1957).

Volcanic eruptions can also be detrimental to marine plankton through (1) hydrolysis of volcanic SO_2 and CO_2 to sulfuric and carbonic acids, resulting in acid rainfall and acidification of oceanic surface waters (Self et al., 2005); (2) leaching of toxic elements such as Pb and Hg from ash, poisoning the aqueous environment (Prosi, 1989; Felitsyn and Kirianov, 2002; Jones and Gislason, 2008); and (3) short-term suppression of planktic productivity through an increase in water turbidity linked to ash suspension (Felitsyn and Kirianov, 2002). Actualistic observations have been insufficient to document such effects on the plankton community for most historical eruptions, although several well-documented instances of effects on nektic organisms have been recorded. For example, the 1912 Katmai eruption in Alaska killed large numbers of salmon in several lakes into which flowed heavy volcanic mud slurries (Eicher and Rounsefell, 1957), and a 1996 eruption in Kamchatka killed the entire fish population of Lake Karym within a few hours (Felitsyn and Kirianov, 2002). While historical volcanic eruptions generally have had more pronounced effects on small freshwater bodies than on larger oceanic watermasses, ancient mega-eruptions such as that at the PTB potentially would have had similar positive and negative effects on ocean-surface biotas.

In the two study sections, pronounced changes in microplankton community compositions are observed in conjunction with each volcanic event (Figs. 7 and 8). The thin black mudstone layers that directly overlie each volcanic ash contain much higher concentrations of acritarchs than are found in the background sediment. This relationship is consistent with acritarchs being a ‘disaster taxon’ that exploited the disturbed environmental conditions developing in the aftermath of each volcanic eruption. Although the exact nature of the volcanically induced environmental changes that triggered acritarch blooms is uncertain, we hypothesize that settling volcanic ash introduced extra nutrients to the ocean surface layer. Additionally, acritarchs may have been better able than other microplanktic organisms to cope with stresses in the immediate post-eruption environment such as watermass turbidity (Algeo and Twitchett, 2010), enhanced fluxes of toxic elements such as Pb (Fig. 7E; Sanei et al., 2012), and reduced dissolved oxygen levels (Shen et al., 2012b).

In contrast to their beneficial effects on acritarchs, volcanic events appear to have been detrimental to the contemporaneous radiolarian community. Radiolarians are abundant in the background sediments of both study sections but nearly absent from the volcanic couplets (Figs. 7 and 8). The reason for the vulnerability of radiolarians to volcanic eruptions is uncertain, but several possibilities can be considered. First, rapid changes in the composition of the phytoplankton community, e.g., from (unfossilized) eukaryotic algae during environmentally stable intervals to a variety of other planktic taxa (including acritarchs) during eruptions, may have caused radiolarians to starve if they were unable to adapt quickly to changes in food supply. Second, zooplankton may have been more physically vulnerable to the effects of ash deposition, e.g., through physical abrasion or chemical toxicity. Third, zooplankton may have been more sensitive to concurrent changes in marine environmental conditions, especially the development of more reducing conditions during many eruptions (Shen et al., 2012a, 2012b). Expansion of the oceanic oxygen-minimum zone and chemocline shallowing (Kump et al., 2005) would have been a likely consequence of stimulation of marine productivity by volcanic nutrients (Algeo et al., 2011a). The negative effect of volcanic eruptions on zooplankton also has been documented in the deepwater Dongpan section, in which both the abundance and diversity of radiolarians decline in proximity to some ash layers (Shen et al., 2012a).

Long-term volcanic effects on microplankton

Intensification of volcanic activity during the latest Permian to earliest Triassic resulted in a change in the pattern of response of the microplankton community. Radiolarians experienced a major regional extinction at the level of the LPME (Fig. 1), disappearing entirely from the study sections (Figs. 7B and 8B). This extinction event is known to have occurred over a wide area, extending, at a minimum, across the eastern Tethys (Feng et al., 2000, 2007; Isozaki et al., 2007; Shen et al., 2012a) and central Panthalassic oceans (Algeo et al., 2010, 2011b). Some radiolarian orders went entirely extinct, e.g., the albaillellarians at the LPME and the latentifistularians during the Early Triassic, whereas other orders recovered and diversified in the aftermath of the PTB crisis, e.g., the entactinarians and spumellarians (Fig. 1). The post-crisis recovery of radiolarian faunas did not begin until the Dienerian (second half of the Early Triassic Induan Stage) and continued until at least the Anisian (early Middle Triassic; Fig. 1).

Acritarchs also experienced a major extinction during the Permian-Triassic transition, although the timing, pattern, and significance of this event are less well understood. All types of acritarchs underwent a major reduction in diversity and abundance at the LPME (Fig. 1), as seen in the study sections (Figs. 7A and 8A) and elsewhere (Lei et al., 2012). However, some types succumbed more rapidly than others: large spherical forms disappeared entirely at or close to the LPME, and small spherical and long-spined forms were sharply reduced at the same time (Fig. 1). However, surviving Paleozoic-type acritarchs were effectively 'dead-clade walking' taxa (Jablonski, 2002; Algeo et al., 2011a) that are considered to have gone completely extinct by the mid-Early Triassic (Fig. 1; Riegel, 2008). Post-Early Triassic acritarchs are unlikely to be direct evolutionary descendants of the forms that dominated late Paleozoic acritarch assemblages (Riegel, 2008).

The spatio-temporal distribution of acritarch types during the Late Permian and Permian-Triassic transition may provide insight into both their ecological roles and the nature of contemporaneous marine environments. At Shangsi, acritarch assemblages were dominated by large spherical forms such as *Dictyotidium* during the Wujiapingian and early Changhsingian and small spherical forms such as *Leiosphaeridia* during the mid to early late Changhsingian (Lei et al., 2013). By the latest Changhsingian, acritarch assemblages were dominated by long-spined and short-spined forms (Fig. 6). Sharp declines are seen among the long-spined forms above Bed 25 (just below the LPME) and among the short-spined forms above mid-Bed 28 (just above the PTB). While the reasons for earlier shifts are uncertain and may be due in part to long-term evolutionary trends, the changes in relative frequencies during the Permian-Triassic transition can be linked to marine environmental stresses. Late Paleozoic acritarchs exhibited a pronounced facies gradient, with small spherical forms predominant in deep-shelf to slope settings, long-spined forms in shallow-shelf settings, and short-spined forms in neritic inner-shelf settings (Fig. 9). The sequential decline of small spherical forms, followed by long-spined and then short-spined forms (Fig. 6), is thus consistent with a progressive encroachment of environmental stresses from the deep ocean onto continental shelves and, eventually, into nearshore regions.

The long-term effects of the Siberian Traps flood basalt eruptions on marine environments have received considerable attention recently. These eruptions resulted in massive releases of the greenhouse gases CO_2 and/or CH_4 (Retallack and Jahren, 2008; Brand et al., 2012), resulting in a very large (~15^0C) increase in tropical sea-surface temperatures (Romano et al., 2012; Sun et al., 2012). This extreme warming event led to strong oceanic stratification (Horacek et al., 2007; Song et al., 2013), contributing to a major expansion of the oceanic oxygen-minimum zone (Algeo et al., 2010, 2011b; Winguth and Winguth, 2012; Feng and Algeo, 2013). Upward movement of the chemocline (i.e., the upper surface of the oxygen-minimum zone; Kump et al., 2005) resulted in episodic eruption of H_2S-rich deepwaters into the ocean-surface layer, which, at least locally, was closely linked to the major biotic crisis at the LPME horizon (Algeo et al., 2007, 2008). Because the upward movement of the chemocline was gradual (i.e., time-transgressive), its effects were felt first by marine biotas in slope and deep-shelf settings and only somewhat later by biotas in shallower settings (Feng and Algeo, 2013). This pattern meant that some nearshore settings were relatively protected from intensifying marine environmental stresses and served as biotic refugia

(Beatty et al., 2008; Zonneveld et al., 2010). In this context, the stratigraphic distribution of acritarchs at Shangsi can be understood as a product of their relative facies preferences, with the taxa favoring nearshore settings (i.e., short-spined forms) surviving for a longer period during the crisis interval than the taxa that lived further offshore .

CONCLUSIONS

Volcanism is likely to have had both positive effects (increased nutrient supply) and negative effects (metal toxicity, lowered seawater pH, increased turbidity) on the microplankton community of Permian-Triassic oceans. The abundances of different microplanktic organisms varied in response to volcanic activity during the latest Permian, with post-eruption increases in acritarchs, possibly due to Fe fertilization, and decreases in radiolarians, possibly due to metal toxicity or changes in food supply. As volcanism intensified during the earliest Triassic, radiolarians experienced a major regional extinction event. Acritarchs exhibited a more complex response, first peaking (reflecting their role as a ‘disaster taxon’) and then declining. The hardiest acritarchs were short-spined forms that persisted in neritic inner-shelf facies after long-spined and small spherical forms had disappeared from deep-shelf and slope facies, suggesting that shallow nearshore regions may have served as refugia during intervals of extreme environmental stress in the Early Triassic.

ACKNOWLEDGMENTS

This work was supported by the 973 program (grant 2011CB808800), the 111 program (B08030), Ministry of Education of China (20110145130001), NSFC (project no. 41073007), China Geological Survey (1212011220796) and the U.S. National Science Foundation (TJA). We thank Prof. Shucheng Xie for improvement the first version of this manuscript. We are grateful to Yu Xiang and Xiaomei Nei for laboratory and field assistance. This paper is a contribution to IGCP Project 572.

REFERENCES

ABELMANN, A., and GOWING, M.M., 1997, Spatial distribution pattern of living polycystine radiolarian taxa-baseline study for paleoenvironmental reconstructions in the Southern Ocean (Atlantic sector): Marine Micropaleontology, v. 30, p, 3-28.

ALBANI, R., BAGNOLI, G., BERNARDEZ, E., GUTIERREZ-MARCO, J.C., and RIBECAI, C., 2006, Late Cambrian acritarchs from the “Túnel Ordovícico del Fabar”, Cantabrian Zone, N Spain: Review of Palaeobotany and Palynology, v. 139, p. 41-52.

ALGEO, T.J., CHEN, Z.-Q., FRAISER, M.L., and TWITCHETT, R.J., 2011a, Terrestrial-marine teleconnections in the collapse and rebuilding of Early Triassic marine ecosystems: Palaeogeography, Palaeoclimatology, Palaeoecology, v. 308, p. 1-11.

ALGEO, T.J., ELLWOOD, B.B., NGUYEN, T.K.T., ROWE, H., and MAYNARD, J.B., 2007, The Permian-Triassic boundary at Nhi Tao, Vietnam: Evidence for recurrent influx of sulfidic watermasses to a shallow-marine carbonate platform: Palaeogeography, Palaeoclimatology, Palaeoecology, v. 252, p. 304-327.

ALGEO, T.J., HENDERSON, C.M., TONG, J.-N, FENG, Q.-L, YIN, H.-F, and TYSON, R., 2013, Plankton and productivity during the Permian-Triassic boundary crisis: An analysis of organic carbon fluxes: Global and Planetary Change, in press. doi:10.1016/j.gloplacha.2012.02.008.

ALGEO, T.J., HINNOV, L., MOSER, J., MAYNARD, J.B., ELSWICK, E., KUWAHARA, K., and SANO, H., 2010, Changes in productivity and redox conditions in the Panthalassic Ocean during the latest Permian: Geology, v. 38, p. 187-190.

ALGEO, T.J., KUWAHARA, K., SANO, H., BATES, S., LYONS, T., ELSWICK, E., HINNOV, L., ELLWOOD, B., MOSER, J., and MAYNARD, J.B., 2011b, Spatial variation in sediment fluxes, redox conditions, and productivity in the Permian-Triassic Panthalassic Ocean: Palaeogeography, Palaeoclimatology, Palaeoecology, v. 308, p. 65-83.

ALGEO, T.J., SHEN, Y.-A, ZHANG, T.-G, LYONS, T.W., BATES, S.M., ROWE, H., and NGUYEN, T.K.T., 2008, Association of ^{34}S-depleted pyrite layers with negative carbonate δ^{13}C excursions at the Permian/Triassic boundary: Evidence for upwelling of sulfidic deep-ocean watermasses: Geochemistry, Geophysics, Geosystems, v. 9, Q04025, 10 pp.

ALGEO, T.J., and TWITCHETT, R.J., 2010, Anomalous Early Triassic sediment fluxes due to due to elevated weathering rates and their biological consequences: Geology, v. 38, p. 1023-1026.

ALROY, J., 2010, The shifting balance of diversity among major marine animal groups: Science, v. 329, p. 1191-1194.

ANDERSON, O.R., BENNETT, P., and BRYAN, M., 1989, Experimental and observational studies of radiolarian physiological ecology: 3. Effects of temperature, salinity and light intensity on the growth and survival of *Spongaster tetras tetras* maintained in laboratory culture: Marine micropaleontology, v. 14, p, 275-282.

AYRIS, P., and DELMELLE, P., 2012, Volcanic and atmospheric controls on ash iron solubility: A review: Physics and Chemistry of the Earth, v. 45-46, p. 103-112.

BEATTY, T.W., ZONNEVELD, J.-P., and HENDERSON, C.M., 2008, Anomalously diverse Early Triassic ichnofossil assemblages in northwest Pangea: A case for a shallow-marine habitable zone: Geology, v. 36, p. 771-774.

BOUIMETARHAN, I., MARRET, F., DUPONT, L., and ZONNEVELD, K., 2009, Dinoflagellate cyst distribution in marine surface sediment off West Africa (17-6^{0}N) in relation to sea-surface conditions, freshwater input and seasonal coastal upwelling: Marine Micropaleontology, v. 71, p.113-130.

BRAND, U., POSENATO, R., CAME, R., AFFEK, H., ANGIOLINI, L., AZMY, K., and FARABEGOLI, E., 2012, The end-Permian mass extinction. A rapid volcanic CO_2 and CH_4-climatic catastrophe: Chemical Geology, v. 322-333, p. 121-144.

CAMPBELL, I.H., CZAMANSKE, G.K., FEDORENKO, V.A., HILL, R.I., and STEPANOV, V., 1992, Synchronism of the Siberian Traps and the Permian-Triassic boundary: Science, v. 258, p. 1760-1763.

DE WEVER, P., O`DOGHERTY, L., and GAAORICAN, S., 2006, The plankton turnover at the Permian-Triassic boundary, emphasis on radiolarians: Eclogae Geologicae Helvetiae, v. 99, Suppl. 1, p. 49-62.

DUGGEN, S., OLGUN, N., CROOT, P., HOFFMANN, L., DIETZE, H., DELMELLE, P., and TESCHNER, C., 2010, The role of airborne volcanic ash for the surface ocean biogeochemical iron-cycle: a review: Biogeosciences, v. 7, p. 827-844.

EICHER, G.J., Jr., and ROUNSEFELL, G.A., 1957, Effects of lake fertilization by volcanic activity on abundance of salmon: Limnology and Oceanography, v. 2, p. 70-76.

EMPSON-MORIN, M.K., 1984, Depth and latitude distribution of Radiolaria in Campanian (Late Cretaceous) tropical and subtropical oceans: Micropaleontology, v. 30, p, 87-115.

EPPLEY, W.R., 1972, Temperature and phytoplankton growth in the sea: Fishery Bulletin, v. 70, p, 1063-1085.

ERWIN, D.H., 1994, The Permo-Triassic extinction: Nature, v. 367, p. 231-236.

ERWIN, D.H., BOWRING, S.A., and JIN, Y.-G., 2002, End-Permian mass-extinctions: a review, *in* Koeberl, C., and MacLeod, K.G., eds., Catastrophic Events and Mass Extinctions: Impacts and Beyond: Geological Society of America Special Papers, v. 356, p. 353-383.

FARABEGOLI, E., and PERRI, M.C., 2012, Millennial physical events and the end-Permian mass mortality in the western Palaeotethys: Timing and primary causes, *in* Talent, J.A., ed., Earth and Life, International Year of Planet Earth: Springer, Berlin, p. 719-758.

FELITSYN, S.B., and KIRIANOV, V.Y., 2002, Mobility of phosphorus during the weathering of volcanic ashes: Lithology and Mineral Resources, v. 37, p. 275-278.

FENG, Q,-L., and ALGEO, T.J., 2013, Evolution of oceanic redox conditions during the Permo-Triassic: Evidence from radiolarian deepwater facies: Earth-Science Reviews, in press.

FENG, Q.-L., and GU, S.-Z., 2002, Uppermost Changxingian (Permian) radiolarian fauna from southern Guizhou, southwestern China: Journal of Paleontology, v. 76, p. 797-809.

FENG, Q.-L., YANG, F.-Q., ZHANG, Z.-F., GAO, Y.-Q., and WANG, Z.-P., 2000, Radiolarian evolution during the Permian and Triassic transition in South and Southwest China, *in* Yin, H.-F, Dickins, J.H., Shi, G.R., and Tong, J.-N, eds., Permian-Triassic Evolution of Tethys and Western Circum-Pacific: Elsevier, Amsterdam, p. 309-326.

FLENLEY, J., 1971, Measurements of the specific gravity of the pollen exine: Pollen et Spores, v. 13, p. 179-186.

FROGNER KOCKUM, P.C., HERBERT, R.B., and GISLASON, S.R., 2006, A diverse ecosystem response to volcanic aerosols: Chemical Geology, v. 231, p. 57-66.

FUNNELL, M.B., 1967, Foraminifera and radiolarian as depth indicators in the marine environment: Marine Geology, v. 5, p. 333-347.

HAMME, R.C., WEBLEY, P.W., CRAWFORD, W.R., WHITNEY, F.A., DEGRANDPRE, M.D., EMERSON, S.R., ERIKSEN, C.C., GIESBRECHT, K.E., GOWER, J.F.R., KAVANAUGH, M.T., PAÑA, M.A., SABINE, C.L., BATTEN, S.D., COOGAN, L.A., GRUNDLE, D.S., and LOCKWOOD, D., 2010, Volcanic ash fuels anomalous plankton bloom in subarctic northeast Pacific: Geophysical Research Letters, v. 37, L19604, doi:10.1029/2010GL044629.

HE, W.-H., FENG, Q.-L., GU, S.-Z., and JIN, Y.-X., 2005, Changxingian (upper Permian) radiolarian fauna from Meishan D section, Changxing, Zhejiang, China, and its possible paleoecological significance: Journal of Paleontology, v. 79, p, 209-218.

HORACEK, M., BRANDNER, R., and ABART, R., 2007, Carbon isotope record of the P/T boundary and the Lower Triassic in the Southern Alps: evidence for rapid changes in storage of organic carbon: Palaeogeography Palaeoclimatology Palaeoecology, v. 252, p. 347-354.

HORWELL, C.J., 2007, Grain-size analysis of volcanic ash for the rapid assessment of respiratory health hazard: Journal of Environmental Monitoring, v. 9, p. 1107-1115.

HUFF, D.W., BERGSTOM, M.S., KOLATA, R.D., 1992, Gigantic Ordovician volcanic ash fall in North America and Europe: Biological, tectonomagmatic, and event-stratigraphic significance: Geology, v. 20, p, 875-878.

IACONO-MARZIANO, G., MARECAL, V., PIRRE, M., GAILLARD, F., ARTEBA, J., SCAILLET, B., and ARNDT, N., 2012, Gas emissions due to magma-sediment interactions during flood magmatism at the Siberian Traps. Gas dispersion and environmental consequences: Earth and Planetary Science Letters, v. 357-358, p. 308-318.

ISOZAKI, Y., 2009, Integrated "plume winter" scenario for the double-phased extinction during the Paleozoic–Mesozoic transition: the G-LB and P-TB events from a Panthalassic perspective: Journal of Asian Earth Sciences, v. 36, p. 459-480.

ISOZAKI, Y., SHIMIZU, N., YAO, J.-X., JI, Z.-S., and MATSUDA, T., 2007, End-Permian extinction and volcanism-induced environmental stress: The Permian-Triassic boundary interval of lower-slope facies at Chaotian, South China: Palaeogeography, Palaeoclimatology, Palaeoecology, v. 252, p. 218-238.

ITAKI, T., 2003, Depth-related radiolarian assemblage in the water-column and surface sediments of the Japan Sea: Marine Micropaleontology, v. 47, p. 253-270.

JABLONSKI, D., 2002, Survival without recovery after mass extinctions: Proc. Nat. Acad. Sci. (U.S.A.), v. 99, p. 8139-8144.

JAVAUX, E.J., MARSHALL, C.P., and BEKKERM, A., 2010, Organic-walled microfossils in 3.2-billion-year-old shallow-marine siliciclastic deposits: Nature, v. 463, P. 934-938.

JIANG, H.-S., LAI, X.-L., YAN, C.-B., ALDRIDGE, R.J., WIGNALL, P.B., and SUN, Y.-D., 2011, Revised conodont zonation and conodont evolution across the Permian-Triassic boundary at the Shangsi section, Guangyuan, Sichuan, South China: Global and Planetary Change, v. 77, p. 103-115.

JIN, Y.-G., WANG, Y., WANG, W., SHANG, Q.-H., CAO, C.-Q., and ERWIN, D.H., 2000, Pattern of marine mass extinction near the Permian Triassic boundary in South China: Science, v. 289, p. 432-436.

JONES, M.T., and GISLASON, S.R., 2008, Rapid releases of metal salts and nutrients following the deposition of volcanic ash into aqueous environments: Geochimica et Cosmochimica Acta, v. 72, p. 3661-3680.

KATZ, M.E., FINKEL, Z.V., GRZEBYK, D., KNOLL, A.H., and FALKOWSKI, P.G., 2004, Evolutionary trajectories and biogeochemical impacts of marine eukaryotic phytoplankton: Annual Review of Ecology, Evolution and Systematics, v. 35, p. 523-556.

KLING, A.S., 1976, Relation of radiolarian distributions to subsurface hydrography in the North Pacific: Deep-Sea Research I, v. 23, p. 1043-1058.

KLING, A.S., and BOLTOVSKOY, D., 1995, Radiolarian vertical distribution patterns across the southern California Current: Deep-Sea Research I, v. 42, p.191-231.

KORTE, C., and KOZUR, H.W., 2010, Carbon-isotope stratigraphy across the Permian- Triassic boundary: A review: Journal of Asian Earth Sciences, v. 39, p. 215-235.

KOZUR, H.W., 1993, Upper Permian radiolarians from the Sosio Valley Area, Western Sicily (Italy) and from the uppermost Lamar Limestone of West Texas: Jahrbuch der Geologischen Bundesanstalt Wien, v. 136, p. 99-123.

KUMP, L.R., PAVLOV, A., and ARTHUR, M.A., 2005, Massive release of hydrogen sulfide to the surface ocean and atmosphere during intervals of oceanic anoxia: Geology, v. 33, p. 397-400.

LAI, X.-L., YANG, F.-Q., HALLAM, A., and WIGNALL, P.B., 1996, The Shangsi section, candidate of the global stratotype section and point of the Permian-Triassic boundary, *in*.Yin, H.F., ed., The Palaeozoic-Mesozoic Boundary, Candidates of the Global Stratotype Section and Point of the Permian-Triassic Boundary: China University of Geosciences Press, Wuhan, China, p. 113-124.

LANGMANN, B., ZAKSEK, K., and HORT, M., 2010a, Atmospheric distribution and removal of volcanic ash after the eruption of Kasatochi volcano: A regional model study: Journal of Geophysical Research, v. 115, D00L06, doi:10.1029/2009JD013298.

LANGMANN, B., ZAKSEK, K., HORT, M., and DUGGEN, S., 2010b, Volcanic ash as fertilizer for the surface ocean: Atmospheric Chemistry and Physics, v. 10, p. 3891-3899.

LEI, Y., SERVAIS, T., FENG, Q.-L., and HE, W.-H., 2012, The spatial (nearshore-offshore) distribution of latest Permian phytoplankton from the Yangtze Block, South China: Palaeogeography, Palaeoclimatology, Palaeoecology, v. 363-364, p. 151-162.

LEI, Y., SERVAIS, T., and FENG, Q.-L., 2013, The diversity of the Permian phytoplankton: Review of Palaeobotany and Palynology, in press.

LI, J., SERVAIS, T., YAN, Y., and ZHU, H., 2004, A nearshore-offshore trend in the acritarch distribution of the Early-Middle Ordovician of the Yangtze Platform, S-China: Review of Palaeobotany and Palynology, v. 130, p. 141-161.

LI, Z.-S., ZHAN, L.-P., ZHU, X.-F., ZHANG, J.-H., JIN, R.-G., LIU, G.-F., SHENG, H.-B., SHEN, G.-M., DAI, J.-Y., HUANG, H.-Q., XIE, L.-C., and YAN, Z., 1986, Mass extinction and geological events between Palaeozoic and Mesozoic era: Acta Geologica Sinica, v. 60, p. 1-15 (in Chinese with English abstract).

LINDENTHAL, A., LANGMANN, B., PAETSCH, J., LORKOWSKI, I., and HORT, M., 2012, The ocean response to volcanic iron fertilization after the eruption of Kasatochi volcano: a regional scale biogeochemical ocean model study: Biogeosciences Discussion, v. 9, p. 9233-9257.

MARTIN, J.H., and FITZWATER, S.E., 1988, Iron deficiency limits phytoplankton growth in the north-east Pacific subarctic: Nature, v. 331, p. 341-344.

MATSUOKA, A., and ANDERSON, O.R., 1992, Experimental and observational studies of radiolarian physiological ecology: 5. Temperature and salinity tolerance of *Dictyocorybe truncatum*: Marine Micropaleontology, v. 19, p, 299-313.

MCLENNAN, S.M., 2001, Relationships between the trace element composition of sedimentary rocks and upper continental crust: Geochemistry Geophysics Geosystems, v. 2, GC000109, doi: 10.1029/2000GC000109.

MOORE, T.C., JR., 1978, The distribution of radiolarian assemblages in the modern and ice-age Pacific: Marine Micropaleontology, v. 3, p, 229-266.

MUNNECKE, A., and SERVAIS, T., 2008, Palaeozoic calcareous plankton: evidence from the Silurian of Gotland: Lethaia, v. 41, p. 185-194.

NICOLL, R.S., METCALFE, I., and WANG, C.-Y., 2002, New species of the conodont genus *Hindeodus* and conodont biostratigraphy of the Permian-Triassic boundary interval: Journal of Asian Earth Sciences, v. 20, p. 609-631.

NONA, S.R.A., CARLOS, M.D., and SUSANA, A., 2000, Nutrient and Temperature Control of the Contribution of Picoplankton to Phytoplankton Biomass and Production: Limnology and Oceanography, v. 45, p, 591-600.

OGDEN, D.E., and SLEEP, N.H., 2012, Explosive eruption of coal and basalt and the end-Permian mass extinction: Proceedings of the National Academy of Sciences (U.S.A.), v. 109, p. 59-62.

OLGUN, N., DUGGEN, S., CROOT, P.L., DELMELLE, P., and DIETZE, H., 2011, Surface ocean iron fertilization: The role of airborne volcanic ash from subduction zone and hot spot volcanoes and related iron fluxed into the Pacific Ocean: Global Biogeochemical Cycles, v. 25, GB4001, doi:10.1029/2009GB003761.

OUYANG, S., and UTTING, J., 1990, Palynology of upper Permian and lower Triassic rocks, Meishan, Changxing County, Zhejiang Province, China: Review of Palaeobotany and Palynology, v. 66, p. 65-103.

PESSAGNO, E.A., Jr., and NEWPORT, R.L., 1972, A technique for extracting radiolaria from radiolarian cherts: Micropaleontology, v. 18, p. 231-234.

PROSI, F., 1989, Factors controlling biological availability and toxic effects of lead in aquatic organisms: Science of the Total Environment, v.79, p. 157-169.

REICHOW, M.K., PRINGLE, M.S., AL'MUKHAMEDOV, A.I., ALLEN, M.B., ANDREICHEW, V.L., BUSLOV, M.M., DAVIES, C.E., FEDOSEEV, G.S., FITTON, J.G., INGER, S., MEDVEDEV, A.Y., MITCHELL, C., PUCHKOV, V.N., SAFANOVA, I.Y., SCOTT, R.A., and SAUNDERS, A.D., 2009, The timing and extent of the eruption of the Siberian Traps large igneous province. Implications for the end-Permian environmental crisis: Earth and Planetary Science Letters, v. 277, p. 9-20.

RENNE, P.R., ZHENG, Z.-C., RICHARDS, M.A., BLACK, M.T., and BASU, A.R., 1995, Synchrony and causal relations between Permian-Triassic boundary crisis and Siberian flood volcanism: Science, v. 269, p. 1413-1416.

RETALLACK, G.J., and JAHREN, A.H., 2008, Methane release from igneous intrusion of coal during later Permian extraction events: Journal of Geology, v. 116, p. 1-20.

RIEGEL, W., 2008, The Late Palaeozoic phytoplankton blackout—Artefact or evidence of global change: Review of Palaeobotany and Palynology, v.148, p. 73-90.

ROMANO, C., GOUDEMAND, N., VENNEMANN, T.W., WARE, D., SCHNEEBELI-HERMANN, E., HOCHULI, P.A., BRÜHWILER, T., BRINKMANN, W., and BUCHER, H., 2012, Climatic and biotic upheavals following the end-Permian mass extinction: Nature Geoscience, v. 6, p. 57-60.

SANEI, H., GRASBY, S.E., and BEAUCHAMP, B., 2012, Latest Permian mercury anomalies: Geology, v. 40, p. 63-66.

SANO, H., KUWAHARA, K., YAO, A., and AGEMATSU, S., 2010, Panthalassan seamount-associated Permian-Triassic boundary siliceous rocks, Mino terrane, central Japan. Paleontological Research, v. 14, p. 295-316.

SASHIDA, K., SALYAPONGSE, S., and NAKORNSRI, N., 2000, Latest Permian radiolarian fauna from Klaeng, Eastern Thailand: Micropaleontology, v. 46, p. 245-263.

SELF, S., THORDARSON, T., and WIDDOWSON, M., 2005, Gas fluxes from flood basalt eruption: Elements, v. 1, p. 283-287.

SERVAIS, T., STRICANNE, L., MONTENARI, M., and PROSS, J., 2004, Population dynamics of galeate acritarchs at the Cambrian-Ordovician transition in the Algerian Sahara: Palaeontology, v. 47, p. 395-414.

SHEN, J., ALGEO, T.J., HU, Q., XU, G.-Z, ZHOU, L., and FENG, Q.-L., 2012b, Volcanism in South China during the Late Permian and its relationship to marine ecosystem and environmental changes: Global Planetary Change, in press, doi: 10.1016/j.gloplacha.2012.02.011.

SHEN, J., ALGEO, T.J., HU, Q., ZHANG, N., ZHOU, L., XIA, W.-C, XIE, S.-C, and FENG, Q.-L., 2012c, Negative C-isotope excursions at the Permian-Triassic boundary linked to volcanism: Geology, v. 40, p. 963-966.

SHEN, J., ALGEO, T.J., ZHOU, L., FENG, Q.-L, YU, J.-X, and ELLWOOD, B.B., 2012a, Volcanic perturbations of the marine environment in South China preceding the latest Permian extinction event and their biotic effects: Geobiology, v. 10, p. 82-103.

SHEN, S.-Z., CROWLEY, J.L., WANG, Y., BOWRING, S.A., ERWIN, D.H., SADLER, P.M., CAO, C.-Q., ROTHMAN, D.H., HENDERSON, C.M., RAMEZANI, J., ZHANG, H., SHEN, Y.-A., WANG, X.-D., WANG, W., MU, L., LI, W.-Z., TANG, Y.-G., LIU, X.-L., LIU, L.-J., ZENG, Y., JIANG, Y.-F., and JIN, Y.-G., 2011, Calibrating the end-Permian mass extinction: Science, v. 334, p. 1367-1372.

SOBOLEV, S.V., SOBOLEV, A.V., KUZMIN, D.V., KRIVOLUTSKAYA, N.A., PETRUNIN, A.G., ARNDT, N.T., RADKO, V.A., and VASILIEV, Y.R., 2011, Linking mantle plumes, large igneous provinces and environmental catastrophes: Nature, v. 477, p. 312-316.

SONG, H.-Y., TONG, J.-N., ALGEO, T.J., HORACEK, M., QIU, H.-O., SONG, H.-J., TIAN, L., and CHEN, Z.-Q., 2013, Large vertical $\delta^{13}C_{DIC}$ gradients in Early Triassic seas of the South China craton: Implications for oceanographic changes related to Siberian Traps volcanism: Global and Planetary Change, in press; doi.org/10.1016/j.gloplacha.2012.10.023.

STROTHER, P.K., 2008, A speculative review of factors controlling the evolution of phytoplankton during Paleozoic time: Revue de Micropaléontologie, v. 51, p. 9-21.

SUN, Y.-D., JOACHIMSKI, M.M., WIGNALL, P.B., YAN, C.-B., CHEN, Y.-L., JIANG, H.-S., WANG, L.-N., and LAI, X.-L., 2012, Lethally hot temperatures during the early Triassic greenhouse: Science, v. 388, p. 366-370.

TAYLOR, S.R., and MCLENNAN, S.M., 1985, The Continental Crust: Its Composition and Evolution. Blackwell, Oxford, 312 pp.

THURMAN, H.V., and TRUJILLO, A.P., 2004, Introductory Oceanography, 10th ed. Pearson, Upper Saddle River, New Jersey, 416 pp.

TYSON, R.V., and FOLLOWS, B., 2000, Palynofacies prediction of distance from sediment source: A case study from the Upper Cretaceous of the Pyrenees: Geology, v. 28, p. 569-571.

VAN DE SCHOOTBRUGGE, B., TREMOLADA, F., ROSENTHAL, Y., BAILEY, T.R., FEIST-BURKHARDT, S., BRINKHUIS, H., PROSS, J., KENT, D.V., and FALKOWSKI, P.G., 2007, End-Triassic calcification crisis and blooms of organic-walled ‘disaster species’: Palaeogeography, Palaeoclimatology, Palaeoecology, v. 244, p. 126-141.

VISHNEVSKAYA, V., 1997, Development of Palaeozoic-Mesozoic radiolarian in the northwestern Pacific rim: Marine Micropaleontology, v. 30, p. 79-95.

WIGNALL, P.B., 2007, The end-Permian mass extinction—how bad did it get?: Geobiology, v. 5, p. 303-309.

WIGNALL, P.B., HALLAM, A., LAI, X.-L., and YANG, F.-Q., 1995, Palaeoenvironmental changes across the Permian/Triassic boundary at Shangsi (N. Sichuan, China): Historical

Biology, v. 10, p. 175-189.WINGUTH, C., and WINGUTH, A.M.E., 2012, Simulating Permian-Triassic oceanic anoxia distribution: implications for species extinction and recovery: Geology, v. 40, p. 127-130.

XIA, W.-C., ZHANG, N., WANG, G.-Q., and KAKUWA, Y., 2004, Pelagic radiolarian and conodont biozonation in the Permo-Triassic boundary internal and correlation to the Meishan GSSP: Micropaleontology, v. 50, p. 27-44.

XIANG, Y., FENG, Q.-L., SHEN, J., and ZHANG, N., 2013, Changhsingian radiolarian fauna from Anshun, Guizhou and its relationship to TOC and paleo-productivity: Science in China Series D (Earth Science), in press.

XIE, S.-C, PANCOST, R.D., WANG, Y.-B, YANG, H., WIGNALL, P.B., LUO, G.-M., JIA, C.-L, and CHEN, L., 2010, Cyanobacterial blooms tied to volcanism during the 5 m.y. Permo-Triassic biotic crisis: Geology, v. 38, p. 447-450.

XU, L., LIN, Y.-T., SHEN, W.-J, QI, L., XIE, L.-W., and OUYANG, Z.-Y., 2007, Platinum group elements of the Meishan Permian-Triassic boundary section: Evidence for flood basaltic volcanism: Chemical Geology, v. 246, p. 55-64.

YANG, J.-H., CAWOOD, P.A., DU, Y.-S., HUANG, H., HUANG, H-W., and TAO, P., 2012, Large igneous province and magmatic arc sourced Permian-Triassic volcanogenic sediments in China: Sedimentary Geology, v. 261-262, p. 120-131.

YANG, Z.-Y., WU, S.-B., YIN, H.-F., XU, G.-R., ZHANG, K.-X., and BI, X.-M., 1991, Permo-Triassic events of South China: Geological Publishing House, Beijing, China, p. 35-64 (in Chinese).

YANG, Z.-Y., YIN, H.-F., WU, S.-B., YANG, F.-Q., DING, M.-H., and XU, G.-R., 1987, Permian-Triassic boundary stratigraphy and fauna of South China: Geological Publishing House, Beijing, China, 378 pp. (in Chinese).

YIN, H.-F, HUANG, S.-J, ZHANG, K.-X., HANSEN, H.J., YANG, F.-Q., DING, M.-H., and BIE, X.-M., 1992, The effects of volcanism on the Permo-Triassic mass extinction in South China, *in* Sweet, W.C., Yang, Z.-Y., Dickins, J.M., and Yin, H.-F., eds., Permo-Triassic Events in the Eastern Tethys: Cambridge University Press, Cambridge, p. 169-174.

YIN, H.-F., JIANG, H.-S., XIA, W.-C., FENG, Q.-L., ZHANG, N., and SHEN, J., under review, The end-Permian regression in South China and its implication on mass extinction: Earth-Science Reviews, submitted in September. 2012.

YIN, H.-F., ZHANG, K.-X., TONG, J.-N., YANG, Z.-Y., and WU, S.-B., 2001, The Global Stratotype Section and Point (GSSP) of the Permian-Triassic boundary: Episodes, v. 24, p. 275-275.

ZHAO, L.-S, CHEN, Z.-Q., ALGEO, T.J., CHEN, J.-P., CHEN, Y.-L., TONG, J.-N., GAO, S., ZHOU, L., HU, Z.-C, and LIU, Y.-S., 2013, Rare-earth element patterns in conodont albid crowns: Evidence for massive inputs of volcanic ash during the latest Permian biocrisis?: Global and Planetary Change, in press; doi.org/10.1016/gloplacha.2012.09.001.

ZONNEVELD, J.-P., BEATTY, T.W., MACNAUGHTON, R.B., PEMBERTON, S.G., UTTING, J., and HENDERSON, C.M., 2010, Sedimentology and ichnology of the Lower Triassic Montney Formation in the Pedigree-Ring/Border-Kahntah River area, northwestern Alberta and northeastern British Columbia: Bulletin of Canadian Petroleum Geology, v. 58, p. 115-140.

FIGURE CAPTIONS

FIGURE 1—Diversity of acritarchs and radiolarians from later Permian to Middle Triassic. Representative acritarch genera are *Dictyotidium* for big spherical forms, *Leiosphaeridia* for small spherical forms, *Veryhachium* and some species of *Micrhystridium* for long-spined forms, and other species of *Micrhystridium* for short-spined forms. Acritarch diversity data from Lei et al. (2012, 2013); radiolarian diversity and range data from Feng et al. (2007), Isozaki (2009), and Shen et al. (2012a). Abbreviations: M-Triassic = Middle Triassic, LPME = latest Permian mass extinction, PTB = Permian-Triassic boundary.

FIGURE 2—(A) Global paleogeography at the Permian-Triassic boundary (~252 Ma). (B) Changhsingian paleogeographic map of South China at the *Clarkina meishanensis* Zone (modified after Yin et al., in review). GSSP = Global Stratotype Section and Point.

FIGURE 3—Field photos from Shangsi section showing the volcanic couplets of ash and mudstone (C1 to C3). AL = argillaceous limestone, VA = volcanic ash, M = mudstone.

FIGURE 4—Field photos from Xinmin section showing (A) volcanic couplets in the full study section, and (B) detailed view of couplets C1 to C5 in a 1-m-thick interval. AL = argillaceous limestone, VA = volcanic ash, BS = black shale.

FIGURE 5—Photomicrographs of microfossils from the Shangsi section. The scale bar is15 m for a-l and 50 m for m. a-e are *Leiosphaeridia microgranifera*; f-h are *Veryhachium hyalodermum* 8: *Micrhystridium stellatum*; i-l: *Micrhystridium breve*; m: radiolarian belonging to order Spumellaria.

FIGURE 6—Concentrations of (A) small spherical acritarch, (B) long-spined acritarchs, and (C) short-spined acritarchs, and (D) total acritarch mass. The concentration data represent the number of individual acritarchs per gram of sediment. Total acritarch mass was calculated as $\rho\times(4/3)\times\pi\times(R^3-r^3)$, where ρ is the average density of acritarch vesicles (an estimate of 1.7 g cm^{-3} was used; cf. Flenley, 1971), and R and r represent the radius of the outside and inside of the acritarch shell, respectively (~15 and 13.5 m for small spherical acritarch, and ~10 and 9 m

for acritarchs with spines; Fig. 4). The age data were base on Shen et al. (2011). Abbreviations: S = (sub) stage, F = formation, Z = conodont zone, B = bed, Lith = lithology, C = cycle; ME = (latest Permian) mass extinction, PTB = Permian-Triassic boundary; (conodont zones) *C*. = *Clarkina*, *H*.= *Hindeodus*, *meishan*.= *meishanensis*; (lithology) L = limestone, AL = argillaceous limestone, VA = volcanic ash, M = mudstone, and C = calcareous mudstone. The purple shaded bars are volcanic ash layers (cm), and the gray shaded bars represent mudstone layers overlying the ash layers. Other details as in Figure 3.

FIGURE 7—Bio- and chemostratigraphic data of Shangsi section: (A) concentration of total acritarchs, (B) concentration of radiolarians, (C) total organic carbon (TOC), (D) Al, and (E) Pb/Al ratios (ppm/%). Concentrations based on the abundance of each fossil component in one gram sample (see text). Other details as in Figures 3 and 6.

FIGURE 8—Bio- and chemostratigraphic data of Xinmin section: (A) concentration of total acritarchs, (B) concentration of radiolarians, (C) total organic carbon (TOC), (D) Al, and (E) element/Al ratios (ppm/%). Concentrations based on the abundance of each fossil component in one gram sample (see text). The units of Pb/Al and Cd/Al are 10^{-4} (ppm/%) and 10^{-6} (100×ppm/%), respectively. Ages were based on Yin et al. (2001) and Shen et al. (2011). Other details as in Figures 3 and 6.

FIGURE 9—Facies and water depth distributions of actitarchs and radiolarians. Based on Feng et al. (2007), Lei et al. (2012), and Feng and Algeo (2013).

FIGURE 10—Interpretative reconstructions of changes in marine environment and microplankton communities during the Permian-Triassic transition. (A) Abundance of radiolarian, and relative normal concentration of different kinds of acritarch in normal deposit preceding the LPME. (B) Higher abundance of acritarch, rare radiolarian and more abundance of organic matter deposit, along with the expansion of OMZ during the volcanic eruptions preceding the LPME. (C) Rare acritarch in the normal environment post the LPME. (D) Relatively enrichment of short-spined acritarch and organic matter along with the expansion of the OMZ during the volcanic eruption post the LPME. SL = sea level, OMZ = oxygen minimum zone.

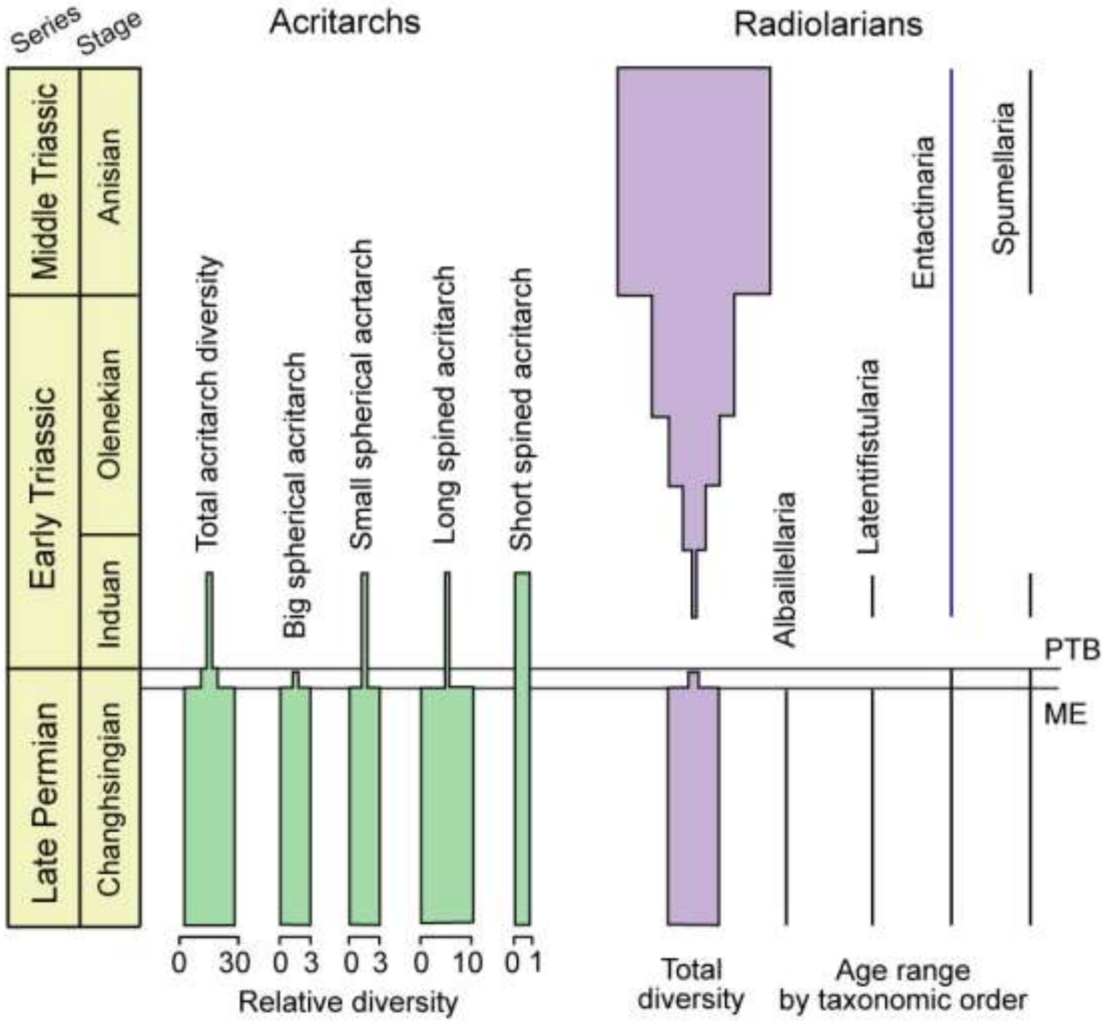
Series
Stage
Acritarchs
Radiolarians
Middle Triassic
Anisian
Early Triassic
Olenekian
Induan
Late Permian
Changhsingian
Total acritarch diversity
Big spherical acritarch
Small spherical acrtarch
Long spined acritarch
Short spined acritarch
Albaillellaria
Latentifistularia
Entactinaria
Spumellaria
PTB
ME
0 30
0 3
0 3
0 10
0 1
Relative diversity
Total diversity
Age range by taxonomic order

FIGURE 1

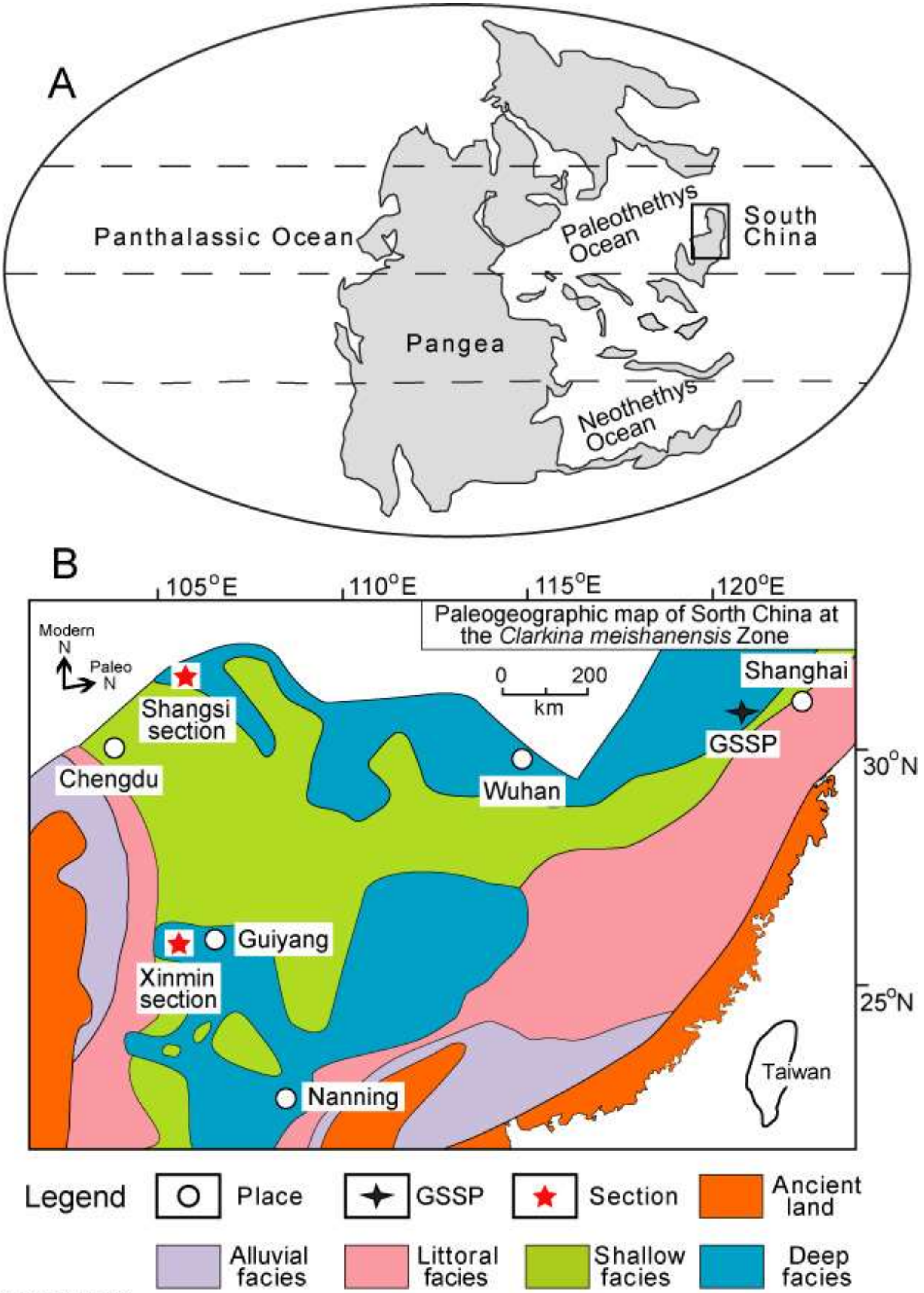
A
Panthalassic Ocean
Paleothethys Ocean
South China
Pangea
Neothethys Ocean
B
105°E
110°E
115°E
120°E
Paleogeographic map of Sorth China at the *Clarkina meishanensis* Zone
Modern N
Paleo N
0
200
km
Shangsi section
Chengdu
Wuhan
Shanghai
GSSP
30°N
25°N
Guiyang
Xinmin section
Nanning
Taiwan
Legend
Place
GSSP
Section
Ancient land
Alluvial facies
Littoral facies
Shallow facies
Deep facies

FIGURE 2

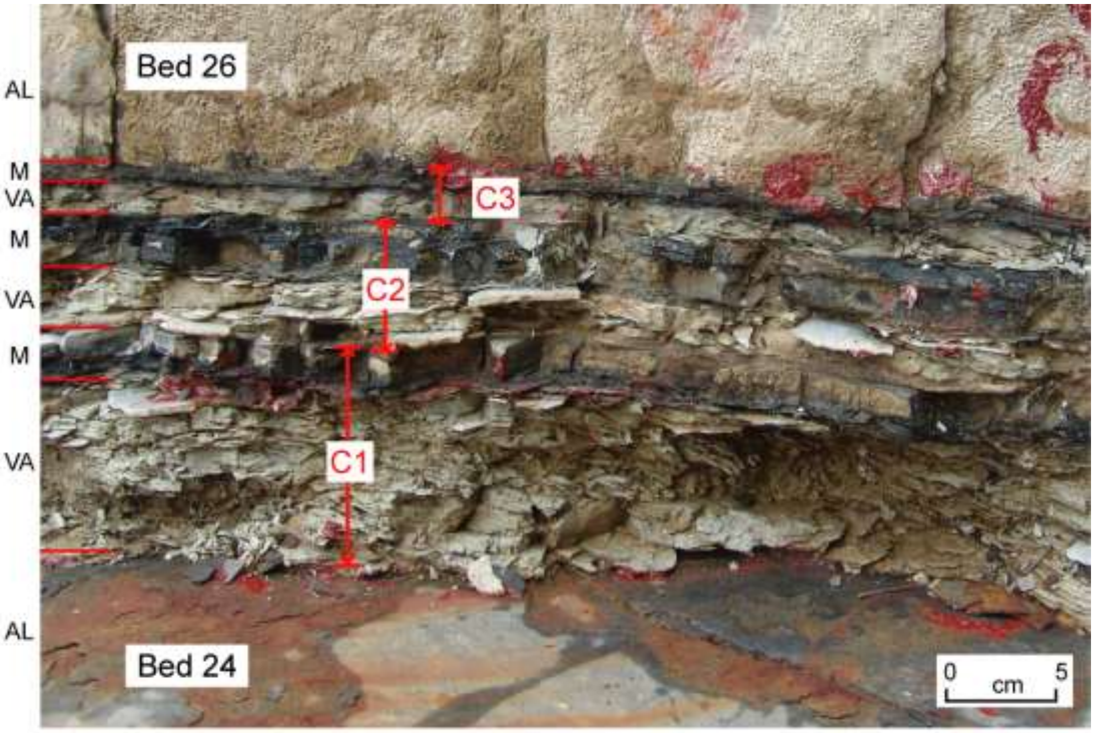

FIGURE 3

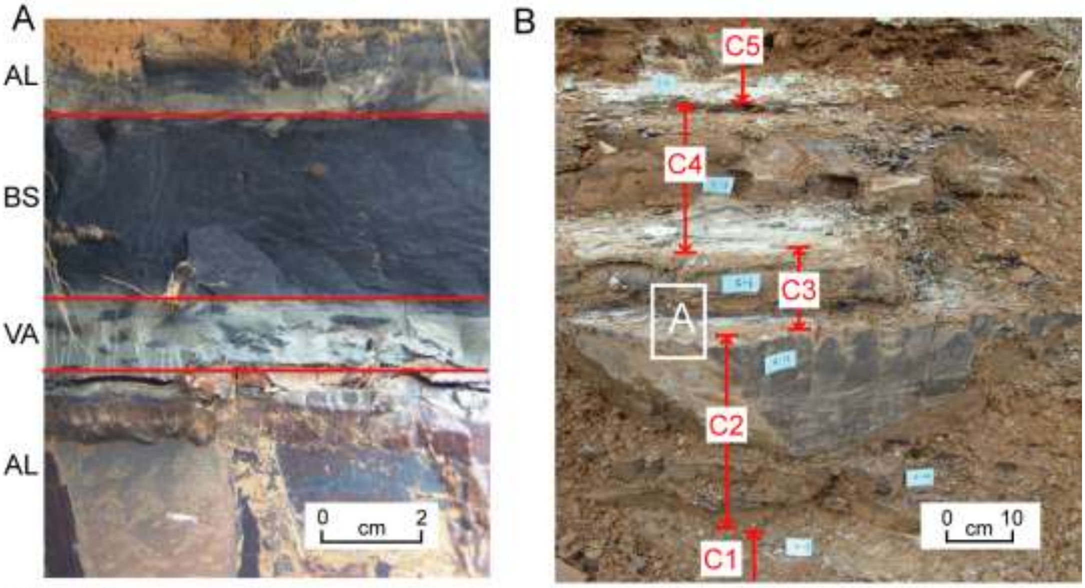

FIGURE 4

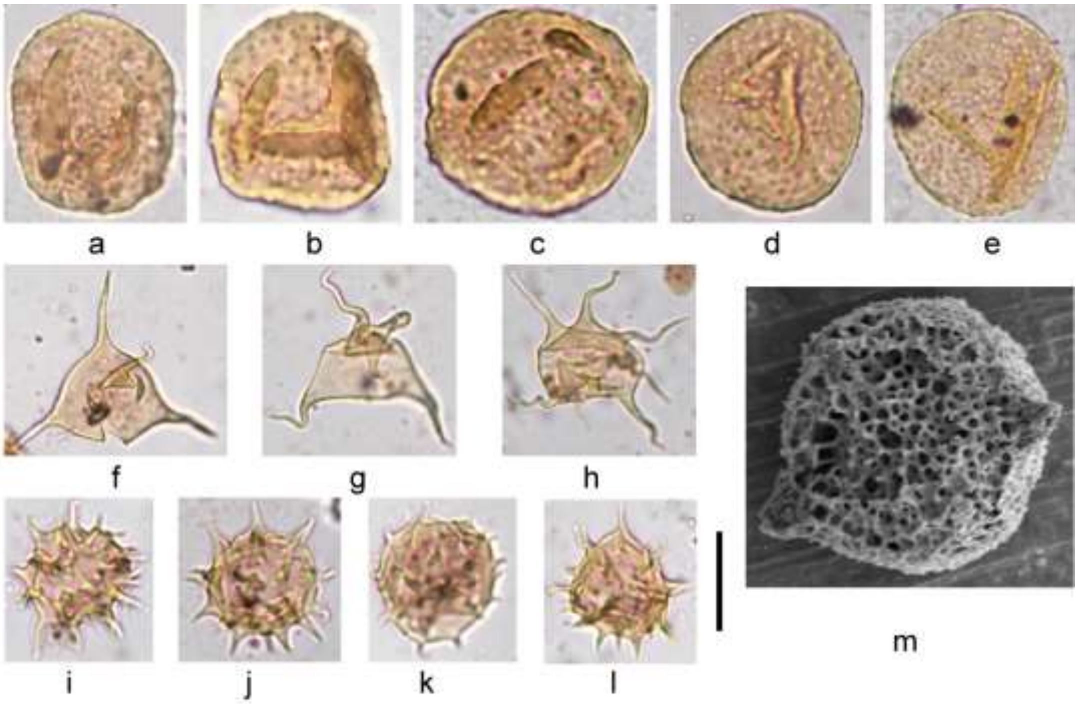

FIGURE 5

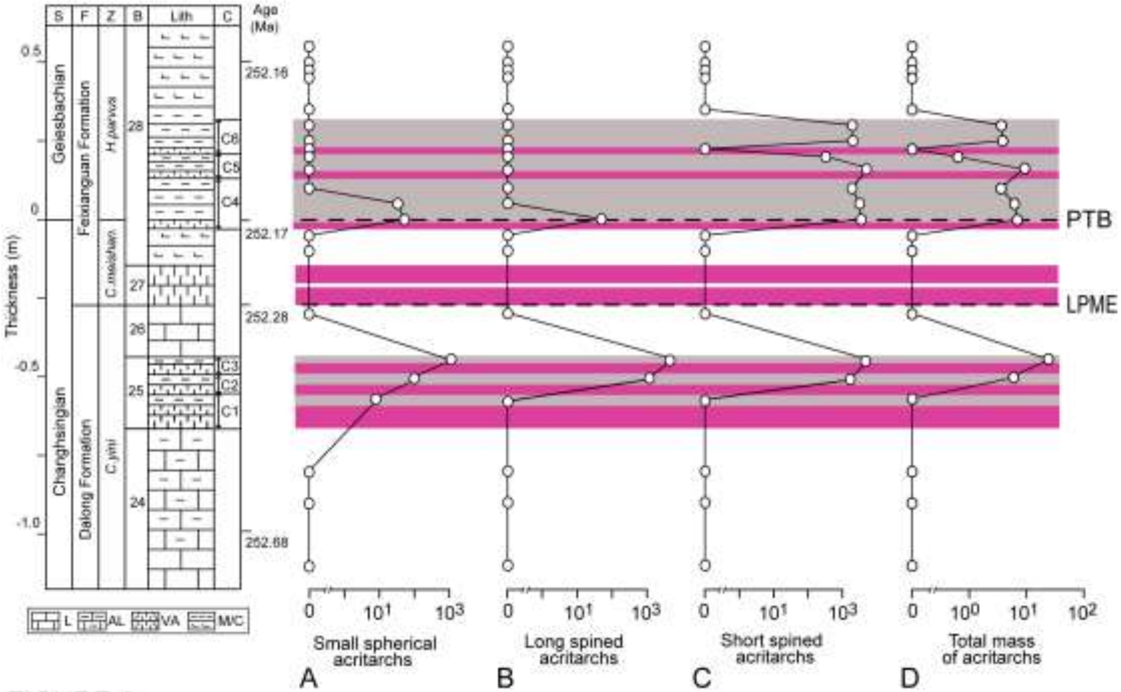

FIGURE 6

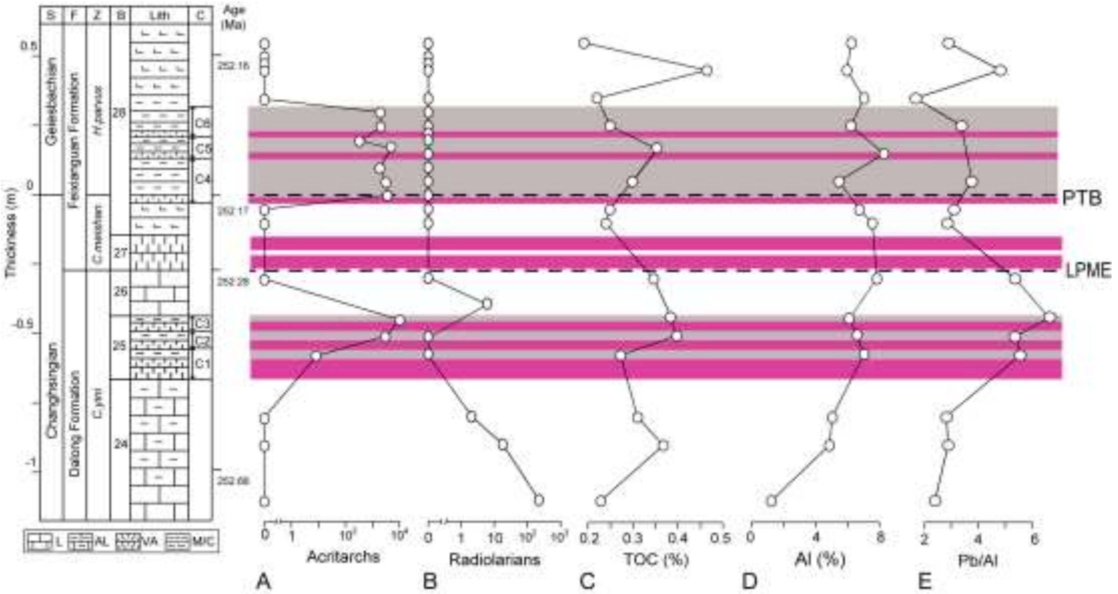

FIGURE 7

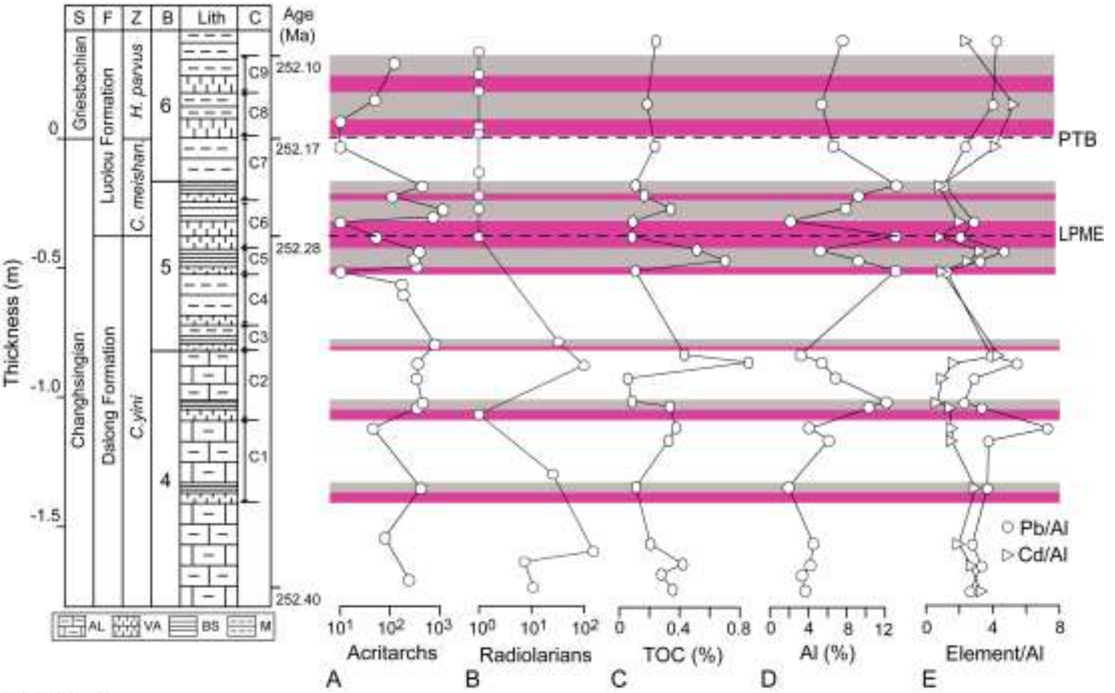

FIGURE 8

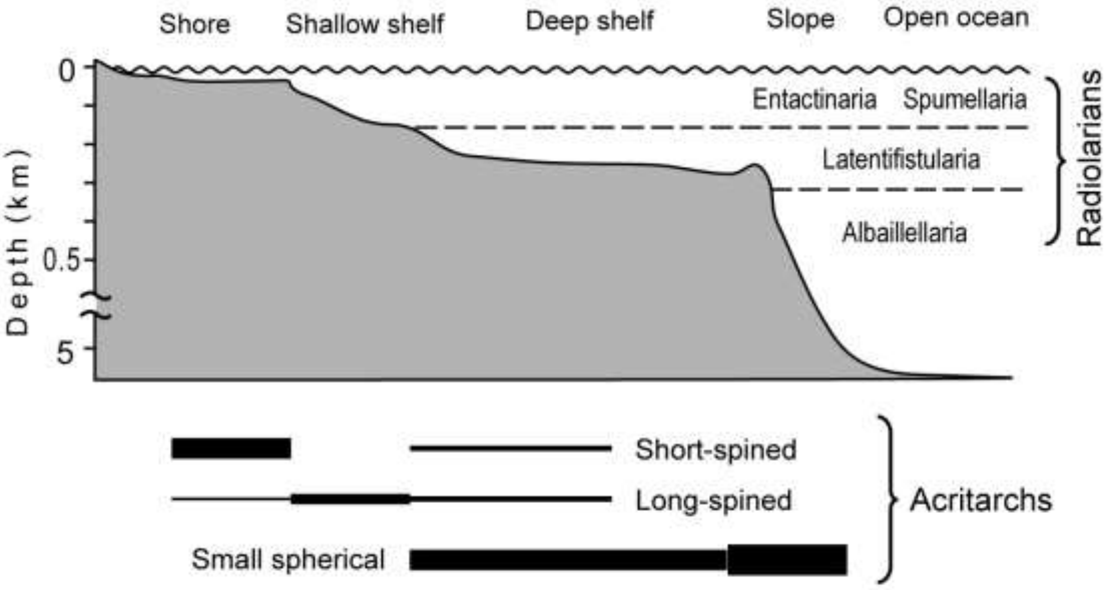
Shore
Shallow shelf
Deep shelf
Slope
Open ocean
Depth (km)
0
0.5
5
Entactinaria
Spumellaria
Latentifistularia
Albaillellaria
Radiolarians
Short-spined
Long-spined
Small spherical
Acritarchs

Figure 9

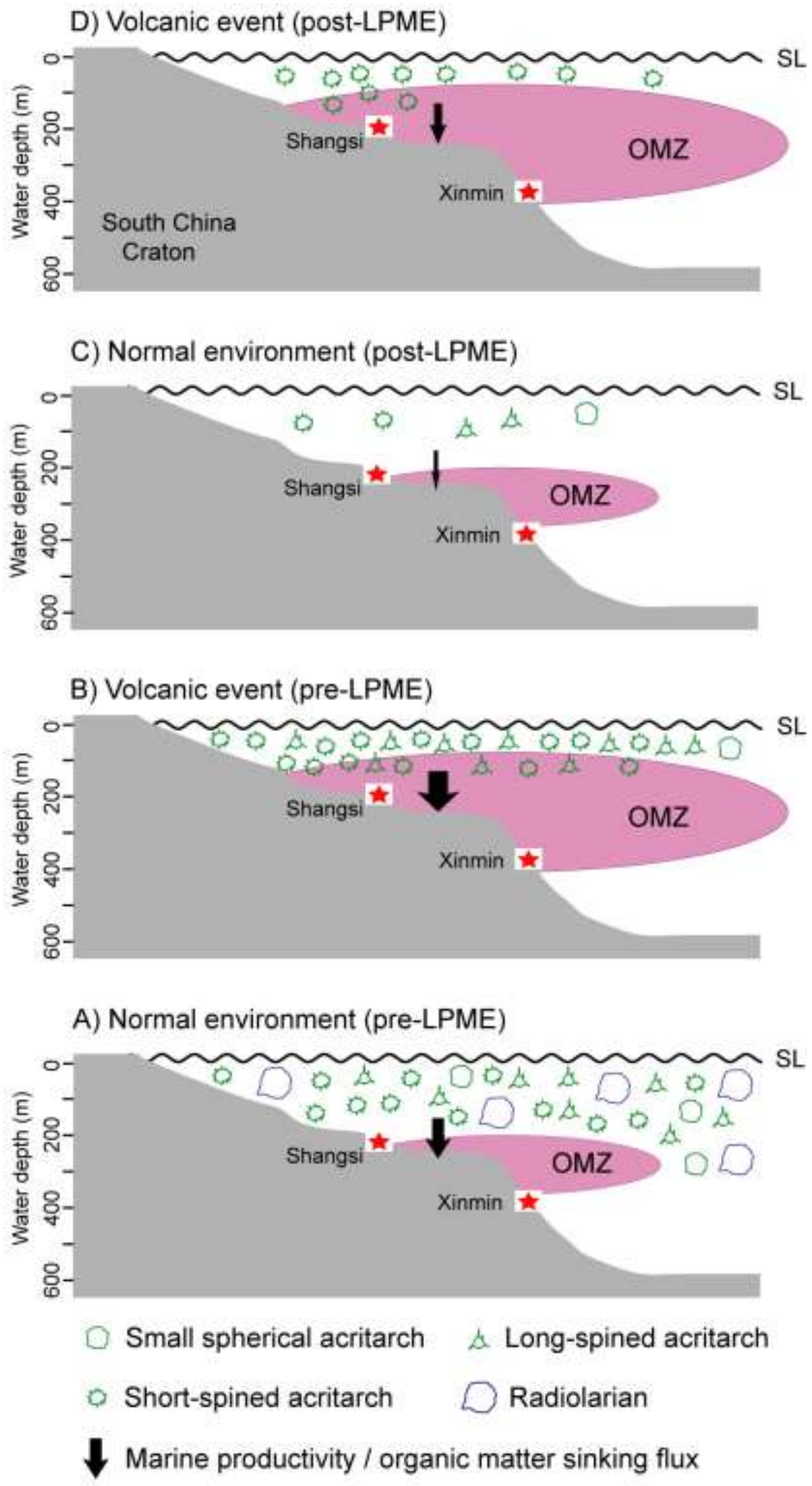
D) Volcanic event (post-LPME)
C) Normal environment (post-LPME)
B) Volcanic event (pre-LPME)
A) Normal environment (pre-LPME)
Water depth (m)
0
200
400
600
SL
OMZ
Shangsi
Xinmin
South China Craton
Small spherical acritarch
Long-spined acritarch
Short-spined acritarch
Radiolarian
Marine productivity / organic matter sinking flux

FIGURE 10